INDC-219

INDC(IND)-003/G

PROCEEDINGS OF THE

Nuclear Physics And Solid State Physics Symposium

1967

NUCLEAR PHYSICS

KANPUR

February 27 – March 3, 1967

ORGANISED BY
PHYSICS COMMITTEE
DEPARTMENT OF ATOMIC ENERGY
GOVERNMENT OF INDIA

Request for copies of this volume should be addressed

to

The Scientific Information Officer,

Bhabha Atomic Research Centre,

Library & Technical Information Section,

2nd floor, Modular Laboratories,

Trombay, Bombay-74.

C O N T E N T S

(Nuclear Physics)

Foreword

The eleventh annual Nuclear Physics and Solid State Physics Symposium sponsored by the Physics Committee of the Department of Atomic Energy was held at the Indian Institute of Technology, Kanpur, during February 28 to March 3, 1967. It was inaugurated by Dr. P.K. Kelkar, Director, Indian Institute of Technology, Kanpur, with Dr. B.D. Nagchaudhuri, Chairman, Physics Committee, D.A.E., presiding.

The number of contributed papers received for the Symposium was overwhelmingly large this year, particularly in Nuclear Physics. This required a slightly different procedure for the presentation of papers. Only about 67 percent of the papers in Nuclear Physics were accepted for full oral presentation and publication in the proceedings. Barring a few papers which were not found acceptable, others were accepted only for discussion, if any, and for publication as abstracts.

The progressive rise of the number of contributions to the Symposium over a period of years is seen from the curves given in the figure on the next page.

For the invited papers and other items of common interest, common sessions were held for the Nuclear Physicists and the Solid State Physicists. For the contributed papers, separate, parallel sessions were held.

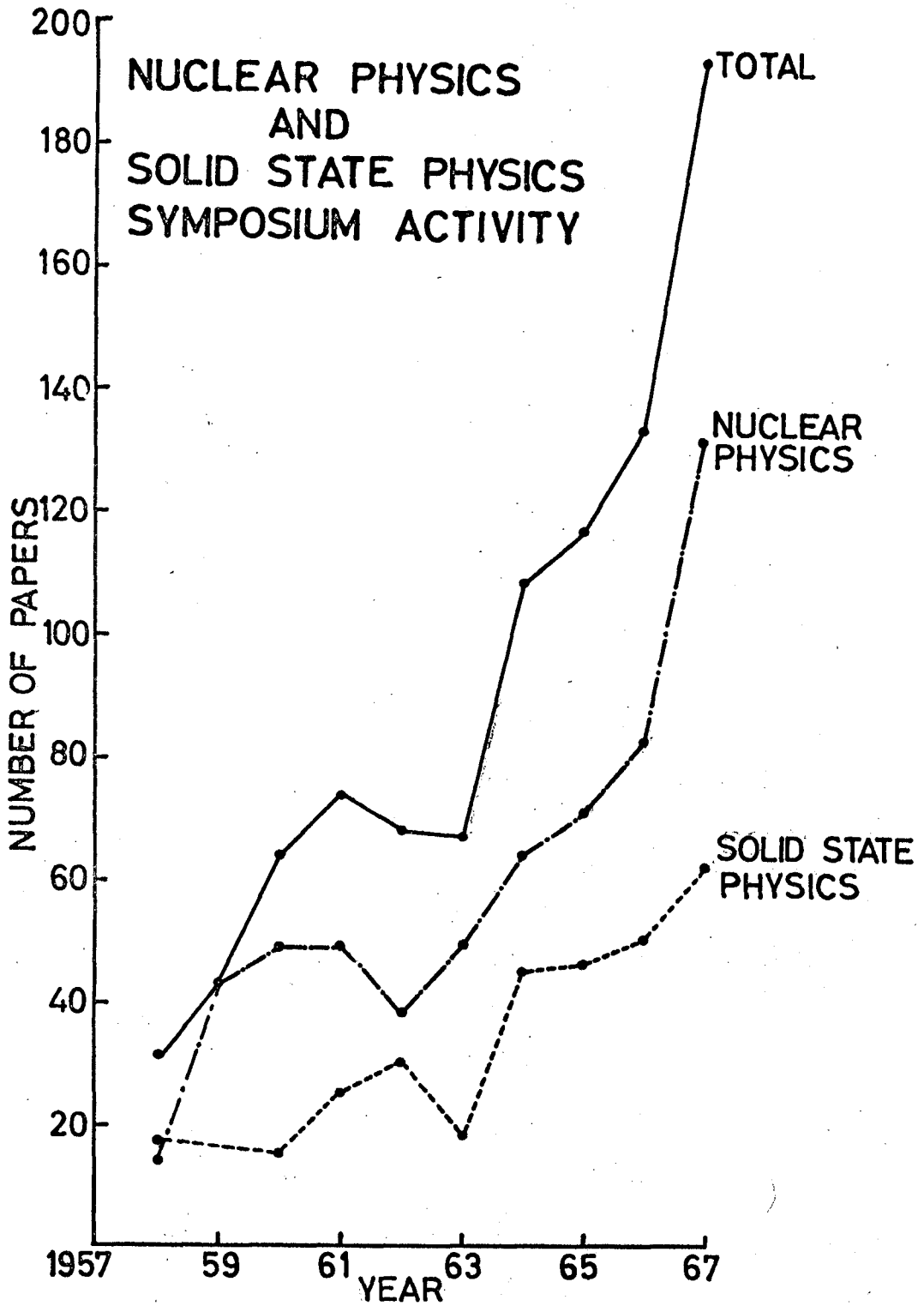
NUCLEAR PHYSICS
AND
SOLID STATE PHYSICS
SYMPOSIUM ACTIVITY
TOTAL
NUCLEAR PHYSICS
SOLID STATE PHYSICS
NUMBER OF PAPERS
200
180
160
140
120
100
80
60
40
20
1957
59
61
63
65
67
YEAR

We wish to thank the Indian Institute of Technology, Kanpur for the warm hospitality and the excellent arrangement during the Symposium.

A.S. Divatia
Convener

SYMPOSIUM COMMITTEE

1.	C. Ambasankaran	B.A.R.C.	
2.	B. Baliga	S.I.N.P.	
3.	H.G. Devare	T.I.F.R.	
4.	A.S. Divatia	B.A.R.C.	(Convener)
5.	M.A. Eswaran	B.A.R.C.	(Sectretary-Nuclear Physics)
6.	K.K. Gupta	T.I.F.R.	
7.	P.K. Iyengar	B.A.R.C.	
8.	V.A. Kamath	B.A.R.C.	(Publication)
9.	J. Mahanty	I.I.T./K.	
10.	S.K. Mitra	T.I.F.R.	
11.	N.S. Satya Murthy	B.A.R.C.	
12.	R.C. Sharma	D.A.E.	
13.	R.M. Singru	I.I.T./K	(Local Secretary)
14.	B.V. Thosar	T.I.F.R.	
15.	R. Vijayaraghavan	T.I.F.R.	(Secretary-Solid State Physics)

---

1. B.A.R.C., Bhabha Atomic Research Centre, Bombay-74.
2. S.I.N.P., Saha Institute of Nuclear Physics, Calcutta- 9.
3. T.I.F.R., Tata Institute of Fundamental Research, Bombay - 5.
4. I.I.T./K., Indian Institute of Technology, Kanpur.
5. D.A.E., Department of Atomic Energy, Bombay - 1.

P R O G R A M M E

February 28, 1967

Inaugural Session

Chairman : B.D. Nagchaudhuri

Inaugural Speech by P.R. Kelkar

NUCLEAR PHYSICS

SESSION - 1.

Chairman : R. Ramanna

SESSION - 2.

Chairman : Y.R. Waghmare

\+ Presented by this author.

* Not for oral presentation.

SESSION - 3.

Chairman : R.P. Singh

SESSION - 4.

Chairman : K.H. Bhatt.

SESSION - 7

Chairman : J. Mahanty

March 2, 1967

SESSION - 8

Chairman : P.P. Kane

SESSION - 9

Chairman : N.V.V.J. Swamy

SESSION - 11

Chairman : P.N. Trehan

SESSION - 12.

Chairman : S. Mukherjee

SESSION - 14.

Chairman : N. Nath.

SESSION - 15.

Chairman : A.M. Ghose.

SESSION - 16.

Chairman : V.K. Deshpande

PLASMA PHYSICS

B.D. Nagchaudhuri
Saha Institute of Nuclear Physics
Calcutta.

The density of ionised matter in plasmas of interest can range from one atom per c.c. in inter-stellar space to $10^{27}/10^{28}$ per cc in the interior of condensed stars such as white dwarfs. This enormous scale factor of 10^{28} perhaps applies to no other class of phenomena in Physics. I will restrict this talk only to a very few and quite limited aspects of the plasma. The major criteria of selection of certain types of plasma for the purpose of this discussion are:

A) We are concerned only with laboratory gaseous plasmas, wholly ionised or partly ionised.

B) The density of the plasmas we would be considering will vary from 10^{7-8} electrons per cc to about 10^{14} per cc. Even this is a fairly large factor.

C) We are interested in plasmas from the point of view of their application as useful devices rather than physical experiments designed to understand the plasma. Let me clarify by saying that we exclude from our discussions such important and provocative aspects of plasma as thermounuclear devices which in their present stage indicate the necessity

of understanding the plasma in greater depth and detail than has so far been done.

Gaseous plasmas lend themselves to many possible devices. Basically these devices depend on the high temperature, the high conductivity and the tensor and non-linear properties (in a magnetic field) of plasma. In fact, as the prospect of the thermonuclear plasma has receded, the plasma physicists and engineers have turned more and more to other applicational aspects of the plasma.

The classic application of the high temperature plasma is the development of plasma torch and electron and ion beam furnances. These devices have proved to be very useful. The Bhabha Atomic Research Centre at Trombay have developed an argon type plasma torch which may be described as a typical high temperature torch. The plasma is created by introducing large radiofrequency power into a jet of argon. The radiofrequency power ionises and heats the argon which may reach the temperature up to around 15,000° to 20,000°C. There are, of course, many problems in the operation of such a device. The coupling between the radiofrequency power source and the plasma is perhpas the most crucial of the various problems involved. Plasmas so formed are partially ionised at a high gas density and with percentage ionisation which may vary from 1-15%. Similar to the plasma torch there is another interesting device in which either electron or ion beam is used. The electron beam torch

can work even at the atmospheric pressure while the ion torch operates only in high vacuum. Large electron or ion currents are accelerated by appropriate voltages and then focussed on to the job. These devices are used in welding and brazing.

To provide the different plasma devices with the necessary electrons and ions various types of ion sources have been developed. Of these the duoplasmatron developed by Von Ardenne (1956) is perhaps the most efficient ion source from the point of view of large extracted currents and high gas efficiency. Usually a very high extraction voltage ($\sim$60 KV) is required for extracting reasonable ion currents from the duoplasmatron. Attempts are being made in our laboratory to reduce the extraction voltage considerably by placing an additional electrode in between the anode and the extractor. With a ring electrode at a few KV positive placed before the extractor a nearly 50% increase of extracted ion current has been recorded at lower voltages. Here the ring produces the necessary ion optical shape to the plasma boundary at the anode orifice so that the ion beam instead of being divergent, becomes fairly collimated at lower extraction voltages. These results will be discussed in another paper to be presented in the symposium.

A very important device using gaseous plasmas is the magnetohydrodynamic (MHD) generator. This device converts

heat into electrical power. Basically the MHD concept was not much different from the conventional turbogenerators. The moving part here is a conducting gas in which emf. is induced when the gas moves across a magnetic field. In contrast to conventional generators, an MHD generator usually produces d.c. power. Several attempts to get a.c. power show that it is more simple and economical to convert the generated d.c. into a.c. by external agencies than to force the generator itself to behave as an a.c. system by methods such as using an a.c. magnet. MHD devices are still in their experimental stage. But the experience already gained with them indicates that, in near future, MHD generators are likely to become big competitors of conventional devices even on a commerical scale. Because of their higher power output per pound weight MHD devices may prove to be more convenient for supersonic and space flights. The possibility of constructing MHD generators with nuclear reactors as heat source is now under study at a number of centres for both space and ground applications.

Another exciting field of plasma research is the ionic and plasma propulsion of space vehicles. When a space vehicle is required to move from a lower to higher orbit or is set out for an interplanetary voyage a very high specific impulse is needed. For example, the optimum specific impulse ranges from 1500 to 5000 seconds for a complete lunar trip and 7500 to 20,000 seconds for interplanetary flights. These values

of specific impulse are inconveniently large for conventional rocket propellents. High specific impulse devices are possible using either an ion beam or a gaseous plasma as the propellent. In the ion propulsion device ions from a suitable ion source are accelerated by an electrostatic field and then ejected from the device in a manner similar to the mass flow from an ordinary rocket. To prevent the ion rocket from acquiring negative charge due to outflow of ions and to stop building up of space charge behind the rocket, the ejecting ion beam should be neutralized. One method of charge neutralization is to inject an equivalent amount of electrons into the ejecting beam. Another suggestion for charge neutralization is the simultaneous or double extraction of ions and electrons from the ion engine. Some efforts in this direction has been made with a duoplasmatron ion source in our laboratory. It has been found that the double extraction gives an increased rate of extracted ions.

Because the plasma is electrically neutral the plasma propulsion device is not affected by the space charge effects as in the case of ion propulsion. A number of plasma propulsion devices have been developed on the basis of heating and acceleration of plasmas by electromagnetic fields. Plasma jets, MHD accelerators, T-tube accelerators etc. are examples of plasma propulsion devices.

Other possible applications of plasma include the construction of microwave components such as attenuators, phase shifts, wave guide filters, etc. and the generation of millimeter waves by harmonic generation using the non-linearity of the plasma in a magnetic field.

TIME VARYING PHENOMENA IN A P.I.G. PLASMA

D.K. Bose, C. Dutta, J.N. Maity, S.N. Sen Gupta
and B.D. Nagchaudhuri
Saha Institute of Nuclear Physics
Calcutta.

ABSTRACT.

The oscillations and fluctuations occurring spontaneously in a P.I.G. discharge in presence of a magnetic field have been studied by means of Langmuir-type probes. The associated signals collected by the probes at different locations within the plasma were analysed by a receiver and an oscilloscope. From the oscillograms recorded the following types of signals were identified:

i) Broad-band noise arising from the random fluctuations of density and potential of the plasma.

ii) Discrete frequency signals associated with some collective phenomena in the plasma.

The origin of these time varying phenomena and their relation with the diffusion of plasma across a magnetic field will be discussed.

EXTRACTION OF POSITIVE IONS AND ELECTRONS SIMULTANEOUSLY FROM A DUOPLASMATRON

D.K. Bose, B.D. Nagchaudhuri and S.N. Sengupta
Saha Institute of Nuclear Physics, Calcutta.

ABSTRACT.

Extraction systems are under investigation which can give high ion currents at lower extraction voltage, for duoplasmatron source. Present arrangement can extract electrons and positive ions simultaneously. Electron extraction is found to improve ion current by almost cent percent. Usual plasma expansion cylinder has been replaced by a copper ring (1" O.D, 3/4" I.D.) placed between the anode and the extractor, and applied either with source potential or electron extraction potential. The extractor 3 mm. away from the ring was applied with ion extraction voltages. Tank plot shows that potential distribution between extractor and anode takes favourable shapes in presence of ring. Ion current is collected in a biased cup. Ion current increases with electron current and becomes almost double and then remains unchanged. A set of data is given:-

P discharge	Arc amp	Magnet amp	Electron extraction potential + kV	Electron current mA	Ion extraction potential -kV	Ion current mA
5×10^{-2}	2	2	0	0	6	2.50
Argon			0.8	1.0	6	2.75
			1.1	2.0	6	3.75
			1.5	3.0	6	4.00
			1.6	10	6	4.25
			1.75	15	6	4.25

Since the ring collects only the electrons and has small dimension, recombination is almost absent. The ring with a slit may be suitable to accelerate the electrons in the form of a beam coaxial with the ion beam which is generally required for beam neutralisation purpose in electrostatic ion energies.

DISCUSSION:

A.S. Divatia: What is the current of + ve ions and - ve ions?

D.K. Bose: For arc 2.0 amp in argon, magnet current 2 amp, $p = 5 \times 10^{-2}$ Torr of discharge, one set of data is as follows: At -6 kv, positive ion current is 4.25 mA while simultanously drawn - ve particle current is about 5 mA at about + 2 kV

applied to the electron extractor, the seperation between the ring, the electron collector and the ion extractor being about 3 mm.

M.P. Navalkar: Is it possible to replace the electro-magnet of duo plasmatron by a permanent one?

D.K. Bose: This of course depends on the arc condition and the extraction voltage. We often need to change the magnetic field to obtain maximum ion current in the collimated form. So it is desired that the magnetic field has to be adjusted.

ON SOME CHARACTERSTICS OF RADIO FREQUENCY PLASMAS

Jayakumar, D.V. Karandikar and M.A. Aziz
Bhabha Atomic Research Centre, Trombay
Technical Physics Division

INTRODUCTION:

Recently a great deal of attention has been directed towards studying the properties of matter, in a state where the matter is so highly ionised that its dynamical equilibrium properties are governed by the free charges created. The radio frequency plasmas deserve special mention, on account of their extensive application in the field of technology. A fruitful study, directed towards inferring the salient parameters of the rf plasma at low and high pressure was conducted in our laboratory.

The atmospheric plasmas have been shown to attain temperatures as high as 30000°K and an electrical conductivity of 100 mho/cm. The tediousness involved in the measurement of such high temperatures by conventional methods is almost too much, particularly when an estimate of the average temperature is enough. The measurement of conductivity and hence the temperature, from the performance characterstics of the generating source proves to be an easier method.

The rf induction plasmas at low pressures and high frequencies have been proved to settle in a non-equilibrium state, as a result of the efficient energy transfer from the field to the

electron and an inefficient transfer from the electrons to the gas atoms. The electron swarm attains a much higher energy than the thermal energy of the gas atoms through collisions, consequent on the fact that the collisions cause the phase of the electron motion to change and as a result, the electron is imparted with more energy from the field, than what it has lost in the collision. The high electron energy gives rise to a high ionisation collision frequency and thus a high conductivity.

THE MEASUREMENTS IN ATMOSPHERIC OF INDUCTION PLASMA:

The value of the electrical conductivity of the induction plasma was arrived at using the method employed by M.C. Gourdine(1). The method is based upon the response of the oscillator frequency to the conductivity of the core material. The dependence is given by the relation

$$\omega = \left[\frac{2\pi C R^2 N^2 \mu_0}{\ell} \frac{\delta}{\sqrt{2} R} \frac{M_1(\beta)}{M_0(\beta)} \sin\left(\theta_1 - \theta_0 - \frac{\pi}{4}\right) \right]^{-1/2}$$

Where ω is the applied angular frequency, C is the Tank capacitance, R is the radious of the core, N and L are the number of turns and length of the tank Coil, respectively. μ_0 is the permeability and σ is the conductivity of the core, M_1 and Mo are Moduli of the Bessel Kelvin functions and $\beta = \sqrt{2} R / \delta$ where $\delta = (2/\sigma \mu_0 \omega)^{1/2}$ The relation between value of ω^2 normalised to the value for infinite conductivity with β, has been delineated in Figure 1.

The experimental values of ω^2, normalised to the value for copper ($\beta > 1000$), for known conductivities agreed well with

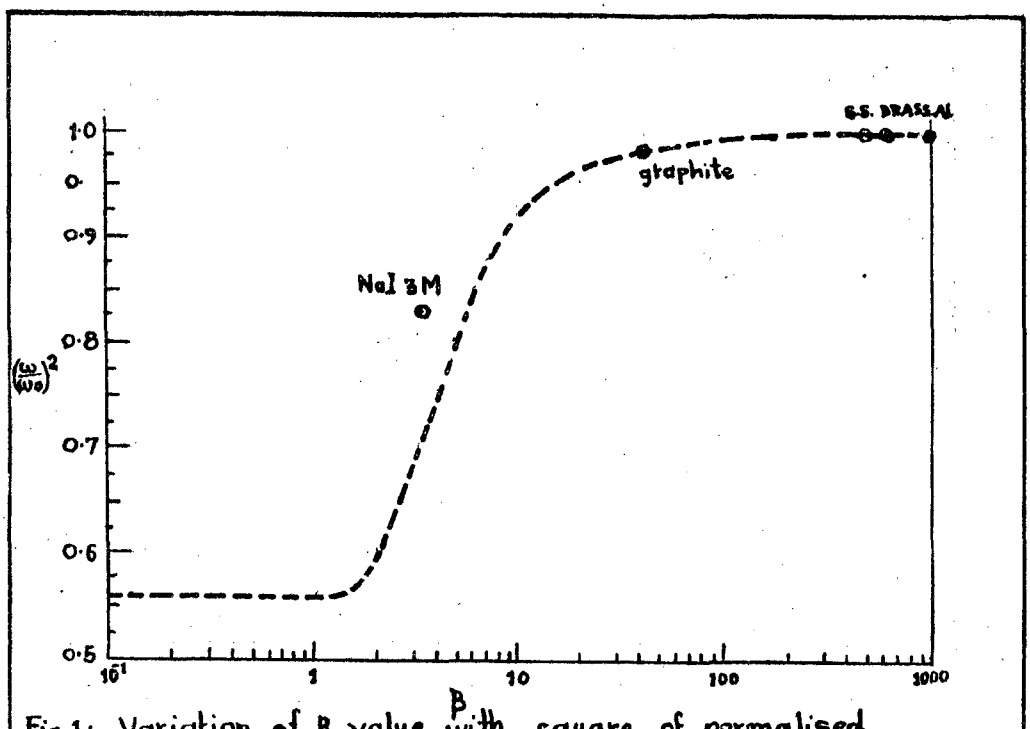

Fig.1:- Variation of β value with square of normalised frequency.

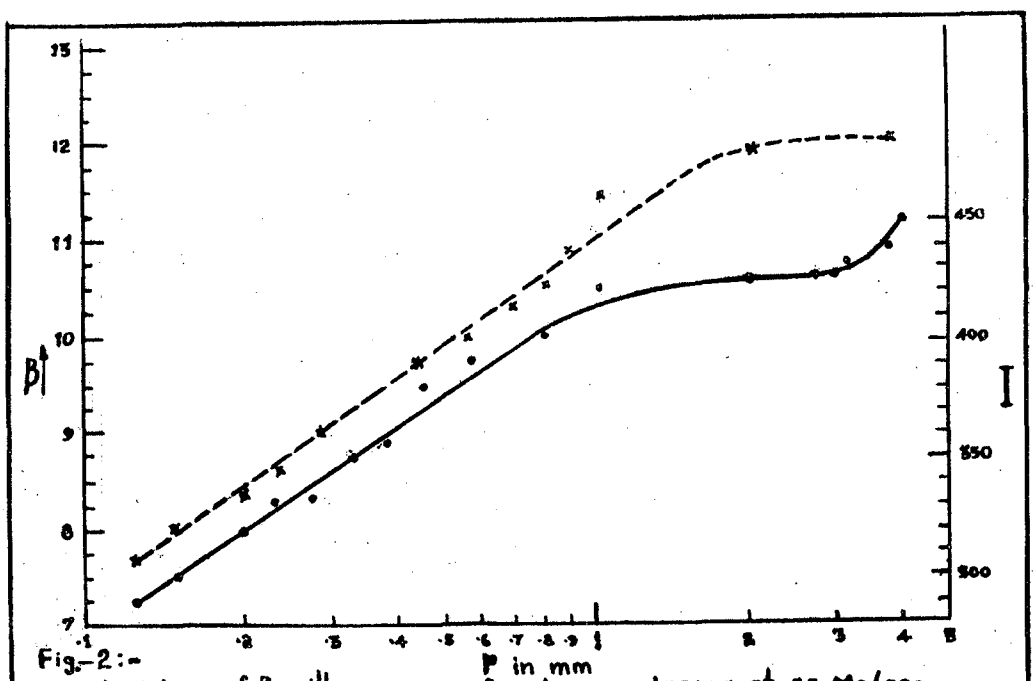

Fig.-2:-
---- Variation of β with pressure for Argon plasma at 36 Mc/sec.
—— Variation of cathode current with pressure for Argon plasma at 36 Mc/sec. and 1000 volts/cm. (Vessel I.D. 25 mm)

the theoretical values, except at very low conductivities, where the added capacity of the circuit increased the frequency.

The conductivity of the Argon Plasma, generated in a vessel of 45 mm i.d, by a 6 K W 6 M c/s oscillatory, was determined from the frequency to be 27.5 mho/cm. The value of the electron temperature was obtained using the calculations of mean free path conductivity by Kantrowitz et. al and Spitzer (2). This agreed with the value predicted by electron density, calculated to be 8.6×10^{16}/c.c. The value of gas temperature inferred from the power measurements, which yielded a power input of 2780 watts in the plasma, agreed with the electron temperature within 10% margin. Thus a good case can be made for the statement that the equilibrium between the species of the plasma exists.

THE rf PLASMA AT LOW PRESSURES:

The principal problem of studying the conductivity of the plasma and the ability of the plasma to load the Oscillator, has been dealt with.

The conductivity of the induction (H type) plasma was computed in the same lines as before. The variation of the conductivity with β and the loading on the oscillator with pressure are shown in Fig. 2. The conductivity of the ring discharge at 1 mm pressure, 700 watt power input, and 36 M c/s applied frequency and in a 26 mm i.d. vessel was 28 mho/cm. It is evident from the low values of power inputs, required for attaining such high conductivities in the case of these plasmas, that the gas temperature is much lower than the electron temperature and this

is backed up by the low intensity of the plasma. This is good news to the MHD enthusiasts as it would greatly minimise the duct wall ablation, if a highly conducting fluid at low temperature is used. The sudden rise in loading of the Oscillator, when the pressure is increased beyond 2.5 mm is indicative of the fact that the transition from the non-equilibrium state to equilibrium takes place and the energy transfer to the atoms is more effective. This has again supported by the sudden increase in the brightness of the Plasma.

The conductivity of the E type plasma was measured from the grid current, which is a function of the conductivity of the load of the work capacitor. The conductivity of the plasma at 1mm pressure 50 watt power input, 34 M c/s frequency and in a 26 mm i.d. tube was .028 mho/cm. The high value of conductivity of the H type Plasma, compared with that in E type is due to the large electron path provided for the electrons Spiralling in the magnetic field.

ACKNOWLEDGEMENT:

Our thanks are due to Mr. C. Ambasankaran who constructively contributed in our work through discussions and Prof. D.Y. Phadke, for his technical help.

REFERENCES:

1. Gourdine M.C., I.E.E. report series No. 4, 16.

2. Cambel, A.B. - Plasma Physics and Magento fluid Mechanics, Mcgrawhill, pp 173 (1963).

J. Basu: Do you consider the complex conductivity of the plasma or only the real part of it? How do you justify neglecting the imaginary part of the conductivity?

Jayakumar: The conductivity measured was the average real conductivity, as it is predicted by the frequency change which is a function of the real conductivity.

RF HEATING OF A CYLINDRICAL PLASMA

J.N. Maiti and J. Basu
Saha Institute of Nuclear Physics,
Calcutta

INTRODUCTION:

It is well known that a plasma behaves as a conductor at low frequencies and as a dielectric at high frequencies. It, therefore, seems appropriate to determine the power that can be fed into a plasma by the standard induction and dielectric heating methods. A uniform plasma of cylindrical geometry is considered for the purpose.

INDUCTION HEATING:

The expression for the power absorbed by a good conductor from an alternating magnetic field is given in the literature (1). By extending the analysis to the case of a plasma which has a complex conductivity $\sigma = \sigma_r + j\sigma_i$ the following formula for the power absorbed per unit length of a cylindrical plasma is obtained.

$$P = \frac{8\pi H_0^2}{B^2} \cdot Ka \cdot \frac{\sigma_r}{\sigma_r^2 + \sigma_i^2} \cdot \frac{M_1(Ka)}{M_0(Ka)} \frac{\sin(\theta_1 - \theta_0 - \phi)}{\sin 2\phi} \qquad (1)$$

where H_0 = impressed magnetic field of frequency ω

a = radius of the plasma column

$k = \left[\omega^2 \mu_0^2 (\sigma_r^2 + \sigma_i^2)\right]^{1/4}$

$$\phi = \frac{1}{2} \tan^{-1} \frac{\sigma_r}{\sigma_i}$$

$$M_1(ka) = \left| J_1(ka,\phi) \right| = \sqrt{w_1^2(ka,\phi) + v_1^2(ka,\phi)}$$

$$M_0(ka) = \left| J_0(ka,\phi) \right| = \sqrt{w_0^2(ka,\phi) + v_0^2(ka,\phi)}$$

$$\theta_1 = \tan^{-1} \frac{v_1(ka,\phi)}{w_1(ka,\phi)}$$

$$\theta_0 = \tan^{-1} \frac{v_0(ka,\phi)}{w_0(ka,\phi)}$$

$$\beta^2 = \left[1 + \frac{\{\omega\mu_0(\sqrt{\sigma_r^2+\sigma_i^2} + \sigma_i)\}^{1/2}}{\sqrt{2}\cdot 120\pi \cdot \sqrt{\sigma_r^2+\sigma_i^2}} \right]^2 + \left[\frac{\{\omega\mu_0(\sqrt{\sigma_r^2+\sigma_i^2} - \sigma_i\}^{1/2}}{\sqrt{2}\cdot 120\pi \cdot \sqrt{\sigma_r^2+\sigma_i^2}} \right]^2$$

The values of w_0, v_0, w_1 and v_1 are given in standard tables (2).

The complex conductivity at a frequency ω is given by (3)

$$\sigma = \sigma_r + j\sigma_i = \frac{\epsilon_0}{\omega^2+\nu^2}\left[\omega_p^2\nu + j\omega(\omega^2+\nu^2-\omega_p^2)\right] \quad (2)$$

where ϵ_0 = permittivity of free space

ω_p = plasma frequency

ν = electron collision frequency.

GOOD CONDUCTOR APPROXIMATION:

In laboratory plasmas ω_p is usually quite high compared to ω or ν. If we now assume $\omega_p \ll \nu$, the plasma acts as a good conductor with $\sigma \simeq \sigma_r = \epsilon_0\omega_p^2/\nu$ and the power absorbed per unit length is given by

$$P = 4\sqrt{\frac{\pi\mu_0}{\epsilon_0}} \cdot H_0^2 \sqrt{(a^2 f)\left(\nu/f_p^2\right)^2} \cdot F \qquad (3)$$

where F is a function of $a^2 f$ and ν/f_p^2.

When $a^2 f < \frac{c^2}{4\pi^3} \cdot \frac{\nu}{f_p^2}$

$$P \simeq \frac{8\pi^5\mu_0}{c^2} \cdot H_0^2 (a^2 f)^2 (f_p^2/\nu) \qquad (4)$$

When $a^2 f > \frac{5c^2}{4\pi^3} \frac{\nu}{f_p^2}$

$$P \simeq 4\sqrt{\frac{\pi\mu_0}{\epsilon_0}} \cdot H_0^2 \cdot \sqrt{(a^2 f)(\nu/f_p^2)} \qquad (5)$$

Fig.1 shows the plot of P in db with repsect to 1 watt against log $(a^2 f)$ for various values of f_p^2/ν, $a^2 f$ and f_p^2/ν being selected so as to cover a wide range of practical systems. For low values of $a^2 f$, the plots correspond to eqn. (4) while for high values they correspond to eqn. (5).

However, the plots in Fig.1 are applicable provided $f \ll \nu$. When f becomes comparable to ν, the exact plot of P deviates from the plot obtained from the good conductor approximation, as shown in Fig.2 for a particular case. P is now found to decrease after reaching a maximum, as the plasma starts behaving more like a dielectric than a conductor.

Plots of P against log (f_p^2/ν) are given in Fig.3 on the basis of the good conductor approximation. It is interesting to find that P has a maximum at

$$f_p^2/\nu \simeq \frac{2.9c^2}{4\pi^3} \cdot \frac{1}{a^2 f} \qquad (6)$$

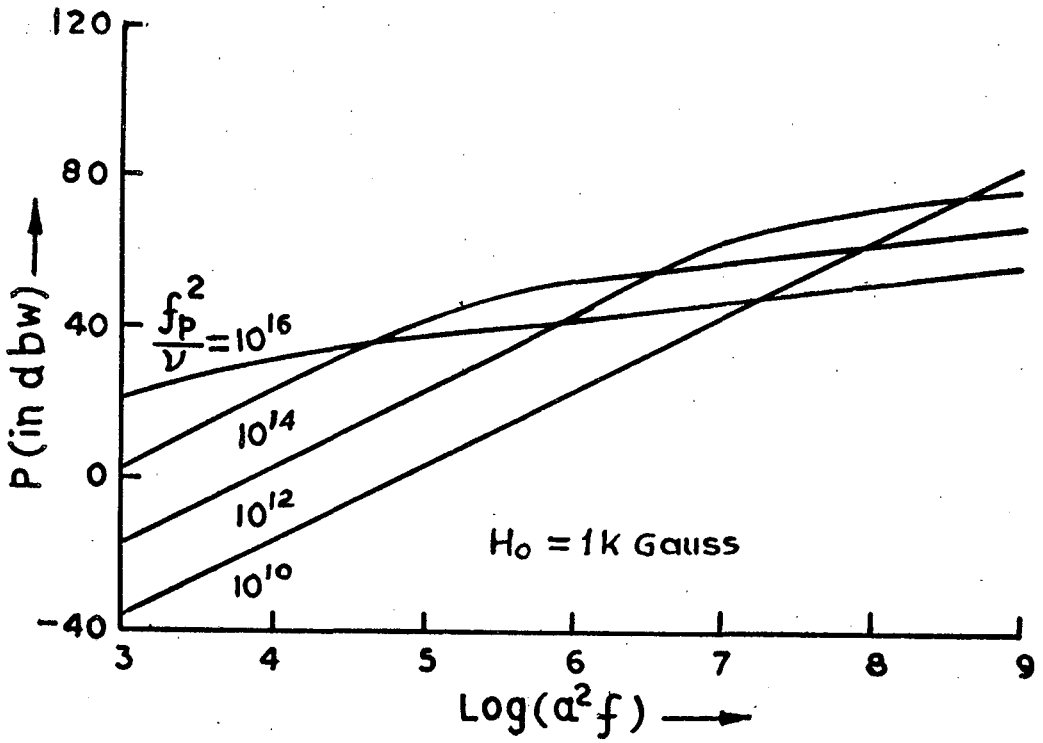
120
80
40
0
-40
P (in dbw)
$\frac{f_p^2}{\nu} = 10^{16}$
10^{14}
10^{12}
10^{10}
$H_o = 1K$ Gauss
3
4
5
6
7
8
9
Log($a^2 f$)

FIG.1.

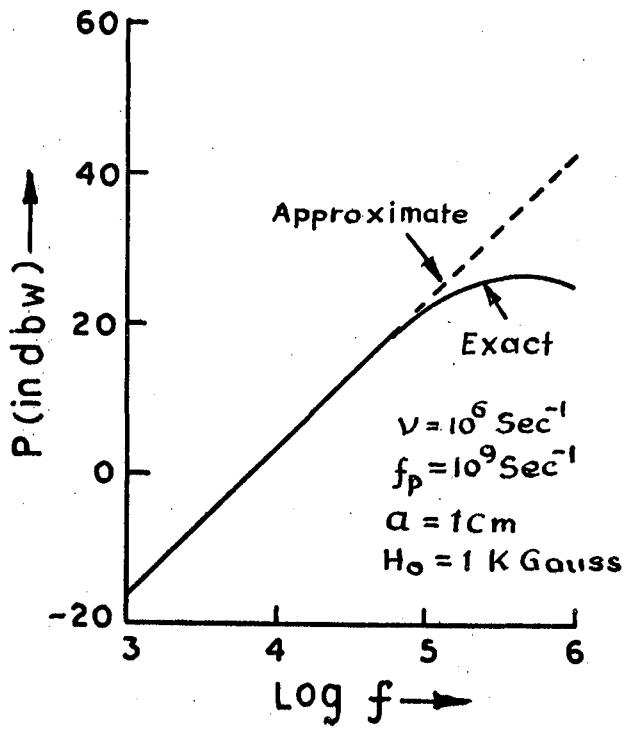
60
40
20
0
-20
P (in dbw)
Approximate
Exact
$\nu = 10^6$ Sec^{-1}
$f_p = 10^9$ Sec^{-1}
$a = 1$ Cm
$H_o = 1$ K Gauss
3
4
5
6
Log f

FIG.2.

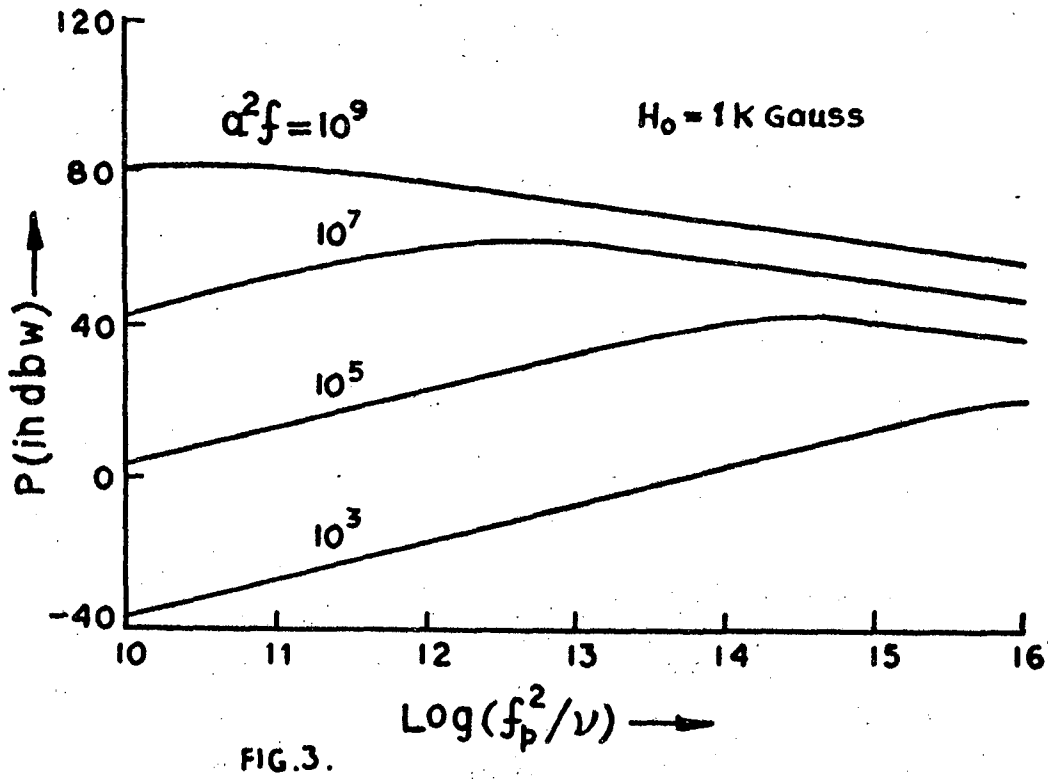

FIG. 3.

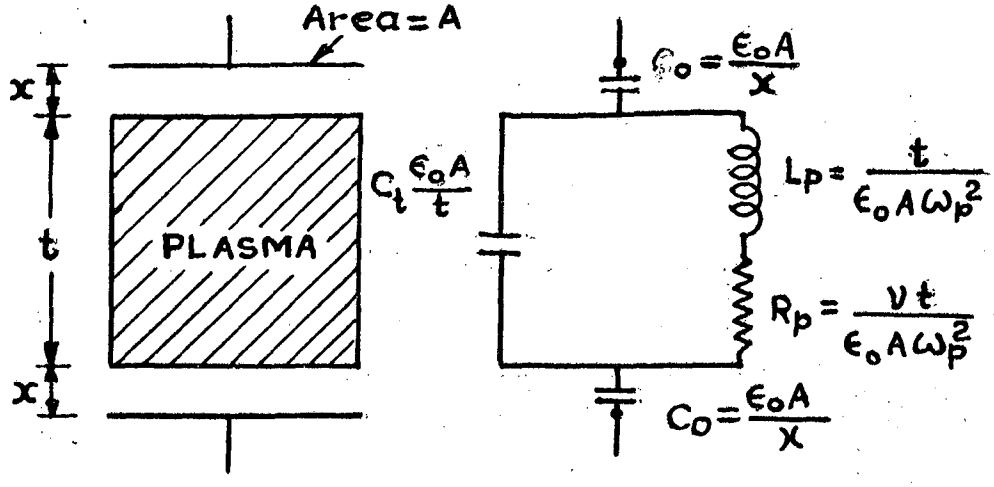

$$\omega_r(\text{Series}) \approx \omega_p \sqrt{2x/(t+2x)}$$

$$P_r\ (\text{Series}) \approx \frac{\omega_p^2 \epsilon_0 A t}{\nu (t+2x)^2} \cdot V^2$$

FIG. 4.

This can be explained by the fact that, as f_p^2/ν rises, the conductivity increases but at the same time the skin depth is reduced.

DIELECTRIC HEATING:

When $\omega \gg \nu$ a plasma can be considered as a dielectric, the complex dielectric constant of which is given by (4)

$$\epsilon = \epsilon_r - j\epsilon_i = 1 - \left(\frac{\omega_p}{\omega}\right)^2 - j\,\frac{\omega_p^2 \nu}{\omega^3} \qquad (7)$$

Let a plasma of cross-section $A = \pi a^2$ and of length t be placed, covering the space between the plates of a condenser. The total power absorbed by the plasma is given by

$$P_t = \frac{\omega \epsilon_0 \epsilon_i A}{t} V^2$$

$$= \epsilon_0 \frac{\omega_p^2 \nu}{\omega^2} \frac{A}{t} \cdot V^2 \qquad (8)$$

where V is the voltage of frequency ω, applied to the condenser plates.

Eqn. (8) shows that, while P_t increases with ω for an ordinary dielectric, it decreases with ω for a plasma.

For low frequencies, on the other hand, most of the voltage drop occurs across the sheaths at the plasma boundaries, and there is little penetration of the field inside the plasma.

It is, therefore, evident that the dielectric method is not generally suitable for heating a plasma.

HEATING AT SERIES RESONANCE:

There is, however, a special case, in which the dielectric method may prove efficient.

Let us consider the system shown in Fig.4, which also shows the equivalent circuit diagram. The circuit has a series resonance at $\omega_r = \omega_p \sqrt{2x/(t+2x)}$, when the power absorbed by the plasma is given by

$$P_r \simeq \frac{\omega_p^2 \epsilon_0 A t}{v (t+2x)^2} \cdot V^2 \qquad (9)$$

This power may be quite considerable.

REFERENCES:

1. Brown, G.H., Hoyler, C.N. and Bierwirth, R.A., 'Theory and Application of Radio-Frequency Heating', p. 29, D. Van Nostrand Company, Inc., (1947).
2. 'Table of The Bessel Functions $J_0(z)$ and $J_1(z)$ for Complex Arguments', Columbia University Press, New York (1947)
3. D.L. Sen Gupta, Proc. IRE 49, 1872 (1961)
4. Ratcliffe, J.A. 'Magneto-Innic Theory', p. 81, Cambridge University Press (1959)

CHARACTERSTICS OF A LOW PRESSURE PIG DISCHARGE

C. Dutta, S.N. Sengupta, J. Basu and B.D. Nagchaudhuri
Saha Institute of Nuclear Physics, Calcutta.

ABSTRACT.

The following discharge characteristics of a cold-cathode ring-anode PIG discharge (pressure $\approx 10^{-5}$ Torr) have been observed.

1) Striking characteristics at magnetic fields ranging from 300 gauss to 1500 gauss.

2) Variation of the discharge current as a function of the discharge voltage and magnetic field, the discharge voltage being varied from 800 V to 1600 V and the magnetic field from 300 gauss to 1500 gauss.

The special features of the characteristics are noted below.

1) The striking voltage is minimum ($\approx$ 850 V) at a magnetic field of about 550 gauss.

2) For the lower range of the magnetic field, the discharge current increases abruptly at a certain value of the discharge voltage, as it is gradually increased. The higher the magnetic field in this range, the lower the voltage at which the effect occurs.

For the higher range of the field, there appears a reverse effect, i.e., the current drops suddenly at a certain voltage.

In the intermediate stage no such effect occurs, and the current varies smoothly with the voltage.

However, there is again an abrupt change in the current when the magnetic field is increased, keeping the voltage constant.

There is also a critical magnetid field at which the discharge current shows a maximum. The higher the discharge voltage, the more prominent the peak at the critical field.

DISCUSSION:

C. Ambasankaran: What is the order of the magnetic field at which the investigation was carried out?

C. Dutta: The critical magnetic field has the value of 540 gauss for argon at a discharge voltage of 1600 volts (pressure $\sim 10^{-5}$ torr). The value was 550 gauss for the residual gas at the same discharge voltage and pressure. The working range of the field was from 300 gauss to 1800 gauss.

COAXIAL PROBE PLASMA DIAGNOSTICS

J. Basu, C. Dutta and S.N. Sengupta
Saha Institute of Nuclear Physics, calcutta

The use of a coaxial probe for determining plasma parameters is suggested. The probe, open at both ends and with the external surface of the outer conductor insulated, is suitable for both dc and rf measurements. It is assumed that the dimensions of the probe are such that the plasma can penetrate fully inside and can be considered to have a uniform annular shape, bounded by the sheaths at the inner conductor and the internal surface of the outer conductor.

The electron temperature and charge density can be obtained by using the coaxial conductors as a dc double probe system with the advantage over the conventional double probe that the results pertain not only to high-energy electrons but also to low-energy ones.

The coaxial geometry is an obvious choice for avoiding stray capacitances in rf measurements. The charge density and electron collision frequency in a plasma can be derived by measuring the impedance of the coaxial probe, placed in the plasma, at two ratio frequencies.

OPTICAL MODEL WITH SEPARABLE POTENTIAL

V.L. Narasimham
Department of Physics
Indian Institute of Technology
Powai, Bombay-76.

ABSTRACT.

The optical potential is given by

$$W = \sum_{i=1}^{A} \langle \phi_0 | G_{0i} | \phi_0 \rangle$$

where G_{0i} is the scattering matrix between the projectile nucleon 'o' and the target nucleon 'i' in the presence of other nucleons. The derivation of the optical potential using Brueckner's theory of nucleus will be discussed. In deriving this the Pauli Principle in the intermediate states of the target nucleus has been taken into consideration.

Not presented.

LOW ENERGY NEUTRON SCATTERING FROM NUCLEI

S. Mukherjee and C.S. Shastry
Saha Institute of Nuclear Physics,
Calcutta.

INTRODUCTION:

The optical model of elastic scattering from nucleons from nuclei is known to be very successful over a wide energy range and for various nuclei covering practically the entire mass table. The striking success of this empirical model is not so well understood physically and in terms of complex system consisting of incident nucleon and target nucleus. This is reflected through the fact that the energy dependence of potential parameters and this dependence on mass number, spin and isospin of the system are known only empirically roughly. The purpose of present investigation is to understand and appreciate the optical model in terms of the physics of the system of particles involved in scattering. For this purpose we use a Regge type representation of the scattering amplitude (1) which is essentially a description of the scattering in terms of poles of S-matrix in angular momentum plane which in turn describe the properties of intermediate compound system consisting of incident nucleons and target nucleus. In the present paper we shall discuss the results obtained by this approach for the low energy scattering of neutrons (.4 to 4.6 MeV) from several

typical nuclei. Rigorous theoretical justifications of the theory will be discussed elsewhere (4).

REGGE POLE REPRESENTATIONS:

Using the rotations of ref. (2) we have the equivalent representations for scattering amplitude $A(k,z)$ corresponding to scattering of a spin zero system with a superposition of Yukawa type potential as

$$A(k,z) = (2ik)^{-1}\sum_{l=0}^{\infty}(2l+1)\left[S_l(k)-1\right]P_l(z)$$

$$= (2k)^{-1}\int_{-\infty}^{+\infty} d\lambda'\lambda'\left[S(i\lambda',k)-1\right]P_{i\lambda'-\frac{1}{2}}(-z)/\cosh\pi\lambda' + i\pi k^{-1}\sum(\alpha_n+\tfrac{1}{2})\, P_n P_{\alpha_n}(-z)/\sin\pi\alpha_n$$

$$= -\frac{1}{\sqrt{2}}\int_{\xi}^{\infty}\left[\int_{-i\infty}^{+i\infty} d\lambda\, e^{\lambda x}\left[\frac{S(\lambda,k)-1}{4\pi k}\right]\right]\frac{\sinh x\, dx}{(\cosh x - z)^{3/2}} - \frac{i}{2k}\sum_{n=1}^{N}\beta_n\left[-\frac{1}{\sqrt{2}}\int_{-\infty}^{\xi} e^{(\alpha_n+\frac{1}{2})x}\frac{\sinh x\, dx}{(\cosh x - z)^{3/2}}\right] + \frac{i\pi}{k}\sum_{n=1}^{N}(\alpha_n+\tfrac{1}{2})P_n\, P_{\alpha_n}(-z)/\sin\pi\alpha_n \qquad (1)$$

N, α_n and β_n are total number, position, and residue of poles of in the half plane $R_e\, l > -\frac{1}{2}$. The first pole representation is given by Regge and second one is a modification of it by Khuri (3). If one neglects the background integrals in these representations, and take partial wave projections, we have, in pole approximation, Regge and Khuri representation $a^R(l,k)$ and $a^K(l,k)$ for partial wave amplitude $a(l,k)$ as

$$a^R(l,k) = (ik)^{-1}\sum_{n=1}^{N}(2\alpha_n+1)\beta_n/\left[(l+\alpha_n+1)(l-\alpha_n)\right] \qquad (2)$$

$$a^K(l,k) = (ik)^{-1}\sum_{n=1}^{N}\beta_n\, e^{(\alpha_n-l)\xi}/(l-\alpha_n) \qquad (3)$$

when sufficient number of $a(\ell, k)$ are known experimentally or can be equivalently calculated from a suitable potential one can solve Eqs. (2) and (3) for various pole parameters and test them for angular distributions of differential cross sections, total cross sections, and leading trajectories. Details of methods of calculations are given in ref: (4). In the next section we shall discuss the various typical results that we obtained from these calculations on low energy (.4 to 4.6 MeV) optical model elastic scattering of neutrons. Our calculations are based on the that can be obtained from the optical potential used by Campbell et al (5).

RESULTS AND DISCUSSION:

In our calculations the following aspects are investigated: (1) The angular distributions of differential cross sections (shape elastic) up to 3 poles approximations in both Regge (R) and Khuri (K) and compare with the exact (E) results. (2) Similarly, total cross sections are evaluated from (K) approximation and compared with exact results. (3) Consitency of pole parameters when one goes from one to two pole, two to three pole approximation are tested and the trajectories generated by poles at various energy points are studied.

Fig.1 to 3 show angular distributions for A_ℓ and Z_n at 1, 2.5 and 4.1 MeV. Fig. 3 shows the total cross sections. From these results we can conclude that in general (K)

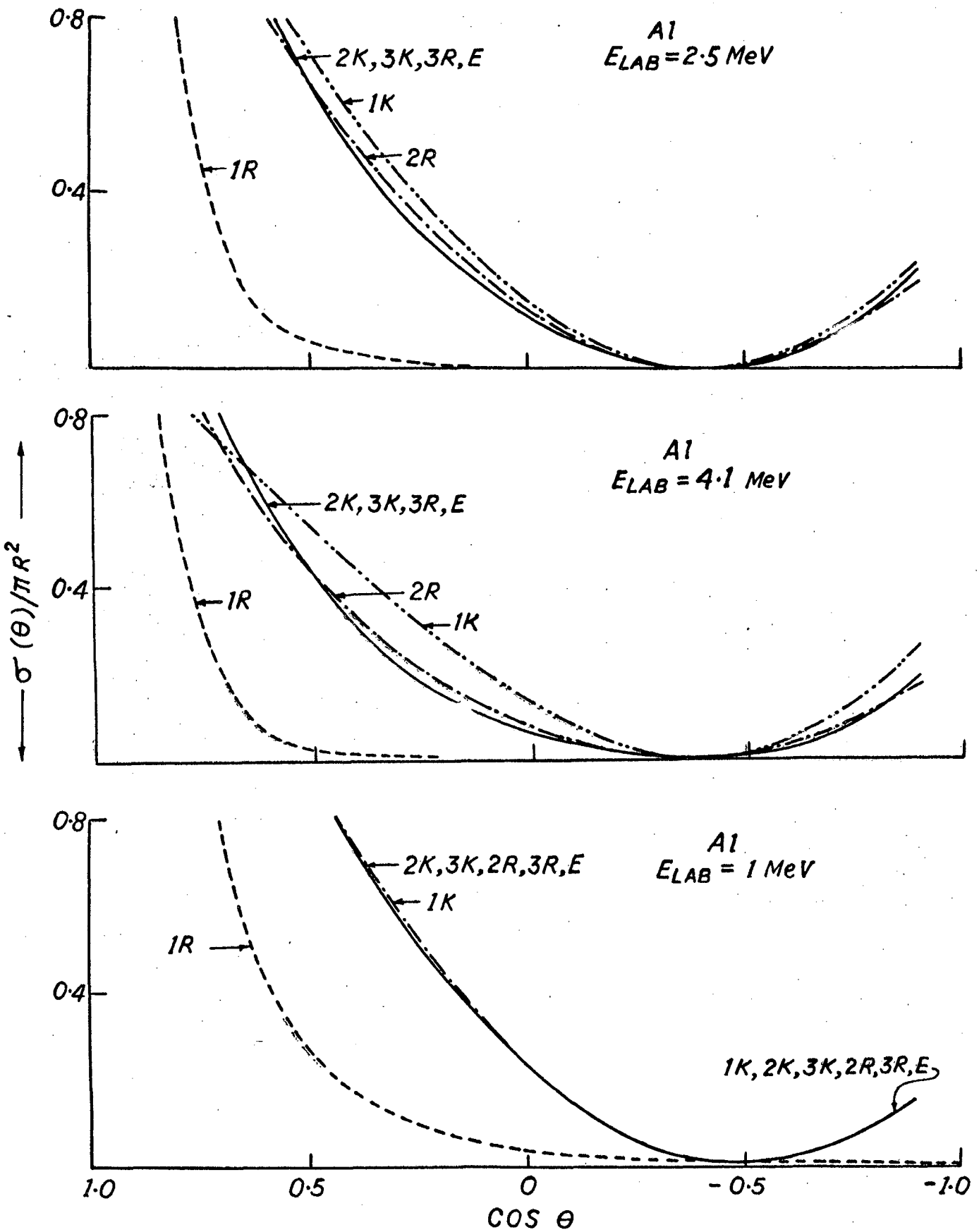
0·8
0·4
Al
E_{LAB} = 2·5 MeV
2K, 3K, 3R, E
1K
2R
1R
0·8
0·4
Al
E_{LAB} = 4·1 MeV
2K, 3K, 3R, E
2R
1K
1R
$\sigma(\theta)/\pi R^2$
0·8
0·4
Al
E_{LAB} = 1 MeV
2K, 3K, 2R, 3R, E
1K
1R
1K, 2K, 3K, 2R, 3R, E
1·0
0·5
0
- 0·5
-1·0
COS θ

FIG. 1

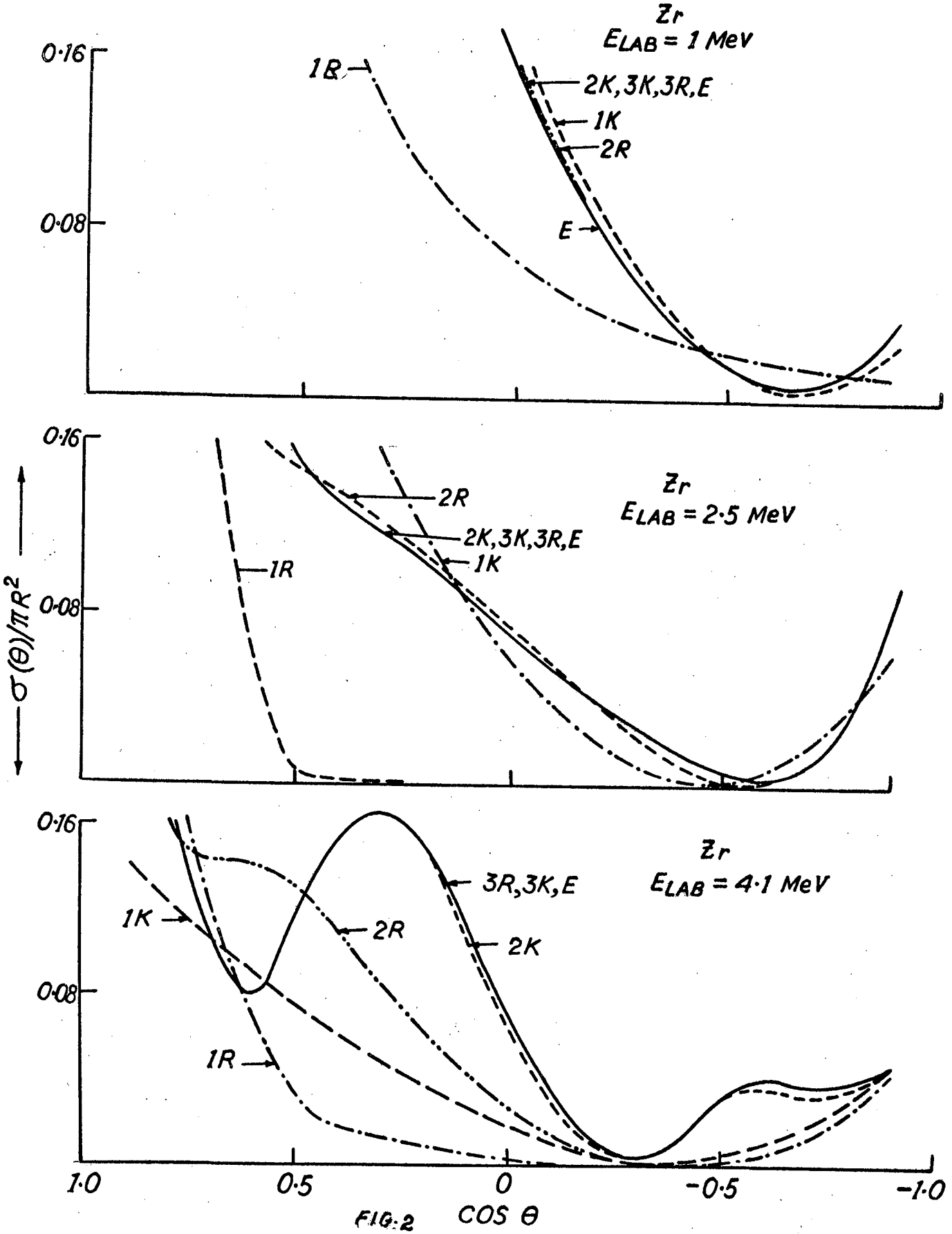
Zr
E_{LAB} = 1 MeV
0·16
0·08
1R
2K,3K,3R,E
1K
2R
E
Zr
E_{LAB} = 2·5 MeV
0·16
0·08
2R
2K,3K,3R,E
1K
1R
$\sigma(\theta)/\pi R^2$
Zr
E_{LAB} = 4·1 MeV
0·16
0·08
3R,3K,E
1K
2R
2K
1R
1·0
0·5
0
-0·5
-1·0
COS θ

FIG. 2

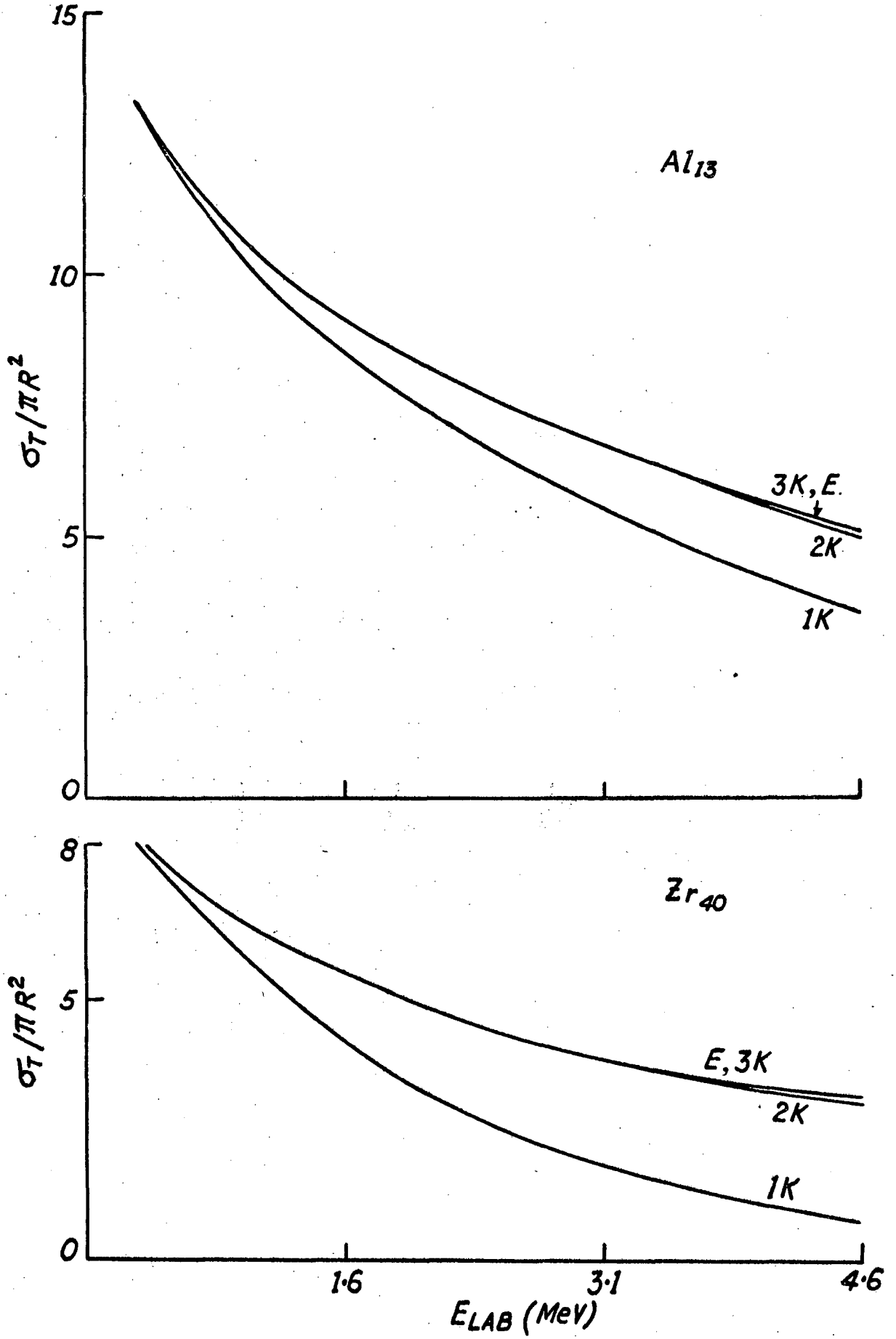
15
10
5
0
$\sigma_T/\pi R^2$
Al_{13}
3K, E.
2K
1K
8
5
0
$\sigma_T/\pi R^2$
Zr_{40}
E, 3K
2K
1K
1·6
3·1
4·6
E_{LAB} (MeV)

FIG. 3

approximation is distinctly superior approximation to (R) approximation and at low energy region 2 pole (K) approximation is sufficient to explain experimental data very satisfactorily. Corresponding (R) approximation mostly gives qualitative features. The deviations from (E) curve are more pronounced for higher energies and heavier nuelei.

The pole approximation obtained at different energies define Regge trajectories. But it is possible that the trajectory obtained from a certain approximation (say one pole) fluctuates drastically from its equivalent trajectory in higher approximation. Whereas if one or two trajectories dominate the scattering then we can expect to obtain this trajectories in practically same postion in all higher approximations. Physically speaking, if levels of the compound nucleus system corresponding to optical potential is having a closely packed structure of levels, none of the level being predominant in scattering, it is not surprising if the poles get drastic fluctuations and no reliable trajectories are generated. On the other hand, if scattering is contributed dominantly by one or two levels, it should be possible to obtain them from pole approximations fairly accurately and consistently. In the light of these remarks if we examine the fig. 4, we find that in (K) approximation consistancy of trajectories is fairly well achieved for $A_{1/2}$, $F_{5/2}$ and $Z_{7/2}$. The trajectories are in the energy range .4 to 4.6 MeV.

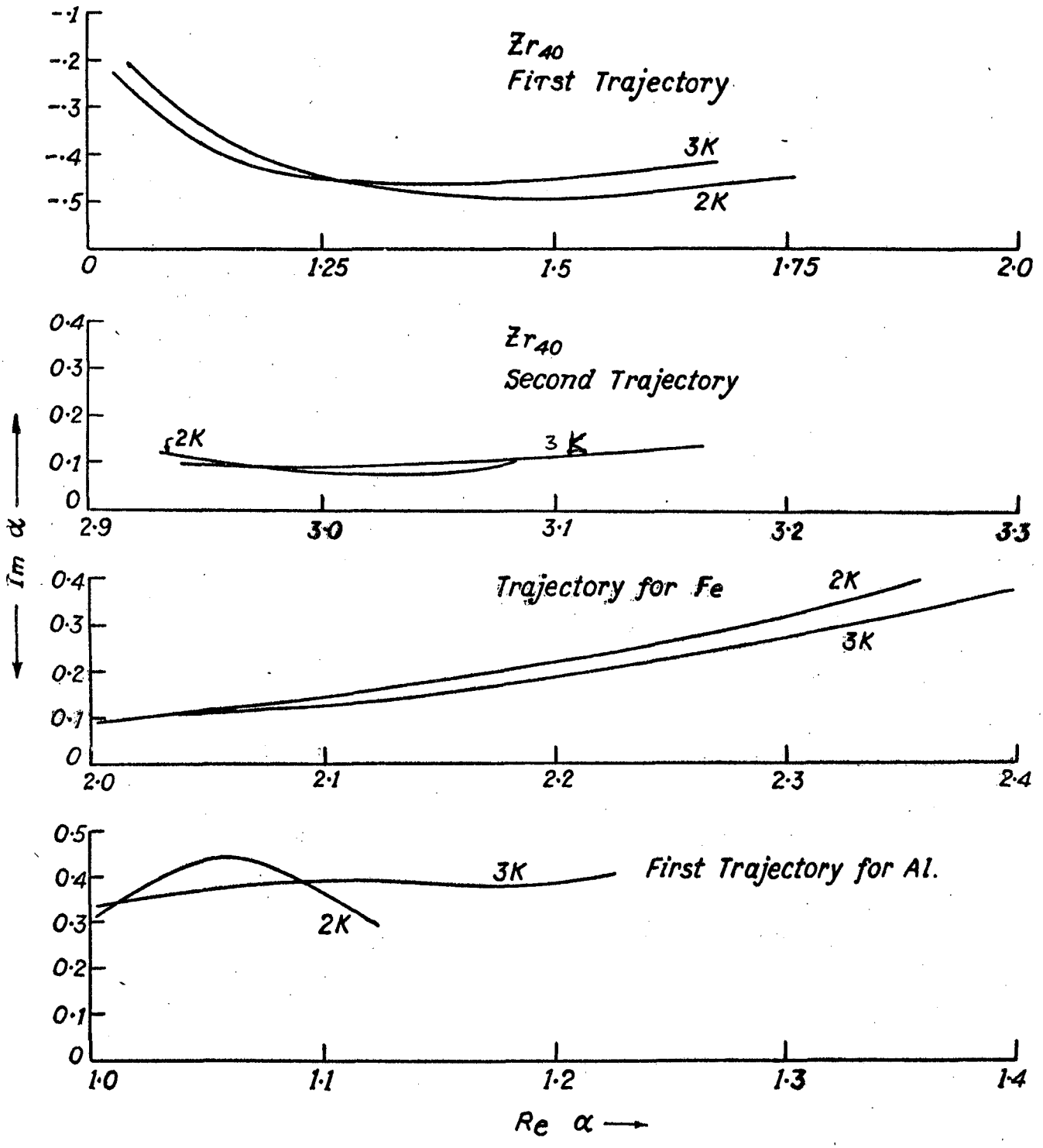
Zr40
First Trajectory
3K
2K
-·1
-·2
-·3
-·4
-·5
0
1·25
1·5
1·75
2·0
Zr40
Second Trajectory
2K
3K
0·4
0·3
0·2
0·1
0
2·9
3·0
3·1
3·2
3·3
Trajectory for Fe
2K
3K
0·4
0·3
0·2
0·1
0
2·0
2·1
2·2
2·3
2·4
3K
First Trajectory for Al.
2K
0·5
0·4
0·3
0·2
0·1
0
1·0
1·1
1·2
1·3
1·4
Im α
Re α

FIG. 4.

In our systematic studies over many nuclei (both medium and heavy) we found that the low energy peaking of total cross sections for some nuclei (Al, Fe , Zr) is explained by one or two leading trajectories. Whereas for some nuclei (Cd, Ag, Cs) when low energy peaking is not pronounced, leading trajectories are not successfully generated. Perhpas in these cases scattering is dominated by too many levels none of them being very predominent to generate a leading trajectory.

These studies show that it is possible to understand the optical model in low energy region from two pole (K) approximation and get leading trajectories for several nuclei which manifest the compound nucleus mechanism this aspect gives strength to the conjucture that it might be possible to understand the predominent contribution to optical model in terms of few leading trajectories having systematic variation with energy and possibly mass. To establish these results, it is necessary to extend our model for different nuclei and higher energies where some improvements and modifications in our theory may be necessary. At higher energies spin orbit forces play a significant part which change the distribution of poles in (4) in angular momentum plane and making the presence of trajectories in 4th quadrant of ℓ plane possible. These investigations constitute the further stage of the work.

REFERENCES:

1. Bottino, A., Longoni, A.M. and Regge. T., Nuovo Ci mento 23, 954 (1962)
2. Newton, R.G. The complex J Plane (W.A. Benjamin, Inc.), 1964
3. Khuri, N.N., Physical Review 130, 429 (1963)
4. S. Mukherjee and Shastry, C.S. (To be published).
5. E. J. Campbell et al, Technical report No. 73, M.I.T. (1960)

DISCUSSION:

B.D. Roy: Does'nt unitarity guarantee that once you have proper threshold condition for the real part, you get it for the imaginary part?

S. Mukherjee: If you had pole approximations only, the answer is no, in general. (example - Khuri representation). We constructed a general representation, where at each pole position, threshold and asymptotic behaviour is guaranteed, without imposing unitarity extreneously on pole forms alone. The general expression is as follows:

$$A(\lambda, K) = \sum \frac{\beta_n}{\lambda - \lambda_n} + f_1(\lambda, K)$$

where $f_1(\lambda, K)$ is the analytic part of $A(\lambda, K)$. It is easily seen that, in the right - half plane, $A(\lambda, K)$ may also be written as

$$A(\lambda, K) = \sum_n \frac{\beta_n F(\lambda_n, \lambda)}{\lambda - \lambda_n} + f_2(\lambda, K)$$

where $F(\lambda', \lambda)$ is such that $F(\lambda, \lambda) = 1$. For example, we may use

$$F(\lambda', \lambda) = g(\lambda)/g(\lambda')$$

where $$g(\lambda) = \exp\left(-\lambda \xi_1 + i \exp(-\lambda \xi_2)\right)$$

$$\xi_i = \cosh^{-1}\left(1 + \frac{\mu_i^2}{2K^2}\right), \quad i = 1, 2$$

It is easily seen that the asymptotic behaviour and threshold behaviour is guaranteed by this form of $F(\lambda', \lambda)$. It may also be noted that $F(\lambda', \lambda) = \frac{2\lambda'}{\lambda + \lambda'}$ gives Regge representation and $F(\lambda', \lambda) = \exp(\lambda' - \lambda)\xi$ gives Khuri representation. The guarantee for asymptotic behaviour does not, however, imply that the background integral is small. We have another prescription for it and it will be reported elsewhere.

OPTICAL WELL SCATTERING OF NEUTRONS FROM NUCLEI

S. Mukherjee and C.S. Shastry
Saha Institute of Nuclear Physics, Calcutta

The usefulness and validity of different pole approximations (1,2 and 3) of neutrons from nuclei in the low energy region (.4 to 4.6 MeV) has been investigated previously (1). There it was found that major contribution to scattering can be analysed in terms of one or two leading trajectories. In this paper we propose to extend our investigation for higher energies and various nuclei. This is necessary because the success of complex angular momentum approach to low energy scattering where only few partial waves are predominent does not guarantee the same at higher energies where many more partial waves dominate. In this present report we restrict our discussion to only three nuclei, namely ^{48}Ti, ^{56}Fe and ^{138}Ba and for the incident neutron energies 6, 10 and 14 MeV. Calculations are carried out as in ref. 1, using the partial waves generated by optical well as described by Hogdson et al (2). In the figures E denotes the result which can be obtained by conventional partial wave methods and capable of reproducing the experimental results. n_R or n_K denotes the results obtained by n (n = 1, 3) pole Regge formula on n pole Khuri formula. If any n is absent it means that the corresponding result is unsatisfactory and can not be presented in a comparable size. The angular distributions correspond to shape

elastic scattering and they are capable of fitting the experimental data since for energy >6 MeV compound elastic effects are small.

Fig.1,2 and 3 shows angular distribution for ^{48}Ti, ^{56}Fe and ^{138}Ba at 6, 10 and 14 MeV of incident neutron energies. To represent many results in a compact space the forward peaking part of angular distribution ($\cos\theta = 1.$ to $\cos\theta = .6$) are omitted. Fig.4 gives the total cross section plots for these nuclei from 2 MeV to 14 MeV along with the results obtained from Khuri approximation. From a careful analysis of these results we can make the following conclusions:

(i) One pole approximation is not satisfactory for higher energies (ii) At 6 MeV 2 approximation is appreciably good for ^{48}Ti and ^{56}Fe. But for the heavy nucleus ^{138}Ba, 2R reproduces very broad qualitative features of angular distribution. Corresponding 2K results are almost similar even-though in the case of ^{138}Ba, 2K improves the results as far as magnitude is concerned but has got a shift in angular distribution. 3K and 3R results agree quite well with exact results. (iii) At 10 MeV 2R results give broad qualitative features of angular distribution whereas 2K results have a marked improvement over 2R results. But for ^{138}Ba, 2K results show, just as for 6 MeV case, an angular shift in the angular distribution and agreement is not very satisfactory. (iv) At 14 MeV 3R gives general qualitative features of angular distribution whereas 3K gives almost quantitative results except for ^{138}Ba. Therefore, a finer improvement over Khuri pole approximation is

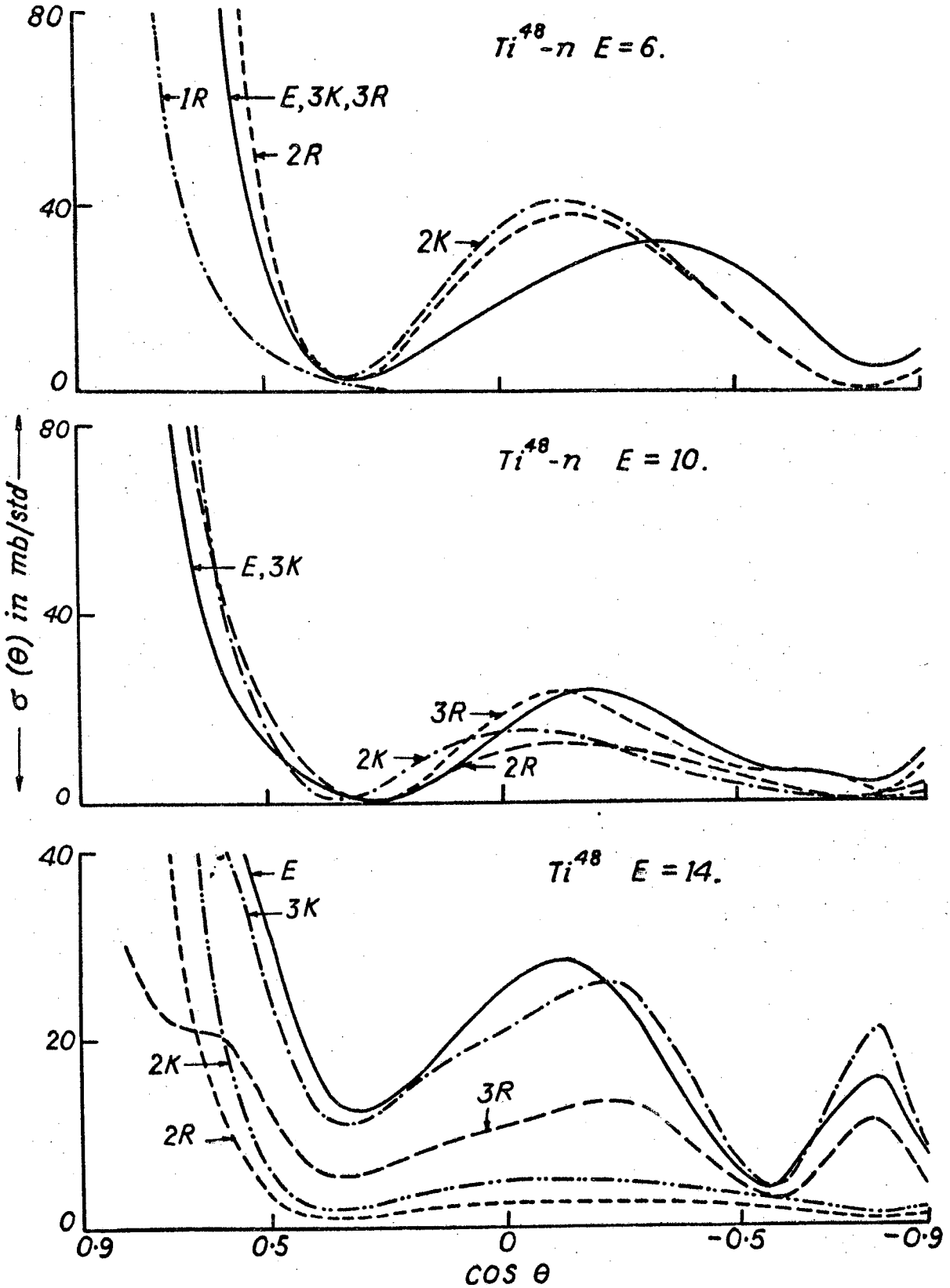
Ti^{48}-n E = 6.
1R
E,3K,3R
2R
2K
Ti^{48}-n E = 10.
E,3K
3R
2K
2R
Ti^{48} E = 14.
E
3K
2K
2R
3R
σ (θ) in mb/std
80
40
0
20
0·9
0·5
0
-0·5
-0·9
COS θ

FIG. 1

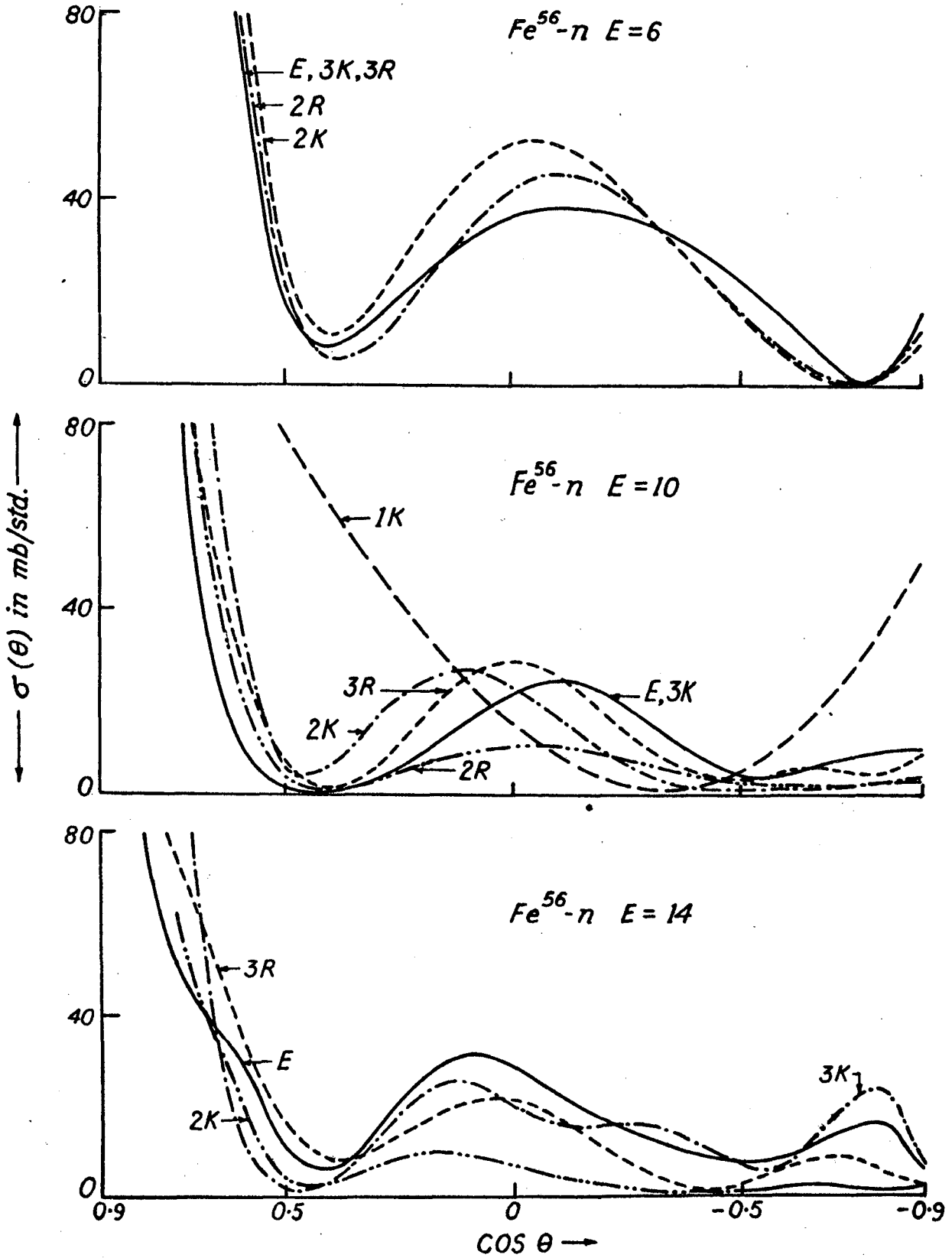
Fe56-n E=6
E, 3K, 3R
2R
2K
Fe56-n E=10
1K
3R
2K
E, 3K
2R
Fe56-n E=14
3R
E
2K
3K
80
40
0
0·9
0·5
0
-0·5
-0·9
COS θ
σ (θ) in mb/std.

FIG. 2

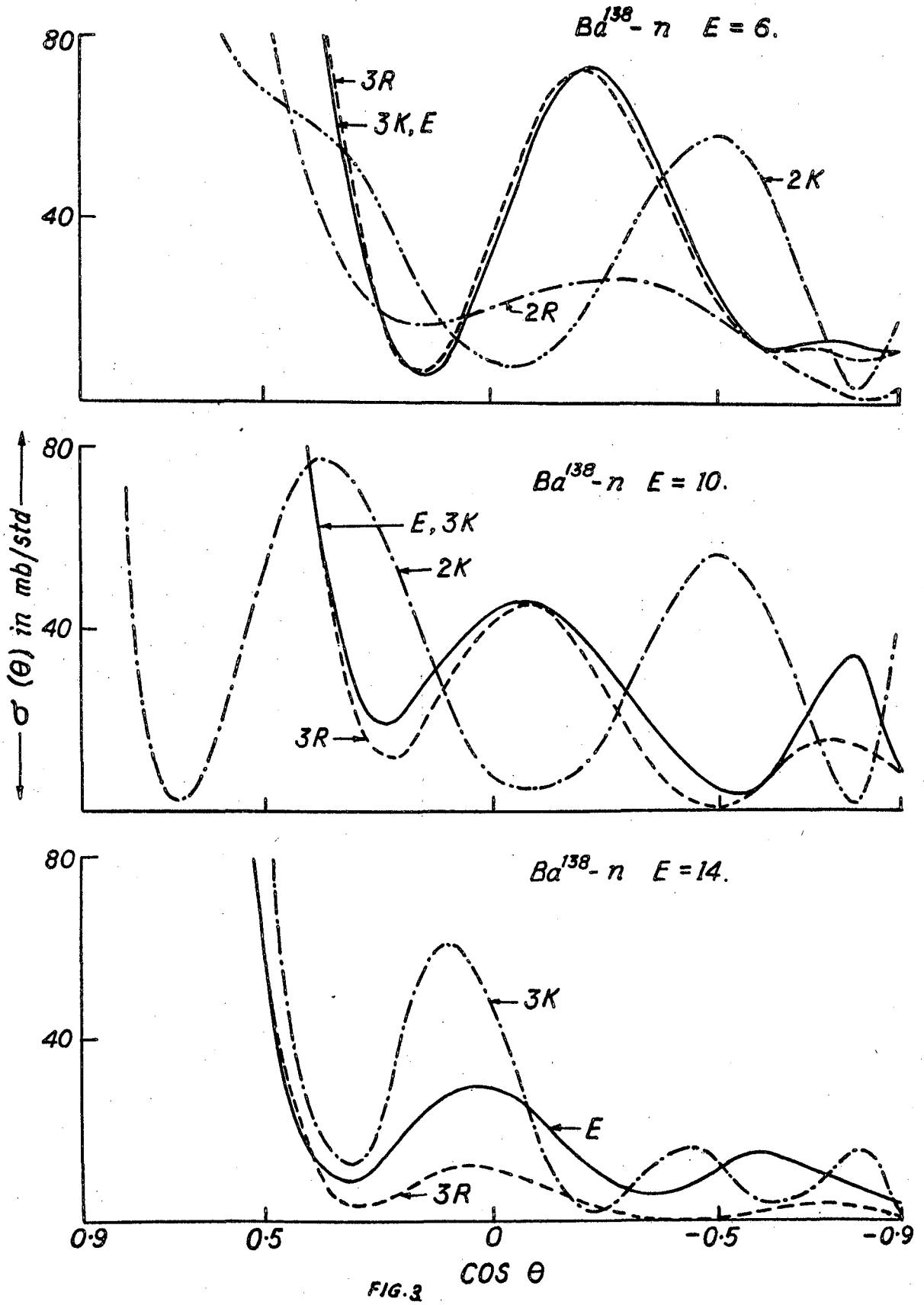
Ba138 - n E = 6.
80
40
3R
3K, E
2K
2R
Ba138 - n E = 10.
80
40
E, 3K
2K
3R
σ (θ) in mb/std
Ba138 - n E = 14.
80
40
3K
E
3R
0·9
0·5
0
-0·5
-0·9
COS θ

FIG. 3

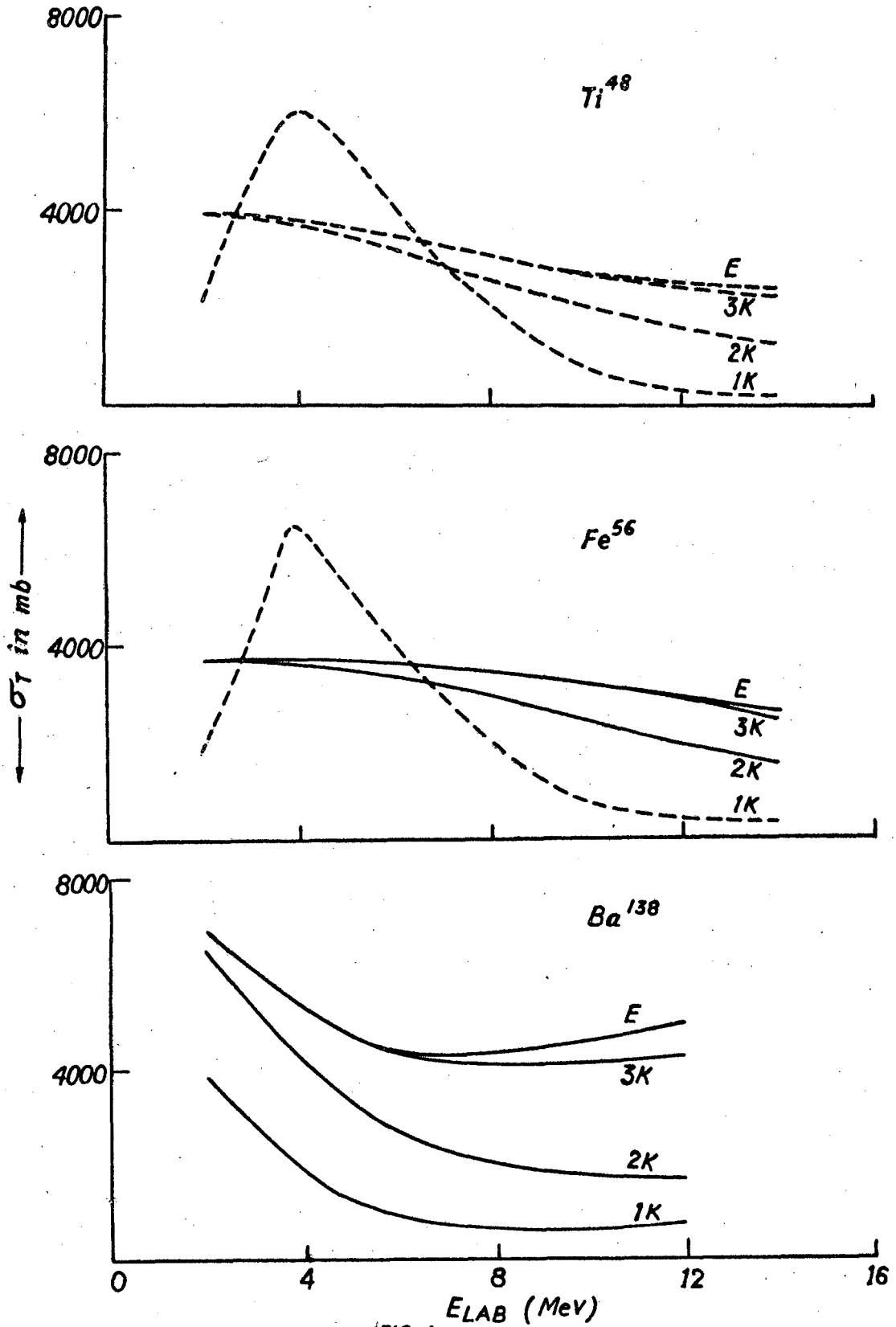
8000
4000
Ti^{48}
E
3K
2K
1K
8000
4000
Fe^{56}
E
3K
2K
1K
σ_T in mb
8000
4000
Ba^{138}
E
3K
2K
1K
0
4
8
12
16
E_{LAB} (MeV)

FIG-4

desirable, especially for heavy nuclei (v) In the total cross section curves 3K gives satisfacotory results and deviations are worse for heavy nucleus.

Fig.5 indicates two leading trajectories for ^{48}Ti and ^{56}Fe which contribute predominently to scattering. Here we have a different way of understanding the optical model phenomena in a systematic way for different neighbouring nuclei and different energies, in contrast to the phenomenological method of obtaining experimental results using general optical potential with varying parameters, the variation being not very systematic. From the typical, trajectories whown in fig.5, and other results (not reported here) it is possible to conclude that there is a systematic basis for optical model for different nuclei and different energies the dominating contribution for which can be represented by a set of leading trajectories which manifest the physical features of the scattering system. In fig.5, the presence of a trajectory on 4th quadrant of angular momentum plane should be understood in the light of discussion given in ref. 1.

Eventhough we could get satisfactory results from 3K for high energies and heavy nuclei it is very desirable to have still better improved approximations. However, one may argue that the improvement can be achieved by including still more number of poles but it is not desirable from the point of simplicity and elegance of approach of having few

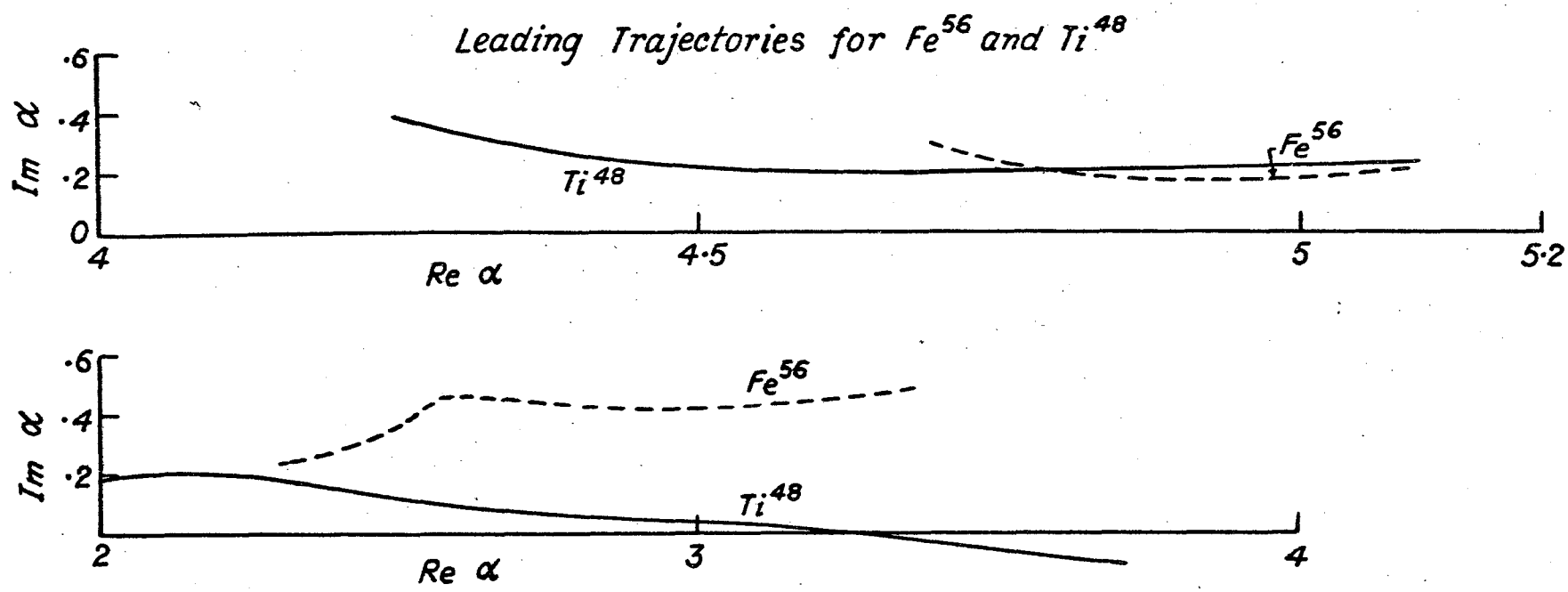
Leading Trajectories for Fe^{56} and Ti^{48}
Im α
·6
·4
·2
0
4
4·5
5
5·2
Re α
Ti^{48}
Fe^{56}
Im α
·6
·4
·2
2
3
4
Re α
Fe^{56}
Ti^{48}

FIG. 5

leading trajectories. The striking improvement of Khuri representation with respect to Regge representation shows that by improving the representation one can obtain much improved results in terms of few (1, 2 or 3) poles. It is also to be noted that deviations from exact curves may be due to: (a) more distant poles in the right half angular momentum plane, (b) the background integral neglected as an approximation. Since the contribution from distant poles is expected to be small, it is background which is mainly to be taken care of. Thus if we could improve upon Khuri representation such that the corresponding background integral is minimised we can hope for still more encouraging results and improved trajectories. This has been achieved (3) and calculations based on this will be discussed in future works.

REFERENCES:

1. S. Mukherjee and C.S. Shastry, Low Energy Neutron Scattering from Nuclei. (Pro. Nucl. Phys. & S.S. Phys. Sym., Kanpur. (1967)

2. D. Wilmore, AERE 4649, The Calculation of Neutron Cross-Sections from Non-local optical model.

3. S. Mukherjee. (To be published).

DISCUSSION:

M.K. Mehta: You mentioned that the poles would represent "intermediate system" resonances. I expect you meant the "compound system" resonances and not the "intermediate structure" resonances discussed by Feshbach et al as "doorway" states.

S. Mukherjee: I meant by poles, the poles of S-matrix that describes the "intermediate system". These poles would correspond to boundstates and resonances that the "intermediate system" may have. A particular class of these resonances correspond to the "doorwary" states of Feshbach.

OPTICAL WELL SCATTERING OF PROTONS FROM NUCLEI

S. Mukherjee and C.S. Shastry
Saha Institute of Nuclear Physics
Calcutta.

ABSTRACT.

Elastic scattering of protons from various nuclei, in the energy range 4 to 20 MeV, are analysed with the use of a modified Regge-representation. The role of background integral in various representation are discussed.

ANALYSIS OF INELASTIC SCATTERING OF 156 MeV PROTONS BY ^{7}Li

J. Mahalanabis
Saha Institute of Nuclear Physics
Calcutta.

ABSTRACT.

The differential cross-section and polarisation in the inelastic scattering of 156 MeV protons by ^{7}Li has already been calculated (1) using impulse approximation and L-s coupled shell-model wave functions constructed from the lowest configuration. The wave functions for the ground state ($\frac{3^-}{2}$) and the first excited state ($\frac{1^-}{2}$) at 0.478 MeV, which are the members of the ^{22}P [3] doublet are then constructed using the fractional parentage method . The shell-model calculations failed to fit the experimental data for the cross-section for the scattering to the 0.478 MeV state. Analysis of the experimental data suggest (2) the application of the rotational model for ^{7}Li nucleus. We have repeated the calculations using the seven-nucleon wave function for the ^{22}P [4+3] states of ^{7}Li, obtained by the generating procedure from the deformed single particle orbitals, which has been shown by Kurath (3) to reproduce the observed

quadrupole moment and the B(E2) strength between the two lowest states in ^{7}Li fairly well. The results obtained are discussed in this paper.

REFERENCES:

1. J. Mahalanabis, Ph.D. Thesis, 1964, London University (unpublished).
2. A.B. Clegg, International Conference on High Energy Physics and Nucl. Structure, Cern - 1963.
3. D. Kurath, Phys. Rev. 140B, 1190 (1965).

To be published in Proceedings of Physical Society, London.

PHOTODISINTEGRATION OF HELIUM WITH VELOCITY-DEPENDENT POTENTIALS

B.K. Srivastava
Physics Department,
Indian Institute of Technology, Kharagpur
and
S.C. Jain
Physics Department
Allahabad University, Allahabad

It is the purpose of the present note to evaluate $\sigma_{int} = \int_0^\infty \sigma(W)\, dW$ (integrated cross section) and $\sigma_b = \int_0^\infty (\sigma/W)\, dW$ (Bremsstrahlung - weighted cross section) by applying the sum rules of Levinger and Bethe (1) as extended by Rustgi and Levinger and using the results of variational calculation of the binding energy of the alpha particle (^4He).

We assume that the gound state of the alpha particle is described by a modified Irving wave function

$$\Psi_0 = N_0 \left\{ \exp\left[-\alpha\left(\sum_{i<j} r_{ij}^2\right)^{\frac{1}{2}}\right] + A \exp\left[-\lambda\left(\sum_{i<j} r_{ij}^2\right)^{\frac{1}{2}}\right]\right\} \Big/ \left(\sum_{i<j} r_{ij}^2\right)^n ; \quad i, j = 1,2,3 \text{ and } 4 \quad \ldots\ldots(1)$$

in which the normalising constant is

$$N_0 = \left[\frac{105 \times 2^{13-8n}}{\pi^4 (8-4n)}\right]^{1/2} \Big/ \left[\alpha^{4n-9} + 2A \left\{ (\alpha+\lambda)/2 \right\}^{4n-9} + A^2 \lambda^{4n-9}\right]^{1/2} \quad \ldots\ldots(2)$$

where α, λ, A and n are the parameters. The effective two-body velocity-dependent potential is the average of potentials in

^1S and ^3S states. It is the same as in our earlier paper (3). For this potential and trial wave function given by Eos. (1) and (2) the variational calculation of the binding energy of the alpha particle gives the best values of the parameters to be

$$n = 0,\ \alpha = 0.90F^{-1},\ \lambda = 1.14F^{-1} \text{ and } A = -1.38 \quad \ldots\ldots\ldots\ldots\ldots(3)$$

and the corresponding value for the binding energy is 30.1 MeV.

The integrated cross section in terms of the summed oscillator strength $\sum n f_{on}$ is expressed (4) by the Eq.

$$\text{int} = (2\pi^2 e^2 \hbar/MC) \sum n F_{on} \quad \ldots\ldots\ldots\ldots\ldots\ldots\ldots (4)$$

$$= (2\pi^2 e^2 \hbar/MC) \quad (\sum n f_{on})_T + (\sum n f_{on})\ \text{static}$$

$$+ (\sum n\ f_{on})\ \text{vel.dep.} \quad \ldots\ldots\ldots\ldots\ldots\ldots (5)$$

where (2, 3)

$$(\sum n\ f_{on})_T = (NZ/A) = 1 \text{ for } {}^4He \quad \ldots\ldots\ldots\ldots\ldots\ldots\ldots\ldots (6)$$

$$(\sum n\ f_{on})_{\text{static}} = -(4M/3\hbar^2)(x+\tfrac{1}{2}y) \langle V_{static}(r_{34})\ r^2_{34} \rangle \quad ..(7)$$

$$(\sum n\ f_{on})_{\text{vel.dep.}} = (V_o)_{\text{vel.dep.}} \left[\langle V_{vel}(r_{34}) \rangle + X_{vel} \langle V_{vel}\ t\ (r_{34}) \rangle \right] \quad \ldots\ldots\ldots\ldots\ldots\ldots(8)$$

$(\sum n f_{on})_T$, $(\sum n f_{on})_{\text{static}}$ and $(\sum n f_{on})_{\text{vel.dep.}}$ are the contributions of the kinetic energy, the static part of the potential and the velocity-dependent part of the potential respectively to the summed oscillator strength. We obtain the above expressions for $(\sum n f_{on})_{\text{static}}$ and $(\sum n f_{on})_{\text{vel.dep.}}$ under the assumption that the static part of the potential contains Majorana and Heisenberg exchange forces (2) (x, and y are the

fractions of Majorana and Heisenberg exchange forces respectively) while the velocity-dependent part has Winger character (3).

We next evaluate $\langle V_{static}(r_{34}) r_{34}^2 \rangle_{00}$, $\langle \omega_s(r_{34}) \rangle_{00}$ and $\langle \omega_t(r_{34}) \rangle_{00}$ for the wave function given by Eqs. (1) and (2) by using the values of integrals given in the appendix of Ref. 3. Finally, using the values of parameters n, α, λ and A [Cf. Eq. (3)] and the potential parameters given in Ref. 3. we obtain from Eqs. (4) - (8)

$$\sigma_{int} = (2\pi^2 e^2 \hbar / MC) \left[1.088 + 1.194 (x + \tfrac{1}{2}y) \right] \quad \ldots\ldots \quad (9)$$

$$= 101.1 \text{ MeVmb for } x + \tfrac{1}{2}y = 0.5 \text{ (Serber mixture)} \ldots \quad (10)$$

$$= 122.6 \text{ McVmb for } x + \tfrac{1}{2}y = 0.8 \text{ (Rosenfeld or Inglis mixture)} \ldots\ldots\ldots\ldots \quad (11)$$

Foldy (5) has shown that for a nucleus whose ground state wave function is completely symmetric in the space coordinates of all the nucleons (as is the case with our modified Irving Wave function for ^{4}He;Cf Eqs(1), the bremsstrahlumg-weighted cross section is related to the mean square radius $\langle r^2 \rangle_{00}$ through the expression

$$\sigma_b = (4\pi^2/3)(e^2/\hbar c) \left[NZ/(A-1) \right] \langle r^2 \rangle_{00} \quad \ldots\ldots\ldots \quad (12)$$

$$\text{where } \langle r^2 \rangle_{00} = (1/Z) \langle \sum_p (\vec{r}_p - \vec{R})^2 \rangle_{00} = R_c^2 - R_p^2 \quad \ldots\ldots \quad (13)$$

In Eq. (13) $\vec{r}_p$ denotes the proton's coordinates, $\vec{R}$ the centre of mass coordinates, R_c^2 and R_p^2 are the mean square radii, of the charge distribution in the nucleus and the proton respectively.

Making use of transformations and method of integration given by Irving (6), we obtain in a straight forward manner the mean square radius of ^4He for the modified Irving wave function ψ_0 [Cf. Eq. (1)] to be

$$\langle r^2 \rangle_\infty = \left[\frac{\pi^4 (10-4n)!\, x^{N_0^2}}{105 \times 2^{19-8n}} \right] \left[\alpha^{4n-11} + 2A \left\{ (\alpha+\lambda)/2 \right\}^{4n-11} + A^2 \lambda^{4n-11} \right] \quad \ldots\ldots\ldots\ldots \quad (14)$$

For the best values of the parameters n, α, λ and A given by Eq. (3), Eq. (14) yields

$$\langle r^2 \rangle_\infty = 2.40\ F^2 \quad \ldots\ldots\ldots\ldots \quad (15)$$

and $$\langle r^2 \rangle_\infty^{1/2} = 1.55\ F \quad \ldots\ldots\ldots\ldots \quad (16)$$

This value of the r.m.s. radius of the alpha particle is in reasonable agreement with those obtained from electron helium scattering experiments (7). Finally Eq. (12) and (15) gives

$$\sigma_b = 3.08\ mb \quad \ldots\ldots\ldots\ldots \quad (17)$$

Table I shows the results of various theoretical calculations (2,8) of σ_{int} and σ_b and lists the current experimental values (9)

We see from table I that for purely central forces without hard core (2) the value of σ_b is very low (0.8 mb). It is satisfactory to note that the present work gives a much better agreement with the experiments (9). For σ_{int} we find that our value for the Serber mixture agrees better with the experiments (9) than that of Goldhammer and Valk (8). The rather large value of Goldhammer and Valk may be attributed to the usually large D state

Table I.

Values of integrated and bremsstrahlung-weighted cross section for ^4He

	σ_{int} (MeVmb) Serber mixture	Rosenfeld or Inglis mixture	σ_b (mb)
Theory[a]	89	106	0.8
Theory[b]	86	102	1.23
Theory[c]	107	---	2.73
Present work	101	123	3.08
Experimental[d]	95±7		2.4±0.15

(a) Ref. 2. with purely central forces without a hard core.

(b) Ref. 2. with central and tensor forces without a hard core.

(c) Ref. 8. Based on two-body interaction having a Serber exchange character with a repulsive core and tensor component.

(d) Ref. 9.

probability of 10.6%. A comparison of our values of σ_{int} with those of Rustgi and Levinger (2) shows that velocity-dependent forces increase σ_{int} by about 14% for the Serber mixture. This is in agreement with the result of Dohnert and Rojo (10), who show that velocity-dependent correlations with Serber mixture increases σ_{int} by 14% for nuclear matter.

In conclusion we remark that a comparison of our results with those of Goldhammer and Valk (8), establishes reasonably well the equivalance of hard core and velocity-dependent potentials in photoeffect calculations for ^{4}He. Also the reasonable agreement of our values with those given by experiments, shows that our wave function [CF. Eqs. (1) and (3)] and two-body potential given in Ref.3 [Cf. Eq. (2) to (7)] are quite good.

REFERENCES:

1. J.S. Levinger and H.A. Bethe, Phys. Rev. 78, 115 (1950)
2. M.L. Rustgi and J.S. Levinger, Phys. Rev. 106, 530 (1957).
3. B.K. Srivastava and S.C. Jain, Phys. Rev. 143, 797 (1966).
4. J.S. Levinger, Nuclear Photodisintegration (Oxford University Press, New York, 1960), Chap.1.
5. L.L. Foldy, Phys. Rev. 107, 1303 (1957).
6. J. Irving, Phil. Mag. 42, 338 (1951)
7. R.W. McAllister and R. Hofstadter, Phys. Rev. 102, 851 (1966); H. Frank, D. Haas and H. Prange, Phys. Letters 19, 391 (1965); R.F. Frosch, R.E. Rand, K.J. Van Oostrum and M.Y. Yearian, Phys. Letters 21, 598 (1966). All these experiments give charge radius of ^{4}He between 1.61F and 1.64F.

8. P. Goldhammer and H.S. Valk, Phys. Rev. 127, 945 (1962)

9. A Gorbunov and V. Spiridonov, Soviet Physics JETP 6, 16 (1958); 7, 596, 600 (1958)

10. L. Dohnert and O. Rojo, Phys. Rev. 136, B396 (1964).

BINDING ENERGY OF HELIUM WITH A VELOCITY-DEPENDENT POTENTIAL

S.C. Jain,
Physics Department
Allahabad University
Allahabad
and
B. K. Srivastava
Physics Department
Indian Institute of Technology
Kharagpur.

ABSTRACT.

We have made a variational calculation of the binding energy of helium, using a two-body velocity-dependent central potential both in ^1S and ^3S states. We have used the two-parameter Irving wave function and its suitable modifications with three and four parameters as trial functions. Our results show that the convergence is rather slow. Obviously the maximum binding energy is obtained for the four parameter wave function. Our maximum value for the binding energy of helium is somewhat greater than the experimental value of 28.2 MeV but is in reasonable agreement with similar calculations of Tang et al using hard core potentials.

DISCUSSION:

S. Mukherjee: Do you consider tensor force in your calculation?

B.K. Srivastava: No. We have used only central forces.

PHOTODISINTEGATION OF DEUTERON

Shankar Mukherjee and Reba Mukherjee
Physics Department,
Banaras Hindu University.

Sum-rule calculations for the photodisintegration of deuteron were earlier carried out by Rustgi (1,2) using simple minded two-body central potential with and without hard core. In the present investigation we have re-evaluated the electric dipole bremsstrahlung weighted cross section and the integrated cross section applying one of the latest two-nucleon phenomenological potential given by Breit et al (3) and a corresponding analytical deuteron wave function suggested recently by Kottler and Kowalski (4). The main object is to test views regarding two-nucleon potential and of the electromagnetic properties of nucleons.

Following Rustgi (1) the electric dipole bremsstrahlung weighted cross section for the photodisintegration of deuteron is given by

$$\sigma_b = \int_0^\infty \frac{\sigma(W)}{W}\, dW = \frac{4\pi^2}{3}\left(\frac{e^2}{\hbar c}\right)\langle r^2\rangle_{00} \qquad (1)$$

where $\langle r^2\rangle_{00}$ denotes mean square radius of the charge distribution of deuteron. Using the radial wave functions u(x) and w(x) of Kottler and Kowalski, we get

$$\langle r^2\rangle_{00} = \frac{1}{4\mu^2}\left[\int_{0.35}^{\infty} x^2\,|u(x)|^2 dx + \int_{0.35}^{3.416} x^2|w(x)|^2 dx + \int_{3.416}^{\infty} x^2\,|w(x)|^2 d\right.$$

$$= 3.81812 \ f_m^2 \qquad (2)$$

Here $x = \mu r$, μ is the inverse Compton wave length of neutral pion and r is the internucleon distance. Therefore the root mean square radius is

$$\sqrt{\langle r^2 \rangle_{00}} = 1.954 \text{ fm} \tag{3}$$

which is in good agreement with the experimental value 1.96 fm obtained from electron scattering experiments. Substituting $\langle r^2 \rangle_{00}$ in equation 1, we get

$$\sigma_b = 3.49 \text{ mb} \tag{4}$$

and $(\sigma_b)_{expt.}$ is 3.9 mb

In the sum-rule calculation of Rustgi (2) it is shown that for central interaction of the form $V(r)\left[1 + x_0 P^M + y_0 P^H\right]$, the integrated cross section for the photodisintegration of deuteron may be written in the form

$$\sigma_{int.} = 30\left[1 - \frac{2}{3}\frac{M}{\hbar^2}(x_0 + y_0)\int \Phi^* V(r) r^2 \Phi \, d\tau\right] \text{ MeV-mb} \tag{5}$$

where x_0 and y_0 are fractions of Majorana and Heisenberg exchange forces present in the two-body interaction and Φ is the ground state wave function of deuteron. In the present investigation we have calculated only the contribution of the one pion exchange potential (OPEP) to the integrated cross section. The effect of other terms in the Yale potential to σ_{int} is under investigation. However, it is expected that major contribution to σ_{int} will come from OPEP. We have used the following form of one pion exchange potential

$$V^{(2)} = -V_0 \left[1 + S_{12}\left(1 + \frac{3}{x} + \frac{3}{x^2}\right)\right] \frac{e^{-x}}{x} \qquad (6)$$

where V_0 = 10.81 MeV. It is apparent that OPEP given above has a strong tensor part and relatively weak central one. It explains high energy nucleon scattering and Iwadare (5) finds that it also ensures agreement with quadrupole moment and binding energy of deuteron. Assuming the same parameters x_0 and y_0 for tensor force and carrying out angular integration and spin summation we get

$$\sigma_{int} = 30 \left[1 + 0.3561 (x_0 + y_0) I \right] \quad \text{MeV-mb} \qquad (7)$$

where the integral I is given by

$$I = \int \left[(u^2 + w^2) + (2\sqrt{8}\, uw - 2w^2)\left(1 + \frac{3}{x} + \frac{3}{x^2}\right)\right] x e^{-x} dx \qquad (8)$$

The numerical estimation of the integral I has been carried out in the CDC 3600 Computer of Tata Institute of Fundamental Research. It is found

$$I = 1.5174 \qquad (9)$$

substituting this value of I in Eq. 7, we get

$$\sigma_{int} = 30 \left[1 + 0.54 (x_0 + y_0)\right] \text{MeV-mb} \qquad (10)$$

The coefficient of ($x_0 + y_0$) is thus 0.54 instead of 0.37 and 0.40 obtained by Rustgi for central force. The values of σ_{int} calculated from Eq. (10) are now given below:

Mixture	x_o	y_o	σ_{int} (MeV - mb) Theo.	σ_{int} (MeV - mb) expt.
Rounfeld	0.93	-0.26	40.8	39
Inglis	0.80	0	43.0	
Serber	0.50	0	38.1	

We conclude from the present calculation that the presence of strong tensor interaction and a mixture of about 7% D-state have enhanced the value of $\sigma_{int.}$ Nevertheless the calculated values are in good agreement with experiment for Rosenfeld and Serber mixtures. Further the agreement of the theoretical values of mean square radius and σ_b of deuteron with experiments tests the validity of the ground state wave function used in the present calculation.

REFERENCES:

1. J.S. Levinger and M.L. Rustgi, Phys. Rev. 106, 607 (1957)
2. M.L. Rustgi, Revista Mex. De Fisica 3, 135 (1957)
3. K. E. Lassila, M.H. Hull, Jr. H.M. Ruppel, F.A. Mc Donald and G. Breit, Phys. Rev. 126, 881 (1962)
4. H. Kottler and K.L. Kowalski, Nuclear Physics 53, 334 (1964)
5. J. Iwadare, S. Otsuki, R. Tamagaki, W. Watari, Progress Theoret. Phys. Suppl. No.3, 32 (1956)

AN OPERATOR DERIVATION OF CERTAIN RECURSION RELATIONS BETWEEN RADIAL MATRIX ELEMENTS OF THE COULOMB FIELD

R.G. Kulkarni and N.V.V.J. Swamy
Department of Physics
Karnatak University
Dharwar-3.

INTRODUCTION:

Pasternack (1) was able to arrive at two different recursion relations between the radial coulomb expectation values for positive and negative integral powers of r. He made use of the contiguous relations between the generalized hypergeometric functions and the result seemed as though it is an accident related to the mathematical structure of the hydrogenic radial wave functions. On the other hand in case of Dirac coulomb matrix elements there is no such recursion relation available.

It is the purpose of this paper to point out that the Pasternack result has a deeper meaning traceable to the symmetry properties of the non-relativistic coulomb field.

The Pasternack result is

$$\langle r^q \rangle = -\frac{n^2 a_0^2}{4Z^2}\left\{\frac{q}{q+1}\left(2l+1+q\right)\left(2l+1-q\right)\langle r^{q-2}\rangle + \frac{8(2q+1)}{a_0(q+1)}\langle r^{q-1}\rangle\right\} \quad \ldots (1)$$

and

$$\left(l+1+\frac{q}{2}\right)\left(l-\frac{q}{2}\right)\left\langle\frac{1}{r^{q+3}}\right\rangle = \frac{2q+1}{q+1}\,\frac{Z}{a_0}\left\langle\frac{1}{r^{q+2}}\right\rangle - \frac{q}{q+1}\,\frac{Z^2}{n^2 a_0^2}\left\langle\frac{1}{r^{q+1}}\right\rangle$$

THE DERIVATION FOR $q \neq 0$

If we define $p_r = \frac{1}{2}(\vec{p}\cdot\hat{r} + \hat{r}\cdot\vec{p})$ where $\hat{r} = \frac{\vec{r}}{r}$

Then we can easily see that for any integer q

$$[ip_r, r^q] = q r^{q-1} \quad \text{(in the units } \hbar = c = 1) \quad \ldots (2)$$

And $[p_r^2, r^q] = -q(q-1)r^{q-2} - 2q r^{q-1} i p_r$ $\quad \ldots (3)$

Now we consider the commutator of r^{-q} with $2m\underset{\sim}{H}$ where H is non relativistic $= \frac{p^2}{2m} - \frac{\alpha Z}{r} + \frac{\vec{L}^2}{2mr^2}$, α being Sommerfeld fine - structure constant. Remembering $\vec{L}^2$ can be written as

$$(\vec{\sigma}\cdot\vec{L}+1)^2 - (\vec{\sigma}\cdot\vec{L}+1) \equiv \underset{\sim}{K}^2 - \underset{\sim}{K}$$

$$\text{i.e. } [r^{-q}, 2m\underset{\sim}{H}] = \left[r^{-q}, p_r^2 + \frac{L^2}{r^2} - \frac{2\alpha Z m}{r}\right] \quad \ldots (4)$$

$L^2 = \underset{\sim}{K}^2 - \underset{\sim}{K}$ is a pure angular operator

and commutes with any power of r.

therefore we get $[r^{-q}, 2m\underset{\sim}{H}] = q(q+1)r^{-q-2} - 2q r^{-q-1} i p_r$ $\quad \ldots (5)$

Taking the expectation value of the equation 5 between the bound state eigen function $|Nlm\rangle$'s We get

$$\langle r^{-q} i p_r \rangle = \frac{q}{2} \langle r^{-q-1} \rangle \qquad \text{---(5a)}$$

Also consider

$$\left[\left[r^{-q}, 2m\underset{\sim}{H}\right], 2m\underset{\sim}{H}\right] = \frac{q(q+1)(q+2)(q+3)}{r^{q+4}} - \frac{4q(q+1)(q+2)}{r^{q+3}} i p_r$$

$$-\frac{4q(q+1)}{r^{q+2}} p_r^2 + \frac{4q(\underset{\sim}{K}^2 - \underset{\sim}{K})}{r^{q+4}} - \frac{4q\alpha z m}{r^{q+3}} \qquad \ldots(6)$$

As we have $p_r^2 = 2m\left(\underset{\sim}{H} - \frac{\underset{\sim}{K}^2 - \underset{\sim}{K}}{2mr^2} + \frac{2z}{r}\right)$ ...(7)

Defining $\chi_\kappa^\mu = \sum_\gamma C^{l\frac{1}{2}j}_{\mu-\gamma,\gamma,\mu} \mathcal{Y}_l^m \chi_{1/2}^\gamma$ ...(7a)

and $|NK\mu\rangle \longrightarrow F_{\mu l} \chi_\kappa^\mu$

We notice

$$\underset{\sim}{H}\mu R |NK\mu\rangle = E_H |NK\mu\rangle \quad |E_n| = \frac{1}{2} m \left(\frac{\alpha z}{n}\right)^2$$

$$\underset{\sim}{K} |NK\mu\rangle = -K |NK\mu\rangle ; \quad l(l+1) = K(K+1) \qquad \text{---(7b)}$$

$$\vec{\sigma}\cdot\vec{r} |NK\mu\rangle = -F_{\mu l} \chi_{-K}^\mu \qquad \text{---(7c)}$$

The operator in equation 6 can be written as

$$\left[\left[r^{-q}, 2m\underset{\sim}{H}\right], 2m\underset{\sim}{H}\right] = \left\{-q(q+1)(q+2)(q+3) + 4q(q+2)(\underset{\sim}{K}^2 - \underset{\sim}{K})\right\} \frac{1}{r^{q+4}} \qquad \text{---(7d)}$$

$$-4q\alpha z m(2q+3)\frac{1}{r^{q+3}} + \frac{4q(q+1)}{r^{q+2}}(-2m\underset{\sim}{H}) + 2q(q+1)\left[\frac{1}{r^{q+2}}, 2m\underset{\sim}{H}\right]$$

Then taking expectation value of both sides with respect to $|NK\mu\rangle$ we see that

$$q(q+2)\{4l(l+1)-(q+1)(q+3)\}\langle \frac{1}{r^{q+4}}\rangle - 4\alpha z m q(2q+3)\langle \frac{1}{r^{q+3}}\rangle - 4q(q+1)2mE_n\langle r^{-q-2}\rangle = 0 \quad ---(8)$$

If $q \neq 0$ we can divide by q and we get finally setting $q \to q-1$

$$\left(l+1+\frac{q}{2}\right)\left(l-\frac{q}{2}\right)\langle r^{-q-3}\rangle = \frac{2q+1}{q+1}\frac{z}{a_0}\langle r^{-q-2}\rangle - \frac{q}{q+1}\frac{z^2}{n^2 a_0^2}\langle r^{-q-1}\rangle \quad ---(9)$$

And it can be shown that the same result holds good for positive powers of r also and can be written in the form

$$\langle r^q\rangle = -\frac{n^2 a_0^2}{4z^2}\left\{\frac{q}{q+1}(2l+1+q)(2l+1-q)\langle r^{q-2}\rangle + \frac{8}{a_0}\frac{2q+1}{q+1}\langle r^{q-1}\rangle\right\} \quad ---(10)$$

Where a_0 is the first Bohr orbit radius $\left(a_0 = \frac{1}{\alpha m}\right)$

So we see that without any appeal to the properties of the contiguous relations of the hypergeometric functions we are able to arrive at the recursion relations based only on operator algebra. The $|NK\mu\rangle$'s are basis vectors (in the subspace of the Hilbert space $\underset{\sim}{H} \to N$) connected with the irreducible representation of the group $O(4) \times SU_2$ and it is important to note that the symmetry of H underlies the Pasternack result.

One of us (R.G.K) is indebted to the D.A.E. for a research grant.

REFERENCES:

1. S. Pasternack, Proc. N.A.S. 23, 91 (1937)

DISCUSSION:

S.C.K. Nair: What is the implication of this on the question of symmetry?

R.G. Kulkarni: Only non relativistic Coulomb problem is invariant under O(4) and only due to that we are able to have a three term recursion relation for the Coulomb expectation value of r^q. The Dirac Coulomb problem is not invariant under O(4) and there is no recursion relation available in that case.

NUCLEAR STRUCTURE STUDIES USING REALISTIC NUCLEON-NUCLEON INTERACTIONS

Yeshwant R. Waghmare
Department of Physics,
Indian Institute of Technology
Kanpur.

For more than thirty years the existance of neutrons and protons as nuclear constituents has been established. From the fact that the protons and neutrons can remain 'inside' a nucleus, it was obvious that the overall nuclear potential must be attractive. However, the nucleon-nucleon potential could not be purely attractive. If this were so there would not have been 'saturation' of nuclear forces. This can be understood in the following way. If the nucleon-nucleon potential were purely attractive and be approximated by a square-well potential of range b and a well depth V_0, a system of A nucleons would 'collapse' to a sphere of radius b/2 and the energy of the nucleons would be proportional to A^2. On the other hand, the potential energy of such a system is proportional to the number of interacting pairs, i.e. A(A-1)/2. This is not compensated by the kinetic energy for the following reason. The kinetic energy of such a system is given by

$$E_0 = \sum \frac{\hbar^2}{2m} K_i^2 \qquad (1)$$

Where $\hbar K_i$ is the momentum of the ith particle. If we assume that all the nucleons are on the surface of the nucleus in which case they all will have the maximum momentum K_f (known

as the 'Fermi momentum') then,

$$E_0 = \frac{\hbar^2}{2m} \cdot \frac{3}{5} A K_f^2 \qquad (2)$$

As $K_f \propto A^{1/3}$, one obtains,

$$E_0 \propto A^{5/3} \qquad (3)$$

It is, therefore, clear that the kinetic energy of the system is not enough so as to compensate the potential energy for the system to be stable. It was also observed from scattering experiments that the 'exchange forces' are not sufficient for such a compensation. Thus, there must be some additional repulsion somewhere. The experimental information about such a repulsion was obtained from the nucleon-nucleon scattering experiments. In these experiments it was observed that the nucleon-nucleon potential is attractive upto a certain distance and then it turns repulsive (Figure (1)). The extension of the repulsive region is $c \sim 0.4$ fermi (1 fermi = 10^{-13}cm.) if one assumes 'infinite repulsion' in this region. The 'infinite repulsion' is, of course, far from reality and is assumed only for mathematical simplifications in nuclear structure calculations. The tendency among physicists these days is to explore the possibility of constructing some better and finite-repulsion potentials which can effectively replace the 'hard core' ones. Attempts to construct non-local, velocity dependent, and 'soft-core' potentials have also been made. However, they have gained only a limited success. It may be mentioned that, recently,

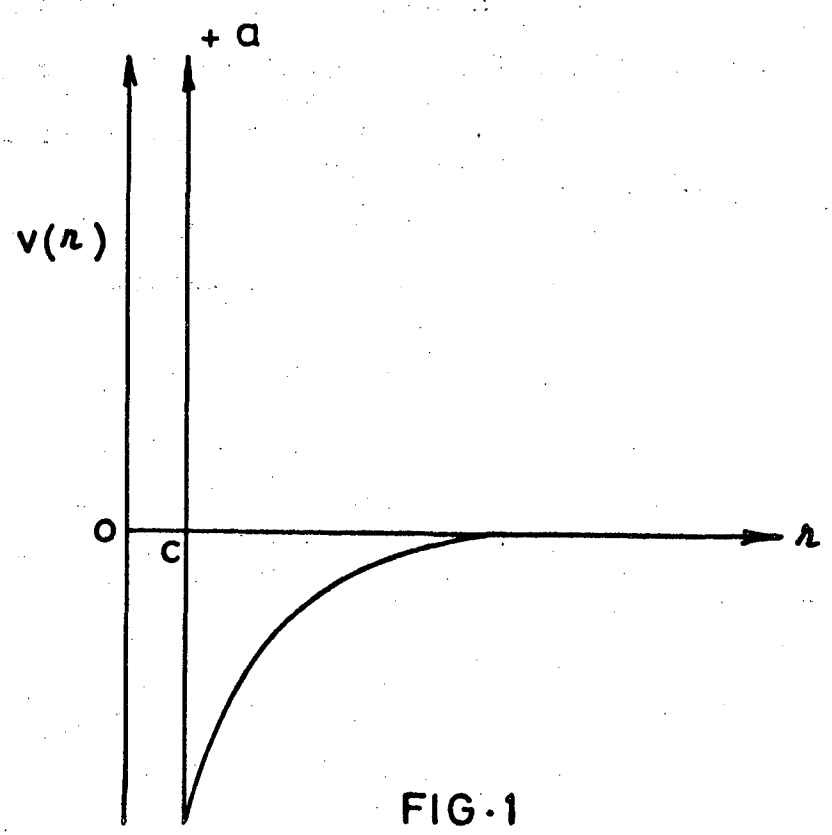

FIG·1

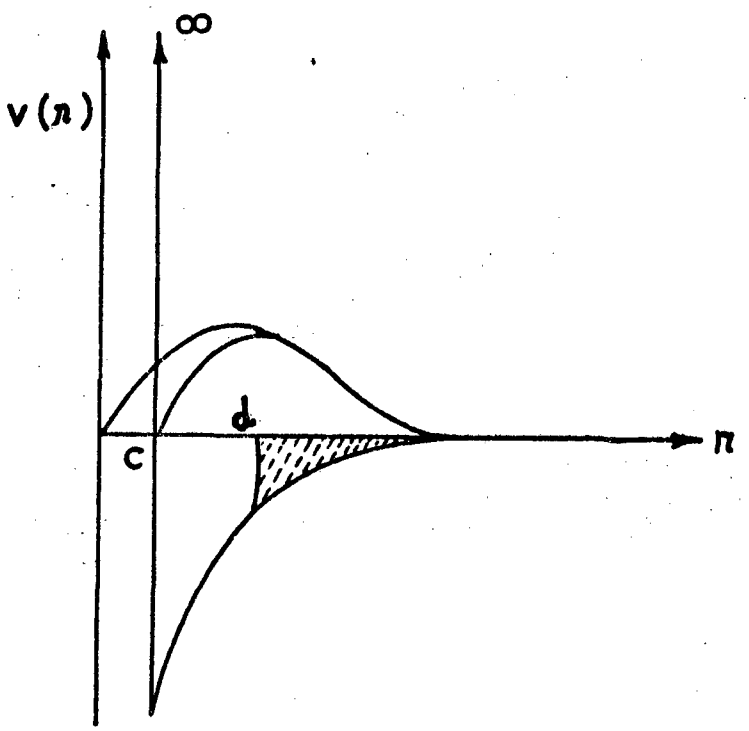

FIG·2

there have also been some attempts to derive the nucleon-nucleon potential from dispersion relations by exchange of mesons. Calculations of nuclear properties with such potentials have not been attempted so far.

Now, when two nucleons interact, their wave functions get modified. Therefore, in calculations one must use modified wave functions and unmodified interaction. Conversely, if unmodified wave functions are used, then the interaction must be modified. The calculations with the modified interaction, which is commenly known as the k-matrix or the reaction matrix, have had only a limited success. It has, therefore, been a general practise for the last ten years to use a 'phenomenological effective interaction' containing few parameters which are fitted to reproduce the experimental results.

If one wants to use the 'realistic potentials' in their form in nuclear structure studies, due to the singular nature of these potentials, one is confronted with the problem of infinities. An elegant approximation method has been proposed by Maszkowski and Scott (1) to deal with this problem. The philosophy of their prescription is as follows. One knows that the overall nucleon-nucleon potential is attractive. One also knows that it possesses strong repulsion at the centre (figure (1)). If one considers only the repulsive part of the potential, then the phase shift due to this part

alone is attractive and the energy is positive. On the other hand, if one takes whole of the potential i.e. repulsion plus all of the attraction, then at low energies, the phase shift is positive. In other words, the attraction more than compensates the repulsion. Thus if one finds that part of the attractive potential which along with the repulsion gives zero phase shift, then the interaction energy is due to the remaining part of the attractive potential alone. In other words, the potential V is divided into a short range part V(s) and a long range part $V^{(\ell)}$ in such a way that the phase shift (and consequently the energy) due to V(s) is zero (figure (2)). Then $V^{(\ell)}$ alone contributes to the interaction energy. The distance d of separation of V(s) and $V^{(\ell)}$ is known as the 'separation' distance. Due to this valuable prescription it became possible to use the 'hard core' potentials in nuclear structure calculations. There are two good potentials of this nature which are derived from nucleon-nucleon scattering experiments, namely, the Hamada-Johnston (2) and the Yale (3) Potential.

However, even if a nucleon-nucleon force were not singular, in shell model calculations one approximates the interaction by considering the effects of only a few shells. One also neglects the renormalization of the effective interaction due to admixture of high-energy orbitals into the

nuclear wave function, which arise from the repulsive nature of the potential. It is not possible to treat these high energy admixtures by a variational principle. However, some prescriptions can be given which would lead to the definition of the effective interaction. This can be achieved by using a unitary model approach (4).

Let us consider a general Hamiltonian,

$$H = \sum_{\alpha\beta} \langle \alpha | t | \beta \rangle a_\alpha^+ a_\beta + \frac{1}{2} \sum_{\alpha\beta\gamma\delta} a_\alpha^+ a_\beta^+ \langle \alpha\beta | V_{12} | \gamma\delta \rangle a_\delta a_\gamma \quad (1)$$

where the potential V_{12} may have a hard core. It is useful to define an effective Hamiltonian in the space of uncorrelated functions as,

$$H_{eff} = e^{-iS} H e^{iS} \quad (2)$$

where e^{iS} a unitary operator. Carrying out a cluster exapansion of H_{eff}, one obtains,

$$H_{eff} = \sum_{\alpha\beta} \langle \alpha | t | \beta \rangle a_\alpha^+ a_\beta + \frac{1}{2} \sum_{\alpha\beta\gamma\delta} a_\alpha^+ a_\beta^+ \langle \alpha\beta | e^{-iS} (t_1 + t_2 - V_{12}) e^{iS} - (t_1 + t_2) | \gamma\delta \rangle a_\delta a_\gamma + \text{-----} \quad (3)$$

Further, in order that one could use harmonic oscillator functions (which are convenient to handle) it is useful to introduce a term,

$$\frac{1}{2} \sum_{\alpha\beta\gamma\delta} a_\alpha^+ a_\beta^+ \langle \alpha\beta | e^{-iS} (U_1 + U_2) e^{iS} - (U_1 + U_2) | \gamma\delta \rangle a_\delta a_\gamma \quad (4)$$

where, U_1 and U_2 are one-body harmonic oscillator potentials; $U_1 = \frac{1}{2} k r_1^2$, $U_2 = \frac{1}{2} k r_2^2$. It may be shown that for the short range correlations the added term has only a small effect on the matrix elements of H_{eff}. These short range correlations are introduced in the wave functions by the unitary operator e^{iS} as,

$$\psi_{n_i, n_j} = e^{iS} \Phi_{n_i n_j} \tag{5}$$

where Φ's are the uncorrelated wave function.

Further more, ψ's can be expanded in a harmonic oscillator basis as,

$$\psi_\alpha(r) = \sum_{n_i} C_\alpha^{n_i} \phi_{n_i}(r) \tag{6}$$

Substitutions of (4)-(6) in (3) gives,

$$H_{eff} = \sum t_{n_1 n_2} a^+_{n_1} a_{n_2} + \frac{1}{2} \sum a^+_{n_1} a^+_{n_2} a_{n_3} a_{n_4} \times \langle \phi_{n_1 n_2} | v(\ell) | \phi_{n_3 n_4} \rangle \tag{7}$$

In equation (5), we have neglected the coupling between different states that arises from tensor force. In other words, e^{iS} induces only central correlations. One also knows that, second order tensor force gives large contribution to the binding energy. Therefore, it must also be included in (7). Thus, H_{eff} can be written more generally as,

$$H_{eff} = \sum t_{n_1 n_2} a^+_{n_1} a_{n_2} + \frac{1}{2} \sum a^+_{n_1} a^+_{n_2} a_{n_3} a_{n_4} \times \langle \phi_{n_1 n_2} | v(\ell) + v_T^{OD} + v_T^{OD} \frac{Q}{e} v_T^{OD} | \phi_{n_4 n_3} \rangle \tag{8}$$

where V_T^{oD} is the off-diagonal tensor force, Q is the Pauli operator and ϵ is the energy denominator. Effective interaction given by (8) can now be used for nuclear structure calculations.

Hartree-Fock calculations using the Yale potential (3) have recently been made (5).

It is clear that the theory gives good results for the single-particle energies, spin-orbit splittings, root-mean-square radius and binding energies. Other calculations such as energy levels and Hartree-Fock for the excited states are in progress. An attempt of deriving phenomenological effective interaction from matrix elements of the realistic potential is being made by Dr. Mehta and myself. They are still to be finished though calculations for the central force for the Yale potential are almost complete.

REFERENCES:

1. S.A. Moszkowski and B.L. Scott, Ann. Phys. 11, 65 (1960)
2. T. Hamada and I. Johnston, Nucl. Phys. 34, 382 (1962), T. Hamada, V. Nakamura, and R. Tomagaki, Prog. Theo. Phys. 33, 769 (1965)
3. K.E. Lassila, M.H. Hull, Jr., H.M. Ruppel, F.A. Mc. Donnald, and G. Breit, Phys. Rev. 126, 881 (1962)
4. C.M. Shakin and Y.R. Waghmare, Phys. Rev. Letters 16, 403 (1965).

5. C.M. Shakin, Y.R. Waghmare and M.H. Hull (To be published).

6. K.A. Brueckner, A.M. Lockett, and M. Rotenberg, Phys. Rev. 121, 255 (1961).

7. A.K. Kerman, J.P. Svenne and F. Villars (Nucl. Phys. 1966)

Table I.

Results of Calculations for ^{16}O using the Yale Potential (b = 2.09 Fermi). Results of other authors are given for comparison.

Quantity	Brueckner et al.[6]	Kerman[7]* et al.	Present Calculations.	Experimental.
B.E./A (without Coulomb and c.m.) in MeV	-	-2.41	-7.75	-
B.E./A (with Coulomb) in MeV	-2.02	-1.44	-6.8	-
B.E./A (with c.m.) in MeV	-	-3.22	-8.58	-
B.E./A (including Coulomb and c.m.) in MeV	-	-2.26	-7.84	-7.98
R.M.S. radius in fm.	2.40	2.38	2.33	-
Charge radius in fm.	2.41	2.42	2.35	2.64
$0p_{3/2}-0p_{1/2}$ splitting in MeV.	4.1	10.2	8.28	(9.0)

* The results reported in this column do not contain second-order corrections.

Table II.

Single particle energies (E) and expansion coefficients (C_s) obtained in calculations for ^{16}O with the Yale Potential.

Particle	State	$0s_{1/2}$	$0p_{3/2}$	$0p_{1/2}$
	E_n	-62.87	-31.28	-22.94
	C_0	.921539	.875073	.893617
Neutron	C_1	- .360736	- .364090	- .315034
	C_2	.143652	.318882	.319692
	E_P	-58.96	-27.54	-19.26
	C_0	.923978	.879652	.899259
Proton	C_1	- .347727	- .347254	- .2955589
	C_2	.159221	.325003	.322428

Table III.

Table of Calculated and Experimental Results for ^{40}Ca with the Yale Potential.

Quantity	Results of BLR[6] (MeV)	Results of Kerman* et al[7]	Present Calculations (MeV)	Experiment (MeV)
B.E./A (without Coulomb and c.m.) in MeV.	-	-	-10.26	-
Coulimb energy/A	-	1.84	1.83	-
Center-of-mass correction/A	-	-0.32	- 0.27	-
Total (B.E./A) in MeV	-3.89	-3.74	- 8.75	-8.55
$0p_{1/2}-0p_{3/2}$ splitting in MeV	-	11.35	6.23	-
$0d_{3/2}-0d_{5/2}$ splitting in MeV	-	7.20	10.93	-
R.M.S. radius in fm	2.88	2.96	2.89	3.52

* The results reported in this column do not contain second-order corrections.

DISCUSSION:

T. Pradhan: Are there interference effects between the two parts of the potential?

S.C.K. Nair (and confirmed by speaker): Yes, there are and these are partly taken care of.

S. Mukherjee:(1) Does the separation distance depend on the states? (2) The operator S is undefined. (3) If S is undefined, how is it that $\tilde{H}$ is hermitian, particularly after truncation at various stages?

Y.R. Waghmare: (1) The separation distance does depend upon the angular momentrum of the state as well as the number of nodes in the wave function for a state. We have calculated matrix elements using these facts. (2) The only restriction on S we put is that it is a two-body Hermitian operator. It's exact structure is known. However, the operator e^{iS} induces short range correlations. (3) We assume that the three-body and higher order contributions to the effective interaction are negligible. This in fact can be noticed if you take Jastron from for the correlation function. In that sense the truncated Hamiltonian can be assumed to be almost Hermitian.

C.S. Warke: In Nuclear spectroscopy the two body interaction depends on the nucleus. Does it, in this case?

Y.R. Waghmare: Yes, it does. The matrix elements we have calculated are density dependent and, therefore, somewhat different for different nuclei.

A.S. Divatia: Is this method selectively applicable to certain types of levels or is it uniformly applicable?

Y.R. Waghmare: In principle this method is quite general.

S.C.K. Nair: (1) Was the separation distance calculated even for making the off-diagonal matrix elements of the short ranged part of the two body interaction zero. (2) Why isit necessary to introduce the S operator?

Y.R. Waghmare: (1) The separation distance was calculated by solving the two equations, namely,

$$\left(t_1 + t_2 + v_1 + v_2 + v_{12}^{(s)}\right) \psi_{n_1 n_2} = \left(\epsilon_{n_1} + \epsilon_{n_2}\right) \psi_{n_1 n_2}$$

$$\left(t_1 + t_2 + v_1 + v_2\right) \phi_{n_1 n_2} = \left(\epsilon_{n_1} + \epsilon_{n_2}\right) \phi_{n_1 n_2}$$

for each state and each number of nodes. The short range correlations in ψ make the contributions from short range part of the interaction zero. (2) The advantage of introducing the S-operator is that, one can make a cluster expansion of the two-body interaction in various states and making the contributions from the short range parts negligible. This can probably be achived in some other way also.

DOUBLET SPLITTINGS USING REALISTIC FORCES

Meera Moorthy and Y.R. Waghmare
Department of Physics
Indian Institute of Technology
Kanpur.

ABSTRACT.

Doublet splittings for T = 0 and T = 1 states are calculated using the matrix elements for the Yale potential of Shakin, Waghmare and Hull. The results are compared with the experiment as well as those obtained by other authors. The implications of configuration mixing is indicated.

DISCUSSION:

S.N. Mukherjee: How large are the off diagonal elements when you include the tensor part? I think neglect of off diagonal terms is not correct because Yale potential has a strong tensor part.

Y.R. Waghmare: The off-diagonal matrix elements of the tensor force are certainly large and we have included those in our tables.

P. Mukherjee: Don't you think that the experimental data on doublet splitting is rather unsatisfactory at present?

Y.R. Waghmare: I am not so sure. If one assigns configurations for the 'doublets' in experimental data, then the theoretical analysis of these doublets alone gives us some idea of relative configuration mixing in the two states which form a doublet.

PHENOMENOLOGICAL POTENTIALS AND REALISTIC FORCES

G.K. Mehta and Y.R. Waghmare
Department of Physics
Indian Institute of Technology, Kanpur

In the past decade most of the nuclear strucutre calculations have been based on phenomenological potentials by considering spin and space exchanges of two particles. These exchanges had the well known Wigner, Majorana, Bartlett and Heisenberg forms. At the same time the experimental as well as theoretical work on nucleon-nucleon potentials revealed that such exchange mixture is inadequate to provide 'saturation'. In order that the nuclear forces saturate, there must be some additional repulsion in the force. In effect, some potentails were developed, such as the Hamada-Johnston (1) and the Yale (2) potential which satisfied the saturation requirement. However, due to their 'singular' nature, any nuclear structure calculations with their direct use are impossible.

Recently, matrix elements of the Yale potential have been calculated by Shaklin et al (3) using the separation technique. The matrix elements of the potential in various states are obtained as a function of the oscillator parameter $b = \sqrt{\hbar/m\omega}$. These matrix elements contain the sum of first and second order contributions from the diagonal elements of all the terms in the Yale potential. An attempt is made here to evaluate the

parameters of the phenomenological potential using the Yale potential matrix elements. It is obvious that if this is possible, then the set of parameters one obtains would be best suited for nuclear strucutre work. Another advantage in this approach is that one uses harmonic oscillator wave-functions (which are conveninent to handle) in evaluating the matrix elements of the two body interaction.

A phenomenological central two - body interaction is written as,

$$H_{12} = (W\,A_W + M\,A_M + B\,A_B - H\,A_H)\,f(r) \qquad (1)$$

where W is the Wigner 'unity' operator, M is the Majorana (space exchange), B is the Bartlett (spin exchange) and H is the Heisenberg (isospin exchange) operator. The A's are the co-efficients signifying contributions due to various exchange forces. For, a definite isospin spin state, one can write (1) as,

$$H_{12} = V_0\left(a'_T + b'_T\,\vec{\sigma}_1\cdot\vec{\sigma}_2\right) f(r) \qquad (2)$$

or

$$H_{12} = \left(a_T + b_T\,\vec{\sigma}_1\cdot\vec{\sigma}_2\right) f(r) \qquad (3)$$

where T = 0 or 1. For f(r) we choose the Gaussian form, namely, $e^{-(r/r_0)^2}$, where r_0 is the range of the potential. The constants a_T, b and r are chosen to give the best agreement of the matrix elements of the potential defined in (2) and the Yale potential matrix elements (3). The closest agreement is obtained for the

following values of these constants:

$$
\begin{aligned}
a_o &= -14.1 \text{ MeV} \\
b_o &= -31.3 \text{ MeV} \\
a_1 &= -25.7 \text{ MeV} \\
b_1 &= +4.9 \text{ MeV} \\
r_o &= 1.4 \text{ fm}
\end{aligned}
\tag{4}
$$

If we use customary normalization, $\frac{1}{V_o}(a - 3b) = 0.6$, we obtain $V_o = -67.30$ MeV. The constants A_W, A_M, A_B and A_H now become,

$$
\begin{aligned}
A_W &= -6.7 \text{ MeV} \\
A_M &= -36.2 \text{ MeV} \\
A_B &= -26.4 \text{ MeV} \\
A_H &= +26.7 \text{ MeV}
\end{aligned}
\tag{5}
$$

Comparison of the calculated matrix elements of the force given by (2) with those obtained from the Yale potential using the constants in (3) is made in table I.

Table I.

Comparison of the phenomenological and calculated "realistic" matrix elements

I_{ne}	Calculated		Phenomenological (Gaussian Integrals)
	T = 0	T = 1	
I_{os}	.0923	.0961	.0894
I_{1s}	.0905	.0826	.0894
I_{2s}	.0762	.0601	.0798
I_{3s}	.0590	.0379	.0711
I_{4s}	.0401	.0167	.0631
I_{op}	.0161	.0179	.0179
I_{1p}	.0271	.0013	.0520
I_{2p}	.0389	- .0273	.0354
I_{3p}	.0521	- .0576	.0387
I_{od}	- .0011	.0058	.0036
I_{1d}	.0102	.0098	.0083
I_{2d}	.0136	.0135	.0121
I_{3d}	.0124	.0166	.0163

From table I we observe that the over all agreement is satisfactory. The discrepancy in p states arises due to the nature of the realistic force. For example, some triplet p-state matrix elements of the Yale potential change sign (3) for $n \geqslant 2$ or 3. In table II a comparison of the present force is made with those obtained by other authors.

Table II.

Comparison of forces obtained by various authors. These are normalized as $(a - 3b)/V_o = 0.6$. Column 2 contains $A_{11} = \frac{1}{V_o}(a + {}^{o}b)$

	Mass Number	A_{11}	V_o (MeV)	r_o (fermi)	Radial shape	Reference
Elliot and Flowers	18	-0.26	-48.3	1.40	Yukawa	(4)
Raz and French	43	+0.20	-30.0	2.70	Gaussian	(5)
True and Ford	206	0.0	-54.1	2.65	Gaussian	(6)
Rosenfeld	16	-0.33	-35.6	1.40	Yukawa	(7)
Band et al	206	+0.26	-60.0	2.00	Gaussian	(8)
Peaslee	16	0.0	-60.0	1.40	Yukawa	(9)
Waghmare	d-s shells	0.40	-68.0	2.06	Gaussian	(10)
Barker	16	0.38	-77.3	1.40	Yukawa	(11)
Present Calculations	--	0.31	-67.3	1.40	Gaussian	

From the analysis it is clear that the parameters in (3) (which include the first and second order contributions of the diagonal part of the forces of the Yale potential) provides a useful phenomenological force for nuclear strucutre claculations with harmonic oscillator wave functions. It is also interesting to note that the "phenomenological-realistic"

force is of shorter range compared to the one generally used (see table II). Calculations of the parameters of the off diagonal tensor force are in progress. However, we feel that this five parameter model is not sufficient to account for the general nature of the realistic force, and a sum of two Gaussians may improve the picture considerably.

REFERENCES:

1. T. Hamada and I. Johnston, Nucl. Phys. 34, 383 (1962)
2. K.E. Lassila, M.H. Hull, Jr., H.M. Ruppel, F.A. McDonald and G. Breit, Phys. Rev. 126, 881 (1962)
3. C.M. Shakin, Y.R. Waghmare and M.H. Hull (To be published)
4. J.P. Elliott and B.H. Flowers, Proc. Roy. Soc. (London) A242, 57 (1957)
5. B.J. Raz and J.B. French, Phys. Rev. 104, 1411 (1956)
6. W.W. True and K.W. Ford, Phys. Rev. 109, 1675 (1958)
7. L. Rosenfeld, Nuclear Forces (North-Holland Pub. Co. Amsterdam, 1948)
8. I.M. Band, Yu. I. Kharitonov, and L.A. Sliv, Nucl. Phys. 35, 136 (1962)
9. D.C. Peaslee, Phys. Rev. 124, 839 (1961)
10. Y.R. Waghmare, Phys. Rev. 134, B1185 (1964)
11. F.C. Barker, Phys. Rev. 122, 572 (1961)

DISCUSSION:

N. Sarma: To what extent are you playing the parameter game?

G.K. Mehta: There are only five parameters as long as one restricts to single Gaussian. By comparing with realistic potential matrix elements we have tried to get a reasonable Phenomenological potential, presumably independent of manipulations.

P. Mukherjee: The plot of E vs b shows that there is no sharp minimum. So, how sensitive, do you think, your parameters are to this oscillator parameter b ?

Y.R. Waghmare (Comment):

The trend of the curve depends upon how many number of nodes are used in the expansion of the orbitals. If large number of nodes are used, you will get a straight line as energy becomes independent of the oscillator parameter b. The matrix elements of the interaction as a function of b, of course, do not have any adjustable parameters.

Y.K. Gambhir (Comment):

I would like to mention the work of Clark and Elliot which is in similar spirit as yours. They take the matrix elements obtained by fitting the observed in the entire mass region for comparison. In their potential they also include the tensor as well as $L S$ terms. They have also done qualitative comparison with the parameters of Hamada Johnston potential.

S.N. Mukherjee: Have you calculated the low lying excited states of some nuclei to test whether the parameters of the potential obtained in the present calculation are reliable.

Y.R. Waghmare: We have as yet not attempted any specific calculations. We have still to calculate the parameters of the tensor forces.

D.K. Sood: What is the procedure for seeking an optimised set of these parameters? Do they comprise a unique set?

K.H. Bhatt (chairman) remarked that errors should be assigned to these numbers and the chi-squared test will give the answer.

STATISTICAL APPROACH TO THE PROBLEM OF CONFIGURATION INTERACTION

Nazakat Ullah
Tata Institute of Fundamental Research,
Bombay-5.

ABSTRACT.

A statistical method is developed to attack the problem of configuration interaction. It is shown that under certain conditions the ground-state properties of a system may not be too much affected by the mixing of higher configurations. An expression has been derived for the mean-square deviation of the expectation value of a quantum mechanical operator in the ground state. Various models are constructed to estimate this meansquare deviation.

Not presented.

ESTIMATION OF THE (t,p) REACTION REDUCED WIDTHS FROM SURFACE-DELTA INTERACTION WAVE-FUNCTIONS

K.V. Chalapati Rao and P. Mukherjee
Saha Institute of Nuclear Physics, Calcutta

Recently, Green and Moszkowski (1) have proposed a surface delta interaction of the type $V(\vec{r}_1-\vec{r}_2)=\delta(\vec{r}_1-\vec{R})\cdot\delta(\vec{r}_2-\vec{R})\cdot V_0$ (I) as an effective interaction between nucleons in nuclei. This is equivalent to a delta interaction in the angular co-ordinates of the interacting particles

$$V_{ik} = -4\pi G\cdot\delta(\Omega_{ik}) \quad ------ \quad (II)$$

with the additional assumption that the radial integrals for the different configurations are all equal for a particular nucleus.

The surface-delta interaction has been applied here to construct the level structures of the nuclei ^{18}O, ^{30}Si, ^{50}Ca and ^{58}Ni. The antisymmetrised matrix elements, in jj-coupling scheme, of the SDI (II) between the states $(j_a j_b)J$ and $(j_c j_d)J$ is given (2) by

$$W_J^A(j_a j_b, j_c j_d) = -\left[(1+\delta_{ab})(1+\delta_{cd})\right]^{-1/2} h_J(j_a j_b)\cdot h_J(j_c j_d)\cdot G$$

where

$$h_J(j_a j_b) = (-)^{j_a+J-1/2}\left\{\frac{[j_a][j_b]}{[J]}\right\}^{1/2}\begin{bmatrix} j_a & j_b & J \\ 1/2 & -1/2 & 0\end{bmatrix} \qquad (III)$$

if l_a+l_b+J is even and zero otherwise. G is the strength of the interaction which is to be adjusted to give fit with

experimental levels. The condition '$l_a + l_b + J$ is even' shows that only natural parity levels will be affected by the interaction.

The configurations mixed in our calculations are : ($1d_{5/2}$, $2s_{1/2}$, $1d_{3/2}$) for ^{18}O; ($2s_{1/2}$, $1d_{3/2}$) for ^{30}Si; ($2p_{3/2}$, $2p_{1/2}$, $1f_{5/2}$, $1g_{9/2}$) for ^{50}Ca and ^{58}Ni. The single particle energies of the above configurations are taken from the experimental levels of the nuclei ^{17}O, ^{29}Si, ^{49}Ca and ^{57}Ni. The fit is satisfactory in all cases except ^{18}O, where the discrepancy is understandable, since core excitation is important in ^{18}O (3).

The SDI wave-functions were used to explain a recent experimental result on (t,p) reactions (4). Data on L = 0 (t,p) transitions show that when the ratio of excited state intensity to ground state intensity σ_{exc}/σ_{gr} is plotted against the neutron number of the residual nucleus, it shows an abrupt fall beyond N = 28.

The differential cross-section for double-transfer reactions is found to be (5) an incoherent sum over L, S, J and T of

$$\sum_M \left| \sum_N G_{NLSJT} \cdot B^M_{NL} (\vec{k}_1, \vec{k}_2) \right|^2 \quad ------ (IV)$$

Here, B^M_{NL} is the transfer amplitude and recent results (5) indicate that it varies slowly from one 0^+-state to another over the entire mass range and the variation may be neglected in finding the ratio of cross-section. G, in eqn. (IV) is the structure factor

given by

$$G_{NLSJT} = g \sum_{\gamma} \beta_{\gamma LSJT} \cdot \Omega_n \cdot \langle n_0, NL; L \mid n_1 l_1, n_2 l_2; L \rangle \quad \text{---} (V)$$

$$g = 1 \quad \text{if } n_1 l_1 j_1 = n_2 l_2 j_2$$
$$= \sqrt{2} \quad \text{otherwise.}$$

The bracket is the Moshinsky bracket. Ω_n gives the overlap of the relative motions of the two nucleons in the residual nucleus and in the nuclide. Its values are calculated following Glandenning (5).

β_γ is the parentage factor connecting the nucleus (A + 2) to A and measures the extent to which the nucleus (A + 2) in the state in which it is formed by the reaction appears as the ground state of the nucleus (A) plus two neutrons in the state $\gamma(=n_1 l_1 n_2 l_2 \text{----}), L, S, J, T$. In the special case when the target is a closed shell nucleus, J = o and

$$\beta_{\gamma LSJT}^{(0,J_2)} = C_{(j_1 j_2) J_2 T_2} \begin{bmatrix} l_1 & 1/2 & j_1 \\ l_2 & 1/2 & j_2 \\ L & S & J \end{bmatrix} \cdot \delta_{JJ_2} \cdot \delta_{TT_2} \quad (VI)$$

Here C's are mixture co-efficients, known from the wave-functions. The ratio of cross-sections is computed as

$$\frac{\left| \sum G \right|^2_{exc}}{\left| \sum G \right|^2_{gr}}$$

for the reactions ^{16}O (t,p) ^{18}O; ^{28}Si (t,p) ^{30}Si, ^{48}Ca (t,p) ^{50}Ca and ^{56}Ni (t,p) ^{58}Ni. The results are given

Table I.

SDI Wavefunctions

Nucleus	Basic States	Excited State	Ground State
^{18}O	$(d_{5/2})^2$	- 0.3691	- 0.9150
	$(s_{1/2})^2$	0.9281	- 0.3533
	$(d_{3/2})^2$	- 0.0497	0.1945
^{30}Si	$(s_{1/2})^2$	0.5616	0.8275
	$(d_{3/2})^2$	- 0.8274	0.5614
^{50}Ca	$(p_{3/2})^2$	- 0.2701	0.9461
	$(f_{5/2})^2$	0.8817	0.1686
	$(p_{1/2})^2$	0.2409	0.1707
	$(g_{9/2})^2$	0.3026	0.2174
	$(p_{3/2})^2$	- 0.2522	0.95291
	$(f_{5/2})^2$	0.8162	0.3030
	$(p_{1/2})^2$	- 0.5198	0.0135

in Tables (1) and (2). It is seen that the ratio exhibits a sharp decrease after N = 28 of the residual nucleus in agreement with experiment. Since the double-transfer reactions are very sensitive to configuration mixing in the residual nucleus, the fair agreement of our results with (t,p) reaction data is an indication that

the surface-delta interaction is a satisfactory effective interaction in the mass region studied.

Table II.

Values of Cross-section ratios

Reaction	
$^{16}O(t,p)^{18}O$	2.6334
$^{28}Si(t,p)^{30}Si$	0.8999
$^{48}Ca(t,p)^{50}Ca$	0.0064
$^{56}Ni(t,p)^{58}Ni$	0.0828

REFERENCES:

1. Green and Moszkowski, Phys. Rev., 139B, 790 (1965)
2. Plastino, Arview and Moszkowski, Phys. Rev., 145, 837 (1966)
3. Engeland, Nucl. Phys., 72, 68 (1965)
4. Hinds et al, Phys. Letters, 21, 328 (1966)
5. Glandenning, Phys. Rev., 137B, 102 (1965)

DISCUSSION:

Y.K. Gambhir: The surface-delta (S-δ) interaction has the same character as the pairing interaction used by Kisslinger and Sorensen (KS). Therefore it will be interesting to see

whether the S-δ with the strength of KS explains all the features you mentioned or not. It will also show, how much this strength has to be modified to explain these features?

K.V. Chalapati Rao: That is true. But the main purpose is to see whether the effect found by Hinds be reproduced by conventional shell model and surface-delta interaction was used only for the sake of simplicity.

MODIFIED NILSSON ORBITALS AND THEIR APPLICATIONS IN THE ANALYSIS OF (d,p) REACTIONS ON EVEN-A RARE EARTH NUCLEI

G. Rama Krishna and P. Mukherjee
Saha Institute of Nuclear Physics, Calcutta

It has been well established that the Nilsson orbitals provide a useful tool for understanding and predicting the observed properties of rare earth nuclei. Subsequent experimental work through (d,p) reactions on these nuclei suggest that the wave functions tabulated by Nilsson do not give correct cross-section ratios among the levels of a rotational band and also that the decoupling parameter for the K = 1/2 bands show a systematic deviation from the values predicted by Nilsson's wave functions. As such an attempt has been made to modify the wave functions incorporating the recently observed single particle states which are much different from those of Nilsson's into the Nilsson Hamiltonian. Figure 1 indicates the fit with the experimental levels in the rare earth region. Nine of the twelve levels are in agreement with χ = 0.033 and μ = 0.35; i(13/2) and h(9/2) levels have been brough into agreement with different sets, indicated in figure 1 by asterisk and cross respectively. The need for a different choice in the case of 'i' levels can be attributed to the fact that i(13/2) level crosses from one major shell to the other with a large spin-orbit splitting and as such needs a large spin-orbit coupling parameter.

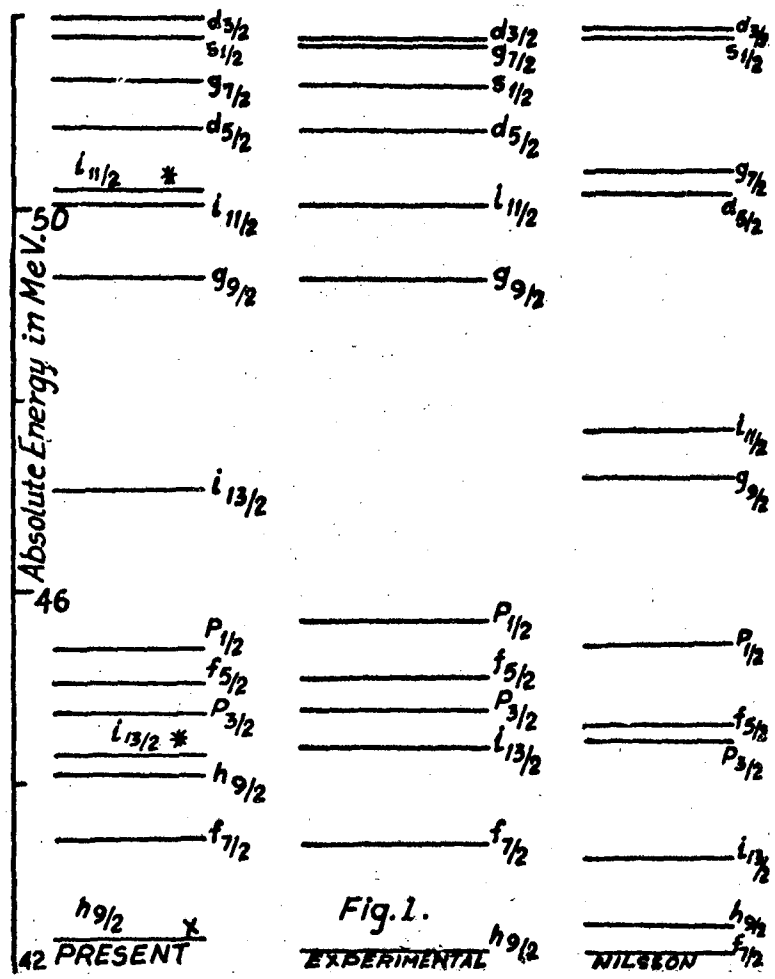
Absolute Energy in MeV.
50
46
42
PRESENT
EXPERIMENTAL
WILSON

Fig. 1.

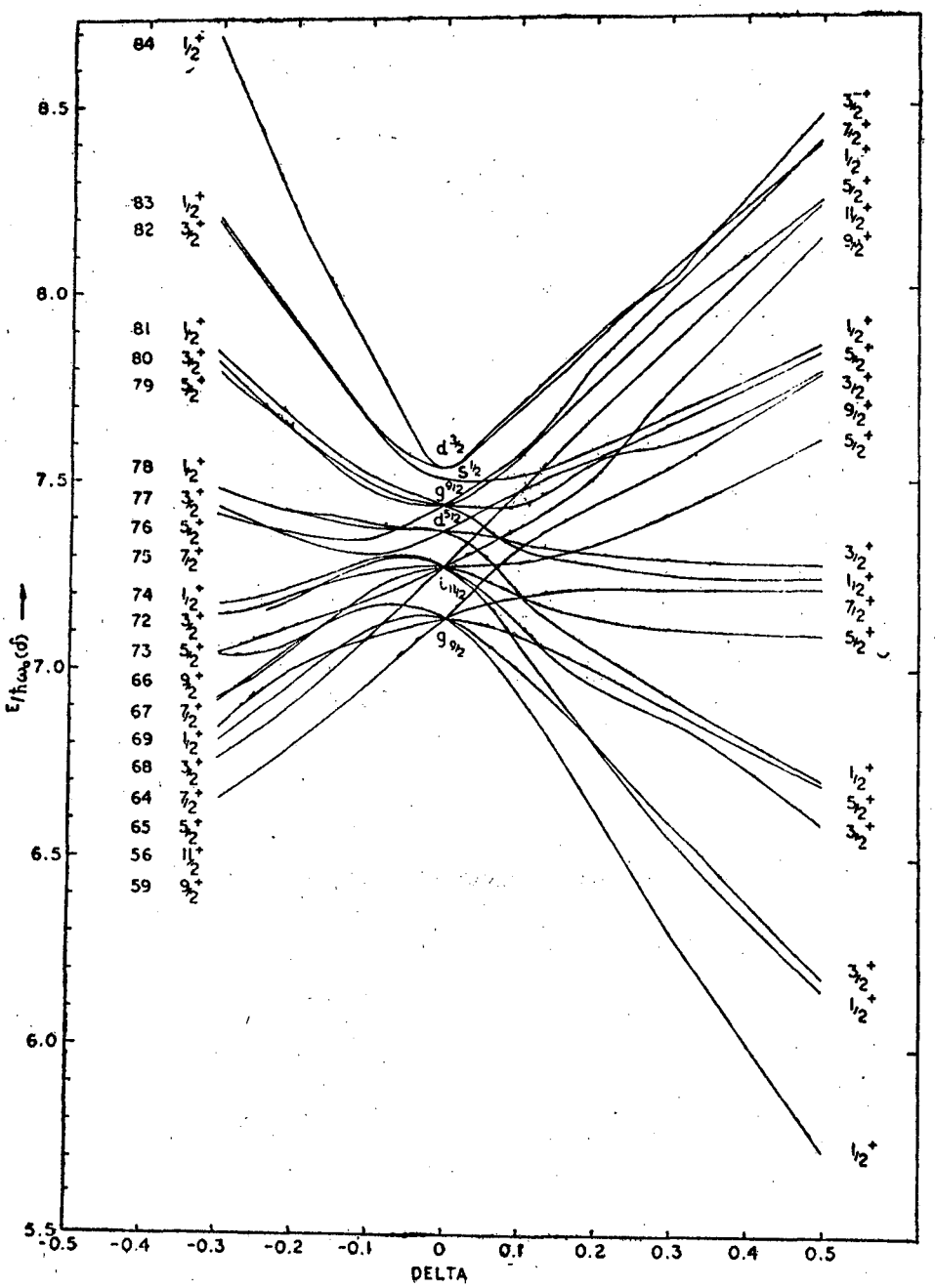
84 1/2+
83 1/2+
82 3/2+
81 1/2+
80 3/2+
79 5/2+
78 1/2+
77 3/2+
76 5/2+
75 7/2+
74 1/2+
72 3/2+
73 5/2+
66 9/2+
67 7/2+
69 1/2+
68 3/2+
64 7/2+
65 5/2+
56 11/2+
59 9/2+
d 3/2
s 1/2
g 9/2
d 5/2
i 11/2
g 9/2
3/2+
7/2+
1/2+
5/2+
11/2+
9/2+
1/2+
5/2+
3/2+
9/2+
5/2+
3/2+
1/2+
7/2+
5/2+
1/2+
5/2+
3/2+
3/2+
1/2+
1/2+
E/ħω0(δ)
8.5
8.0
7.5
7.0
6.5
6.0
5.5
-0.5
-0.4
-0.3
-0.2
-0.1
0
0.1
0.2
0.3
0.4
0.5
DELTA

Fig. 2.

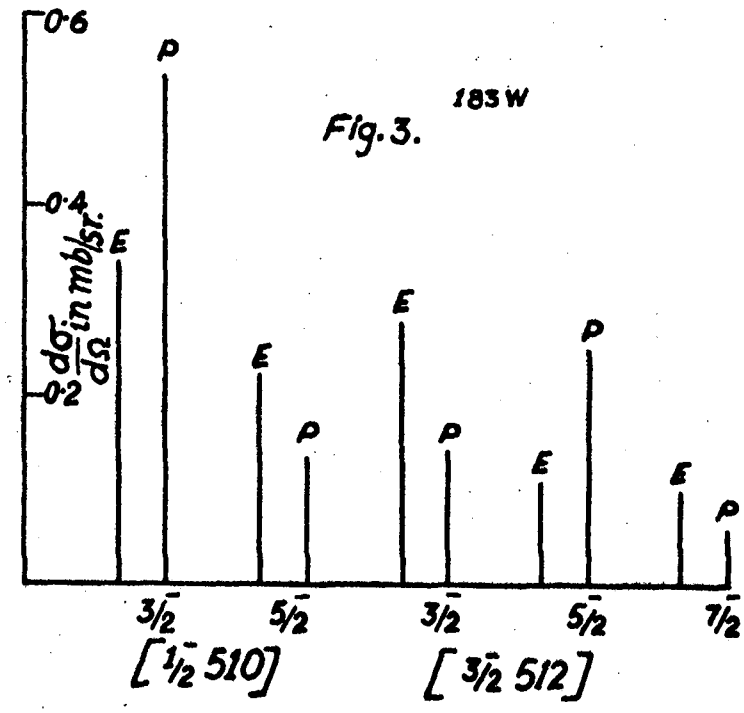
0·6
0·4
0·2
$\frac{d\sigma}{d\Omega}$ in mb/sr.
183W
E
P
E
P
E
P
E
P
E
P
3/2⁻
5/2⁻
3/2⁻
5/2⁻
7/2⁻
[1/2⁻ 510]
[3/2⁻ 512]

Fig. 3.

The single particle states have been calculated with this Hamiltonian and these are found to be much different from those of Nilsson as can be seen from figure 2 which is a plot of $E/\hbar\omega_0(\delta)$ vs. deformation δ for the N = 6 shell. The decoupling parameters have been calculated with our wave functions for the different K = 1/2 bands and these are found to have a better trend of variation towards the experimental value. The cross-section ratios for the (d,p) reactions have been calculated for different rotational bands in 165 DY, 177 Yb, 179 Yb and 179 Hf. A typical result is shown in figure 3 where E is the experimental yield and P the calculated cross-section. Similar calculations are in progress for other rare-earth nuclei.

REFERENCES:

1. S.G. Nilsson, Kgl Danske Videnskab. Selskab, Mat. Fys. Medd., 29, No.16 (1965)

   B.R. Mottelson and S.G. Nilsson, Kgl Danske Videnskab Selskab, Mat. Fys. Skrifter 1, No. 8 (1959)

2. Michel N. Vergnes and R.K. Sheline, Phys. Rev., 132, 1736 (1963)

   R.K. Sheline, et al., Phys. Rev., 136, B351 (1964)

DISCUSSION

S.N. Mukherjee: How do you know that ^{209}Po is sphencial while adjusting κ and μ?

G. Ramakrishna: Stripping reaction data indicate that the states are purely shell model states.

S. Mukherjee: Why do you put all the stress on the coefficients C_j's and not on ϕ_ℓ's?

G. Ramakrishna: This is essentially a structure effect, so it has to do with the spectroscopic factor. We know ϕ_ℓ very accurately from DWBA analysis.

A QUASI-PARTICLE FORMALISM FOR EXCITED BAND IN EVEN-EVEN NUCLEI

Harish Chandra and L. Satpathy
Saha Institute of Nuclear Physics
Calcutta.

ABSTRACT.

Application of the Hartree-Bogolyubov theory to the deformed nuclei yields the single quasi-particle energy spectra and a set of quasi-particle wave function. This solution has been used to deduce R.P.A. equations for studying the excited bands of the deformed even-even nuclei. The calculation in s-d and p-f shell is in progress.

ALPHA-ALPHA INTERACTION POTENTIAL

Rajagopal Shanta
Saha Institute of Nuclear Physics,
Calcutta.

1. INTRODUCTION

The elastic scattering of α particles by ^{4}He has been studied at a wide range of laboratory energies from 150 keV to 120 MeV (1). However the present investigation is restricted to c.m. energies $E \leqslant 12$ MeV because for these energies the phase shifts are more or less well determined. Further, the s, d and g partial waves alone contribute to the scattering at these energies.

Russel et al., (2) and Heydenberg and Temmer (3) have discussed the qualitative features of the α-α potential from the energy dependence of the phase shifts at low energies. Above 200 keV the nuclear S wave interaction begins to contribute starting at δ_0 near π and smoothly decreasing with increasing energy and eventually becoming negative at about 10 MeV. This behaviour of the δ_0 phase shift indicates that there must be some spatial region in which the interaction potential is more repulsive than the Coulomb potential. The d wave phase shift first begins to contribute at 1.25 MeV. As the energy increases it begins to deviate from zero in the positive direction at an energy corresponding to an impact parameter of 5 F, and then passes through resonance. Above the resonance the $\ell=$ beaming negative at an impact parameter of 1 - 2F. This feature indicates that the interaction has a repulsive core of radius 1 - 2F. At about 6 MeV, the g wave in the positive direction at an impact parameter of 5F and then passes

through resonance. The behaviour of d and g waves indicates that the outermost effect of the nuclear potential must be attractive followed by a Coulomb potential outside the range of the nuclear forces.

The investigations of Van der Spuy and Pienaar (4) indicate that the phase shift data for α-α scattering cannot be represented by a velocity independent interaction potential even in the low energy domain. However their results indicate that a strongly ℓ-dependent repulsive core and an outside ℓ-independent attractive square well potential yield a reasonable fit to the experimental phase shifts for c.m. energies < 3 MeV. Using such an interaction potential it is investigated whether it is possible to fit the $\ell = 0$, 2 and 4 phase shifts for c.m. energies $\lesssim 12$ MeV.

2. RESULTS AND DISCUSSION

Assuming an infinite repulsive core of radius $r_I = 1.8$ F, an attractive square well potential of depth 9.5 MeV and an outer interaction radius $r_N = 4$F, a reasonably good fit is obtained for the S wave phase shifts upto E (C.M) = 12 MeV. This can be seen from fig. 1. With the same value of r_N and V but $r_I = .8$ F, the d wave phase shifts were calculated. The experimental δ_2 phase shift increases smoothly upto E (C.M.) = 5.44 MeV and then begins to fall monotonically whereas the calculated values show a steady increase upto 8.9 MeV and then a slow increase upto 12 MeV (fig.2). The g wave phase shifts were calculated with the same values of r_N and V but $r_I = 0$. The experimental δ_4 phase shift just begins to contribute at about 6 MeV and then increases in the positive

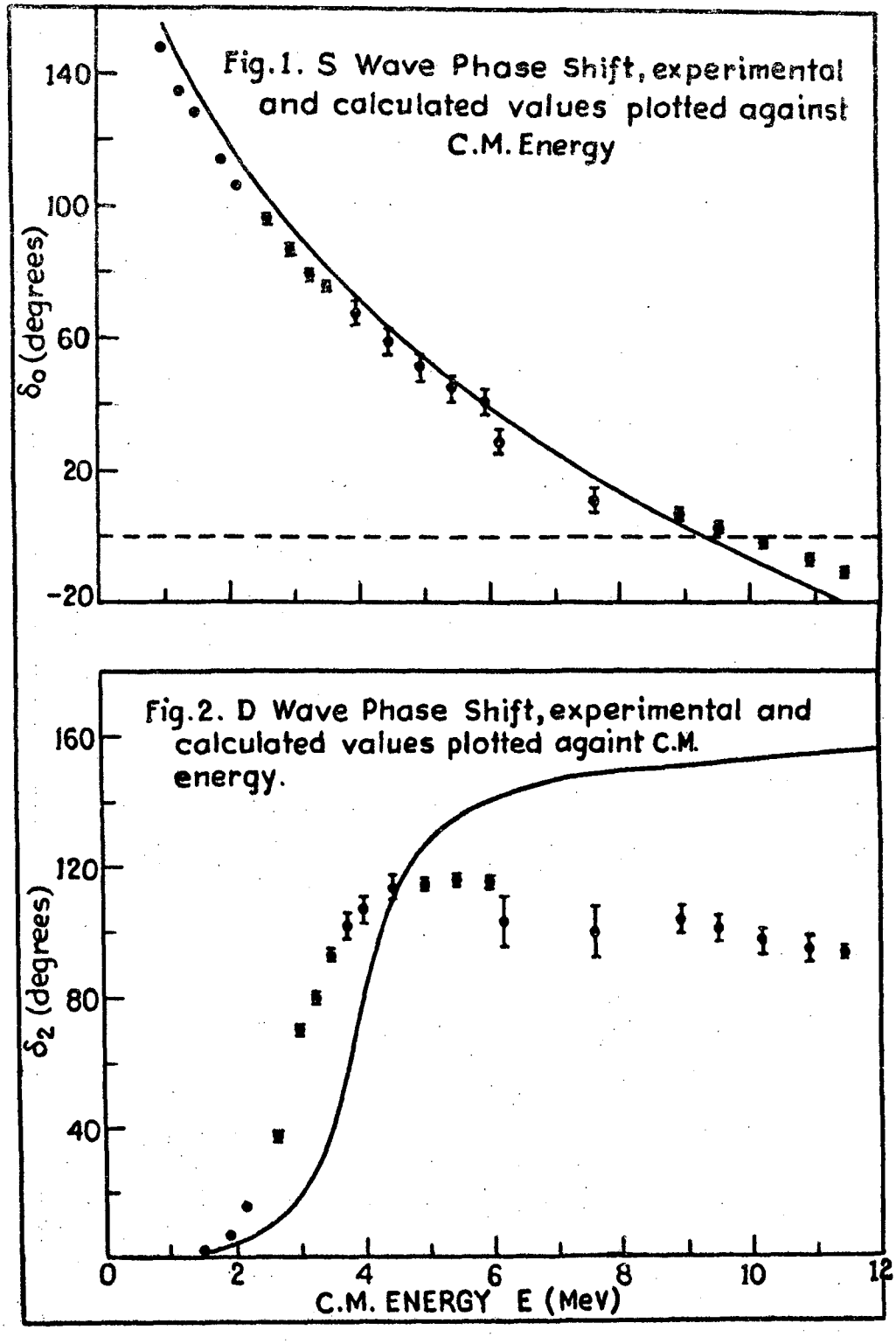

Fig.1. S Wave Phase Shift, experimental and calculated values plotted against C.M. Energy

Fig.2. D Wave Phase Shift, experimental and calculated values plotted againt C.M. energy.

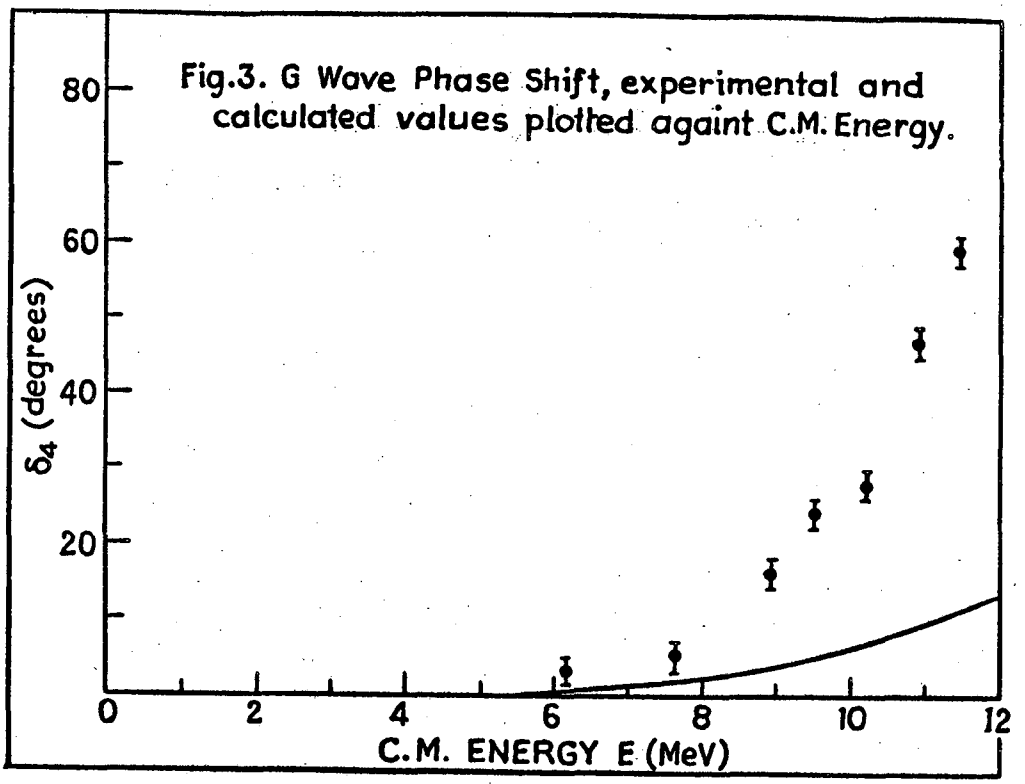

Fig.3. G Wave Phase Shift, experimental and calculated values plotted againt C.M. Energy.

direction. The calculated values of δ_4 phase shift also increase with increase in energy but rather slowly compared to the experimental values (fig.3). These results indicate that the potential is not sufficiently attractive to reproduce δ_4^{exp}

Ali and Bodmer (5) have used a superposition of repulsive and attractive Gaussian shapes for the nuclear part of the potentials. They have first determined the attractive part of the potential by fitting the δ_4 phase shift. Then keeping the attractive part ℓ-independent they have fitted the δ_0 and δ_2 phase shifts by varying the repulsive part. A similar procedure is being attempted in the present case also.

REFERENCES

1. P. Darriulat et al., Phys. Rev. 137, B 315 (1965) and references (9-11) there in.
2. J.L. Russel et al., Phys. Rev. 104, 135 (1956)
3. N.P. Heydenbug and G.M. Temmer, Phys. Rev. 104, 123 (1956)
4. E. Van der Spuy and H.J Pienaar, Nuclear Physics 7, 397 (1958)
5. S. Ali and A.R. Bodmer, Nuclear Physics 80 (1966)

DISCUSSION:

P. Mukherjee: Did you take into account the states of ^{8}Be in your α-α scattering analysis?

Rajagopal Shanta: ^{8}Be has the following low lying states 0^+ at .094 MeV, 2^+ at 2.99 MeV and 4^+ at 11.79 MeV.

S.N. Mukherjee: What about the binding energy of ^{8}Be?

Rajagopal Shanta: I did not calculate the binding energy. I calculated only the phase shifts.

AN EVEN-Odd ANOMALY AT LOW ENERGIES

M.Z. Rehman Khan and Israr Ahmed
Department of Physics
A.M.U. Aligarh
U.P. India

ABSTRACT.

Evidence for an even-odd anomaly which suggests a higher strength of the real part of the optical potential for odd mass nuclei is briefly discussed. Sitenko's theory which seems fairly satisfactory in explaining the difference between the imaginary parts of the optical potential of even and odd mass nuclei is found to encounter serious difficulties in predicting the real part of the potential. Our attempt to explain the even-odd anomaly in the strength of the real part has not been entirely satisfactory. Work to improve the situation is presently in progress.

Not presented.

ON HIGH ANGULAR MOMENTUM RESONANCES IN NEUTRON CROSS-SECTIONS AT LOW ENERGIES

Q.N. Usmani and M.Z.R. Khan
Department of Physics
Aligarh Muslim University, Aligarh

An attempt has been made to investigate the high angular momentum resonances in neutron cross-sections at low energies. In this connection the Feshbach, Peaslee, and Weisskopf (1,2) theory was applied to the scattering of neutrons from a square well potential. We found that their expansion of the logarithmic derivative does not converge for high values of ℓ in the neighbourhood of the resonance energies. It, therefore, needs modification.

For a real square well potential we define resonance when the cross-section reaches its maximum value i.e. when $\delta_\ell = \pi/2$. It can easily be seen that for the phase shift to become $\pi/2$ the following relation should be satisfied

$$f = 1 + X \frac{j'(X)}{j(X)} = 1 + x \frac{n'(x)}{n(x)} = B_{s\ell} \quad \text{(Say)} \ldots\ldots (1)$$

where,

$$X^2 = (X_0^2 + x^2), \quad X_0^2 = \frac{2m}{\hbar^2} V R^2, \quad x^2 = \frac{2m}{\hbar^2} E R^2.$$

V being the depth of the potential.

For very low energies the relation (1) reduces to $B_{s\ell} = -\ell$, which is the same as assumed by several authors e.g (3,4). Feshbach, Peaslee, and Weisskopf have assumed $f_\ell = 0$ as their resonance condition. It is, therefore, obvious that this would hold rigorously for S-waves only.

Since W is a small quanity we have retained the condition (1) as the resonance condition for a complex square well potential i.e. we formally define a resonance when the phase - shift becomes $\pi/2$ with W = 0. The effect of W is to shift the resonance slightly and this can be conveniently taken into account.

We have derived the required formulae, valid in the neighbourhood of the resonance, by expanding the logarithmic derivative (treated as a function of energy and ς ($=\frac{W}{V}$) at r = R around the resonance energy and $\varsigma = 0$, retaining terms upto second order in ς . The total cross-section $\sigma_t^{(l)}$ for the lth partial wave has been calculated to be

$$\sigma_t^{(l)} = \frac{\pi(2l+1)}{k^2}\left[\frac{\Gamma_{nl}\{\Gamma_l \cos 2\xi_l - 2(E-E_s'+\lambda_{sl})\sin 2\xi_l\}}{(E-E_s'+\lambda_{sl})^2+(\frac{1}{2}\Gamma_l)^2} + 4\sin^2\xi_l\right] \quad \text{-----(2)}$$

where

$\Gamma_{nl} \equiv \frac{2S_l\hbar^2}{mR^2}$ is the neutron width;

$\Gamma_l \equiv \Gamma_{nl} + 2W$ is the total width;

$E_s' = E_s - S^2\left(\frac{\partial^2 f_l}{\partial S^2}\right)_{E_s,S=0} \Big/ \left(\frac{\partial f_l}{\partial E}\right)_{E_s,S=0}$ is defined to be the actual resonance energy (scattering cross-section is maximum at E'_s and E_s is one of the roots of the equation(1).

$$\lambda_{sl} \equiv (B_{sl} - \Delta_l) \Big/ \left(\frac{\partial f_l}{\partial E}\right)_{E_s,S=0}$$

$(B_{sl} - \Delta_l)$ at low energies can be approximated to

$$- \frac{(2l+1)\, x^{4l+2}}{[(2l-1)!!]^2 [(2l+1)!!]^2}$$

Absorption cross-section in the resonance region is

$$\sigma_c(l) = \frac{\pi(2l+1)}{k^2} \frac{2W\Gamma_{nl}}{(E-E_s'+\lambda_{sl})^2+(\frac{1}{2}\Gamma_l)^2} \quad ------ (3)$$

If one considers the logarithmic derivative as a function of R and ϱ and expands it around $R = R_s$ and $\varrho = 0$, where R_s is the value of R which shows resonance behaviour with respect to R for a fixed energy, one finds that

$$\sigma_t(l) = \frac{\pi(2l+1)}{k^2}\left[\frac{\Gamma_{nl}^R\{\Gamma_l^R \cos 2\xi_l - 2(R-R_s'+\lambda_{sl}^R)\sin 2\xi_l\}}{(R-R_s'+\lambda_{sl}^R)^2+(\frac{1}{2}\Gamma_l^R)^2} + 4\sin^2\xi_l\right] \quad ------ (4)$$

$$\sigma_c(l) = \frac{\pi(2l+1)}{k^2} \frac{\Gamma_{nl}^R(\Gamma_l^R - \Gamma_{nl}^R)}{(R-R_s'+\lambda_{sl}^R)^2+(\frac{1}{2}\Gamma_l^R)^2} \quad ------ (5)$$

where $\Gamma_{nl}^R \equiv \frac{2S_l R_s}{X_s}$; $\Gamma_l^R \equiv \left(\frac{W}{V} + \frac{2S_l}{X_s}\right)R_s$; $R_s' \equiv \frac{R_s - S^2\left(\frac{\partial f_l}{\partial S^2}\right)_{R_s, S=0}}{\left(\frac{\partial^2 f_l}{\partial R}\right)_{R_s, S=0}}$

$$\lambda_{sl}^R \equiv (B_{sl} - \Delta_l) \Big/ \left(\frac{\partial f_l}{\partial R}\right)_{R_s, S=0}$$

X_s is one of the roots of the equation (1)

One can also derive the formula for the strength function, $\frac{\langle \gamma_n^l \rangle}{D}$ where $\langle \gamma_n^l \rangle$ is the average neutron reduced width and D is the average level distance.

At low energies, for typical optical parameters, our resonance condition (1) can be satisfied upto $l = 7$, i.e. a real optical-potential would exhibit resonances upto $l \simeq 7$ in scattering.

At resonance the contribution to total scattering cross-section of ℓth partial wave is $\frac{4\pi(2\ell+1)}{k^2}$ which for low energies would mean a great jump over the background. However, we found that at low energies the realistic value of W practically wipes out the contribution of high angular momentum resonances. For example, if we demand $\ell = 5$ to contribute significantly at about 1 MeV, it would be possible only if W is a few electron volts (where as the realistic value of W is of order 1 - 2 MeV at very low energies). Here, it would be probably interesting to point out that it seems to be generally believed that at low energies high partial waves are entirely insignificant due to centrifugal barrier. But as we have mentioned above high partial waves contribute significantly for a sufficiently small W.

The average width of a many body high angular momentum resonance is extremely small compared to the average width of a S-wave resonance. A rough estimate shows that for a medium nucleus near 1 MeV the average widths of high angular momentum $(\ell \simeq 5)$ resonances would be of the order of an election volt. Thus their experimental investigation would be a very difficult task. It, therefore, seems desirable to predict the situation where these are most pronounced.

In the sprit of Lane, Thomas and Wigner (5) we should expect that the best situation is where the high angular momentum single particle levels appear. Thus, our considerations can be of some help in the experimental investigation of many body high angular momentum resonances.

As a further application of our proceedure we have studied the validity criterion (for S-wave the validity criterion has been discussed by Brown (6) of the intermediate Model (Lane, Thomas and Wigner) for high partial waves. For a medium light nucleus and $\ell = 5$ we find $E_s - E_{s'} \sim 38$ MeV. This means $E_s - E_{s'} \gg W$, indicating the validity of the intermediate model for high partial waves.

We have made calculations for a complex square well potential. They are of very general nature. It is, therefore, reasonable to suppose that the realistic diffusness will not change their basic nature.

The work which we have reported here is in a preliminary stage. We are going to apply it to some other situations.

REFERENCES:

1. Feshbach, Peaslee, and Weisskopf; Phys. Rev. Vol 71 No.3, 145 (1947)
2. Blatt and Weisskopf; Theoretical Nuclear Physics: Chap.VIII
3. Lane and Thomas, Revs. Mod. Phys. Vol 30, 257 (1958)
5. Lane, Thomas, and Wigner; Phys. Rev, Vol. 98, No.3, 693 (1955)
6. Brown, Rev. Mod. Phys. Vol. 31, No. 4, 893 (1959)

^{6}Li AS A THREE BODY SYSTEM

M.S. Shah
Physical Research Laboratory, Ahmedabad-9

and

A.N. Mitra
Physics Department, University of Delhi.

^{6}Li has been treated as a three body system consisting of a structureless α-particle, a proton and a neutron interacting through non-local separable potentials. Onlu the central s-state and p-state interactions are taken for N-N and α-N potentials respectively. These are as follows.

$$\langle q | v_{NN} | q' \rangle = -\frac{\lambda_{np}}{2\mu_{np}} g(q) g(q')$$

and

$$\langle q | v_{\alpha N} | q' \rangle = -\frac{\lambda_{\alpha N}}{2\mu_{\alpha N}} f(q) f(q') \, 3\vec{q}\cdot\vec{q}'$$

The parameters λ_{np} and β_{np} for triplet and singlet states are taken from (1), whereas $\lambda_{\alpha N}$ and $\beta_{\alpha N}$ are taken from (2).

We have utilised the same procedure for ^{6}Li as in Mitra's earlier paper (3). Additional compelxity arises here compared to ^{3}H due to the different masses of the nucleon and the α-particle, and the p-wave nature of α-N interaction.

It is well known that the ground state 1^+ of ^{6}Li is L = 0, S = 1. So T = 0 N-N force enters into the Schrödinger equation for this state. The excited 0^+ state which is known to

be L = 0, S = 0 will be described only by T = 1 N-N force. Following the same notations as given in (3) the wave-function for ^{6}Li is represented by two Spectator functions G(p) and $\vec{p}$ F (p) which describe the α-particle and one nucleon wave-functions with respect to two other particles respectively. These Spectator functions satisfy two coupled one dimensional integral equations but due to the simplicity of the problem in our case reduce to only one integral equation.

This integral eighenvalue equation is solved on IBM 1620 by constructing 16 x 16 matrix and then trying to find out the maximum eigenvalue $\lambda_{\alpha N}^{-1}$ i.e. minimum value of $\lambda_{\alpha N}$ for different values of the binding energy for the ground state 1^+, and then this number is compared with the experimentally derived two body parameter. The numbers are quoted in Table - I. The experimental two-body value of $\lambda_{\alpha N}$ gives overbinding for ^{6}Li (5.6 MeV Compared to observed 3.7 MeV). This may be due to the neglect of tensor force. If only the central part of more realistic N-N force which includes also the tensor force (4) is taken, then this force binds ^{6}Li only by about 1.2 MeV. This suggests the importance of the tensor force. Our results should be compared with Austern and Wackmann (5). The results also indicate that the change in $\lambda_{\alpha N}$ by 2% to 2.5% changes the binding energy by about 15% to 20%. However the wave-function F' (p) = p^2F(p) does not show appreciable change for these different values of binding energy.

Table I

$\lambda_{\alpha N}(\text{expt}) = 0.3818\ \alpha_d$ $\qquad \alpha_d = 2.316 \times 10^{12} cm^{-1}$

Binding Energy (MeV)	6.22	5.39	4.56
$\lambda_{\alpha N}$ in units of α_d	0.3888	0.3797	0.3687

It is nice to know that these potential parameters do not give any other excited bound state. The 0^+ excited state is bound by 0.2 MeV. The eigenvalue equation is again solved for the T = 1 singlet state parameters. At E_b = 0.46 MeV the minimum $\lambda_{\alpha N}$ (maximum $\lambda_{\alpha N}^{-1}$) turns out to be 0.3933 α_d. This may be compared with $\lambda_{\alpha N}$ = 0.3818 α_d and E_b = 0.2 MeV.

In concluding we can say that L = 0 states of ^6Li are well explained by this model.

REFERENCES:

1. Yamaguchi and Yamaguchi, Phys. Rev. 95, 1628 (1954)
2. Mitra, Bhasin and Bhakar, Nucl. Phys. 38, 316 (1962)
3. Mitra A.N. Nucl. Phys. 32, 529 (1962)
4. Yamaguchi and Yamaguchi, Phys. Rev. 95, 1635 (1954)
5. Austern and Wackmann, Nucl. Phys. 30, 529 (1962)

DISCUSSION:

P. Mukherjee: Are the parameters of α-N scattering real?

M.S. Shah: They are assumed to be real, and derived by least squares fit to $p_{3/2}$ and $p_{1/2}$ phase shifts.

PION ABSORPTION IN ^{3}HE

M.S. Shah and S.P. Pandya,
Physical Research Laboratory, Ahmedabad-9.
and
A.N. Mitra
Physics Department, University of Delhi.

Study of pion absorption in light nuclei is expected to yield detailed information on nuclear correlations. Absorption of π^- in ^{3}He has been calculated by Diwakaran (1) and Cheon (2) using different models. We present here a calculation of the ''deuteron mode'' ($\pi^- + {}^3He \rightarrow n + d$) which is a part of a more elaborate programme of studies of pion interactions in nuclei.

We assume that pion is absorbed from the s-orbit in the ^{3}He atom. Pion - nucleon interaction is chosen to be a sum of one-body operators as in (2).

$$H = G\left(-\frac{\mu_\pi}{m_n}\right) \sum_{i=1}^{3} \left(\underset{\sim}{\tau_i} \cdot \underset{\sim}{\phi(i)}\right)\left(\vec{\sigma_i} \cdot \vec{p_i}\right) \quad (1)$$

where G is the strength of the interaction, σ, τ and p are the spin, i-spin and momentum operators for the nucleon and ϕ is the pion wavefunction. We have dropped the usual pion - momentum terms, since they make no contribution to capture from s-orbit.

To take account of the symmetries of the three-body wavefunctions, this interaction is expressed in terms of three-body operators of correct symmetries (3). We then obtain

$$H = \frac{2}{27}\left(-\frac{\mu_\pi}{m_n} G\right)\Big[(\tau_s \cdot \phi^s)(\sigma' \cdot p' + \sigma'' \cdot p'') + (\tau' \cdot \phi^s)(\sigma^s \cdot p' + \sigma'' \cdot p' + \sigma' \cdot p'') + (\tau'' \cdot \phi^s)(\sigma^s \cdot p'' + \sigma' \cdot p' - \sigma'' \cdot p'')\Big] \quad (2)$$

The wavefunction of ^{3}He is assumed to be $^2S_{1/2}$, (3)

$$\Psi(^3He) = \frac{1}{\sqrt{2}}\left(\chi' \mathcal{J}'' - \chi'' \mathcal{J}'\right)\psi^s(P_1 P_2 P_3) \quad (3)$$

The momentum wavefunction ψ^s is obtained à la Mitra (4) using s-state, spin-independent, non-local separable nucleon-nucleon interaction with parameters as given by Yamaguchi (5), except that the spin-independent strength parameter is now chosen to be

$$\lambda = \tfrac{1}{2}(\lambda_s + \lambda_t)$$

For the final state wavefunction we only consider T = 1/2, S = 3/2 state, i.e.,

$$\Psi(n+d) = \frac{1}{\sqrt{2}}\left(\psi' \mathcal{J}'' - \psi'' \mathcal{J}'\right)\chi^s \quad (4)$$

The wavefunctions (3) and (4) are suitably normalised.

For ψ' we chose the form (3)

$$\psi' \sim \left[\frac{\delta(\vec{P}_3 - \vec{K})\, g(P_{12})}{P_{12}^2 + \alpha_d^2} - \frac{\delta(\vec{P}_2 - \vec{K})\, g(P_{31})}{P_{31}^2 + \alpha_d^2}\right] \quad (5)$$

α_D^2 is the binding energy of deuteron, and g (p) is given in (5). The matrix element, after evaluating spin and i-spin integrals, countains the momentum-space integral $\langle \psi' | p' | \psi^s \rangle$. The calculation is straightforward and yields for the reaction rate.

$$W = (1.15,\ 1.59,\ 1.95) \times 10^{15}\ \text{sec}^{-1}$$

where the three values are obtained with ^{3}He wavefunctions giving binding energy 6.22, 8.29 and 10.36 MeV. The correlations in the initial as well as final states have been introduced by taking proper account of the realistic nuclear interaction. This differs from the procedure of Diwakaran and Cheon.

REFERENCES:

1. Diwakaran, Phys. Rev. 139, B 387 (1965)
2. Cheon, Phys. Rev. 145, 794 (1966)
3. Verde, Handbuch der Physik 39, 144.
4. Mitra, Nucl. Phys. 32, 529 (1962)
5. Yamaguchi and Yamaguchi, Phys. Rev. 95, 1628 (1954)

DISCUSSION:

V.S. Mathur: Don't you think that the contribution of the mixed symmetric state would be significant in your calculation?

M.S. Shah: For the mixed symmetry state, final n-d state can have symmetric spatial component but the form of interaction does not allow this final state. So the final state will be the same as it is described in the paper, so mixed symmetry state which is 2% will contribute same percentage to the calculated one.

S.N. Mukherjee: Do the pion absorption cross section depends significantly on the size of the trinucleon system?

M.S. Shah: With the different binding energy of ^{3}He the capture rate does not vary drastically. On the same spirit I would like to say that the size of tri-nucleon system will affect the capture rate very little.

ON THE NUCLEAR STRUCTURE EFFECTS IN THE PHOTO PRODUCTION OF POSITIVE PIONS FROM ^{16}O+

V. Devanathan
University of Virginia
Charlottesville, Virginia

K. Sreenivasa Rao
Matscience, Madras

and

S.C.K. Nair
Saha Institute of Nuclear Physics, Calcutta

The photoproduction of positive pions from ^{16}O in which the residual nucleus is left either in its ground state or in one of the low lying excited states is analysed in the impulse approximation. The details of the nuclear physics involved is put in by means of (i) the crude single particle-hole model, (ii) the particle-hole model in the Tamm-Dancoff approximation and (iii) the R.P.A. model (the latter two taken from the work of Fillet and Vinh Mau). It is found that the total cross section in the single particle-hole model is about 15% larger than calculated either with the R.P.A. or T.D.A. wave functions. However, to get good agreement with the experimental result the hypothesis of surface production of pions needs to be invoked. It is stressed that the proper theoretical justification for this is lacking at the moment. It is also pointed out in this paper that the probability for the final nucleus being left

---

+ To be published in Nuclear Physics.

in one of the collective states which will subsequently decay by nucleon emission is large as compared with the process in which a non-collective state is involved.

FINAL STATE INTERACTIONS IN THE DECAY OF LIGHT HYPERNUCLEI

K.N. Chaudhari, S.N. Ganguli and N.K. Rao

Tata Institute of Fundamental Research, Colaba, Bombay-5

In this paper an attempt has been made to study excited states of ^{5}Li, ^{8}Be and ^{9}B from decay of hypernuclei $^5_\Lambda$He, $^8_\Lambda$Li and $^9_\Lambda$Be. These hypernuclei are produced from interactions of slow K^- mesons with emulsion nuclei (C, N, O and Ag, Br). Results are as follows.

<u>$^5_\Lambda$He:</u> This hypernucleus results from the binding of Λ^0 hyperon to an alpha particle. It decays mainly according to the scheme $^5_\Lambda He \rightarrow \pi^- + p + {}^4He$. The striking features exhibited by the experimental data are: (a) a strong forward peaking between the line of flight of the α-particle and the direction of emission of the π^- meson in the π-p rest system, and (b) a double peaking in the momentum distribution of $|P_{\pi p}|$ (see fig.1). These have led Dalitz to suggest that the decay could be dominated by strong interactions between the particles present in the final state. The solid curve in fig. 1 is due to Byers and Cottingham who have taken into account in their calculation the known p-^{4}He nuclear interaction. The experimental phase shift analysis of p - ^{4}He indicates the existence of a sharp $P_{3/2}$ resonance at 1.8 MeV and a broad $P_{1/2}$ state between 5 and 10 MeV above the $P_{3/2}$ state. By comparing the experimental data with the predictions of Byers and Cottingham, it is concluded that the decay of $^5_\Lambda$He can be described by a two step process: $^5_\Lambda He \rightarrow \pi^- + {}^5Li^*$, $^5Li^* \rightarrow p + {}^4He$, with a transition predominantly to the 1.8 MeV, $3/2^-$ level of ^{5}Li.

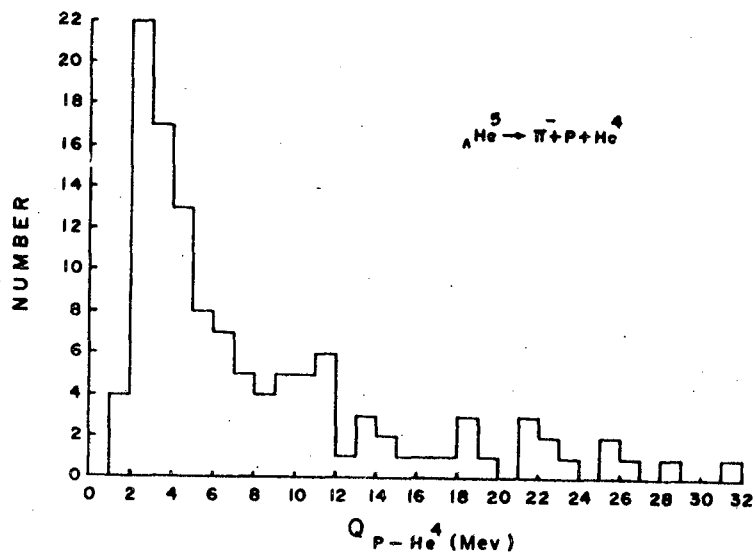
NUMBER
$_{\Lambda}He^{5} \rightarrow \pi^{-} + P + He^{4}$
$Q_{P-He^{4}}$ (Mev)

FIG. 1 (b)

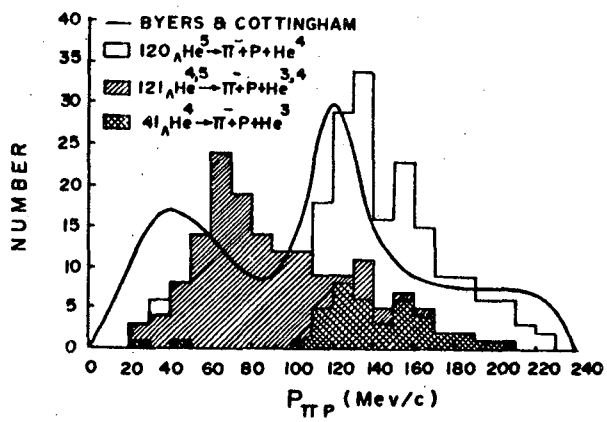
BYERS & COTTINGHAM
120 $_{\Lambda}He^{5} \rightarrow \pi^{-} + P + He^{4}$
121 $_{\Lambda}He^{4,5} \rightarrow \pi^{-} + P + He^{3,4}$
41 $_{\Lambda}He^{4} \rightarrow \pi^{-} + P + He^{3}$
NUMBER
$P_{\pi P}$ (Mev/c)

FIG - 1 (a)

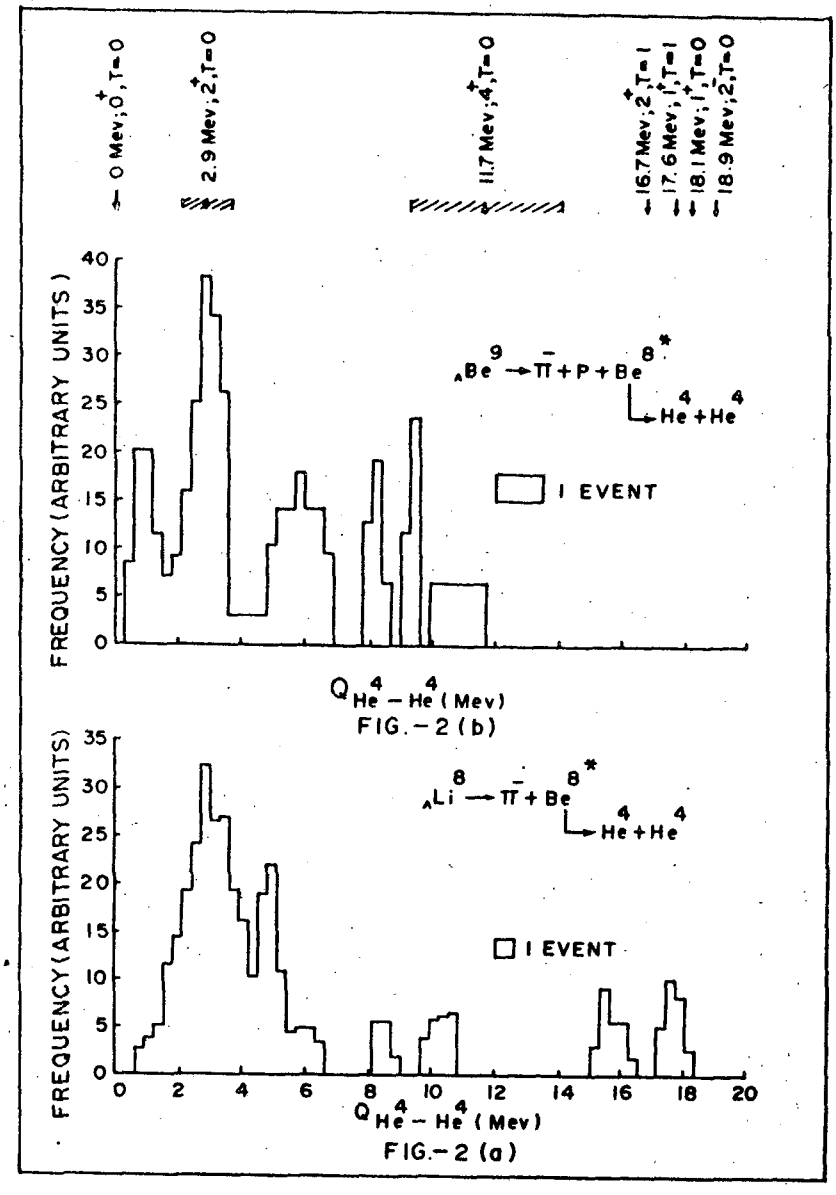
0 Mev; 0+, T=0
2.9 Mev; 2+, T=0
11.7 Mev; 4+, T=0
16.7 Mev; 2+, T=1
17.6 Mev; 1+, T=1
18.1 Mev; 1+, T=0
18.9 Mev; 2-, T=0
FREQUENCY (ARBITRARY UNITS)
$_{4}Be^{9} \rightarrow \pi^{-} + P + Be^{8*}$
$\rightarrow He^{4} + He^{4}$
1 EVENT
$Q_{He^4 - He^4}$ (Mev)
FIG.-2 (b)
FREQUENCY (ARBITRARY UNITS)
$_{4}Li^{8} \rightarrow \pi^{-} + Be^{8*}$
$\rightarrow He^{4} + He^{4}$
1 EVENT
$Q_{He^4 - He^4}$ (Mev)
FIG.-2 (a)

$^{8}_{\Lambda}Li$: This hypernucleus is due to the binding of Λ^{0} to a ^{7}Li core. From a sample of 30 $^{8}_{\Lambda}Li$ decaying according to the scheme $^{8}_{\Lambda}Li \rightarrow \pi^{-} + {}^{4}He + {}^{4}He$ a study of final state interaction has been made. For these events Q values of the two alpha particles in their rest system are computed and the result is shown in fig.2 (a). From this figure one sees the pronounced peak at 2.9 MeV of ^{8}Be excited state of 2^{+} and a short peak around 17 MeV. This has led various groups to postulate that $^{8}_{\Lambda}Li$ decays essentially via two step process, namely, $^{8}_{\Lambda}Li \rightarrow \pi^{-} + {}^{8}Be^{*}$, $^{8}Be^{*} \rightarrow {}^{4}He + {}^{4}He$.

$^{9}_{\Lambda}Be$: The core of this hypernucleus is ^{8}Be which is unstable; but since the presence of Λ^{0} hyperon in a nucleus increases the binding energy, and so it is possible to form $^{9}_{\Lambda}Be$. This hypernucleus decays mainly via the channel: $^{9}_{\Lambda}Be \rightarrow \pi^{-} + {}^{1}H + {}^{4}He + {}^{4}He$. The following final state interactions can be studied from its decay:

(a) $^{9}_{\Lambda}Be \rightarrow \pi^{-} + {}^{9}B^{*}$, $^{9}B^{*} \rightarrow p + {}^{8}Be^{*}$; $^{8}Be^{*} \rightarrow {}^{4}He + {}^{4}He$

(b) $^{9}_{\Lambda}Be \rightarrow \pi^{-} + {}^{9}B^{*}$, $^{9}B^{*} \rightarrow {}^{4}He + {}^{5}Li^{*}$, $^{5}Li^{*} \rightarrow p + {}^{4}He$

(c) $^{9}_{\Lambda}Be \rightarrow \pi^{-} + p + {}^{8}Be^{*}$, $^{8}Be^{*} \rightarrow {}^{4}He + {}^{4}He$

(d) $^{9}_{\Lambda}Be \rightarrow \pi^{-} + {}^{4}He + {}^{5}Li^{*}$, $^{5}Li^{*} \rightarrow p + {}^{4}He$

From a sample of 11 $^{9}_{\Lambda}Be$ we have tried to study type (c) final state interaction and the result of Q value of ^{4}He, ^{4}He in its rest frame is shown in fig.2(b). This clearly again depicts 2.9 MeV level of $^{8}Be^{*}$. More statistics is needed to study the other three type of final state interactions.

HYPERNUCLEI OF MASS NUMBER A = 7

K.N. Chaudhari, S.N. Ganguli and N.K. Rao
Tata Institute of Fundamental Research Centre
Colaba, Bombay-5.

ABSTRACT.

Hypernuclei are those where Λ-hyperon is bound to nuclear fragments; Λ-hyperon can be bound to the ground as well as excited states of nuclei. The study of hypernuclei will reveal information of the binding of Λ to the various levels of nuclei and the nature of Λ-nucleon interaction.

It is known that the presence of Λ hyperon in a nucleus increases the binding energy by about 0.9 MeV per nucleon for a nuclear core of zero spin. This is sufficient to stabilise some aggregates of nucleons which have no bound states. For example, the nucleus ^{6}Be is unstable against break up into ^{4}He + 2p by 1.4 MeV, where as $^{7}_{\Lambda}$Be is stable against break up into $^{5}_{\Lambda}$He + 2p by about 0.5 MeV. Therefore it is often possible to know from study of hypernuclei, groups of nucleons that cannot otherwise exist as stable structure can be formed in the presence of Λ-hyperon.

In this paper we discuss hypernuclei of mass number A = 7 of isotopic spin T = 1. ^{6}He, ^{6}Li* and ^{6}Be are members of T = 1

triplet. The principle of charge symmetry implies the same binding energy for Λ in ${}^{7}_{\Lambda}He$ and ${}^{7}_{\Lambda}Be$ as they are mirror hypernuclei. But the experimental observation gives a broad distribution for the binding energy of Λ in ${}^{7}_{\Lambda}He$. Understanding of this aspect in terms of nuclear levels of ${}^{6}Be$ is discussed in this paper.

ALPHA PARTICLE SCATTERING

M.K. Mehta
Bhabha Atomic Research Centre
Trombay, Bombay.

As is quite obvious from the title, I am going to talk about only one class of nuclear reactions generally classified as the "Alpha Particle Scattering". Like all other subjects these days, there will not be enough time to go into a detailed exposition of this field, but what I hope to do is to bring to your notice the type of work going on and indicate the contribution which it has already made to our knowledge of nuclear phenomena.

What makes an alpha particle different from other light projectiles is the absence of the spin. As I shall indicate later, this absence of spin makes the analysis of scattering experiments much simpler, especially for low bombarding energies.

The comparatively greater mass of the alpha particle brings in larger ℓ values to a compound nucleus. Thus, states with higher spin can be excited in alpha particle scattering than can be done with protons of the same energy. The high coulomb barrier seen by an alpha particle actually works to an advantage in the following manner; In light and medium heavy

nuclei at excitation of about 15 MeV the density of states is expected to be fairly high, and a proton scattering excitation function would show a very large number of peaks making it very difficult to study individual resonances. On the other hand because of the large coulomb barrier for alpha particles, only those states which have large alpha particle widths would show up as resonances in alpha particle scattering, making it possible to study these individually. Again, I shall elaborate on this point a little later.

Another property of the alpha particle, which has made it a useful tool, is the strong absorption by the nuclei, the intraction being confined largely, to the nuclear surface. This has enabled Prof. J.S. Blair to understand and interpret the alpha particle scattering in terms of a rather simple model.

Generally speaking alpha particle scattering experiments can be divided into three catagories. All experiments involve the measurements of excitation functions and angular distributions of elastically and inelastically scattered alpha particles. The classification into three catagories is on the bases of the type of analysis used to bring out the relevant information. It is understandable that the bombarding-energy which I shall from now on refer to as E_α will be an important factor in this consideration. The three regions are:

(a) The resonance Region - (Van-de-Graaff region) up to $E_\alpha = 5.5$ MeV.

(b) The Average-Potential Model Region - (Cyclotron Region) $E_\alpha > 20$ MeV.

(c) The intermediate Region - (Tandem Region) E_α from 5 to 20 MeV.

As in all other classifications there are no sharp boundaries between these regions.

(a) <u>The Resonance Region.</u>

This region is characterized by excitation curves which excibit a few resonances. Individual resonances can be analyzed using the Briet Winger single level dispersion theory. A typical example is the $^{16}O(\alpha\alpha)^{16}O$ experiment done at Columbia in 1960 by Mc-Dermott and others (1). Fig.1 shows the excitation curves they have measured using an ^{16}O gas target in a differentially pumped gas scattering chamber. The differential cross sections are accurate to within 5% measured with resolution between 2 to 5 keV. It is in such cases that the zero spin of the alpha particle has been most useful in the interpretection of the data. To write down the most general expression for the differential cross section for elastic scattering is beyond the scope of this talk. The expression in the simplified form due to the zero channel spin is

$$\left(\frac{d\sigma}{d\Omega}\right)_{cm} = \frac{1}{k^2}\left|-\left(\frac{1}{2}\right) n \csc^2\theta/2 \, e^{in\log\csc^2\theta/2} + \sum_{\ell}(2\ell+1)P_\ell(\theta)\, e^{i\alpha_\ell}\, e^{i\delta_\ell}\sin\delta_\ell\right|^2$$

$$n = \frac{zz'e^2}{\hbar v} \qquad \alpha_\ell = 2(\sigma_\ell - \sigma_0)$$

where k is the wave number, n is the coulomb parameter = $\frac{22'c^2}{\hbar v}$

The δ_ℓ in the above expression is written as $\delta_\ell = \beta_\ell - \phi_\ell$ where ϕ_ℓ is called the 'hard sphere' potential phase shift, and β_ℓ the resonance phase shift. The B.W. single level approximation gives $\beta_\ell = \tan^{-1} \frac{\Gamma_{\lambda\ell}}{2(E_R - E)}$ where $\Gamma_{\lambda\ell}$ is the so called full width at half maximum. Over and above the assumption of an isolated single level, only one channel-the elastic scattering channel, is assumed to be open. These assumptions mean that only one value of ℓ will contribute to the width $\Gamma_{\lambda\ell}$ (λ= channel number). Thus the sum over ℓ in the scattering amplitude reduces to only one term corresponding to the partial wave that excites the resonance. If the data are taken at c.m. angles which correspond to zeros of various Legndre Polynomials, then the resonance which is due to a particular ℓ value will not appear at all at the angle where the Legendre Polynomial of that ℓ order is zero. The first figure has a number of cases where this is classically illustrated. So just the vanishing of a resonance at a particular angle immediately determines the ℓ value for the partial wave that excities that resonance. The spin of the level J = $\ell + s$ where s is the channel spin given by the vector sum of the target and the projectile

spins. This is zero in the present case.

Therefore $J = \ell$ and $\pi = (-1)^{\ell} = (-1)^{J}$ thus knowledge of ℓ immediately gives the spin and parity of the compound nuclear level that produces the resonance. Because $\pi = (\ -\ )^{J}$ only the natural parity levels will be excited in this reaction, i.e. if the parity is conserved in nuclear interaction. To determined the resonance energy E_R, the width Γ_{ℓ} and the reduced width $\gamma_{\lambda\ell}^2 = \frac{A_{\ell}^2}{2k} \cdot \Gamma_{\lambda\ell}$ (where $A_{\ell}^2 = F_{\ell}^2 + G_{\ell}^2$) detailed shape fits to the resonance at the measured angles have to be calculated. The lines drawn through the points in the Fig.1 are actual fits calculated in this manner. One can seee how good they are. These fits are very sensitive to the change in level parameters, and thus determine these parameters uniquely. What I have shown here is almost an ideal case for the resonance region. If we just carry the same experiment to higher E_{α}, the single level and the single channel approximations are stretched to the limit. This is illustrated in the next Fig.2 where the same experiment was carried to E_{α} = 10 MeV, at the Florida State University by my colleague Dr. Hunt and I. The data were taken actually at ten angles, the figure shows 5 of these. Upto E_{α}=10 MeV the single channel approximation is still reasonably valid but as you can see the number of resonances is large. Even then the vanishing of the resonance terms at various angles enabled us to assign spin and parity to a large number of levels by carefull examination

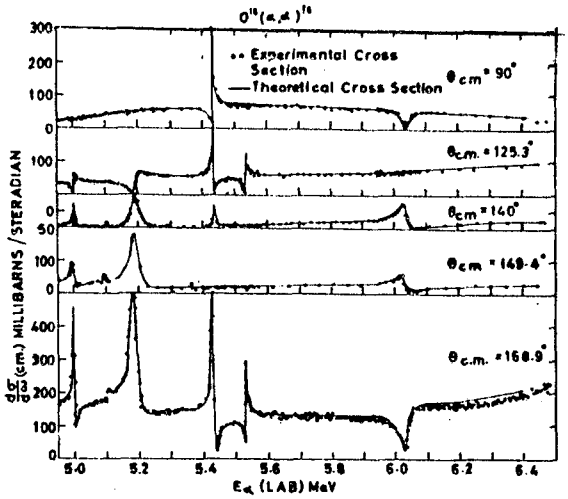

Fig. 1

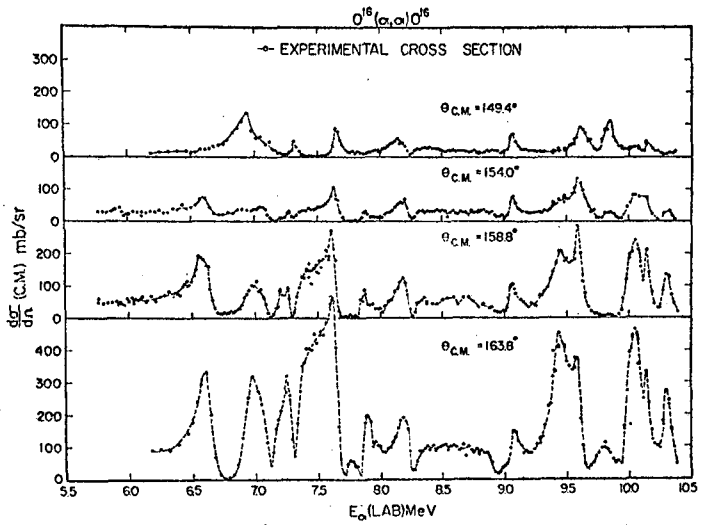

Fig. 2

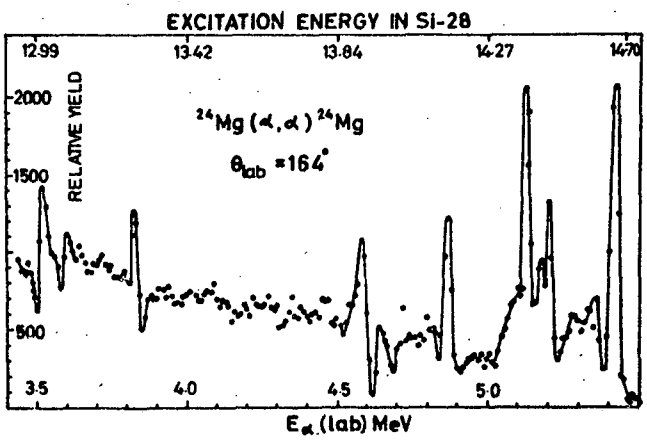

Fig. 3

of the data taken at 10 angles.

If one goes to a slighly heavier nucleus and stays below $E_\alpha = 5.5$ MeV, the situation is again similar. Here the high coulomb barrier seen by the alpha particles works to our advantage. Let me elaborate on this.

The resonance contribution to the differential cross section can be written as

$$\left(\frac{d\sigma}{d\Omega}\right)_{R\ell} \propto \frac{\Gamma_{\lambda\ell}^2}{(E-E_R)+(\frac{1}{2}\Gamma)^2}\left\{P_\ell(\theta)\right\}^2$$

the partial width is $\Gamma_{\lambda\ell}$, Γ being the total width

and $\Gamma_{\lambda\ell} = 2k\,\gamma_{\lambda\ell}^2\,A_\ell^{-2}$ where A_ℓ^{-2} is called the penetrability Γ is the total width of the level.

Now let us take a specific example of $^{24}Mg + \alpha$. The coulomb barrier in this case is about 5.2 MeV. There is a paper by Mr. Kerekatte in the next session which will describe this in more detail. With 5 MeV alphas we go to an excitation of about 13 MeV in the compound nucleus ^{28}Si. We have investigated the same compound nucleus by the $^{27}Al + p$ channel and found that in a range of 1.5 MeV interval there are about 35 peaks in the excitation functions. But when we look at it through the alpha channel the small penetrability A_ℓ^{-2} will

make the Γ_λ small i.e. the resonance contribution due to the level to the differential cross section also will be small as it is proportional to Γ_λ^2. Only those levels for which the reduced widths γ_λ^2 are large, i.e. for those level whose partial alpha widths are large enough to overcome the effect of the coulumb barrier, will show up as resonances. Thus the alpha beam will pick out only these strong levels which will be relatively fewer in number. This again makes the individual resonance analysis possible. I shall show the next Fig.3 to illustrate this point. This Fig. shows the excitation function measured at 90° for the eleastic scattering of alpha particle from ^{24}Mg upto 5.5 MeV E_α. This work was reported at this symposium last year in Bombay (2). The managable number of resonances are now being investigated individually by measuring the excitation curves in their neighbourhood at four angles representing the zeros of the Lyendre Polynomials, I shall show one example of a resonance in the next Fig.4 where we have been able to assign the parity of the level as 4^+ from the vanishing of the anomaly.

(b) <u>The Cyclorton or the Average Potential Region;</u>

What was considered so far was the one extreme of isolated resonances and a single reaction channel. The other exteme would be the one where the excitation energy is so high that we are practically in a continnum, or where the direct reactions predominate.

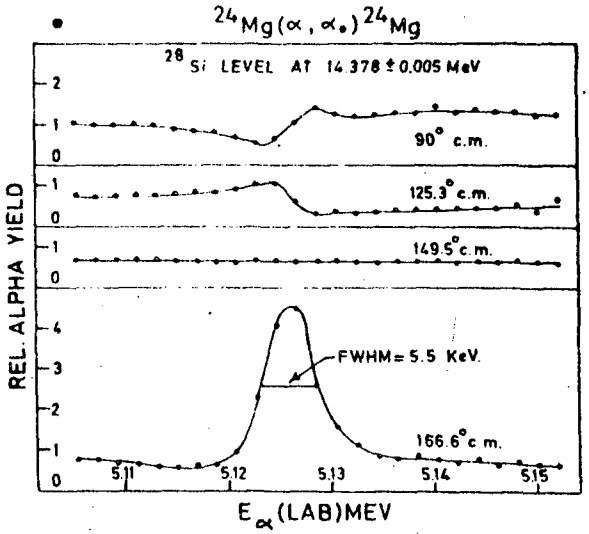

Fig. 4

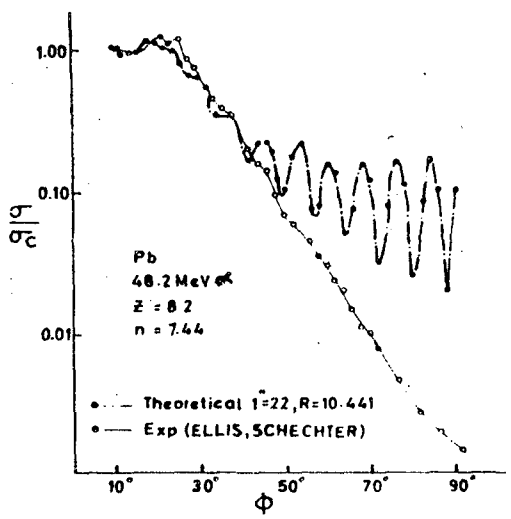

Fig. 5

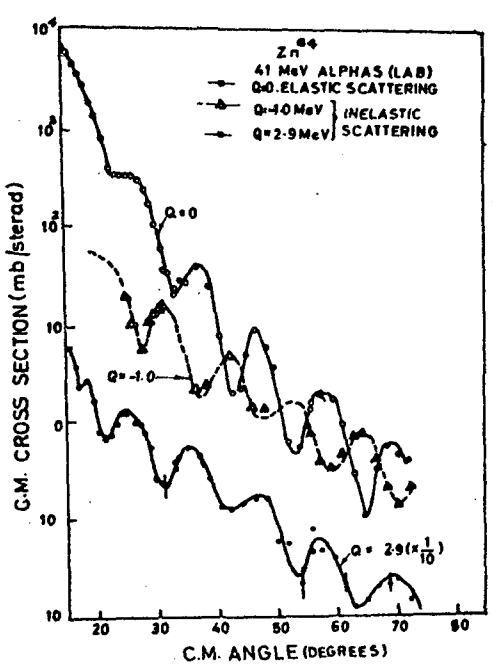

Fig. 6

The data in this region generally consist of angular distributions measured at fixed energies with beams obtained from cyclotrons with the energy spread of the order of 100 keV or more. A number of models are used to fit the data and extract the nuclear information. A good review of the work done upto 1960 in this region has been given by Eisberg and Porter (3). Igo (4) and his cowerkers have used the optical model to interprete the data. A major conclusion they have come to is that the alpha particles are strongly obsorbed at the surface of the nucleus. The work of J.S. Blair (5) and coworkers at the University of Washington in Seattle has been very outstanding in this energy region. Prof. Blair (6) has developed a model which depends on the assumption-based on experimental observation-that alpha particles are strongly absorbed by nuclei. I shall briefly indicate the basic ideas of this model.

Fundamental assumption of this model is that the motion of the alpha particles can be described classically i.e. the alpha particle and the target nucleus can be picutred as spheres with distnict radii. Coupling this with the absorption idea, one can use strightforward Fraunhofer diffraction interpretation and deduce this model. The other way is to do this in terms of the phase shifts. I shall discuss the phase shift approach here. For the above mentioned classical criterion to be valid the necessary condition is that the

reduced wave length $\lambda\!\!\!^{-} = \frac{\hbar}{mv}$ is much smaller than the nuclear demension R. The model is most successfully used for E_α of around 40 MeV and medium and heavy weight nuclei as targets. This makes the ratio $\lambda\!\!\!^{-}/R$ smaller than 1/10.

Blair's first sharp cut off model assumed that those alpha particles which strike a nucleus are totally absorbed and those which miss the nucleus undergo only coulomb scattering. This leads to a condition on the phase shifts for each partial wave.

The elastic scattering differential cross section can be written as

$$\frac{d\sigma(\theta)}{d\Omega} = |f(\theta)|^2$$

$$f(\theta) = (2ik)^{-1} \sum_{l=0}^{\infty} (2l+1)(\eta_l - 1) P_l(\theta)$$

and $\eta_l = 0$ would mean that the partial wave with that particular l value will be totally absorbed. Thus the Blair condition would give

$$\eta_l = 0 \quad \text{for } l \leq l'$$
$$\eta_l = e^{2i\sigma_l} \quad \text{for } l > l'$$

where σ_l is the coulomb phase shifts given by

$$\sigma_l = \arg\Gamma(1+l+in) = \sigma_0 + \sum_{l''=1}^{l} \tan^{-1}\left(\frac{n}{l''}\right)$$

The value l' depends on the interaction radiers R and is given by

$$\hbar l'(l'+1) = 2mR^2\left(E - \frac{zz'e^2}{R}\right)$$

This can be derived from classical Rutherford orbits. This sharp cut off model was able to fit many experimental results for small angles, but introduced violent oscillations at larger angles. The stringent sharp cut off condition was then replaced by a diffused cut off condition (6). With this modification the model was very successful. The modification involves changing the Blair conditions on η_ℓ. Here the η_ℓ is given by

$$\eta_\ell = A_\ell \exp\left[2i\left(\sigma_\ell + \delta_\ell\right)\right]$$

where σ_ℓ is the coulomb phase shift as before, but now a nuclear phase shift is introduced, which is

$$\delta_\ell = \delta_0\left\{1+\exp\left[(\ell-\ell_\delta)/\Delta\ell_\delta\right]\right\}^{-1} \quad \text{and} \quad A_\ell = \left\{1+\exp\left[(\ell_A-\ell)/\Delta\ell_A\right]\right\}^{-1}$$

Thus in place of the only adjustible parameter R of the sharp cut off model, we now have five parameters ℓ_A, $\Delta\ell_A$, $\delta_0 + \ell_\delta$ and $\Delta\ell_\delta$

In Fig.5, one of the sharp cut off fits is shown. The fitting at the forward angle is quite good but the oscillation at more back ward angles are not so prominent in the experiment. Even then the phasing seems to agree with the theory. The Seattle group has carried out this type of analysis over a wide range of A. The fits are quite sensitive to the R values. The radius values they find over a range of A from

^{58}Ni to ^{238}U lie very closely on a straight line when plotted against $A^{1/3}$ The straight line can be expressed very well by (5)

$$R = 1.414\ A^{1/3} + 2.190 \text{ in fermis.}$$

Before I show the smooth cut off fits let me illustrate the situation for the inelastic scattering. Fig.6 shows the typical experimental results. The outstanding features are that the inelastic cross sections are comperable with the elastic cross section and the oscillations are either in phase or out of phase depending on the parity of the excited states. The envelope of the inelastic cross section drops less slowly.

An extenstion of the Blair model to the inelastic scattering with an 'adiabatic' assumption has been very successful in explaining the above features (5). The adiabatic assumption means that the collective parameters are considered frozen during the time of collision so that the inelastic cross section can be calculated from the elastic scattering amplitudes.

In the last five or six years a number of parallel model has been developed for treating the elastic and the inelastic scattering of high energy alphas mainly on the strong absorption theme. Blair and his group at Seattle and Satchlar's group at oak Ridge have been mainly responsible for this. Those treatments effectively consider the scattering as a direct process. The names given to these models are, the damped Fraunhofer diffrection, the distorted wave Born approximation, the Austern-Blair parametorized phase shift, the coupled

channel optical model and such (5). The Seattle group has shown that the first three models essentially give the same results (6), but the Austern-Blair Parameterized phase shift (5,7) treatment is preferable. According to this the amplitude for single excitation from a ground state of spin zero to an excited state of spin I, projection M is

$$f_{IM,00}(\theta) = \frac{1}{2} i (\beta_I R) \sum_{\ell \ell'} i^{\ell-\ell'} (2\ell'+1)^{1/2} \exp[i(\sigma_\ell + \sigma_{\ell'})]$$
$$\times (\ell' I 00 | \ell 0)(\ell' I -M M | \ell 0) \left(\frac{\partial \eta_{\bar{\ell}}}{\partial \ell}\right) Y_{\ell'}^{-M}(\theta, 0)$$

where η_ℓ is the same as mentioned earlier and derivative of η_ℓ is evaluated at $\bar{\ell} = (\ell + \ell')/2$

$\beta_I R$ are the transition amplitudes.

Fig. 7 shows a typical and very successful aplication of this model.

The experiment is the scattering of 48 MeV alpha particles from ^{48}Ca. R.J. Peterson (6) has been able to assign spin, parity and calculate the transition amplitudes for more than ten lowest lying states of ^{48}Ca.

A vigoarous programme of research is going on in this field. Before I go away from this region I would like to mention an off-shoot of this work. The Austern-Blair model gives a definite phase relationship between the elastic and the inelastic differential cross sections. This model is as I mentioned earlier a direct reaction model. A compound

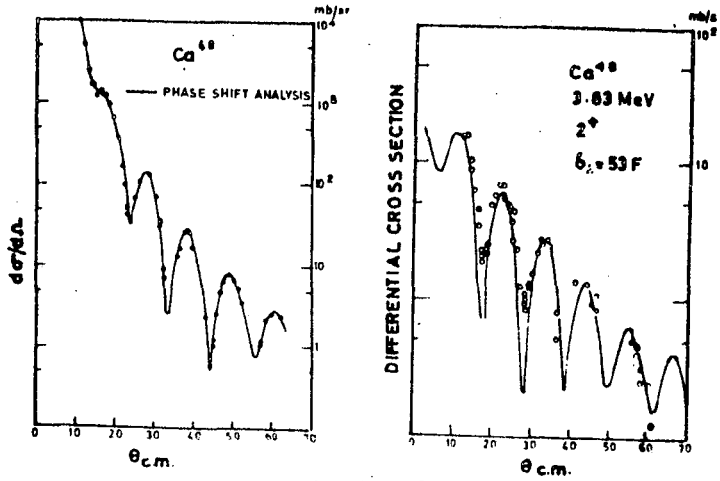

Fig. 7

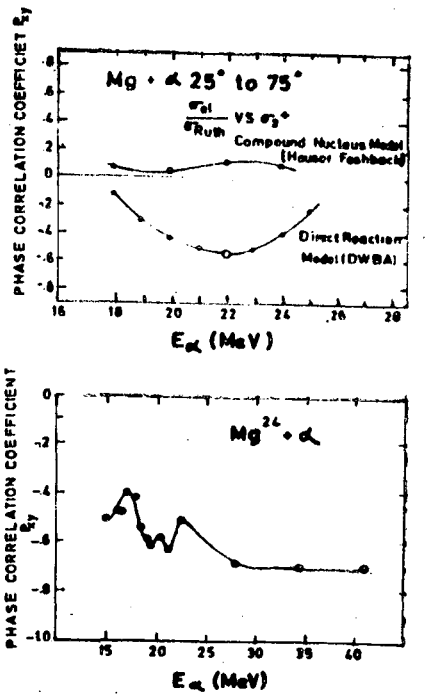

Fig. 8

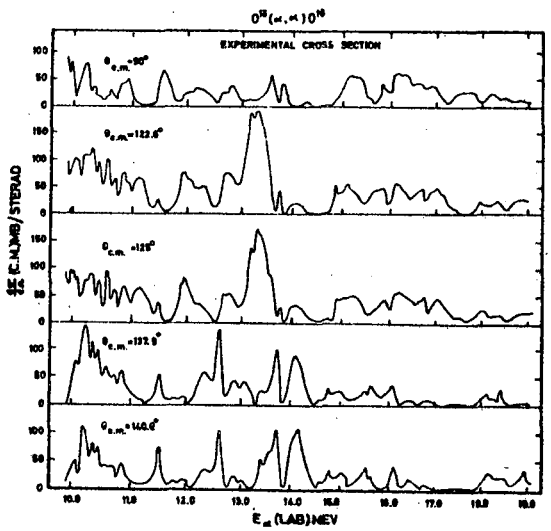

Fig. 9

nuclear model (statistical model) would give a random phase relationship between these two. Based on this concept Braithwaite and others (8), again at Seattle, define what they call the "phase correlation coefficient" between the elastic and the inelastic differential cross section at a fixed energy. Using DWBA methods they calculate the variation in this co-efficient as a function of E_α assuming a hundred percent direct raction. Using Hauser Feshback model they calculate the same thing for a pure CN reaction. Fig.8, shows their calculated and the experimental results for the case of $^{24}Mg(\alpha,\alpha')^{24}Mg$ reaction. The calculated CN coefficient is very small as expected and a pure CN reaction would give values fluctuating about this as an average. The calculated DR value is-ve and much larger in amplitude. The actual experimental case indicates a large-ve co-efficient for $E_\alpha > 20$ MeV which starts fluctuating and decreasing for E_α bellow 20 MeV. One can infer that this is the transition region from CN to DR. Thus such investigations are likely to determine quantitatively the ratio of the contribution from the two reaction mechanisms in the transition region.

(c) <u>The Intermediate Region:</u>

I shall now go over to the third region-the so called "Intermediate Region" which may as well be called the Tandem Region, as this was investigated only after the tandems were developed and precisely variable alpha energies upto 20 MeV were made available. As the name itself implies this is

a region where none of the previous two extremes is fully justified. This is because a large number of reaction channels are open, and possibility of exciting a large number of CN levels ferbids a resonance analysis. The second extreme of excitation to the continnum region or a direct reaction is not fully valid because the excitation curves reveal resonance like structure. Let me illustrate this by showing Fig.9 which again shows work done by Dr. Hunt and I at the Florida State University (9). This is further extension-from 10 to 19 MeV-of the $^{16}O(\alpha\alpha)^{16}O$ work which I showed in a previous Fig. There is distinct resonance behaviour all the way upto E_{α}=19 MeV. Work done with a cyclotron at 18.3 MeV at Indiana (10) previous to our work was left uninterpreted as no optical parameters could be found to fit the angular distribution expecially at the backward angles. This is not surprising in view of the resonance that we discovered around 18.3 MeV which is quite prominent at the backward angles as shown in Fig.10. No amount of either Blair model or optical model juggling could fit the angular distributions measured on prominent resonances. Only when specific resonance terms were added to the smooth cutoff Blair-Model, satisfactory fits were obtained. This is illustrated in Fig.11, where two angular distributions measured on two prominent resonances are shown. The improvement in the fits, specially for the backward angles

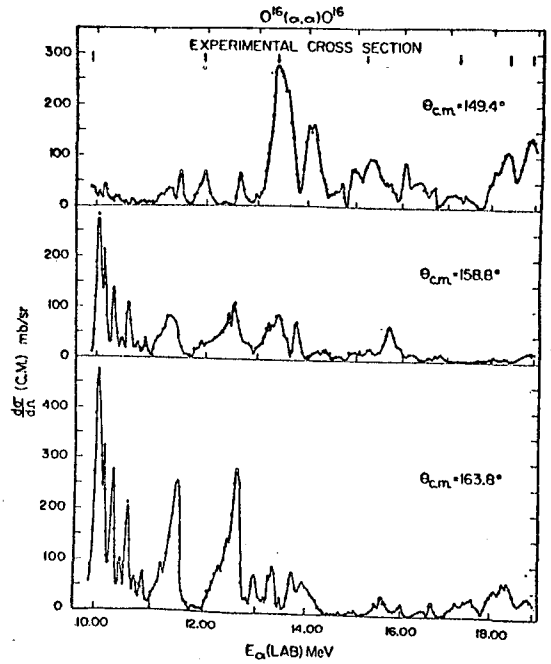

Fig. 10

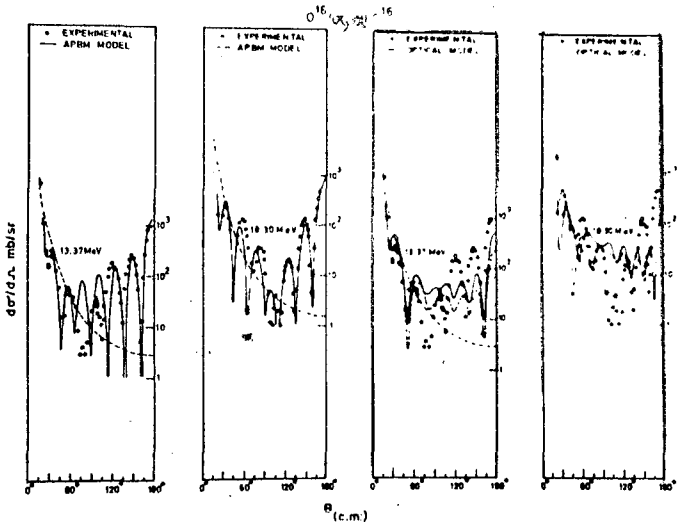

Fig. 11

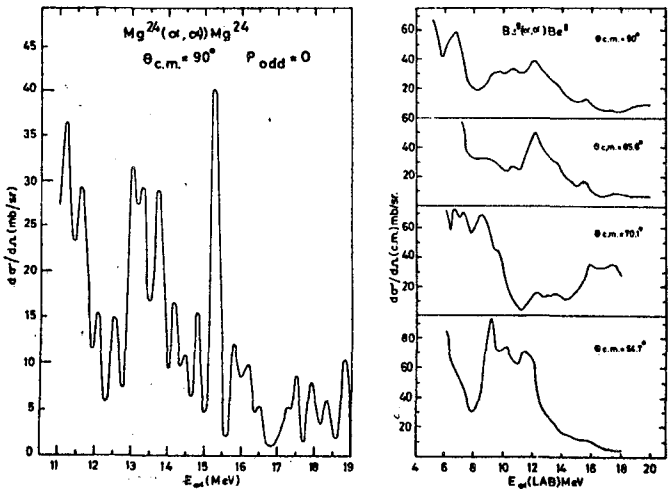

Fig. 12

is very noticable over the optical model fits. A 7^- resonance phase shift for the 13.37 MeV case and a 6^+ resonance phase shift with a small mixture of 7^- and 8^+ neighbouring resonances for the 18.3 MeV case, were required to yield the acceptable fits. Thus again spin parity assignments to such highly excited states are possible with this technique.

On the other hand in case of $^9Be(\alpha,\alpha)^9Be$ and $^{24}Mg(\alpha,\alpha)^{24}Mg$ the Florida State University group working under Prof. R.H. Davis (11) has found a different situation. The excitation curves that they have measured are shown in the next Fig.12, where again resonance like structure is visible but not quite as narrow as in the oxygen case. They found that the angular distributions could be fitted over a wide range of energy by a set of optical parameters which were energy dependent on a relatively simple manner. However to get better fits at backward angles a term coupling the target spin with the incident alpha particle orbital angular momentum ℓ was necessary for the $^9Be + \alpha$ case. This is illustrated in the Fig.13.

Fairly satisfactory optical fits could be obtained for $^{24}Mg + \alpha$ case also even ~~even~~ for angular distributions measured on and off a prominent structure without much change in the optical parameters. This is possible because unlike the ^{16}O case the differential cross section does not rise as high at the most backwards angles. An example of such a fit is also shown in Fig.13.

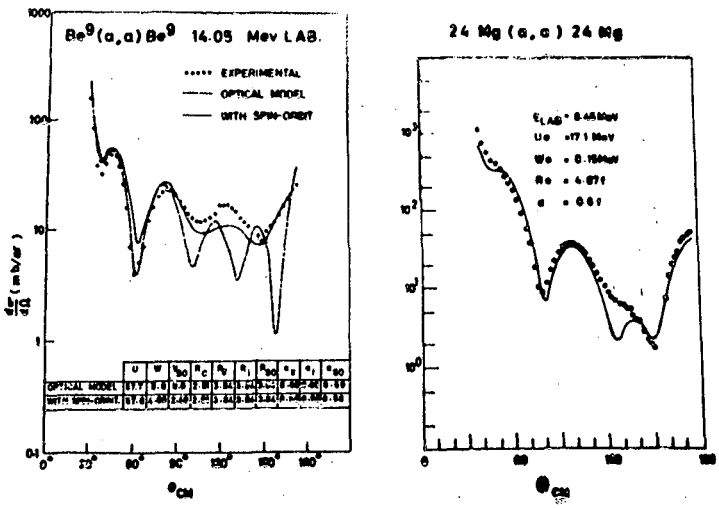
Be9(α,α)Be9 14.05 Mev LAB.
EXPERIMENTAL
OPTICAL MODEL
WITH SPIN-ORBIT
24 Mg (α,α) 24 Mg

Fig. 13

One would expect a large value of W on the strong absorption base, but as the Fig. shows for the ^{24}Mg case a very small W is required for the fit. We shall see the importance of this point shortly.

All the above considerations are for the angular distributions, however, to describe the behaviour of the differential cross section as a function of E_α, one can not get away from the structure observed in the excitation functions. For the oxygen case it can be said with confidence that the structure represents resonances due mostly to individual levels whose spin and parity, can be determined from a resonance plus average potential analysis.

A general expression can be written for such an analysis in the following way (11);

$$f(\theta) = \frac{1}{2ik} \sum_{l} (2l+1) S_l P_l(\cos\theta)$$

where

$$S_l = e^{2i\eta_l} - 1 - i e^{2i\eta_l} \sum_{R} \frac{\Gamma_0}{E - E_R + \frac{1}{2} i\Gamma}$$

here the quantity η is the potential phase shift and could be calculated from the optical potentials or from the smooth cut off Blair Model, Γ is the total width for the level generating the resonance at E_R and Γ_0 is the partial width for reemission into the entrance channel.

However the structure in the $^{24}Mg + \alpha$ case can not be explained by such comparatively narrow levels as no specific resonance terms are required in the angular distribution fits.

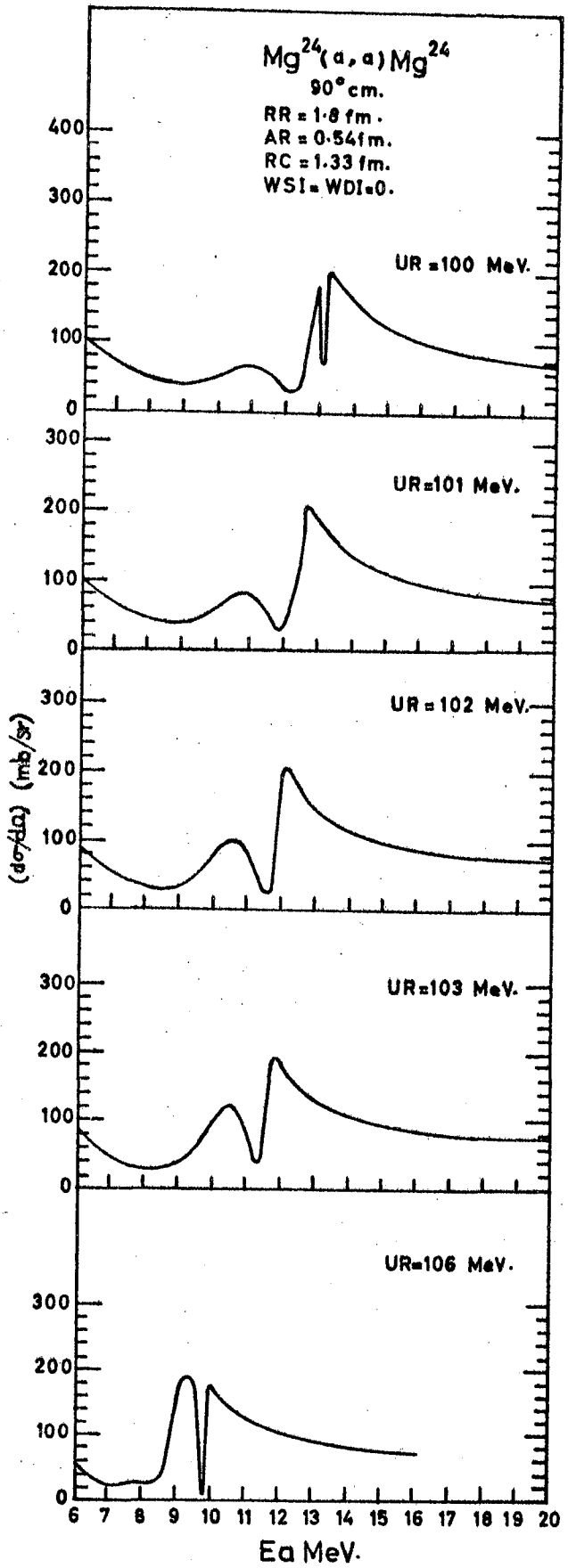
Mg24(α, α)Mg24
90° cm.
RR = 1·8 fm.
AR = 0·54 fm.
RC = 1·33 fm.
WSI = WDI = 0.
UR = 100 MeV.
UR = 101 MeV.
UR = 102 MeV.
UR = 103 MeV.
UR = 106 MeV.
(dσ/dΩ) (mb/sr)
Eα MeV.

Fig. 14

In order to see the type of excitation functions the optical potentials by themselves would generate, the FSU group has carried out extensive calculations with various sets of optical potential determined from angular distributions fits. They found that if a very small value of W-the imaginary potential-is used, the excitation function does show rather gross resonance like structure as shown in Fig.14. However the experimental excitation curves have structure, which is not so gross. These resonances would be due to compound nuclear states which have widths intermediate between the narrow multinuclear excitation levels and the gross-giant-potential resonances. The word "Intermediate States" have been coined for this, and more and more evidence is now forthcoming for the existance of such states. Fashback and his coworkers (12) at MIT have developed a 'Doorway' states idea which represents excitation of "two particle one hole" configurations. However these states need not be restricted to such excitations only. D. Robson at FSU has suggested a model (11) which is based on an extension of the R matrix theory by Lane and Robson (13). In this model the intermediate states modify the optical potentials in the following manner.

$$U = U_o + \alpha^2 \sum_d \frac{E_d - E}{(E_d - E)^2 + W_d^2}$$

$$\text{and } W = W_o + \alpha^2 \sum_d \frac{W_d}{(E_d - E)^2 + W_d^2}$$

where the U_0 and Wo are the constant real and imaginary parts of the wood-saxon potential. The 'doorway' state resonance energies and widths are E_d and W_d. The parameter α^2 couples the single particle-the potential - resonance to the doorway states. Calculation based on this model results in excitation curves shown in Fig.15. In these calculation existance of doorway states of the same widths spaced at constant separation D is assumed. The intermediate width modulation of the potential resonance is quite noticable. So the attempts, though not fully successful, seem to be in the right direction.

Above are a few examples of the experimental information available and methods used to tackle it in this "intermediate" region.

CONCLUDING REMARKS:

I have now covered the subject of alpha particle scattering in a range of E_α from less than one MeV upto 40 MeV. I have also tried to show what, even now, can be done with a small Van de Graaff. It is obvious that with higher energy Tandems and the AVF cyclotrons a large amount of new information will be available which would help us in understanding the reaction mechanism itself and in cases like the Austern-Blair Model, would even give the spectroscopic information about low lying levels. A successful intermediate structure analysis would tell us about the structure of compound nuclei at high excitation energies.

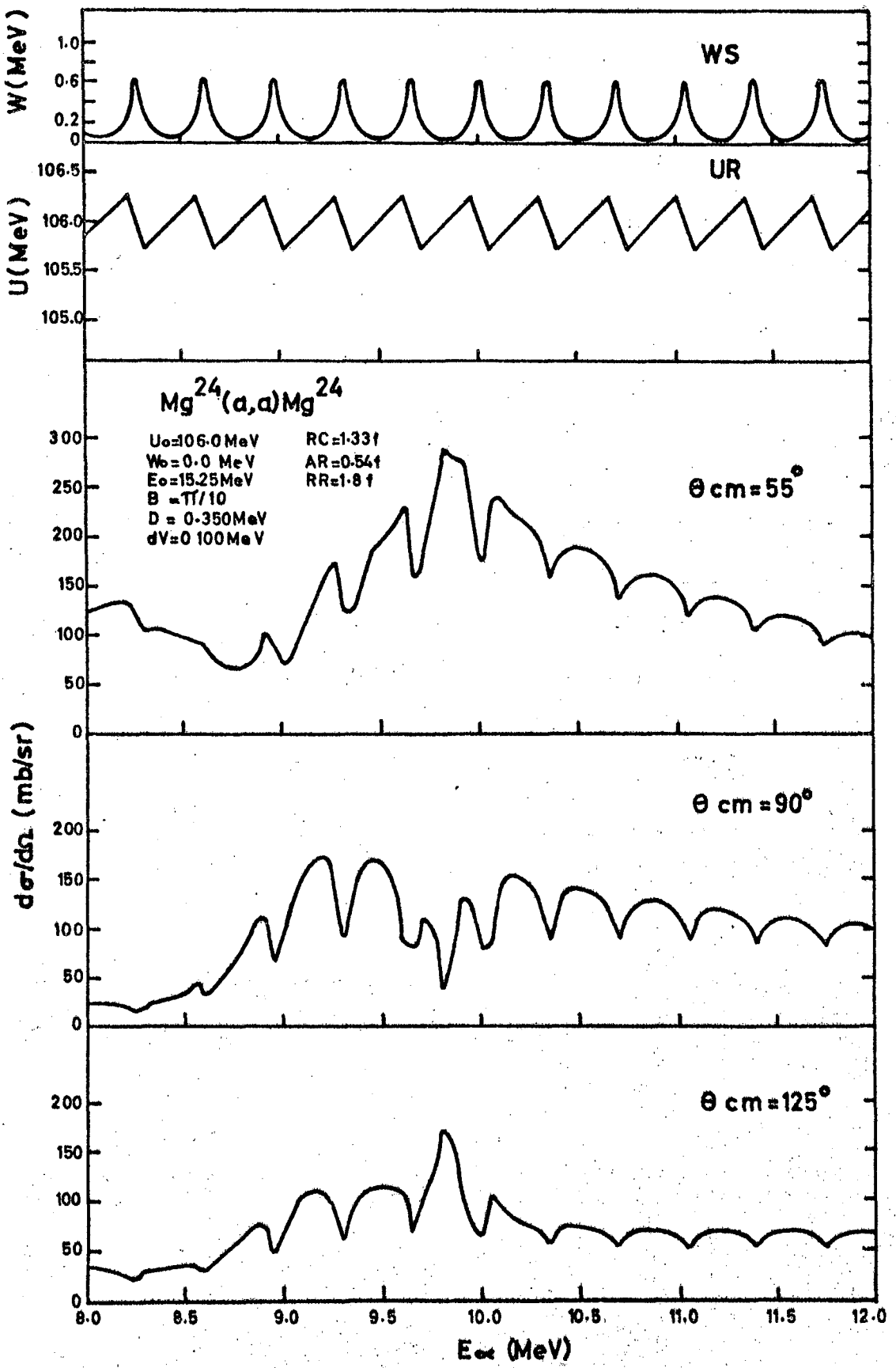
W(MeV)
WS
U(MeV)
UR
Mg24(α,α)Mg24
Uo=106.0 MeV
Wo=0.0 MeV
Eo=15.25MeV
B =π/10
D = 0.350MeV
dV=0.100MeV
RC=1.33f
AR=0.54f
RR=1.8f
θ cm=55°
θ cm=90°
θ cm=125°
dσ/dΩ (mb/sr)
Eα (MeV)

Fig. 15

By choosing a few examples I have tried to indicate the amount of effort being put into these studies and the nuclear information that these efforts have already generated and are likely to generate in future.

Thank you,

REFERENCES:

1. L.C. McDermott, K.W. Jones, H. Smotrich and R.E. Benensar, Phys. Rev. 118, 175 (1960)
2. S.S. Kerekatte, M.K. Mehta, A.S. Divatia and K.K. Sekharan, Proceedings, of the Nuclear Physics and Solid State Physics Symposium Bombay, P.120 (1966)
3. R.M. Eisberg and C.E. Parter, Rev. Modern Phys. 33, 190 (1961)
4. G. Igo and R.M. Thales, Phys. Rev. 106, 126 (1957)
   G. Igo. Phys. Rev. 115, 1665 (1959)
5. J.S. Blair, Lectures on Nuclear Interactions, Herceg-Nove 1962 Vo.II (Federal Nuclear Energy Commission of Ugoslavia, Belgrade 1964)
   J.S. Blair, Lectures on Reaction with strongly Absorbed Particles. (Tata Institute of Fundamental Research, Bombay 1966)
6. R.J. Peterson, Phys. Rev. 140, B1479 (1965)
7. N. Austern and J.S. Blair, Ann. Phys. (N.Y.) 33, 15 (1965)

8. W.J. Braithwaite, J.G. Gramer and R.A. Hinrichs, Annual Report of the Nuclear Physics Laboratory (University of Washinginton, Seattle, June 1966) P.14.

9. M.K. Mehta, W.E. Hunt and R.H. Davis, To be Published in Phys. Rev.

10. J.C. Corelli, E. Blailer, and D.J. Tandem, Phys. Rev. 116, 1184 (1959)

11. R.H. Davis, Proceedings of the Symposium on Recent Progress in Nuclear Physics with Tandems, edited by W. Hering (Max-Plank-Institute for Nuclear Physics, Heidelberg, 1966)

12. H. Feshbach, A.K. Kerman and R.H. Lemmer, Compte Rendus Du Congress International de Physique Nucleaire, Vol II, Paris, France, P.693 (1964)

13. A.M. Lane and D. Robson, (to be published).

DISCUSSION:

P. Mukherjee (Comment):-

I would like to point out that in the case of inelastic scattering, simple Blair analysis is not very helpful for parity determinations and the interference effects are very important.

STUDY OF LEVELS IN ^{28}Si

S.S. Kerekatte, A.S. Divatia, M.K. Mehta,
K.B. Nambiar and K.K. Sekharan
Bhabha Atomic Research Centre, Trombay

Some excited levels in ^{28}Si, lying in the 14 MeV region, have been studied by the technique of elastic scattering of alpha particles by ^{24}Mg. The target was a thin layer of enriched (99.96%) ^{24}Mg oxide, deposited on a thin carbon film. The reaction spectra were recorded, simultaneously, at four angles, using semiconductor surface-barrier detectors. The excitation function was measured in 2 to 5 keV steps, over seven resonances corresponding to excited levels in ^{28}Si at 13.912, 13.963, 14.160, 14.417, 14.378, 14.448 and 14.627 MeV. These resonances were reported by us at last year's symposium (1).

In the scattering of alpha particles by a zero-spin nucleus such as ^{24}Mg, only states having spins and parties 0^+, 1^-, 2^+, 3^-, etc. can be excited in the compound nucleus. The highest energy of the alphas available from the accelerator, being 5.5 MeV, states of spin higher than 5 cannot be excited, due to quantum mechanical considerations. The differential cross-section thus includes sums over partial waves having angular momenta ℓ = 0 to 5 only. Since, each partial wave includes a Legendre polynomial as a factor, angles of observation were selected for which the polynomials vanish. The spectra were recorded at the centre of mass angles 90°, 125.3°, 149.5° and 166.6°. Therefore,

the following conditions are satisfied in this experiment:

1. A $J = 0^+$ resonance ($\ell = 0$ partial wave) will be present at all the four angles with equal intensity, since $P_0(\cos\theta) = 1$ for all θ.

2. All odd spin, parity resonances $J = 1^-, 3^-, 5^-$ ($\ell = 1,3,5$ partial waves) will be absent at $90^\circ_{cm.}$ (since $P_\ell(\cos 90^\circ) = 0$ for odd values of ℓ), but will be present at the other three angles.

3. A $J = 2^+$ resonance ($\ell = 2$ partial wave) will be absent at $125.3^\circ_{c.m.}$ (since $P_2(\cos 125.3^\circ) = 0$), but will be present at the other three angles.

4. A $J = 4^+$ resonance ($\ell = 4$ partial wave) will be absent at $149.5^\circ_{c.m.}$ (since $P_4(\cos 149.5^\circ) = 0$), but will be present at the other three angles.

5. All the resonances (i.e. $J = 0^+, 1^-, 2^+, 3^-, 4^+, 5^-$) will be present at the backward angle $166.6^\circ_{c.m.}$) since, none of the Legendre polynomials with $\ell \leq 5$ vanish at this angle. Also, all these polynomials attain their maximum value as θ approaches 180°, so that even weak resonances show up easily at backward angles.

By taking data at four angles, it was possible to assign spins and parities to some resonances by means of the five conditions above. From the figures, it can be seen that the resonances at the lab. energies of 5.126 and 5.170 MeV, (corresponding

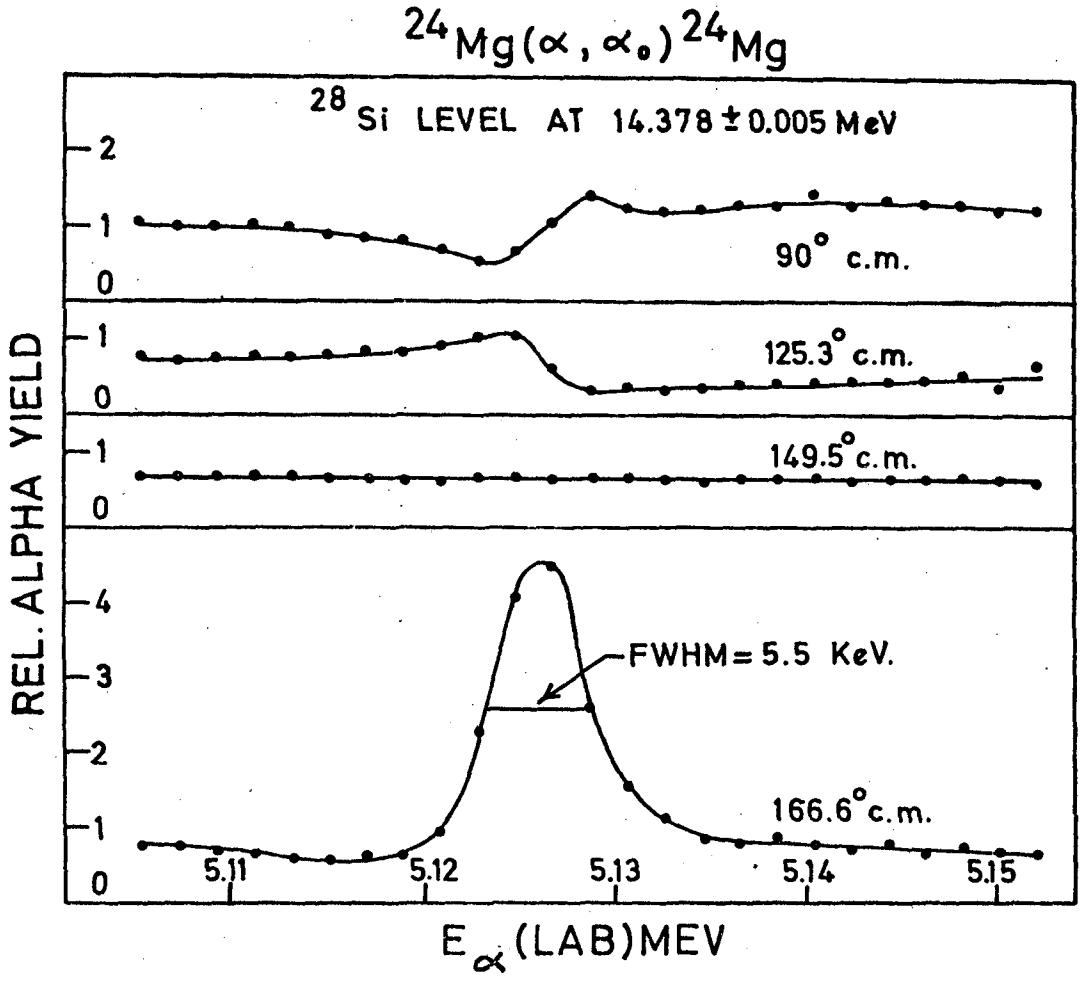
$^{24}Mg(\alpha,\alpha_0)^{24}Mg$
^{28}Si LEVEL AT 14.378 ± 0.005 MeV
90° c.m.
125.3° c.m.
149.5° c.m.
FWHM = 5.5 KeV.
166.6° c.m.
REL. ALPHA YIELD
5.11
5.12
5.13
5.14
5.15
E_α (LAB) MEV

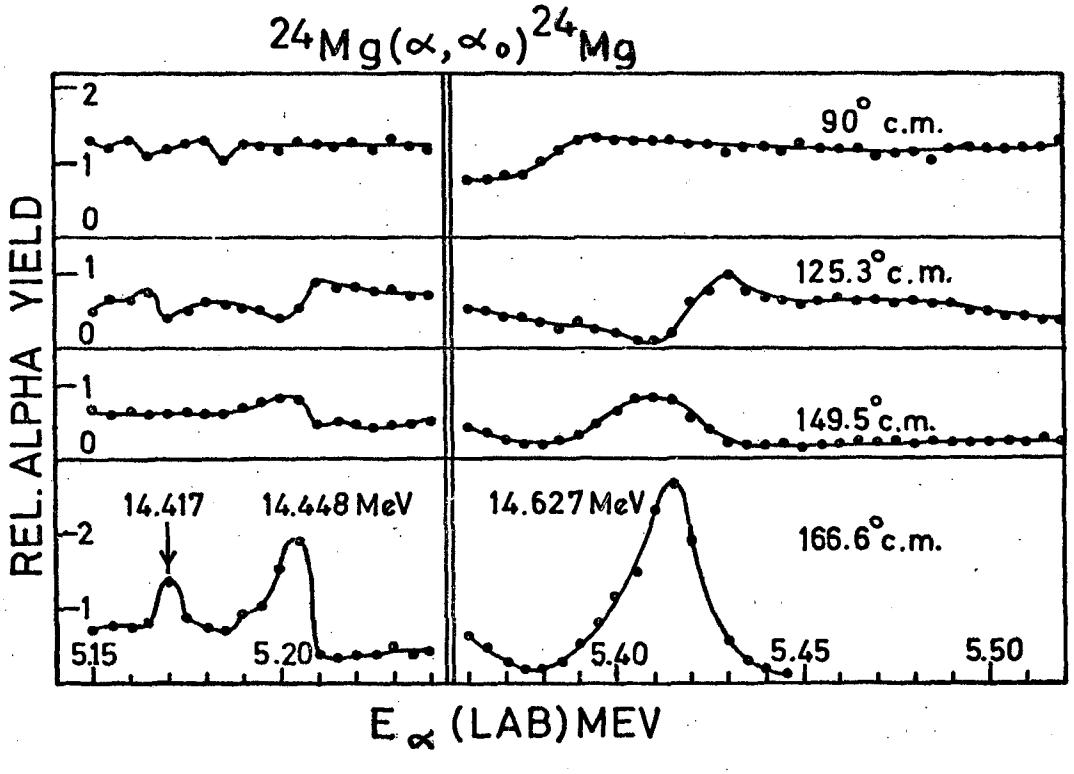
$^{24}Mg(\alpha,\alpha_0)^{24}Mg$
90° c.m.
125.3° c.m.
149.5° c.m.
14.417
14.448 MeV
14.627 MeV
166.6° c.m.
REL. ALPHA YIELD
5.15
5.20
5.40
5.45
5.50
E_α (LAB) MEV

to levels in ^{28}Si at 14.378 and 14.417 MeV), can be assigned a spin and parity of 4^+. Similarly, the resonances at the lab. energies of 5.205 and 5.415 MeV (corresponding to levels in ^{28}Si at 14.448 and 14.627 MeV), can be assigned odd spin and parity. It will be necessary to take data at angles at which P_3 and P_5 are zero, in order to clarify the last two assignments.

Incidentally, the 14.417 MeV resonance has seven data points over the peak whose FWHM = 5.5 keV. If it is assumed that this width is due almost entirely to the target thickness (^{24}Mg layer), it means that the target is less than 5.5 keV thick, which is extremely thin for solid targets in alpha particle scattering work. A shape analysis will be done in order to confirm the spin and parity assignments, and to obtain the resonance parameters.

REFERENCES:

1. S.S. Kerekatte, et al, Proc. Nucl. Phys. & Sol. State Phys. Symp., Bombay, 120 (1966)

THE 6.57 MEV LEVEL IN ^{10}B

K.B. Nambiar, M.K. Mehta S.S. Kerekatte,
K.K. Sekharan and M. Balakrishnan
Bhabha Atomic Research Centre, Trombay

ABSTRACT.

The 6.57 MeV level in ^{10}B is being studied by the elastic scattering of alpha particles from ^{6}Li (1). Since the level appears well isolated from the neighbouring ones, the spin and parity can be determined by the application of the single level resonance theory, though the channel spin 1 involved in the reaction makes the problem rather complicated. Angular distributions were obtained over the corresponding resonance at E_{α}(lab.) = 3.50 MeV, from $\theta_{c.m.} = 50^{\circ}$ to $\theta_{c.m.} = 132^{\circ}$. The excitation curves at four laboratory angles, viz., 43°, 56°, 71° and 84° corresponding to the zeres of the Legendre polynomials P_4, P_3, P_4 and P_2 respectively, where obtained for the energy range E_{α}(lab.) = 3.00 MeV to E_{α}(lab.) = 4.42 MeV. The resonance structure at E_{α}(lab.)=3.11 MeV which was observed by us previously does not appear in any of the four excitations we obtained this time. The shape of the resonance at E_{α}(lab.) = 3.50 MeV is found to change radically with the scattering angle and moreover, the corresponding energy level in ^{10}B is believed to have positive parity and spin (2) between one and three. Therefore a shape fitting analysis of the resonance is being done for determining the spin and parity of the level.

REFERENCES:

1. D.K. Sathe, K.B. Nambiar, A.S. Divatia and M.K. Mehta, Proceedings of the Nuclear Physics and Solid State Physics Symposium, Bombay 123 (1966)

2. P.D. Forsyth, A.R. Kundson and F.C. Young Technical Report 515 (1965)

ANGULAR DISTRIBUTION STUDIES ON $^{56}Fe(p,p'\gamma)$ RADIATIONS *

P.N. Trehan and P.C. Mangal
Panjab University
Physics Department,
Chandigarh-14

The $(p,p'\gamma)$ reaction is a useful means for studying the properties of excited nuclear levels of medium weight nuclei. In particular it is found that the cross section for the exitation of the low lying levels is favourable and, therefore, a measurement of the cross section and angular distribution of the $(p,p'\gamma)$ radiations can yield good information about the character of these states and the character of the gamma radiations associated with them. In case of ^{56}Fe measurement of absolute cross section of various $(p,p'\gamma)$ radiations was done and has been already reported (1). In the present paper a brief discussion of some of the ^{56}Fe $(p,p'\gamma)$ radiation angular distribution studies is made.

The experiment was to measure the yields of the $(p,p'\gamma)$ radiations from ^{56}Fe target for proton bombarding energies ranging from 4.8 MeV to 6.0 MeV. A self-supporting target of ^{56}Fe with 99.7% enrichment and 3.02 mg/cm^2 thickness was kept at 45° with respect to the incident proton beam. A

* This work has been done in collaboration with Dr.D.M. Van Patter of Bartol Research Foundation under the sponsorship of U.S. Air Force Office of Scientific Research and National Bureau of Standards, Washington D.C.

platinum foil was placed immediately behind ^{56}Fe target to ensure complete stopping of the proton beam.

The experimental geometty was the same as reported in the earlier publications (2,3). The $(p,p'\gamma)$ radiations were detected with a 3" x 3" NaI(Tl) detector and recorded with a RIDL-400 channel analyser. A similar 3" x 3" NaI(Tl) detector located at 90° with the incident beam was used as a monitor for the angular distribution measurements. The angular distributions were studied at 0°, 30°, 55° and 90°. In some cases a study was also made at 150° to verify the symmetry of angular distribution about 90°. The γ-ray spectra, taken at various angles, were analysed by usual peeling off method. The photopeak counts of the γ-ray for a given observation angle, thus obtained, after being corrected for the dead time losses of the analyser, were normalized to the observed monitor counts. This procedure eliminates uncertainities in the angular distribution measurements such as due to target nonuniformities. By a computer programme the least square fit of these numbers to the angular distribution function $W(\theta) = 1 + A_2P_2(\cos\theta) + A_4P_4(\cos\theta)$ gave values of A_2 and A_4 together with their root mean square deviations. The values of A_2 and A_4 were corrected for the finite solid angle of the detector using the tables given by Davisson and Gossett (4). No correction has been made for the finite dimensions of the source.

Theoretical angular distribution calculations have been made using Satchler's theory (5) and suitable optical model potential (6). The transmission coefficients for these calculations upto 5.5 MeV for both incident and out going protons were available.

Figure (1) shows the level scheme of ^{56}Fe that was proposed on the basis of $(p,p'\gamma)$ measurements. The assignment of various γ-rays has recently been checked by $(p'-\gamma)$ coincidence measurements(7).

Figure (2) shows the angular distribution of γ-rays from the first two excited states of ^{56}Fe, at $\overline{E}_p$ = 5.395 and 4.733 MeV. There is a fair agreement between the theoretical and experimental angular distribution for 0.845 MeV 2^+ (E2)0^+ and 1.24 MeV 4^+ (E_2) 2^+ transitions. It should be noted that the correction for the cascade feeding has been applied to the theoretical predictions which changes the angular distribution calculated for the direct excitation of the level.

Fig.3 (a) shows the angular distribution for 1.81 MeV γ-ray at $\overline{E}_p$ = 4.733 and 5.395 MeV. The 1.81 MeV γ-ray from 2.658 MeV level has been uniquely identified as $2^+(M_1,E_2)2^+$ by Dagley et al (8) from the gamma-gamma angular correlation measurements in the decay of ^{56}Mn. The present results are compared with the theoretical predictions for a mixing ratio

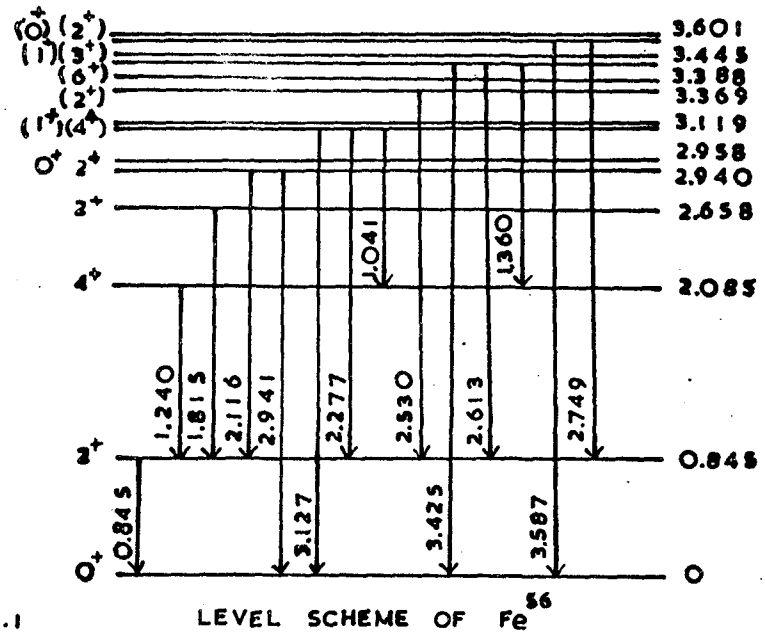

FIG. 1 LEVEL SCHEME OF Fe^{56}

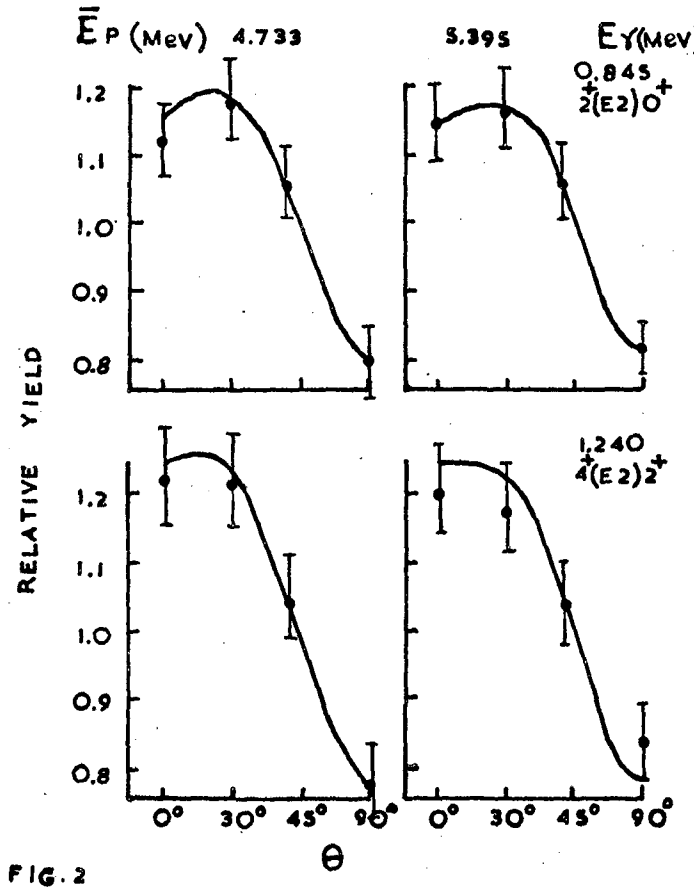

FIG. 2

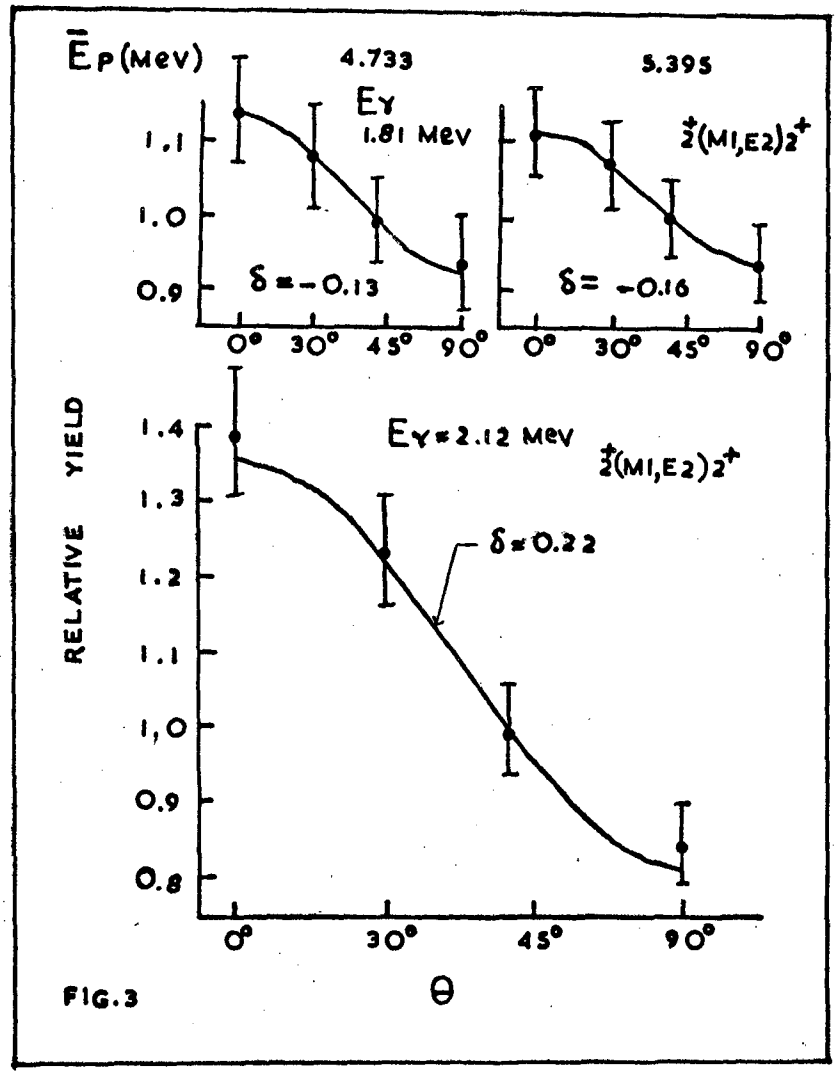
$\bar{E}_p$ (Mev)
4.733
5.395
E_γ
1.81 Mev
$\frac{+}{2}(M1,E2)2^+$
1.1
1.0
0.9
δ = −0.13
δ = −0.16
0°
30°
45°
90°
RELATIVE YIELD
1.4
1.3
1.2
1.1
1.0
0.9
0.8
E_γ = 2.12 Mev
$\frac{+}{2}(M1,E2)2^+$
δ = 0.22
θ

FIG. 3

$\delta = -0.13$ and -0.16 for $\overline{E}_p = 4.733$ and 5.395 MeV respectively. This yields an average value of $\delta = -0.15 \pm 0.04$. This value agrees well with the value of $\delta = 0.15 \pm 0.02$ obtained from radio activity measurements, since the sign of δ for $(p,p'\gamma)$ study should be reversed due to the reversal of the order of $2^+(M_1,E_2)\ 2^+$ mixed transition.

The 2.12 MeV γ-ray is expected to have contributions from the deexcitation of 2.958(2+) and 2.940(0+) MeV level to 0.845(2+) MeV level. The total excitation cross section, obtained experimentally for these two levels, is found to agree very well with the theoretical cross section if we assume the above mentioned spins for these two levels. To obtain the yield of 2.12 MeV γ-ray, only from 2.958 MeV level, we have removed the expected isotropic component of 2.12 MeV γ-ray deexciting 2.940 MeV level and also we have corrected for the 2.96 MeV γ-ray contribution. These corrections have been made on the basis of the ratio of the theoretical cross sections. Fig.3 (b) shows the angular distribution for this γ-ray for $\overline{E}_p = 5.395$ MeV. Taking this transition (8) to the $2^+(M_1,E_2)2^+$ we get the value of mixing ratio $\delta = 0.22 \pm 0.04$ which agrees with the value of $\delta = -0.28 \pm 0.02$ obtained from radio activity measurements.

Table (1) shows the theoretical and experimental values of A_2 and A_4 for various gamma ray transitions discussed so far. This table also shows the spin assignments to various levels obtained on the basis of angular distribution measurements.

The angular distribution of 3.445 and 3.60 MeV gamma rays have also been studied. The comparison of experimental results with theoretical angular distribution favours a spin of 1^+ for one of the members of the doublet at 3.445 MeV and 2^+ for one of the members of the doublet at 3.60 MeV.

Table I.

Angular distribution results for $^{56}Fe(p,p'\gamma)$ reaction, with values of A_2 and A_4 described by $W(\theta)=1+A_2P_2(\cos\theta)+A_4P_4(\cos\theta)$

E MeV	$\bar{E}_p$ MeV	Experimental A_2	Experimental A_4	Theoretical a) A_2	Theoretical a) A_4	Assigned Transitions
0.84	4.733	0.323±0.008	-0.194±0.011	0.309	-0.150	$2^+(E_2)0^+$
	5.395	0.277±0.009	-0.132±0.012	0.280	-0.136	
1.24	4.733	0.360±0.019	-0.134±0.024	0.360	-0.132	$4^+(E_2)2^+$
	5.395	0.278±0.004	-0.082±0.005	0.375	-0.113	
1.81	4.733	0.131±0.034	0.009±0.038	0.124	-0.0008	$2^+(M_1,E_2)2^+$
	5.935	0.120±0.020	-0.008±0.024	0.125	-0.0012	=-0.15±0.04
2.21	5.395	0.362±0.016	0.026±0.027	0.362	-0.0004	$2^+(M_1,E_2)2^+$ =0.22±0.04

a) The theoretical values of A_2 and A_4 listed for $2^+(M_1,E_2)2^+$ transition correspond to the values chosen for the mixing ratio δ.

REFERENCES:

1. Proceedings of the Nuclear Physics and Solic State Physics Symposium 98 (1966)
2. D.M. Van Patter, R. Rikmenspoel and P.N. Trehan Nucl. Phys. 27, 467 (1961)
3. A.K. Sen Gupta and D.M. Van Patter, Nucl. Phys. 50, 17 (1964)
4. C.R. Gossett and C.M. Davisson, Bull. Am. Phys. Soc. 7, 9 (1962).
5. G.R. Satchler, Phys. Rev. 109, 1198 (1956); errata 111, 1747 (1958)
6. R.K. Mohindra and D.M. Van Patter Phys. Rev. 139, B274 (1964)
7. D.M. Van Patter - Private Communication.
8. P. Dagley, M.A. Grace, J.M. Gregory and J.S. Hill, Proc. Roy. Soc. (London) 250, 550 (1959)

DISCUSSION:

M.P. Navalkar: Were the experimental results corrected for efficiency of γ detector?

P.C. Mangal: Yes.

P. Mukherjee: Did you take into account the absence (or presence) of (p,γ) and (p,α) reactions?

P.C. Mangal: At the energies we worked we did not have much trouble from these reactions, as their cross sections were very small.

M.L. Sehgal: Are the spins of the levels known from conversion co-efficient measurements? If so, how do they compare with your values?

P.C. Mangal: Spins of some of the levels have been checked up by internal conversion coefficient measurements. These agree with our results. Our results discussed in this paper for spin agree with some recent ($\alpha, \alpha'\gamma$) measurements.

S.K. Gupta: One can recognise the gamma rays from ($p, p'\gamma$) reaction by varying the proton energy and indentify the gamma rays from inelastic scattering.

P.C. Mangal: The indentification was done in two ways. (1) By varying the E_p of the protons, we could assign the gamma rays to various levels. (2) Also the assignment of the gamma rays was checked using ($p'-\gamma$) coincidence using charge particle semi-conductor detector.

S. Mohan Bharathi: Did you try to measure the relative intensities of the gamma rays? This may give you an idea as to whether the transition probabilities from vibrational levels are enhanced or not?

P.C. Mangal: This has been done and we have some results which are not checked up for the vibrational levels.

K.V.K. Iyengar: You have measured δ-s (i.e) mixing ratios for a particular transition at two different energies. They are different. Should they vary? If so why, particularly when you say you have taken account of all transitions from higher states cascading through it.

P.C. Mangal: The value of δ that we have measured for 1.81 and 2.12 MeV gamma rays are expected to show the same value for different proton energies. There is no problem from higher levels as the levels at 2.958 and 2.6 MeV are not found to be fed from higher levels at the proton energies we have done our experiments.

S.K. Gupta: (i) How do you justify the angular distribution measurement only at four angles for determining the Legendre Polynomial coefficients? Normally the number of points on the angular distribution should be twice the No. of coefficients?
(ii) Have you checked up the isotropy of the geometry and corrected for it?

P.C. Mangal: (i) We wanted to determine A_2 and A_4 coefficients for which we found that measurements at four angles were fairly enough. In some case we ran at five angles and we did not find any difference from the measurement done with four angles.
(ii) We checked up the isotropy of our set up and we found that this was $\leq 3\%$. We did correct for it.

STUDY OF THE 1.94 MeV STATE IN ^{27}Mg BY MEANS OF THE REACTION $^{26}Mg(d,p\gamma)^{27}Mg$

M.A. Eswaran, N.L. Ragoowansi and K.K. Sekharan
Bhabha Atomic Research Centre
Trombay, Bombay.

As a continuation (1) of the studies on the properties of the low-lying excited states in ^{27}Mg the 1.94 MeV third excited state has been studied by proton-gamma ray angular correlation measurements in the reaction $^{26}Mg(d,p\gamma)^{27}Mg$ employing the Litherland and Ferguson (2) method which is independent of any assumption regarding reaction mechanism. The experimental details are described in ref (1). The de-excitation gamma ray spectrum in coincidence with the protons feeding the 1.94 MeV state, detected at 0° to the beam is shown in Fig.1. The angular correlation data, for the combined (0.98 + 0.96) MeV gamma ray peak due to the two transitions 1.94 → 0.98 MeV and 0.98 → 0 MeV, are plotted in Fig.2.

This represents the sum of the following two angular correlations:

(a) Angular correlation of the gamma ray due to the transition 1.94→0.98 MeV in coincidence with the protons feeding the 1.94 MeV state.

(b) Angular correlation of the gamma ray due to the transition 0.98→0 MeV in coincidence with the

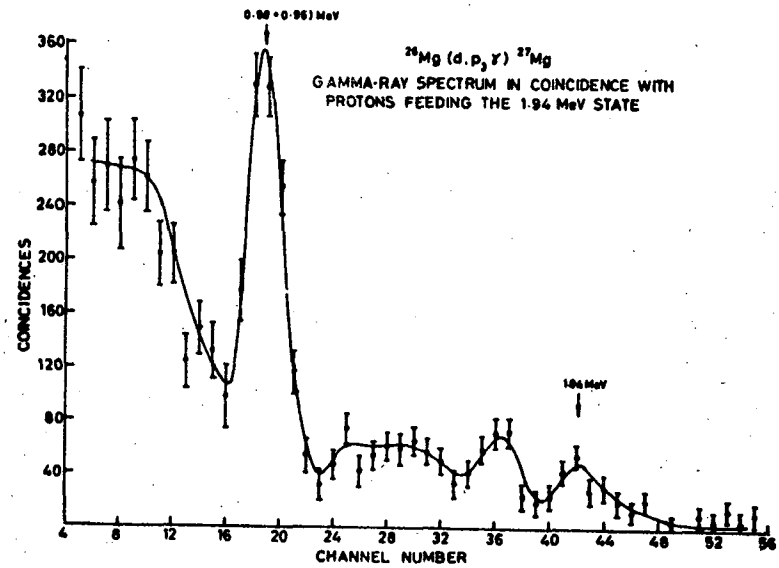
0·98 + 0·96) MeV
^{26}Mg (d, p$_3$ γ) ^{27}Mg
GAMMA-RAY SPECTRUM IN COINCIDENCE WITH
PROTONS FEEDING THE 1·94 MeV STATE
1·94 MeV
CONCIDENCES
CHANNEL NUMBER

FIG-1

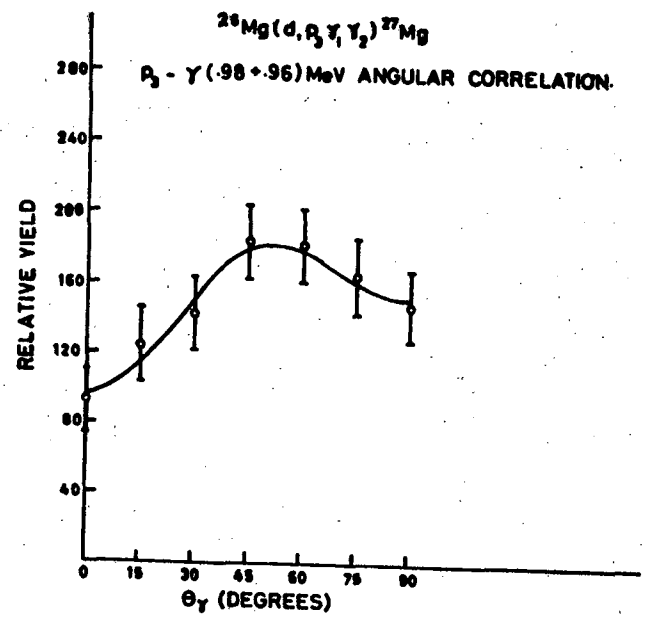
^{26}Mg(d, p$_3$ γ$_1$ γ$_2$) ^{27}Mg
p$_3$ - γ (·98 + ·96) MeV ANGULAR CORRELATION.
RELATIVE YIELD
θ$_γ$ (DEGREES)

FIG-2

protons feeding the 1.94 MeV state with the intermediate gamma ray due to the 1.94 → 0.98 MeV transition unobserved.

The data were analysed by a method (3) similar to the one used for 'method I' of Litherland and Ferguson. The correlation functions for (a) and (b) can be put in the following forms from the expressions quoted in ref (4).

$$W_a(\theta_\gamma) = \sum_{m, L_1, L_1'} P(m)\, \delta_1^{P_1} \sum_K C^0_{K0}(J_1, J_2, L_1, L_1', m) \sqrt{2K+1}\, Q_K P_K(\cos\theta) \quad \text{---(1}$$

and

$$W_b(\theta_\gamma) = \sum_{m L_1 L_1' L_2 L_2'} P(m)\, \delta_1^{P_1} \delta_2^{P_2} \sum_M C^0_{0m}(J_1, J_2, J_3, L_1, L_1', L_2, L_2', m) \sqrt{2M+1}\, Q_M P_M(\cos\theta) \quad \text{--- (2)}$$

where all the quantities are as defined in ref. (4) J_1, J_2 are the spins of the three states 1.94, 0.98 and 0 MeV of ^{27}Mg and δ_1 and δ_2 are the quadrupole to dipole mixing amplitude ratio of the first and second gamma rays due to 1.94 → 0.98 and 0.98 → 0 MeV transitions respectively. P (m) is the population parameter of the magnetic substate 'm' of the 1.94 MeV state of spin J_1. The combination of two angular correlations (a) and (b) is represented by sum of the above two equations (1) and (2) i.e. $W_a(\theta_\gamma) + W_b(\theta_\gamma)$ with the constant term of each of these equations being normalized to unity.

A computer programme was written for the CDC-3600 computer of T.I.F.R. to carry out the analysis of the data which proceeds through a linear least squares fit of the data points using the above equations with magnetic substate population parameters P (m) as the unknowns. The values of

magnetic substates m are limited to 1/2 and 3/2 due to the 0° detection of the protons in the reaction (2). The vector addition coefficients C^0_{Ko} and C^0_{oM} were obtained from the tables of Smith (4). The spins J_2 and J_3 for the states 0.98 and 0 MeV are known to be (1) (5) 3/2 and 1/2. Hence the fit is performed for a fixed spin value J_1 of the 1.94 MeV state, and for fixed values of δ_1 and δ_2. The fit is repeated over the ranges of δ_1 and δ_2 appropriate to the spin value chosen for J_1 with the multipolarities being limited to quadrupole and dipole. In the programme δ_1 and δ_2 are taken as $\tan\tau_1$ and $\tan\tau_2$ where τ_1 and τ_2 are varied from -90° to $+90^\circ$ in steps of 5°. The result of this fitting is a series of χ^2 values for various combinations of δ_1 and δ_2 for each spin choice for J_1. χ^2 is given by

$$\chi^2 = \sum_i [Y(\theta_i) - w(\theta_i)]^2 / \sigma^2(\theta_i) \qquad \text{---(3)}$$

where $\sigma(\theta_i)$ is the uncertainty assigned to the gamma ray yield $Y(\theta_i)$ at angle θ_i due to counting statistics. The minima in χ^2 lead to conclusions about spin assignments. These fits were obtained for choice of 1/2, 3/2, 5/2 and 7/2 for J_1.

This analysis showed that χ^2 values were insensitive to variations in δ_2. Choosing a vlues (6) of 0.176 for δ_2 the χ^2 plots are shown as a function of τ_1 (= arctg. δ_1) in Fig.3 for various spin choices J_1 for the 1.94 MeV state. This analysis shows that spin value of 5/2 can be assigned

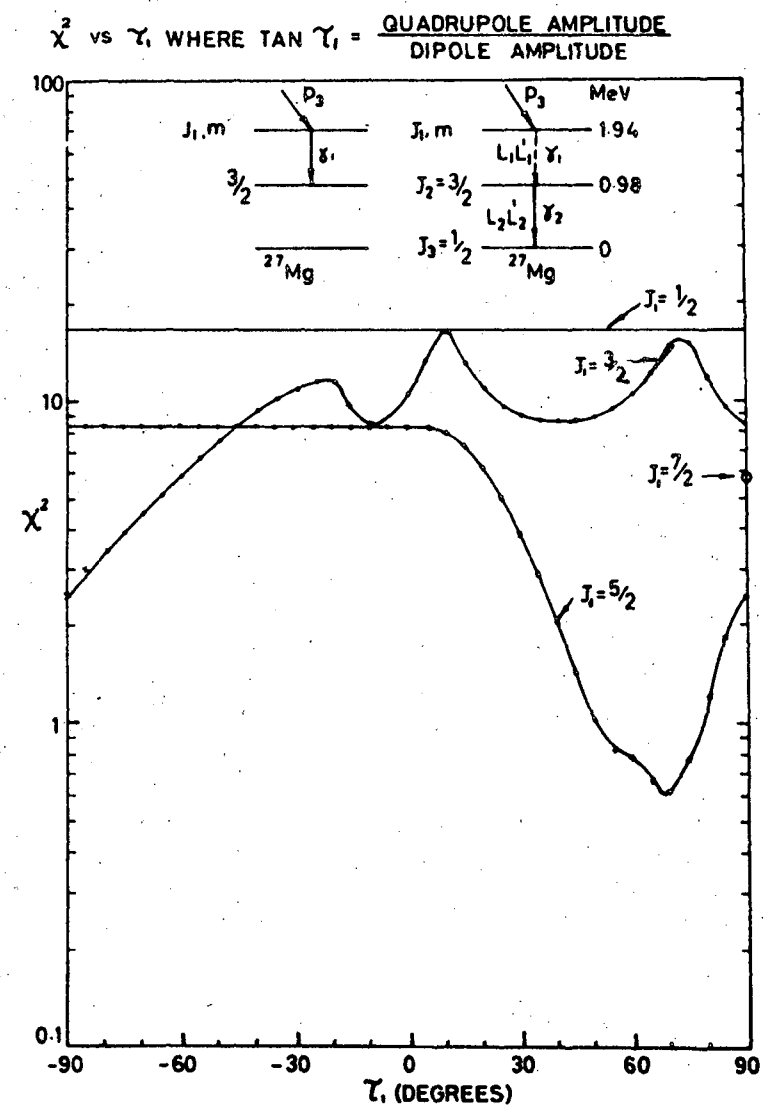
χ² vs τ₁ WHERE TAN τ₁ = QUADRUPOLE AMPLITUDE / DIPOLE AMPLITUDE
100
10
1
0.1
χ²
-90
-60
-30
0
30
60
90
τ₁ (DEGREES)
P₃
J₁, m
γ₁
3/2
²⁷Mg
MeV
1.94
0.98
0
J₂ = 3/2
J₃ = 1/2
L₁L₁'
L₂L₂'
γ₂
J₁ = 1/2
J₁ = 3/2
J₁ = 7/2
J₁ = 5/2

FIG-3

to the 1.94 MeV third excited state. Further measurements are planned to be made to determine conclusively the value of multipole mixing ratio of the gamma ray due to the $1.94 \rightarrow 0.98$ MeV transition. From the coincidence spectrum in Fig.1, the cascade to cross over branching ratio of 1.94 MeV state (i.e) $I(1.94 \rightarrow 0.98)/I(1.94 \rightarrow 0)$ is estimated to be 2.0 ± 0.3.

In conclusion it is observed that the spin sequence and level energies of the states at 0, 0.98 and 1.94 MeV are consistent with the expectation that they form the members of the ground state rotational band.

REFERENCES:

1. M.A. Eswaran, Proc. of N.P. and S.S.P. Symposium, Bombay, 114, (1966); Bull. Am. Phys. Soc. II (3), 406 (1966)
2. A.E. Litherland and A.J. Ferguson, Can. J. Phys. 39, 788 (1961)
3. C. Broude and M.A. Eswaran, Can. J. Phys. 42, 1300 (1964)
4. P.B. Smith in Nuclear Reactions, Vol.II ed. by P.M. Endt and P.B. Smith, North-Holland Pulb. Co. Amsterdam, 248 (1962)
5. P.M. Endt and C. van der Leun, Nuclear Physics, 34, 1 (1962)
6. J.M. Lacambra, D.R. Tilley and N.R. Roberson, Physics Letters, 20, 649 (1966)

DISCUSSION:

M.L. Sehgal: How does the ratio of cascade to the cross-over compare with the Weisskopf estimate?

M.A. Eswaran: Weisskopf estimate will give predominant M1 transition so that cross over E2 transition will be negligible. But the cascade to cross over ratio we observed is 2, as mentioned earlier.

P. Mukherjee: Did somebody determine the spin (and parity) of the 1.94 MeV level by firing the γ and taking the corresponding proton angular distribution?

M.A. Eswaran: No. Recently proton-gamma ray angular correlation measurements have been reported in the literature, by detecting the protons at the angle corresponding to stripping peak and measuring gamma ray angular correlation. Using plane wave analysis, it is reported that spin of 5/2 is preferred for this 1.94 MeV level. This analysis is dependent on assumption regarding the mechanism of the reaction. However, in the experiment reported in the present paper, the analysis is independent of any assumption regarding reaction mechanism.

PROTON-GAMMA RAY ANGULAR CORRELATION MEASUREMENTS IN THE REACTION $^{24}Mg(d,p_3\gamma)^{25}Mg$

M.A. Eswaran, N.L. Ragoowansi and P.C. Mitra,
Bhabha Atomic Research Centre,
Trombay, Bombay.

ABSTRACT.

To obtain direct evidence for the spin of the 1.61 MeV state in ^{25}Mg, the level was excited in the reaction $^{24}Mg(d,p\gamma)^{25}Mg$ using 2.1 MeV deuteron beam and detecting the outgoing protons feeding the state, at 0° to the beam in an ORTEC surface barrier detector, the angular correlation of the subsequent 1.61 MeV de-excitation gamma ray was measured. Measurements were analysed by a computer program based on the Litherland and Ferguson (1) method which is independent of any assumption regarding reaction mechanism. Results can be fitted with a spin choice of 3/2 or 7/2 for the state. Spin value 7/2 for this 1.61 MeV state agrees with the expectation from other evidences. For this spin value the values of quadrupole to dipole mixing amplitude ratio parameter $|\delta|$, for which the data could be fitted are 0.18 and 2.14. The value of 0.18 for $|\delta|$, is consistent with the known lifetime (2) of the 1.61 MeV level.

REFERENCES:

1. A.E. Litherland and A.J. Ferguson. Can. J. Phys. 39, 788 (1961)

2. P.M. Endt and C. van der Leun Nucl. Phys. 34, 1 (1962)

STUDY OF THE ENERGY LEVELS OF ODD MASS ISOTOPES OF In, Ag, Rh, AND Nb BY THE INELASTIC SCATTERING OF PROTONS

V.R. Pandharipande, K.G. Prasad and R.P. Sharma
Tata Institute of Fundamental Research
Colaba, Bombay.

The excited states of odd mass In, Ag, Rh and Nb nuclei are studied from the inelastic scattering of protons of energy 3.5, 4 and 4.5 MeV. These nuclei lie in the near spherical region and have 1, 3, 5 and 9 proton holes respectively near the magic number 50. In this region the excited states are expected to arise due to the coupling of the collective and particle excitations, and the inelastic scattering data is very helpful in the study of their nature. The (p,p') and (d,d') spectra have also been studied earlier (1,2).

The present work mainly concerns with the study of the de-excitation of the above mentioned excited states with the help of high resolution Ge(Li) detector. A suitable arrangement for the use of Ge(Li) detector at liquid air temperature was made and the gamma spectra in each case were recorded by placing the detector assembly behind the target. The gamma spectra obtained by bombarding metallic silver foil with 4 and 4.5 MeV protons are shown in Fig.1. In these spectra the contributions from general background and those from (p,p'γ), (p,n) and (p,γ) reaction were separated. The photopeaks at the energy 504, 695, 845, 1015 and 1365 keV were due to general

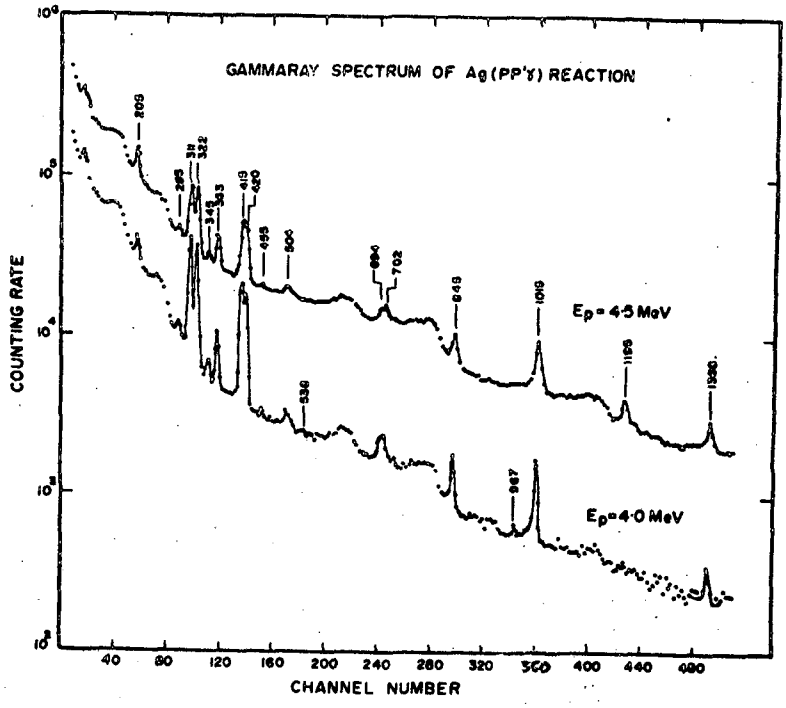
GAMMARAY SPECTRUM OF Ag(PP'γ) REACTION
COUNTING RATE
CHANNEL NUMBER
Ep=4·5 MeV
Ep=4·0 MeV
40
80
120
160
200
240
280
320
360
400
440
480

FIG.1

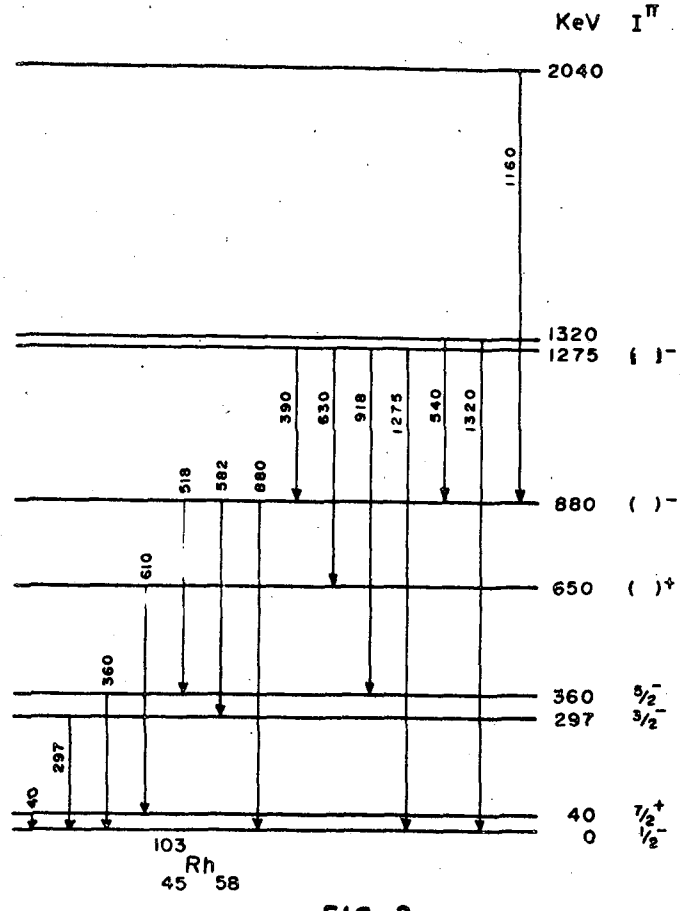
KeV
Iπ
2040
1320
1275
880
650
360
297
40
0
1/2−
7/2+
5/2−
3/2−
1160
390
630
918
1275
540
1320
518
582
880
610
360
297
40
103
45 Rh 58

FIG. 2

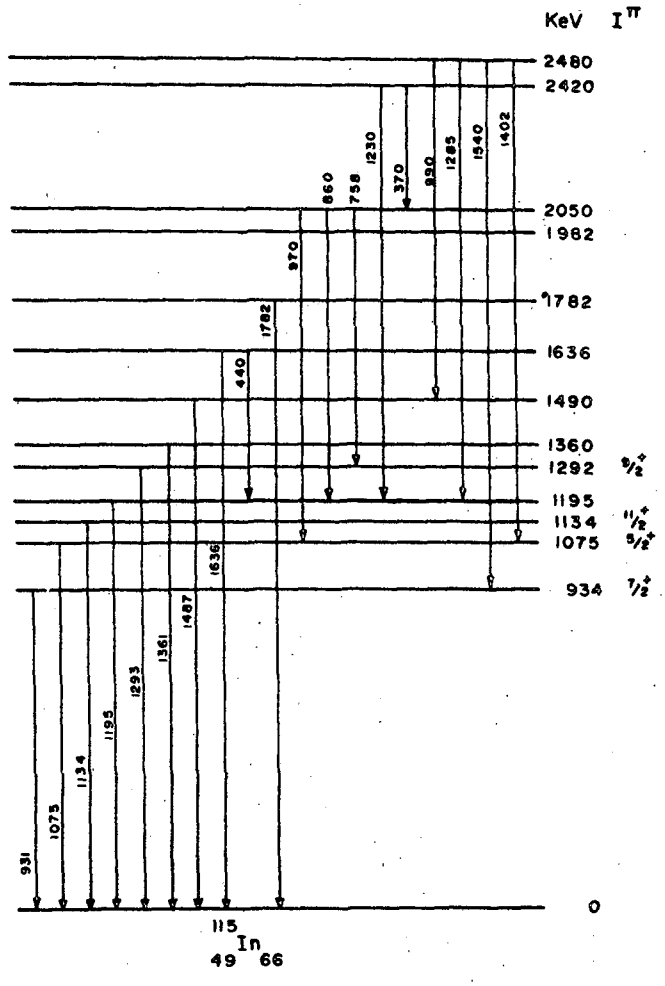
KeV
I^{π}
2480
2420
2050
1982
1782
1636
1490
1360
1292
1195
1134
1075
934
0
$9/2^+$
$11/2^+$
$5/2^+$
$7/2^+$
931
1075
1134
1195
1293
1361
1487
1636
440
1782
970
860
758
1230
370
890
1285
1540
1402
$^{115}_{49}In_{66}$

FIG. 3

background and those at 204 and 285 keV were due to (p,n) reaction. No gamma rays were observed due to (p,γ) reaction. In a similar way other spectra were analysed.

The accurate determination of the energy of the gamma transitions from the above spectra has helped in establishing the decay of the excited states in In, Ag, Rh and Nb nuclei. The energy levels of Rh (spec pure natural Rh containing 100% ^{103}Rh) are shown in Fig.2. The levels at 297 and 360 keV are the well known $3/2^-$ and $5/2^-$ members of the doublet formed due to the coupling of 2^+ state with the odd proton in the $1/2^-$ state. As is evident in the decay scheme (Fig.2), considering the decay and the relative intensity of the gamma transitions the level at 1275 and 880 keV are of negative parity while the 650 keV level appears to be of positive parity.

The excited states in In are shown in Fig.3. Here the levels extend upto 2480 keV. In the energy region 0 $\rightarrow$ 934 keV, the excitations due to inelastic scattering of protons are not observed, because in this region the levels mainly decay to $1/2^-$ isomeric state of In and are predominantly single particle in character. Above 900 keV there is a group of levels which decays to the ground state, while those in the region of 2 MeV decay to these levels. In the former case one expects a multiplet of 5 members

arising due to the coupling of the proton hole in the $9/2^+$ ground state with the first 2^+ state. In the first group of 7 excited states, 5 may be the members of this multiplet, but the nature of the other two is difficult to ascertain.

In a similar way the excited states of Ag and Nb have been studied. In all these cases a group of levels has been observed to decay to the ground state while another group higher in energy decays predominantly to the first group of levels. It may be possible that the higher group of excited states might be arising due to the coupling of second 2^+ state with the odd particle in the ground state. The calculations of the excitation functions will throw some light in this respect. Further work is in progress to clarify this point.

REFERENCES:

1. B.L. Cohen and A.G. Rubin, Phys. Rev. 111, 1568 (1958)
2. B.L. Cohen and R.E. Price, Phys. Rev. 123, 283 (1961)

DISCUSSION:

P. Mukherjee: Can you quote the error in your relative intensity near 1 MeV? What is the background count?

R.P. Sharma: In the high energy region, since the detector is only 2 mm thick the efficiency is small and the statistics is poor, so the error in intensity will be of the order of 10%.

S.S. Kapoor: What was the energy resolution, and did you use any FET preamplifier to improve the resolution?

R.P. Sharma: The resolution was 6 keV FWHM for the 661 keV transition. FET has not been used.

P.N. Tiwari: (1) What is the thickness of the depletion of the detector? (2) How the single escape and double escape peaks were taken into account? (3) But if there are some new levels?

R.P. Sharma: 2 M.M. (2) The single and double escape peak positions can be determined by subtracting 510 and 1020 keV from the observed high energy gamma ray. Most of the gamma rays have been observed in the energy range of ~1 MeV where double escape is not possible and the single escape peaks are not prominent. (3) In case where both the escape peaks are present and they happen to coincide with the gamma rays of that energy then their contribution can be determined by standard monoenergetic gamma ray sources.

K.K. Suri: Assignment of $11/2^+$ spin to the 1135 keV level in In is still controversial. Do your experimental observations confirm the $11/2^+$ spin assignment to this level?

R.P. Sharma: The $11/2^+$ spin assignment has not uniquely been made. It has been done from the earlier angular correlation measurements and by the process of elimination.

N. Nath: Have you seen any effect of neutrons in the Ge(Li) detector arising out of the (p,n) reactions in the target?

R.P. Sharma: Such effect is not observed. Also the cross section for (p,n) is quite small as is seen from the observed intensity of the gamma rays due to this reaction.

COULOMB EXCITATION OF ^{127}I

S.H. Devare, P.N. Tandon and H.G. Devare
Tata Institute of Fundamental Research
Colaba, Bombay.

The level scheme of ^{127}I nucleus is fairly well known from radioactive decay (1,2), and is shown in fig.1. The spins of various levels and the E2/M1 ratios of various gamma transitions arising from different levels have been measured by directional correlation and conversion coefficient measurements respectively (1,3). The mean lives of 58 keV and 203 keV have been measured by delayed coincidence measurements (4) and the mean life of 418 keV level is measured by resonance fluorescence studies (5). The magnetic moments of 58 and 203 keV levels have been measured by employing perturbed correlation technique (6,7). It was therefore thought desirable to observe the Coulomb excitation spectra of this nucleus and get the reduced E2 transition probabilities directly. This type of work was previously carried out by Davis et al (8) using PbI_2 target and scintillation spectrometer. As the level scheme of this nuclide was not known that time, the $B(E2)$ values calculated could contain considerable error. Moreover it is clear from fig.2 that there are various gamma rays too close in energy to be resolved by any NaI(Tl) crystal. We have repeated the same experiment using a proton beam of the 5.5 MeV Van de Graaff

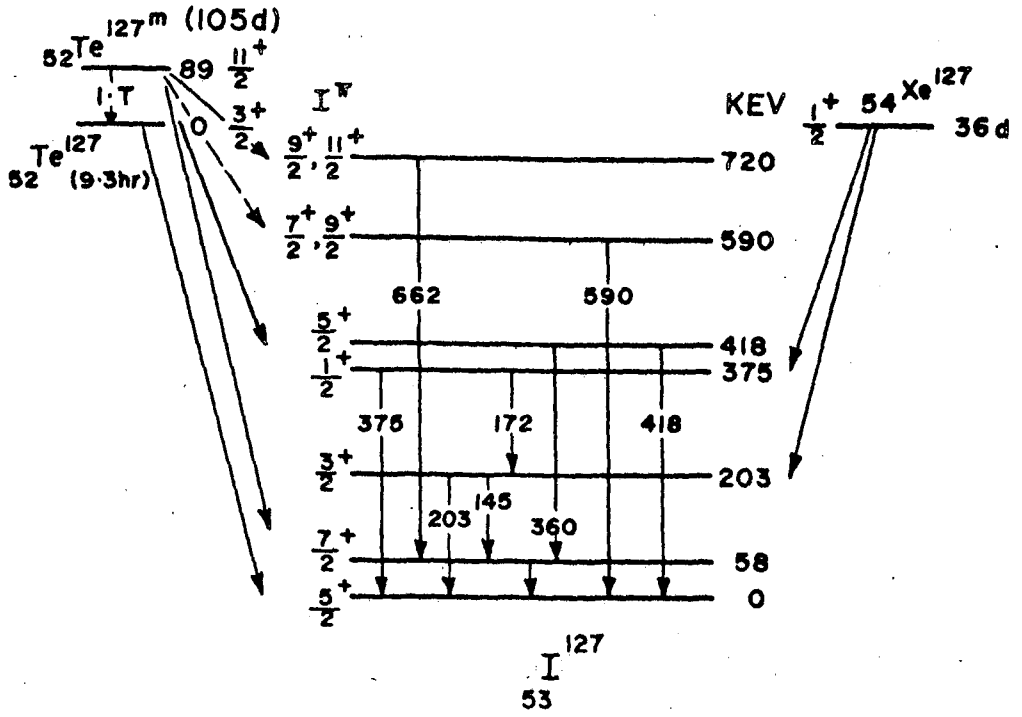
52Te127m (105d)
89 11/2+
I.T
52Te127 (9.3hr)
0 3/2+
I127
KEV
1/2+ 54Xe127
36d
9/2+, 11/2+ 720
7/2+, 9/2+ 590
662
590
5/2+ 418
1/2+ 375
375
172
418
3/2+ 203
203
145
360
7/2+ 58
5/2+ 0
I127
53

FIG. 1

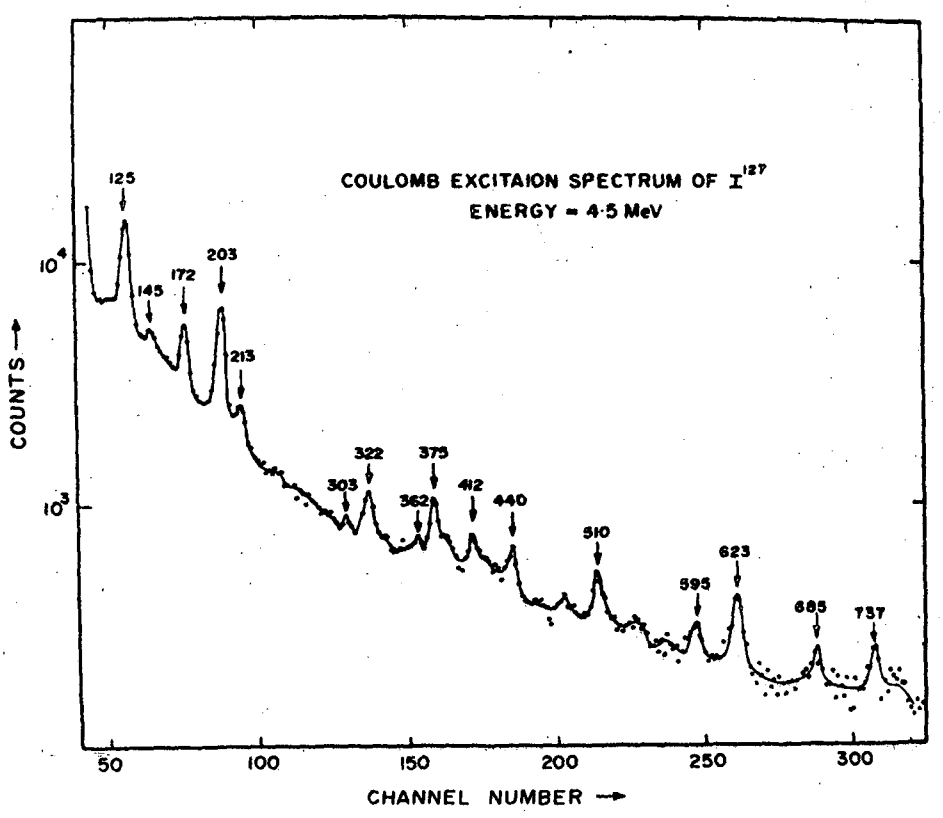
COULOMB EXCITAION SPECTRUM OF I127
ENERGY = 4·5 MeV
COUNTS →
CHANNEL NUMBER →
10^4
10^3
50
100
150
200
250
300
125
145
172
203
213
303
322
362
375
412
440
510
595
623
685
737

FIG. 2

accelerator at Trombay. The spectra were observed by means of a Li - drifted Ge detector having a resolution of ~7 keV. Various proton beam energies ranging from 4 to 5 MeV were utilised in the experiment. The spectrum observed at beam energy 4.5 MeV is shown in Fig.2. The gamma rays of energy 145, 172, 203, 215, 360, 375, 413 and 590 keV are known from radioactive decay. In order to get the yields of various gamma transitions for different beam energies, the photopeak counts after taking into account the background contribution were corrected for absolute photopeak efficiencies of various gamma rays. These were determined independently for our detector by using standard sources of known strength. Thisyield was further corrected for the branching ratios which were already known from the decay scheme measurements. The excitation yield for various levels thus calculated was checked with the theoretical yields at various beam energies assuming E2 excitation. They agree well within errors. Such analysis was carried out for three main levels in ^{127}I i.e. levels 203 keV, 375 keV and 418 keV. From the known yield/incident proton, the reduced E2 transition probabilities $B(E2)_{ex}$ were calculated from the formula given in ref. (9). Then knowing the gamma ray branching from these levels and E2/M1 ratios from various transitions, the mean lives of the levels could be calculated. The results obtained are summarized in table I and compared with experimentally measured

mean lives of various transitions. The agreement seems to be fairly good within the experimental error which would be about 20%. This large error is due to poor statistics in the photopeaks as the targets were very volatile and one had to give very short runs to make sure that the beam is viewing a thick target.

REFERENCES:

1. J.S. Geiger, Phys. Letters 7, 48 (1963) and Phys. Rev. To be published.
2. R.L. Anble and W.H. Kelly, Nuclear Physics 73, 25 (1965)
3. S. Jha and R. Leonard, Phys. Rev. 136, B,1585 (1964)
4. J.S. Geiger and R.L. Graham, Nuclear Physics 89, 81 (1966)
5. H. Langhoff, Nuclear Physics 63, 425 (1964)
6. P.N. Tandon, S.H. Devare and H.G. Devare, Proceedings of the Congres International de Physique Nucléaire, Paris (1964), Part II, Page 56.
7. A.G. Svensson, R.W. Sommerfeldt, L.O. Norlin and P.N. Tandon, Nuclear Physics - To be published.
8. R.H. Davis, A.S. Divatia, D.A. Lind and R.D. Moffat, Phys. Rev. 103, 1801 (1956)
9. K. Alder, A. Bohr, T. Huus, B.R. Mottelson and A. Winther, Rev. Mod. Phys. 28, 432 (1956)

Results of Coulimb Excitation in ^{127}I

Level Energy (keV)	Incident Proton Energy (MeV)	Mean $B(E2)_{ex}$ $10^{-50} e^2 Cm^4$	Mean life τ (sec)	$\frac{B(E2)d}{B(E2)s.p}$
203	4, 4.5, 4.75	3.51	7×10^{-10}*	9.9
375	4, 4.5, 4.75	3.91	3.61×10^{-11}	22
418	4.75	1.92	4.3×10^{-12}**	3.6

* Assuming E2 admixture to be 21% (Ref.1)

** Assuming E2 admixture to be 0.7% (Ref.5)

DISCUSSION:

P. Mukherjee: Did you check by monitoring the elastic proton the stability of your target thickness?

S.H. Devare: No. However, we had kept the target thickness sufficiently large so that the beam was incident on a thick target even though a part of it evaporated. Secondly we kept the target at liquid air temperature to reduce the evaporation rate.

S.K. Gupta: Why did you prefer to look for the gamma rays rather than the protons? The proton detector efficiency may compensate for the thin target?

S.H. Devare: For such measurements we would need a target of thickness 50 $\mu g/cm^2$. We are not sure that such a thin target would last even for a few minutes under proton bombardment. However, the energy lost in the material is quite small and if the backing has good conductivity the target may last long enough. We would try this next time.

GAMMA RAYS FROM $^{55}Mn(p,n\gamma)^{55}Fe$ REACTION

K.V.K. Iyengar, B. Lal and S.K. Gupta
Tata Institute of Fundamental Research,
Colaba, Bombay-5.

There has been considerable interest in the level structure of the $^{55}_{26}Fe$ nucleus and it has been extensively studied (1-8) using different reactions. Until some time ago all the measurements on the levels of ^{55}Fe had established the existence of only two levels below 1 MeV viz. at 0.413 and 0.933 MeV. Ramavataram (9) and also Maxwell and Parkinson (1) were able to give a fairly satisfactory theoretical description of the position and spin of the levels of ^{55}Fe as known till then. Kim (10) found evidence for two additional levels in ^{55}Fe at 0.510 and 0.680 MeV by a study of the neutrons from $^{55}Mn(p,n)^{55}Fe$ reaction. Alevra et al. (11) reported the appearance of a neutron group corresponding to the 0.510 MeV level of ^{55}Fe.

We have carried out a search for the 0.510 and 0.680 MeV levels of ^{55}Fe generated in the $^{55}Mn(p,n)^{55}Fe$ reaction by detecting the gamma-rays from the reaction employing the high resolution available from Ge(Li) detector. The Ge(Li) detector had a FWHM $\approx$8 keV for 662 keV gamma-rays. Manganese metal of high chemical purity evaporated onto thin gold backing was used as the target. The thickness of the target was 700 $\mu g/cm^2$. The 5.5 MV Van de Graaff accelerator at Bhabha Atomic Research Centre, Trombay, was used as the source of

protons. In fig.1 are shown the spectra due to interaction of 2.40 MeV protons with (i) manganese, and (ii) target backing and (iii) due to interaction of 1.43 Mev neutrons from T(p,n) reaction (of about the same energy as that of neutrons to ground state of ^{55}Fe from $^{55}Mn(p,n)^{55}Fe$ reaction at E_p=2.40 MeV). The 0.412, 0.932 and 1.316 MeV gamma-rays are from ^{55}Fe. The 0.510 and 0.680 MeV gamma-rays do not seem to be present in the spectrum due to interaction of protons with Mn to an intensity greater than 5% of that of the 0.413 MeV gamma rays. The origin of the 0.439 MeV gamma rays is not known.

In fig.2 are shown the spectra due to interaction of protons with Mn target at 2.45, 3.00 and 3.50 MeV. The 0.933, 1.322 and 1.413 MeV gamma-rays begin to appear as the prton energy exceeds the thresholds for excitation of the respective levels. Their intensity also increases with proton energy. As would normally be expected in the case when the 0.510 and 0.680 MeV levels are generated in this reaction no prominent peaks at the regions correspomding to 0.510 and 0.680 MeV gamma rays showed up even at the higher proton energies. However, the spectrum in the region of 0.680 MeV gamma-rays is complicated by the presence of the Compton hump of 0.933 MeV gamma-rays and the 0.690 MeV conversion electron line due to inelastic scattering of neutrons from ^{72}Ge in the Ge(Li) detector itself. To eliminate the 0.690 MeV gamma-rays arising from $^{72}Ge(n,n'\gamma)$ and thus to reduce the background in the region of 0.680 MeV gamma-rays, a spectrum was

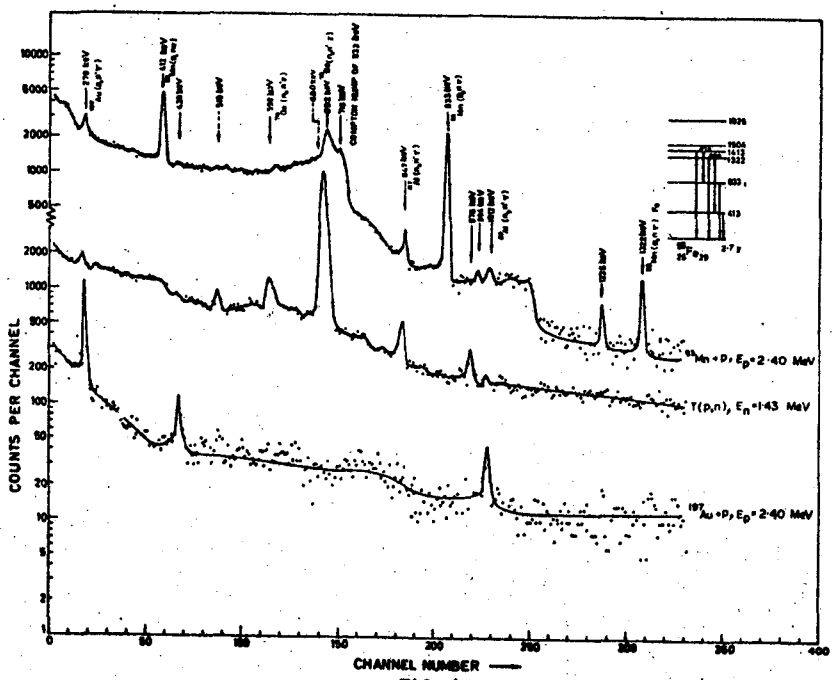
COUNTS PER CHANNEL
CHANNEL NUMBER
^{55}Mn + P, E_p = 2·40 MeV
T(p,n), E_n = 1·43 MeV
^{197}Au + P, E_p = 2·40 MeV

FIG. 1

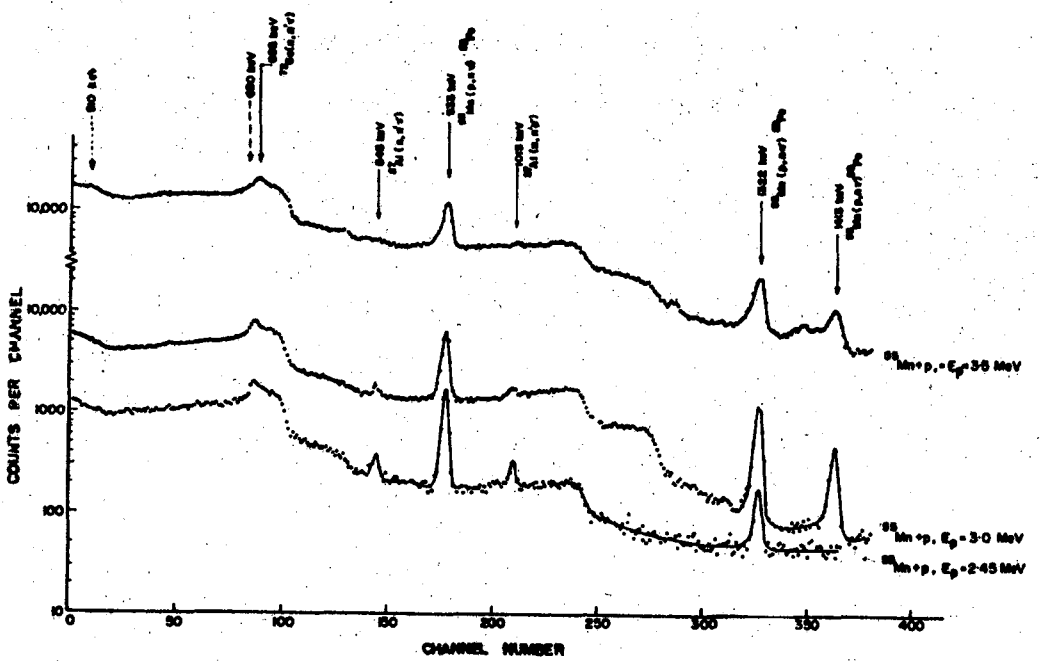
COUNTS PER CHANNEL
CHANNEL NUMBER
^{55}Mn + p, E_p = 3·5 MeV
^{55}Mn + p, E_p = 3·0 MeV
^{55}Mn + p, E_p = 2·45 MeV

FIG. 2

taken with NaI(Tl) scintillator of 7.5 cm x 7.5 cm at E_p=2.40 MeV and is shown in fig.3. No positive evidence for the presence of the 0.680 MeV gamma-ray is avilable from this spectrum either.

The angular distributions of the 0.933, 1.322 and 1.413 MeV gamma-rays from $^{55}Mn(p,n)^{55}Fe$ reaction were measured at E_p = 2.40 and 3.50 MeV using Ge(Li) detector. The full energy peak due to 0.933 MeV gamma-ray produced in the reaction and detected by 7.5 cm x 7.5 cm NaI(Tl) crystal was selected in the single channel analyser for monitoring the yield of the reaction. A stable current integrator was used for measuring the proton flux incident on the target. The measured angular distributions (corrected for losses due to attenuation in the target backing and holder) are presented in fig.4 along with the curves calculated from the statistical theory of Satchler and Sheldon (12-14). Absolute cross-sections were computed from the measured yield by determining the full energy peak efficiency of the Ge(Li) detector by comparing its performance with a NaI(Tl) crystal of known full energy peak efficiency. The measured cross-sections are in better agreement with the theoretical predictions at E_p = 2.40 MeV than at E_p=3.50 MeV. This deviation at higher bombarding energy is felt to be essentially due to the contribution to the intensity of concerned gamma-rays from higher levels by cascade transitions (which have not been taken into account) through the levels responsible for the gamma-rays of interest. On the whole the agreement between the measured and theoretically predicted

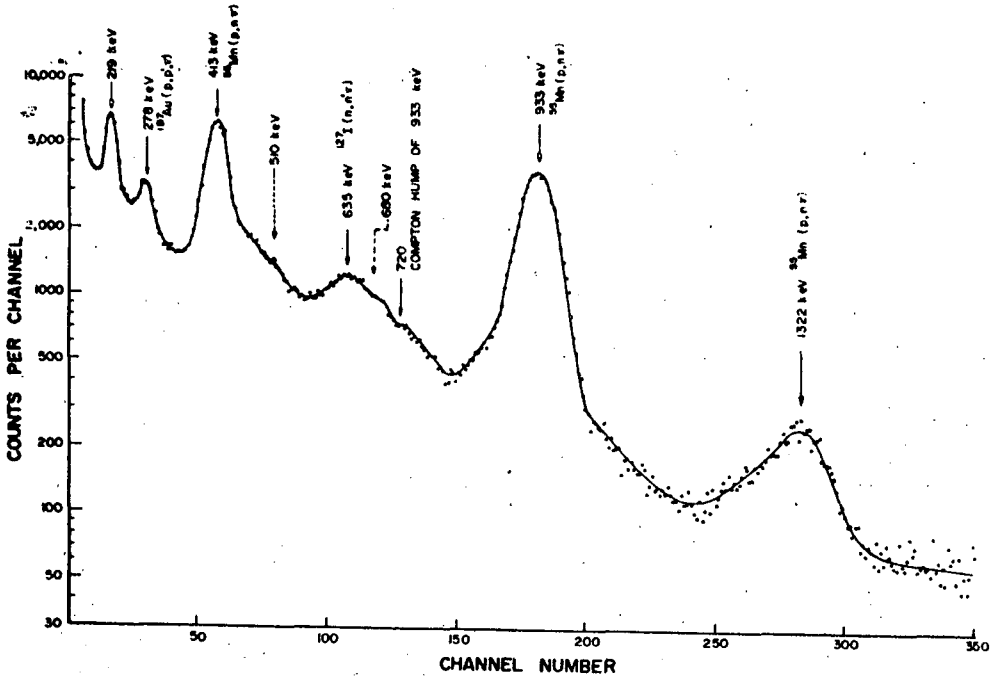
COUNTS PER CHANNEL
CHANNEL NUMBER
279 keV
279 keV
413 keV
50 keV
633 keV
680 keV
720
COMPTON HUMP OF 933 keV
933 keV
1322 keV

FIG. 3

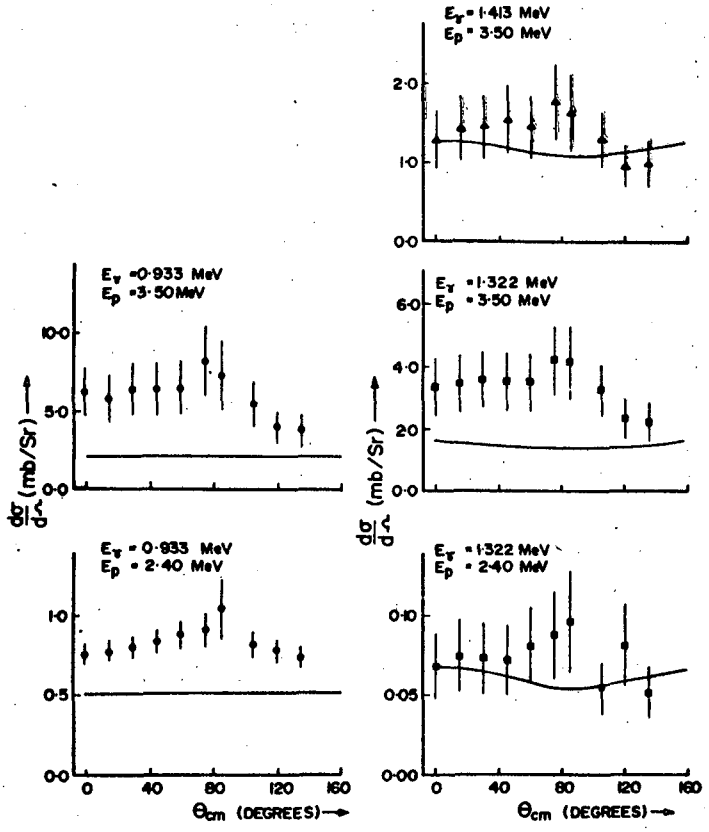
Eγ = 1·413 MeV
Ep = 3·50 MeV
Eγ = 0·933 MeV
Ep = 3·50 MeV
Eγ = 1·322 MeV
Ep = 3·50 MeV
Eγ = 0·933 MeV
Ep = 2·40 MeV
Eγ = 1·322 MeV
Ep = 2·40 MeV
dσ/dΩ (mb/Sr)
θcm (DEGREES)

FIG. 4

angular distributions is quite satisfactory within the limits of errors on the measured cross sections which are $\sim\pm$ 40%. The angular distributions are almost isotropic within the limits of experimental errors. We conclude from these observations that the reaction proceeds through the compound nucleus and that the random phase approximation is valid for the compound nucleus ^{56}Fe at excitation energies of about 13 MeV.

REFERENCES:

1. J.R. Maxwell and Parkinson, Phys. Rev. 135, B82 (1964)
2. R.H. Fulmer and A.L. McCarthy, Phys. Rev. 131, 2133 (1963)
3. A. Sperduto and W.W. Buechner, Phys. Rev. 134, B142 (1964)
4. P.H. Stelson and W.M. Preston, Phys. Rev. 82, 655 (1951)
5. R.A. Chapman and C.L. Stattery, Phys. Rev. 105, 633 (1957)
6. A.J. Elwyn and H.H. Landon, Phys. Rev. 112, 1200 (1958)
7. C.A. Whitten, E. Kashy and J.P. Schiffer, Nuclear Physics 86, 307 (1966)
8. B. Lobkowicz, H. Guhl and P. Marmier, Helv. Phys. Acta. 31, 320 (1958)
9. K. Ramavataram, Phys. Rev. 132, 2255 (1963)
10. H.J. Kim, Phys. Letters 5, 138 (1963).
11. A. Alevra, R. Dumitreschu, I.R. Lukas, .M. Magela, N. Martalogw, D. Plostinaru, E. Trutia, I. Vilcov and N. Vilcov, Rev. Roum. Phys. 10, 593 (1965)

12. E. Sheldon, Revs. Mod. Phys. 35, 795 (1963)

13. E. Sheldon, Phys. Rev. 133, B732 (1964)

14. E. Sheldon and D.M. Van Patter, Revs. Mod. Phys. 38, 143 (1966)

SEARCH FOR THE LEVEL AT 803 keV IN ^{51}Cr

K.V.K. Iyengar, B. Lal, S.K. Gupta and M.D. Deshpande
Tata Institute of Fundamental Research
Colaba, Bombay -5.

ABSTRACT.

A search for the level at 803 keV in ^{51}Cr first observed by Bjerregaard et al (1). in the reaction $^{50}Cr(d,p)^{51}Cr$ was made in the reaction $^{51}V(p,n)^{51}Cr$ by observing the direct gamma rays from the proton bombardment of vanadium with a Ge(Li) detector in the proton energy range 2.31 to 3.10 MeV. The level at 803 keV is expected to be excited at energies higher than E_p = 2.35 MeV as the Q value for this reaction is - 1.534 MeV. The intensity of the 803 keV gamma rays was found to be lesser than 2 per cent of the intensity of the gamma rays from the first excited level at 747 keV in ^{51}Cr at E_p = 2.6 MeV. Also, no variation in the intensity of the 803 keV gamma rays was observed with change in the proton energy. If the 803 keV level is excited in this reaction then the low intensity of the 803 keV gamma-ray has only to be accounted by the decay of the level almost entirely through the 747 keV level. However, the neutron group corresponding to this level in the reaction $^{51}V(p,n)^{51}Cr$ should have been observed by Ferguson (2), (if the level was excited) which is not the case. We therefore conclude that the level at 803 keV is at least not generated in the $^{51}V(p,n)^{51}Cr$ reaction.

REFERENCES:

1. J.H. Bjerregaard, P.F. Dahl, O. Hansen and G. Sidenius, Nuclear Physics 51, 641 (1964)

2. A.T.G. Ferguson and E.B. Paul, Nuclear Physics 12, 426 (1959)

TOTAL AND PARTIAL WIDTHS FOR LEVELS IN ^{17}O

A.S. Divatia, K.K. Sekharan and M.K. Mehta
Bhabha Atomic Research Centre
Trombay, Bombay.

The total cross section for the reaction $^{13}C(\alpha,n)^{16}O$ has been measured earlier (1) in the incident alpha energy range 1.95 - 5.57 MeV, using a 4π neutron detector. By an analysis of the resonances observed the total widths for 16 levels in ^{17}O in the excitation energy region 7.9 to 10.5 MeV have been determined. The partial widths Γ_α and Γ_n along with the corresponding reduced widths γ_α^2 and γ_n^2 for 4 of these levels have also been obtained.

For the wide resonances the total width Γ was obtained directly from the experimental width Γ_{exp} and target thickness T since

$$\Gamma_{exp}^2 = \Gamma^2 + T^2$$

The spread in the incident beam energy was negligible. For the isolated resonances which were narrow compared to the target thickness Richard's leading edge method (2) was used for evaluating the total widths. The total widths evaluated for various resonances are given in Table I. The error in the widths has been estimated for each resonance separately and takes account of the error involved in the procedure for determining the width.

Table I.

Peak total cross sections and total widths of levels in ^{17}O

Resonance energy E_α MeV	Excitation energy in ^{17}O E_x MeV	Peak total cross sections $^{13}C(\alpha,n)^{16}O$ mb	Total level width (C.M.) Γ keV
2.08	7.94	46.4	$79^b \pm 10$
2.25	8.07	75.0	$71^b \pm 8$
2.41	8.19	68.7	$71^b \pm 5$
2.61	8.34	43.6	$9^a \pm 3$
2.68	8.40	45.2	$4^a \pm 3$
2.77	8.47	37.9	$7^a \pm 3$
2.81	8.50	82.0	$5^a \pm 3$
3.07	8.69	52.7	$50^b \pm 3$
3.32	8.89	105.2	$101^b \pm 3$
3.42	8.96	93.1	$21^b \pm 3$
3.65	9.14	6.7	$4^a \pm 3$
3.72	9.19	23.5	$4^a \pm 3$
4.12	9.50	17.3	$8^a \pm 3$
4.42	9.73	75.6	$15^a \pm 3$
(4.49)	(9.78)	--	---
4.62	9.88	67.0	$5^a \pm 3$
(4.77)	(9.99)	(23.2)	----
(4.85)	(10.05)	(22.9)	----
5.04	10.20	113.1	$50^b \pm 3$
5.29	10.39	147.7	----
5.41	10.49	197.4	----

The partial widths of 4 resonances at E_α equal to 2.68, 2.81, 3.72 and 4.62 MeV have been obtained using the relationship of Gove (3),

$$\frac{2\epsilon}{\lambda^2} y(\infty,\infty) = \frac{(2J+1)}{(2I+1)(2i+1)} \sum \frac{\Gamma_\alpha \Gamma_n}{\Gamma}$$

where

ϵ = stopping power of the target in units of energy times cm^2/atom.

λ = centre of mass wave length of the incident particle in centimetre.

$y(\infty,\infty)$ = the step in the thick target yield in units of reactions per incident particle.

J = the total angular momentum of the compound nucleus level.

i,I = the spin angular momentum of the incident and the target nucleus respectively.

Γ, Γ_α, Γ_n = the total width, the partial alpha width and partial neutron width, respectively.

Since the target thickness is substantially greater than the natural width of these levels it is possible to use this expression for evaluating the product of the partial widths Γ_α and Γ_n. Further Γ_α and Γ_n are related, since $\Gamma_\alpha + \Gamma_n = \Gamma$.
Considering the penetrability effect one may assume Γ_n greater than Γ_α. It is then possible to solve for both Γ_α and Γ_n.
In addition the reduced widths and the ratio of the reduced width

to the Wigner limit as a percentage could be calculated from the following expressions

$$\Gamma_s = 2 P_l \gamma_s^2 \qquad (2)$$

$$\theta_s = \frac{100 \gamma_s^2}{3\hbar^2/2 m_s a_s^2} \qquad (3)$$

where P_l is the penetrability factor for the l th partial wave, γ_s^2 is the reduced width of the level for the channel s, θ_s is the reduced width in terms of the Wigner limit expressed as a percentage and m_s and a_s are the reduced mass and channel radius respectively. The reduced widths and reduced widths in terms of the Wigner limit calculated in this way are given in Table II.

It is not possible to make a comparison of the reduced width with theoretical estimate since the excitation energy is very high and theoretical estimates are very difficult to make.

REFERENCES:

1. K.K. Sekharan, A.S. Divatia, M.K. Mehta and S.S. Kerekatte, Proc. Nucl. Phys. and Solid State Phys. Sym., Bombay, 93 (1966)
2. H.T. Richards, in Nuclear Spectroscopy, Part A, edited by F. Ajzenberg-Selove (Academic Press Inc., New York, 1960) chap. I.D., p 123.
3. H.E. Gove, in Nuclear Reactions, edited by P.M. Endt and M. Demeur (Inter Science Publishers, Inc., New York, 1959) Vol I. chap. 6, p.302.

Table II.

The partial widths and reduced widths for levels in ^{17}O

Resonance Energy, E_α	J^a	ℓ_α	Γ_α keV	γ_α^2 keV	ℓ_n	Γ_n keV	γ_n^2 keV	Precentage of Wigner limit θ_α	θ_n
2.68	$5/2^+$	3	0.16	2.3	2	3.84	1.6	0.365	0.058
2.81	$5/2^-$	2	0.43	1.3	3	4.57	5.0	0.206	0.182
3.72	5/2	2	0.14	0.11	3		3.1	0.017	0.113
		3		0.31	2	3.86	1.3	0.049	0.047
4.62	9/2	4	0.30	0.82	5	4.70	100	0.130	3.635
		5		4.57	4		12	0.725	0.436

DISCUSSION:

S.K. Gupta: Have you applied the leading edge method to determine Γ for wider resonances? This will give a further verification of leading edge method.

A.S. Divatia: The leading edge method is well established and we do not need to test the method.

R.K. Tandon: Can we obtain some information about quantum No., spin and parities of the energy levels?

A.S. Divatia: We can obtain information about the widths. To get more information, angular distributions of the neutrons will be required. This is not possible with a 4π neutron counter.

N. Nath: have you considered trying different thicknesses of the target to cross-check on the adequancy and accuracy of the leading edge analysis method?

A.S. Divatia: No. But we have assigned sufficiently large errors to take care of the inaccuracies in the leading edge method.

S.S. Kapoor: In these cases, where the observed width is of the same order as that due to the target thickness, what are the uncertainities in the derived widths?

A.S. Divatia: As you may note from the tables, the error is as high as 3 keV, when the total width is 4 keV.

P. Mukherjee: Did someone measure the $^{16}O(n,\gamma)^{17}O$ reaction?

A.S. Divatia: Some measurements exist, but it is difficult to get an exact overlap with the same excitation energy region. It should be noted that Γ_{rad} is small.

R.S. Kaushal: Why do you not consider Γ_{rad} in the expression of the total observed level width?

A.S. Divatia: Γ_{rad} can be safely assumed to be small here, as compared to Γ_{α} and Γ_{n}.

THE ABSOLUTE CROSS SECTIONS OF (t,p) AND (^{3}He,p) REACTIONS

V.S. Mathur* and J.R. Rook
Nuclear Physics Laboratory, Oxford.

In this paper we wish to present the results of a DWBA calculation for the absolute cross sections of (t,p) reaction on ^{16}O using Ohmura's hard-core wavefunction (1,2) to describe the internal structure of the triton, which is known to reproduce the size as well as the binding energy of this particle. Besides this we also offer an explanation as to why the absolute cross sections of (p, ^{3}He) and (p,t) reactions, leading to analogue isobaric states of the residual nuclei, are equal (3,4) (apart from the momentum and isospin factors) despite considerable difference in the size of these two particles.

In the DWBA, the cross section of the stripping process A(a,b)B is given by (5).

$$\frac{d\sigma}{d\Omega} = \frac{\mu_a \mu_b}{(2\pi\hbar^2)^2} \frac{k_b}{k_a} |M|^2$$

where μ_a and μ_b are the reduced masses of the incident and outgoing particles a and b and $\underline{k_a}$ and $\underline{k_b}$ their momenta. The matrix element M of the process is given by (5)

$$M = J \int d\underline{r_a} \int d\underline{r_b}\, U_b^-(k_b, r_b) \langle B, b | V | A, a \rangle U_a^+(\underline{k_a}\, \underline{r_a})$$

where $\underline{r_a}$ and $\underline{r_b}$ are the relative coordinates of a and b with

---

* Present Address : Department of Physics, Benaras Hindu University, Varanasi - 5.

respect to the target and the residual nuclei respectively, and J is the Jacobian of transformation to these coordinates from the natural coordinates $\underline{r}_{xA}$ and $\underline{r}_{bx}$, x being the particle transferred in the reaction. $\langle B,b|V|A,a\rangle$ is the matrix element of the interaction causing the stripping taken between the internal states of the colliding pairs. To evaluate this matrix element we make two assumption: (1) Within the residual nucleus, the relative motion part of the wavefunction of the transferred particles is a much more slowly varying function of their relative distance than its counterpart when these particles are part of the triton. This simplifies the overlap integral.
(2) The other approximation is the 'zero range' approximation which is usually made in the stripping calculations. This amounts to approximating the $\underline{r}_{bx}$-dependent part of $\langle B,b|V|A,a\rangle$ by a delta function. The justification for this approximation is that the two-body interaction responsible for this rearrangement is short-range one.

This gives finally:

$$\langle B,b|V|A,a\rangle = \sum (s_A \sigma_A j \xi | s_B \sigma_B)(s\sigma l\lambda | j\xi)\, \theta_{s_A s_B}(j s l l_1 l_2)\, g\, \delta(\underline{r}_{bx}) \left[\psi^*_{s,\lambda_1}(\underline{r}_{xA}),\ \psi^*_{l_2\lambda_2}(\underline{r}_{xA})\right]_{l\lambda},$$

where $\theta_{s_A s_B}$ is the two-particle fractional parentage coefficient, $\psi_{l,\lambda_1}(\underline{r}_{xA})$ is the single particle shell model wavefunction of a transferred particle, the bracket implies that the two wave functions inside it are coupled so as to give the angular momentum specified by the subscripts, $j\xi$ is the total angular momentum

transferred in the reaction and the various Clebsch, Gordan coefficients appearing in the formula take account of the angular momentum couplings. On substituting this gives finally, apart from a factor ρ, the formula obtained by Rook and Mitra (6) for the angular distribution of the protons in the (t,p) reaction which they derived considering the triton to be a point particle. The factor ρ^2 with which Rook and Mitra's DWBA results must be multiplied to give the absolute cross section, contains information regarding the triton structure. We calculated this factor using Ohmura's wavefunction

$$\Psi = \prod_{i>j} \left[e^{-\mu(r_{ij}-D)} - e^{-\nu(r_{ij}-D)} \right]$$

with their best values of the parameters and and the two-body force parameters tabulated by them to fit the low energy data. For the optical potentials of the triton and proton we used the parameters derived from the elastic scattering data and used earlier by Glover and Jones(7) to reproduce the angular distribution of the outgoing protons in this reaction. Our results are tabulated in Table I.

We now discuss a comparison between the absolute cross sections of (p,t) and (p,^{3}He) reactions leading to analogue isobaric states. Calculation with a simple Gaussian wavefunction indicates that the cross sections would differ considerably even if the rms charge radii of the triton and ^{3}He were slightly

different. Experimentally the rms charge radius of ^{3}He is appreciably larger than that of the triton and yet, according to the experiments of Cerny and Pehl (3) and Detraz et al (4) with 43.7 MeV protons, the absolute cross sections of (p,^{3}He) and (p,t) reactions on ^{16}O and ^{9}Be leading to analogue isobaric states of ^{14}O(gs,0^+, T=1) and ^{14}N*(2.31 MeV, 0^+, T = 1) respectively in the first case and ^{7}Be* (10.79 MeV, T = $\frac{3}{2}$) and ^{7}Li(11.13 MeV, T = $\frac{3}{2}$) respectively in the second case, are nearly identical apart from the well known momentum and isospin factors. We have tried to explain this in terms of the mixed symmetric wavefunction

$$\Psi = \phi_0 u + (\phi_1 v_2 - \phi_2 v_1)$$

suggested by Schiff (8) to explain the difference in the electromagentic form factors of ^{3}H and ^{3}He and subsequently used by Davey and Valk (12) to explain their size difference. We have shown that if the two-body interaction is spin dependent and isospin conserving, then we obtain using the mixed symmetric wavefunction

$$g(^3H) = g(^3He) = \frac{1}{2}\int \left(3V'(r_{12}) + V^0(r_{12})\right)(u - v_1)\, d\tau$$

where V' is the spin triplet potential and V^0 is the spin singlet potential.

The quantititive calculations, using the mixed symmetric wavefunction with a hard-core, are in progress.

Table I.

Calculated and experimental values

Hard core radius r_D (fm)	Binding energy of ^3H (MeV)	E_c (MeV)	rms charge radius (fm)	$(\sigma_{int})_{E1}$ (MeV.mb)	$(\sigma_{-1})_{E1}$ (mb)	g^2 (MeV^2.fm^6)	Maximum cross section (mb sr)
0.00	10.26	0.936	1.59	RI a):62.4 S b):54.0	1.80	19.3 10^6	20.0
0.20	8.81	0.835	1.67	RI :64.8 S :55.5	2.06	31.4 10^6	32.5
0.40	7.52	0.746	1.74	RI :67.0 S : 56.9	2.29	54.4 10^6	52.2
0.60	5.79	0.636	1.81	RI : 69.7 S : 58.6	2.52	89.8 10^6	93.1
Experimental values (c)	8.49	0.764	1.68±0.17	62± 6	2.53±0.19		25±3

a) RI: Rosenberg-Inglis mixture of exchange forces.

b) S : Serber mixture of exchange forces.

c) Refs (9,10,11)

REFERENCES:

1. T. Kikuta (Ohmura), M. Morita and M. Yamada, Prog. Theor. Phys. 15, 222 (1956)
2. T. Ohmura, Prog. Theor. Phys. 22, 34 (1959)
3. J. Cerny and R.H. Pehl, Phys. Rev. Lett. 12, 619 (1964)
4. C. Detraz, J. Cerny and R.H. Pehl. Phys. Rev. Lett. 14, 708 (1965)
5. G.R. Satchler, Nuclear Physics 55, 1 (1964)
6. J.R. Rook and D. Mitra, Nuclear Physics 51, 96 (1964)
7. R.N. Glover and A. D.W. Jones, Physics Lett. 18, 165 (1965)
8. L.I. Schiff, Phys. Rev. 133B, 803 (1964)
9. H. Collard et al, Phys. Rev. Lett. 11, 132 (1963)
10. R. Middleton and D.J. Pullen, Nuclear Physics, 51, 63 (1964)
11. V.N. Fesitov, A.N. Gorbunov and A.T. Vanfalomeav, Nuclear Physics 71, 305 (1965)
12. P.O. Davey and H.S. Valk, Phys. Letters, 7, 335 (1963)

PERTURBED ANGULAR CORRELATIONS

H.G. Devare
Tata Institute of Fundamental Research
Colaba, Bombay.

In this talk, I shall try to give an overall picture of perturbed angular correlations (PAC). This subject has been attracting considerable attention in recent years and quite interesting work is being done in this field. Though detailed theoretical treatment of PAC was available as early as 1953 (1), experimental work could make progress only during the last ten years or so. By 1963, there was so much activity in this field that an international conference on this subject was held at Uppsala. Since then many new techniques have been introduced for the study of PAC and, what is more important, the scope of their application has been considerably widened. Thus the next international conference on this subject to be held this year in Asilomar, California, includes also nuclear orientation and Mossbauer effect. A review of the work in this field prior to 1963 is available in the proceedings of the Uppsala conference (2) and I wish to devote the present talk mainly to the more recent work. However, for the sake of completeness, I shall briefly indicate the various perturbation mechanisms and their effect on angular correlations.

In the case of a gamma ray cascade, detection of the first gamma ray in a particular direction causes an unequal m substate population with respect to this direction in the intermediate level. The second gamma ray then has, in general, an unisotropic distribution given by

$$W(\theta) = 1 + A_2 P_2 (\cos \theta) + A_4 P_4 (\cos \theta)$$

in most cases. The angular correlation coefficients A_2 and A_4 depend only on nuclear properties like spins of the states involved and multipolarity of the gamma rays. The experimentally determined values of A_2 and A_4 can be used to get information about the nuclear properties provided the angular correlation is not perturbed. Any change in the m state population during the lifetime of the intermediate state gives rise to a perturbation of the angular correlation. The interaction of the nuclear electromagnetic moments with extra-nuclear fields causes transitions between the m substates and is responsible for PAC. Thus, PAC provide us a tool for the study of this interaction. Measurement of the electromagnetic moments of shortlived nuclear excited states is also possible using PAC techniques. These techniques have shown in recent years considerable promise as a probe for the study of the hyperfine and crystal fields.

We need to consider only the interactions of the magnetic dipole moment μ and electric quadrupole moment Q with external magnetic field and electric field gradient respectively. The interaction can be considered static if the direction and

intensity of the field remains constant for a time which is long compared to the lifetime of the intermediate state. Otherwise, we get a time dependent interaction. A static magnetic field H acting on a magnetic dipole moment μ removes the degeneracy of the m states and the energy difference between adjacent states in $\Delta E_m = gH\mu_N = \hbar\omega_L$ where g is the ratio μ/I for the intermedate state, μ_N is nuclear magneton and ω_L is the Larmor frequency. Classically, the nucleus precesses about the field direction with the frequency ω_L. The quadrupole moment will interact with an electric field gradient which can be denoted by Vzz in the case of a symmetric field gradient and the energies of m states in this case are,

$$E_m = \frac{3m^2 - I(I+1)}{4I(2I-1)} eQV_{zz}$$

The energy differences between adjacent states are not constant here and +m and -m states have the same energy. Thus quadrupole interaction gives rise to many precession frequenceis and both clockwise and anticlockwise precessions are present. As a measure of the strength of the quadrupole interaction, we would use the lowest precession frequency given by $\omega_e^0 = \frac{3}{4I(2I-1)}\frac{eQ}{\hbar}V_{zz}$ for integer I and $\omega_e^0 = \frac{3}{2I(2I-1)}\frac{eQ}{\hbar}V_{zz}$ for half integer I. It is convenient to consider the perturbing effects in terms of the precession frequencies ω_L and ω_e^0.

This page is missing

distribution with a width σ about a mean value $\overline{\omega_\ell^\circ}$. The attenuation coefficients have been calculated (5) taking into account this effect, for various values of the parameter $\delta = \sigma / \overline{\omega_\ell^\circ}$. A typical example of such studies is the differential measurement for a polycrystalline ^{181}Hf source, by Sommerfeldt et al (6) who get a good fit for the observed time dependence of the anisotropy with a proper choice of δ and the asymmetry parameter η. Once one gets the strength of the hyperfine interaction from such studies one can find the quadrupole moment of the excited state if the components of the crystal field are known. In general it may be more instructive to calculate the crystal field gradients using a value for the quadrupole moment of the excited state derived from some nuclear model.

Let us now consider the time dependent perturbations. Magnetic interactions of this type are due to the hyperfine fields which change their direction at random because of the change in the orientation of the electron spin caused by the spin-lattice interaction. Time dependent quadrupole interactions can arise in liquids because of the instantaneous field gradients due to the various configurations of the ions surrounding the nuclei emitting the gamma rays. Such configurations last, on the average for a time τ_c the correlation time, and keep on changing because of the random motion of the ions. Abragam and Pound (1) have treated this problem

considering each such configuration to produce a small perturbation. They show that the attenuation coefficients have the form $G_k(t) = e^{-\lambda_k t}$ and the integrated coefficients, $G_k = 1/1+\lambda_k \tau_N$ The λ_k depends on the average strength of the interaction and the correlation time τ_c or the relaxation time τ_s for magnetic interactions. Such an exponential attenuation of anisotropy has been observed by differential angular correlation measurements in several cases. Recently, Dillenburg and Maris (7) have suggested that there is also a possibility that the perturbation in the time dependent case may be the result of only a few interactions each producing a large effect. In such a case the first order theory used by Abragam and Pound is not applicable. From a more general treatment of the problem, they conclude that $G_k(t) = \sum_i \epsilon_{ki} e^{-\lambda_i t}$ where ϵ_{ki} are normalized to unity and the number of coefficients $\lambda_i = I$ or $I - \frac{1}{2}$. Some work has been reported (8) to support this theory but the evidence cannot be considered to be conclusive. It should be noted that even though perturbations may be present in liquids they are usually very small compared to solid sources as the correlation time τ_c is very small $\sim 10^{-11}$ sec. for dilute liquids. Even in solid sources, perturbations are more or less absent in cubic lattices.

It is sometimes possible to reduce the perturbations by means of a decoupling magnetic field in the direction of one

of the detectors. In the case of attenuations due to static hyperfine coupling, the decoupling field causes the magnetic moment of the electron shell to precess round it. One then gets the nuclear analogue of the Paschen Back effect with the I-J coupling completely broken and the perturbation is removed. Usually, J is coupled to the lattice or the liquid environment and for such case larger decoupling fields are required. However, if the crystal fields of the solid cause the hyperfine coupling to be anisotropic, it is not possible to remove the perturbation with a decoupling field. In the case of static quadrupole interaction it is possible to reduce the perturbation provided the decoupling field produces a precession frequency $\omega_L \gg \omega_Q^0$. The attenuations in liquid sources caused by time-dependent quadrupole interactions cannot be removed by decoupling fields.

The biggest contribution of the PAC techniques has been to the measurement of the magentic moments of excited states. One studies the PAC in an external magnetic field perpendicular to the plane of detectors. Using the differential method, very good accuracy can be achieved for such measurements. Moreover, with this technique, one determines ω_L directly and one need not know the angular correlation coefficients, effects of interfering cascades, attenuation or even the half life of the excited state. However, such differential measurements are possible only in a few cases where the intermediate

state has a sufficiently long lifetime $\gtrsim$ 5 ns. If this method has to be used for very long half lives of about a few m sec, limitations are set by the following factors: (1) one must have a time to amplitude convertor which is linear over a very wide range and has a good time resolution (2) one has to use a very weak source to keep the chance coincidence rate low as one uses very large resolving times (3) one has to select a proper environment for the source so that perturbations do not wipe off the angular correlation for several half lives of the intermediate state. The method of digital analysis of PAC (9) gets over the first limitation by direct digitization of the delay between the two gamma rays at 1 C H_z digitizing rate and storing on magnetic tape. A computer analysis of the Fourier transform of the time spectrum gives the resonance frequency quite accurately.

In a majority of the cases the intermediate state has a small half life so that only the integral method can be used. Here, the shift $\omega_L \tau$ is measured either by studying the whole angular correlation in the magnetic field or indirectly by observing the change in the coincidence counting rate at a suitable angle by reversing the field. One has, of course, to find the angular correlation coefficients in the same geometry, correct for interfering cascades and know the half life of the intermediate level. For smaller half lives quite large magnetic fields are needed to have an observably large

effect. Recently, the large hyperfine fields on impurity atoms in ferromagnetic lattices have been used for this purpose. The technique is applicable to cases with half lives of a few picosec, like the 2^+ virtrational states of spherical nuclei. A systematic study of such g factors of vibrational states is of considerable interest from the point of view of nuclear models. It is, of course necessary to know the hyperfine field from some other measurement like Mossbauer studies. Conversely, one can use PAC to study hyperfine fields on nuclei where the g factor of the excited state is known. Recently Matthias and Shirley have used this technique with the differential method for the study of hyperfine fields in unmagnetized ferromagnetic hosts (10). The domains in such a case are randomly oriented giving rise to an unisotropic static magnetic interaction provided the spin relaxation time is sufficiently long. Under such conditions the angular correlation is given by

$$W(\theta, t) = \sum_k A_k G_k(t) P_k(\cos\theta)$$

where

$$G_k(t) = \frac{1}{2k+1} \sum_N \cos N\omega_L t$$

Though there is some resemblance here with the case of quadrupole interaction in a polycrystalline source, the main differences are that only one frequency ω_L and its harmonics are present and secondly there is no dependence on I the intermediate state spin. Using this technique, they got the value

of H = 65.3 ± 1.6 acting on cadmium in a nickel lattice. This method is applicable to a wide range of fields from a few kg to several hundred kg.

The study of the hyperfine field on Ru and Cd in nickel lattice by Matthias and Shirley (11) illustrates nicely the application of PAC techniques to solid state problems. They use the differential method to study the temperature dependence of the hyperfine field below the Curie point and the dependence on the polarizing field above the Curie temperature. They show that the hyperfine field on Ru does not follow the lattice magnetization curve whereas in the case of Cd it does. This is interpreted on the basis of a local moment on Ru in the nickel lattice. The dependence of the internal field on the applied field shows an effect analogous to Knight shifts but considerably larger.

In another recent experiment (12) the Berkeley group have observed NMR for an excited nuclear state using PAC techniques. For such an experiment to succeed it is necessary that (1) the m substate splitting produced by the magnetic field should be large compared to the natural line width of the nuclear level; i.e. $\omega_L \tau \gg 1$ (2). The r.f. field must be strong enough to cause transitions in magnetic substates in time $\sim \tau$; i.e. $g H_{rf} \sim \frac{1}{\tau}$ and (3). There should not be present any other perturbing factors to attenuate the anisotropy. The main difficulty in

such an experiment was the very high r.f. fields that would be necessary. To overcome this, the enhancement of the r.f. field in a ferromagnetic lattice was used. The ^{100}Pd source was diffused in a very thin Ni foil ($\sim 10^{-4}$ cm) and a polarizing field of 100 gauss applied along the direction of one detector the other detector being at 180°. An r.f. field of 3 gauss was applied at right angles and the frequency varied. Resonance condition was detected by a fall in the coincidence counting rate. Combining the resonance frequency obtained in this work viz. 322.5 ± 3 MHz and the known value of the g factor (9) g = + 2.151 ± 0.004, the value of the hyperfine field on Rh in Ni is found to be 197 ± 2 kg.

A similar technique is used by the Japanese group (13) to measure the magnetic moment of ^{17}F which has a half life of 66 sec. Because of the long half life, one does not need large values of r.f. field and the enhancement in ferromagnetic lattice is not necessary. The activity is produced by $^{16}O(d,n)^{17}F$ reaction at 2.3 MeV incident energy. The ^{17}F ions recoiling from the target have polarization perpendicular to the plane of reaction. The perturbation of the asymmetry of the positrons emitted from these polarized nuclei is used to detect the NMR. It is necessary to see that the polarization persists for a sufficiently long time. This is achieved by a decoupling magnetic field parallel to the polarization direction along which the positrons are detected. In addition, quadrupole perturbations

are avoided by using CaF_2 crystals which have cubic lattice to stop the ions. They get a value of $\mu = 4.7224 \pm 0.0012$ nm. By this technique it is possible to incorporate in PAC at least to some extent the accuracy of NMR. The technique appears to have wide applicability to the long lived states excited in nuclear reactions.

Finally, I wish to consider the implantation technique developed recently at Copenhagen (14,15) in which the recoil energy given to nuclei in the coulomb excitation process is used to embed them in a ferromagnetic lattice. A thin target $\sim$ 50 to 100 $\mu gm/cm^2$ is evaporated directly on a thin foil of iron or any other material in which the recoiling nuclei are to be implanted. The Coulomb excitation is done by oxygen ions accelerated in a Tandem Van de Graaff to about 36 MeV. Only the nuclei recoiling in the forward direction in the backing foil are selected by detecting the corresponding backscattered oxygen ions with a ring type solid state detector. In such a case the recoil energy is quite large being around 10 MeV and the stopping time is around 10^{-13} sec. The recoiling nuclei de-excite from states with half-lifes of the order of a few pico-seconds after coming to rest. The angular distribution of the de-excitation gamma rays is studied in coincidence with the backscattered ions with a field of about one kg applied to the foil perpendicular to the plane of detection. The requirement of coincidence

with the backscattered ions not only reduces considerably the background but causes the angular distribution of the gamma rays to be highly anisotropic. This makes it possible to observe the rotation $\omega_L \tau$ even in cases where the half lives are small. Grodzins (16) has recently used this technique to measure the g factors of vibrational 2^+ states in even-even Te isotopes from ^{120}Te to ^{128}Te. The mean lives in these cases vary from 4 to 13 ps and $\omega_L \tau$ values of about 1 to 2 per cent were observed. Assuming the internal field to be 610 $\pm$ 20 kg from Mossbauer effect, the g-factors were calculated. The interesting result is that these values are much larger than predicted by the various models and it seems necessary to revise our ideas regarding the nature of these levels. Another interesting application of this technique is by Boehm, Hagemann and Winther (15) for the study of internal fields on rare-earths in iron. They excite the 4^+ state and study of the angular distribution for the $4^+ \rightarrow 2^+$ gamma ray. The g factors and the lifetimes of the 4^+ states are computed from the known values for the 2^+ states assuming the validity of the rotational model. The conclusion of these studies is that the fields are positive for rare earths in the first half of the 4f shell and become negative in the second half. This indicates an antiferromagnetic coupling of the rare earth and iron magnetic moments.

The implantation technique allows one to study the fields on impurty atoms in host lattices in extremely small concentrations which is not possible by any other method. The only doubtful point is whether the recoiling nuclei go in the host lattice substitutionally and whether all of them see the same field. It would be interesting to check this by a Mossbauer experiment combined with implantation technique. This technique seems to be a quite promising and powerful tool and is sure to come into wider use.

In conclusion I would say that the perturbed correlation techniques have been fairly well developed now and promise to be useful as a tool for the study of solid state problems also.

REFERENCES:

1. A. Abragam and R.V. Pound, Phys. Rev. 92, 943 (1953)
2. Perturbed Angular Correlations, Ed. by E. Karlsson, E. Matthias and K. Siegbahn, North Holland Publication (1964).
3. M. Salomon, L. Bostrom, T. Lindqvist, M. Perez and M. Zwanziger, Ark, Fysik 27, 97 (1964)
4. E. Matthias, W. Schneider and R.M. Steffen, Ark. Fysik 24, 97 (1963).
5. E. Matthias, W. Schneider and R.M. Steffen, Physics Letters , 4, 41 (1963).

6. R.W. Sommerfeldt, T.W. Cannon, L.W. Coleman and L. Schecter, Phys. Rev. 138, B763 (1965)

7. D. Dillenburg and Th. A.J. Maris, Nucl. Phys. 33, 208 (1962)

8. M. Salomon, R. Ballestero and M. Zwanziger, Ark. Fysik 26, 521 (1964)

9. E. Matthias and D.A. Shirley, U.C.R.L. Report 16779 (1966) unpublished.

10. E. Matthias, S.S. Rosenblum and D.A. Shirley, Phys. Rev. Letters, 14, 46 (1965)

11. E. Matthias, S.S. Rosenblum and D.A. Shirley, U.C.R.L. Report 16342 (1965) unpublished.

12. E. Matthias, D.A. Shirley, M.P. Klein and N. Edelstein, Phys. Rev. Letters, 16, 974 (1966)

13. K. Sugimoto, A. Mizobuchi, K. Nakai and K. Matuda, J. Phys. Soc. Japan, 21, 213 (1966)

14. F. Boehm, G.B. Hagemann and A. Winther, Physics Letters 21, 217 (1966)

15. L. Grodzins, R. Borchers and G.B. Hagemann, Phys. Letters, 21, 214 (1966).

16. R.R. Borchers, J.D. Bronson, D.E. Murinck and L. Grodzins, Phys. Rev. Letters 17, 1099 (1966)

INVITED TALK

PROJECTED HARTREE-FOCK SPECTRA FOR FINITE NUCLEI

Chindhu S. Warke
Tata Institute of Fundamental Research
Colaba, Bombay-5.

There is abundant experimental information available about finite nuclei. However, theory is far behind. We all know that there are two main obstacles that come in the way of development of theories of real nuclei (excluding nuclear matter). One is the strong short range forces and the other the finite size of the system. There are however some theories available which deal with the first problem. Amongst these Moscowaski-Scott (1) (MS) approach is easier to handle and looks more promising. Other approaches include those of Brueckner (2), Bethe's spectral (3) method, and Shakin and Waghmare's (4) canonical transformation (which can be considered equivalent to MS method). All these approaches as we know are directly applicable only to doubly closed shell nuclei which are not degenerate. Recently an attempt has been made by Brown and Kuo (5) to extend these approaches to obtain the effective interaction for open shell nuclei. Here we will not go into the details of these theories since we avoided this difficulty by taking a phenomenological effective interaction instead of starting from the free two nucleon interactions.

Even if we know the effective hamiltonian we yet do not have ways to solve the many-body system with finite size. In such circumstances one naturally investigates models which will reproduce the maximum experimental information. The most fruitful model which has enjoyed great popularity is the shell model proposed by Mayer and Jenson. In order to avoid the above difficulty one further approximates the model by treating the particles in the closed shells as inert. Even further one assumes that the outer particles can only be in a few single particle orbitals. The finite size is reflected in constructing good angular momentum states for large number of nucleons. One of the main formal problems of the shell model theory is the construction of antisymmetric N-particle wave functions with good angular momentum and finding out the one and two body matrix elements with respect to this wave function. This problem is also being investigated by group theoretical methods (6). Based on physical intuition and good guess there are various other models proposed in order to avoid this many-particle difficulty. The basic ones amongst these are Bohr and Mottelson's (7) deformed rotating nucleus for even-even case, with the possibility of equilibrium deformation $\beta_e = 0$ or $\beta_e \neq 0$; a modification due to Nilson and Mottelson (8) for $\beta_e \neq 0$ in order to treat the odd-A nuclei. Similar extensions are also made for $\beta_e = 0$ and for other types of deformations.

Here we want to discuss a method that allows us to carry out the calculations for a large number of nucleons outside the closed shells. The tests of this method would be: (1) It should reproduce results corresponding to configuration mixing calculations for few nucleons. (2) It should also reproduce results similar to Bohr-Mottelson model for large number of nucleons. (3) Further the method should have a consistent success over a whole range of nuclei and as general a validity as possible.

It has been investigated by Redlich, Kurath and Picman (9), and later on by others (9) that the wave functions generated from the deformed single particle orbitals have a remarkable similarity to the wave functions of the configuration mixing calculations. These wave functions were obtained from the projection of the angular momentum J from the determinental wave function constructed from Nilson type single particle orbitals. It is however natural to take the deformed single particle orbitals from the Hartree-Fock (HF) theory. It is our aim to find out whether the HF theory together with the angular momentum projection is a useful approximation to the configuration mixing calculations which become rapidly too complicated as the number of particles and the number of shells increase.

Since we will be concerned mainly with the study of the projected spectra, we will assume that we have solved the HF problem and obtained the determinantal state Φ_K of A nucleons.

The single particle HF orbitals thus obtained are of the following form

$$\Phi_{m_i p_i} = \sum_{j_i} C^{j_i}_{m_i p_i} \, |j_i \, m_i \, p_i\rangle$$

Let us now define the projected state

$$\Psi^{I}_{MK} = P^{I}_{MK} \, \Phi_K$$

where the projection operator is

$$P^{I}_{MK} = \frac{2I+1}{16\pi^2} \int \left[\mathcal{D}^{I\,*}_{MK}(\alpha\beta\gamma) + (-1)^{I-K} \mathcal{D}^{I\,*}_{M-K}(\alpha\beta\gamma) \right] \times e^{-i\alpha J_z} e^{-i\beta J_y} e^{-i\gamma J_z} d\Omega \qquad \text{---(2)}$$

The energy defined by the expectation value of the total Hamiltonian (H) with respect to Ψ^{I}_{MK} is denoted by E^{I}_{K}. It is expected that these E^{I}_{K} are approximately the observed low-lying excited states of the nucleus under consderation. There are no valid proof of this statement except that these E^{I}_{K} have the variational character in them. First one would like to investigate the general properties of such spectra. Though we will not prove it here, we take them from Ref. (10).

$$E^{I}_{K} = h^{I}_{K} / p^{I}_{K}$$

where

$$\begin{bmatrix} h^{I}_{K} \\ p^{I}_{K} \end{bmatrix} = \int_0^{\pi/2} \left[d^{I}_{KK}(\theta) + (-1)^{I-K} d^{I}_{K-K}(\theta) \right] \langle \Phi_K | \begin{bmatrix} H \\ 1 \end{bmatrix} e^{-iJ_y\theta} | \Phi_K \rangle \, d\cos\theta \qquad \text{---(3)}$$

In Eq. (3) we observe that the possible nuclear spins are $I = 0, 2, 4, .. I_{max}$ for $K = 0$ band and $I = K, K+1, ..$ I_{max} for $K \neq 0$ band. One can also prove that the ordering of

the spectra would be according to (10)

$$E_K^I \lesseqgtr E_K^{I'} \text{ for } I < I' \quad \text{if } E_K^I = K \lesseqgtr E_K^{HF} \qquad \text{--- (4)}$$

Thus one observes that in order to obtain any resemblance with the experimental situation our interaction and input single particle energies must satisfy the condition $E_K^I = K < E_K^{HF}$.

It may happen that the two bands K and K′ may come close to each other; in that case we have to generalize the wave function to be projected (11). It is obvious to take the projected wave function

$$\psi_M^I = a\psi_{MK}^I + b\psi_{MK'}^I \qquad \text{--- (5)}$$

and to find out a and b by minimizing the expectation value of H. Thus with this technique we can calculate the projected spectra for any number of particles outside the closed shell.

We can also calculate the binding energies of these nuclei (11) assuming that the core is inert except that the core-nucleon contribution to the binding energy is λ (a constant) per particle. With this assumption the binding energy BE of the nucleus (core + A) is

BE (core + A) = BE (core) + λA - Projected ground state energy of A nucleons.

In order to test this approach, mere agreement with the spectra and binding energy is not a sensitive test. Besides,

this one should test the wave function by calculating magnetic moments, quadrupole moments, transition probabilities, ft values in β-decay, nuclear form factors in electron scattering, and the single particle reduced widths in (d,p) reactions (12). We should note that all the above quantities are such that we know the interactions involved with the nucleus very well except in (d,p) reactions. However, here we know that the results do not depend critically on the nucleon-nucleus interaction except at low incident energies. This program is under investigation by Dr. Gunye and myself at TIFR. The preliminary results are very encouraging.

There are some disadvantages in this approach (12). It may happen some times that the wave functions may not have good isotopic spin T. However it is our belief that in the low lying states the mixture of the excited iso-spin states would be very small due to the variational character of the HF wave function. Secondly one should also investigate how much these projected states would change if one takes into account the effect of higher shells. The results of the application of the above method to few cases are shown in the following diagrams and in the tables . (a) are calculated and (b) are the experimental values.

LOW LYING ENERGY LEVEL OF 2S-1d SHELL NUCLEI

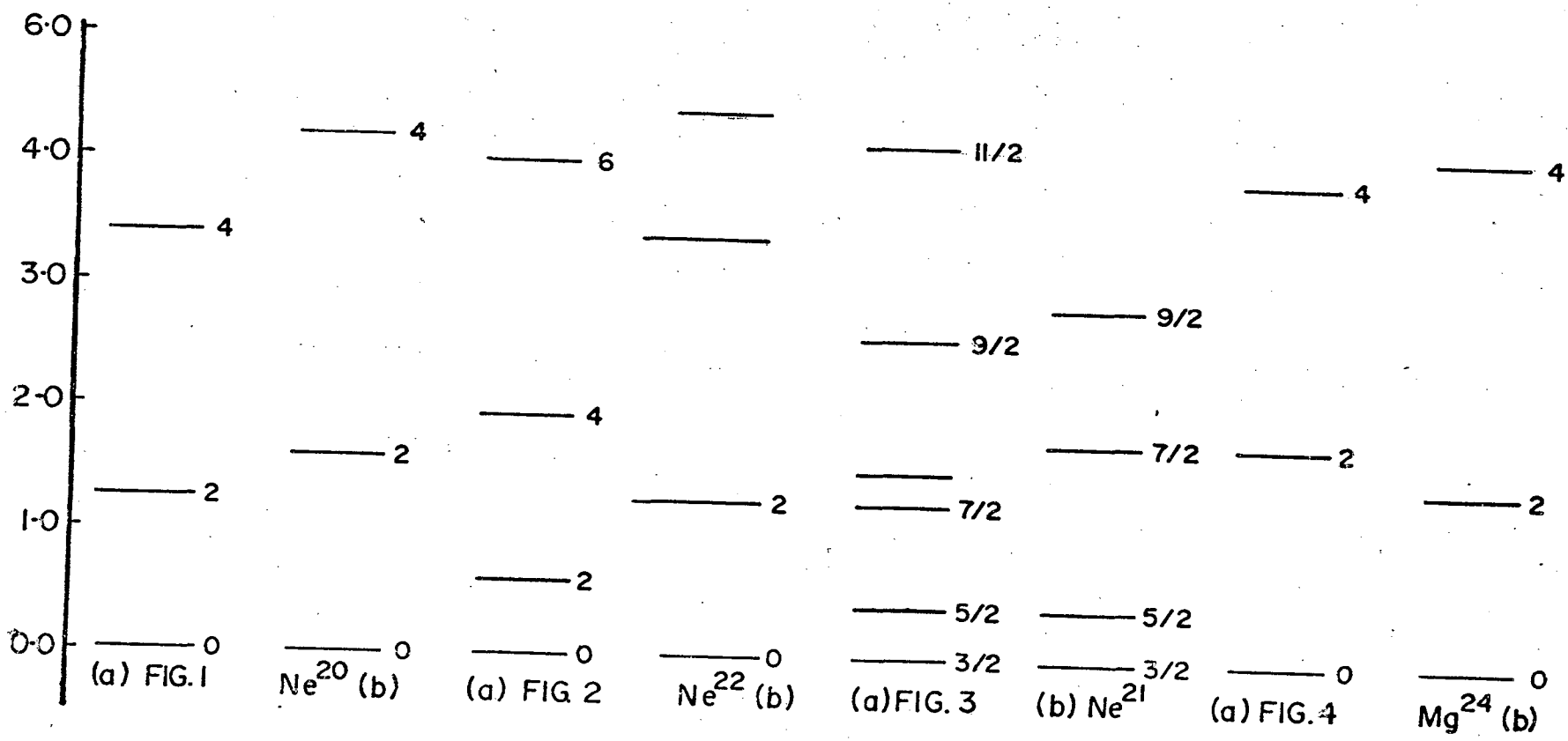

TABLE I
BINDING ENERGIES

NUCLEUS	EXPERIMENTAL BINDING ENERGY (^{16}O) Mev	CALCULATED BINDING ENERGY (^{16}O) Mev
^{20}F	26·78	26·78
^{20}Ne	33·27	35·02
^{21}Ne	40·02	40·56
^{22}Ne	50·39	48·02
^{22}Na	46·77	48·65
^{23}Na	59·18	57·19
^{24}Na	66·14	64·23
^{24}Mg	70·88	69·47
^{25}Al	73·18	77·09

TABLE II
QUADRUPOLE MOMENTS

NUCLEUS	EXPERIMENTAL QUADRUPOLE MOMENTS $e(10^{-24}\ cm^2)$	CALCULATED QUADRUPOLE MOMENTS $e_p = 1{\cdot}5e$ $e_n = 0{\cdot}5e$ $e(10^{-24}\ cm^2)$
^{20}F	-----	0·081
^{21}Ne	0·093	0·097
^{23}Na	0·097	0·105
^{25}Mg	0·22	0·18
^{33}S	−0·064	−0·043
^{35}S	0·054	0·025
^{35}Cl	−0·080	−0·10

TABLE III
MAGNETIC MOMENTS

NUCLEUS	EXPERIMENTAL MAGETIC MOMENTS (BOHR MAGNETONS)	CALCULATED MAGNETIC MOMENTS (BOHR MAGNETONS)
^{20}F	2 · 09	1·54 (1·73)
^{21}Ne	- 0 · 662	-0·571 (0·848)
^{22}Na	1 · 746	1·747 (1·73)
^{23}Na	2 · 218	2·11 (0·124)
^{24}Na	1 · 69	1·586 (1·73)
^{25}Al	- - - -	3·367 (4·793)
^{25}Mg	-0 · 855	-0·583 (-1·913)
^{32}P	-0 · 252	-0·39 (0·44)

TABLE IV
HALF-LIVES OF LEVELS

NUCLEUS	$T_{1/2}(J_f)$ EXPERIMENTAL (SECONDS)	$\frac{B(E2)_{cal.}}{B(E2)_{sp}}$	$T_{1/2}(J_f)$ CALCULATED (SECONDS)	FIRST EXCITED STATE J_f	GROUND STATE J_f
^{19}F	$8·7 \times 10^{-8}$	3 · 2	$11·1 \times 10^{-8}$	5/2	1/2
^{20}Ne	$5·3 \times 10^{-13}$	14 · 0	$10·9 \times 10^{-13}$	2	0
^{21}Ne	$(1·3 \pm 1·1)\ 10^{-13}$	6 · 9	$1·3 \times 10^{-12}$	5/2	3/2
^{23}Na	$10·0 \times 10^{-13}$	7 · 2	$3·9 \times 10^{-13}$	5/2	3/2
^{24}Mg	$10·0 \times 10^{-13}$	15 · 0	19×10^{-13}	2	0
^{25}Mg	$1·7 \times 10^{-14}$	5 · 6	$0·55 \times 10^{-14}$	7/2	5/2
^{28}Si	$5·1 \times 10^{-13}$	7 · 0	$8·97 \times 10^{-13}$	2	0
^{31}P	$1·5 \cdot 10^{-13}$	2 · 0	$0·92 \times 10^{-13}$	3/2	1/2

REFERENCES:

1. S.A. Moszkowski and B.L. Scott, Ann. Phys. 11, 657 (1960)
2. K.A. Brueckner, J.L. Gammel and H. Weitzner, Phys. Rev. 110, 431 (1958)
3. H.A. Bethe, B.H. Brandow and A.G. Petchek, Phys. Rev. 129, 225 (1963)
4. C. Shakin and Y.R. Waghmare, Phys. Rev. Letts. 16,403 (1966)
5. G.E. Brown and T.T.S. Kuo, Nucl. Phys. A92, 481 (1967)
6. J. Flores and M. Moshinsky, Nucl. Phys. A93, 81 (1967)
7. A. Bohr and B.R. Mottelson, Dan. Mat. Fys. Medd. 27, No.16 (1953)
8. B.R. Mottelson and S.G. Nilson, Dan. Mat. Fys. Medd. 1, No.8 (1959)
9. M. Redlich, Phys. Rev. 110, 468 (1958)
   D. Kurath and L. Picman, Nucl. Phys. 10, 313 (1959)
   M.K. Banerjee and C.A. Levinson, Phys. Rev. 130, 1036 (1963)
   W.H. Bassichis, B. Giraud and G. Ripca, Phys. Rev. Letts. 13, 52 (1965).
   I. Unna, Phys. Rev. 132, 2225 (1963)
   I. Kelson, Nucl. Phys. 89, 387 (1966)
10. C.S. Warke and M.R. Gunye, to appear in Phys. Rev.
11. M.R. Gunye and C.S. Warke, to appear in Phys. Rev.
12. C.S. Warke and M.R. Gunye, to be published in the Phys. Rev.

DISCUSSION:

S.S. Jha (Comment):-

If I understand Dr. Warke's work correctly, what he means is that in his work the number and values of the parameters are fixed once for all, unlike configuration mixing calculations. In that sense his method seems to be simpler and more promising to fit a wide range of experimental results for different nuclei.

Y.R. Waghmare: Do you get the signs of quadrupole and magnetic moments out of the theory?

C.S. Warke: Yes.

Indra Mani Govil: Did you try this model to explain ℓ forbidden M_1 transition and what do you expect, whether you can explain these transitions or not?

C.S. Warke: We do not calculate these since we are working in the s-d shell. I do not know whether these also would come out to be reasonable or not.

Y.R. Waghmare: As I understand the basic philosophy of Hartree-Fock theory is to make one-particle one-hole diagrams zero. How do you account for particle-hole contributions arising from core excitations?

C.S. Warke: I feel this effect is partially included once you take a phenomenological two nucleon interaction. For the outer nucleons of course, the off diagonal HF potential would be zero and the next contribution would be from second order in the potential, only for outer nucleons.

L. Satapathy: Some of the excited states obtained by projecting from the ground state band, may be having same energy, as the state projected from the excited band. What is you comment on this?

C.S. Warke: Where the two bands are lying farther, that is, their separation is larger than the projected energy separation then usually one does not come across with this difficulty. In most of the calculations of low lying states this happens only when the bands are close. In this case one has to take into account the band mixing.

Y.K. Gambhir: You remarked in your talk the results obtained by you in the framework of your model are better than the configuration mixing results of the shell model. My feeling is, that the configuration mixing (CM) results must be more accurate than the results obtained by your model, because you are making all the approximations which are made in the CM and besides that more approximations are made in your model. Of course, it is essential to construct such models because CM calculations are not practical for more than four nucleons. In fact CM calculation results should be used in testing the accuracy of such a model.

C.S. Warke: I remarked it on the basis of possibility of extending the accuracy of this method. It is possible to make this approach accurate enough so that it would give results even better than configuration mixing. I agree that at this stage it is to be compared with shell-model configuration mixing.

I disagree with you that such calculations would be tested from configuration mixing calculations. I can do better job than configuration mixing though these calculations do'nt have this accuracy. Any way if your question is simply about the point, which is better, at this stage, I will say neither you nor we can answer it now, unless you have carried out configuration mixing calculations for 8-9 particles in the s-d shell.

BAND-MIXING CALCULATIONS IN ^{25}Al

M.R. Gunye
Bhabha Atomic Research Centre, Trombay, Bombay

INTRODUCTION:

The Hartree-Fock (HF) calculations with a phenomenological inter-nucleon residual interaction are carried out for the K = 5/2 and K = 1/2 bands in ^{25}Al. The low-lying excited states built on these bands are obtained by projecting out good angular momentum states from the deformed axially symmetric HF states. The interaction employed in the calculation is of the form,

$$v(i,j) = \underset{\sim}{\tau_i} \cdot \underset{\sim}{\tau_j} \left(a + b\, \underset{\sim}{\sigma_i} \cdot \underset{\sim}{\sigma_j}\right) V_0 \; \frac{\exp\left(-r_{ij}/\mu\right)}{r_{ij}/\mu} \qquad ..(1)$$

with μ = 1.37 f. V_0 is the strength of the interaction. The radial wave-functions used in the calculation of matrix elements are those of harmonic oscillator with size parameter $\sqrt{\hbar/m\omega}$ = 1.65 f.

The intrinsic state of the system is the axially symmetric determinantal HF state ϕ_K characterized by the band quantum number K. This intrinsic state is composed by superposition of states with good angular momentum J. The energies E^J_{KK} of these states are extracted from ϕ_K by angular momentum projection. We define two relevant quantities

$$h^J_{KK'} = \langle \phi_K | H P^J_{KK'} | \phi_{K'} \rangle \qquad \ldots (2a)$$

$$P^J_{KK'} = \langle \phi_K | P^J_{KK'} | \phi_{K'} \rangle \qquad \ldots (2b)$$

where $P^J_{KK'}$ is the usual projection operator for angular momentum. The projected energies E^J_{KK} are then given simply by

$$E^J_{KK} = h^J_{KK} / p^J_{KK} \qquad \ldots (3)$$

If the HF energies E^{HF}_K and $E^{HF}_{K'}$ corresponding to the two bands K and K′ are close, as in the case of K = 5/2 and K′ = 1/2 bands in ^{25}Al, then the projected energies must be corrected due to band-mixing. The wave-function Ψ^J_M for the state J will then be approximated by a linear combination

$$\Psi^J_M = a_1 \Psi^J_{MK} + a_2 \Psi^J_{MK'} \qquad ---(4)$$

where $\Psi^J_{MK} = P^J_{MK} \phi_K / (p^J_{KK})^{1/2}$, and similarly $\Psi^J_{MK'}$. The energy ε^J of the state with angular momentum J is then given by

$$\varepsilon^J = (a_1^2 E^J_{KK} + a_2^2 E^J_{KK'} + 2 a_1 a_2 E^J_{KK'}) / (a_1^2 + a_2^2 + 2 a_1 a_2 q^J_{KK'}) \qquad ---(5)$$

where E^J_{KK}, $E^J_{K'K'}$ are given by eq. (3) and

$$E^J_{KK'} = h^J_{KK'} / (p^J_{KK} p^J_{K'K'})^{1/2} \qquad ---(6a)$$

$$q^J_{KK} = p^J_{KK'} / (p^J_{KK} p^J_{K'K'})^{1/2} \qquad ---(6b)$$

Minimizing ε^J with respect to a_1 and a_2 in eq. (5) one gets the corrected energy

$$\varepsilon^J = \left\{ \tfrac{1}{2}(E^J_{KK} + E^J_{K'K'}) - A \pm \left[\tfrac{1}{4}(E^J_{KK} - E^J_{K'K'})^2 + (E^J_{KK'})^2 + B \right]^{1/2} \right\} / C \qquad ---(7)$$

where

$$A = q^J_{KK'} E^J_{KK'} \quad , \quad C = 1 - (q^J_{KK'})^2$$

$$B = E^J_{KK} E^J_{K'K'} (q^J_{KK'})^2 - (E^J_{KK} + E^J_{K'K'}) q^J_{KK'} E^J_{KK'}$$

RESULTS:

The single particle energies of $d_{5/2}$, $d_{3/2}$ and $s_{1/2}$ states are fixed by the strength $\alpha = -2.48$ MeV of the spin-orbit force. By employing $V_0 = 45$ MeV, $a = .10$ and $b = .233$ in eq. (1), the calculated energy spectra from $K = 5/2$ and $K' = 1/2$ bands in ^{25}Al are shown in fig. a. The calculated spectra with $V_0 = 42.5$ MeV, $a = .056$ and $b = .233$ are shown in fig. e. Since the two bands and the projected energies are quite close, the interaction between the projected states with the same angular momentum must be taken into account. The calculations for ^{25}Al are, however, very lengthy, even considering the projection from an individual band since we are dealing with 9 particles outside the ^{16}O core. In particular the band-mixing calculations described above are quite involved and hence some approximations are sought. The overlap integral $P^{J}_{KK'}$ is neglected and the interband energy term is simplified. The resultant energy spectrum after taking into account the band-mixing by the approximate method is shown in fig. b (for parameters corresponding to fig. a) and in fig.d (for parameters corresponding to fig. e). The experimental spectrum is shown in fig. c. The agreement between the calculated and the experimental spectrum is quite fair. Moreover, the calculated spectra are not so sensitive to a slight change in the exchange character or the strength of the two-body interaction as can be seen from fig. b and fig. d.

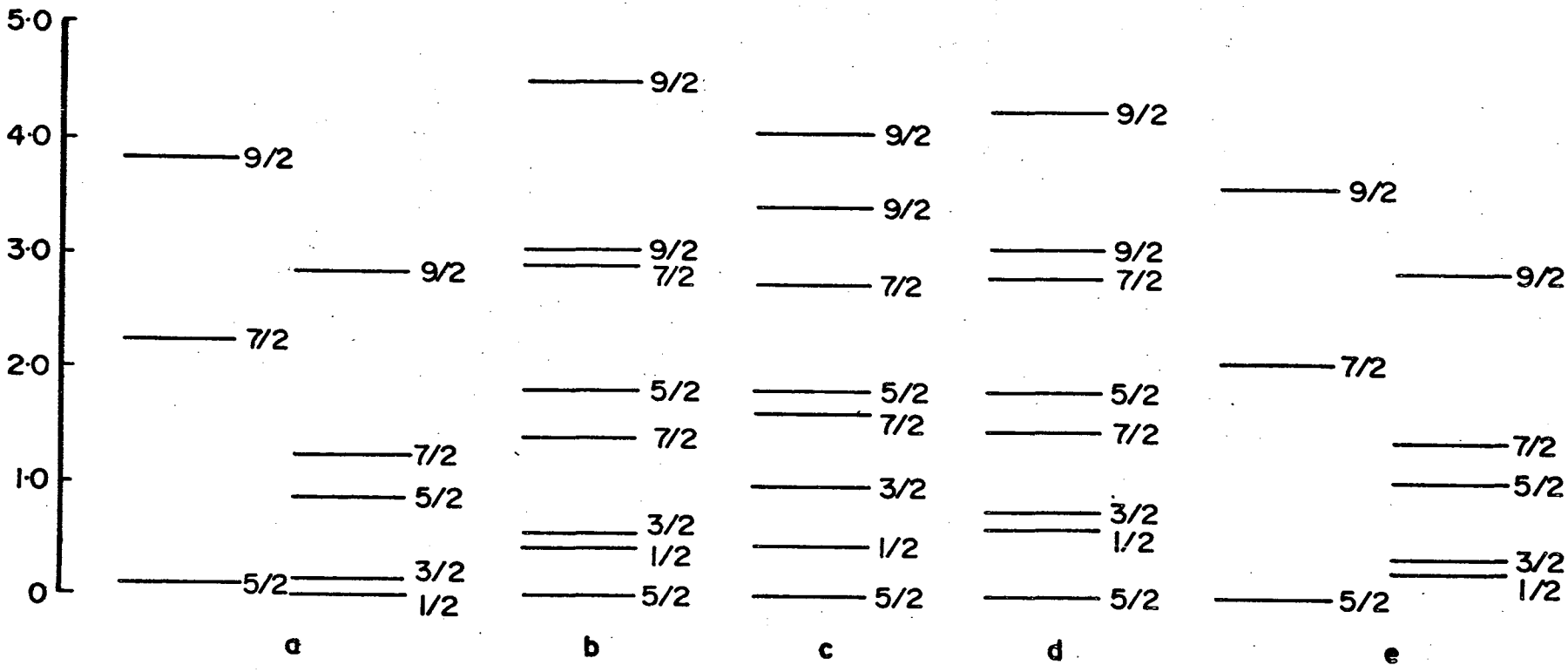
5·0
4·0
3·0
2·0
1·0
0
9/2
7/2
5/2
9/2
7/2
5/2
3/2
1/2
a
9/2
9/2
7/2
5/2
7/2
3/2
1/2
5/2
b
9/2
9/2
7/2
5/2
7/2
3/2
1/2
5/2
c
9/2
9/2
7/2
5/2
7/2
3/2
1/2
5/2
d
9/2
7/2
5/2
9/2
7/2
5/2
3/2
1/2
e

DISCUSSION:

S. Ramamurty: What is the exact energy of interaction of bands which you assumed?

M.R. Gunye: We have not assumed any interaction energy between the bands as this sort of assumption is not needed in our formalism.

S.C.K. Nair: I would like to know the magnitude of the band mixing coefficient.

M.R. Gunye: In the calculations reported here, we do not need to know the values of a_1, and a_2 (band-mixing coefficients) specifically and hence they are not evaluated; however, they can be easily obtained.

L. Satapathy: (1) If one first does a non-axial calculation for ^{25}AI and then projects out, will it be different than the present result? (2) According to this calculation, will ^{25}Mg have a different result?

M.R. Gunye: (1) The intrinsic state employed in our calculations is axially symmetric Hartree-Fock state. However, some effect of non-axial terms is taken into account in the evaluation of $h^{J}_{KK'}$. If one has to start from a non-axial HF state, this formalism would have to be modified. (2) No. The results of ^{25}Mg and ^{25}AI would be very similar.

SU_4 SCHEME FOR CONFIGURATION MIXING ACROSS MAJOR SHELL AND THE "MONOPOLE" BREATHING MODE

S.B. Khadkikar
Tata Institute of Fundamental Research
Colaba, Bombay - 5.

ABSTRACT

The model interaction in the group classification of the shell model states under a single (2, 0, 0) irreducible representation of the group SU_4 is analysed. This interaction was introduced in a previous paper. It is shown that the resonance level in ^4He has a possible description in terms of the collective monopole oscillation called as "breathing"mode , the model interaction could be responsible for such a collective behaviour in the same way the quadrupole-quadrupole interaction is responsible for the collective rotation in Elliot's SU_3 Scheme.

Not presented

MIXED-PARITY ORBITALS FOR THE LIGHT NUCLEI

J.C. Parikh and Nazakat Ullah,
Tata Institute of Fundamental Research,
Colaba, Bombay-5.

ABSTRACT.

We have looked into the problem of obtaining the mixed-parity orbitals for the 1p-shell nuclei. Using an exact self-consistent solution, it is shown that no parity mixed orbitals can be obtained for the ground-state band of ^{16}O using a reasonable two-body force. Preliminary calculations on ^{14}N show that a mixed-parity solution can be obtained only if the strength of central force is taken to be three times the usual strength. The role of time reversal invariance in connection with the mixed parity orbitals will also be discussed.

Not presented.

ONE- AND THREE-QUASI-PARTICLE STATES OF THE Ni ISOTOPES

Y.K. Gambhir and Ram Raj
Saha Institute of Nuclear Physics, Calcutta.

The well-known Super conductivity (BCS or pairing) model of the nucleus neatly takes into account the strong pairing interaction between nucleons by the Bogoliubov-Valatin transformation resulting in quasi-particles. The model interprets the first few excited states of singly closed shell (SCS) odd nuclei as independent quasi-particle excitations with respect to the new quasi (BCS) vacuum $|0\rangle$ which physically describes the ground state of the neighbouring even-even nuclei. The further refinement obviously consists of the configuration mixing treatment of residual interaction $\overline{H}_{QP}$ between quasi-particles. Most up-to-date description of the collective vibrational states of SCS even-even nuclei in this model is given in terms of two- (TDA and RPA(1)) and four- (HRPA(2) and MTDA(3)) interacting quasi-particles. While SCS odd nuclei are described in terms of one- and three-interacting quasi-particles.

$\overline{H}_{QP}$ is symbolically written as

$$\overline{H}_{QP} = H_{22} + H_{31} + H_{13} + H_{40} + H_{04} \text{ ---------- } (1)$$

where suffices with H's denote the number of creation and annihilation quasi-particle operators respectively and their explicit forms are given in reference (3).

The properly antisymmetric ortho-normal states for three quasi-particles can easily be constructed by the standard shell-model technique (seniority). Only H_{22} part of $\overline{H}_{QP}$ which conserves the number of quasi-particles will contribute to the **matrix** elements in the pure three quasi-particle sub-space. The general matrix elements of H_{22} between three-quasi-particle states can easily be calculated with the help of one- particle fractional parentage coefficients (fPC).

The non-conserving part of $\overline{H}_{QP}$ will connect the different quasiparticle subspaces. The part $H_{31}(H_{13})$ will contribute in the mixing of three-(one) and one-(Three) quasi-particle subspaces. The evaluation of these mixed matrix elements require all the quasi-particle states in the second quantized form. The second quantized varsion of three-quasi-particle basis is straightforward except for the case where all the three quasi-particles are in the same angular-momentum states and can be written as

$$|ab_{J_1,c;JM}\rangle = N(abc;J_1J)\left\{A^{+}(abJ_1),\alpha_c^{+}\right\}_M^J|0\rangle \quad ---(2)$$

where N is the normalization constant and α_α^+ creates (annihilates) quasiparticel in the state $\alpha(nljm)$. The $A^+(abJM)$ is the pair creation operator for the quasiparticles in the angular momentum states 'a' and 'b' coupled to a total angular momentum J with projection M defined as

$$A^{+}(abJM) = \sum_{\alpha\beta}\begin{bmatrix} a & b & J \\ \alpha & \beta & M \end{bmatrix}\alpha_\alpha^{+}\alpha_\beta^{+} --- \quad (3)$$

the notation [ ] denotes a Clebsch-Gordan coefficient. The case with a = b = c in equation (2) requires a special treatment because the operators

$$\{A^{+}(aaJ_1), \alpha_a^{+}\}^{J}_{M} \text{ and } \{A^{+}(aaJ_2), \alpha_a^{+}\}^{J}_{M} \text{ --- } \quad (4)$$

are not generally independent; in otherwords they are redundant and non-orthonormal. Therefore, one to one correspondence has been established between the second quantized version and the seniority classification of states and is given by the following simple relation

$$|a^3 J v M\rangle = \left\{\sqrt{3!}\,\langle a^2 J_1, a; J \| a^3 J v\rangle\right\}^{-1} \{A^{+}(aaJ_1)\alpha_a^{+}\}^{J}_{M}|0\rangle \quad (5)$$

for the case where there is no repeatition of the same J with the different seniority (v). The symbol $\langle \| \rangle$ appearing in eqn. (5) is the one fpc.

We have evaluated the mixed matrix elements by expressing $H_{3i}\alpha_i^{+}|0\rangle$ in terms of three-quasi-particle states and then utilising the ortho-gonality relations and equation (5). In a similar way the ground state correlations (H_{40} and H_{04} of $\overline{H}_{QP}$) can be included.

In the actual numerical calculations the nucleons outside the ^{58}Ni core are considered. The unperturbed single-particle energies 0.0, 0.78 and 1.08 MeV for the $2p_{3/2}$, $1f_{5/2}$ and $2p_{1/2}$ orbitals have been taken from the experimental spectra of ^{59}Ni. The BCS equations are solved for all the odd-Ni isotopes using the numbers listed in references (4) obtained

by directly fitting the observed level energies, as effective two-body matrix elements. The dimensions of the various matrices for $1/2^-$, $3/2^-$, $5/2^-$, $7/2^-$, and $11/2^-$ states are 5 x 5, 10 x 10, 10 x 10, 6 x 6, 5 x 5 and 1 x 1 in the pure three quasiparticle subspace and 6 x 6, 11 x 11, 11 x 11, 6 x 6, 5 x 5 and 1 x 1 in the mixed space respectively.

The spurious states arising due to the non-conservation of the number operator by the Bogoliubov Valatin transformation must be projected out before the diagonalization of the various matrices.

The results for all the odd NI isotopes are arranged in table I. The first few states of all these isotopes are well described in terms of one-quasi-particle excitations. Considerable improvement is achieved for the excited states in the mixed quasi-particle space (MIX). There are very small quasi-particle admixtures except for the first $1/2^-$ states of ^{59}Ni and ^{61}Ni where mixing coefficients are 15% and 10% respectively. The effect of ground state correlations on the energy spectra is quite small, the maximum energy shift is less than 5%. These results in mixed one- and three-quasi-particle space (MIX) are very close to those obtained by the exact shell-model calculations (EXACT). This reflects the accuracy of the proposed formalism.

Thus the proposed Extended Tamm-Dancoff Approximation (ETDA) for the description of the states of odd-A nuclei is quite accurate.

Table I.

Level Spectra of odd-Ni isotopes.

		LEVEL ENERGY IN MEV.					
	J^{π}	$1/2^-_1$	$1/2^-_2$	$3/2^-_1$	$3/2^-_2$	$5/2^-_1$	$5/2^-_2$
59 Ni	PURE	.54	.93	0	.64	.24	1.17
	MIX.	.51	1.07	0	1.25	.26	1.28
	EXACT.	.30	1.11	0	.83	.21	-
	EXPT.	.47	1.32	0	.89	.34	-
61 Ni	PURE.	.19	.58	.05	.48	0	.65
	MIX.	.12	.73	.01	.71	0	.75
	EXACT.	.02	-	0	-	0	.90
	EXPT.	.28	-	0	-	.07	.91
63 Ni	PURE.	.04	.69	.31	.49	0	.63
	MIX.	0	.83	.23	.67	0	.67
	EXACT.	0	1.18	.24	.90	.01	-
	EXPT.	0	1.01	.16	.53	.09	-
65 Ni	PURE.	0	1.23	.64	.71	.11	.97
	MIX.	0	1.28	.57	1.02	.12	1.00
	EXACT.	.05	-	.53	.76	0	-
	EXPT.	.06	-	.32	.70	0	-

REFERENCES:

1. M. Baranger, Phys. Rev. 120, 957 (1960); this work lists all other earlier publications.
2. M. Savoia, J. Sawicki and A. Tomasini, Nuovo Cimento 32, 991 (1964)
   G. Do Dang and A. Klein, Phys. Rev. 133, B257 (1964)
   T. Tamura and T. Udagawa, Nucl. Phys 53, 33 (1964)
3. M.K. Pal, Y.K. Gambhir and Ram Raj, to be published in Phys. Rev.
4. R.D. Lawson, M.H. MacFarlane and T.T.S. Kuo, Phys. Letters 22, 168 (1966).

DISCUSSION:

Mukherjee: How do you know if the $\frac{1}{2}^-$ (states) in Ni, as designated by you as $\frac{1}{2}^-_1$ and $\frac{1}{2}^-_2$ are the correct designation? Do you have the s.p. strengths for these states to support your assumption?

Y.K. Gambhir: Well, we have described these states as the superposition of one - and three - quasiparticle states. In this space the order of the matrix in 5 x 5 and hence we get five $\frac{1}{2}^-$ states and the lowest ones are compared with the experimentally observed levels. We have simply compared the spin and the energy. However, as far as the s.p. strength is concerned one should calculate the spectroscopic factors, but that is altogether a different story, because we did not say that these are s.p. states. We have approximately taken into account the configuration mixing arising due to the residual interaction for all the nucleons present outside the assumed ^{56}Ni core.

L. Satapathy: How was the shell model calculation performed on ^{65}Ni?

Y.R. Gambhir: These shell-model results are quoted from the paper of Lauson et al. They did not mention the details in their paper. In fact it indicates that they have considered all the configurations possible for ^{65}Ni in which all the nucleons outside the ^{56}Ni core are distributed among $2p_{3/2}$, $2p_{1/2}$ and $1f_{5/2}$ single particle orbitals in all possible ways.

TWO AND FOUR PARTICLE SHELL MODEL SPECTRA

Ram Raj and Y.K. Gambhir,
Saha Institute of Nuclear Physics
Calcutta.

ABSTRACT.

Exact shell-model calculations for nuclei having two-(^{58}Ni) and four-(^{60}Ni) particles in the active shell model orbitals have been made using various interactions namely, (1). The surface-delta interaction, the conventional Serber exchange with Yukawa radial dependence and a potential having exchange mixture similar to the Rosenfeld mixture with Yukawa radial dependence. (2). An approximate reaction matrix obtained by using the Hamada-Johnston and non-local separable Tabakin potentials as free two-body interaction. The results are compared with those obtained by using the numbers for two-body matrix elements determined by directly fitting the observed level energies combined with the reaction matrix theory. The overlap of the BCS projected wave functions with the exact shell model ground state wave functions and the odd-even mass differences obtained from the pairing theory are calculated and discussed.

INVERSE GAP EQUATION AND EFFECTIVE INTERACTIONS

Y.K. Gambhir
Saha Institute of Nuclear Physics
Calcutta.

ABSTRACT.

Calculations based on the Inverse Gap Equation (IGE) method are made first with the phenomenological two-body interactions known to give excellent results in the shell-model picture for nuclei in the 2p-1f region. Slight departure of the force strength from unity and the smooth variation of the Hartree-Fock spectrum with mass number thus obtained provides the validity of this model in this region. The pairing nature of the various interactions like (1) The surface-delta, a potential having exchange mixture similar to the Rosenfeld mixture with Yukawa radial dependence and (2) An approximate reaction matrix obtained by using the Hamada-Johnston and non-local separable Tabakin potentials as free two-body nucleon interaction, is studied. The results of the Tamm-Dancoff Approximation (TDA) obtained by using the various quantities determined by the IGE model are discussed with those obtained by using the corresponding quantities of the conventional BCS theory.

SHELL MODEL SPECTRA IN ODD MASS INDIUM ISOTOPES

V.R. Pandharipande
Tata Institute of Fundamental Research,
Colaba, Bombay-5.

It is knwon that the δ function residual interaction gives singularly large values for the matrix element $\langle j_1 j_2 J | V | j_3 j_4 J \rangle$ when J is an extreme value $j_1 \pm j_2$ or $j_3 \pm j_4$. It was shown (1) that by modifying the δ function interaction for such states having an extreme value of J one can emperically define an effective residual interaction to reproduce the spectra of many two particle nuclei with few parameters. The interaction proposed is defined by its matrix element as follows:

$$\langle j_1 j_2 J | V | j_3 j_4 J \rangle = \alpha_J \, V \langle j_1 j_2 J | \delta(r_1 - r_2) \left[1 - \beta + \beta(\sigma_1 \cdot \sigma_2)\right] | j_3 j_4 J \rangle$$

$\alpha_J = 1$, if J is not an extreme value $j_1 \pm j_2$ or $j_3 \pm j_4$

$\alpha_J = a + b\,J$, if J is an extreme value $j_1 \pm j_2$ or $j_3 \pm j_4$

The two particle spectra of many nuclei are calculated with this interaction using harmonic oscillator wave functions and simple shell model configurations used by Talmi and co-workers (2) in their investigations. A good agreement is obtained for the following values of the parameters and this is shown in fig.1 and fig.2.

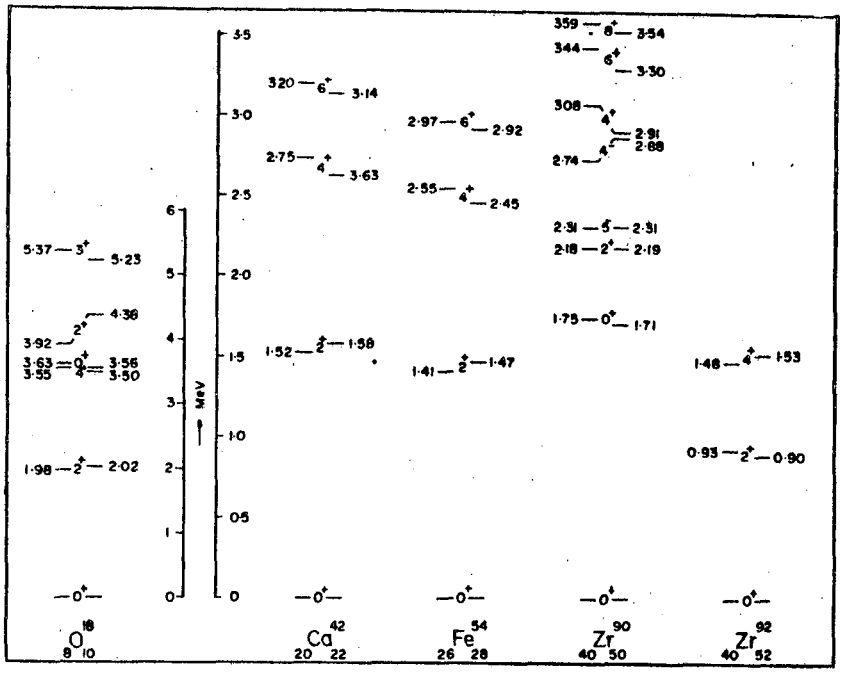
MeV
$O^{18}_{8\ 10}$
$Ca^{42}_{20\ 22}$
$Fe^{54}_{26\ 28}$
$Zr^{90}_{40\ 50}$
$Zr^{92}_{40\ 52}$

FIG. 1

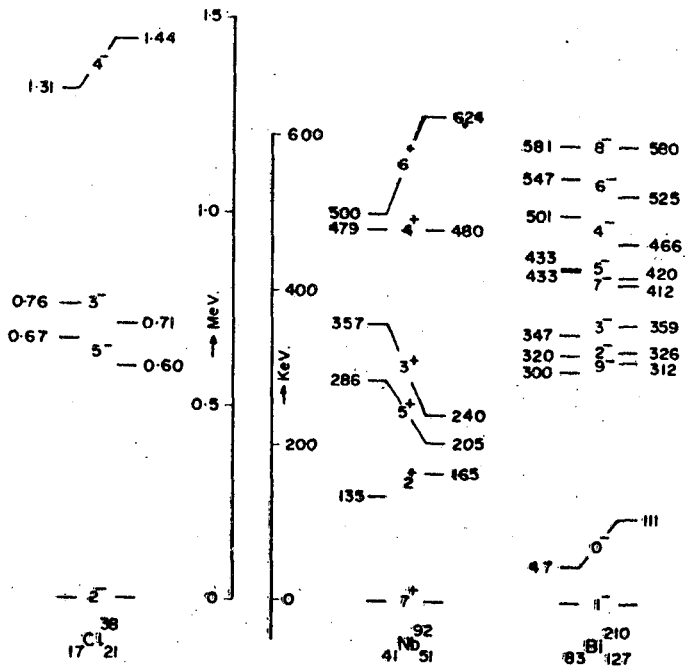
MeV.
KeV.
$Cl^{38}_{17\ 21}$
$Nb^{92}_{41\ 51}$
$Bi^{210}_{83\ 127}$

FIG. 2

$$V = 1630 \text{ MeV fm}^3$$
$$a = 0.42$$
$$b = 0.05$$
$$\beta = 0.1$$

The spectra of even Tin and odd mass Indium isotopes are calculated with this interaction. The neutrons predominantly fill the h11/2 and 1d3/2 orbitals in going from ^{116}Sn to higher Tin isotopes. So the first shell model approximation to the spectra of these Tin isotopes should be that of two neutrons in h11/2 and 1d3/2 orbitals. This agreement is very good.

In the ground state of odd mass Indium isotopes the proton hole is in the g9/2 orbital. By coupling this hole with the 2^+ state in the Tin core one can get a multiplet of five positive parity states with spins from 5/2 to 13/2. Some of these states are known in ^{115}Sn and ^{117}In in the region of one MeV. In the weak coupling model of de-Shalit (3) one assumes that in the states of this multiplet the neutron wave function is the same as that for the 2^+ state in Tin. If this is denoted by ψ^n_{2+} then the energies $\langle \psi^n_{2+} g_{9/2}^{-p} J | V_{np} | \psi^n_{2+} g_{9/2}^{-p} J \rangle$ can be calculated using the ψ^n_{2+} obtained in the previous calculation in Tin. This calculation, however, does not give good agreement.

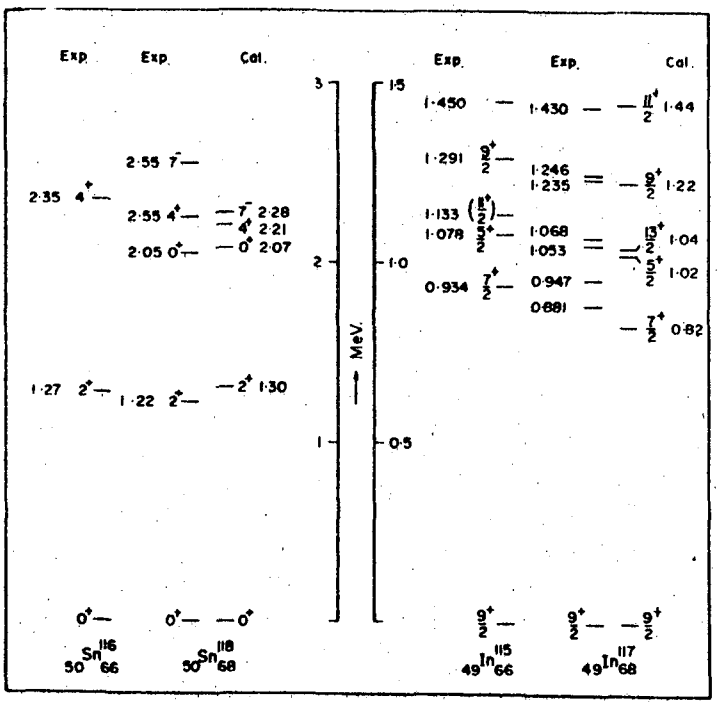
Exp.
Exp.
Cal.
Exp.
Exp.
Cal.
3
2
1
1·5
1·0
0·5
MeV.
2·35 4+
2·55 7−
2·55 4+
2·05 0+
7− 2·28
4+ 2·21
0+ 2·07
1·27 2+
1·22 2+
2+ 1·30
0+
0+
0+
1·450
1·291 9/2+
1·133 (11/2+)
1·078 5/2+
0·934 7/2+
1·430
1·246
1·235
1·068
1·053
0·947
0·881
11/2+ 1·44
9/2+ 1·22
13/2+ 1·04
5/2+ 1·02
7/2+ 0·82
9/2+
9/2+
9/2+
9/2+
50Sn116 66
50Sn118 68
49In115 66
49In117 68

FIG.3

We find that the non diagonal matrix elements, of the neutron proton interaction of the type $\langle \psi_J^n g_{9/2}^{-p} J | V_{np} | \psi_{J\neq J}^n g_{9/2}^{-p} J \rangle$ connecting states with different neutron spins, are small. Such matrix elements have the product of two 6j symbols in their geometrical factors and in the summation over the intermediate spin J (np) these do not in general add in phase. Hence a better approximation could be to diagonalise the interaction between states like $| J_1^n J_2^n (2^+) j^{-p} J |$ restricting the neutron spin to two. These results are shown in fig.3. The agreement is fair. From this calculation we find that the neutron wave function is different in the various states of the multiplet and differs considerably from that in the 2^+ state of Tin. Graeffe et al (4) have also pointed out, by examining the experimental data on these levels, that the weak coupling model may not be well applied in these isotopes and that the n-p interaction may have considerable effect on the neutron wave functions in Indium.

REFERENCES:

1. V.R. Pandharipande, Proc. of Nucl. Phys. and Solid State Phys. Symp. 146, (1966)
2. I. Talmi, Rev. Mod. Phys. 34, 704 (1962)
   N. Auerbach and I. Talmi, Nucl. Phys. 64, 458 (1965)
3. A. de-Shalit, Phys. Rev. 122, 1530 (1961)
4. G. Graeffe, C.W. Tang, C.D. Coryell and G.E. Gordon, Phys. Rev. (149) 384 (1966)

SPIN ORBIT INTERACTION AND REGIONS OF DEFORMED NUCLEI

J.C. Parikh
Tata Institute of Fundamental Research, Bombay-5.

and
K.H. Bhatt
Physical Research Laboratory, Ahmedabad-9.

We discuss here a simple procedure which seems to enable one to understand in a qualitative way, why nuclei in some regions of the nuclear periodic table are deformed whereas in others they are not.

Nuclei are considered to be 'deformed' when they have rotational energy sequence. In general, the nuclei whose spectra exhibit well developed rotational sequence, have large intrinsic quadrupole moment. Hence, if a nucleus is 'deformed' enough to exhibit rotational spectrum, the nucleons in it must be filling single particle orbits which have large intrinsic quadrupole moments.

We surmise therefore, that a given nucleus will be 'deformed' if the energy sequence of the spherical single particle states, as determined by the spin-orbit interaction is such that the residual interactions between extracore nucleons, can generate self consistant orbits with large quadrupole moments.

We thus expect the spin-orbit interaction to play an important role in determining whether the nuclei in a given region of the periodic table will be deformed or not, even when the residual interaction is assumed to have the tendency to form

deformed nuclei. This point seems to have received little attention.

<u>The 1d - 2s shell</u>. Nuclei in the beginning of this shell are known to be 'deformed'. So let us start with the deformed view point. Consider the nucleons moving in a Q_0^2 quadrupole field.

The single particle states of the nucleons in a Q_0^2 field can be labled by the values of $\nu = \langle l_z \rangle$, the expectation value of the component of the orbital angular momentrum along the symmetry axis and ε the eigen value of the intrinsic quadrupole moment (in units of $\hbar/mw$) (2).

The six single particle states $\varphi(\nu, \varepsilon)$ of the 1d-2s shell in a Q_0^2 field are,

$$\varphi(0,4) = \frac{1}{\sqrt{3}} (\sqrt{2}\ do - So)$$
$$\varphi(\pm 1, 1) = d \pm 1$$
$$\varphi(\pm 2, -2) = d \pm 2$$
$$\varphi(0, -2) = \frac{1}{\sqrt{3}} (\sqrt{2}\ So + do)$$

Here d_ν and s_ν are Harmonic oscillator eigenfunctions for the 1d and 2s states with $\langle l_z \rangle = \nu$

The orbit $\varphi(0,4)$ lies the lowest in energy. It has the <u>largest</u> possible value for the intrinsic quadrupole moment for a single particle in the s - d shell. Note that it contains more of the d, than the s state.

Now let us look at the situation from the spherical point of view. The enrgy sequence of the single particle states in the

spherical potential with spin orbit interaction is $d_{5/2}$ - $s_{1/2}$ - $d_{3/2}$. Let us suppose that the residual interactions between nucleons have a tendency to produce a Q_0^2 field. In that case, as we start filling the s - d shell, the main result of the residual interaction between the nucleons, will be to generate deformed single particle states. These deformed states should necessarily contain more of the d than the s state, in view of the ordering of the spherical single particle states.

We see therefore, that the single particle energy sequence $d_{5/2}$ - $s_{1/2}$ - $d_{3/2}$ due to the spin orbit interaction is such as to allow the formation of deformed orbits of the type $\varphi(0,4)$, having large quadrupole moment.

It is not surprising therefore that nuclei in the beginning the d-s shell show rotational spectra. In addition, we can also 'see' some interesting details regarding these nuclei.

1) The nucleus $^{19}_{9}F_{10}$ is more deformed than $^{19}_{8}O_{11}$. It must be. The two neutrons and the proton in ^{19}F can all occupy orbit of the type $\varphi(0,4)$ having the largest intrinsic quadrupole moment. The third neutron in ^{19}O must occupy an orbit of the type $\varphi(\pm 1, 1)$ (Nilsson K = 3/2 orbit) (3), which has a significantly smaller quadrupole moment than $\varphi(0,4)$. Similarly the nucleus ^{20}Ne should be and is, more deformed than ^{20}O.

It is apparent that the nuclei having both protons and neutrons outside closed shell can have a larger intrinsic quadrupole moment because, in that case it is possible to put the maxium number of nucleons in the orbit having large ε. Thus

the fact that large deformations result when both protons and neutrons are present, seems to be mainly due to (the effect of) the Pauli principle, and perhaps only secondarily due to the extra deformation producing ability of the p - n residual interaction.

2) The nucleus ^{23}Na is more deformed than ^{25}Na. Note that the two extra neutrons of ^{25}Na must occupy an orbit of the type $\varphi(\pm 2, -2)$ (Nilsson = 5/2 orbit) having a negative intrinsic quadrupole moment. Thus the quadrupole moment of ^{25}Na must be less than that of ^{23}Na (by at least four units).

The 1f-2p shell: The single particle energy sequence due to the spin orbit interaction is $f_{7/2}$ - $p_{3/2}$ - $f_{5/2}$ and $p_{1/2}$, with a separation of about 2 MeV between the $p_{3/2}$ and $f_{7/2}$ states.

The single particle states in a Q_0^2 field are

$$\varphi_0 = \varphi\begin{pmatrix} \nu & \varepsilon \\ 0 & 0 \end{pmatrix} = \frac{1}{\sqrt{5}}\left(\sqrt{3}\, f_0 + \sqrt{2}\, P_0\right)$$

$$\varphi_{\pm 1} = \varphi\begin{pmatrix} \pm 1 & 3 \end{pmatrix} = \frac{1}{\sqrt{5}}\left(2 f_{\pm 1} - P_{\pm 1}\right)$$

$$\varphi_{\pm 2} = \varphi\begin{pmatrix} \pm 2 & 0 \end{pmatrix} = f_{\pm 2}$$

$$\varphi_{\pm 3} = \varphi\begin{pmatrix} \pm 3 & -3 \end{pmatrix} = f_{\pm 3}$$

$$\varphi'_{\pm 1} = \varphi\begin{pmatrix} \pm 1 & -3 \end{pmatrix} = \frac{1}{\sqrt{5}}\left(f_{\pm 1} + 2 P_{\pm 1}\right)$$

$$\varphi'_0 = \varphi\begin{pmatrix} 0 & 6 \end{pmatrix} = \frac{1}{\sqrt{5}}\left(\sqrt{2}\, f_0 - \sqrt{3}\, P_0\right)$$

The orbit φ'_0 having the largest quadrupole moment in the f - p shell contains more of the p than the f state.

As we start filling the f - p shell, the main result of the inter-nucleon interaction, which we have assumed to have a

tendency to deform the nucleus, would be to generate self consistent deformed orbits of the type φ_2 or $\varphi \pm 1$ having a larger amount of the f than the p state. It is clear that the spin-orbit interaction will prevent the formation of deformed orbits like φ_0' having a large quadrupole moment, in the beginning of the f - p shell. Thus, contrary to the s-d shell nuclei we do not expect (nor observe) the nuclei just filling the f-p shell to exibit rotational spectra.

If we the nucleus $^{56}_{28}Ni_{28}$ as a closed 'core', in which the $f_{7/2}$ subshell is completely filled, the spherical single particle states available to the nucleons outside it have the energy sequence $p_{3/2} - f_{5/2} - p_{1/2}$. The separation between the $f_{5/2}$ and $p_{3/2}$ states is only 780 keV. The deformed self consistent orbit with k = 1/2 generated when nucleons are added to ^{56}Ni will have the f-p admixt

possible ε . The nucleus $^{60}_{30}Zn_{30}$ with the two protons and neutrons occupying such an orbit. It is thus quite likely that ^{60}Zn (like ^{20}Ne) would be 'deformed' enough to exibit a rotational spectrum. It would be of interest to do an explicit shell model calculation of ^{60}Zn energy levels, since it might be difficult to observe these energy levels experimentally.

Larger quadrupole moments can not be built up in this region of nuclei. Consider $^{59}_{28}Ni_{31}$. The first two neutrons can occupy an orbit like φ_0' but the third one must occupy an orbit like φ_1' (Nilsson k = 3/2 orbit), which has a negative intrinsic quadrupole moment ($\varepsilon = -3$). Thus the intrinsic quadrupole

moment of ^{59}Ni (also ^{60}Ni) would tend to decrease compared to that of ^{58}Ni. It seems therefore that the occurrence of a rotational spectrum, though possible in this region, will be sensitively dependent on the number of particles out side ^{56}Ni core.

This is in contrast to the situation in the beginning of the s-d shell where the $\nu = 1$ orbit has $\varepsilon = 1$, which has the same sign as the quadrupole moment $\varepsilon = 4$ for the $\nu = 0$ orbit. It is (perhaps) for this reason that 'rotational' behaviour builds up and persists in the s-d shell and is not observed in the f-p shell.

It is amusing to compare the spectra of $^{56}_{26}Fe_{30}$ and $^{58}_{26}Fe_{32}$. From our discussion, the intrinsic quadrupole moment of the two neutrons in ^{56}Fe will be larger (by six units!) than that of the four neutrons in ^{58}Fe. The spectrum of ^{56}Fe (0^+, 2^+ (0.34 MeV), 4^+ (2.08) MeV) is more 'rotational', that of ^{58}Fe (0^+, 2^+ (0.80 MeV), 2^+ (1.66 MeV) looks like a 'vibrational' one.

One can understand in a similar way why many nuclei in the higher shells do not exhbit rotational spectra.

REFERENCES

1. I. Kelson and C. A. Levinson, Phys. Rev. 134, B 269 (1964)
   C. A. Levinson 'Lectures on Hartree Fock Theory and its applications to Nuclei, Tata Institute of Fundamental Research, Bombay (1964).
2. J.P. Elliott, Proc. Roy. Soc. (London) A245, 128 (1958)
3. S.G. Nilsson, Kgl. Dansk Videnskab. Selskab, Mat-Fys. Medd. 29, No.16 (1955).

INTRINSIC STATES IN $^{42}_{20}Ca_{22}$ AND $^{58}_{28}Ni_{30}$.

K.H. Bhatt
Physical Research Laboratory, Ahmedabad-9.
and
J.C. Parikh
Tata Institute of Fundamental Research, Bombay-5.

Shell model calculations of the wavefunctions of states in ^{42}Ca and ^{58}Ni are recently done (1). The extra 'core' neutrons in Ca are constrained to be in the $f_{7/2}$ and $p_{3/2}$ orbits only, while those of Ni are confined to the $p_{3/2}$, $f_{5/2}$ and $p_{1/2}$ states. It is shown here that these wavefunctions are just projections with definite angular momenta, of axially symmetrically deformed intrinsic states. χ_K, where K is the angular momentum along the symmetry axis.

PROJECTION FROM AN INTRINSIC STATE

States Ψ^I_{MK}, with angular momentum I and, projection M along the space fixed z axis, can be projected (2) from by the Hill - Wheeler integral.

$$\Psi^I_{MK}(x) = N^I_K \int D^I_{MK}(R)\, \chi_K(Rx)\, dR \qquad (1)$$

N^I_K is a normalization constant.

Axially symmetrically deformed single particle states can be written as

$$\varphi_K = \sum_j c_{jk}\, \psi_{jk} \quad \text{with} \quad c_{j,-k} = (-)^{j-k} c_{jk} \quad (2,3)$$

where ψ_{jk} are the spherical single particle states. A sketch of the energy sequence of Nilsson like (3) states is shown in the figure.

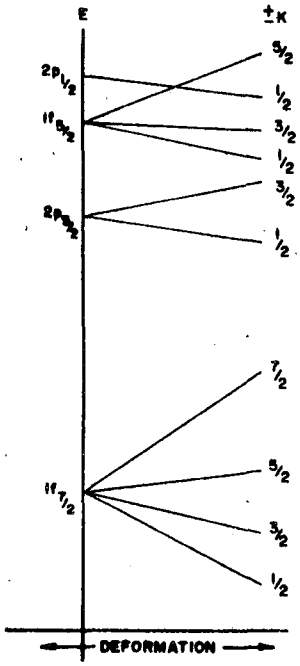

$$\varphi^{(2)}_{1/2} = \frac{1}{\sqrt{5}}\left[\sqrt{3}\left\{a\,\psi_{p_{\frac{3}{2}\frac{1}{2}}} + \sqrt{1-a^2}\,\psi_{p_{\frac{1}{2}\frac{1}{2}}}\right\} - \sqrt{2}\,\psi_{f_{\frac{5}{2}\frac{1}{2}}}\right]$$

$a = -0.927$

$$\varphi^{(1)}_{1/2} = \frac{1}{\sqrt{5}}\left[2\,\psi_{f_{\frac{7}{2}\frac{1}{2}}} - \psi_{p_{\frac{3}{2}\frac{1}{2}}}\right]$$

The antisymmetrized intrinsic states of ^{42}Ca and ^{58}Ni should be formed by putting the two extra core neutrons in the $k=\pm 1/2$ orbits indicated in the figure as $\varphi^{(1)}_{1/2}$ and $\varphi^{(2)}_{1/2}$ respectively. The states with definite angular momenta I generated from such an intrinsic state $\chi_{K=0}$ are

$$\Psi^{I}_{MK} = \sum_{j_1 j_2} A(j_1 j_2;\ k_1 k_2 K;\ I)\ \Phi^{I}_{M}(j_1 j_2) \qquad (4)$$

Here Φ^{I}_{M} is an antisymmetric two particle wavefunction.

The configuration mixing coefficients A are given by $A(j_1 j_2; k_1 k_2 K; I) = N^{I}_{K}\, C_{j_1 k_1}\, C_{j_2 k_2}\, (j_1 j_2 k_1 k_2 | IK) b$ (5) where $(j_1 j_2 k_1 k_2 | IK)$ is a clebsh-gordan coefficient and the constant $b = 1$ if $j_1 \neq j_2$ and $b = \sqrt{2}$ if $j_1 = j_2$. The values of $k_1 k_2$ and K are 1/2, - 1/2 and 0 respectively.

CHOICE OF THE INTRINSIC STATES

To determine the best values of the coefficients c_{jk}, we could vary their values to maximize the overlaps of the generated wavefunctions with the shell model ones. We suggest a method of determining these coefficients in analogy with the structure of the single particle states in the quadrupole field, in the absence of spin orbit interaction. These orbits in a Q_0^2 field are labled by $\nu = \langle lz \rangle$ and $\varepsilon = \langle Q_0^2 \rangle$ the quadrupole moment. The orbits with $\nu =$ 0 and 1 are

$$\varphi_0 = \varphi\left(\overset{\nu}{0},\overset{\varepsilon}{0}\right) = \frac{1}{\sqrt{5}}\left(\sqrt{3}\, f_0 + \sqrt{2}\, P_0\right)$$

$$\varphi_{\pm 1} = \varphi(\pm 1, +3) = \frac{1}{\sqrt{5}}\left(2 f_{\pm 1} - P_{\pm 1}\right)$$

$$\varphi'_{\pm 1} = \varphi(\pm 1, -3) = \frac{1}{\sqrt{5}}\left(f_{\pm 1} + 2 P_{\pm 1}\right)$$

$$\varphi'_0 = \varphi(0, 6) = \frac{1}{\sqrt{5}}\left(\sqrt{2}\, f_0 - \sqrt{3}\, P_0\right)$$

Here f and p are the Harmonic Oscillator states with $\langle lz \rangle = \nu$. The first two states, containing a larger amount of the f than the p state would be appropriate for constructing the intrinsic state for ^{42}Ca, the latter two for ^{58}Ni. We suggest that from among the two states which can contribute to the formation of a k = 1/2 orbit, we should choose the one having larger quadrupole moment ε. Thus the f-p admixture in $\varphi^{(1)}_{1/2}$ may be taken to be the same as in φ_1: Similarly the f-p admixture in $\varphi^{(2)}_{1/2}$ may be taken to be the same as in φ_0'.

<u>Intrinsic State For ^{42}Ca</u>. A k = 1/2 orbit restricting the particle to the $f_{7/2}$ and $p_{3/2}$ states is

$$\varphi^{(1)}_{1/2} = C_{7/2\ 1/2}\ f_{7/2\ 1/2} + C_{3/2\ 1/2}\ p_{3/2\ 1/2}.$$

Taking the f-p admixture the same as in φ_1 we get

$$\varphi^{(1)}_{1/2} = \frac{1}{\sqrt{5}}\ (2\ f_{7/2\ 1/2} - p_{3/2\ 1/2}) \qquad (6)$$

We use eq.3 to obtain $\varphi^{(1)}_{-1/2}$ and then eq. 5 to generate the wave functions.

<u>Intrinsic State For ^{58}Ni</u>. A k = 1/2 orbit restricting the particle to the $p_{3/2}$, $f_{5/2}$ and $p_{1/2}$ states is

$$\varphi^{(2)}_{1/2} = C_{3/2\ 1/2}\ p_{3/2\ 1/2} + C_{5/2\ 1/2}\ f_{5/2\ 1/2} + C_{1/2\ 1/2}\ p_{1/2\ 1/2}$$

We can take the f-p admixture to be the same as in φ_0' if we define

$$\varphi^{(2)}_{1/2} = \frac{1}{\sqrt{5}}\left\{\sqrt{3}\,(a\ p_{3/2\ 1/2} + \sqrt{(1-a^2)}\ p_{1/2\ 1/2}) - \sqrt{2}\,f_{5/2\ 1/2}\right\} \qquad (7).$$

We use eq.3 to obtain $\varphi^{(2)}_{-1/2}$ and eq.5 to generate the wave-functions. The parameter a(=-0.924) is fixed by equating the ratio

of the coefficients of the $p^2_{3/2}$ and $p_{3/2}\ p_{1/2}$ components of the I=2 generated and shell model wavefunctions.

DISCUSSION

The overlaps of the generated and shell model wavefunctions shown in the table under column 1,

	Ni Overlap		Ca Overlap	
I	1	2	1	2
0	0.990	0.983	0.988	0.996
2	0.958	0.989	0.967	0.997
4	0.997	0.999	0.892	0.970,

are quite good for Ni and good for Ca. The reason for the poorer agreement for Ca lies in our neglect of the effect of the spin orbit interaction while defining the generating orbits. We took the f-p admixture in $\varphi^{(1)}$ and $\varphi^{(2)}$ to be the same as in φ_1 and φ_0'. The f-p admixture in these latter orbits is obtained assuming that the f and p states are degenerate. In the presence of spin orbit splitting, we should expect that in $\varphi^{(1)}$ the amount of the $p_{3/2}$ state should be reduced since the $f_{7/2}$ is lower than the $p_{3/2}$ state. Similarly in $\varphi^{(2)}$ the amount of $f_{5/2}$ should be reduced. Since the $(p_{3/2}, p_{1/2})$ - $f_{5/2}$ splitting is much smaller than the $p_{3/2}$ - $f_{7/2}$ splitting, we expect the error we made in our choice of $\varphi^{(1)}_{1/2}$ to be larger than that for $\varphi^{(2)}_{1/2}$.

The overlaps given in the table under column 2 were obtained by using the generating orbits

$$\varphi^{1}_{1/2} = 0.958\ f_{7/2\ 1/2} - 0.287\ p_{3/2\ 1/2} \text{ and}$$

$$\varphi^{2}_{1/2} = 0.840\ (a\ p_{3/2\ 1/2} + \sqrt{(1-a^2)}\ p_{1/2\ 1/2}) - 0.542\, f_{5/2\ 1/2},$$

$$a = -0.924.$$

in which the f-p admixture has been modified to obtain the best overall agreement with the shell model wavefunctions.

The overlaps $\langle \varphi^{1}_{1/2} | \varphi^{(1)}_{1/2} \rangle$ and $\langle \varphi^{2}_{1/2} | \varphi^{(2)}_{1/2} \rangle$ are 0.985 and 0.993 respectively reflecting the accuracy of the method suggested here for determining the structure of the intrinsic states of nuclei.

REFERENCES:

1. S. Cohen, R.D. Lawson, M.H. Macfarlane, S.P. Pandya and M. Soga (Private communication from S.P. Pandya). T. Engeland and Osnes Phys. Letters 20, 424 (1966)

2. J.P. Elliott. Proc. Roy.Soc.(London) A 245, 128 (1958)

3. S.G. Nilsson, Kgl. Dansk Videnskab. Selskab, Mat-fgs Medd. 29, No. 16 (1955)

THE STRUCTURE OF LOW-LYING STATES OF EVEN-EVEN NUCLEI IN THE NEIGHBOURHOOD OF Sn

K.H. Bhatt
Physical Research Laboratory
Navarangpura,
Ahmedabad - 9.

ABSTRACT.

It is suggested that the low-lying states of even-even nuclei in the neighbourhood of the tin isotopes may be more properly describable in terms of the weak coupling between the low-lying states of the protons and neutrons rather than in terms of the collective quadrupole vibrations of the nuclei which imply a strong coupling between the protons and the neutrons.

THE GENERATING PROCEDURE AND THE STRUCTURE OF THE LOW LYING STATES OF NUCLEI

J.C. Parikh,
Tata Institute of Fundamental Research Centre
Colaba, Bombay-5.

and

K. H. Bhatt,
Physical Research Laboratory
Navarangpura,
Ahmedabad-9.

ABSTRACT.

The wave functions of the low lying states of $^{39}_{18}A_{21}$, $^{40}_{18}A_{22}$, $^{51}_{22}Ti_{29}$, $^{52}_{22}Ti_{30}$, $^{93}_{42}Mo_{51}$, $^{94}_{42}Mo_{52}$, $^{93}_{42}Nb_{52}$ have been obtained by projecting them from deformed intrinsic states in which both the protons and the neutrons are restricted to single j shells only. Thus for example the protons in $^{40}_{18}A_{22}$ are considered to be $d_{3/2}$ and the neutrons are considered to be in the $f_{7/2}$ shell. The projected wave functions are shown to have good overlaps with the corresponding shell model ones.

A SHELL MODEL STUDY OF ^{42}Ca AND ^{43}Ca ENERGY LEVELS

K. Sreenivasa Rao
Matscience, Madras,

and

S.C.K. Nair and S.K. Singh
Saha Institute of Nuclear Physics
Calcutta

A conventional shell model calculation of the energy levels in ^{42}Ca and ^{43}Ca is done with the over simplified 'realistic' interaction of Kallio and Koltveit. The state dependence of the separation distance is taken into account, so also the correction to the two body matrix elements stemming from the polarisation of the ^{40}Ca core. Comparison is made between our results and the recently published similar calculations and with the experimental numbers.

COLLECTIVE NATURE OF 1.29 MEV 2^+ STATE OF ^{116}Sn

S. Sen
Saha Institute of Nuclear Physics, Calcutta

The tin isotopes have drawn attention of many nuclear physicists, theoretical as well as experimental, because of its single closed shell (Z = 50) nature. The ^{116}Sn nucleus contains 50 protons and 66 neutrons. Theoretical calculations on nuclear structure of ^{116}Sn have been done by many authors (1,2) using a pairing interaction in short range residual nuclear force calculations. In this calculation we have used a very simplified model in order to explain the collective nature of the first excited 2^+ state of ^{116}Sn without recourse to any pairing force calculation. In the case of ^{116}Sn, 16 neutrons outside the closed shell, filling $1g_{7/2}$, $2d_{5/2}$, $3s_{1/2}$ states are assumed to form a closed shell core and we limit ourselves to only neutron excitation without including any isobaric spin formalism.

Methods of Calculation and Results:

We took $1p$-$1h$ neutron states as our basic states and matrix elements were calculated using δ-function interaction $-V_0\, \delta(\vec{r}_1 - \vec{r}_2)$.

Hole-particle matrix elements of δ-function interaction between j-j coupled antisymmetrized states are given by

$$V_{int} = A\,(j_1 j_2 J)\, A(j_3 j_4 J) + B(j_1 j_2 J)\, B(j_3 j_4 J)$$

where

$$A(j_1 j_2 J) = \sqrt{\tfrac{1}{2} I V_s}\; (-1)^{l_1+l_2+j_1} \sqrt{\frac{[j_1][j_2]}{[J]}} \begin{bmatrix} j_1 & j_2 & J \\ \frac{1}{2} & -\frac{1}{2} & 0 \end{bmatrix}$$

$$B(j_1 j_2 J) = \sqrt{\tfrac{1}{2} I V_s}\; (-1)^{l_1+l_2+j_1+j_2} \sqrt{\frac{[j_1][j_2]}{[J]}} \begin{bmatrix} j_1 & j_2 & J \\ \frac{1}{2} & \frac{1}{2} & 1 \end{bmatrix}$$

where V_s is the strength of the singlet-spin potential

$J = 2J + 1$, $\begin{bmatrix} j_1 & j_2 & J \\ \frac{1}{2} & -\frac{1}{2} & 0 \end{bmatrix}$ etc are Clebsch-Gordan coefficients,

ℓ_1, ℓ_2 are the orbital angular momenta corresponding to states 1 and 2 etc., and

$$I(n_1\ell_1, n_2\ell_2, n_3\ell_3, n_4\ell_4) = \frac{1}{4\pi}\int_0^\infty R_{n_1\ell_1} R_{n_2\ell_2} R_{n_3\ell_3} R_{n_4\ell_4} r^2 dr$$

where $R_{n\ell}$ is the radial wavefunction. Harmonic oscillator wavefunctions with oscillator parameter 'b' adjusted to 2.18 fm to fit r.m.s. radius of ^{116}Sn have been used. The matrix was diagonalised in order to get different eigen-values.

Transition probabilities for different gamma-transitions were calculated using the normalised eigenfunctions for first excited 2^+ and second excited 2^+ state from the following formula:

$$T(L) = \frac{8\pi(L+1)}{L[(2L+1)!!]^2} \frac{1}{\hbar}\left(\frac{\Delta E}{\hbar c}\right)^{2L+1} B(L\sigma)$$

where T(L) = transition probability (in sec^{-1}) for gamma rays of a given multipolarity L

ΔE = transition energy and $B(L\sigma)$ the reduced transition probability given by

$$B(L\sigma) = \frac{1}{2J_i+1}\left|\langle J_i \| M^L \| J_f\rangle\right|^2$$

Results obtained with strength of the δ-force $Vs/4\pi b^3$=22 MeV and different configurations entering into the calculations are given in table I, II, III and IV. The unperturbed energies of the various configurations have been determined very accurately from the experimental data (3) on ^{117}Sn and ^{115}Sn and from work of Cohen (4) et al.

Table I.

Unperturbed energies of one hole, one particle configurations entering in the $J = 2^+$ state calculation of Sn-116.

Configurations	Unperturbed Energies in MeV.
1. $1\ g^{-1}_{7/2}\ 2\ d_{3/2}$	3.97
2. $2\ d^{-1}_{5/2}\ 2\ d_{3/2}$	3.62
3. $3\ S^{-1}_{1/2}\ 2\ d_{3/2}$	2.59

Table II.

Normalised wavefunctions for first excited 2^+ and second excited 2^+ state of Sn-116

State	$1\ g^{-1}_{7/2}\ 2d_{3/2}$	$2\ d^{-1}_{5/2}\ 2\ d_{3/2}$	$3\ S^{-1}_{1/2}\ 2\ d_{3/2}$
First 2^+	- .1338	+ .7632	+ .6335
Second 2^+	+ .064	+ .4143	- .9025

Table III.

Calculated and Experimental level positions over ground state in MeV.

State (J, π)	Calculated	Experimental
First 2^+	1.29	1.29
Second 2^+	2.63	2.12
4^+	3.10	3.06

Table IV.

Calculated and experimental transition probabilities for different gamma transitions for two different values of effective charge of neutron

	Calculated values $e_n^{eff} = 1$	$e_n^{eff} = 1.5$	Experimental
T(E2) from first 2^+ to ground state T(M1) from second 2^+ to first 2^+	$.25 \times 10^{12} sec^{-1}$	$.56 \times 10^{12} sec^{-1}$	$1.4 \times 10^{12} sec^{-1}$
T(E2) from second 2^+ to ground state	1.8	.8	1

All the experimental results have been taken from Ref. 5.

REFERENCES:

1. Kisslinger and Sorensen, Kgl. Danske Videnskab Selskab Mat. Fys. Medd. 32, No.9 (1960)
2. R. Arvien, E. Baranger, M. Veneroni, M. Baranger and V. Giuet, Phys. Letters, 4, 119 (1963)
3. Landolt-Bornstein, Energy Levels of Nuclei A = 5 to A = 257 (1961)
4. B.L. Cohen : Private Communication
5. H.H. Bolotin : Phys. Rev. 136B, 1557 (1964)

PERCOMPOUND AND COMPOUND PARTICLES OF DECAY IN NUCLEAR REACTIONS

E. Kondaiah, K. Parthasaradhi and V.V.G. Sastry
The Laboratories For Nuclear Research
Andhra University, Waltair.

In the present paper, we have analysed the data on $^{80}Se(p,n)^{80}Br$ (1), $^{94}Zr(p,n)^{94}Nb$ (1), $^{118}Sn(p,n)^{118}Sb$ (2), $^{122}Sn(p,n)^{122}Sb$ (3), $^{40}Ca(n,\alpha)^{37}A$ (4), $^{56}Fe(n,\alpha)^{53}Cr$ (4), $^{58}Ni(n,\alpha)^{55}Fe$ (4), $^{27}Al(n,p)^{27}Mg$ (5), (6) and $^{59}Co(n,p)^{59}Fe$ (5),(7), on the same lines as Griffin (8) did using the "exciton" model and plotted $N(E_o).W_p(E_o)$ as a function of U for all the cases; only some typcial graphs are presented in Figure 1; here $N(E_o)$ stands for the number of particles having energy E_o and $W_p(E_o)$ is the corresponding probability for "prestatistical decay" of the compound nucleus.

The following observations may be made on an examination of Figure 1.

(i) Usually one expects direct interactions to predominate at forward angles and give rise to high energy particles of decay; this analysis shows that direct interaction, if it is defined to include all the "prestatistical decay" particles, does seem to predominate even at high excitation energies U, corresponding to low energies of emitted particles; this is borne out by the absence of significant rise at high U in Figure 1 (a), (d), (h), (j) and (k). So the thumb rule of attributing forward peaks in angular distributions to direct interactions may not , after all, be incorrect.

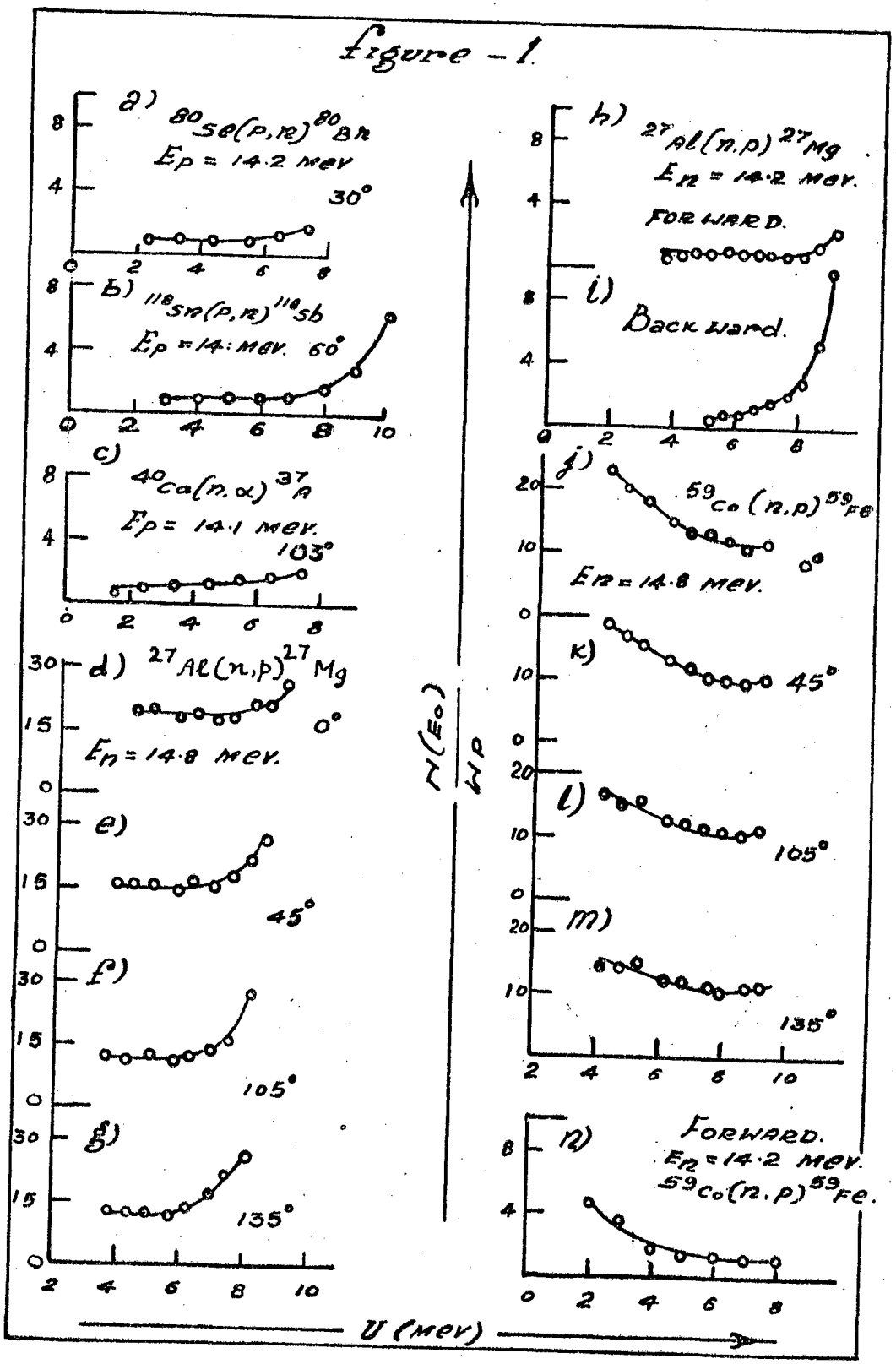
figure - 1.
a) 80Se(p,n)80Br
Ep = 14.2 mev
30°
b) 118Sn(p,n)118Sb
Ep = 14 mev. 60°
c) 40Ca(n,α)37A
Ep = 14.1 mev.
105°
d) 27Al(n,p)27Mg
0°
En = 14.8 mev.
e)
45°
f)
105°
g)
135°
h) 27Al(n,p)27Mg
En = 14.2 mev.
FORWARD.
i)
Backward.
j) 59Co(n,p)59Fe
0°
En = 14.8 mev.
k)
45°
l)
105°
m)
135°
n)
FORWARD.
En = 14.2 mev.
59Co(n,p)59Fe.
σ(E0)
WP
U (mev)

(ii) For $^{118}Sn(p,n)^{118}Sb$ reaction (Fig. 1 (b)), the curve obtained by us from the distribution at 60° is similar to the one reported by Griffin (8); $^{122}Sn(p,n)^{122}Sb$ also shows similar behaviour. It seems in the case of Sn isotopes, the statistical decay of the compound nucleus predominates even at forward angles at high excitation, U, of the residual nucleus Sb; Sn has a closed shell for protons and one might further explore whether similar effects can be seen in (p,n) reactions in the case of other closed shell nuclei.

(iii) In the case of (n,α)reactions analysed by us, Fig.1 (c) the statistical decay particles appear to be small even at back angles (103°); this may be due to the Coulomb barrier effects.

(iv) It is interesting to see how the present analysis ties up with the conventional notion that as one proceeds from forward to backward angles, the statistical compound-nuclear decay particles predominate over the direct interaction contributions; this fact is clearly brought out in Figs. 1 (d) to (g) from analysis of the $^{27}Al(n,p)^{27}Mg$ data (5) and in Fig. 1 (h) and (i) from an analysis of the same reaction using the data of Nair et al (6). The data of Mohindra and Hans (5) was taken with a counter telescope that did not resolve the individual groups whereas the data of Nair et al (6) was taken using Nuclear emulsions which has shown clear peaks at the high energy end of the particle spectrum emitted at forward angles. It may be mentioned that we have taken the continuous smooth distribution under the peaks for our analysis whenever such peaks are clearly visible in the spectra reported. Both the data (5), (6) show that statistical compound-nuclear

decay predominates at back angles in the high U region.

(v) The analysis of $^{59}Co(n,p)^{59}Fe$ data (5) presented in Fig. 1 (j) to (m) as well as the analysis of data (7) on the same reaction presented in Fig. 1 (n) show a rise at low U; in the latter data (7) the individual peaks are clearly visible and have been taken into account by us.

One might expect such a rise at low U (high energies of emitted particles) due to special processes like the knock off, if they are not properly taken into account by the "exciton" model of Griffin (8), however, the persistent rise at low U in Fig. 1 (j) to (n) at all angles is rather surprising. It may, however, be noted that the rise at low U in Fig. 1 (j) to (m) diminishes as one goes from 0° to 135° showing the relative importance of compound-nuclear particles at back angles.

In conclusion, one might say that Griffin (8) has given an additional method of testing the presence of direct interaction contributions in the emitted particle spectrum and understanding the same as a natural consequence of the "excition" model.

REFERENCES:

1. Y. Sajiet et al.
EANDC-50-S, Article 20, International Conference on the study of nuclear structure with neutrons held at Antwerp, Belgium (1965)

2. R. Wood, R. Borchers, and H. Benachall, Nucl. Phys. 1, 71, 529 (1965)

3. R.R. Borchers et al., Reference 1, Article 119.

4. M. Bormann et al., Reference 1, Article 110

5. R.K. Mohindra and H.S. Hans., Nucl. Phys. 44,597 (1963)

6. K.G. Nair et al., Nucl. Phys. 26, 193 (1961)

7. W. Jack and A. Ward., Proc. Phys. Soc., 75, 833 (1060)

8. J.J. Griffin, Phys. Rev. Letters, 17,9,478 (1966)

DISCUSSION:

S.K. Gupta: (1) Where do you put the precompound emission on time scale? (2) How much precompound part has been observed in the data analysed by you?

E. Kondaiah: (1) The time scale extends right from the time connected with the usual direct interaction (that is $\sim 10^{-22}$ sec) upto the time of statistical equilibrium decay, which may be anywhere up to a million times longer. (2) It is not possible to give an absolute value of the direct intraction contribution or even the ratio of the D.I/C.N. by this method of analysis. The only thing one can say is whether there is a large contribution of C.N. (statistical) decay over the precompound decay in the experimental energy distribution. If there is such a large contribution of the statistical decay particles at high U (excitation energy of the residual nucleus) then it is justified to use the spectrum to obtain statistcal parameters such as Temperature etc. from the portion of the spectrum where such

a steep rise occurs. If this type of analysis does not show a large enough region where the C.N. (statistical) component predominates, it is doubtful whether such an energy spectrum can be used to obtain statistical parameters.

FLUCTUATION ANALYSIS OF THE COMPOUND NUCLEUS LEVELS OF ^{52}Cr

C.M. Lamba, N. Sarma and N.S. Thampi
Bhabha Atomic Research Centre
Trombay, Bombay
and
D.K. Sood and V.K. Deshpande
Indian Institute of Technology
Kanpur.

A brief account of all possible aspects of the fluctuation theory as applied on the reaction "elastic scattering of protons from ^{51}V" is presented in this work.

Excitation functions at angles (100°, 120°, 140°, 160°) covering energy range 4.005 to 5.515 in steps, δE of 5 keV are measured with an experimental resolution, ρ of 1 keV and two of them are shown in Fig.1. The cross section for inelastic proton and alpha groups was too small to cross background barrier.

1.1. AUTO CORRELATION ANALYSIS FOR FULL RANGE OF DATA:

Auto-correlation functions (1) for total energy range, were calculated. It is found that $C_p(\epsilon)$ does not fluctuate about ϵ axis but has a linear modulation imposed on it. This behaviour is attributed to energy dependent non fluctuating process. In such a case the modified auto correlation function (1) is a Lorentzian displaced by an amount $K_0'(\epsilon)$ from ϵ axis. $K_0'(0)$ is a measure of modulation. The form of $K_0'(\epsilon)$ could not be calculated accurately but is visually estimated to be a

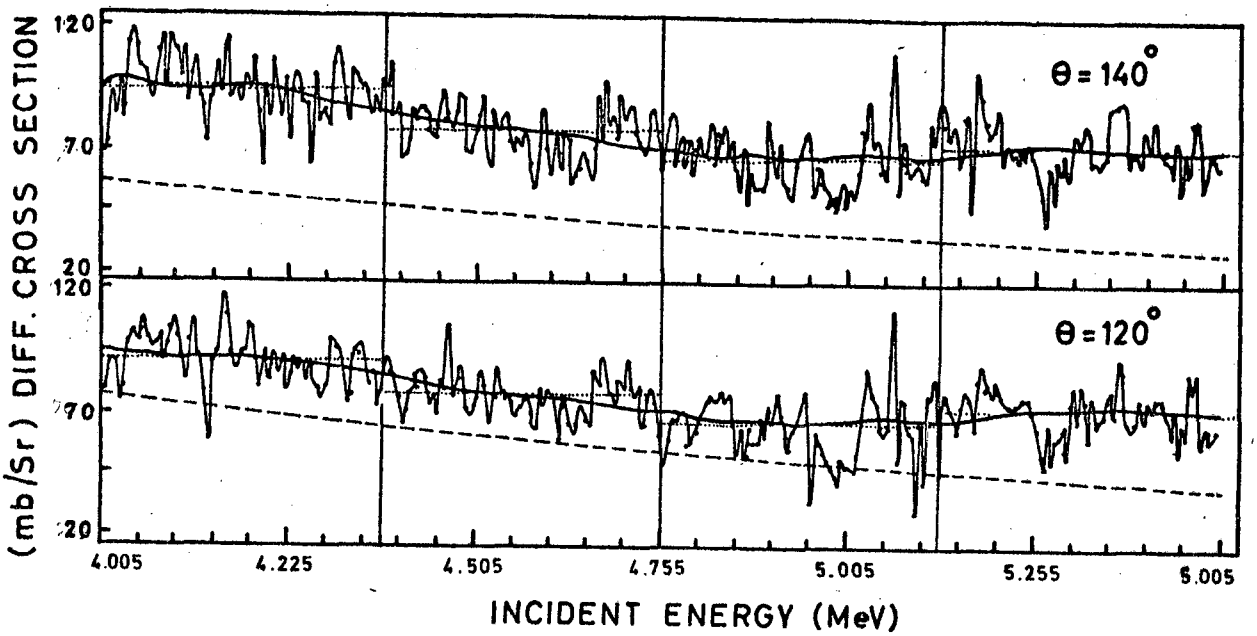

FIG-1

TABLE I

θ_{LAB} DEG.	$C_p(0)$	$K_o'(0)$	$C_p(0)-K_o'(0)$	$C_p^q(0)$	$\Delta C_p(0)$	Γ_{RAW} (KeV)	Γ_{CORR} (KeV)	Γ_q (KeV)	Γ_{CORTI} (KeV)	$\frac{\Delta\Gamma}{\Gamma}$
100	0.0636	0.0512	0.0124	0.0166	±0.0040	22.4	3.5	4.0	3.6	±0.084
120	0.0348	0.0164	0.0184	0.0206	±0.0048	17.3	3.5	4.4	4.0	±0.084
140	0.0422	0.0222	0.0200	0.0236	±0.0048	34.5	4.0	4.1	4.3	±0.084
160	0.0583	0.0300	0.0283	0.0363	±0.0065	24.0	3.5	4.0	4.4	±0.085

straight line. This shows the presence of strong modulation. The width Γ_{RAW} (ignoring modulation) and Γ_{CORR} (corrected for modulates) are shown in Table I.

The modulation effects are eliminated by taking local average of Q points of energy width $q\Gamma$. The value of $q\Gamma$ is chosen from the q dependence of $C_p^q(0)$. The agreement of $C_p(0)$ and $(C_p(0) - K_0'(0))$ (Cf. Table I) shows that this metod elimination modulation effects. The level width Γ_q are also shown.

In Fig. 1, the averaged cross section $\sigma_q(E_i)$ for $q\Gamma$ = 400 keV and Rutherford scattering cross sections are shown with thick and dotted lines respectively. Minimum at 4.955 MeV at all angles gives an idea of the presence of intermediate structure of width 900 keV. However, considering that $\sigma_q(E_i)$ comprises of so many other factor it is not possible to isolate intermediate structure.

2.1. DETERMINATION OF Γ BY VARIABLE ENERGY RESOLUTION METHOD:

The autocorrelation analysis is not a very sensitive tool when $\delta E > \rho$ and $\delta E > \Gamma$. As it has been made sure that $C_p(0)$ and probability histograms (section 5.1) do not vary with step size a method proposed by Corti is a more reliable tool for extracting Γ. (To ensure that two excitation functions of 151 points each were constructed at each angle with δE = 10 keV using alternate points). $C_p(\rho)$ the normalised variance decreases

rapidly as ρ increases, the rate of decrease depending on ρ/Γ. By successive application of formula

$$\sigma_r(E_i) = \frac{1}{r}\sum_{j=i}^{j=i+r-1} \sigma(E_j)$$

new excitation functions with worse resolutions are obtained. If square resolution function, $\rho_0 = \delta E$ new resolution for the rth operation is $r\rho_0$. In the present case $\rho_0 < \delta E$ so for $r = 1, 2, 3$ ..... excitation functions are assumed to have resolutions $\rho_0, 2\delta E, 3\delta E$ - - - -

The function $C_p(\rho)$ is fitted with Gibb's formula (2) for various ρ values. This function is very sensitive to the value of ρ chosen. The values of Γ obtained are shown in Table I as Γ_{CORTI}.

3.1. CROSS CORRELATIONS:

Angular cross correlations were calculated and a rise with increasing $q\Gamma$ is found and is ascribed to modulation effects. We find that cross correlations for (100°, 120°), (100°, 140°,), (100°, 160°,) are .703, .6076 and .4906 respectively.

Theoretical estimate of coherence angle when Y_D is high is difficult to make.

4.1. The energy is then divided in four equal parts (shown by vertical lines in Fig. 1, because firstly Y_D is less dependent on energy over a smaller range so that probability distribution

analysis to get N, Y_D assuming Y_D constant is justified and secondly a systematic variation of C(o) & Γ can be studied.

4.2. The auto correlation analysis for 4 parts separately has indicated the following.

(i) As $\sigma_q(E_i)$ does not differ from $\langle\sigma(E_i)\rangle_p$ (dotted lines parallel to energy axis in Fig.1.), $K'_0(0)$ is small and functions $C_p^q(E)$ and $C_p(E)$ are identical.

(ii) $C(0)$ varies very much within energy range thus showing variation of Y_D over energy range assuming N constant

(iii) Γ does not vary with energy within the error of 0.8 keV.

5.1. PROBABILITY DISTRIBUTION:

32 sets of experimentally normalised probability histograms $P_\theta^{Ex}(\gamma)$ for full range considering local averages are found quite similar. As N is quite large increase in either N or Y_D produces similar effects. As a result large number of (N, Y_D) sets fit experimental distributions equally well. These sets were restricted by following constraints.

(a) N does not vary through an energy block

(b) $\sigma_D \geq \langle \sigma_{Ruth} \rangle$

(c) such (N, Y_D) sets should give a $C(0)$ value which agrees to experimental one within errors. The following are the best sets.

Angle	N	Part (1) Y_D	Part (2) Y_D	Part (3) Y_D	Part (4) Y_D
100°	24 ± 3	0.85 ± 0.05	0.85 ± 0.05	0.60 ± 0.10	0.70 ± 0.10
120°	20 ± 3	0.83 ± 0.03	0.87 ± 0.05	0.50 ± 0.10	0.75 ± 0.05
140°	20 ± 3	0.80 ± 0.07	0.75 ± 0.05	0.60 ± 0.12	0.70 ± 0.07
160°	15 ± 3	0.76 ± 0.04	0.67 ± 0.05	0.53 ± 0.08	0.67 ± 0.06

As expected by theory N falls at backward angles. Theoretical value of N at 90° is 128 in this present reaction. This prediction of theory is not at all satisfactory as from data N exp = $\frac{1}{C_p^2(0)}$ at 100° is 60 and any direct process Y_D will lower N exp. further.

CONCLUSIONS:

(1) A large range (energy and angle) of data must be studied so that modulation, which standard theory does not describe, may become apparent.

(2) Γ obtained by different methods agree well but Corti's method is found to be more reliable in present circumstances.

(3) For local averages proper averaging interval should be chosen.

(4) Probability distribution analysis shows that it is meaningful to distinguish direct and compound contributions even at high excitations where compound nucleus lives for a very small time.

(5) Probability histograms and normalised variance are unaffected by step size provided sample is large enough.

REFERENCES:

1. B.W. Allardyce et al, Nucl. Phys. 35, 193 (1966)

2. M. Corti et al, Energia Nucleare 13, 312 (1966)

3. T. Mayer Kuckuk, Experimental Evidence of Statistical Fluctuations, Hercegrovi Lectures.

STUDY OF THE STRUCTURE IN THE EXCITATION FUNCTIONS FOR THE REACTIONS $^{27}Al(p,\alpha_0)^{24}Mg$ AND $^{27}Al(p,\alpha_1)^{24}Mg^*$

M.K. Mehta, A.S. Divatia, S.S. Kerekatte and K.K. Sekharan
Bhabha Atomic Research Centre
Trombay, Bombay.

ABSTRACT.

In continuation of previous work (1), the yields from the reactions $^{27}Al(p,\alpha_0)^{24}Mg$ and $^{27}Al(p,\alpha_1)^{24}Mg^*$ have been measured at a few angles for the range of proton bombarding energy from 4 to 5.5 MeV. The excitation functions reveal a gross structure on which finer variations are superimposed. A cross-correlation analysis is under progress to determine whether the strong resonance like structures are indeed resonances representing individual levels in the compound nucleus ^{28}Si and not the so called Ericson fluctuations.

REFERENCES:

1. M.K. Mehta and A.S. Divatia, Proceedings of the N.P. and S.S.P. Symposium Bombay 80 (1966).

$^{51}V(p,n)^{51}Cr$ REACTION BETWEEN 1.56 AND 5.53 MEV

K.K. Sekharan, M.K. Mheta and A.S. Divatia
Bhabha Atomic Research Centre
Trombay, Bombay.

The total neutron yield for the $^{51}V(p,n)^{51}Cr$ reaction has been measured in the incident proton energy range 1.56 to 5.53 MeV using a 4π neutron counter. A thin Vanadium metal target evaporated on to a thick tantalum backing was bombarded with protons, the incident protons being monitored by a current integrator. The step in which the yield was measured varied from 6 to 10 keV. The excitation function a part of which is shown in figure 1 shows a number of peaks which are overlapping. The dots are the total cross section values obtained by a separate measurement using a thick target.

$^{51}V+p$ in the incident energy range 1.56 to 5.53 MeV leads to an excitation energy of about 12 to 16 MeV in the compound nucleus ^{52}Cr which is the statistical region. The data was, therefore, analysed on the basis of the fluctuation theory. Since the neutron yield increases rapidly with the incident energy the data was split into three ranges of energy namely 1.56 - 2.55, 2.55 - 3.84 and 3.84 - 5.53 MeV. The auto correlation function $C(\epsilon)$ was evaluated using the equation

$$C(\epsilon) = \frac{\Delta E}{E_2 - E_1} \sum_{E_1}^{E_2} \left(\frac{\sigma(E_i)}{\langle \sigma(E_i) \rangle} - 1 \right) \left(\frac{\sigma(E_i + \epsilon)}{\langle \sigma(E_i + \epsilon) \rangle} - 1 \right)$$

for the three energy ranges separately for various values of the averaging interval, δ. In figure 2 C(0) is shown as a function

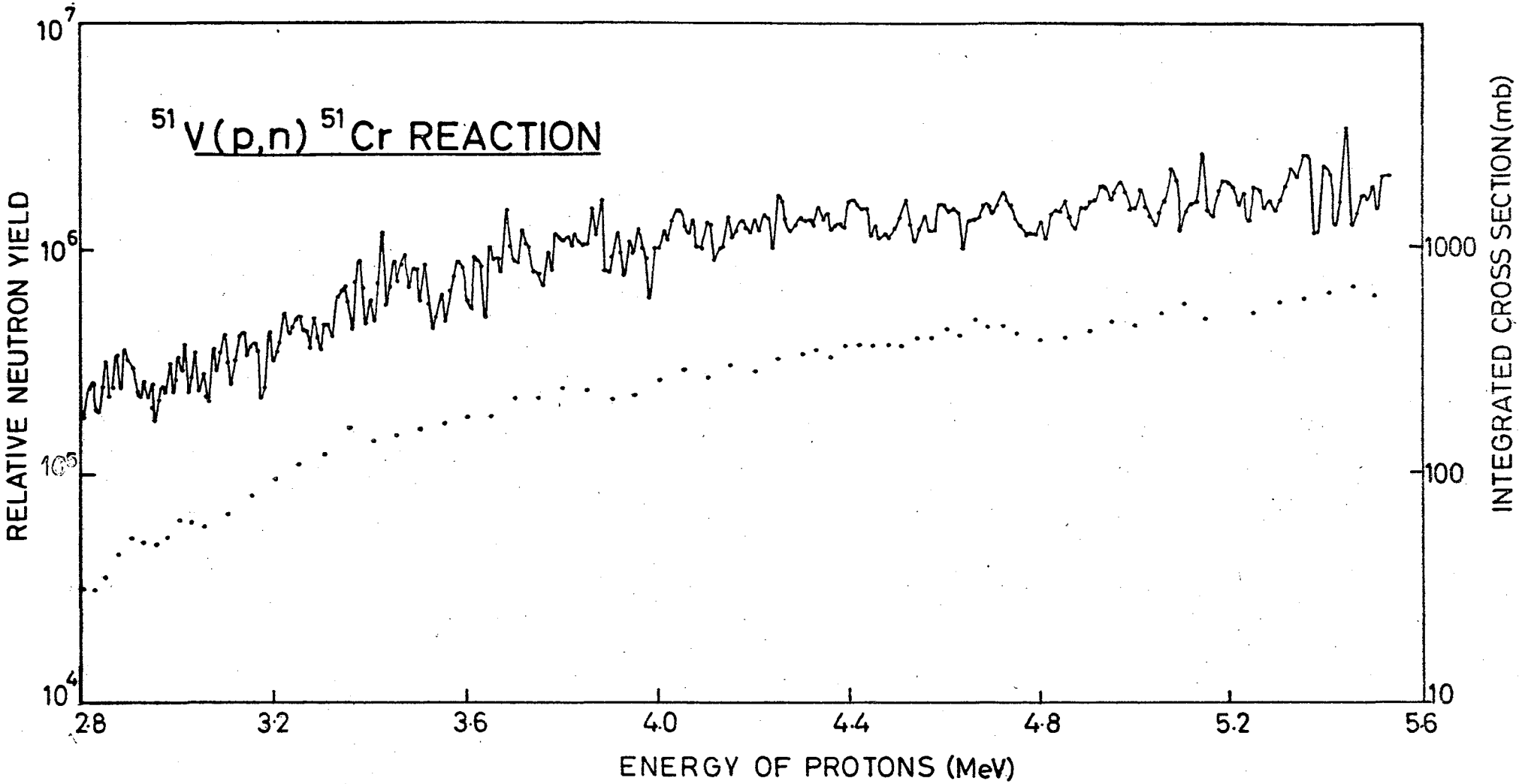
$^{51}V(p,n)^{51}Cr$ REACTION
RELATIVE NEUTRON YIELD
10^7
10^6
10^5
10^4
INTEGRATED CROSS SECTION (mb)
1000
100
10
2·8
3·2
3·6
4·0
4·4
4·8
5·2
5·6
ENERGY OF PROTONS (MeV)

FIG. 1

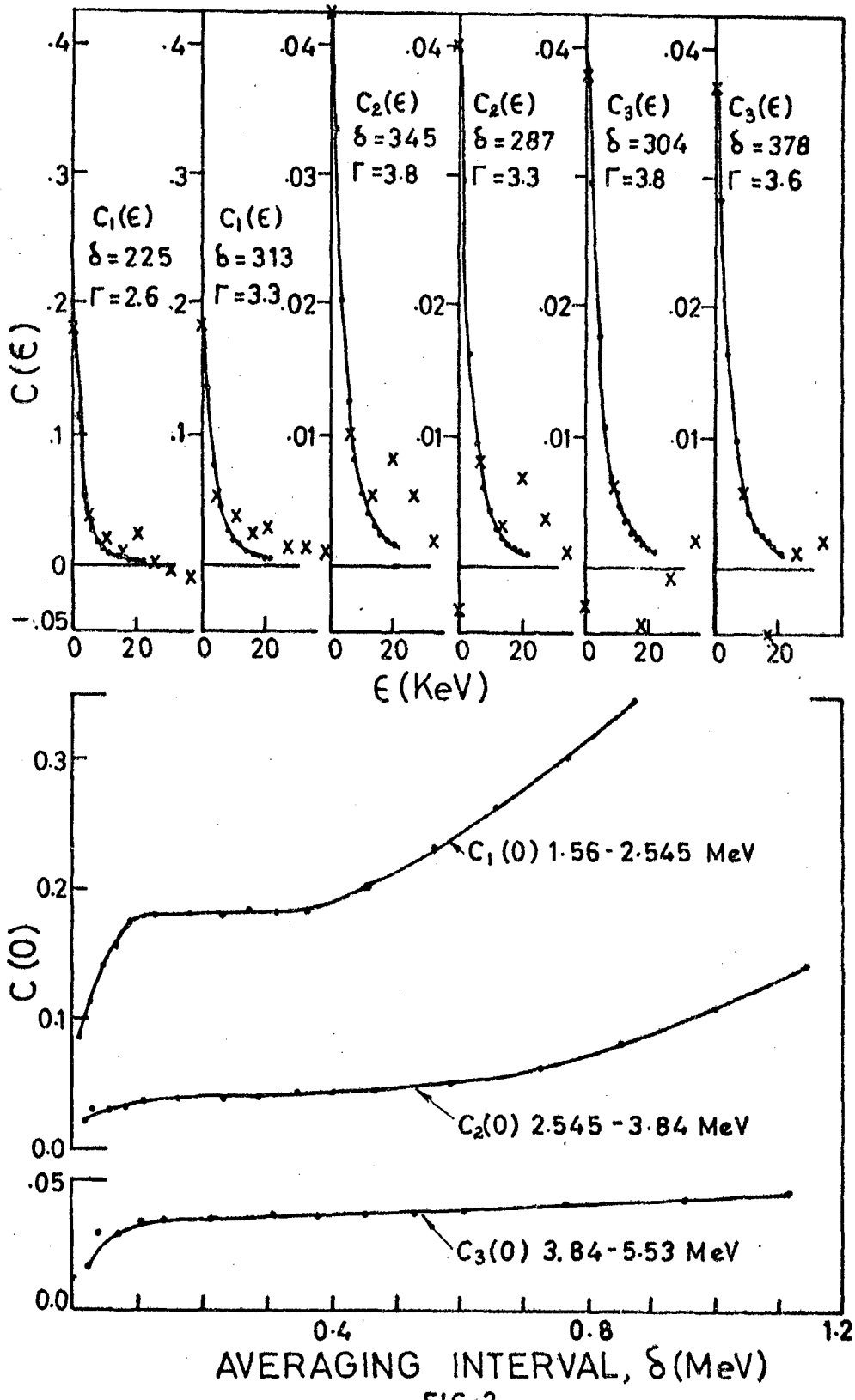
C(ε)
C₁(ε) δ=225 Γ=2.6
C₁(ε) δ=313 Γ=3.3
C₂(ε) δ=345 Γ=3.8
C₂(ε) δ=287 Γ=3.3
C₃(ε) δ=304 Γ=3.8
C₃(ε) δ=378 Γ=3.6
ε (KeV)
C(0)
C₁(0) 1.56-2.545 MeV
C₂(0) 2.545-3.84 MeV
C₃(0) 3.84-5.53 MeV
AVERAGING INTERVAL, δ(MeV)

FIG-2

of δ for the three energy ranges. C(0) remains constant for a certain range of values of δ for all the three curves. Averaging interval is chosen from this range for evaluating the average width, Γ. In the upper portion of figure 2, C (ϵ) against small values of ϵ is plotted for averaging intervals equal to 225,313,287,345, 304 and 378 keV. Crosses are the experimental points. The dots are the calculated values using the formula $C(\epsilon)=C(0)\frac{\Gamma^2}{\Gamma^2+\epsilon^2}$ where Γ is the average level width. Since the energy step in which the neutron yield is measured is large compared to the average width obtained there are only two or three experimental points which lie on the Lorentzian. Since there are only two or three points on the curve error as much as $\pm$ 50% of Γ could be assigned to the value of Γ though the F.R.D. error is much smaller.

In the present experiment the experimental resolution, ρ is about 1.5 keV which is less than the average width Γ and the energy step ΔE. In an ideal case for which fluctuation analysis is applied ρ and ΔE should be less than Γ. Corti et.al(1) have developed a method of extracting Γ where $\Gamma < \rho$. For applying this method a necessary condition is that ΔE should be equal to ρ. In the present experiment since ρ is less than ΔE Corti's method was not applied.

The average width, Γ obtained for levels in the ^{52}Cr nucleus in the excitation energy range 12 to 16 MeV is 3.5 keV.

REFERENCES:

1. M. Corti, M.G. Marcazzan, L. Milazzo Colli and M. Milazzo, Energia Nucleare, 13, 312 (1966).

FLUCTUATIONS IN THE INTEGRATED CROSS SECTION OF THE REACTION $^{45}Sc(p,n)^{45}Ti$

K.V.K. Iyengar and S.K. Gupta
Tata Institute of Fundamental Research, Colaba, Bombay-5.

and

K.K. Sekharan, M.K. Mehta and A.S. Divatia
Bhabha Atomic Research Centre, Bombay-74

The integrated cross section of the reaction $^{45}Sc(p,n)^{45}Ti$ was measured in the incident proton energy range 2.910 - 5.250 MeV, corresponding to the excitation energy range 13.195 - 15.485 MeV in the compound nucleus ^{46}Ti. Scandium evaporated onto thick aluminium was used as the target. Its thickness was determined by observing the shift of the $^{27}Al(p,\gamma)^{28}Si$ resonances at 1.38 MeV due to the energy lost by the proton beam while traversing through the scandium. The over all experimental energy resolution was $\approx$ 3.5 keV (taking the thickness of the target into account) around 4 MeV the mean incident energy. This scandium target was placed at the centre of 4π geometry neutron counter (1) consisting of a BF_3 counter paraffin assembly, and was bombarded by protons from the 5.5-MV Van de Graaff accelerator at Bhabha Atomic Research Centre, Trombay, The yield of the neutrons was measured as a function of the proton bombarding energy in steps of 5 keV starting from the threshold at 2.910 to 5.250 MeV and is shown in fig.1. These measurements were repeatedly checked to ensure the reproducibility of the data. The neutron yield shows a large number of fluctuations. Since at the excitations reached

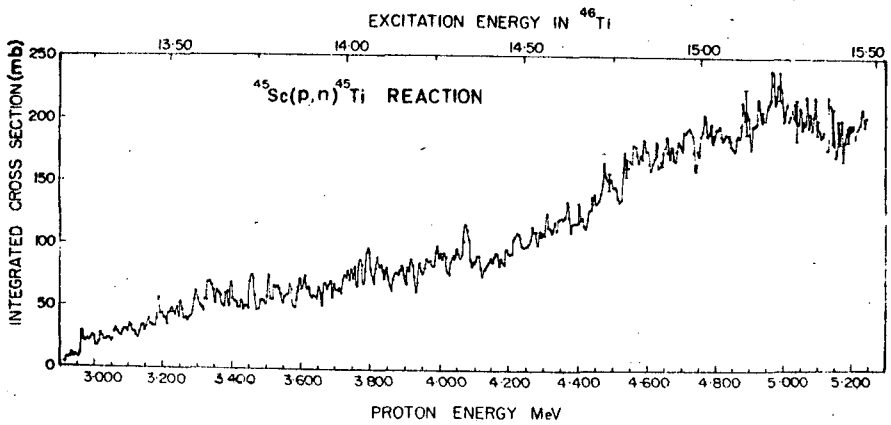

FIG-1

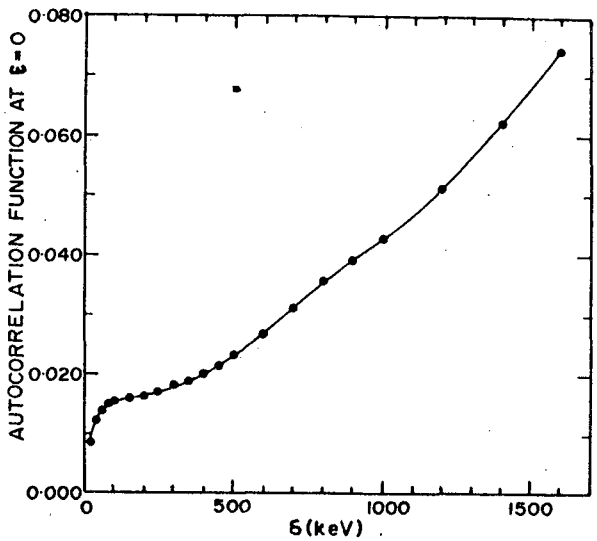

FIG-2

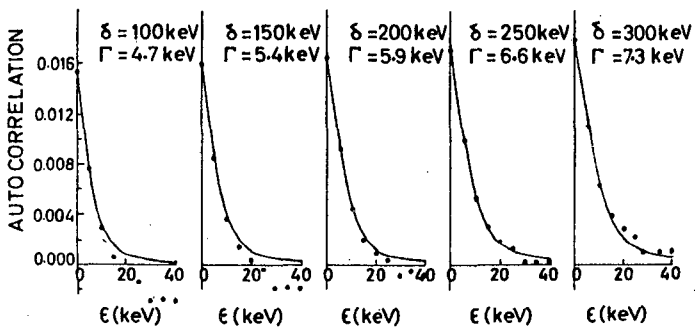

FIG-3

in the present experiment $\langle\Gamma\rangle/D$ is expected to be $\gg 1$ on theoretical considerations a fluctuation analysis of the data was carried out. Only the data in the energy range 2.940 - 4.890 MeV was used for the fluctuation analysis as the reproducibility was poor beyond 4.900 MeV. The fluctuations in the reaction cross-section are superimposed on an average cross section which increases from 18 mb to 208 mb over the energy interval 3.000 - 4.890 MeV. This increase in the average cross section is essentially due to the effect of increasing penetrability for protons. The absolute error on the measured cross section is 25%. The rather low amplitude of the fluctuations could be due to the damping by the large number of open neutron reaction channels and the high target spin of 7/2. The observed neutron yield which is due to contributions from neutrons leading to all energetically allowed states of the residual nucleus ^{45}Ti has been however assumed to be mainly due to the neutron groups feeding the ground state and the first excited state of ^{45}Ti at 25 keV, and that their energies are the same. The autocorrelation function

$$c(\varepsilon) = \frac{\Delta E}{E_2 - E_1} \sum_{E=E_1}^{E_2} \frac{\left[\sigma(E+\varepsilon) - \langle\sigma(E+\varepsilon)\rangle\right]\left[\sigma(E) - \langle\sigma(E)\rangle\right]}{\langle\sigma(E+\varepsilon)\rangle\langle\sigma(E)\rangle}$$

where ε is the energy increment, $\langle\ \rangle$, a total average over the averaging interval δ, ΔE the energy step in which data is taken, E_1 and E_2, the initial and final energies of the energy interval chosen for analysis, was calculated for various averaging intervals δ. Singh et al (2), have discussed in detail the need and

the criteria for choosing properly the averaging interval δ, especially when the cross section itself is a function of bombarding energy. In fig.2 is shown the dependence of C(0) on δ. It can be seen that C(0) remains fairly constant over the interval 100-300 keV. The coherence width Γ was determined for δ's in the interval 100-300 keV by linear least squares fitting of the data to the expression $C(\varepsilon) = C(0) \frac{\Gamma^2}{\Gamma^2 + \varepsilon^2}$. The curves so obtained are shown in fig.3 and the values of Γ vs δ are presented in table 1.

Table I

Coherence energy for a number of averaging intervals δ obtained in fig. 4.

δ (keV)	Γ (keV)
80	4.1
100	4.7
150	5.4
200	5.9
250	6.6
300	7.3

The FRD errors on the Γ were estimated using the curves and relations given by Gibbs (3). Thus a mean value of 6 $\pm$ 1 keV

was obtained for the coherence width Γ in the compound nucleus ^{46}Ti at the mean excitation energy of 14.3 MeV. This value is in complete conformity with the value of 8 keV obatined by Bamberger (4) and Richter et al (5) for the same nucleus ^{46}Ti at the mean excitation energy of 19 MeV. The value obtained for Γ in the present experiment lies well within the limits of 1.5 - 23 keV predicted by Corti et al (6) for this nucleus on theoretical considerations.

REFERENCES:

1. K.K. Sekharan, M.Sc. Thesis, Bombay University, unpublished(1966)
2. P.P. Singh, R.E. Segel, L. Meyer-Schutzmeister, S.S. Hanna and R.G. Allan, Nuclear Physics 65, 577 (1965)
3. W.R. Gibbs, Phys.Rev. 139, B1185 (1965)
4. A. Bamberger, Diploma Arbeit, Heidelberg, to be published (1965)
5. A. Richter, A. Bamberger, P.Von Brentano, T. Mayer-Kuckuk and W. Von Witsch, 21a, 1001 (1966)
6. M. Corti, M.G. Marcazzan, L. Milazzo Colli, M. Milazzo, Energia Nucleare 13, 312 (1966)

DISCUSSION:

D.K. Sood: What are the errors on the values of Γ you have determined? Gibbs estimate of FRD errors is almost obsolete by now. I feel the FRD errors should have some variation with the value of moving averaging interval?

K.V.K. Iyengar: You may be right. But Gibbs FRD errors are for a stationary excitation function or rather when C(o) is not a function of averaging interval. What we do in this method, is to obtain C(o) as a function of averaging interval, choose the region where it is almost independent of δ and use it to determine Γ. The errors are obtained then using Gibbs relations. Since C(o) is almost independent of δ for the δ ranges chosen, Gibbs expressions and results must still hold good. We do not think it is inapplicable under the conditions stated above.

D.K. Sood: You showed a plot of systematic variation of Γ with A. Don't you think your value $\langle\Gamma\rangle$ is rather high in the context of the general variation shown?

K.V.K. Iyengar: The relation quoted by me was an empirical one. Our value is in full conformity with the systematics within the error quoted by us.

STOCHASTIC THEORY OF FISSION

R. Ramanna and V.S. Ramamurthy
Bhabha Atomic Research Centre
Trombay, Bombay.

Fragment mass asymmetry in low energy fission of heavy nuclei has so far defied a rigorous theoretical explanation. It has been shown earlier (1,2) that it is possible to give a description of the fission process as a stochastic process. It was also shown that by introducing nuclear structure effects in the description it is possible to explain the systematics in the fragment mass distributions.

Reviewing the proposed mechanism, a heavy nucleus given sufficient energy to overcome the energy barrier for the fission process, passes over the barrier, after which division into two parts becomes imminent. However, scission takes place much later, and in view of the experimental evidence for the influence of the fragment structure effects on the fission process, one can assume that as the fissioning nucleus proceeds towards the scission point, certain grouping of the contituent nucleons into two parts takes place. These two groups gradually start exhibiting properties of their own. They, however, retain a nuclear interaction between them and hence do not fly apart due to the Coulomb repulsion. As a result of the nuclear

interaction, the two groups can also change their identity i.e continuous regrouping of the nucleons also takes place in time, which is assumed to proceed through nucleon exchanges. Since we are interested in the final distribution of the fragment masses, one can specify the configuration of the fissioning nucleus at any instant t, by specifying the number of nucleons in either group. The division process can now be completely described by a set of probabilities.

I_M = the probability that the fissioning nucleus has a configuration with mass M on one side at any instant t.

F_M = the probability that the fissioning nucleus has a configuration with mass M as the same side at instant $t + \Delta t$, where Δt is the unit of time.

$P_{M,M'}$ = the probability that the fissioning nucleus having a configuration with mass M on one side goes over to one with mass M' on the same side, in unit time Δt.

These probabilities are related as

$$F_M = \sum_{M'} I_{M'} P_{M'M}$$

Assuming that only single nucleon transfers take place and that steady state is reached before scission takes place, one gets

$$I_M = \omega_M = I_{M-1} P_{M-1,M} + I_M P_{M,M} + I_{M+1} P_{M+1,M}$$

where ω is the observed mass distribution. Making use of the relation

$$P_{M,M-1} + P_{M,M+1} + P_{M,M} = 1$$

one gets

$$\frac{\omega_{M+1}}{\omega_M} = \frac{P_{M,M+1}}{P_{M+1,M}}$$

To evaluate the transition probabilities, we consider the process to take place in two steps.

(i) The nucleon releases itself from the structure of one side and

(ii) Attaches itself to the other side

Hence $P_{M,M-1} = P_D\, P'_A\, T_D\, (1-P'_D\, P_A\, T'_D)$

$P_{M,M+1} = P'_D\, P_A\, T'_D\, (1-P_D\, P'_A\, T_D)$

$P_D\, P'_A$ and $P'_D\, P_A$ represents the statistical weights for the respective processes and are given by the level density of the fissioning nucleus after the exchange. T_D and T'_D are expected to include the structure effects of the two sides involved in the exchange.

To evaluate T_D we examine the potential seen by a nucleon along the symmetry axis of the fissioning nucleus (Fig.1). Prior to the saddle point, where there is no indication of a separation into two groups, the potential energy diagram is that of a deformed nucleus. On the other hand near the scission point, the fissioning nucleus can be approximated

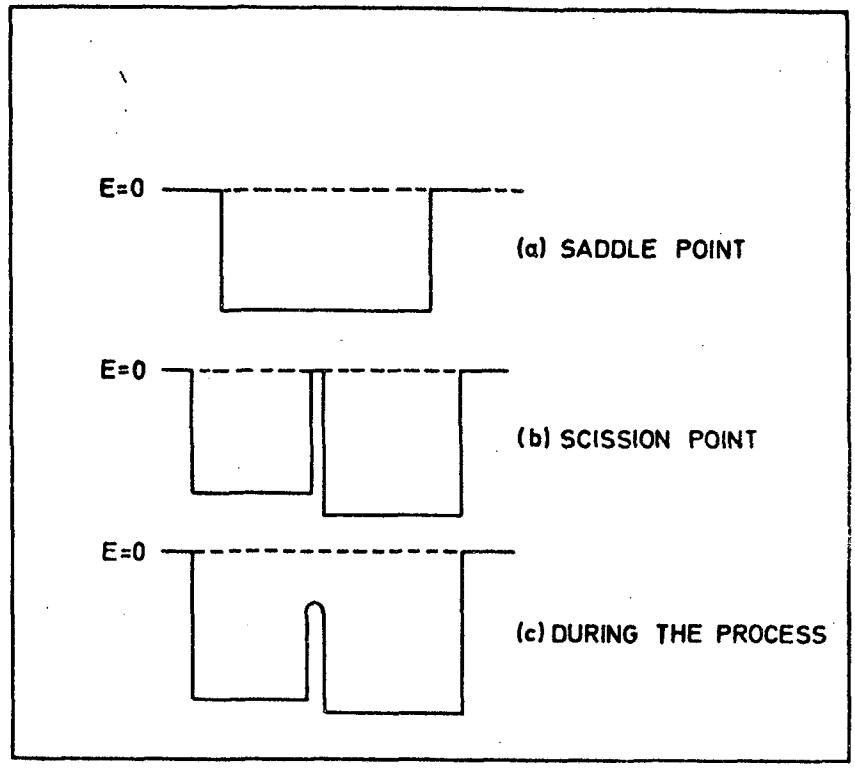
E=0
(a) SADDLE POINT
E=0
(b) SCISSION POINT
E=0
(c) DURING THE PROCESS

FIG. 1

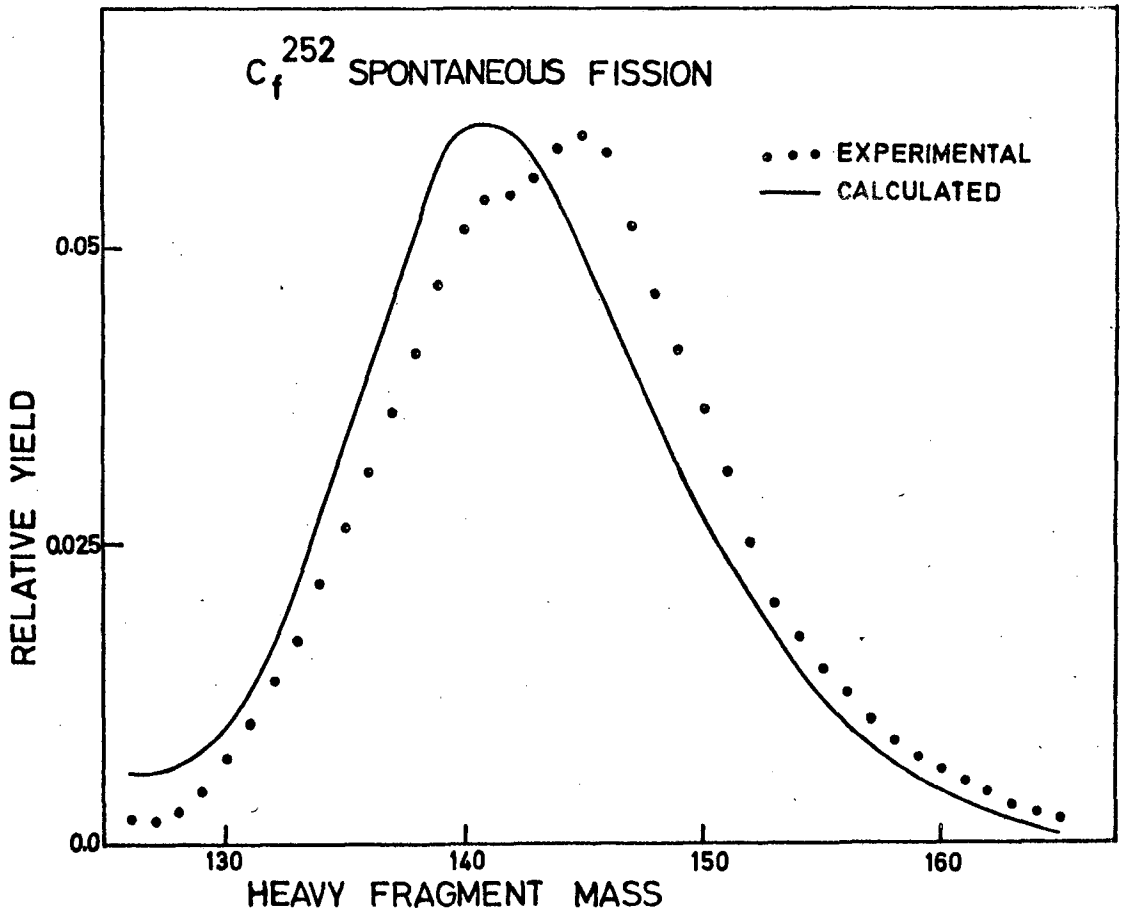
C_f^{252} SPONTANEOUS FISSION
EXPERIMENTAL
CALCULATED
RELATIVE YIELD
0.05
0.025
0.0
130
140
150
160
HEAVY FRAGMENT MASS

FIG. 2

by two independent nuclei in contact and the potential energy diagram is as shown. Hence during the process one would expect a growing barrier, separating the two groups of nucleons. The probability T_D can then be taken to represent the penetration probability of a nucleon through this barrier. Hence T_D will depend on the energy state of the transferred nucleon and the nature of the barrier.

Since at present, no information is available on the spectrum of energy states of a nucleon in a deformed nucleus, we assume that all the nucleons on the average have an energy-E, where E is the average binding energy of a nucleon in the nucleus, given by the semiempirical mass formula. To evaluate the penetration factor through the barrier we make use of Hill's expression for an inverted parabola to give the functional form.

$$T = \frac{1}{1+\exp\left[E/\hbar\omega\right]} \simeq \exp\left(-E/\hbar\omega\right)$$

where $\hbar\omega$ is a constant, characterising the nature of the barrier.

To evaluate E we make use of the mass formula as given by Mayer and Swiatecki (3) according to which ABE = $(ABE)_{\text{Liquid drop}}$ + $(ABE)_{\text{shell}}$ + deformation. The first term refers to a spherical liquid drop, and the second term takes care of the deformation and shell structure effects and has to be evaluated for deformations pertinent to the fission process. A static study of the scission configuration has shown that the deformable nuclei are deformed more at scission. Hence we write

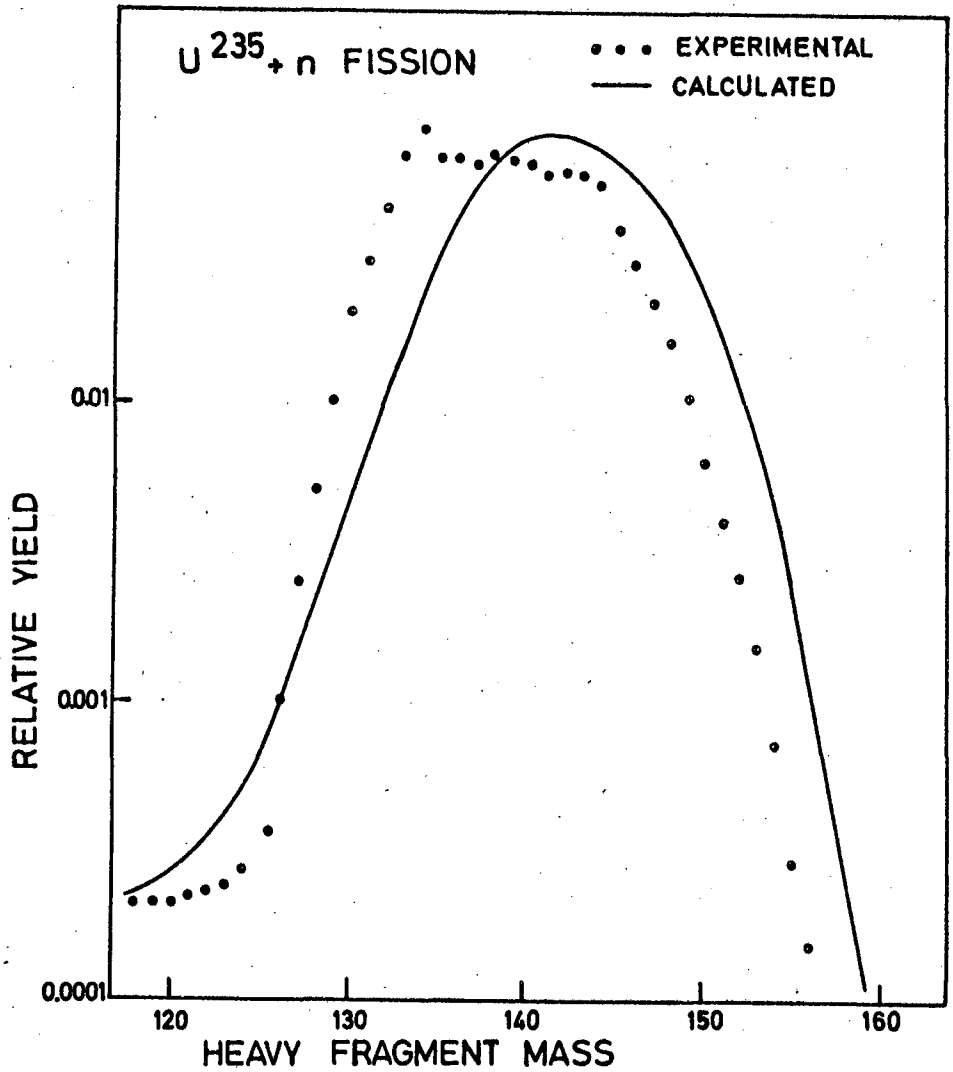
U 235 + n FISSION
EXPERIMENTAL
CALCULATED
RELATIVE YIELD
0.01
0.001
0.0001
120
130
140
150
160
HEAVY FRAGMENT MASS

FIG. 3

$$ABE = (ABE)_{L.D.} + K\,(ABE)_{shell + deformation}$$

where K is a constant and the second term is evaluated for ground state deformations.

The resulting mass distribution in the case of ^{252}Cf spontaneous fission and neutron induced fission of ^{235}U are shown in Figs. 2 and 3, with $K = 6$

Another intersting possibility, suggested by the above investigations is the study of charge distribution in fission. So far we have assumed that the charges divide in the ratio of the masses. However if one writes the probabilities in terms of the number of neutrons and protons, one can treat the problem as a two dimensional random walk, in which case one can study the charge distribution also. The possibility is being investigated.

REFERENCES:

1. R. Ramanna, R. Subramanian and Raju.N. Aiyer, Nuclear Physics 67, 529 (1965).
2. R. Ramanna and V.S. Ramamurthy Physics Letters 21, 437 (1966).
3. W.D. Myers and W.I. Swiatecki, Nuclear Masses and deformations, UCRL-11980 (1965).

DISCUSSION:

R.S. Kaushal: Do you get any idea about induced fission, if so can you apply it to explain mass distribution of induced binary fission?

V.S. Ramamurthy: The proposed mechanism applies to all fission processes irrespective of the trigger used to supply the necessary energy.

Shankar Mukherjee: By taking into account the charge of the transferred nucleon, is it possible to predict charge distribution in fission?

V.S. Ramamurthy: Yes, though claculations would be more involved.

R.K. Tandon: In the experimental results, what is plotted in the Y axis for relative yield? How were these experimental results obtained?

V.S. Ramamurthy: The relative yield plotted in the Y axis represents the fraction of the total number of fission events, giving rise to mass divisions, characterised by the mass of the heavy fragment. The simplest method of measuring the masses of the fragments is to simultaneously measure the energies of the two fragments. Conservation of momentum requires

$$M_1/M_2 = E_2/E_1$$

$M_1 + M_2$ = Mass of the fissioning nucleus. Hence M_1 and M_2 can be inferred.

ANGULAR ANISOTROPY OF FISSION FRAGMENTS IN 3 MeV NEUTRON INDUCED BINARY AND TERNARY FISSION OF ^{235}U

D.M. Nadkarni
Bhabha Atomic Research Centre
Trombay, Bombay.

To understand the mechanism of ternary fission, fission accompanied by long range alpha particles (LRA), it is important to know at what stage of the process these particles are emitted. The measurement of fragment angular distributions in ternary fission can be expected to provide an understanding about the stage at which LRA are emitted. Previous measurements (1) of angular distribution of fragments in ternary indicated that the anisotropies in binary and ternary fission are different. In the present work using solid state detectors the anisotropy of fragments in ternary fission of ^{235}U induced by 3 MeV neutrons has been measured.

EXPERIMENTAL SET-UP:

Two diffused-junction type solid state detectors were used to detect fission fragments emitted along and at right angles to the incident neutron beam direction and the third solid state detector was kept very close to the fissile target to detect LRA in nearly 2π geometry. (Fig.1) ^{235}U target was 1 mg/cm^2 thick on a 8 mg/cm^2 Al backing which allowed only

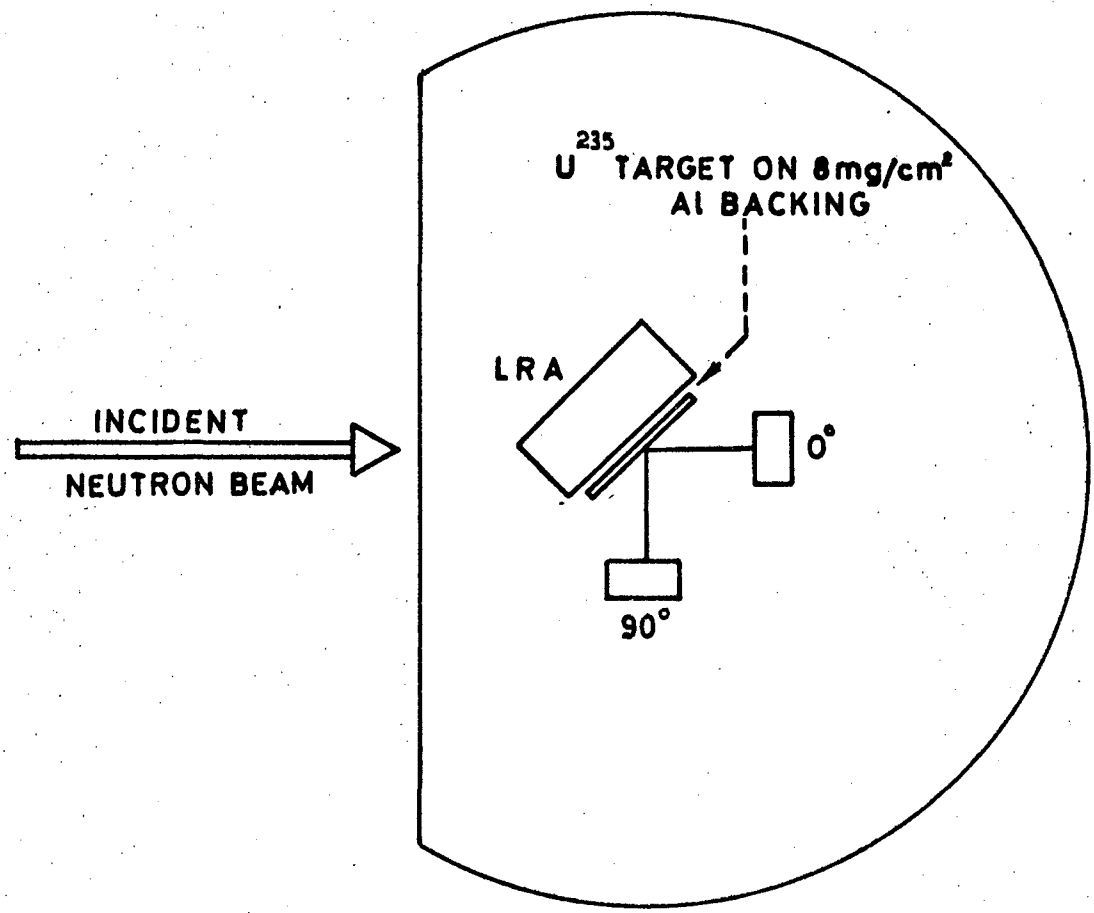
U^{235} TARGET ON 8mg/cm²
Al BACKING
LRA
INCIDENT
NEUTRON BEAM
0°
90°

LRA to reach the back detector. 3 MeV neutrons were produced with $T(p,n)^3He$ reaction using the 5.5 MeV Van-de-Graaff Accelerator. The very low cross-section for fast neutron induced ternary fission necessitated keeping the fragment detectors near the target resulting in poor angular resolution ($\approx 35^\circ$). The spectra of fission fragment kinetic energy in 0°-and 90°-detectors in coincidence and anti-coincidence with the LRA pulse were recoreded simultaneously in four 100-channel analyzers. Efficiency correction factors for 3 MeV neutron induced binary and ternary fission were made using the isotropic fragment distribution in thermal neutron induced binary and ternary fission. The thermal neutron measurements were carried out by surrounding the fission chamber with paraffin blocks and keeping the chamber configuration constant. About 810 events of 3 MeV neutron induced ternary fission and about 1590 events of thermal neutron induced ternary fission were recorded in a series of runs lasting nearly 100 hours.

RESULTS:

The results of these measurements are (i) Binary fragment anisotropy $(N(0^\circ)/N(90^\circ)) = 1.04 \pm 0.01$
(ii) Ternary fragment anisotropy $(N(0^\circ)/N(90^\circ)) = 0.87 \pm 0.06$
(iii) The ternary to binary cross-section ratio was found to be about 50% and 25% lower for 3 MeV neutron fission as compared to thermal neutron fission, in the 0° and 90° directions

respectively. (iv) The decrease in the average kinetic energy of ternary fission fragments compared to that of binary fragments was found to be approximately equal (14 ± 3 MeV) both in the thermal and 3 MeV neutron induced fission.

The rather low binary anisotropy is attributed to the poor angular resolution as well as to the variation of the neutron flux across the fissile target. The binary fragment anisotropy was separately measured for the case where the neutron flux is nearly uniform across the fissible target and was found to be 1.107 ± 0.017. Using the values of binary anisotropies measured in the present work and that reported by Simmons and Henkel (2), approximate correction for the angular resolution and non-uniform flux of neutrons across the target have been made to the ternary fission data. The corrected ternary anisotropy was found to be (0.91 ± 0.07).

DISCUSSION:

It is of interest to correlate (n,α) anisotropy in 3 MeV neutron induced ternary fission of ^{235}U (3) with the anisotropy of ternary fragments measured in the present work. According to the Evaporation Model (1) the angular distribution of LRA is given by

$$n_\alpha(\theta) \approx 1 + \frac{\alpha^2 \overline{I^2}\,\overline{l^2}}{2} \cos^2\theta \approx a + b\cos^2\theta$$

Imposing on this the condition that LRA and ternary fission fragments are emitted at right angles to each other, the ternary fragment angular distribution obtained is $n_{tf}(\theta) \approx a + \frac{1}{2}\sin^2\theta$. Using the LRA anisotropy (3) of 1.32 ± 0.12 this gives for the ternary fragment anisotropy a value of 0.86 ± 0.05 which is in fair agreement with the value obtained in the present measurements. The results of the present work suggest that due to the emission of LRA the K-distribution at the scission stage in ternary fission is different from that in binary fission.

REFERENCES:

1. R. Ramanna, K.G. Nair and S.S. Kapoor, Phys. Rev. 129, 1350 (1963); D.M. Nadkarni, Proc. Nucl. Phys. Symposium, P.35 (1966).
2. J.E. Simmons and R.L. Henkel, Phys. Rev. 120, 198 (1960)
3. V.A. Hattangadi, T. Methasiri, D.M. Nadkarni, R. Ramanna and P.N. Rama Rao, SM-60/71, IAEA Symposium, on Phys & Chem. of Fission, Salzburg (1965).

DISCUSSION:

S. Mukherji: You mention that αs come out first and then fission occurs. Are we right in talking about fission after α comes out from the neck? After what time (from α emission moment) does fission occur?

D.M. Nadkarni: It is precisely for the reason that it is not possible to find directly from experiments whether α-s are emitted before or after scission that the present measurements on angular distribution of ternary fission fragments were made. I believe we are right in talking about α-s coming out from the neck region of fissioning nucleus towards the last stages of scission and being emitted in the region between the heavy fission fragments as shown by the (α, f), (n,α) and $(n,\alpha f)$ correlations. As α-s come at the last stages of fission, the time between the α emission and subsequent snapping is not definitely known but it must be pretty short ($\sim 10^{-22}$ sec). Further work on this in future, it is hoped, will answer this question.

Question: What is the cross section for $^{235}U(n,\alpha)$ reaction at 3 MeV?

D.M. Nadkarni: Measurements of (n,α) at these incident neutron energies have not yet been reported, as far as I know. For thermal neutron case at least the (n,α) cross-section is an order of magnitude smaller than $(n,\alpha f)$ cross-section.

R.K. Tandon: What is expected to be the energy of incident neutron beam bombarding uranium target?

D.M. Nadkarni: The incident neutron energy is about 3 MeV with a spread of about 100 keV.

S. Mohan Bharathi: What is the error in your measurement?

D.M. Nadkarni: These are preliminary results as mentioned earlier and anisotropy $N(0^\circ)/N(90^\circ)$ mentioned was 1.07 ± 0.02; the error quoted is statistical error only. Corrections due to finite angular resolution and non uniform neutron flux over the uranium target have not yet been made. This correction is expected to decrease the 90° peaking of the ternary fission fragment angular distribution by about 5% roughly. However, accurate corrections to the data will be made in future.

S.K. Gupta: How do you identify the alpha particle coming from the fission? It can very well be ^3He or ^3He.

D.M. Nadkarni: The α particles were not identified as such but it has been very well established by earlier workers, that most of the light charged particles emitted ($\sim$ 95%) are alpha particles.

KINETIC ENERGY DISTRIBUTION OF FISSION FRAGMENTS IN THE FISSION OF ^{235}U INDUCED BY NEUTRONS IN THE ENERGY REGION: THERMAL TO 2 MeV.

D.M. Nadkarni and B.R. Ballal
Bhabha Atomic Research Centre
Trombay, Bombay.

ABSTRACT.

Studies on the angular distribution of fission fragments have indicated a large pairing gap of about 2.7 MeV in the transition state spectra of heavy even-even fissioning nuclei. To study the possible dependence of fission fragment average kinetic energy $\overline{E}_k$, on the nature of the transition states, $\overline{E}_k$ has been measured in the fission of ^{235}U induced by neutrons of energy ranging from thermal to 2.1 MeV. A gridded ionization chamber filled with pure Argon was used to measure $\overline{E}_k$ and monoenergetic neutrons were generated with $T(p,n)^3He$ reaction using the 5.5 MeV Van-de-Graaff Accelerator, the neutron energy spread being about 100 keV. The ion chamber calibration was done using thermal neutron fission, recording the fission spectrum on a 100 channel analyser. Measurements were made at 22 different energies in this region with 2.5×10^4 to 7.5×10^4 events being recorded at each of these energies. The measured $\overline{E}_k$ was corrected for the centre of mass motion. $\overline{E}_k$ was found to

remain constant within about 0.6% ($\approx$ 1 MeV) in this region. However, a slight decrease of $\overline{E}_k$ of the order of about 700 keV, was observed at $E_n \approx$ 370 keV and 870 keV and a slight increase of about 900 keV was observed at $E_n \approx$ 650 keV and 1240 keV as compared to $\overline{E}_k$ for thermal neutron fission. Although these variations could be due to statistical fluctuations the possibility that these are associated with the nature of transition spectrum cannot be ruled out. The results of Blyumkina et al (1) who observed increase of $\overline{E}_k$ at $E_n \approx$ 770 keV and a decrease at $E_n \approx$ 400 keV and those of Mather et al (2) who observed small peaks in $\overline{\nu}$ Vs E_n data at $E_n \approx$ 230 keV and 840 keV followed by a decrease at $E_k \approx$ 700 keV and 930 keV compare well with the present measurements.

REFERENCES:

1. Yu. A. Blyumkina et al. Nuclear Physics 52, No.4, 648 (1964)
2. D.S. Mather et al. Phys. Rev. 133, No. 6B, B 1403 (1964)

P-WAVE NEUTRON FISSION OF ^{235}U

G.K. Mehta
Department of Physics
Indian Institute of Technology, Kanpur

and

J.M. Lebowitz and E. Melkonian
Department of Physics
Columbia University, New York

INTRODUCTION

A correlation between the observed mass distributions of fission fragments and the spin and parity of the compound nucleus is expected from the "channel-theory" of Aage Bohr (1). According to Bohr's theory the nucleus at the saddle point is relatively unexcited, as most of the excitation energy goes into the deformation, and should have well defined states. The ordering of these states with energy can be guessed from studies of nuclei at their equilibrium deformation. For an even-even nucleus low lying states are $0^+, 2^+, 4^+$ etc. followed by 1^-, 3^- etc. at higher excitation energies. If we take the accepted assignment of $7/2^-$ for ^{235}U then we can build up a spin of 3^- or 4^- for the compound nucleus with slow neutron absorption. Considering the case where the compound nucleus is formed in a 3^- state, the nucleus has to pass through the saddle point which corresponds to this spin value which is few hundred keV higher than the lowest saddle point (0^+) available. If on the other hand, the compound nucleus is formed in the 4^- state then the barrier which is to be surmounted is much higher, may be 1 or 2 MeV higher than the 3^- barrier. So one expects that fission

on taking place through these two channels might bear some differences which can be experimentally detected. There is some experimental evidence of this kind of correlation. One also expects that fission proceeding through an even parity saddle point would show a more symmetric mass distribution (higher valley in mass distribution curve) than that proceeding through an odd parity state.

If the neutron energy is increased so that the p-wave interactions become probable then one can excite even parity levels in addition to 3^- and 4^-. In this case it is reasonable to believe that the symmetric fission yield should be more than for s-wave neutrons. Rae, Margolis and Troubetskoy(2) have calculated the partial wave fission cross-section (upto $l = 3$) for ($^{235}U + n$). According to their calculations the p-wave interaction predominates in 100 keV to 500 keV region, and both p and d waves contribute appreciably from 500 keV to ~1 MeV. Radiochemical measurements have been made by Cunnighame, Kitt and Rae (3) in this region. They found that the mass distribution is more asymmetric in the 65 keV to 125 keV region than thermal mass distribution and above 200 keV the symmetric fission yield increases. The result between 65 and 125 keV was contrary to what one would expect from simple channel theory. We have made an attempt to make these measurements using back-to-back solid state detectors.

Any change in mass distribution should reflect in the total kinetic energy distributions. According to the correlation found in the previous work (4), lower mean kinetic energy should correspond to higher valley (more symmetric fission) and higher mean kinetic

energy to lower valley (less symmetric fission). Also wider total kinetic energy distribution should lead to more symmetric fission(5).

In the results presented here the widths of kinetic energy distributions and the valleys of mass distribution curves are examined for several neutron energies and compared with the corresponding thermal neutron values.

EXPERIMENT:

Neutrons were produced by the Li(p,n) reaction using protons from Columbia University 5.5 MeV Van de Graaff. For 60 keV neutrons backward angle was used. The thickness of the lithium target varied from 20 keV to 100 keV depending upon the neutron energy desired, keeping the energy spread of the neutron beam reasonable. The fission chamber consisted of a back-to-back arrangement of surface barrier silicon detectors. The detectors were fabricated in the laboratory on a thin mica mount so as to keep the scattering minimum. A thin layer of $^{235}U(50\mu gm/cm^2)$ was evaporated on one of the detectors. The fission fragment from both the detectors were recorded in coincidence on a 2-Parameter data acquisition system. The data were recorded directly on magnetic tape and processed on IBM 7090 computer. Measurements were made at 60 keV, 120 keV, 200 keV, 300 keV, 500 keV, 750 keV, 1.0 MeV, 1.5 MeV and 2.0 MeV neutron energies. A thermal neutron run was taken after each change in neutron energy to keep check on over-all performance of detectors and the electronic system. Unfortunately a part of 60 keV run and the entire 120 keV data was lost while transferring the data from one magnetic tape to other. Consequently the results

presented here do not include these two energies. About 40,000 events were recorded for each run.

RESULTS AND DISCUSSION:

In the computations we normalized the two peaks in the kinetic energy distribution curves to line up at 68.4 MeV and 99.6 MeV. This way one avoids the problem of keeping track of drifts in the electronic system from one run to another. However, in doing so we missed the information about the dependence of mean kinetic energy of fission fragments on the neutron energy. In order to get this information one has to go back to the raw data and normalize the runs using the information from the thermal runs which were taken after each run. This has not been done as yet.

The counts in the valley of mass distributions corresponding to different energies of incident neutrons are normalized and presented in Table I. It must be mentioned that the mass distributions obtained by using solid state detectors are usually distorted because of inherent problems associated with these detectors. So the results on the symmetry of fission should be taken with caution. Nevertheless the variations observed are well outside the statistical deviations and the data for all the thermal runs is consistent. Therefore, it gives us some confidence in these numbers.

The widths of total kinetic-energy distributions were determined, at several heights, for each neutron energy. These are listed in table II. We observe from these tables that the symmetric fission yield increases in the energy range of 750 keV to 1.0 MeV and decreases again at higher energies but remains greater than the thermal value. Similar trend is observed in the widths of the

kinetic energy distributions also. This shows a clear correlation between the valley of mass distribution and the total kinetic energy distribution. Our plan is to repeat some measurements and confirm our findings and also get the data in the 60 keV to 120 keV region again before drawing any definite conclusions.

Table I

Relative Probability of Symmetric Fission

No.	Neutron Energy	Normalized counts in the valley of Mass Distributions
1.	200 keV	758± 32
2.	300 keV	722± 27
3.	500 keV	719± 27
4.	750 keV	898± 42
5.	1.0 MeV	958± 47
6.	1.5 MeV	805± 30
7.	2.0 MeV	815± 39
8.	Thermal (average of all runs)	738± 19

Table II.

Width (W) of the total Kinetic-Energy-Distributions.

No.	Neutron Energy	W at $\frac{7^{th}}{10}$ of Max.	W at ½ Max.	W at $\frac{1^{th}}{10}$ of Max
1	200 keV	16.07*	25.34	47.47
2	300 keV	17.20	25.25	47.28
3	500 keV	17.34	25.59	46.82
4	750 keV	18.40	26.63	47.55
5	1.0 MeV	18.48	26.65	48.65
6	1.5 MeV	16.80	24.43	46.77
7	2.0 MeV	18.56	25.51	47.17
8	Thermal (average of all runs)	17.94	25.3	47.13

* Errors in W are of the order of 1%.

REFERENCES:

1. A. Bohr, Paper P/911, Proc. Intern. Conf. Peaceful uses of Atomic Energy, Geneva (1955).
2. E.R. Rae, B. Mangolis and E.S. Troubetskoy, Phys. Rev. 112, 492 (1958)
3. J.G. Cunninghame, G.P. Kitt and E.R. Rae, Nucl. Phys. 27, 154 (1961)
4. G.K. Mehta and E. Melkonian, Transactions American Nuclear Society Vol 6, 262 (1963)
5. E. Melkonian and G.K. Mehta, Proc. Intern. Symposium on Physics and Chemistry of Fission, Salzburg, Vol.II, 355 (1965)

DISCUSSION:

S. Mukherjee: Was there a simultaneous counting in the peak region? There might be a simultaneous lowering in the counts in the two regions due to decrease in fission cross section.

G.K. Mehta: Yes, this was done.

N. Sarma: Do you observe any correlation between the values you have and the total σ_f variation with energy?

G.K. Mehta: No.

R. Rangarajan: How did you ascertain that $\ell = 1$ is predominating?

G.K. Mehta: Rae et al have made calculations on partial wave fission cross section. According to that in the region of neutron energy 65 keV to 125 keV $\ell = 1$ wave predominates.

ENERGY DISTRIBUTION LIGHT CHARGED PARTICLES FROM THERMAL FISSION OF ^{235}U, ^{239}Pu AND SPONTANEOUS FISSION OF ^{252}Cf.

V.A. Hattangadi
Bhabha Atomic Research Centre, Trombay.

The energy spectra of the light charged particles emitted in the fission of various nuclides have been studied in the past using different detection techniques (1-5). However, owing to the poor counting statistics involved in such measurements most of the results reported are not, in general, consistent except, probably, in the case of thermal fission of ^{235}U, which is the most widely studied nucleus. As it would be interesting to know if there is any dependence of the charged particle spectrum on the fissibility of the fissioning nucleus, we have measured, using a semiconductor detector, the energy spectra of long range charged particles emitted in the thermal fission of ^{235}U, ^{239}Pu and in the spontaneous fission of ^{252}Cf. Since more than 97% of the charged particles emitted in fission are the long range alpha particles they will be referred to as such in the following text.

EXPERIMENTAL ARRANGEMENT AND METHOD:

The experimental arrangement, shown in Fig.1. consisted of essentially a xenon filled gas scintillation chamber. The target foil, prepared by coating the fissible material on an

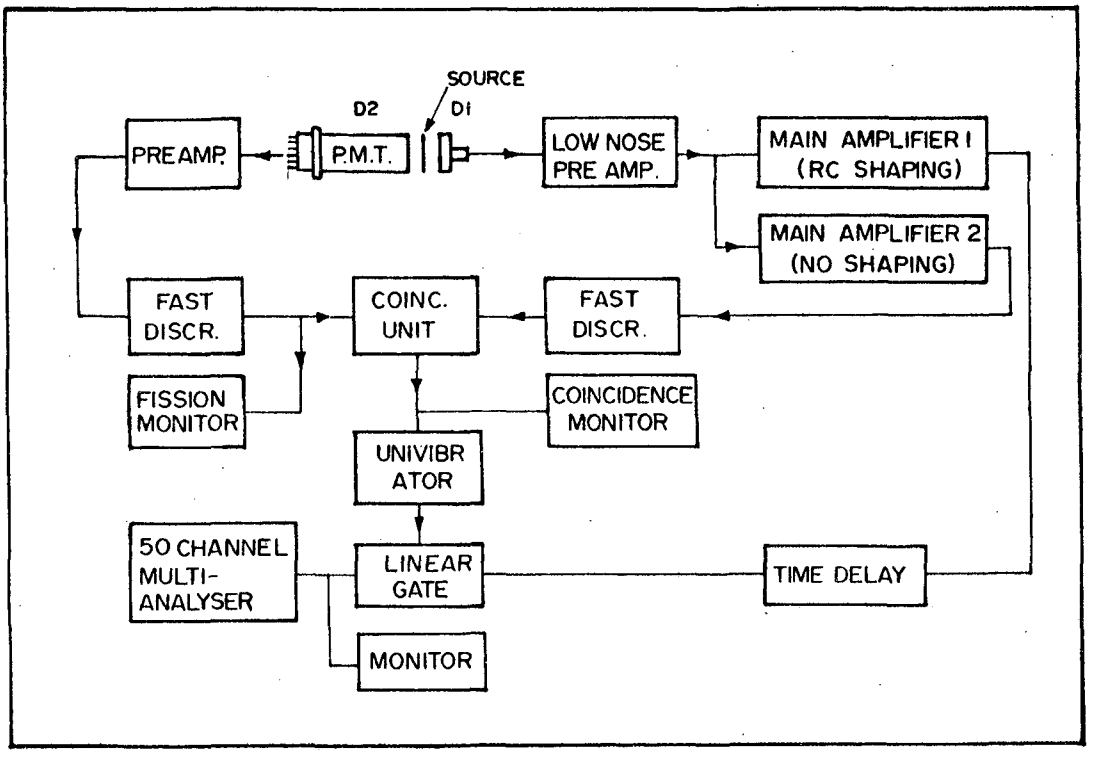

BLOCK DIARAM OF ELECTRONIC EQUIPMENT

FIG-1

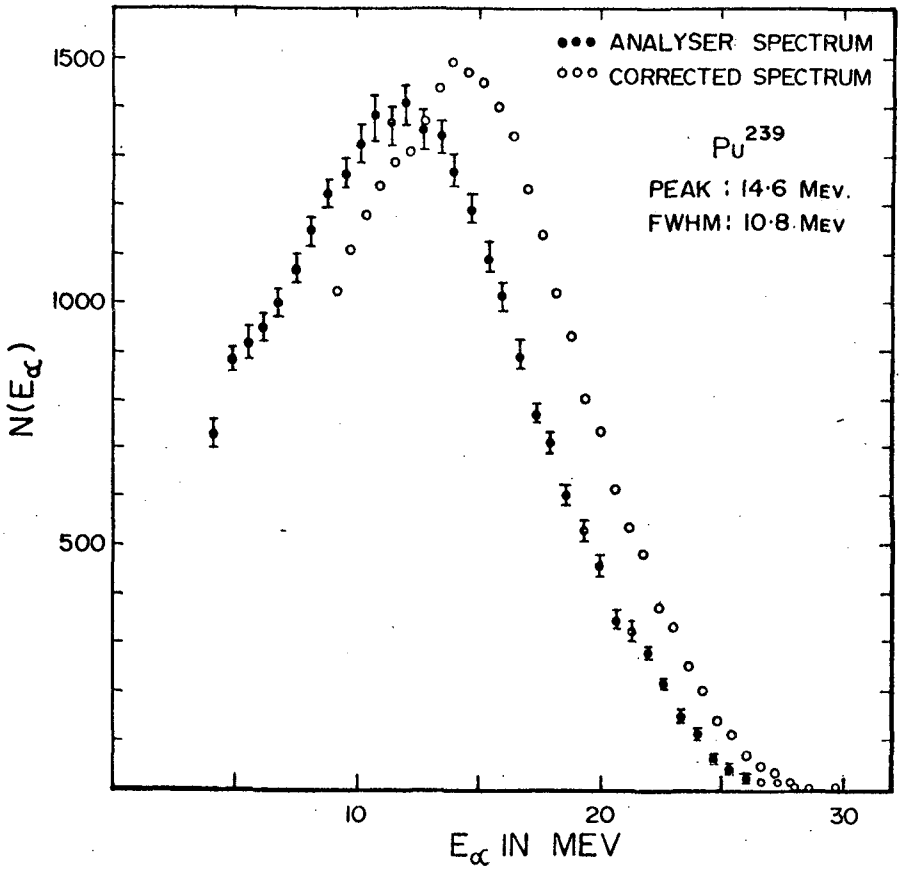

FIG. 2

aluminium backing was mounted in the chamber facing the photo multiplier tube. The chamber was filled with pure Xenon to a pressure of only about 25 mm of Hg, so that, because of their different stopping powers, the fissions could be detected well above the pile-up noise due to the high natural alpha activity of the source. A surface barrier type semiconductor detector, mounted behind the target foil, detected the long range alpha particles after they traversed through the aluminium backing which was of sufficient thickness to stop all the fission fragments and the natural alpha particles from the source. When operated at 80 Volts, the semiconductor detector had a depletion depth of 320 μm, which is sufficient to stop alpha particles of energies up to 28 MeV. The chamber was irradiated inside a beam hole of the thermal column of the Apsara Reactor, wherein the thermal neutron flux is 10^7 nv/ cm^2/sec.

The amplified signals from the two detectors were fed, through a pair of fast discriminators, to a coincidence circuit whose output was used to gate the input to a 50 channel multichannel analyser that recorded the alpha particle spectrum. The analyser channels were calibrated in terms of energy using standard alpha particle sources. The data were collected over a number of short runs, the overall gain of the entire set up being monitored with a precision mercury relay pulser; such of the runs, during which a gain drift was observed, were rejected. Thus, a total of about 50,000 ternary events, on the

average, were included in the analysis for each nucleus studied.

RESULTS AND ANALYSIS:

The observed energy spectrum of the long range alpha particles was corrected for the loss of energy by the alpha particles in the aluminium backing which depends upon, both, the incident energy and the range of the particle in the aluminium. The corrections were made by first constructing a response matrix, $[R]$, each element of which represented the probability of an alpha particle of energy, Ei emerging out of the aluminium foil with a residual energy, Er. This was done by making numerical Monte-Carlo calculations using the CDC - 3600 computer. The actual energy spectrum of the long range alpha particles was then obtained by solving the following equation:

$$\left(E_r\right) = [R] \cdot \left(Ei\right)$$

However, in order to avoid oscillatory solutions-a normal occurence in such problems (6) -- both the sides of the above equation were pre-multiplied by the transpose of the response matrix before the solution of the transformed equation could be found by the Gauss-Sidel Iteration method (7). This procedure leads to a solution which, upon passing through the original response matrix, yields a least square fit to the analyser spectrum (8).

The corrected energy spectrum of the long range alpha particles in the case of ^{239}Pu fission is shown in Fig.2, together with the observed analyser spectrum. The spectrum

shows a peak at 14.8 MeV ± 0.6 MeV. This is not in agreement with the results of Perfilor et. al (9) who found, using photographic emulsion technique, the peak at 17 MeV and a width of 7.5 MeV (FWHM). The results in the case of the nuclides ^{235}U and ^{252}Cf are tabulated below and as can be seen they are in general agreement with the published results.

Compound Nucleus	PRESENT WORK		PRESENT WORK		
	Peak	FWHM	Peak	FWHM	Ref:
^{236}U	15.0 MeV	10.6 MeV	15.0 MeV	10.7 MeV	(10)
^{252}Cf	14.8 MeV	12.0 MeV	15.0 MeV	13.0 MeV	(11)

REFERENCES:

1. E.W. Titterton; Nature, 168, 590 (1951)
2. K.W. Allen and J.T. Dewan; Phys. Rev. 75, 337 (1949)
3. R.A. Nobles; Phys. Rev. 126, 1508 (1962)
4. J.C. Watson; Phys. Rev. 121, 230 (1961)
5. M.L. Muga, H.R. Bowman and S.G. Thompson; Phys. Rev. 121, 270 (1961)
6. R. Gold; Argonne National Lab. Rep. No. ANL - 6984 (1964)
7. "Principles of computations", P. Calisgaert; Addison-Wesley P 154 (1965)

8. R.W. Detenbeck; I.E.E.E. Trans. Nucl. Sci.; NS-9,344 (1964)

9. N.A. Perfilov, Z.I. Solov'eva, R.A. Filov, S.I. Khlbenikov; Sov. Phys. JETP, 17, 1232 (1963)

10. C.B. Fulmer and B.L. Cohen; Phys. Rev. 108, 370 (1957)

11. Z. Frenkel (Preprint) (1965).

DISCUSSION:

S. Mukherji: What were the source thickness and collimation angle? What α source was used for standardizing the detector?

V.A. Hattangadi: Source thickness was 75 μgm/cm^2 and collimation angle, 5°. Standard Cf α source was used.

ANGULAR DISTRIBUTION OF THE PROMPT-GAMMA RAYS IN THE SPONTANEOUS FISSION OF ^{252}Cf.

S.S. Kapoor, V.S. Ramamurthy,
P.N. Rama Rao and S.R.S. Murthy
Bhabha Atomic Research Centre
Trombay, Bombay.

The gamma rays emitted by fission fragments provide a powerful tool for studying the de-excitation mechanism of nuclei with high angular momentum. In addition, though the initial stages of the gamma cascade are primarily statistical in nature due to the high level densities involved, the last stages of de-excitation are expected to proceed through discrete states, including collective states of the fragments. These low energy transitions are expected have a high probability for internal conversion, giving rise to conversion electrons and X-rays. Hence a simultaneous study of the gamma rays, X-rays and the electrons emitted from the fragments can yield information on the low lying states of these nuclei i.e. one can study the spectroscopy of neutron-rich nuclei, not easily accessible by other means. However, a knowledge about the initial fragment spin is necessary to analyse the fragment de-excitation. Fragment-gamma angular correlations can provide this information.

We have studied the anisotropy, the gamma rays emitted by the fragments in spontaneous fission of ^{252}Cf, with respect

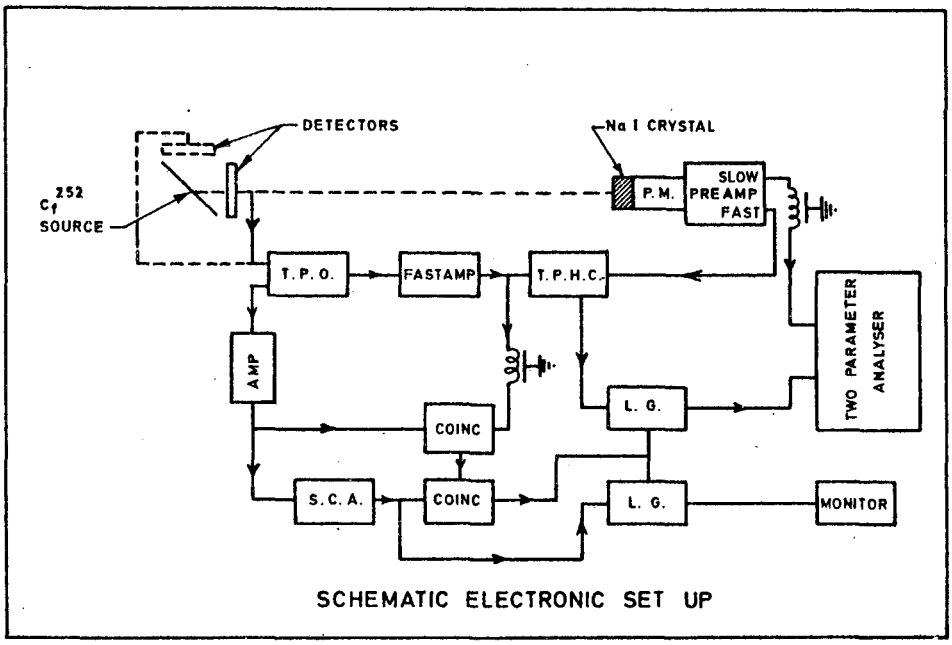
DETECTORS
Na I CRYSTAL
C_f^{252} SOURCE
P.M.
SLOW PREAMP FAST
T.P.O.
FASTAMP
T.P.H.C.
AMP
COINC
L.G.
TWO PARAMETER ANALYSER
S.C.A.
COINC
L.G.
MONITOR
SCHEMATIC ELECTRONIC SET UP

FIG. 1

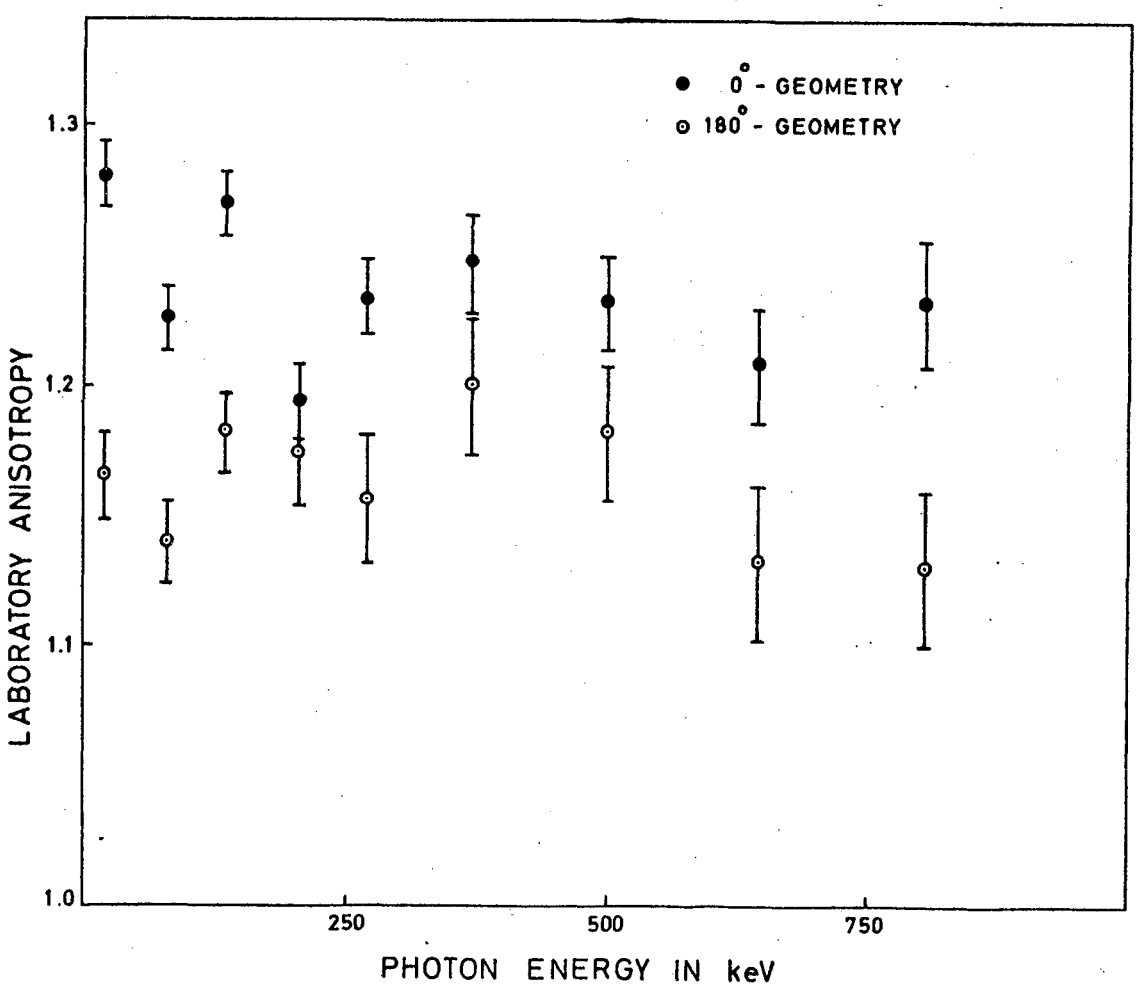
0° - GEOMETRY
180° - GEOMETRY
1.3
1.2
1.1
1.0
LABORATORY ANISOTROPY
250
500
750
PHOTON ENERGY IN keV

FIG. 2

to the direction of fragment motion, for various gamma ray energy groups. The experimental set up is as shown in figure (1). Two semiconductor detectors kept at right angles to each other and at a distance of 3 cms from a ^{252}Cf fission source of strength 5×10^5 fission/minute detected the fission fragments. The associated gamma rays were detected by a NaI(Tl) crystal-photomultiplier assembly, situated at a distance of about 50 cm from the fission source and placed in line with one of the fragment detectors. Time of flight method was used to ensure complete elimination of the prompt neutrons from getting recorded, since these are known to be highly anisotropic. The fast negative pulse from the anode of the photomultiplier and a fast pulse derived from the fragment detector using a Time - Pick-off unit were fed to a Time-to pulse-height-converter, (TPH). The output of TPH, and the dynode pulse from the photomultiplier, carrying the information about the energy of the gamma ray were fed to a two-parameter analyser, to record the time of flight spectrum for different gamma ray energy groups. The full width at half maximum of the gamma peak in the Time of Flight spectrum was about 8 ns. and all counts having a flight time less than 20 ns. were taken as gamma rays. The experiment was repeated with the fragment detectors at 0°, 90°, and 180° with respect to the gamma ray direction. The observed Laboratory anisotropies $N(0^\circ)/N(90^\circ)$ and $N(180^\circ)/N(90^\circ)$ are shown in fig.2, where $N(0^\circ)$, $N(90^\circ)$ and $N(180^\circ)$ are the number of gamma rays per

fission detected at respective angles. The results seem to indicate a small but noticeable variation of the gamm ray anisotropy with the gamma ray energy. However, since the observed variation is small, the pulse height spectrum has to be corrected for the response of the NaI(Tl) crystal to extract the exact variation of the gamma ray anisotropy with energy. The analysis is in progress.

The gross anisotropy irrespective of the gamma-ray energy is also of interest. When the observed laboratory anisotropy is corrected for the effect of fragment motion (1), a value of $(0.16 \pm .01)$ is obtained for the anisotropy $\left(\frac{N(0) - N(90^\circ)}{N(90^\circ)}\right)$ in the fragment system, assuming that the light and the heavy fragments emit equal number of gamma rays. This is considerably higher than the value of $(0.11 \pm .01)$ observed for the fission of ^{235}U, induced by thermal neutrons (1,2). This indicates that the average angular momentum of the fragments in the spontaneous fission of ^{252}Cf is higher than that in thermal fission of ^{235}U. This is consistent with the fact that the fragments in ^{252}Cf fission emit more energy in the form of gamma rays than those in ^{235}U thermal fission, although the average neutron binding energy is nearly the same in both cases. Such an increase in the energy emitted in the form of gamma rays from nuclei with higher spin is expected on the basis of higher competition between neutron and gamma emission due to larger spin.

REFERENCES:

1. S.S. Kapoor and R. Ramanna, Phys. Rev., 133, 598 (1964)

2. K. Skarsvag and I. Singstad, Nucl. Phys. 621, 103 (1965)

DISCUSSION:

S.K. Gupta: You have various fission fragments involved in the final gamma emission and this is a highly complex situation. How will you explain this theoretically?

S.S. Kapoor: Well, we will be measuring the anisotropies for various specified masses shortly, to resolve the complexity.

S. Mohan Bharathi: Was the fragment energy determined by time of flight technique?

S.S. Kapoor: No, the gamma rays were separated from prompt neutrons by time of flight method.

CROSS SECTION FOR SOME FAST NEUTRON INDUCED REACTIONS AND THE STATISTICAL MODEL

P.N. Tiwari* and E. Kondaiah**
Tata Institute of Fundamental Research
Bombay - 5, India.

INTRODUCTION:

Although large amount of work has been devoted for the measurements of the fast neutron induced reaction cross section (1) the field is far from complete because the cross sections for most of the rare reactions like (n,t) and (n,d) have not yet been measured; even the cross sections for many reactions like (n,p), (n,α) and (n,2n) reported by different authors for the same reaction differ from each other by a factor of about two or more(2).

Majority of the cross sections for the fast neutron induced reactions have been measured by the activation technique. But this technique has not been so extensively used for the measurements of cross sections for the rare reactions, because the activities produced in such reactions are small and therefore, difficult to measure. However this method can be used to measure small cross sections, if one uses large material for irradiation, high efficiency of detection, low back ground of the counting set up and gamma counting, apart from the higher flux and the longer

* Present address: Department of Physics, Banaras Hindu University, India.

** Present address: Department of Nuclear Physics, Andhra University, India.

period of irradiation and counting. Gamma counting offers double check (peak position and half-life) on the activity under measurement and the corrections for source absorption and scattering are not that serious as in the case of beta counting.

Based on these ideas a cross section measuring set-up was built (3). Using this set-up some of the (n,p), (n,α), (n.t) and (n,d) cross sections have already been measured and reported (4). The same set up has been used to measure some cross sections on spec pure potassium.

<u>Cross sections for the $^{39}K(n,2n)^{38}K_{g.s.}$, $^{41}K(n,p)^{41}Ar$ and $^{41}K(n,\alpha)^{38}Cl$ reactions</u>:- The two consecutive gamma ray spectra of the irradiated spec-pure K_2Co_3 recorded each for 7.6 min did not confirm the earlier reported half-life (5) of $^{38}K_{g.s.}$ In order to determine this half-life accurately, the decay curve of the activities produced by irradiating spec-pure K_2Co_3 was followed in such a way as to give maximum weightage to $^{38}K_{g.s.}$ activity. This was done by following the decay of 0.51 MeV photopeak, produce by the annihilation of β^+ emitted by $^{38}K_{g.s.}$ The contribution of longer lived activities (^{41}Ar and ^{38}Cl) in the decay curve are so small that even if one makes some mistake in subtracting these contribution, there will not be any appreciable change in the slope of the shortest lived activity in the present case. On the analysis of this curve by least square fit, the half-life of $^{38}K_{g.s.}$ was found to be 8.9 $\pm$ 0.14 min which does not agree with its previously reported value of 7.6 min (5).

The 0.51 MeV and 1.29 MeV photopeaks were used for the determination of the cross sections of the $^{39}K(n,2n)^{38}K_{g.s.}$ and $^{41}K(n,p)^{41}Ar$ reactions respectively. The 1.6 MeV photopeak can not be used for the determination of the cross section for the $^{41}K(n,\alpha)^{38}Cl$ reaction because the single escape peak of 2.16 MeV gamma ray in the present case being emitted both by ^{38}Cl and $^{38}K_{g.s.}$ falls in this region. Therefore in order to measure this cross section, a gamma ray spectrum was taken after complete decay of $^{38}K_{g.s.}$ activity. The 2.16 MeV photopeak from this spectrum was used for the determination of the cross section for the $^{41}K(n,\alpha)^{38}Cl$ reaction. The cross sections for the $^{39}K(n,2n)^{38}K_{g.s.}$ $^{41}K(n,p)^{41}Ar$ and $^{41}K(n,\alpha)^{38}Cl$ were found to be 2.6 ± 0.4 mb, 50 ± 6 mb and 46 ± 6 mb respectively.

The cross sections for all the (n,p), (n,α) and (n,2n) reactions measured by us have been calculated on the basis of the statistical model of the nuclear reaction, using optical potential penetrabilities. On this model the cross section σ (a,b) of the reaction

x(a,b)y

is given by (6);

$$\sigma(a,b) = \sigma_c(E_a) \frac{(2S_b+1)\mu_b \int_0^{E_{max}} E_b \sigma_c(E_b) W(U) dE}{\sum_b (2S_b+1)\mu_b \int_0^{E_{max}} E_b \sigma_c(E_b) W(U) dE}$$

where $\sigma(E_a)$ is the cross section for the formation of the compound nucleus, when the particle 'a' with energy E_a strikes the

target nucleus 'x', S_b and μ_b are the spin and the reduced mass of the emitted particle 'b', E_b its energy, $\sigma_c(E_b)$ is the inverse cross section, W(U) is the level density of the residual nucleus at the excitation energy U, $U = E_a + Q(a,b) - E_b - \delta$. [$E_a$ is the energy of the incident particle, Q(a,b) is the Q value of the reaction, δ is the pairing energy]. The summation extends over all the particles that may be emitted in the reaction. $E_{max} = E_a + Q(a,b) - \delta$.

In the present calculations, the probability of decay of the compound nucleus by emission of particles other than neutron, proton and alpha have been assumed to be neglible. The compound nucleus formation cross sections for the neutron and proton as the incident particle, have been taken from the optical potential calculation of Mani et.al (7), (8) and that for alpha from the optical potential calculations of Huizenga et. al (9). The form of level density term was taken as (10)

$$W(U) = c \exp 2(aU)^{\frac{1}{2}}$$

The Q values were taken from the Nuclear data table (11) and pairing energy (δ) from Cameron's table (12).

The calculation was performed for the various values of the level density parameter on the CDC-3600 computor of our institute. The agreement between theoretical and experimental values for the most of the cross sections studied in this work was found to be good with the level density parameter a = A/8, where A is the mass number of the product nucleus. This comparison is shown in table 1. It can be noticed from table 1, that the experi-

mental and theoretical values of the cross sections for the (n,p) reactions agree very well except for the $^{41}K(n,p)^{41}Ar$ reaction. That part of the cross section which is not accounted for by the statistical model may be attributed to the direct interaction.

The measured cross sections for all the three (n,α) reactions are higher than the corresponding theoretical values. Here also the excess cross section may be attributed to the direct interaction. However, it is not possible to arrive at this conclusion with any certainity because of following reasons. The inverse cross sections for the (n,α) reaction were determined by interpolation not only for various energies but for various nuclei also, because the Huizenga and Igo table (9) gives total reaction cross sections for only few nuclei in the region of the recent work. Moreover, it is known that a slight change in the optical potential parameters changes the transmission coefficient appreciably (9), particularly if the energy of the emitted alpha particle is below the barrier height, which is the case in all the presently studied (n,α) reactions. Therefore the absence of good agreement between the measured and theoretical values should not be taken seriously.

Out of the two (n,2n) cross section, the agreement between experiment and theorey is quite good for the $^{48}Ca(n,2n)^{47}Ca$ reaction. In the other case $\left[^{39}K(n,2n)^{38}K_{g,s}\right]$ the measured cross section corresponds to ground state only where as the theoretical one gives the total cross section for the (n2n) reaction. The disagreement is not only because of this but also because the energy

of the incident neutron (14.2 ± 0.2 MeV) is very close to the Q value (13.08 MeV) of this reaction. In such a case, a slight change in Q value will change the cross section by an order of magnitude.

REFERENCES:

1. CINDA (July 1, 1966) Neutron Data Compilation Centre, Columbia University.
2. Jeromimo, J.M.F. et al Nucl. Phys. 47, 225 (1963)
3. Tiwari, P.N. and Kondaiah, E., Nucl. Inst. and Meth. 42,118 (1966)
4. Tiwari, P.N. and Kondaiah, E., Nuclear Physics and Solid State Physics symposium 1966.
5. Nuclear Data Sheets, National Academy of Science-National Research Council, Washington, D.C., (1960-65)
6. Ericson, T. Advances Phys., 9, 425 (1960)
7. Mani, G.S., et al, Report C.E.A. n^0 2379 (1963)
8. Mani, G.S., et al, Report C.E.A. n^0 2380 (1963)
9. Huizenga, J.R. and Igo, G. Nucl. Phys. 29, 462 (1962)
10. Blatt, J. and Weisskopf, V.F., Theoretical Nuclear Physics (John Viley, Inc., New York 1952)
11. Everling, F. et al, Nuclear Data Tables Part I (Published by Nat. Acad. Sci. Nat. Res. Council, Washington, D.C. (1960)
12. Cameron, A.G.W., Can. J. Phys. 36, 1040 (1958)

Table 1.

Reactions	Cross sections measured in mb	Cross section calculated in mb, with a/ A 8
$^{27}Al(n,p)^{27}Mg$	71 ± 9	82.3
$^{42}Ca(n,p)^{42}K$	193 ± 24	203.1
$^{43}Ca(n,p)^{43}K$	93 ± 12	78.7
$^{44}Ca(n,p)^{44}K$	20 ± 8	13.4
$^{41}K(n,p)^{41}Ar$	50 ± 6	20.1
$^{27}Al(n,\alpha)^{24}Na$	115 ± 5	45.31
$^{44}Ca(n,\alpha)^{41}Ar$	35 ± 3	1.4
$^{41}K(n,\alpha)^{38}Cl$	46 ± 6	33.4
$^{48}Ca(n,2n)^{47}Ca$	900 ± 108	1010.1
$^{39}K(n,2n)^{38g}K$	2.6 ± .4	~6. (total)

DISCUSSION:

A. Chatterjee (Comment):-

(1) I notice that the shifted Fermi gas model corrects only for pairing, not for shell effects. (2) The nuclei chosen are almost sure to show direct effects.

Question: Does ^{38}K have an isomeric state?

P.N. Tiwari: Yes, of about .9 second half life.

MEASUREMENTS OF NEUTRON CAPTURE CROSS SECTIONS AT AN AVERAGE NEUTRON ENERGY OF 25 keV

P.N. Tiwari, S.N. Chaturvedi and N. Nath
Department of Physics
Banaras Hindu University
Varanasi-5

ABSTRACT

A low counting set-up has been built employing specially shielded well type NaI(T1) Scintillation crystal. Using this set-up in conjunction with the 1 curie Sb-Be Neutron source obtained from Bhabha Atomic Research Centre, Trombay, the cross sections for some of the (n,γ) reactions have been measured by the activation technique. The $^{197}Au(n,\gamma)^{198}Au$ reaction with $\sigma = 640 \pm 25$ mb at $E_n = 23.8$ keV has been used as the standard reaction in these measurements.

MEASUREMENTS OF THE CROSS SECTIONS FOR THE (n,d) AND (n,t) REACTIONS WITH ENRICHED Ca ISOTOPES

P.N. Tiwari * and E Kondaiah **

Tata Institute of Fundamental Research Centre
Colaba, Bombay-5.

ABSTRACT.

Cross Sections for the $^{43}Ca(n,d)^{42}K$ and $^{40}Ca(n,t)^{38}K_{g.s}$ reactions have been measured at $E_n = 14.2 \pm 0.2$ MeV by activation technique using enriched isotopes. The cross sections for these reactions were found to be 1300 μb and 190 $\pm$ 24 μb respectively. The method adopted for the measurements of present (n,d) cross sections can be used for measuring large number of such cross sections that are not measured till now.

---

* Present address - Physics Department,
Banaras Hindu University.

** Present address - Nuclear Physics Department,
Andhra University.

FAST NEUTRON REACTION CROSS SECTIONS AT 14 MeV IN SOME RARE-EARTH ISOTOPES

P. Rama Prasad, J. Rama Rao and E. Kondaiah
Laboratories for Nuclear Research,
Andhra University, Waltair.

INTRODUCTION:

A survey of the 14 MeV neutron-induced reaction cross sections reveals the fact that such measurements are relatively rare in the rare-earth region of isotopes. Even in cases where there is more than one measurement of cross section of a particular reaction, there is wide scatter, by a factor of four, among the various values reported. Further, the discovery of new isomeric states in some nuclides rendered the previous cross section measurements inaccurate. Lastly, there are many cases in rare-earth isotopes where the (n,p) and (n,α) cross sections have not been measured so far. A systematic investigation is, therefore, undertaken in this region using 14.2 MeV neutrons and the activation technique. Natural samples in their oxide form are supplied by the Chemistry Division, BARC, Bombay, with chemical purity better than 99.9%.

EXPERIMENTAL DETAILS:

The 14.2 $\pm$ 0.2 MeV neutrons are obtained from the Cockcroft-Walton Accelerator of TIFR, Bombay, employing the $T(d,n)^4He$ reaction. The neutron flux ranged from $\sim 10^7$ to 10^3 neutrons per cm^2 per sec. In all the experiments, the samples for irradiation

were enclosed in cylindrical polyethylene containers, wrapped outside with aluminum foil for monitoring the flux. Optimum bombarding times are used for each sample so as to obtain maximum activity of the radioisotope of interest with a minimum of other unwanted activities. The cross section measurements are made by absolute gamma counting using a well type NaI(Tl) scintillation spectrometer (1) and TMC 1024-channel pulse height analyzer. Simultaneously with the recording of the γ-ray spectra, the half life of the activity is also followed in a wide window single channel analyzer-scaler-timer unit. This affords unique identification of the reaction product.

The cross sections reported here are measured relative to the standard $^{27}Al(n,\alpha)^{24}Na$ reaction whose cross section is taken as 115 $\pm$ 5 mb. In cases where the half-life of the experimental activity is very short, the 9 mt. $^{27}Al(n,p)^{27}Mg$ reaction measured by us is taken as the standard with a cross section of 71 $\pm$ 7 mb.

Results are summerised in the table.

DISCUSSION:

<u>$^{142}Nd(n,2n)^{141\,m,g}Nd$</u>: The short-lived metastable state formed in this reaction decays to the ground state through 0.75 MeV isomeric transition with a half-life of 64 sec. Recently the individual cross section for this isomeric state has been reported by Broadhead et al (2) but no attempt was made to measure the ground state cross section and isomeric ratio. Again, there

is a discrepancy of about 50% in the values of the total cross section reported by earlier investigators (3). We have measured both the cross sections as well as the isomeric ratio. Our value of the isomeric cross section 571 ± 60 mb agrees well with that of Broadhead et al.viz. 545 ± 60 mb. The ground state cross section has been measured by us to be 1957 ± 200 mb. However, our total ($\sigma_m + \sigma_g$) cross section 2528 mb differs significantly from the most recent measurement of 1670 mb (4) but agrees well with the value of 2411 ± 200 mb reported by Rayburn et al.(5). In our case, the isomeric ratio, defined as σ_m/σ_g comes out to be 0.29

<u>$^{153}Eu(n,2n)^{152m_1,m_2}Eu$:</u> The existence of the isomeric state with half-life of 96 min. (m2) was first reported by Kirby and Kavanagh (6) and confirmed by Takahashi et al. (7); but no measurement of the isomeric cross section has so far been made. For the 9.3 hour metastable state (m_1) the two values of the cross section reported in literature are in wide disagreement with each other by a factor of four. We have measured the cross section of the m_2 state to be 295 ± 50 mb. Our value of m_1 cross section, 873 ± 90 mb agrees with that measured by Wille and Fink (8) within experimental errors.

<u>$^{159}Tb(n,2n)^{158m}Tb$:</u> The interest in this reaction is the relatively short half-life of 11 sec. of the metastable state which decays to the stable ground state through 111 keV isomeric transition. There is only one measurement of this isomeric cross section (2)

reported in literature. In view of the very short half life, sufficient precaution should be taken to see that much of the activity is not lost before the irradiated sample is transferred to the counting system. In our case, we have made use of an automatic quick delivery system. In our case, we have made use of an automatic quick delivery system to achieve this end. A microswitch, operating automatically with the stoppage of irradiation, releases the sample in the target room and simultaneously triggers an electronic timer so as to enable an accurate determination of the time elapsed before counting is started. Transit times of the order of 10 to 11 secs could thus be achieved with this system. To follow the half life use is made of the Model 214 Multiscaler unit of the TMC 1024 channel analyzer with the **preset** time at 1 sec. The prominent k-x ray peak at 45 keV is used for the determination of the cross section employing the latest values of α_k = 56 and α_{tot}= 106 reported by Schmidt-Ott et al (10). Our cross section value for this isomeric state is 238 $\pm$ 40 mb which is larger than that reported by Broadhead et al. This discrepancy can in part be explained by the difference in the values of the conversion coefficients used in the two investigations.

<u>$^{160}Gd(n,2n)^{159}Gd$:</u> While looking for $^{158}Gd(n,\gamma)$ reaction in natural Gadolinium, this 18 hours activity is easily formed in large intensity by virtue of the very high cross sections for (n,2n) reaction in these regions. Incidentally, therefore, this

cross section is measured by us to be 1675 ± 160 mb, which agrees within experimental errors with the literature values (8,9,11).

$^{158}Gd(n,\alpha)^{155}Sm$: There is no report of cross section measurement for this reaction in literature. By studying the characteristic 105 keV γ-rays of ^{155}Sm decaying with a half-life of 24 min, we have measured the cross section as 1.4 ± 0.25 mb. The large error is due to the uncertainties in the extrapolation procedures used for obtaining the absolute efficiency.

$^{75}As(n,p)^{75m,g}Ge$: Although Arsenic is not a member of the rare-earth group of elements, we are presenting the results of our measurements on the isomeric and the ground state reactions in view of the reported large discrepancy in the experimental and C.N. theoretical values of the isomeric ratio indicating a strong predominance of the direct interaction process. Our value of σ_m agrees fairly with that of Fukuzawa (13) while our σ_g is smaller, giving a slightly higher isomeric ratio, viz. 0.5. This value is still smaller by a factor of 10 than that predicted on the basis of compound nuclear model thus confirming the prominence of direct reaction contribution.

The γ-ray detection efficiencies for the well-crystal used in the present investigation have been taken from ref. (12) for all γ-ray energies above 140 keV. For γ-rays of lower energy, extrapolation procedures are employed taking into account the source absorption effects. Owing to the uncertainties involved

TABLE OF CROSS-SECTIONS

$E_n = 14.2 \pm 0.2$ MeV.

Reaction Studied	σ in mb obtained by us	σ in mb given in literature.	Ref:
$^{27}Al(n,p)^{27}Mg$	71 ± 7	71 ± 10.6	1
$^{142}Nd(n,2n)^{141m}Nd$	571 ± 60	545 ± 60	2
$^{142}Nd(n,2n)^{141g}Nd$	1957 ± 200	2060 ± 200	8
		2411 ± 200	5
$^{153}Eu(n,2n)^{152m_2}Eu$	295 ± 50	1650 ± 165	4

$^{153}Eu(n,2n)^{152m_1}Eu$	303 ± 90	750 ± 200	8
		164 ± 25	9
$^{158}Gd(n,\alpha)^{155}Sm$	1.4 ± 0.25	---	
$^{160}Gd(n,2n)^{159}Gd$	1675 ± 160	1470 ± 820	11
		1450 ± 300	8
		1725 ± 170	9
$^{159}Tb(n,2n)^{158m}Tb$	238 ± 40	160 + 19	2
$^{75}As(n,p)^{75m}Ge$	8 ± 1	10 ± 2	13
$^{75}As(n,p)^{75g}Ge$	16 ± 2	25 ± 5	13

in this, large errors are associated with the cross section measurements in $^{159}Tb(n,2n)$, $^{153}Eu(n,2n)^{152m}{}_2Eu$ and $^{158}Gd(n,\alpha)$ reactions. Experiments are in progress to extend the efficiency measurements on this crystal down to the X-ray region.

REFERENCES:

1. P.N. Tiwari and E. Kondaiah, Proceedings of the Nuclear Physics Symposium, p.60 (1966)
2. K.G. Broadhead, D.E. Shanks and H.H. Heady, Phys. Rev. 139, B 1525 (1965)
3. M. Bormann, Nucl. Phys. 65, 257 (1965)
4. J.T. Grissom, D.R. Koehler and W.L. Alford, Phys. Rev. 142, 725 (1966)
5. L.A. Rayburn, Phys. Rev. 122, 168 (1961)
6. P. Kirby and T.M. Kavanagh, Nucl. Phys. 49, 300 (1963)
7. K. Takahashi, M. McKeown and G, Scharff-Goldhaber, Phys. Rev. 137, B 763 (1965)
8. R.G. Wille and R.W. Fink, Phys. Rev. 118, 242 (1960)
9. C.S. Khurana and H.S. Hans, Nucl. Phys. 28, 560 (1961)
10. W.D. Schmidt-Ott, F. Smend and A. Flammersfeld, Z. Physik, 184, 310 (1965)
11. E.B. Paul and R.L. Clarke, Can. J. Phys. 31, 271 (1953)
12. P.N. Tiwari and E. Kondaiah, Nucl. Inst. & Methods, 42, 118 (1966)
13. Fumio Fukuzawa, Jour. Phys. Soc. Japan, 16, 2371 (1961)

DISCUSSION:

A. Chatterjee: (1) What sort of calculations of the statistical model did you do? (2) Do the isomeric ratios agree with the statistical model? (3) Have you any comment to make on the low (n,α) cross section of Gadolinium?

J. Rama Rao: (1) None yet, results are preliminary. (2) We have yet to make theoretical calculations. (3) The order of the cross-section value is correct. There is no other experimental result for comparison .

MEASUREMENT OF (n,2n) CROSS SECTIONS OF FAST NEUTRONS

Arun Chatterjee, A. Nath and A.M. Ghose
Nuclear Physics Laboratory
Bose Institute
Calcutta

(n,2n) cross sections of several nuclei have been measured absolutely by measuring the absolute value of the fast neutron flux by a heavily biased plastic scintillator and the absolute value of the positron activity using an absolutely calibrated high resolution coincidence spectrometer.

The measurement of the fast neutron flux has been carried out by the following procedure developed in our laboratory. A small cylindrical plastic phosphor 1.25 cm. in height and 2.5 cm. in radius has been used in these measurements. The size of the detector reduces the efficiency of detection for γ-rays and the recoil proton spectrum above 10 MeV is due entirely to the incident neutrons. The quantitative relationship between the fast neutron flux and the number of recoil protons above a suitable bias has been taken from our theory of fast neutron response of organic scintillators (1).

The samples have been irradiated using the Bose Institute neutron generator keeping the deuteron energy confined to 130 keV. The irradiations were carried out in the forward direction and the incident neutron energy was thus 14.8 $\pm$ 0.1 MeV.

The measurement of the positron activity has been carried out by feeding the pulses from NaI/Tl scintillators into a fast amplifier using EFP 60 secondary emission tubes and a 6AK5 limiter. A slow-fast coincidence circuit of fast resolution slightly greater than 3ns has been used. Absolute calibration of the spectrometer has been carried out using secondary standard sources of the same dimensions as the samples. The secondary sources have been calibrated by using reference sources available through the courtesy of N.B.S., U.S.A.

Table I shows the experimental (n,2n) cross sections obtained in the present work as well as those obtained by other workers in this field.

The estimated error in our measurements is of the order of ± 10%. Further experiments with better geometrical arrangement is in progress and the present data should be considered as only provisional.

(n,2n) Cross Sections of nuclei for 14 MeV neutrons

Nuclei	E_n (MeV)	Cross Section (in mb)	Exp.
^{19}F	14.1	38.9 ± 2.3	Cevolani & Petralia
	14.4	51.9 ± 9	Rayburn
	14.6	53.0 ± 4	Csikai
	14.3 ± .1	49.4 ± 5.0	Chatterjee, Mitra & Ghose
	14.8 ± .1	46.3 ± 4.6	Present Work

Nuclei	E_n (MeV)	Cross Section (in mb)	Exp.
^{63}Cu	14	556 ± 28	Yasumi
	14.1	409 ± 25	Cevolani & Petralia
	14.37 ± 0.15	448 ± 24	Weigold & Glover
	14.4 ± 0.3	503 ± 57	Rayburn
	14.6 ± 0.1	514	Csikai
	14.8	507 ± 45	Ferguson & Thompson
	14.8	548 ± 10	Grimeland, Kjellsby & Vines
	14.8 ± 0.1	544 ± 54	Chatterjee et al
	14.8 ± 0.1	509 ± 51	Present Work
^{64}Zn	14	119 ± 14	Yasumi
	14.1	105 ± 7	Cevolani & Petralia
	14.3	107	Weigold & Glover
	14.4	167 ± 17	Rayburn
	14.6	201 ± 13	Csikai
	14.8 ± 0.1	174 ± 17.4	Chatterjee et al
	14.8 ± 0.1	165 ± 17	Present Work
^{69}Ga	14.1	735 ± 44	Cevolani & Petralia
	14.1	923 ± 92	Rayburn
	14.8	1070 ± 107	Khurana & Hans
	14.8 ± 0.1	1013 ± 101	Chatterjee et al
	14.8 ± 0.1	950 ± 95	Present Work

Nuclei	E_n (MeV)	Cross Section (in mb)	Exp.
^{107}Ag	14	458 ± 51	Yasumi
	14.1	734 ± 44	Cevolani & Petralia
	14.1	889 ± 89	Rayburn
	14.5	657 ±102	Khurana & Hans
	14.8 ± 0.1	562 ± 56	Chatterjee et al
	14.8 ± 0.1	535 ± 54	Present Work

REFERENCES:

1. Arun Chatterjee and A.M. Ghose, Trans. Bose Inst. 29,(2) (1966)
2. Cevolani and Petralia, Nuovo Cimento, 26, 1323 (1962)
3. L.A. Rayburn, Phys. Rev. 122, 168 (1961)
4. Yasumi, J. Phys. Soc. Japan. 12, 443 (1957)
5. Weigold and Glover, Nucl. Phys. 32, 106 (1962)
6. Fergusson and Thompson, Phys. Rev. 118, 228 (1960)
7. Khurana and Hans, Nucl. Phys. 28, 560 (1961)
8. Grimeland et al. Phys. Rev. 137, B879 (1965)
9. Csikai, J. Atomkei Kozlemanyk Report 8, (Kotet) 79 (1966).

A SURVEY OF RESULTS OF (n,p) CROSS SECTIONS OF 14 MEV NEUTRONS IN LOW-Z NUCLEI

B. Mitra
Bose Institute, Calcutta

We previously reported (1) a few 14 MeV (n,p) cross sections of low-Z nuclei and we have measured a few more in pursuing our programme of systematic measurements. The measured nuclei range between $8 \leqslant Z \leqslant 33$. These data will be presented along with the results of comparison of them with other experimental and semi-empirically calculated data according to statistical model calculations. A survey of our results vis-a-vis results of experimental (n,p) cross sections of different workers has been attempted.

It appeared to us that a systematic set of data reported from a single laboratory would be more suitable for comparison, instead of scattered data reported by various groups. It has been found that the only existing such systematic data are those old data of Paul & Clarke (1) and those of D.L. Allan (3). Even a search through a compilation made by Chatterjee (4) convinces us that no other laboratory's systematic measurement exists upto date. We do not propose to discuss Paul and Clarke's less accurate data, but compare our data with those of Allan.

Allan obtained his results of (n,p) cross section by emulsion plate technique, while our data are activation analysis data. Although the two sets were obtained by

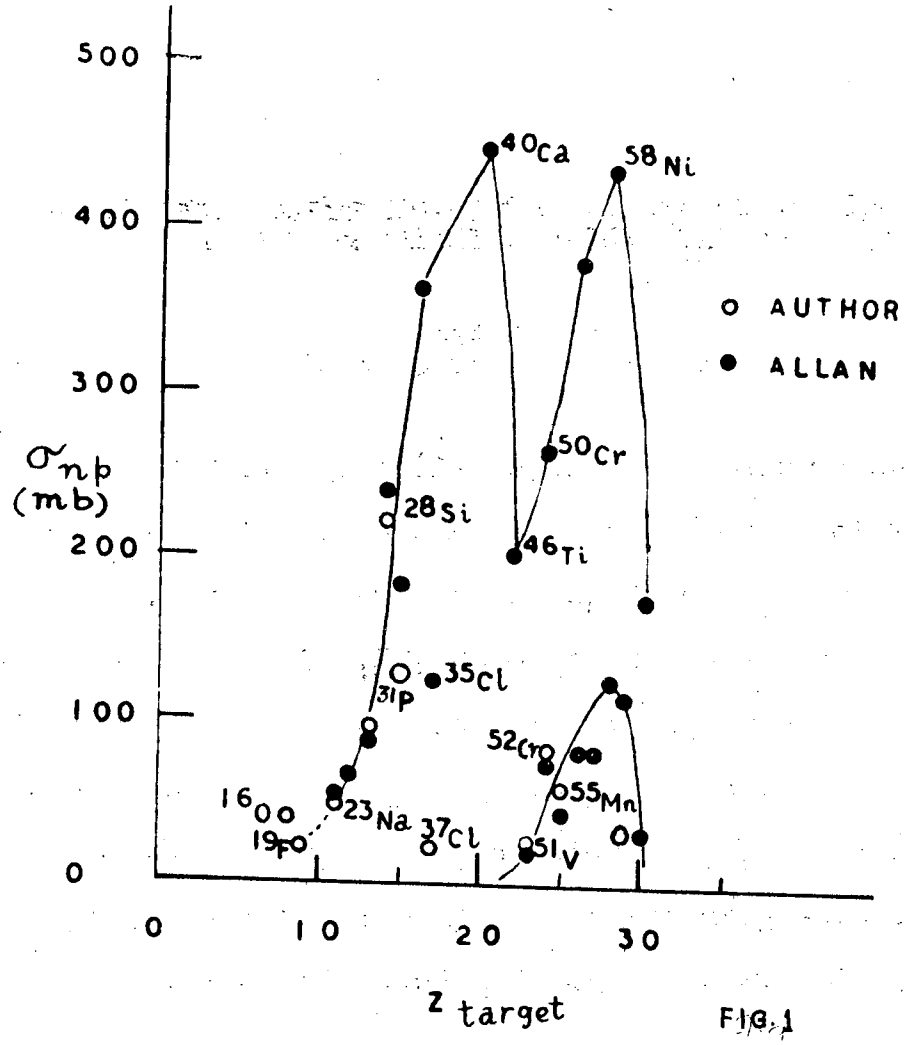
500
400
300
200
100
0
σ_{np} (mb)
0
10
20
30
Z target
AUTHOR
ALLAN
40Ca
58Ni
50Cr
46Ti
28Si
31P
35Cl
52Cr
55Mn
51V
16O
19F
23Na
37Cl

FIG. 1

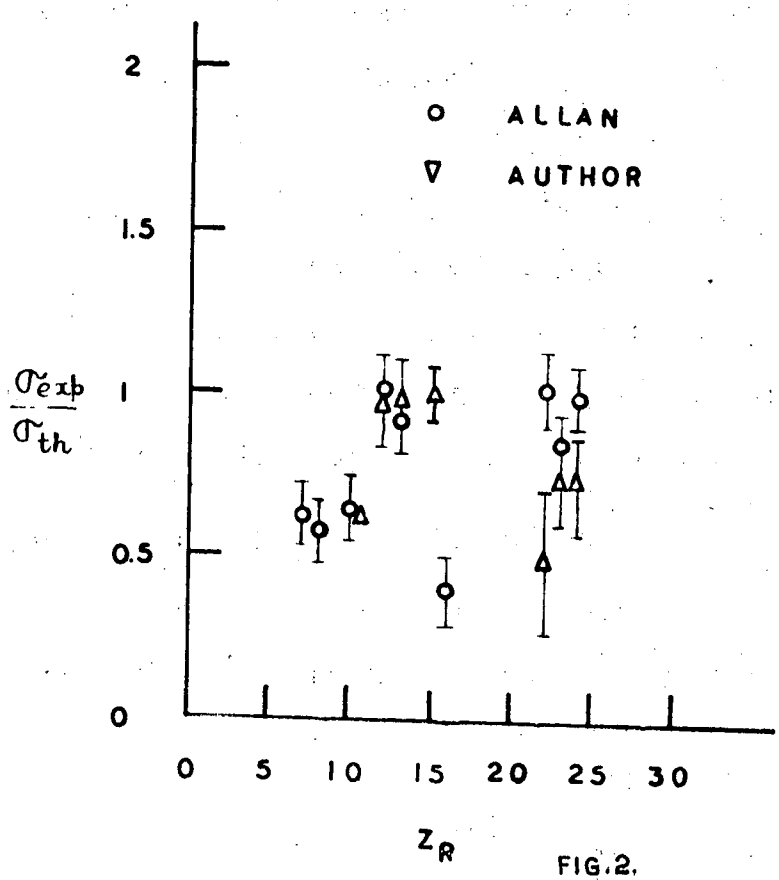
2
1.5
1
0.5
0
$\frac{\sigma_{exp}}{\sigma_{th}}$
ALLAN
AUTHOR
0
5
10
15
20
25
30
Z_R

FIG. 2.

diversely different techniques, yet it was gratifying to notice that barring one or two cases, the agreement in the two sets, in both the absolute magnitude of the values and the trend, are remarkable (Fig.1). The curve showing dependence of $\sigma_{n,p}$ on closed neutron shell structure, has been drawn by Allan, where our data have been fitted. The comparison shows that for a number of nuclei the agreement is surprisingly good. Only in the case of phosphorus ^{31}P, the dispersion is a bit large, - Allan's value being $\simeq$ 184 $\pm$ 14mb. While our activation analysis value is 140 $\pm$ 14 mb. However this disagreement is also not as large as to cast any doubt about presence of bias in either of the measurements, and the general agreement is held to be good. In case of ^{37}Cl, there is no data in Allan's but our data appears in a place where the ratio of $\sigma_{n,p}$ of ^{35}Cl and ^{37}Cl (Allan has data for ^{35}Cl) is as the ratio appears to be in case of neighbouring isotopes of other nuclei.

The plate data of Allan was obtained at lab. angle 120° to the deuteron beam and admittedly they have no direct interaction contribution. But the cross section values should come out to be large owing to (n,np) contribution.

The result of comparison of our values with Gardner's (5) predicted cross sections is shown in Fig.2. This shows that the agreement with Gardner's semiempirically obtained cross sections is not too good. Gardner in obtaining his semiempirical parameters depended upon selected values and he did not average the scattered cross section obtained by various workers. In contradiction to Gardner's formula, which is claimed to be

obtained according to statistical model, Levkovskii (6) proposed another formula with only one empirical parameter, and which is claimed to be derived not strictly according to statistical model. In Fig.3 a comparison of our data with Levkovskii's has been attempted. The agreement here also is not so good. The dip at $Z_{target} = 20$ is conjectural and the gross trend cannot be said to indicate any shell effect.

Attempts to add proton-shell effect to other structural effects in statistical model calculations has been made by Chatterjee (7) in case of (n,p) cross section. He obtained a shell dependent level density formula, starting from Bloch-Rosenzweig formula. Then he tried to fit the computed cross section values with values obtained by averaging of scattered experimental data. He justifies the averaging by citing experiments of excitation function measurement of few nuclei where nearly no fine structure was obtained at the best resolution of $\simeq 60$ keV. In Fig.4 is shown the attempt to fit our values of $\sigma_{n,p}$ in low Z nuclei with the computed curve of Chatterjee. The fit is not very good. Therefore it appears that systematic cross sections obtained from a single set of measurements do not show the expected proton shell effects in their trend. In this connection to find out how far it is justified to have averaged cross sections for such fit, we performed

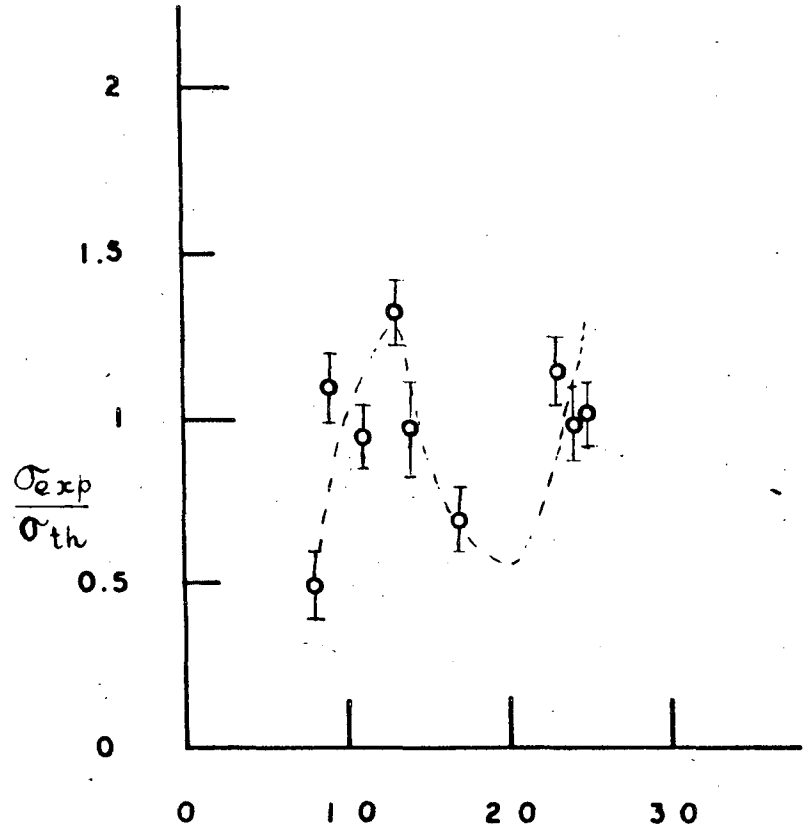

FIG. 3

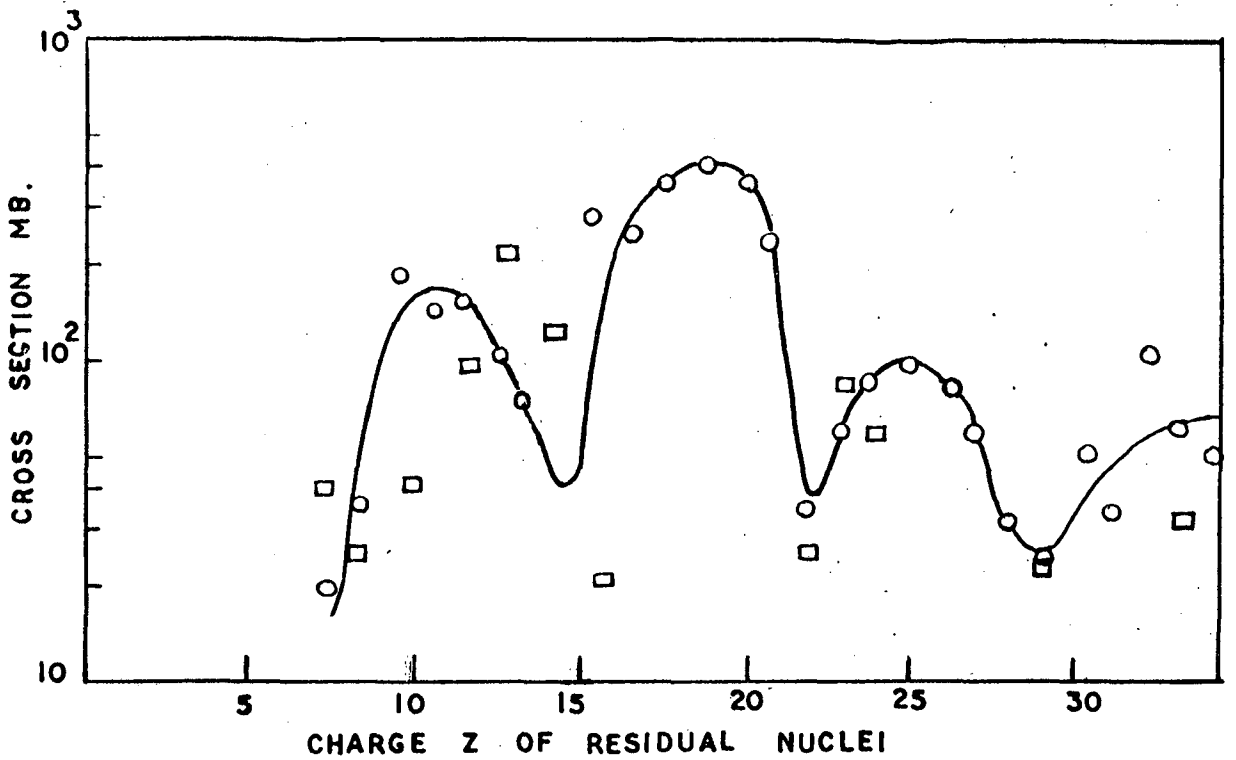

CIRCLES ARE CHATTERJEE'S CALCULATED VALUES USING SHELL DEPENDENT LEVEL DENSITY. SOLID CURVE DRAWN BY HIM.

SQUARES ARE PRESENT EXPERIMENTAL VALUES.

FIG. 4

experiments, even in our "poor-resolution" way. We have measured (n,p) cross sections of ^{31}P, ^{37}Cl, ^{65}Cu and ^{75}As at En = 14.1 ± .1 and E_n = 14.8 ± 0.02 MeV respectively; while the value of ^{31}P is not yet obtained as a conclusive one, the table I shows the values of other three nuclei. It may be seen that even in this poor resolution experiment, there exists fluctuations in cross section values at energy fluctuation of 0.7 MeV. The values obtained are relative to σ(n,2n) values of ^{63}Cu, the excitation function of which reaction has been carefully done by Csikai (8). We have used Csikai's experimental curve, extrapolated upto 14.8 MeV. The result for ^{75}As is rather startling since it represents a factor of two change. Values of ^{37}Cl also represents a trend, which does not explain a very low value of it, $>$5 mb at a higher energy $\simeq$ 17 MeV. A scope for renewed excitation function measurement exists in this energy range of 13 - 17 MeV, for this nucleus, - as well as for ^{75}As. Meanwhile Cuzzocrea and Nottarigo (9) also discount any proton shell effect in experimental σ(n,p).

Therefore, from our obtained data, and their concurrence with experimental data of Allan, we generally conclude that the semi empirical theories so far developed to predict σ(n,p) do not account for the experimental cross section values in the low Z region.

REFERENCES:

1. Mitra and Chose, Proc. Nucl. Phys. Symp. Cal.(1965)
2. Paul and Clarke, Can. J. Phys. 31, 267(1953)
3. Allan, Nucl.Phys. 24, 274(1961)

4. Chatterjee, Nucleonics, (1965) August.

5. Gardner, Nucl. Phys. 29, 373 (1962)

6. Levkovskii, JETP, 18, 213 (1964)

7. Chatterjee, Nucl. Phys. 60, 273 (1964)

8. Csikai, Ph. D. Thesis (1966)

9. Cuzzocrea and Nottarigo, Int. Conf. Antwerp, EANDC-50-S, Cont 115, (1965)

Table 1.

Nucleus	E_n MeV	σ_{np} mb author	σ_{np} mb literature
^{37}Cl	14.1 ± 0.18	21 ± 3	18 ± 8 Cohen & White
	14.8 ± 0.02	25 ± 3	31 ± 7 "
			<5 at E_n = 17.5 ± .25 Mani et al.
^{65}Cu	14.1 ± 0.18	19 ± 2	26 ± 7 Borman
	14.8 ± 0.02	26 ± 3	22 ± 7 "
^{75}As	14.1 ± 0.18	15 ± 4	20.7 ± 1.5 Bayhurst & Prestwood
	14.8 ± 0.02	33 ± 3	15.9 ± .36 "

ISOMERIC CROSS SECTION RATIOS FOR (n,2n) REACTIONS AT 14.8 MEV

R. Prasad and D.C. Sarkar
Department of Physics, Muslim University, Aligarh

1. INTRODUCTION:

In an nuclear reaction where the residual nucleus has an excited level of measurable half-life, the extent to which each isomer is populated in the reaction may be expressed by the isomeric cross section ratio. Since isomers differ in their spin, it is possible to calculate this cross section ratio theoretically using the spin density relation due to Bethe (1) and Bloch (2). This involves the spin distribution parameter σ. Many measurements of the parameter have been performed (3 - 10), but the situation is still far from satisfactory due to the lack of data.

We have measured the isomeric cross section ratios experimentally by following the activities produced in samples due to (n,2n) reactions at 14.8 MeV. The experimentally measured and the theoretical values of the isomeric cross section ratios were compared to find the probable value of the spin distribution parameter σ.

2. MEASUREMENTS:

The details of neutron production, sample prepration and of the irradiation technique have already been described previously (11,12). Cross-sections were measured with respect to

the $^{56}Fe(n,p)^{56}Mn$ reaction.

The residual nuclei in the reactions $^{35}Cl(n,2n)^{34m}Cl$, $^{45}Sc(n,2n)^{44}Sc$ and $^{92}Mo(n,2n)^{91m,g}Mo$ decay partially through positron emission. Cross sections for these reactions have been found by following their activities by the end-window beta counter. For a check in case of $^{92}Mo\ (n,2n)^{91m}Mo$, the cross section has also been measured by following the decay of 658 keV gamma ray arising from the isomeric transition of ^{91m}Mo. A 3.8cm x 3.8 cm NaI(Tl) crystal coupled to a photomultiplier tube has served as the gamma ray detector. As the half life of ^{91m}Mo is short, the window width and the base line of the gamma ray spectrometer were adjusted to include the 658 keV gamma ray. The two values of the same cross section obtained in this way were found to agree well with in the experimental errors. Necessary corrections have been applied for the contribution of the isomeric state to the decay rate of the ground state in molybdenum. The details of measurements for the reactions $^{35}Cl(n,2n)^{34g}Cl$ and $^{115}In(n,2n)\ ^{114g}In$ are given elsewhere (12).

3. CALCULATIONS AND RESULTS:

Isomeric ratios are theoretically calculated from the method developed by Vandenbosch and Huizenga (15,16). Neutron transmission coefficients for these calculations are taken from ref. (17). Isomeric ratios for different values of σ are calculated in steps of 0.5. The parameter has also been calculated from the relations (10) $\sigma_{mg}^2 = \frac{I}{\hbar^2} T = \frac{2}{5} mR^2 T/\hbar^2$

In table 1 are given the observed cross sections and their half-lives Isomeric ratios for these reactions are listed in table 2. The best value of parameter σ is found by comparing the calculated values to those found experimentally. For chlorine and scandium, the probable value of σ is found to be 4 $\pm$ 1. In cases of indium and molybdenum the value of σ is 6.5 $\pm$ 1 and 8.5 $\pm$ 1.5, which is higher than the general value 4 $\pm$ 1. In these calculations we have considered only the dipole emission. Bishop (9) has shown that the cross section ratio is quite sensitive to the polarity of gamma rays. In the last column of table 2 are given σ_{mg}. It can be seen that there is some agreement between σ_{mg} and σ_{mg}.

Table 1

Activation cross sections for 14.8 MeV neutrons.

Reaction	Half-life	Observed cross sections (mb)
$^{35}Cl(n,2n)^{34m}Cl$	33 min	12 $\pm$ 2
$^{35}Cl(n,2n)^{34g}Cl$	1.7 sec	7.3 $\pm$ 1.5
$^{45}Sc(n,2n)^{44m}Sc$	2.4 d	150 $\pm$ 11 a)
$^{45}Sc(n,2n)^{44g}Sc$	4.0 h	100 $\pm$ 10
$^{92}Mo(n,2n)^{91m}Mo$	66 sec	51 $\pm$ 10
$^{92}Mo(n,2n)^{91g}Mo$	16 min	205 $\pm$ 25
$^{115}In(n,2n)^{114m}In$	50 d	1585 $\pm$ 79 b)
$^{115}In(n,2n)^{114g}In$	72 sec	360 $\pm$ 40

a) Ref. 13) : b) Ref. 14)

Table 2.

Isomeric pair	Target spin	Competing level spin		Isomeric ratio highspin/total spin	σ_{prob}	σ_{rho}
$^{35}Cl(n,2n)^{34m,g}Cl$	3/2	0	3	0.64 ± 0.02	2.5	2
$^{45}Sc(n,2n)^{44m,g}Sc$	7/2	2	6	0.60 ± 0.01	4.5	2.25
$^{92}Mo(n,2n)^{91m,g}Mo$	0	1/2	9/2	0.80 ± 0.1	8.5	3.82
$^{115}In(n,2n)^{114m,g}In$	9/2	1	5	0.84 ± 0.01	6.5	4.44

REFERENCES:

1. H.A. Bethe, Revs. Mod. Phys. 9, 84 (1937)
2. C. Bloch, Phys. Rev. 93, 1094 (1954)
3. S.K. Mangal and P.S. Gill, Nucl. Phys. 41, 372 (1963)
4. S.K. Mangal and P.S. Gill, Nucl. Phys. 49, 510 (1963)
5. J.H. Carver, G.E. Coote and T.R. Sherwood, Nucl. Phys. 37, 449 (1962)
6. A.C. Douglas and N. MacDonald, Nucl. Phys. 13, 382 (1958)
7. C.T. Hibdon, Bull. Am. Phys. Soc. 3, 48 (1958)
8. S.K. Mangal and C.S. Khurana, Nucl. Phys. 69, 158 (1965)
9. C.T. Bishop, ANL-6405
10. L. Katz, L. Peace and H. Moody, Can. J. Phys. 30, 476 (1952)
11. R. Prasad, D.C. Sarkar and C.S. Khurana, Nucl. Phys. 85, 476 (1966)
12. R. Prasad, D.C. Sarkar and C.S. Khurana, Nucl. Phys. 88, 349 (1966)

13. L.A. Rayburn, Phys. Rev. 122, 168 (1961)

14. J.R. Prestwood and B.P. Baythurst, Phys. Rev. 121, 1438 (1961)

15. J.R. Huizenga and R. Vandenbosch, Phys. Rev. 120, 1305 (1960)

16. R. Vandenbosch and J.R. Huizenga, Phys. Rev. 120, 1313 (1960)

17. B.T. Field et al., Fast Neutron Data Project NYO - 636 (1961)

18. T. Ericson, Nucl. Phys. 11, 481 (1959)

DETECTION MECHANISM IN SEMICONDUCTOR COUNTERS

R.Y. Deshpande
Technical Physics Division
Bhabha Atomic Research Centre, Bombay

I. INTRODUCTION:

The use of semiconductor detectors in the field of nuclear spectroscopy has been well-established during the past few years (1). The unrivalled energy resolution and speed of response obtainable with these detectors have led to their quick acceptance in nuclear physics research. These detectors are essentially solid-state ionization chambers and can be tailored to suit the requirements of several specific problems. Thus starting from a simple dielectric counter like a gold-plated silicon slab cooled to liquid helium temperature, we have surface barrier, diffused junction, lithium-drifted silicon and germanium and dE/dx - types of detectors. Efforts in the preparation of high-Z materials like GaSb and CdS for the fabrication of high-efficiency γ-detectors are also being pu (2). Through an increase in Z (from 32 in Ge to 51 in Sb) these materials can improve photoconversion efficiency by an order of magnitude over the present values.

Basic processes right from the passage of charged particles through the detectors medium to the formation of signal at the output of the detector have been fairly well understood. Charged particles traverse the detector medium dissipating their energy through a multitude of inelastic collissions with

the atomic electrons. These high-energy electrons then produce electron-hole pairs and lattice phonons. Finally, Collection of the liberated charge gives a signal in proportion to the amount of energy deposited by the incident particle in the sensitive volume of the detector.

The statistics of energy loss, of charge production and collection, and of background noise and formation of signal, have also been extensively studied. A fairly completed picture of all these processes is now emerging. Thus for the case of thick absorbers (the case where the particle range is smaller than the width of the detector) van Roosbroeck (3) has developed a theory relating the quantum yield, statistical deviation and Fano factor. Experimental confirmation of the theory can be considered to be very good. On the other hand, direct verification of Landau-effect in silicon detectors by Maccabee et al (4) confirms Vavilov's theory (5) of fluctuation of energy loss in thin absorbers.

Recently several review articles have been written covering the various aspects of detection with these counters (6). In the present review we shall however confine ourselves chiefly to the fundamental processes governing the detection mechanism in junction-type counters. We shall exclude simple conduction or dielectric-type of counters. Also, we shall not consider the details of producing sensitive columns, including rectification processes, in the detector medium. An attempt is

therefore made to present a consistent picutre of the detection mechanism only in junction-type counters. We shall consider the processes of creation of electron-hole pairs in the detector-medium, collection of the liberated charge, and the detector noise limitations on the energy resolution capabilities. Wherever possible the theoretical results are compared with the experimental values. While doing so it should however be pointed out that considerable spread in the experimental values, and at times contradictory results, have been reported in the literature. This could of course be attributed to a variety of factors including the very art of fabrication of the detectors.

II. ENERGY PER ELECTRON-HOLE PAIR:

Average energy expended by the incident particle in producing a charge pair in a detector medium is a quantity of fundamental interest in assessing the resolution capability of a particular detector. Semiconductor counters derive their advantage in that they require very small energy ($\sim$3.5 eV) to produce one electron-hole pair. Theoretical approach in analyzing the factors determining ϵ is essentially the study of the whole problem of interaction of radiation with matter. Thus ϵ, which is a grand average of a large number of ionization processes, includes in it the minimum energy required to produce an electron-hole pair plus the energy imparted to the lattice phonons.

Shockley (7) has developed a simple phenomenological model to account for the processes determining ϵ. The incident energy can be accounted in three ways:

(i) Threshold energy E_{th} required to produce an electron-hole pair. This is one of the adjustable parameters in Shockley's theory and will be about E_g, the band-gap of the semiconductor.

(ii) Phonon energy rE_R imparted to the lattice. For every impact ionization producing an electron-hole pair r phonons of highest frequency, the Raman phonons, corresponding to the energy E_R are produced. r is another adjustable parameter.

(iii) Residual energy or the final energy E_f unable to produce an electron-hole pair. This energy is spent in the production of low frequency phonons corresponding to phonons with non-vanishing wave-vectors in the Brillouin zone picutre of the semiconductor. For parabolic energy surfaces Shockley estimates this contribution to be $1.2E_{th}$.

Thus summing up all the three contributions to ϵ shockley predicts that

$$\epsilon = 2.2\ E_{th} + r\ E_R.$$

Using the experimental values of E_{th}, r and E_R Shockley has calculated ϵ. In the case of Ge and Si the

values of E_R have been determined by the neutron diffraction experiments and are E_R = 0.063 eV for silicon (8) and 0.037 eV for germanium (9). r is determined from Vavilov's data (10) of enhanced photo-quantum yield in these crystals; r = 17.5 phonons per ionising collision in Si and 57 in Ge. Then choosing $E_{th} = E_g$ (E_g = 1.1 eV for Si and 0.66 eV for Ge at 300°K) he predicts ϵ = 3.5 eV for Si and 3.6 eV for Ge.

Several authors (11) have experimentally determined the values of ϵ for both Ge and Si, and for various ionising radiations. Some of these results are given in Table I. The general agreement with values predicated by Shockley's simple model is surprisingly good and lends support to the mechanism postulated by him. However, as pointed out by Fano (12), Shockley's theory postulates an energy loss mechanism for the incident high energy particle through a branching process at the end of which electron-hole pairs and lattice phonons are created. This is not wholly consistent with the present theory of interaction of radition with matter where the main excitations are of a collective plasma type. This should necessitate further theoretical study to clarify the point.

Pertinent to the theory of ϵ is also the question of its temperature dependence. It has been observed by several authors (13) that the pulse height for a monoenergetic source decreases on cooling the detector. None of the terms in Shockley's formula exhibit any rapid variation with temperature

and it should be possible to account any ϵ -variation with temperature through $E_g(T)$. Measurements on with temperature in the range 6 - 77°K have been carried out by Dodge et al. They find that the temperature dependence of ϵ can be well explained by the Shockley theory through the temperature dependence of the energy gap.

Thus it can be said that, apart from the point raised by Fano, the Shockley theory, considering its simplicity, does predict reasonably accurate ϵ - values and the temperature dependence of ϵ.

Intimately connected with the average energy per electron-hole pair is also the question of Fano factor F. Based on what he calls the "crazy carpentry" model van Rooshroeck (3) has carried out elaborate analytical and Monte Carlo calculations of yield, variance and Fano factor. Essentially again, it is the same branching process through which the incident high energy particle loses its energy and produces electron-hole pairs and optical phonons. Theoretically, the relative quantum yield is defined by $Y = E_{th}/\epsilon$, the percentage of ϵ - energy which goes in the production of electron-hole pairs. The dependence of Y and F is then related to the ratio $R = r\, E_R/E_{th}$, the ratio of energy loss to phonons to the ionization threshold energy. The results of his calculations are given in Fig. 1. Using the values of r, E_R and $E_{th} = E_g$ as given above, we can calculate R and then Y and F. Or, conversely,

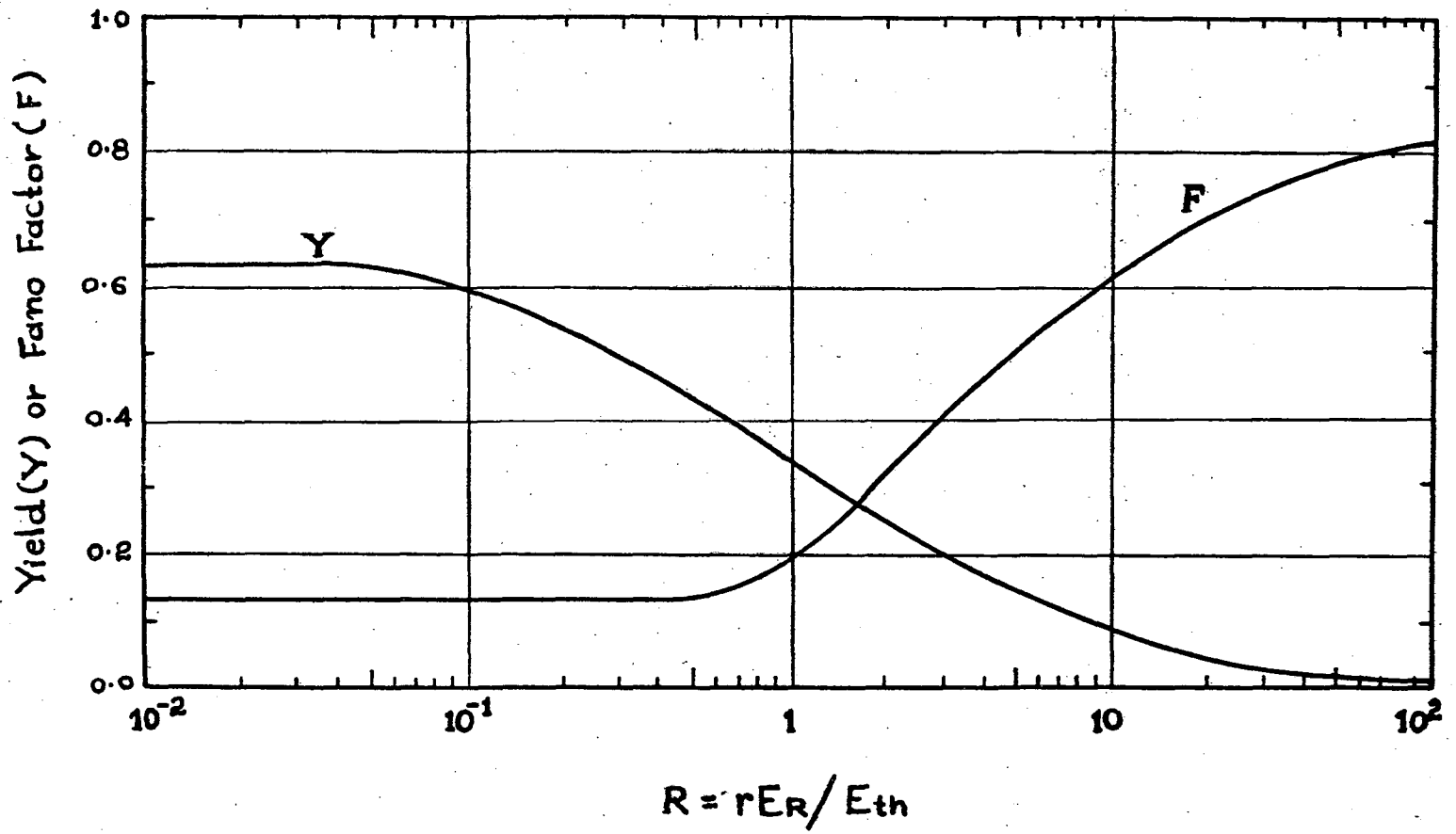

Fig. 1. Yield (Y) and Fano Factor (F) related to the ratio of energy loss to phonons to the ionization threshold energy (R)

R = 17.5 x 0.063/1.1 = 1 for silicon (300°K), and

R = 57 x 0.037/0.74 = 2.85 for germanium (77°K).

using the experimental values of ϵ or F we can calculate the other quantities. Of course in all these calculations an assumption is made that $E_{th} = E_g$.

Experimental determination of ϵ and F has been done by several authors (14). Alongwith some of the values of F are also given in Table I. As is obvious, there seems to be a considerable spread in the values reported in the literature and at this stage nothing definite can be said regarding the exact values. In any case the theory can easily take care of the spread through the adjustable parameters E_{th} and r. Thus a variation of R = 1 - 3 gives a variation in Y = 0.35 - 0.20 and in F = 0.20 - 0.40. To this extent the theory is entirely consistent with the experimental results. However, further accuracy can be obtained only by defining the precise nature of the threshold energy E_{th}.

III. CHARGE COLLECTION PROCESSES:

The faithful collection of the total liberated charge in the sensitive volume of the detector is of course essential to obtain reliable information about the incident particle. The dynamics of charge collection is highly complicated by several processes, some of them competing with each other. We shall briefly consider some of these factors in the following.

Firstly, it is necessary that the dense charge cloud formed along the track of the indident particle should seperate so as to enable to extract the information from the charge pairs. In the initial stages the external field cannot act on the plasma and separation takes place only by diffusion under a high carrier concentration gradient. Soon the external field starts sweeping the carriers at the tail of the diffusion profile and through plasma erosion completes the charge seperation. Hence-onward charge collection begins. Generally the time constant for charge seperation, the plasma time, is sufficiently short ($< 10^{-8}$ sec) so as not to impose limitations on timing possibilities. Also, it will not lead to any serious loss of charge either through direct recombination or recombination via recombination centres; the time constants for the recombination processes are always much greater than 10^{-6} sec.

However, both during the charge seperation and charge collection stages it is necessary that the medium be capable of holding the excess free charge for times long enough to complete these processes. The nature of the medium is characterized by the dielectric relaxation time τ_d and the excess charge decays with time t as $\exp(-t/\tau_d)$. Obviously should be greater than t so as to ensure that very little charge is dielectrically dissipated in the detector medium. In a practical situation the time constant that need be compared with τ_d is the carrier

transit time t_r across the device; other time constants are generally much shorter than t_r. Assuming no field-dependent mobility and constant field $t_r = W/\mu E = W^2/\mu V$, where W is the width of the depletion layer, μ the carrier mobility, E the electric field, and V the applied reverse bias. Typically $t_r > 10$ nsec for both Ge and Si counters. On the other hand, $\tau_d = 1.1(\rho K/4\pi) \times 10^{-12}$ sec where ρ is the resistivity and K the deelctric constant. For intrinisic Si (K = 12 and $\rho = 10^5$ ohm-cm at room temperature) $\tau_d = 10^{-7}$ sec and for intrinsic Ge (K = 16 and ρ = 50 ohm-cm) $\tau_d = 5 \times 10^{-11}$ sec. This clearly indicates the necessity of cooling Ge counters to low temperature in order to reduce the free carrier density so as to increase the resisitivity and hence τ_d. Here it may also be pointed out that, as against silicon, although germanium can be purified to almost intrinsic conditions it is still essential to produce thick Ge counters by the perfect lithium compensation techniques. The reason is, as in insulators, the dielectric relaxation time is governed by the uncompensated impurity centres possessing charge. The effective screening length, the Debye length, is tremendoysly reduced by these active charge centres thus restricting the movement of the free charge. Therefore on cooling if these charge centres are not frozen, the Ge(li) counters would fail to operate. A familiar situation of reduced Debye length occurs in photo-conductors.

Another point that need be considered in connection with the relaxation time is its optimization. Although too low a value is ruled out due to the dissipation of charge in the detector medium, too high a value will lead to incomplete charge collection due to the finite bandwidth of the amplifier. It is therefore quite likely that the liquid nitrogen temperature for the operation of Ge(Li) counters may not be the optimum temperature. This should also probably explain the recent observations made by El-Shishini and Zobel (15).

After assuring that there is complete charge seperation and that the detector medium will not eat away the excess charge before it is collected, we should consider other factors which are likely to shunt the charge collection. Miller and Gibson (16) have studied in considerable detail the problem of charge collection efficiency, defined by $\eta = Q_c/Q_L$ where Q_c is the collected charge and Q_L the liberated charge. They find that the important mechanism limiting the full collection is the trapping of the charge during its transit to the respective electrode. In fact the charge collection process in an electric field is described by the equation (17)

$$\Delta Q_c = Q_L \ \Delta x/W$$

where ΔQ_c is the collected charge when it moves over a distance Δx in the electric field. As is clear from this equation, full collection of the charge will be restricted by the inability

of the charge to traverse the entire distance W. Assuming that we are dealing with a constant-field (as in PIN detectors) and field-independent mobility situation, the distance Δx covered in its lifetime τ by a free carrier is $\Delta x = \mu E \tau$. Similarly, expressing W in terms of transit time $t_r = W/\mu E$, charge collection efficiency is given by $\eta = \tau/t_r$. After taking care of the charge lost or immobilized in time t_r, the fraction of this charge is $\left[1-\exp(-t_r/\tau)\right]$, we have

$$\eta = (\tau/t_r)\left[1 - \exp(-t_r/\tau)\right]$$

For $t_r > \tau$ charge collection is very poor. On the other hand, when $t_r < \tau$, η can be written as

$$\eta = 1 - (t_r/2\tau) = 1 - (W^2/2\mu V \tau).$$

The importance of large reverse biases for good collection efficiency is obvious from this equation; also is obvious the necessity of high lifetime material. In devices prepared with techniques which are likely to introduce a high concentration of recombination or trapping centres, as in diffused silicon detectors, charge collection will be rather poor. The preparation of new materials to the level of perfection of Ge and Si should also be emphasied here.

Pertinent to the processes of charge collection is the subject of pulse formation at the detector output end. But we will not consider it in any detail as it has been reviewed

thorughly by Goulding (6). However, it should be pointed out that the requirement of low resistivity material for fast risetime (18) should not clash with the requirement of high dielectric relaxation time for complete charge collection.

IV. LIMITATIONS TO ENERGY RESOLUTION:

Although not directly connected with the physics of detection, several statistical processes need be considered to assess the full usefulness of a semiconductor detector for nuclear spectroscopy. From this point of view it may be stated that as compared with the statistics of energy loss, of creation of electron-hole pairs, and of charge seperation and collection, the statistics of background processes are more important. Thus the problem of the electronics of a semiconductor counter is the one of maximization of signal to noise ratio. It may be pointed out here that although noise is highly undesirable, the occurrence of the detector noise predominantly in the low frequency region of the noise spectrum is a very happy circumstance (19); it enables to design high-pass filters for the optimization of the signal to noise ratio.

Apropos optimization of signal to noise ratio, the detector and the amplifier system must be considered together. Gouldingand Hansen (20) attribute the energy spread of a monoenergetic line to two important sources of noise, viz. the input tube shot noise and the current noise. For a single differentiating and integrating time constant τ_a of the amplifier,

the tube shot noise decreases with increasing τ_a whereas the current noise increases with increasing τ_a. Therefore there exists an optimum amplifier time constant for which the best energy resolution could be obtained. Thus the use of a field-effect transistor cooled to liquid nitrogen temperature along-with Ge(Li) detector (21), through a decrease in the shot noise, improves the γ- ray resolution to 0.7 keV.

In characterizing the noise-behaviour of the detector, Goulding and Hansen have used the reverse current (leakage current) as the parameter determining the detector noise. Although it is a good and simple criterion, it fails to show the details of the noise distribution. It is therefore necessary to trace the origin of the noise to the basic processes going on in a reverse-biased p-n junction (22). The reverse current itself depends upon the carrier generation and recombination through the agency of deep recombination centres. The charge fluctuation at the recombination centres is compensated by an equal charge fluctuation in the free carrier densities. This is passed on as noise, with a fluctuation time constant τ_f in the external circuit. Using the Shockley-Read-Hall(23) statistics the noise spectrum associated with this charge fluctuation has been analyzed by Sah (24) for the depletion region of the field-effect transistor. We have extended the theory of Sah to the case of detectors (19). It is shown that the noise power spectrum, defined as the mean square noise per unit bandwidth,

for a detector-amplifier system is given by

$$\langle E^2_{da}\rangle = \langle E^2_{dt}\rangle \quad (2/\pi)\left[x/(1 + x^2)\right] \left[a\, x^2/(1 + a\, x^2)^2\right].$$

In this expression $\langle E^2_{da}\rangle$ is the mean square detector-amplifier noise expressed in keV^2; $\langle E^2_{dt}\rangle$ is the total mean square detector noise (in keV^2 per unit sensitive colume of the detector) in the absence of the amplifier; $x = \omega \tau_f$, $\Delta x = \Delta\omega \tau_f$ and $a = \tau_a^2/\tau_f^2$ with ω the angular frequency where the noise is measured, τ_a the amplifier time constant and τ_f the fluctuation time constant. With a cut-off frequency defined by $x = x_c$ ($x_c = \omega_c \tau_f = 2\pi f_c \tau_f = 2\pi \tau_f/\tau_c$) lying well beyond the maximum of the noise spectrum as given by the above equation, $\langle E^2_{da}\rangle$ can be easily integrated from $f = f_c$ to ∞. The total mean square noise is then given by

$$\langle E^2_{dat}\rangle = \langle E^2_{dt}\rangle \quad (2/\pi)/(3a x_c^3)$$

$$= \langle E^2_{dt}\rangle \quad (1/\ 12\pi^4)(\tau_c^3/\tau_a^2 \tau_f)$$

As is clear from this equation, energy resolution is extremely sensitive to the various time constants and therefore to the factors that determine these time constants.

The noise expression derived here is quite general and be used for any junction-type detector. However, to calculate the resultion it is necessary to have certain information about the recombination centres. It is thus necessary to know

the density, the energy level, and the electron - and hole-capture cross-sections. Unfortunately this information is completely lacking for most of the devices except for diffused silicon detectors. Using the available data for silicon and taking a typical case of $a = 10^{-2}$ ($\tau_f = 7\mu sec$, $\tau_c = 0.7\mu sec$), $x_c = 10^2$ ($\tau_c = 0.45\mu sec$), $\langle E_{dt}^2 \rangle = 10^9$ keV^2 per unit volume ($\rho = 1000$ ohm-cm), $W = 10^{-2}$ cm and area of the detector = 1 cm^2, the energy resolution is $\langle E_{dat} \rangle = 15$ keV. This seems to be a reasonable value agreeing with the experimentally observed best resolutions (6).

So far we have been considering the generation-recombination noise in the bulk of the semiconductor. Of course processes continuously occur on the surface of the semiconductor and in several instances decisively determine the usefulness of the device. But any attempt in estimating the contribution to noise from this source is completely hampered by the aweful ignorance about the surface. Several factors alter the characteristics in many ways. Thus to enumerate just a few example: adsorption of polar molecules will induce surface states which can act as traps or recombination centres; presence of charge will either attract or repel the free charge from the bulk thus giving rise to spurious capacitive effects; formation of inversion layer on the p-n junction will prevent application of large reverse biases. However, a workable control over the surface properties can be obtained by chemical treatments,

by thermal cycling in different ambients, by the application of electric fields during, say, cooling of the Ge(Li) detectors, or by several combinations of these processes. In essence, surface control is an art and recipes have to be worked out for specific problems.

V. CONCLUDING REMARKS:

In the foregoing discussion we have been considering only a few of the basic aspects connected with the details of detection in a semiconductor counter. The detector literature is replete with several effects and defects -- just to mention one of each category we have the ion channeling effect (25) and the fission fragment pulse height defect (26). Therefore whille trying to present a consistent picutre of the detection mechanism it was felt necessary to confine to those aspects having direct bearing on the subject matter. Although this is a difficult procedure, as several aspects are inter-related to each other, a heavy selection of topics had to be made.

Finally, before closing this review we should like to make a mention of the possibility of a proportional solid-state counter. A noiseless p-n junction detector operated in a multiplying mode should show improvement in energy resolution because of the effective reduction in the average energy to produce an electron-hole pair. But noise considerations are quite serious and seem to preclude the possibility of such a

device (27). However, Locker and Huth (28) have recently introduced a new concept of detection of high speed singnals even in the presence of excessive noise. They use an avalanching untoured surface-type silicon detector coupled to a tunnel diode for the detection of extremely low energy events. With their scheme they have been able to detect x-rays down to 1.49 keV. This corresponds to the detection of a pulse of 400 electrons introduced into the avalanche detector. Further work in this field will be watched with great interest.

Table I.

Experimental values of the average energy per electron-hole pair (ϵ) and Fano factor (F)

ϵ (eV)	F	Temperature T°K	Type of Radiation	Reference
Si				
3.61	-	300	5.477 MeV - α	Bussolati et al, Phys. Rev. 136 A, 1756 (1964).
3.79	-	300	365 keV-e	
3.55	-	300	Independent of radiation	Goulding, Nucl. Instr. and Meth. 43, 1 (1966).
3.53	-	297	4.82,5.30 MeV-	Buys, Nucl. Instr. and Meth. 42, 329 (1966).
3.61 - 3.86	-	300 - 20	5.477 MeV- α	Emery and Rabson, Phys, Rev. 140 A, 2039 (1965).
3.79 - 5.22	-	300 - 20	1.06 MeV-e	
3.72	-	6 - 77	1.06 MeV-e	Dodge et al Phys. Rev. Letters 17, 653 (1966).
Ge				
2.85	0.38 - 0.50	77	122-2614 keV- γ	Ewan and Tavendale Can. J. Phys. 42, 2286 (1964)
2.93	0.23 - 0.35	77	122-2754 keV- γ	Antmann et al Nucl. Instr. and Meth. 40, 272 (1966).
2.3	0.13 - 0.16	77	122-10,000 keV- γ	Mann et al NS-13, 252 (June 1966).

REFERENCES:

1. J.M. Hollander, Nucl. and Meth. 43, 65 (1966)
2. J.W. Mayer, Nucl. Instr. and Meth. 43, 55 (1966)
   W.L. Hansen, Lawerence Rad. Lab. Private Communication (1966)
3. W. van Roosbroeck, Phys. Rev. 139A, 1702 (1965)
4. H.D. Maccabee, M.R. Raju and C.A. Tobias, IEEE Trans. Nucl. Sci. NS-13, 176 (June 1966).
5. P.V. Vavilov, Soviery Phys. JETP 5, 749 (1957)
6. See, for example, F.S. Goulding, Nucl. Instr. and Meth. 43, 1 (1966).
7. W. Shockley, Solid-State Electron. 2, 35 (1961).
8. H. Palevsky, D.J. Hughes, W. Kley, and E. Tunkelo, Phys. Rev. letters, 2, 258 (1959)
9. B.N. Brockhouse and P.K. Iyengar, Phys. Rev. 111, 747 (1958).
10. V.S. Vavilov, J. Phys. Chem. Solids 8, 223 (1959)
11. See references given with Table I.
12. U. Fano, Ann. Rev. Nucl. Sci. 13, 1 (1963).
13. W. R. Dodge, S.R. Domen, T.F. Leedy, and D.M. Skopik, Phys. Rev. Letter, 17, 653 (1966).
    F.E. Emery and T.A. Rabson, Phys. Rev. 140A, 2089 (1965).
14. See references given with Table I.
15. M.M. El-Shishini and W. Zobel, IEEE Trans. Nucl. Sci. NS-13, 359 (June 1966).
16. G.L. Miller and W.M. Gibson, Nuclear Electronics I, 477 (IAEA, Vienna, 1962).

17. G. Cavalleri, G. Fabri, E. Gatti and V. Svelto, Nucl. Instr. and Meth. 21, 177 (1963).

18. P.A. Tove and F. Falk, Nucl. Instra and Meth. 29, 66 (1964).

19. R.Y. Deshpande, Nucl. Instr. and Meth, 46, 255 (1967)

20. F.S. Goulding and W.L. Hansen, Nucl. Instr. and Meth 12, 249 (1961).

21. L. Glad, Nucl. Instr. and Meth, 37, 327 (1965).

22. C.T. Sah, R.N. Noyce, and W. Shockley, Proc. IRE 45, 1228 (1957).

23. W. Shockley and R.T. Read Jr. Phys. Rev. 87, 835 (1952). R.N. Hall, Phys. Rev. 87, 387 (1952).

24. C.T. Sah, Proc. IEEE 52, 795 (1964).

25. W.M. Gibson, IEEE Trans. Nucl. Sci. NS-13, 162, (June 1966)

26. H.W. Schmitt, W.M. Gibson, J.H. Neiler, F.J. Walter, and T.D. Thomas, Physics and Chemistry of Fission I, 531 (IAEA, Vienaa 1965).

27. R.H. Baitz and F.M. Smits, IEEE Trans. Nucl. Sci. NS-13, 198 (June 1966).

28. R.J. Locker and G.C. Huth, Appl. Phys. Letters, 9, 227 (1966).

DISCUSSION:

R. Ramanna: Can you tell us something about the present status of position sensitive detectors?

R.Y. Deshpande: These detectors were interoduced in 1963 and presently several laboratories are working on them. However, non-linear effects seem to be quite serious and compromises have to be made to obtain good resolution.

P.N. Tiwari: What is maximum depletion layer of Li-Ge detector obtained so far?

R.Y. Deshpande: About 15 mm. More appropriately, sensitive volumes upto 54 cm^3 have been reported.

P.K. Patwardhan: What about non-linear effect you may encounter when using tunnel diode systems for noise discrimination?

R.Y. Deshpande: The proportional solid-state counter I have described is essentially a digital detector.

A HIGH RESOLUTION X-RAY SPECTROMETER USING LITHIUM DRIFTED SILICON DETECTOR FOR NUCLEAR CHARGE DETERMINATION

S.S. Kapoor and P.N. Rama Rao
Bhabha Atomic Research Centre,
Trombay, Bombay.

In the recent years, the semiconductor detectors are being increasingly used for the high resolution gamma ray and X-Ray spectroscopy. This has been made possible by the technological advances in the fabrication of totally depleted thick detectors, which in addition to giving high resolution also have good detection efficiencies.

The present paper describes a photon spectrometer set up at Trombay for the determination of nuclear charges by measuring the characteristic X-Ray energies. In particular this set up is planned to be used for the study of nuclear charge distribution in fission by physical means. The complete set up consists of a cooled Lithium drifted silicon detector, a cooled field effect transiter mounted on the top of the detector, a low noise preamplifer and a main amplifer connected to a multichannel analyser.

Fig.1 shows the mounting arrangement. The cold finger is maintained at the liquid nitrogen temperature by a L type cryostat (2). The detector is attached to a Aluminium ring which is separated from the cold finger by means of three

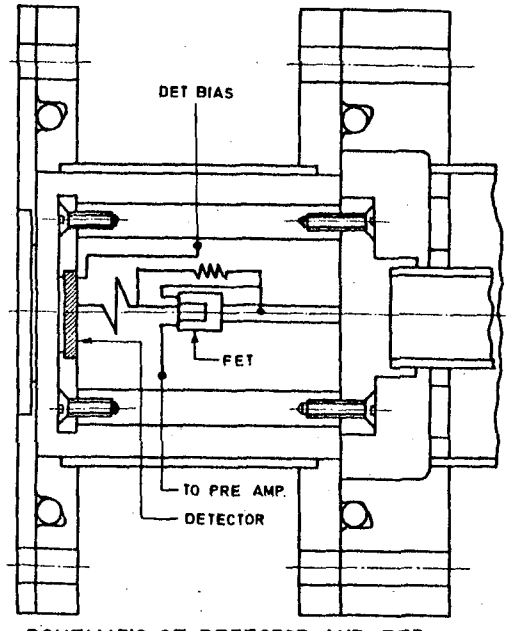

SCHEMATIC OF DETECTOR AND FET

FIG. 1

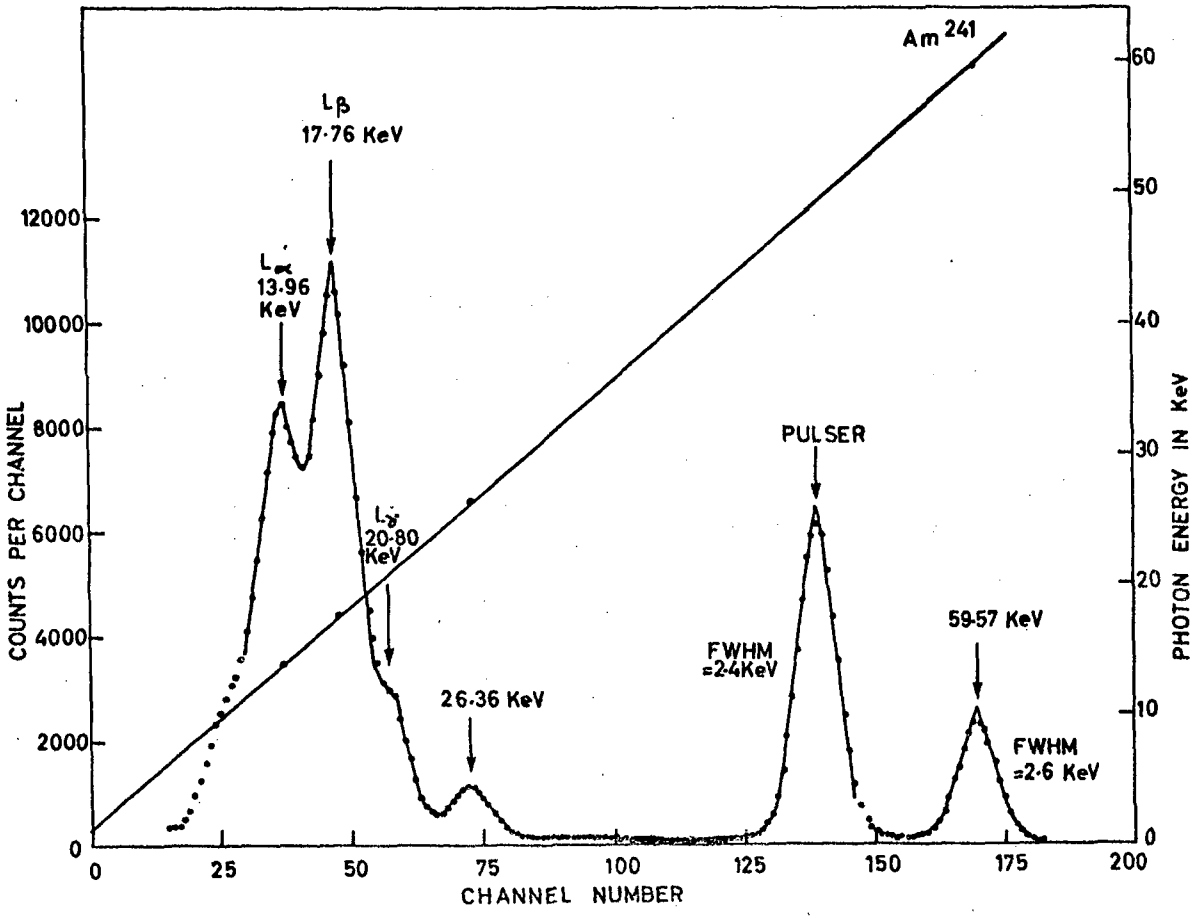

FIG. 2

ceramic rods which electrically isolate the detector and also provide the necessary heat leak to maintin the detector at about - 140 °C, which was found to be the optimum temperature for best resolution. A n - channel field effect transistor attached to the cold finger and cooled to liquid nitrogen temperature is connected to the detector with a spring loaded contact. The FET is followed by a preamplifier of the type developed by Elad and Nakamura (2). The chamber containing the detector and the field effect transistor is evacuated to a pressure of about 1 x 10^{-7}mm of Hg, by an ion pump. The detector was operated at a reverse bias of 300 volts for optimum energy resolution performance.

Fig.2 shows the spectra of gamma rays and L-X Rays emitted by ^{241}Am. The energy resolution as measured in terms of full width at half maximum of 59.57 keV line is found to be 2.6 keV. Fig.3 shows the spectra of X-Rays and gamma rays emitted from the sources of ^{137}Cs, ^{133}Ba, ^{153}Gd and ^{57}Co. The spectra of K - X Rays of Ag, excited by the 59.57 keV gamma rays of ^{241}Am is also shown along with the positions of peaks expected for the neighbouring elements. From Fig.3 it is evident that from the observed peak positions in the X-Ray spectra, it ispossible to unambigously determine the charge of the emitting nucleus. Though further improvement in the energy resolution is desired, even with the present energy

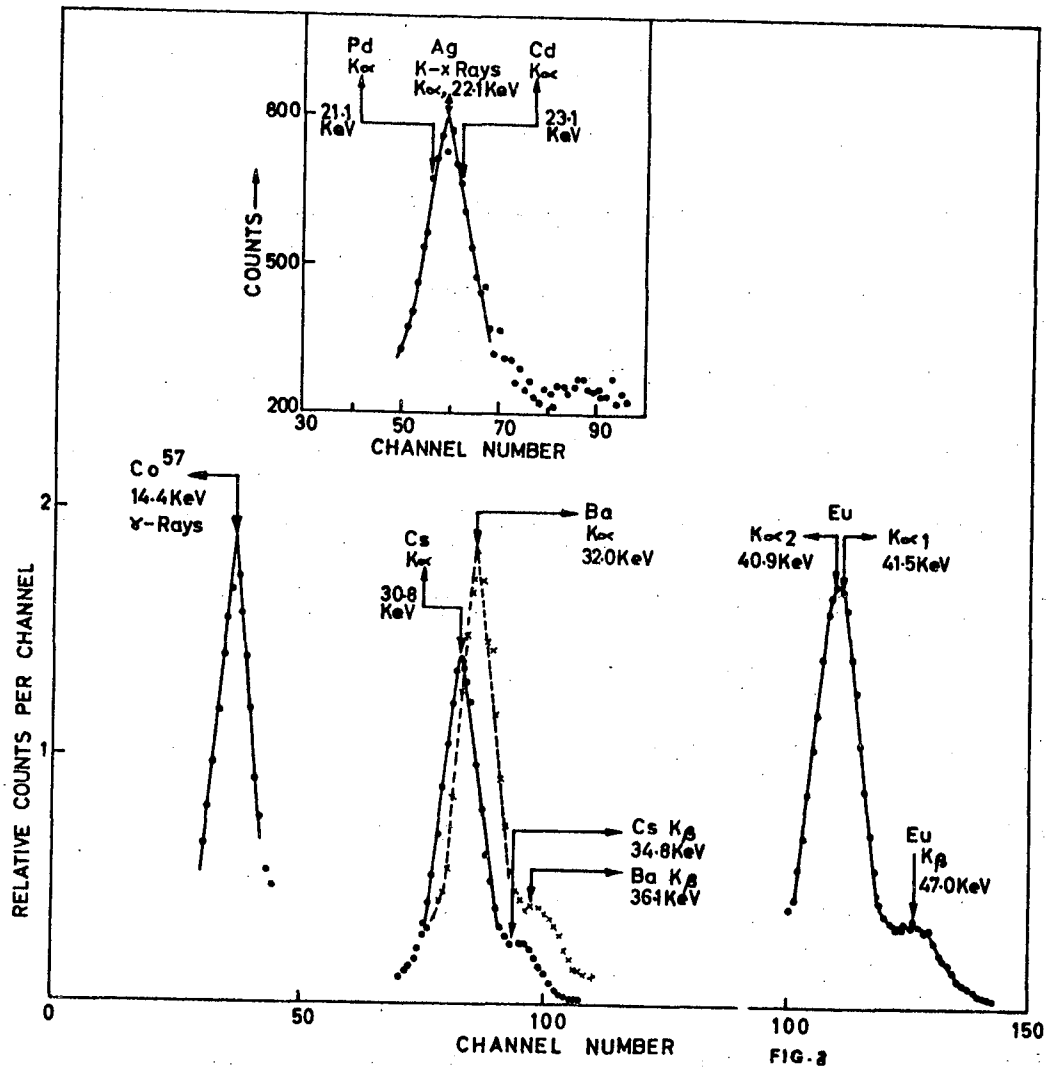
Pd
Kα
Ag
K-x Rays
Kα, 22·1KeV
Cd
Kα
21·1
KeV
23·1
KeV
800
500
200
COUNTS
30
50
70
90
CHANNEL NUMBER
Co 57
14·4KeV
γ-Rays
Cs
Kα
30·8
KeV
Ba
Kα
32·0KeV
Cs Kβ
34·8KeV
Ba Kβ
36·1KeV
Eu
Kα2
40·9KeV
Kα1
41·5KeV
Eu
Kβ
47·0KeV
RELATIVE COUNTS PER CHANNEL
2
1
0
50
100
CHANNEL NUMBER
100
150

FIG. 3

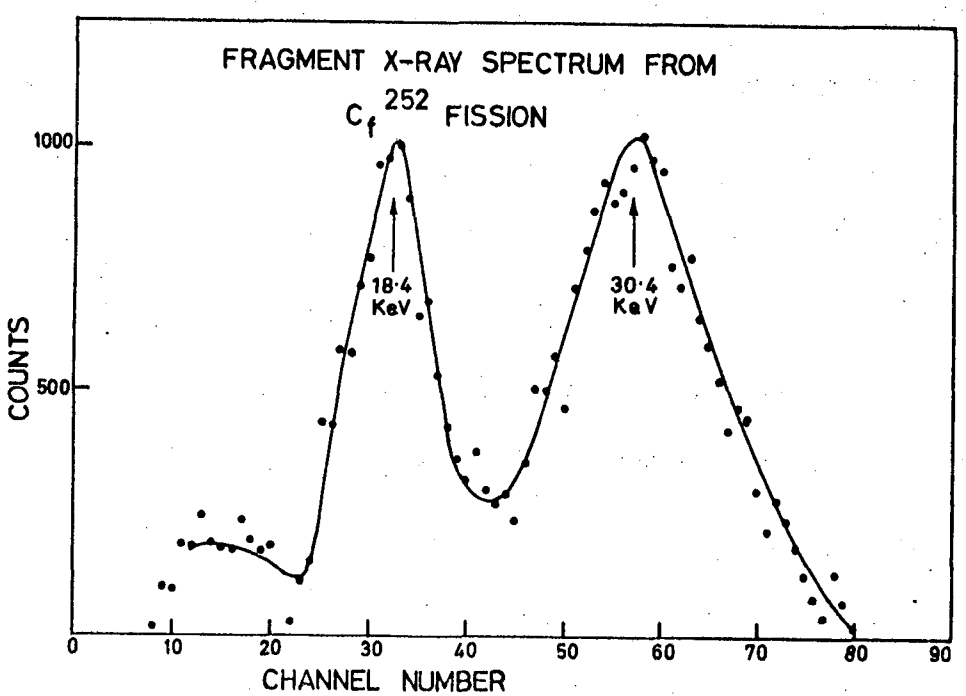
FRAGMENT X-RAY SPECTRUM FROM
Cf 252 FISSION
1000
500
COUNTS
18·4
KeV
30·4
KeV
0
10
20
30
40
50
60
70
80
90
CHANNEL NUMBER

FIG. 4.

resolution the system can be used for non-destructive identification of elements by exciting their X-Rays by an external gamma source, and recording the spectra of the emitted X-Rays.

The system is planned to be used for the study of prompt K X - Rays emitted by fission fragments to enable a physical determination of the charges of the fragments. The spectra of K - X Rays emitted by the fragments in the spontaneous fission of ^{252}Cf, as obtained by this set up, is shown in Fig.4.

Further improvements in the preamplifier system including choise of proper FET are now being attempted to further improve the energy resolution.

REFERENCES:

1. E. Fugene Miner, UCRL - 11946 (1965)
   H.R. Bowman, E.K. Hyde, S.G. Thompson and R.C. Jared, UCRL - 16485 (1965)
2. E. Elad and M. Nakamura, Nuclear Instruments and Methods, 42, 315 (1966)

DISCUSSION:

P.K. Patwardhan: Have you studied the contribution of drift and noise separately on the line width broadening contributed by the preamplifier?

S.S. Kapoor: Since in some cases we took spectra for only about a few minutes, the drift obviously could not play significant role in giving the observed spread.

A. Chatterji: In accumulating about 1000 counts at the peak in the ^{252}Cf fission, what was the running time? About a day's run?

S.S. Kapoor: Yes, 7 to 8 hours.

P.P. Kane: You mentioned something about coincidences in connection with your work. Can you clarify this point?

S.S. Kapoor: The coincidences are those between the γ-rays from fission fragments and characteristic K X-rays.

S. Mohan Bharathi: Did you try to measure the temperature at the position of the detector?

S.S. Kapoor: We have made use of the work done at Berkely in this connection.

B. Lal: What is the reason for choosing Lithium drifted silicon detector and not the Lithium drifted Germanium detector? I feel the resolution and efficiency wise the Germanium Lithium drifted detectors are better than silicon detector?

S.S. Kapoor: Li drifted silicon detectors have a much narrower window, and, therefore, are better for low energy photon measurements.

ON THE DETERMINATION OF CONVERSION RATIOS USING SEMI-CONDUCTOR DETECTORS

L.R. Khare
Physics Department
Indian Institute of Technology, Kanpur

ABSTRACT.

Conversion ratios, conversion electron spectrum, γ-spectrum and the decay schemes of some unclides (like ^{148}Sm) were studied with great accuracy using fast-slow coincidence, 512-channel analyzer and a NaI(Tl) γ-spectrometer. The beta-detector was a Molechem Si p-n junction detector (depth 2μ, resistivity 20,000 ohm.cm, are 20 mm^2 and a leakage current=1.5μ.amp at the maximum reverse bias of 250 volts).

The resolution of the entire β-spectrometer vs. reverse bias applied V was examined using the 624 keV K-conversion line of ^{137}Cs with the detector at room and dry ice temperatures. Cooling improves the resolution, being 1.8 percent at 250 volts reverse bias and dry ice-temp., at which the system wasoperated for all measurements. There is an increase in the pulse-height response of the detector with increasing V for a given line; its graph is obtained by noting the channel in which the line peak was lying. A graph was plotted between the total energy absorption efficiency (being the ratio of the counts at the applied rev. bias V to that at 250 Volts) vs. $(V)^{\frac{1}{2}}$. For the above type detector depletion width W and V are related as:

$W = 0.3\ (\rho V)^{\frac{1}{2}}$ microns, where ρ is the resistivity in ohm-cm.

The detector was calibrated using standard sources and pulse ht. response vs. particle energy was found to be linear. Conversion ratios found by our method agree very closely with the values of other workers, who used lens, magnetic and other spectrometers.

MEASUREMENT OF CAPTURE GAMMAS FROM RESONANCE ABSORBERS USING LEAD SPECTROMETER

K. Chandramoleswar, M.P. Navalkar, M.R. Phiske,
D.V.S. Ramakrishna and S.K. Sadavarte
Bhabha Atomic Research Centre, Trombay, Bombay

INTRODUCTION:

The principle of lead spectrometer which has been built at BARC in connection with an IAEA research contract project, has been described in our previous papers (1,2). In brief it consists in injecting short bursts of fast neutrons in a lead assembly at time t = 0 which slow down with time as a result of elastic collisions with lead nuclei. Becuase of the large mass number (M = 207) monoenergetic neutrons with a narrow spread about mean energy are obtained as a function of time elapsed from t = 0. An absorber and detector placed at the centre of the assembly, in conjunction with a multichannel time analyser gives reaction rates in the absorber due to monoenergetic neutrons.

When the neutron energy is high, it can be shown that the mean energy and dispersion of the distribution are given by

$$\langle t_f \rangle = \frac{1+\mu}{1-\frac{1}{3}\mu} \cdot \frac{\lambda}{\mu v} \qquad \text{--------- (1)}$$

$$D_f = \frac{2}{3}\mu \cdot t_f^2 \qquad \text{--------- (2)}$$

When μ, λ and v are the inverse mass number, scattering mean free path of lead and the neutron velocity respectively.

However when the neutron energy approaches the energies associated with thermal exitation of moderator nuclei, the dispersion is no longer energy independent and can be calculated using time moments as given by Williums (3).

$$t(E) = t_f \left[1 + c(\mu) \frac{K\bar{T}}{E} \right] \qquad \ldots\ldots(3)$$

$$D(E) = D_f \left[1 + B(\mu) \frac{K\bar{T}}{E} \right] \qquad \ldots\ldots(4)$$

Where $C(\mu)$ and $B(\mu)$ are the positive functions of inverse mass (μ) and $\bar{T}$ is the measure of kinetic energy of the nucleus.

The measurements of gamma ray intensities from isolated resonances of various absorbers at energies where thermal motion influences the slowing down process have been made to verify the above relations and the results are reported in this paper.

EXPERIMENTAL:

The measurements were carried out using samples of Ag, Au, Ta, Ho etc. A thin plastic scintillator was used in conjunction with a 40 channel time analyser to record capture gamma rays. The detector was covered with a bismuth shield of 2 m.m thickness to avoid detection of transition and activation gammas. The capture gamma intensity I_γ, was normalized to neutron density I_B measured with a 1/v detector such as BF_3. If I_γ be the counting rate with resonance absorber then

$$I_\gamma(t) \propto \iiiint^{\mu' t_0 t'_\infty} \left(1 - e^{-n'\sigma_A(E)\frac{x'}{\mu'}}\right) v\, n(E,t)\, dE\, d\mu'\, dt_0\, dt_1 \qquad \text{-------}(5)$$

Where t_0 is the burst width

t_1 is the channel width

n' is the no. of atoms of the absorber element per cc.

$\sigma_\Delta(E)$ is the doppler broadened cross section.

x is the thickness of the absorber.

RESULTS AND CONCLUSIONS:

(I_γ/I_B) as a function of time for each element was calculated using expressions (1-5). In order to save computation time the doppler broadened cross section was replaced by an analytical expression given by Fraser (4). Column III of Table I shows calculated values of half widths (full width at half maximum) taking dispersion as given by expression (2) with nuclei considered free and at rest (natural broadening), where as column IV incorporates effects due to thermal motion in addition to natural broadening and column V due to natural broadening, thermal motion and admixture of oxygen in lead. It has been verified by density measurements and ultrasonic testing that blow holes are present and are introduced as a result of casting. The experimental results of (I_γ/I_B) were plotted as a function of time and the typical curves for Ta and Ho are shown in Figures (1) & (2). The column VI of the Table I gives the experimental values of the half widths. It is seen from the Table that the experimental half width for all the elements, even taking errors into account are much higher than the widths calculated for pure lead without

FIG. 1 (I_γ / I_B) AS A FUNCTION OF 't' FOR Ta.

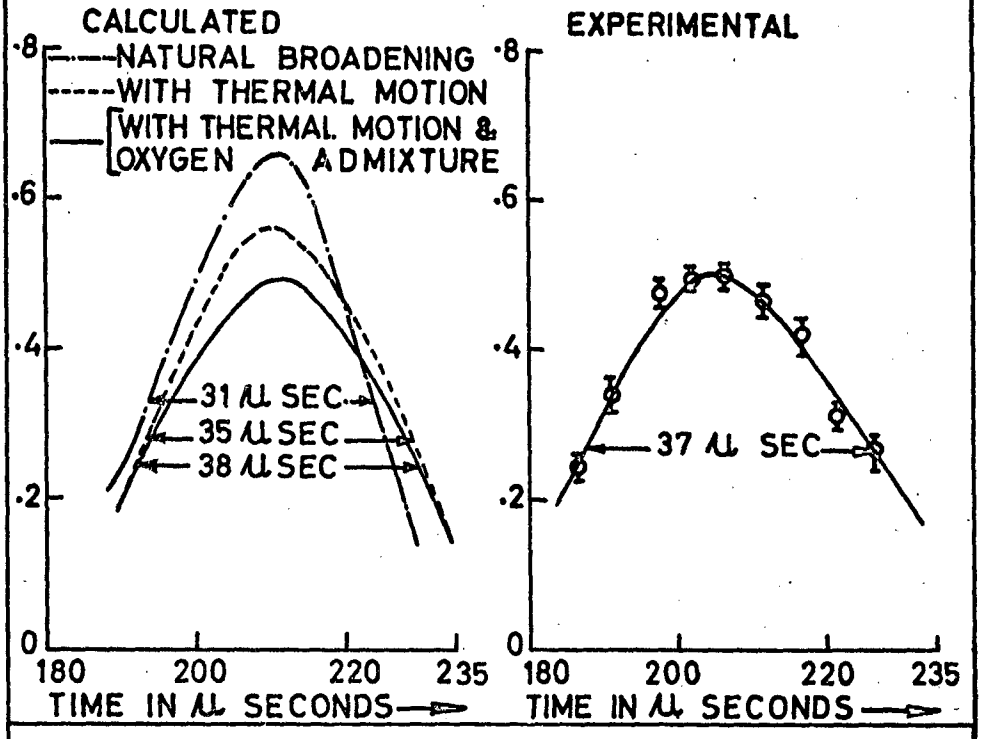

FIG. 2 (I_γ / I_B) AS A FUNCTION OF 't' FOR Ho.

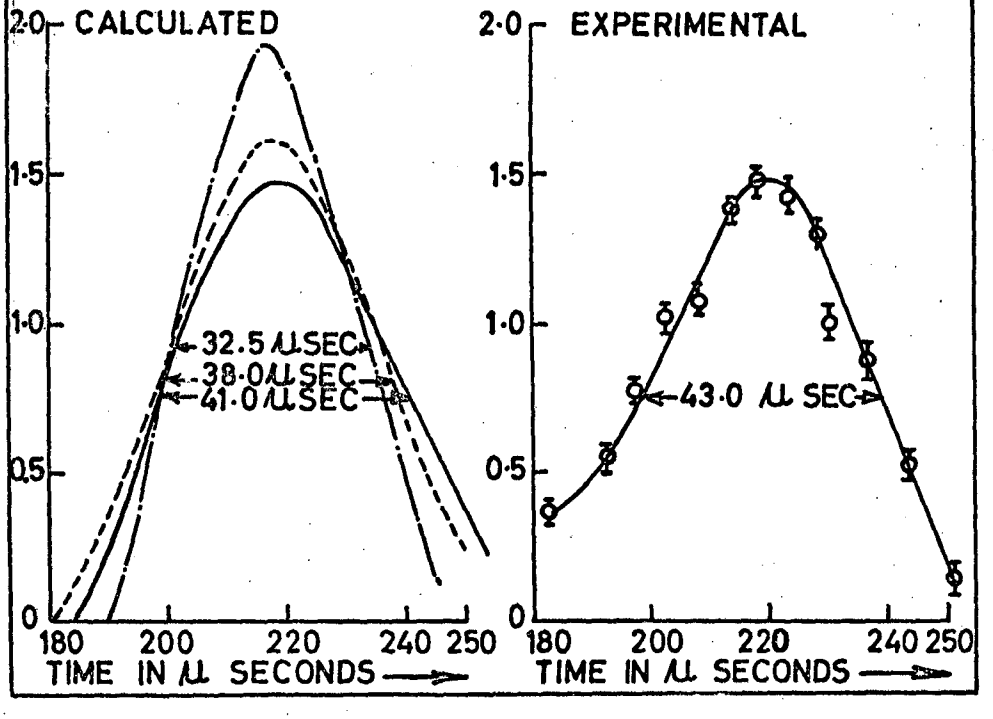

taking into account the broadening caused by thermal motion. An admixture of oxygen (5×10^{-3} per lead atom) has been used for calculations. The difference between columns IV and V of Table I is not appreciable and is of the same order as the experimental error on the determination of the half widths. The effect of admixture could have been seen at higher energies where broadening due to thermal motion which is a predominant factor at low energies is much less. Even with the present experimental errors it can be said that there is better agreement between the experimental values of half widths and the calculated ones taking into account effects of thermal motion and admixture than those calculated with thermal motion alone.

REFERENCES:

1. K. Chandramoleswar, M.P. Navalkar, R. Ramanna, D.V.S. Ramakrishna and K.R. Subbaramu, Nuclear Physics and Solid State Physics Symposium (1964).

2. K. Chandramoleswar, M.P. Navalkar, M.R. Phiske, D.V.S. Ramakrishna, J.V. Ramanna and S.K. Sadavarte, Nuclear Physics and Solid State Physics Symposium (1966).

3. M.M.R. Williums, Nucl. Sci. Eng. 19, 221 (1964).

4. J.S. Fraser, AECL 1744, Part A, (1963)

TABLE I

Capture ray measurements (Half Widths)

	Isotope of the element having resonance	Resonance energy Eo in ev	Calculated half width in μ-secs. due to natural broadening and averaged over burst and channel width.	Calculated half width in μ-secs. due to natural broadening, thermal motion and averaged over burst and channel widths.	Calculated half width in μ-secs. due to natural broadening, thermal motion and averaged over burst and channel widths.	Experimental values of half widths in μ-secs.
1.	Ag^{109}	5.2 ev	31	33	37	41 ± 10%
2.	Au^{197}	4.9	31	35	39	41 ± "
3.	Ta^{181}	4.28	31	35	38	37 ± "
4.	Ho^{165}	3.92	32.5	38	41	43 ± "
5.	Tb^{159}	3.35	35.5	43.5	44.5	40 ± "
6.	In^{115}	1.46	62	139	144	140 ± "
7.	Rh^{103}	1.26	89	122	124	130 ± "

DISCUSSION:

G.V. Acharya: (1) Does your computation take into account, the shadowing effect of resonances? (2) Are your calculations valid for thick films and anisotropic beams?

D.V.S. Ramkrishnan: (1) This does not arise in our case. (2) As can be seen from the equation, absorption probability takes care of the thickness and isotopy is taken care of by cos θ term.

M.P. Navalkar (Comment):-

The resonances are isolated resonances and the width of the resonance is of the order of 2 ev. If we take the case of any element, say, silver we find that two resonances (5 eV and 16 eV) are separated and hence there is no interference from the resonance other than the desired one.

THERMAL NEUTRON CAPTURE GAMMA-RAYS FROM $^{59}Co(n,\gamma)^{60}Co$ AND $^{159}Tb(n,\gamma)^{160}Tb$ REACTIONS

K. Sriramamurty, Ch. Suryanarayana,
D.L. Sastry and Swami Jnanananda.
Laboratories for Nuclear Research,
Andhra University, Waltair.

INTRODUCTION:

Theoretical as well as experimental studies of odd-odd nuclei seem to be particularly interesting since they provide information about the residual neutron-proton interaction. Most of the odd-odd isotopes cannot be studied by the general technique of radioactive decay, since they are not populated by beta-decay and hence reactions of the type (n,γ) and (d,p) are taken recourse to.

The present studies concern with the level structures of $^{60}_{27}Co_{33}$ and $^{160}_{65}Tb_{95}$ odd-odd isotopes, the former belonging to the medium-mass region and the latter belonging to the deformed mass region of atomic nuclei, Neutron capture gamma rays from ^{60}Co have been earlier reported, but coincidence and angular correlation studies are undertaken, since no excited state spin assignments have been given earlier. Information on ^{160}Tb is scanty, and we have undertaken to study the low energy part of ^{160}Tb decay scheme using gamma-gamma coincidence measurements.

EXPERIMENTAL DETAILS:

We planned to use the E-12 beam hole of the 40 MW Cirus at Trombay. Internal and external collimation has been

done and the necessary shield structure erected. The beam is filtered for gamma-rays by a 6" long bismuth plug at the core-end and further by a 4" long bismuth at the reactor wall-end. In order to enable the effective removal of the sizeable fast-neutron content, several selected quartz crystals are cored and faced to the 3.5" diameter neutron column, for a length of 8".

Thin samples of specpure materials are used for singles and coincidence studies in the low-energy region. In the case of cobalt, the sample is a foil of ½" diameter and in the case of Terbium, Terbiumoxide powder is sandwitched uniformly in between very thin cellophane and filter papers of ½" diameter. The back-ground contributed due to cellophane is quite small, and is taken account of. For angular correlation studies, Cobalt in the form of a right circular cylinder, ½" long and 5 cm. in diameter, is employed.

The neutron beam, collimated to 1" in diameter with an intensity of 10^6 neutrons/sec/cm^2 at the target position, leaves the shielding through 1.5" i.d.B_4C tube (shielded outside with lead and paraffin), to be further attenuated and led to the beam-catcher. The target is looked at by two scintillators each mounted on RCA 6810A photomultiplier tubes, well shielded by lead, B_4C, paraffin and Li_2CO_3 and the shielding layout is as shown in figure 1. The scattered neutrons are prevented to enter the crystals by enriched $^6Li_2CO_3$ at their faces. The

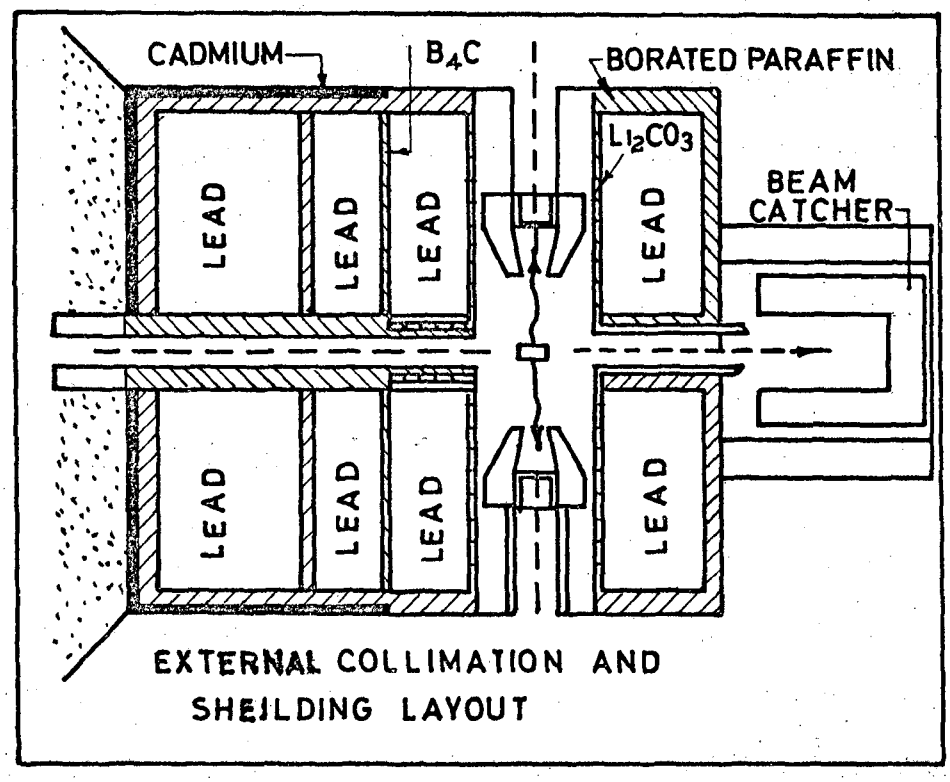

EXTERNAL COLLIMATION AND SHEILDING LAYOUT

background is found to be 2,500 counts/per sec. over an integral bias of 50 keV.

The spectrometer utilises a transistorized fast-slow triple coincidence assembly with a resolving time of 30 nsec. The singles and coincidence spectra are taken using the TMC 400 multichannel analyser of the Van de Graaff Laboratories. For angular correlations the movable counter in the vertical plane is controlled and automated by the electronic control unit.

EXPERIMENTAL RESULTS:

The single spectra are observed with scintillation counter which has a resolution of 8.4% for the 662 keV ^{137}Cs peak.

The low energy spectrum of ^{60}Co is found to have energy components of 60 -, 158 -, 230 -, 280 -, 390 -, 450 -, 510 -, and 550 keV. The coincidence spectra are taken by gating each of these components.

Calculations for estimation of the intensities from which the branching ratios may be obtained are programmed on CDC 3600 at T.I.F.R.

The low energy spectrum of ^{160}Tb contains 76, 98, 145, 185, 223, 253, 292, 340, 416 and 640 keV lines and coincidences of each of these lines with others are investigated.

The observed gamma energies and their coincidence modes for the low energy part are listed in Table I.

The nucleus ^{60}Co has 27 protons and 33 neutrons and according to shell model the proton configuration may be given as $(1f_{7/2})^{-1}$ and the neutron configuration as $(f_{5/2})^{2}_{0}(p_{3/2})^{-1}$. For the odd-group model the ground and low-lying configurations for ^{60}Co may be resulting due to the $(f_{7/2})^{-1}$ proton hole and the $(p_{3/2})^{-1}$ neutron hole. Such a coupling will result in a set of levels with spins 2^+, 3^+, 4^+, 5^+, the ordering of which will be sensitive to the nature of the residual proton-neutron interaction and theoretical calculations aiming at achieving the level ordering have been attempted by several authors.

The deformed ^{160}Tb nucleus may be theoretically described by the Nilsson model and the ground state has a spin of 3^-, with the configuration given as $(411\uparrow + 521\uparrow)$. Nilsson and Mottelson have also given energy levels in terms of Nilsson orbitals for odd proton and odd neutron. The present experiment is an attempt to compare theoretical conclusions with experimental observations. Since the computer calculations have not been ready this discussion may be termed as incomplete. The results are expected to be communicated soon after the computer calculations are over.

Table I.

The observed low energy gamma rays together with their coincidence modes.

^{60}Co		^{160}Tb	
Energy of the gamma ray in keV	Energy components with which coinc. are obtained in keV	Energy of the gamma ray in keV	Energy Components with which coinc. are obtained in keV
60	158, 230, 450, 510, 550	76	145, 185, 253, 292, 340, 640
158	60, 280	98	145, 185, 253
230	60, 280, 510	145	76, 98, 185, 292, 416
280	158, 230	185	76, 98, 145, 185, 340
390	550	223	416
450	60	253	76, 98
510	60, 230	292	76, 145
550	60, 390	340	76, 185

STUDY OF THE A(n,p)Cl REACTION

M.L. Jhingan, Roshan Rivetna* and E. Kondaiah
Tata Institute of Fundamental Research
Colaba, Bombay.

A preliminary report on the study of the A(n,p)Cl reaction induced by 14 MeV neutrons is presented here. A modified version of Allan's Camera (1) was used for this study. Ilford K2 emulsions of 400 microns thickness were used as detectors. The geometrical set up is shown in fig.1. The cylindrical chamber was lined with lead coated graphite to stop protons from the brass walls of the chamber. The chamber was filled with chemically pure argon gas at one atmospheric pressure. The protons from the A(n,p)Cl reaction were recorded in the emulsion plate placed at the centre bottom of the chamber. An identical exposure with vacuum inside the chamber served as the background.

An area of 1 cm x 1 cm at the centre of the emulsion was scanned. Tracks originating from the surface of the emulsion and having dip angles less than 10° were measured to ensure that the effective gas volume elements were the same at all angles. Further, only tracks lying above 3.8 MeV were scanned. The space angle and energy of each track was calculated with the help of the CDC 3600 Computer of T.I.F.R. The corrections for divergence of neutron beam and loss of

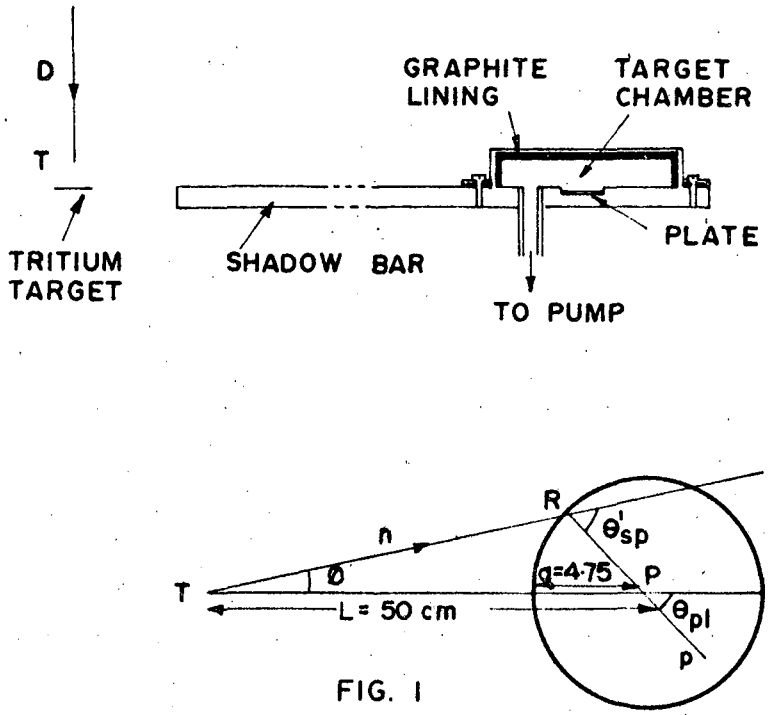
D
T
TRITIUM TARGET
SHADOW BAR
GRAPHITE LINING
TARGET CHAMBER
PLATE
TO PUMP
R
n
θ'_{sp}
T
Ø
q=4·75
P
L= 50 cm
θ_{pl}
p

FIG. 1

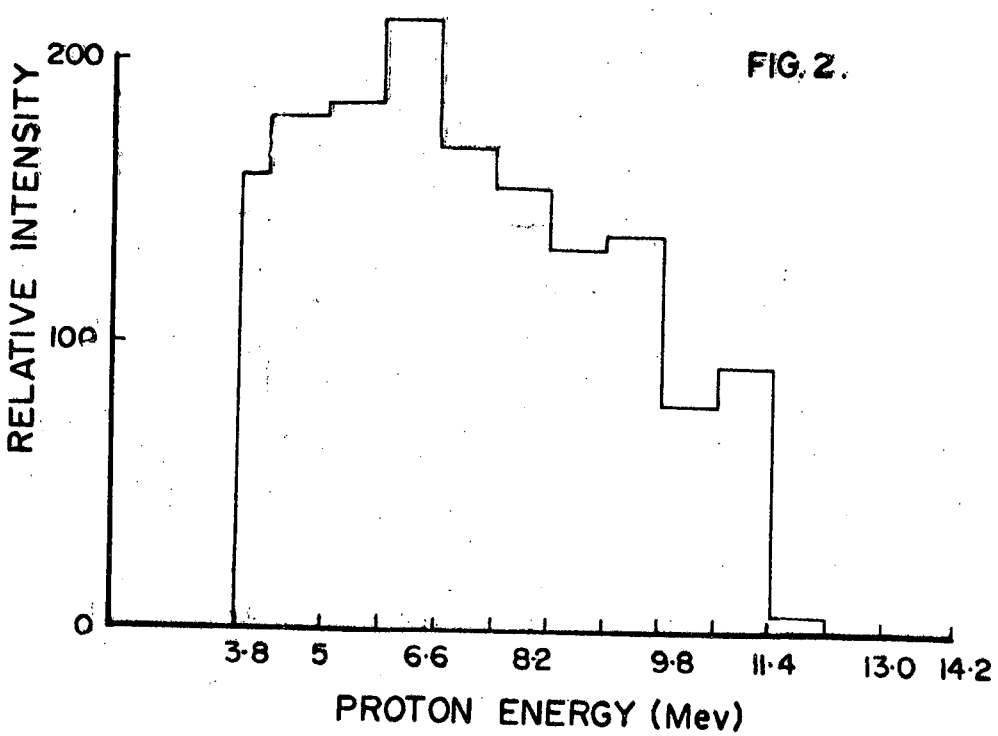
FIG. 2.
RELATIVE INTENSITY
200
100
0
3·8
5
6·6
8·2
9·8
11·4
13·0
14·2
PROTON ENERGY (Mev)

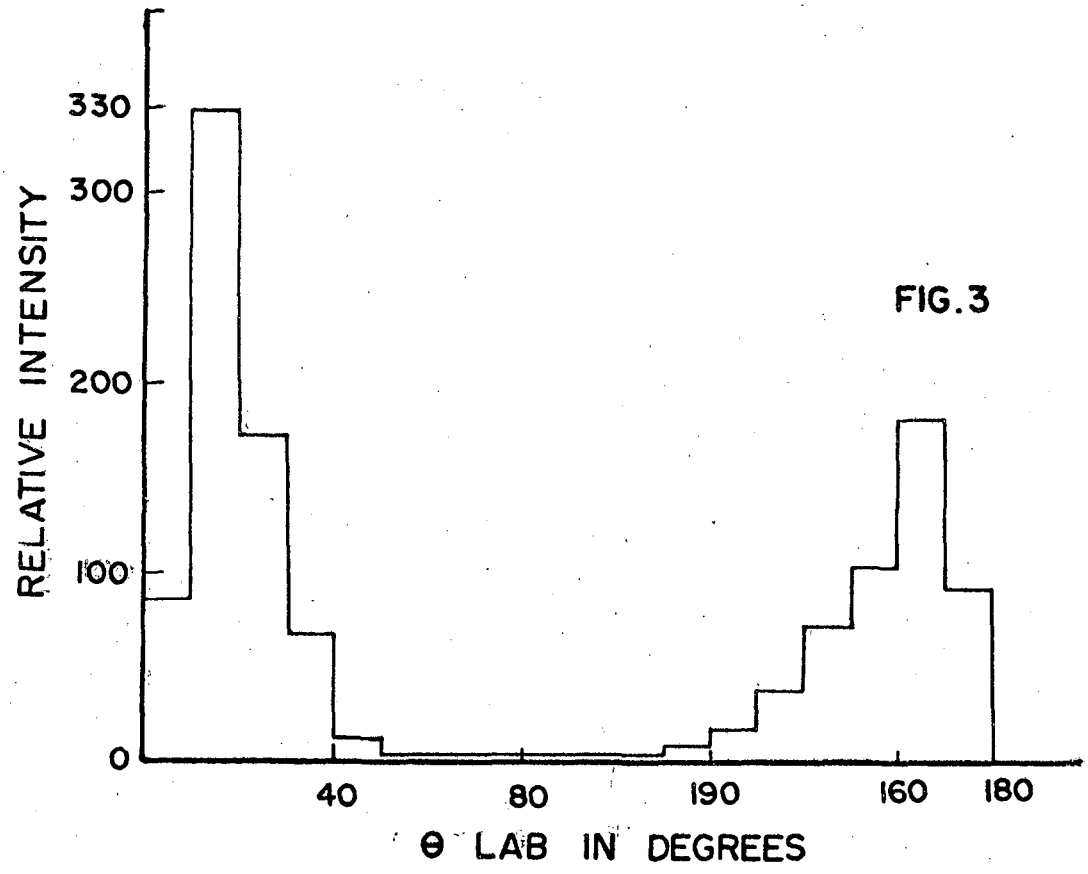
RELATIVE INTENSITY
330
300
200
100
0
40
80
190
160
180
θ LAB IN DEGREES

FIG.3

energy were applied. Due to extended target geometry, the energy resolution was not very good. At a proton energy of 8 MeV, the uncertainty in energy was $\pm$ 0.5 MeV.

Fig.2 shows the energy distribution of protons arising from the A(n,p)Cl reaction. The Q value for the $^{40}A(n,p)^{40}Cl$ reaction is 6.7183 MeV and the natural abundance of ^{40}A is 99.6%. So, one should not expect tracks above 7.3 MeV But, in fig.2, quite a good number of tracks are present above 7.3 MeV. These may be due to the contribution from the $^{36}A(n,p)^{36}Cl$ reaction for which the Q value is 0.0690 MeV. The abundance of ^{36}A is only 0.36%, but the $^{36}A(n,p)^{36}Cl$ reaction has a cross section 16 times larger than that for the $^{40}A(n,p)^{40}Cl$ reaction, as reported by Gardner (2). Further, it is possible that most of the contributions due to the $^{40}A(n,p)^{40}Cl$ reaction may be lying below 3.8 MeV, while the $^{36}A(n,p)^{36}Cl$ reaction will contribute quite a bit in higher energy region. We are trying to analyse this point further. Fig.3 shows the angular distribution of the tracks lying above 3.8 MeV.

REFERENCES:

1. E. Kondaiah and R. Patell, Nuovo Cimento, 42, 297 (1966)

2. D.G. Gardner, Nucl. Phys. 29, 373 (1962)

---

* On Leave

Present address: Professor and Head of the Department, Laboratories for Nuclear Studies, Andhra University, Waltair.

DISCUSSION:

S.K. Gupta: The percentage of ^{36}Ar is very small and even a factor of 16 cannot account for it. This indicates that the $^{36}Ar(n,p)^{36}Cl$ must be much larger?

M.L. Jhingan: This may be due to the fact that ^{40}Ar may contribute mostly in the energy region of 3.8 MeV or lower while $^{36}Ar(n,p)$ may contribute mostly in the energy region more than 3.8 MeV. We are trying to analyse this point further.

EVALUATION OF NEUTRON CROSS-SECTIONS ON THE BASES OF OPTICAL AND STATISTICAL MODELS

S.B. Garg
Reactor Engineering Division
Bhabha Atomic Research Centre, Trombay

The phenomenological appraoch to Optical model (1), (2) is being widely used to understand the nucleon-nucleus interactions for heavy and medium weight nuclei both in the intermediate and high energy regions. Optical model combines in it the aspects of the strong interaction (compound nucleus model) and single particle theories (shell model). It provides a mechanism to applied scientists to interpolate and extrapolate measured quantities like total and elastic cross-sections. It determines the "shape elastic" and "reaction" cross-sections. The latter must be divided into elastic and inelastic components using statistical theory of Hauser and Feshbach (3). Thus

$$\sigma_t = \sigma_{se} + \sigma_r \quad \text{(Optical Model)}$$

$$\sigma_r = \sigma_{ce} + \sigma_{ine} \quad \text{(Statistical Theory)}$$

The description of neutron-nucleus interactions is of great interest to those who are engaged in the design of nuclear power reactors and in particular the knowledge of elastic and inelastic cross-sections together with their angular distributions is quite significant in determining their neutronic behaviour.

The Optical model combined with the statistical theory can be profitably employed to obtain information on elastic and inelastic scattering even in those regions where measurements are

lacking. To calculate inelastic cross-sections the knowledge of the energy levels of the target nucleus is essential. Any uncertainty in the energy levels - their spins and parities would be reflected in these calculations. From the predicted angular distributions one can obtain $\bar{\mu}$ - the average cosine of the scattering angle in the Laboratory system and then the transport cross-section which is a key to reactor calculations according to the following relation:

$$\sigma_{tr} = \sigma_t - \bar{\mu}\,\sigma_{el}$$

In the optical model analysis the Schrödinger eqn. is numerically solved to obtain η_{lj} - the relative amplitude of the outgoing wave with the following complex potential:

$$V(r) = -Uf(r) - iWg(r) - V_{so}\,h(r)\,l\cdot\sigma$$

where

$$f(r) = \left[1 + \exp\left(\frac{r-R}{a}\right)\right]^{-1} \qquad \text{(Saxen form)}$$

$$g(r) = \exp\left[-\left(\frac{r-R}{b}\right)^2\right] \qquad \text{(Gaussian form)}$$

$$h(r) = \left(\frac{\hbar}{\mu_\pi c}\right)^2 \frac{1}{r}\frac{df(r)}{dr} \qquad \text{(Thomas form)}$$

$$R = rA^{1/3}$$

The transmission coefficients T_{lj}, "shape elastic" and "reaction" cross-sections are then given by

$$T_{lj} = 1 - |\eta_{lj}|^2$$

$$\sigma_{se}(\theta) = \pi\lambda\!\!\!^{-2}\left[\sum (2l+1)(1-\eta_{lj})\frac{P_l(\cos\theta)}{\sqrt{4\pi}}\right]^2$$

$$\sigma_r = \pi\lambda\!\!\!^{-2}\sum (2l+1)\,T_{lj}$$

On the basis of Hauser-Feshbach theory (4) the inelastic cross-section and its angular distribution are given by

$$\sigma(E,E') = \frac{\pi \lambda\!\!\!^{-2}}{2(2I_0+1)} \sum_{\ell j} T_{\ell j}(E) \sum_{J} (2J+1) \frac{\sum_{J'\ell'} T_{\ell' j'}(E')}{\sum_{p j''\ell''} T_{\ell'' j''}(E'_p)}$$

$$\sigma(E,E',\theta) = \frac{\lambda\!\!\!^{-2}}{4} \frac{1}{2(2I_0+1)} \sum_{j\ell} T_{\ell j}(E) \sum_{J} (2J+1)^2 \frac{\sum_{j'\ell'} T_{\ell' j'}(E')}{\sum_{p j''\ell''} T_{\ell'' j''}(E'_p)}$$

$$\times \sum_{L\ \mathrm{even}} (-1)^{I-I'} Z(\ell' j'\, \ell' j', \tfrac{1}{2}L)\, Z(\ell j\, \ell j, \tfrac{1}{2}L)$$

$$\times\ W(J j' J j', I' L)\, W(J j J j, I \ell)\, P_\ell(\cos\theta)$$

CALCULATIONS:

In the present work we have computed neutron cross-sections for Cr, ^{58}Ni, ^{60}Ni, Zr, Mo and Cd which find a frequent use in reactors in the MeV region with the ABACUS-2 Code (5). In the analysis of Cr, ^{58}Ni, ^{60}Ni we have used the Saxon form of potential both for the real and imaginary parts and have not included the spin-orbit term since it only affects the polarization and angular distributions which we have not cared to fit-the data being very meagre. The local optical parameters scanned to give good fits to the measured total cross-sections in the energy region 0.1 to 4.0 MeV for Cr, ^{58}Ni and ^{60}Ni are given below:

Cr

U = 45.0 MeV; a = 0.5 fm; V_{so} = 0; r = 1.45 fm and the values of W chosen are

(i) $E = 0.5$ MeV ; $W = 6.0$ MeV

(ii) $0.5 < E \leqslant 4.0$ MeV ; $W = 4.0$ MeV

^{58}Ni & ^{60}Ni

U = 45.0 MeV; a = 0.5 fm; V_{so} = 0 and the values of r and W are

(i) $0.1 \leqslant E \leqslant 0.5$ MeV ; $W = 18$ MeV ; $r = 1.45$ fm

(ii) $0.5 < E \leqslant 1.5$ MeV ; $W = 5$ MeV ; $r = 1.45$ fm

(iii) $1.5 < E \leqslant 3.5$ MeV ; $W = 5$ MeV ; $r = 1.35$ fm

(iv) $3.5 < E \leqslant 4.0$ MeV ; $W = 4$ MeV ; $r = 1.35$ fm

Below 0.5 MeV cross-sections show fluctuations and thus it is not possible to obtain sufficiently energy averaged data to make optical model calculations which are meaningful. The calculated and measured cross-sections are compared in Table I. In these computations the attempt has been to find average optical parameters which can give reasonable fits in certain energy regions rather than to find point-parameters which give the best fit to individual energy points. Using these parameters and the energy levels from the data sheets we have calculated elastic and inelastic cross-sections.

In the case of Zr, Mo and Cd cross-sections have been calculated in the energy range 1.0 to 10.0 MeV. Five parameters U,W,a,b and r were varied to obrain best fits by keeping Vso fixed at zero. The calculated and measured data are compared in Table II. We have not calculated compound elastic and inelastic cross-sections for these materials since we have not had an adequate information on their energy levels. We have used the Gaussian form of potential for the imaginary part and the Saxon form of potential for the real part. The parameters searched are given below:

<u>Zr</u>

(i) $E = 1.0$ MeV ; $U = 40$ MeV; $W = 10$ MeV ; $a = b = 0.5$ fm ; $r = 1.555$ fm

(ii) $2 \leq E \leq 10.0$ MeV; $U = 40$ MeV; $W = 10$ MeV; $a = b = 0.6$ fm; $r = 1.25$ fm

<u>Mo</u>

(i) $E = 1.0$ MeV; $U = 40$ MeV ; $W = 9$ MeV ; $a = b = 0.5$ fm ; $r = 1.51$ fm

(ii) $2 \leq E \leq 10.0$ MeV; $U = 40$ MeV ; $W = 14$ MeV ; $a = 0.6$ fm ; $b = 0.5$ fm
$r = 1.25$ fm

<u>Cd</u>

(i) $E = 1.0$ MeV ; $U = 60$ MeV; $W = 14$ MeV; $a = b = 0.5$ fm ; $r = 1.56$ fm

(ii) $1 < E \leq 2.0$ MeV; $U = 60$ MeV; $W = 14$ MeV ; $a = b = 0.5$ fm ; $r = 1.35$ fm

(iii) $2 < E \leq 4.0$ MeV ; $U = 60$ MeV ; $W = 14$ MeV ; $a = b = 0.5$ fm; $r = 1.31$ fm

(iv) $4 < E \leq 10.0$ MeV; $U = 45$ MeV ; $W = 8$ MeV ; $a = b = 0.5$ fm; $r = 1.25$ fm

REFERENCES:

1. H. Feshbach et al, Phys. Rev. 96, 448 (1954)

2. P.E. Hodgson, The Optical Model Elastic Scattering.

3. W. Hauser and H. Feshbach, Phys. Rev. 87, 366 (1952)

4. E.H. Auerbach and S.O. Moore, Phys. Rev. 135, B895 (1964)

5. E.H. Auerbach; ABACUS - 2 Code - BNL 6562.

DISCUSSION:

E. Kondaiah (Comment):-

Rosen has fitted a large amount of polarization and other data using nucleon-nucleon optical potential whose dependence on the energy and other parameters such as A and Z is explicitly given. The various potentials used in your calculations may be explained in terms of Rosen's potentials.

A.S. Divatia: Have you compared these parameters with those obtained by Rosen from polarization experiments? How do they compare?

S.B. Garg: We have not cared to compare our parameters with those of Rosen, the reason being that Rosen obtained parameters on protons by fitting the polarization and elastic scattering data and the parameters can vary quite a bit if all these phenomena are to be represented well.

Table I.

E (MeV)	Cr		^{58}Ni		^{60}Ni
	Claculated σ_t	Measured σ_t	Calculated σ_t	Measured σ_t	Calculated σ_t*
0.5	3.27	3.27	3.91	3.83	3.96
0.8	3.01	2.80	3.50	3.42	3.56
1.0	3.11	2.76	3.38	3.34	3.41
1.5	3.38	3.10	3.24	3.25	3.23
2.0	3.52	4.14	3.22	3.21	3.29
2.5	3.55	3.60	3.32	3.20	3.37
3.0	3.54	3.70	3.34	3.33	3.39
3.5	3.49	3.76	3.36	3.39	3.39
4.0	3.43	3.80	3.47	3.45	3.50

* All cross-sections are in barns

Table II.

E (MeV)	Zr		Mo		Cd	
	Calculated σ_t	Measured σ_t	Calculated σ_t	Measured σ_t	Calculated σ_t	Measured σ_t *
1.0	7.24	7.20	6.60	6.60	6.65	6.70
2.0	4.23	4.80	4.20	5.10	5.65	5.50
2.5	4.44	4.50	4.21	4.50	5.12	5.00
3.5	4.33	4.30	4.08	3.95	4.25	4.20
4.5	4.00	4.00	3.86	3.80	4.13	4.10
5.0	3.84	3.90	3.76	3.80	4.30	4.10
6.5	3.73	4.05	4.0	3.95	4.23	4.10
7.5	4.21	4.20	3.99	4.00	4.10	4.10
8.0	4.27	4.30	3.93	4.05	4.05	4.10
9.0	4.16	4.40	3.80	4.10	4.00	4.20
10.0	3.94	4.30	3.66	4.20	4.07	4.40

* All cross-sections are in barns

THE GYROMAGNETIC RATIO OF 379 keV LEVEL OF ^{169}Tm

A.K. Nigam and R. Bhattacharyya ,
Saha Institute of Nuclear Physics,
Calcutta.

INTRODUCTION:

The g - factor of the 118 keV level of ^{169}Tm has been measured by Manning and Rogers (1,2) but the g - factor for the 379 keV level has not been reported so far. We have employed the Differential - Delay Reverse-Field method (3) for the measurement of the g - factor of this level. The half-life (4) of this isomeric level is 50 ns. The g - factor is determined by studying the perturbed angular correlation under the external magnetic field in the direction perpendicular to the plane of the correlation measurement.

EXPERIMENTAL METHOD:

The time-dependent angular correlation function in a magnetic field is

$$W(\theta, \pm H, T) = \alpha_0 + \alpha_2 \cos 2(\theta \pm 2\omega T) + \alpha_4 \cos 4(\theta \pm \omega T)$$

where ω, the Larmor - precession frequency of the intermediate state magnetic moment is given by

$$\omega = -g \mu_N \frac{H_{eff}}{\hbar}$$

where $H_{eff} = \beta H_{app}$ and β is the paramagnetic effect correction factor.

The coincidence time-spectra are carried out at two angles $\Theta_1 = \frac{5\pi}{8}$ and $\Theta_2 = \frac{7\pi}{8}$ with the direction of the applied magnetic field up and down. We denote these as W_1^+, W_1^-, W_2^+, W_2^-, where $W_{1,2}^{\pm}$ is the notation for $W(\Theta_{1,2}, \pm H, T)$. We calculate the following expression

$$F(T) = \frac{(W_1^+ - W_1^-) + (W_2^+ - W_2^-)}{(W_2^+ - W_1^+) + (W_2^- - W_1^-)}$$

which reduces to a very simple form for angles $\frac{5\pi}{8}$ and $\frac{7\pi}{8}$ if the influence of the finite resolving time is neglected, i.e. $(\tau_0 \ll \tau, \tau_0 \ll T)$

$$F(T) = \tan 2\omega T$$

The observation of $F(T)$ with different delay T, gives rise to an experimental tan θ - curve. Each point of this experimental curve can be used for the determination of the Larmor-precession frequency and hence the g-factor without any knowledge of the α-coefficients and the half-life of the level.

EXPERIMENTAL DETAILS:

The measurements were performed with a liquid source in the form of $YbCl_3$ in HCl solution in a small perspex capsule of 1/8" dia x 1/8" length, placed in the pole gap of 1/8" of the magnet operated at a magnetic field B = $\pm$ 12870 gauss. Experimental $W_{1,2}^{\pm}$ were obtained with a conventional

Fast-Slow coincidence circuit of resolving time 15 ns, by introducing a variable delay T in the fast channel corresponding to 93 keV radiation with the magnetic field direction up and down.

RESULTS:

The perturbed angular correlation was studied with the 93-63 keV cascade (Fig.I). These radiations do not give well separated peaks. The respective regions were selected in order to have negligible contribution of other radiations. The half-life of the level was measured under this condition and a value of 51 ns was obtained in agreement with previous reports (4).

On account of the finite resolving time of the coincidence circuit the function $F(T)$ is distorted in the vicinity of the zero time. The results of our measurements are shown in Fig.2. The Larmor-precession frequency for each point of the Fig.2, was calculated and the mean value of ω was found to be $(0.851 \pm 0.034) \times 10^8$ sec^{-1}. As Tm is a rare-earth element, the effective magnetic field due to the paramagnetic effects (5) at the site of the nucleus is 5.08 times the applied field. With the values of ω and the effective field, the gyromagnetic ratio is calculated giving

$$g = 0.272 \pm 0.021$$

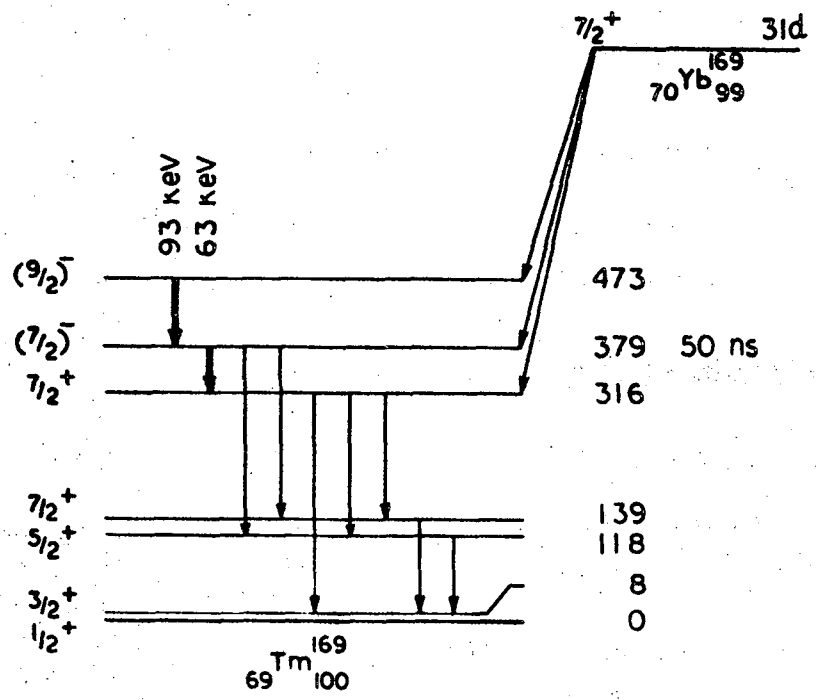
7/2+
31d
70Yb169 99
93 keV
63 keV
(9/2)-
473
(7/2)-
379
50 ns
7/2+
316
7/2+
139
5/2+
118
8
3/2+
0
1/2+
69Tm169 100

FIG. 1

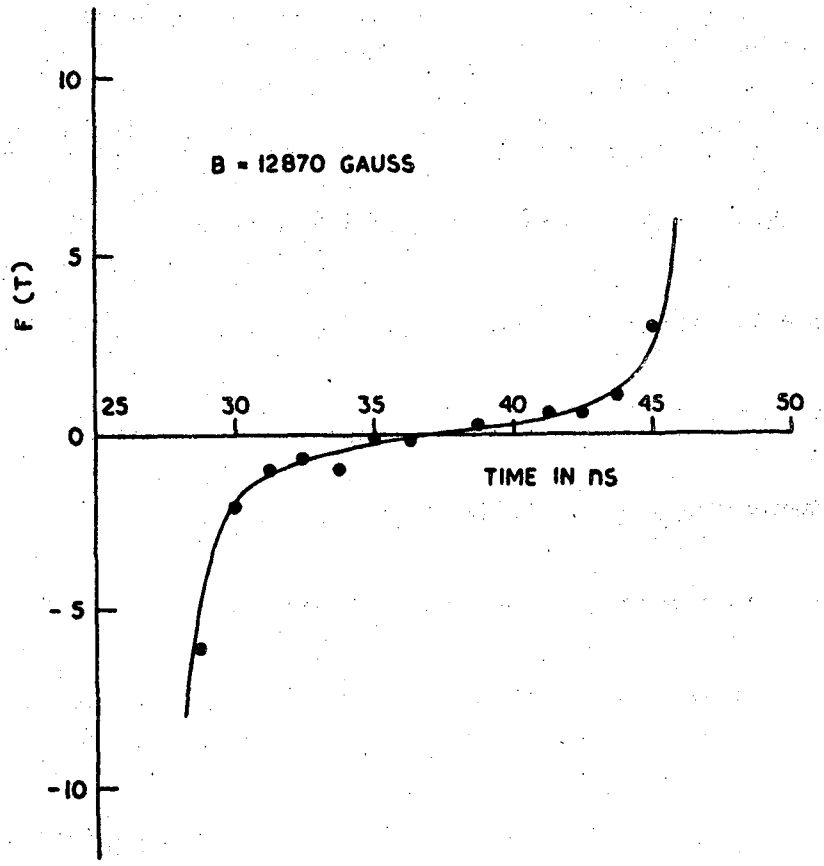
B = 12870 GAUSS
F (T)
10
5
0
-5
-10
25
30
35
40
45
50
TIME IN ns

FIG. 2

Taking into account the diamagnetic correction (6) for Tm, we obtain

$$g = 0.274 \pm 0.021$$

REFERENCES:

1. Manning and Rogers, Nuclear Physics, 19, 675 (1960)
2. Koicki et al., Phys. Rev., 143, 148 (1966)
3. Bozek et al., Physics Letters, 1, 126 (1962)
4. Mihelieh et al., Phys. Rev., 103, 1285 (1955)
5. Gunther and Lindgren, in "Perturbed Angular Correlations" ed, by E. Karlsson et al, (North-Holland Publishing Co., Amsterdarm (1964))
6. Fuller and Cohen, Nuclear Moments, Appendix I to Nuclear Data Sheets (1964)

DISCUSSION:

C.V.K. Baba: Have you tried to understand the value on the basis any model? The value seems to be very small for an odd proton state.

A.K. Nigam: The value seems to be low. The experiment will be repeated using other possible techniques and then the calculated result will be compared.

G.N. Rao: Did you measure the unperturbed angular correlation coefficients of the 379 keV state?

A.K. Nigam: As it does not appear explicitely in the formula of g - factor, it is not necessary here.

H.G. Devare: The time resolution used is not mentioned. How much was τ_c?

A.K. Nigam: The resolving time of the slow-fast coincidence circuit was 15 ns.

I.M. Govil: Did you take into account the effect due to time dependent quandrupole interaction?

A.K. Nigam: It is expected to be very low.

NUCLEAR 'g' FACTOR OF THE 57 keV STATE IN ^{143}Pr

P.N. Tandon, S.H. Devare and H.G. Devare
Tata Institute of Fundamental Research
Colaba, Bombay.

The nuclear 'g' factor of the 57 keV state of ^{143}Pr has been measured using the perturbed angular correlation technique. This level is known to decay with a half life of 4.17 nano sec. as measured by Graham et al (1). This level is strongly populated by a 293 keV gamma transition. The 293-57 keV γ-γ angular correlation is found to have a large anisotropy. All these factors make it rather easy to measure the magentic moment of this state. There are a few measurements on the magnetic moment of this state (2-4) but they disagree considerably. The disagreement is mainly because of the paramagnetic correction factor β which enhances the magnetic field seen at the nucleus. This factor is different for different ionic states of the daughter nucleus after the parent β decay. Hence it is very essential to know the final ionic state of the daughter nucleus. In the present measurement this difficulty is overcome by using the parent activity in different ionic states and then establishing the ionic state of the daughter nuclei from the existing data.

Sources of ^{143}Co were obtained by irradiating enriched $^{142}CeO_2$ in CIRUS. Two different types of sources were made

(a) the powder was reduced by HBr, dried and then finally dissolved in dil. Hcl. In this the activity is in $CeCl_3$ form and the ionic state is 3^+. (b) the powder was used as such in CeO_2 form and the activity is in 4^+ ionic state.

The angular correlation of the 293-57 keV cascade was measured on an automatic set up with both type of sources. The source was kept in between the pole tips, in the same geometry as for the $\omega\tau$ measurement. The value of the A_2 coefficient uncorrected for geometry, obtained are

$$A_2 \text{ (liquid source)} = 0.092 \pm 0.006$$

$$A_2 \text{ (powder source)} = 0.106 \pm 0.005$$

This shows that the liquid source has attenuations. The powder source, CeO_2 being cubic, does not seem to show perturbations. To check for the possible time dependent attenuations the differential angular correlation was done using a time to amplitude converter. Fig.1 shows the anisotropy as a function of time. Fig.1(A) corresponds to liquid source, the solid line being the least squares fit. Fig.1(B) corresponds to the powder source, which clearly shows that there are no perturbations present. The integral attenuation coefficient G_2 for the liquid source obtained is $G_2 = 0.75 \pm 0.07$.

For the measurements in the magnetic field, the detectors were placed at an angle of 135°. The data was collected automatically. The time taken for a fixed number of

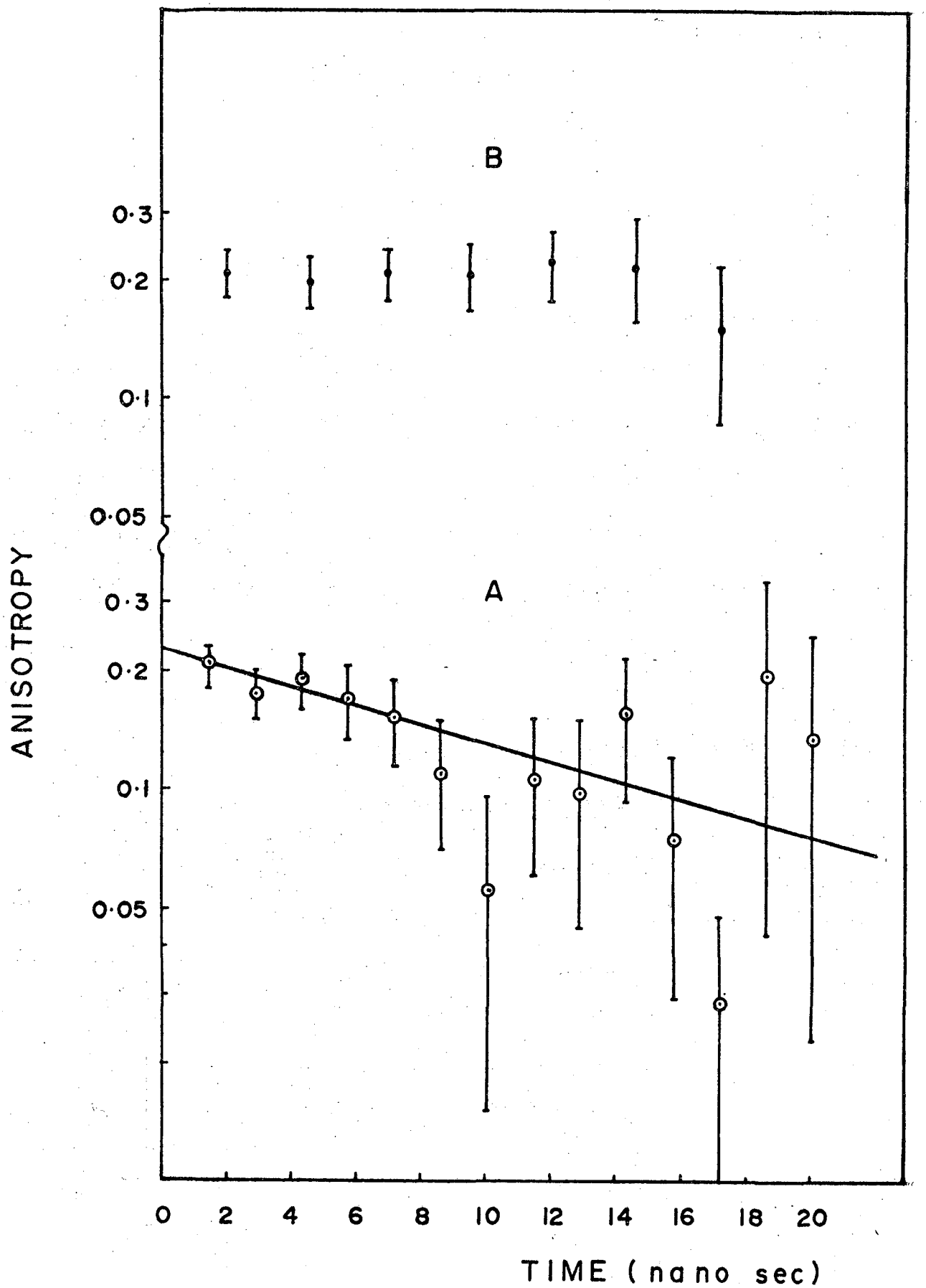
B
A
0·3
0·2
0·1
0·05
0·3
0·2
0·1
0·05
ANISOTROPY
0
2
4
6
8
10
12
14
16
18
20
TIME (nano sec)

coincidence counts was recorded. The quantity 'R' defined as

$$R = 2\frac{N_c(up) - N_c(down)}{N_c(up) + N_c(down)}$$

was experimentally determined. This quantity can be expressed in terms of C_2 and $\omega\tau$ as

$$R_{135^\circ} = \frac{4\, C_2\, G_2\, \omega\tau}{1 + (2G_2C_2\omega\tau)^2}$$

The table summarises all the measurements made

Field (Kg)	Source form and intial ionic state.		R	$G_2\, g\beta$
8.5	Powder	4^+	0.077 ± 0.004	2.03 ± 0.57
5.6	Powder	4^+	0.061 ± 0.004	$1.52 + 0.18$ $- 0.15$
5.6	Liquid	3^+	0.061 ± 0.005	$2.00 + 0.62$ $- 0.31$

The large error in $G_2\, g\beta$, is mainly due to the fact that these values of 'R' lie on a very flat portion of R vs. $\omega\tau$ curve.

From the measurements at 5.6 Kg and 8.5 Kg field, using the powder source, one gets the value of $g\beta = 1.58 \pm 0.12$, this being the overlap between the two values for the powder source and G_2 being equal to one. It is seen that this value

of 'g' for powder source agrees with that for the liquid source the final state of Pr ion is 3^+ (β =2.0) and for powder source is 4^+ (β = 1.4). This is again supported by the work of Zmora et al (2) who have shown that Ce in liquid sources goes to 3^+ ionic state in Pr no matter whether one starts with a 3^+ or a 4^+ state. However, as is shown in the present measurement, CeO_2 goes to 4^+ state in Pr and remains in this state at least till the mean life of the 57 keV state which is about 6 nano sec. One then gets for the value of 'g' from the powder source measurements as

$$'g' = 1.13 \pm 0.08$$

in very good agreement with that of Zmora et al (2). The spin of 57 keV state being 5/2, the value of μ = 2.83 $\pm$ 0.2. This value will agree with other measurements (3,4) if one corrects for 'β' properly.

REFERENCES:

1. R.L. Graham, J.M. Hollander and P. Kleinheinz Ncul. Phys. 49, 641 (1963)
2. H. Zmora, S. Ofer and M. Rakavy Nucl. Phys. 89, 225 (1966)
3. H.J. Korner, K. Auerbach, J. Braunsfurth, U. Ortabasi and Heisenberg Comptes Rendus de Congres International Physique Nucleaire Vol.II, 481 (1964)
4. R.M. Levy, UCRL, 11663 (thesis)

DISCUSSION:

I.M. Govil: The CeO_2 may have some lattice imperfection due to the decayed Pr nuclei. Did you see that the anisotropy is not affected by quadrupole interaction with some frequency distribution?

P.N. Tandon: The differential correlation using powder source clearly showed that there are no pertirbations at least up to 20 ns.

MAGNETIC MOMENT OF THE 1290 keV ($3/2^-$) STATE IN ^{59}Co

Y.K. Agarwal, C.V.K. Baba and S.K. Bhattacherjee
Tata Institute of Fundamental Research,
Colaba, Bombay.

AB STRACT.

The life time and the magnetic dipole moment of the 1290 keV ($3/2^-$) state in ^{59}Co have been measured to be $T_{\frac{1}{2}} = (0.59 \pm 0.02)$ nsec. and $\mu = 1.90 \pm 0.35$ n.m. The electromagnetic properties of the 1100 keV and the 1290 keV states have been explained by assigning a mixture of $p_{3/2^-}$ and $\left\{ f_{7/2}, 2^+; 3/2^- \right\}$ configurations to the 1100 keV and 1290 keV states.

DISCUSSION:

P. Sen: What is the slope of your prompt curve? Is it with plastic scintillator?

Y.K. Agarwal: The slope is $\sim$0.2 ns. Plastic scintillators were used.

FERMI MATRIX ELEMENTS IN MEDIUM AND HEAVY NUCLEI

S.K. Mitra and H.C. Padhi
Tata Institute of Fundamental Research,
Colaba, Bombay.

ABSTRACT.

A compilation has been made of measurements of Fermi matrix element M_F in different regions of the periodic table. The presently available data are reviewed in the light of isospin impurities of nuclear wave-functions.

FERMI TO GAMOW-TELLER MATRIX ELEMENT RATIOS IN ALLOWED BETA TRANSITIONS IN ^{56}Co, ^{58}Co AND ^{134}Cs.

S.K. Bhattacherjee, S.K. Mitra and H.C. Padhi,
Tata Institute of Fundamental Research Centre
Colaba, Bombay.

ABSTRACT.

The angular correlation asymmetry parameter for circularly polarised gamma rays following allowed beta decay has been measured for three nuclei ^{56}Co, ^{58}Co and ^{134}Cs. The polarimeter employed the usual forward Compton scattering of gamma rays. The measured asymmetry parameter A and the Fermi to Gamow-Teller matrix element ratio X in these decays are as follows:

	A	X
^{56}Co	0.014 ± 0.022	0.131 ± 0.030
^{58}Co	- 0.16 ± 0.04	- 0.008 ± 0.050
^{134}Cs	- 0.072 ± 0.018	0.213 ± 0.025

THE NUCLEAR COUPLING SCHEME OF ^{121}Sb and ^{123}Sb

M.C. Joshi
Tata Institute of Fundamental Research
Colaba, Bombay-5.

Our previous investigations (1,2) on the nuclear levels of ^{121}Sb and ^{123}Sb using different nuclear reactions (^{3}He,d), (dd) and (^{16}O,^{16}O'γ) suggested an appreciable coupling between the odd proton and the core - the semi-magic nuclei of Tin. It was suggested that there should be four levels of spin $7/2^+$, $9/2^+$, $9/2^+$ and $11/2^+$ at about one MeV of excitation energy present in both the nuclei. And these levels have large components of one phonon coupled to two shell model states $1g_{7/2}$ and $2d_{5/2}$. There are four levels observed in ^{123}Sb at about the expected energy region whereas only two were observed in ^{121}Sb. If the other two levels have a very large amplitude of one phonon coupled to $g_{7/2}$ shell model state one does expect them to be excited in the reactions mentioned above. One may expect them to be populated in the radio-active decay of high spin isomer ^{121m}Te $(11/2^-) \xrightarrow{EC.} {}^{121}$Sb.

It was an object of this brief note giving a further clarification on this point. In the ^{121}Sb (dd') measurements the energies of the levels at (1024 $\pm$ 5) keV and (1143 $\pm$ 5) keV were determined with the magnetic spectrograph. The energies of the γ rays (1024 $\pm$ 5) and (1141 $\pm$ 3) keV observed in the coulomb excitation of ^{121}Sb (^{16}O,^{16}O'γ) were measured using a Ge(Li) detector. The levels 1024 and 1143 keV which were

strongly excited in the inelastic scattering measurements decay directly to the ground level with a branching less than 10%. Whereas in a study of the radio-active decay of ^{121m}Te the levels at 1141 and 1038 keV have been porposed by Aubley et al (3) based on their $\gamma\gamma$ coincidence measurements using NaI(Tl) crystal and proportional counters as detectors. Although the levels proposed in the decay scheme work are very close to those observed in the inelastic scattering measurements their decay mode is different. These two levels decay mainly to the 35 keV ($7/2^+$) level. There are no direct transitions to the ground level observed. It is concluded that the 1141 and the 1033 keV levels proposed in the radio-active decay measurements are not the same as those observed in the inelastic scattering measurements and it is further suggested that these are the two missing members of the four levels as expected above. In view of this interesting feature of the levels it was very necessary to study the singles spectrum of the γ rays using a Ge(Li) detector in order to redetermine the level positions more accurately.

Tellurium activities were produced by irradiating Antimony oxide with 20 MeV deuterons from the cyclotron of the Institute of Atomic Physics Stockholm. Several months after irradiation the Te activities were chemically separated. After repeated separation the γ ray spectrum was taken with

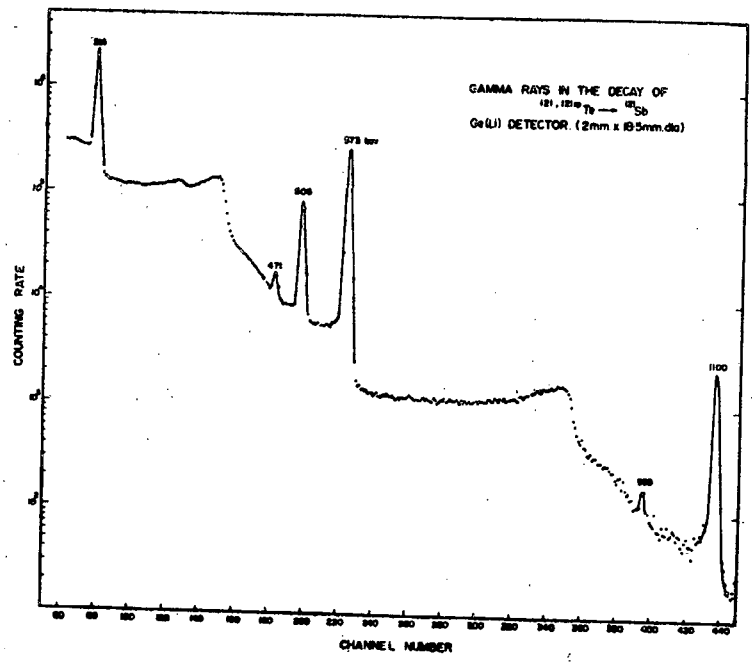
GAMMA RAYS IN THE DECAY OF
Ge(Li) DETECTOR. (2mm x 19.5mm.dia)
COUNTING RATE
CHANNEL NUMBER
1100

FIG. 1

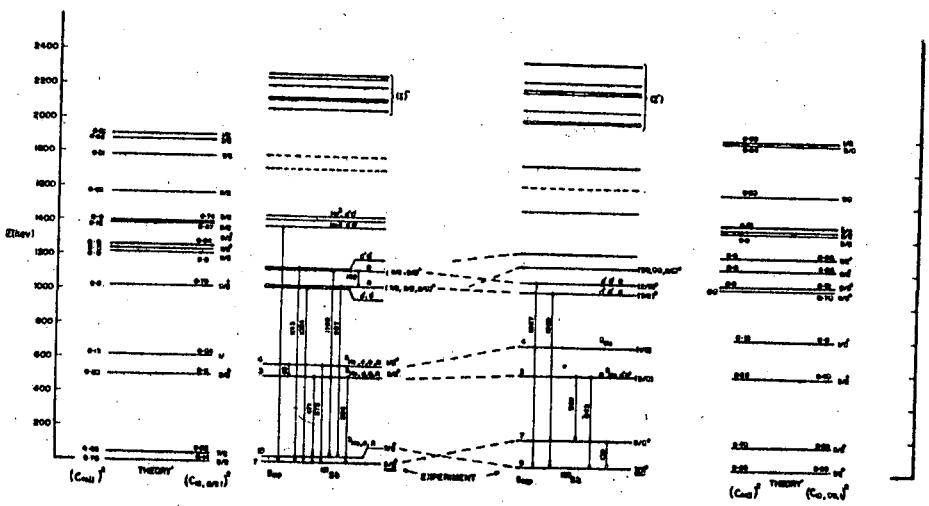
E(kev)
THEORY
EXPERIMENT
THEORY

FIG. 2

a Ge(Li) detector (2mm x 18.5 mm dia) which is shown in Fig.1. The γ-rays 471, 506, 573, 997, 1100 keV (with an error of $\pm$ 3 keV) were observed. There is an evidence for the existence of a weak γ-ray of 997 keV which had been shown in the $\gamma\gamma$ coincidence measurements by Auble et al (3). One can rely on the extensive $\gamma\gamma$ coincidence measurements by these workers. The decay scheme is taken as well established. According to new energy determination of the γ-rays the levels populated in the radio-active decay are placed at 1032 $\pm$ 5 and 1135 $\pm$ 5 keV. It is to be noted that the decay mode of these two levels is similar to the corresponding levels at 1029 keV ($9/2^-$, $11/2^+$) 1087 keV ($11/2^+$, $9/2^+$) in ^{123}Sb.

This clarification regarding the levels around 1 MeV gives a further support to the theoretical description of ^{121}Sb and ^{123}Sb by P.D. Barnes and C. Ellegaard (4) which is shown in the Fig.2.

REFERENCES:

1. P.D. Barnes, C. Ellegaard, B. Herskind and M.C. Joshi, Phys. Letters, 23, 266 (1966).
2. M.C. Joshi and B. Herskind, Proc. International Conference on Nuclear Physics, Gatlinberg (1966)
3. R.L. Auble and W.H. Kelly, Nucl. Phys. 58, 337 (1964)
4. P.D. Barnes and C. Ellegaard, Reported at the Int. Conf. on Nucl. Phys. (1966) and Private communication.

DISCUSSION:

J. Varma: The new γ-ray peak is too sharp giving an impression that it is more accidental than real. Only, if the peak is present in other similar observations it should be regarded as real.

M.C. Joshi: Presence of the weak γ-ray peak is certain from other measurements.

DECAY OF ^{182}Ta *

P.C. Mangal, S.P. Sud and P.N. Trehan
Department of Physics,
Panjab University
Chandigarh.

ABSTRACT.

The decay of ^{182}Ta has been studied by using a sum Peak coincidence spectrometer in almost 4π geometry. This spectrometer is found to be a good tool for investigating the low intensity cascading gamma rays because the coincidence detection efficiency in this spectrometer is the highest and the set up is fairly insensitive to the minor electronic drifts. From the sum peak coincidence spectra, run for a sufficiently long time by setting the integral bias at 80 KeV, two some peaks at 580 and 1740 keV are observed which are inaddition to the sum peaks arising because of the summing of the well established double or triple cascades in ^{182}W. The sum peak at 580 keV which arises because of the summing of 229 and 351 keV γ-rays indicates a level at 680 keV. This is further confirmed by the observance of a small peak at 680 keV cascade deexciting the 680 keV level. A sum peak at 1740 keV can be explained only

---

* This work has been done under the sponsorship of National Bureau of standards, Washington, D.C.

by assuming a new level at 1740 keV. This level deexcites by atriple cascade of 1410-229-100 keV. Since in 4π geometry chance summing is increased to a large extent, to take care of this contribution in the region of 1810 keV, the sum peak coincidence spectrum has been run by setting the integral bias at 390 keV. After substraction of this spectrum from the first spectrum a sum peak at 1740 keV shows up more clearly which strongly indicates the existance of a new level at 1740 keV.

THE LEVEL STRUCTURE OF $^{117}_{49}In$

K.G. Prasad, V.R. Pandharipande and R.P Sharma,
Tata Institute of Fundamental Research,
Colaba, Bombay.

The energy levels of one proton hole ^{117}In are studied in the decay of 2.8 hr ^{117}Cd and ^{117m}Cd. Since itis energetically possible to feed the levels upto about 2.5 MeV in ^{117}In in this decay, it is suitable for investigating the nature of various types of excitations such as single particle, collective and those due to breaking of a neutron pair etc.

The gamma-ray spectrum was studied with a Ge(Li) detector of 6.5 keV FWHM after purifying the irradiated sample by ion exchange method. The gamma-rays in the decay of ^{117}Cd are seen to extend upto 2412 keV. The 155, 553 and 710 keV gamma rays are found to be due to the 1.8 hr decay of ^{117}In to ^{117}Sn.

In our earlier work (1,2) we had reported an extensive beta-gamma, gamma-gamma coincidence studies in order to establish the level scheme of ^{117}In. In the present work we have carried out some more gamma-gamma coincidences in the light of many new gamma rays previously not observed.

The life time of 658 keV level has been measured to be 55 nsec using the cascade 88-345 keV. We had earlier reported the measurement of the life time of 746 keV state as 4.9 nsec.

The level scheme of ^{117}In is shown fig.1. The various levels are established by fitting the gamma-ray intensities, gamma-gamma and beta-gamma, coincidence data. The spin and parity of the ground state and the 313 keV isomeric state are known to be $9/2^+$ and $1/2^-$ respectively. We have measured the angular correlation of 1306-274 keV cascade and found the spin and parity of 588 keV level to be $3/2^-$.

The spin and parity of 658 keV level is established as $5/2^-$ because it is fed by a $9/2^-$ level at 1997 keV and there is a transition from 658 keV level to $1/2^-$ level.

The spin and parity of the 746 keV level can be $5/2^-$, $3/2^-$ or $3/2^+$ from the log ft value. However, if it is $5/2^-$, then the β-γ directional correlation of the 1800 keV beta group and the following 435 keV ray should show an anisotropy of about 50%. We have measured this beta gamma directional correlation and found it to be not more than 5%. In order to see if there is any attenuation of the directional correlation we have also measured the differential beta gamma directional correlation. The analysis does not show any large anisotropy. So we conclude that the probable spin and parity of this level to be either $3/2^+$ or $3/2^-$.

The levels from 880-1430 keV have one common feature. They all decay to the ground state. These may be due

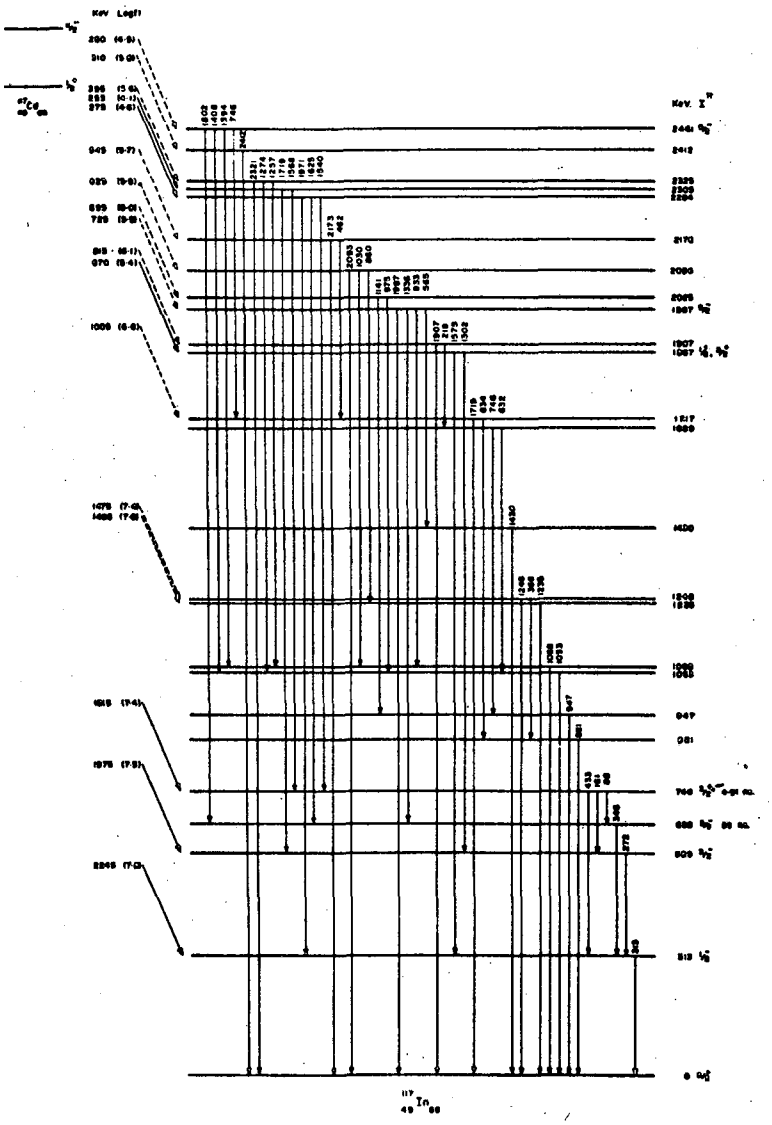

FIG. 1

to the coupling of g9/2 hole to the ^{118}Sn 2^+ state. If this is the case then 5 levels are expected. The origin of the two extra levels is very difficult to understand. In this context it is worthwhile mentioning that a similar situation occurs in ^{115}In.

There are many negative parity states around 2 MeV. These may be due to the coupling of the octupole excitation with the g9/2 hole. The other possibility is due to the breaking up of a neutron pair and formation of the three particle states. The pairing energy incidentally is 2 MeV in this region. The measurement of half life of these levels may throw some light on the nature of these levels.

REFERENCES:

1. R.P. Sharma, K.P. Gopinathan and S.R. Amtey, Phys. Rev. 134, B730 (1964)
2. V.R. Pandharipande, K.G. Prasad, R.M. Singru and R.P. Sharma, Phys. Rev., 143, 740 (1966)

EXCITED LEVELS IN ^{61}Co FROM THE DECAY OF ^{61}Fe

S.C. Gujrathi and S.K. Mukherjee
Saha Institute of Nuclear Physics
Calcutta.

ABSTRACT.

Irradiation of enriched ^{64}Ni samples with the 14.8 MeV neutrons was found to produce an activity of 5.8 ± 0.5-min half-life which was assigned to ^{61}Fe. The assignment was confirmed by following the decay of the iron activity separated from the irradiated samples of spec-pure nickel. The scintillation spectrometer studies showed that gamma rays of energies 130, 170, 230, 295, 400, 1010 and 1180 keV and beta groups of maximum energies 2800 ± 100 (31%), 2630 ± 100 (54%) and 2500 ± 100 (13%) keV were decaying with a half-life of 5.8 min. The gamma-gamma and the beta-gamma coincidence studies were performed which showed the existence of the excited levels at 1010, 1180, 1305 and 1410 keV in ^{61}Co. A decay scheme of ^{61}Fe is proposed and the results are discussed in the light of the single-particle shell model.

To be published in Phys. Rev.

LIFETIME MEASUREMENTS OF THE EXCITED STATES OF ^{46}Ti, ^{84}Rb, ^{99}Tc, ^{162}Dy, ^{164}Er and ^{196}Au

B. Sethi and S.K. Mukherjee
Saha Institute of Nuclear Physics
Calcutta.

The measurement of lifetimes of excited states of some nuclei has been performed using the delayed coincidence technique. All measurements were carried out with RCA 7850 Photomultipliers. For detecting beta rays, 2.5 cm dia x 3 mm thick NE 810 plastic scintillator was used, whereas for gamma-ray detection NE 102 scintillators of various sizes e.g. 2.5 cm dia x 5 cm long and 5 cm dia x 5 cm long were used. When the half life to be measured was sufficiently long 5 cm x 5 cm NaI(Tl) phosphors were employed. For detection of low energy x-rays and γ-rays 3.75 cm dia x 2 mm thick NaI(Tl) scintillator was used. The output of the time-to-pulse-height converter was analysed by means of a 512 channel analyzer. The time calibration was performed with respect to the velocity of gamma rays. The dalys introduced by the cables were found to agree within 2% with the values calculated from their characteristic constants.

The life-times of the nuclear levels in various cases were determined from the slope as well as the moment analysis of the delayed curves. The moment analysis in all cases

was carried out on a computer. Moments upto the third order were used in the analysis.

MEASUREMENTS AND RESULTS:

1. ^{46}Ti. The lifetimes of the second excited states of ^{46}Ti and ^{60}Ni were compared by using beta- gamma coincidence. The sources of ^{46}So and ^{60}So were prepared by depositing them over areas of about 1 sq.mm. on mylar foils. The radiations were detected in plastic scintillators and the measurements were done alternately with the two sources, using the same geometry in each case. For each measurement the source was kept in contact with the beta detector. The alternate sets of beta were separately recorded. The moment analysis of the data leads to a value of 10 ps, with a statistical error of about 80%, for the difference between the half lives of the 4^+ states of ^{46}Ti and ^{60}Ni. Therefore, it is concluded that the difference between their half lives is less than 20 ps.

2. ^{84}Rb. The half life of the 250 keV state of ^{84}Rb was determined by measuring the delay between the conversion electrons of the 216 keV transition and the 250 keV gamma rays. The source used was the 20 min. isomer of ^{84}Rb produced by (n,2n) reaction with 14 MeV neutrons on natural rubidium. The value of the half life from three independent measurements was $(3.08 \pm 0.55) \times 10^{-10}$ sec.

3. ^{99}Tc. The excited states of ^{99}Tc are populated in the beta decay of ^{99}Mo. The 67 hour ^{99}Mo was produced by (n,2n) reaction with fast neutrons on enriched ^{100}Mo. By measurement of delay between the 450 keV beta group and the 740 and 730 keV gamma rays, the half life of the 920 keV level of ^{99}Tc was found to be less than 10^{-10} sec, in agreement with the finding of Meiling et al (1). The half life of the 181 keV level was determined from the slope of delayed curve and found to be 3.40 ± 0.10 ns.

4. ^{162}Dy. The half life of the 1155 keV level of ^{162}Dy was also determined by measurement of the beta-gamma delay. The detectors used were the same as in previous cases. The parent activity was that of ^{162}Tb (7.5 min) produced by (n,p) reaction on enriched ^{162}Dy. The 1155 keV state of ^{162}Dy is fed by the 1450 keV (80%) beta group. The most intense gamma ray emitted in the de-excitation of this level has 265 keV energy. The delay of this gamma ray with respect to the feeding beta rays was measured in order to determine the half life of the 1155 keV level. The half life was found to be (2.10 ± 0.40) x 10^{-10} sec.

5. ^{164}Er. The half life of the 90 keV level of ^{164}Er was determined by measurement of the delay of the 90 keV gamma ray with respect to the 875 keV beta rays from the ^{164}Ho decay. The source, $^{164m\&h}$Ho (39.0 & 23.9 min.), was produced by

$^{165}Ho(n,2n)^{164}Ho$ reaction with 14 MeV neutrons. The half life of the 90 keV level of ^{164}Er, taking the mean of four measurements, was found to be $(1.52 \pm 0.06) \times 10^{-9}$ sec.

6. ^{196}Au. Measurement of the half life of the 85 keV level of ^{196}Au was attempted by detecting the 188 keV gamma rays feeding the 85 keV level and the Lx-rays emitted in the de-excitation of this level by internal conversion. Both radiations were detected by means of NaI(Tl) scintillators. The source used was the 9.7 hour ^{196m}Au produced by $^{197}Au(n,2n)^{196}Au$ reaction with fast neutrons. Separate runs were given for genuine and random coincidences. It is concluded from a series of measurements that the half life of the 85 keV level of ^{196}Au is greater than 4 μsec.

The results of all measurements are summarised in the following table.

Table I.

NUCLIDE	LEVEL	PARENT ACTIVITY	RADIATIONS SELECTED	HALF LIFE	
				PRESENT WORK	EARLIER MEASUREMENTS
$^{162}_{66}Dy_{96}$	1155 keV	^{162}Tb (7.5^{m})	β^- 1450 keV. γ 265 keV.	$(2.10 \pm 0.40) \times 10^{-10}$ sec.	.....
$^{164}_{68}Er_{96}$	[illegible] keV	164m & g Ho (39.0 and 23.9 min)	β^- 875 keV. γ 90 keV.	$(1.52 \pm 0.06) \times 10^{-9}$ sec.	1. $(1.4 \pm 0.5) \times 10^{-9}$ sec. Brown & Becker (7). 2. $(1.732 \pm 0.003) \times 10^{-9}$ sec. Boer et al (8) 3. $(1.43 \pm 0.05) \times 10^{-9}$ sec. Fossan et al (9).
$^{196}_{79}Au_{117}$	35 keV	^{196m}Au (9.7^{h})	γ 133 keV Lx-ray	$> 4 \mu$sec.	$> 0.5 \mu$sec. NDS(1962).

Table I.

NUCLIDE	LEVEL	PARENT ACTIVITY	RADIATIONS SELECTED	HALF LIFE: PRESENT WORK	HALF LIFE: EARLIER MEASUREMENTS
$^{46}_{22}Ti_{42}$	2006 keV	^{46}Sc (84^{d})	β^- 357 keV γ 1119 keV	$<$ 20 ps	1 30 ps Azuma (2) 2. 5 ps Lee et al (3)
$^{84}_{37}Rb_{47}$	250 keV	^{84m}Rb (20^{m})	ce 216 keV 250 keV.	$(3.08 \pm 0.55) \times 10^{-10}$ sec.	.....
	920 keV	^{99}Mo (67^{h})	β^- 450 keV γ 780 & 740 keV	$<$ 1 x 10^{-10} sec.	$<$ 1×10^{-10} sec. Meiling et al (1)
$^{99}_{43}Tc_{56}$	181 keV	^{99}Mo (67^{h})	β^- 450 keV. γ 181 keV	$(3.40 \pm 0.10) \times 10^{-9}$ sec.	1. $(3.5 \pm 0.3) \times 10^{-9}$ sec. Lehmann et al (4) 2. $(3.575 \pm 0.05) \times 10^{-9}$ sec. Bodenstedt et al (5) 3. $(3.53 \pm 0.05) \times 10^{-9}$ sec. Andrade et al (6) 4. $(3.45 \pm 0.06) \times 10^{-9}$ sec. Meling et al (1).

REFERENCES:

1. W. Meiling and F. Stary, Nucl. Phys. 74, 113 (1965)
2. R.E. Azuma, Phil. Mag. 46, 1031 (1955)
3. Y.K. Lee and C.S. Wu, Phys. Rev. 132, 1200 (1963)
4. P. Lehmann and J. Miller, Compt. Rend. 240, 1525 (1955)
5. E. Bodenstedt, E. Matthias and H. J. Korner, Z. Physik 153, 423 (1959)
6. P.D.R. Andrade et al., Nucl. Phys. 66, 545 (1965)
7. H.N. Brown and R.A. Becker, Phys. Rev. 96, 1372 (1954)
8. T.J. De Boer, E.W. Ten Napel and J. Blok, Physica 29, 1013 (1963)
9. D.B. Fossan and B. Herskind, Nucl. Phys. 40, 24 (1963).

DISCUSSION:

N.N. Ajitanand: How was the time resolution in your system measured? What was the type of converter used?

B. Sethi: The time resolution in our system was measured from the full width at half maximum of the prompt curve. The time-to-amplitude converter was a transistorised one, using a tunnel diode memory as its main element.

I.M. Govil: What is the time resolution for β-γ coincidences, I mean, for a specified energy and channel width?

B. Sethi: The time resolution for β-γ coincidence depends on the ranges of energies selected. A typical value of the time resolution, i.e. FWHM, with the beta rays in the energy range 200 to 250 keV and gamma rays selected with 800 to 1000 keV energy loss in the scintillator, is 6.8×10^{-10} sec.

LIFETIME OF THE 531 keV STATE IN ^{147}Pm

M.T. Rama Rao, V.V. Ramamrthy and V. Lakshminarayana
Laboratories for Nuclear Research
Andhra University, WALTAIR.

INTRODUCTION:

The lifetime of the 91 keV state in ^{147}Pm populated by the beta decay of ^{147}Nd was determined (1) accurately. The ground and the 91 keV state spins being 7/2 and 5/2 respectively, the M1 transition probability was determined and the large hindrance observed was atrributed to 1-forbidenness. The detailed wavefunctions for these two states are recently furnished by Kisslinger and Sorenson (2). In an attempt to study the structure of the second 5/2 + state at 531 keV in ^{147}Pm, its halflife is measured employing a time-to-pulse height converter similar to that of Green and Bell (3).

EXPERIMENTAL DETAILS:

The experimental arrangement consists of 2 photomultiplier crystal combinations (RCA 6810A and NE-102 Plastic scintillators) in a conventional fast-slow coincidence arrangement. The fast pulses are taken from the anodes, limited with E88CC tubes and clipped with RG 63-U cables. The slow channels receive pulses from the eighth dynodes. The time-to-height converter is based on 6BN6 operated conventionally at reduced potentials. The resultant time spectrum is recorded on 100 channel analyser gated by slow channel coincidence putput. The prompt resolution curve obtained

with a ^{60}Co source yielded a full width at half maximum of 7.6×10^{-10} sec. and intrinsic slope of 8.02×10^{-11} sec. The centroid shift method is employed for the measurement of the meanlife, the prompt source being ^{60}Co. The beta spectrum feeding the 531 keV state in the energy interval 225-300 keV is accepted in the early channel and the compton edge of the 531 keV gamma is accepted in the late channel. The resultant time spectrum is shown in Fig. 1. together with the spectrum obtained with ^{60}Co under similar conditions. The centroid shift estimated as a mean of 5 independent determinations is given by $(1.2 \pm 0.22) \times 10^{-10}$ sec which corresponds to the meanlife of the 531 keV state. No attempt seems to have been made earlier to determine this lifetime. Hans (4) et. al. however fixed an upper limit to the life of this state as 0.6 ns.

DISCUSSION:

The experimental M1 and E2 transition probabilities are estimated from the meanlife reported above employing the mixing ratio of Westernberger (5) et. al. and the known (6) branching ratio (R) of the transition ($\delta^2 = 0.95$ and $R = 100/121$) and given below:

$$T(M1) = (3.60 \pm 0.60) \times 10^9 \text{ sec.}^{-1}$$

and $$T(E2) = (3.24 \pm 0.55) \times 10^9 \text{ sec.}^{-1}$$

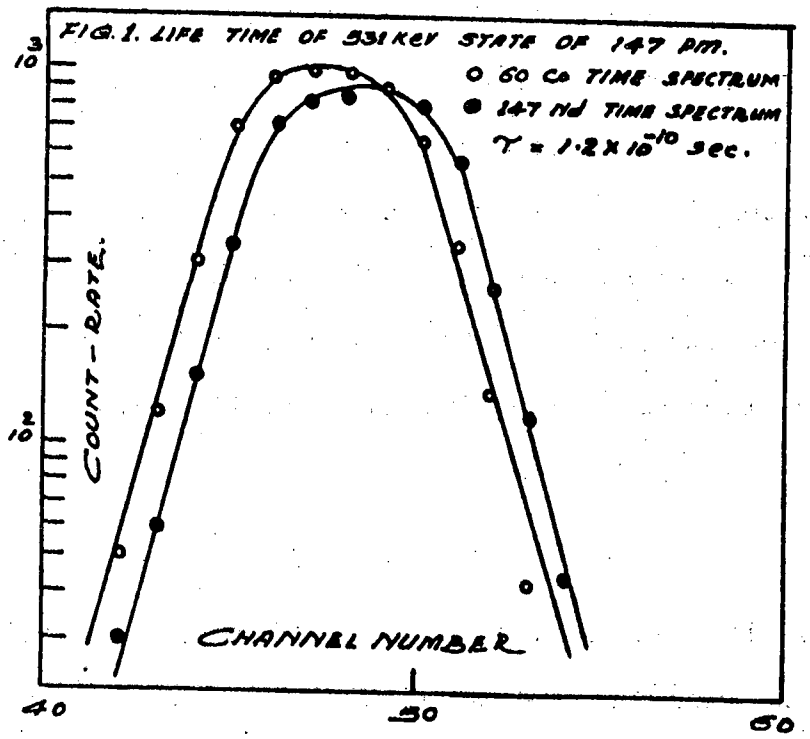
FIG. 1. LIFE TIME OF 531 KeV STATE OF 147 Pm.
○ 60 Co TIME SPECTRUM
● 147 Nd TIME SPECTRUM
τ = 1·2 x 10^-10 sec.
COUNT - RATE.
10^3
10^2
CHANNEL NUMBER
40
50
60

The corresponding values from the single particle estimates are given by

$$T(M1) = 7.2 \times 10^{12}\ sec^{-1}$$

$$T(E2) = 8.21 \times 10^{8}\ sec^{-1}$$

the hindrance in M1 and the enhancement in E2 being about 2000 and 4 respectively. The M1 hindrance in this case may be due to the 1-forbiddenness (as in the case of the 91 keV transition) or to the description of the 5/2 + state at 531 keV as of collective type. A pure de-Shalit type of wave-function however requires considerable E2 enhancement which is not observed in the present case. It thus appears that the KisslingerSorenson type of wave function may be assumed and the particle and collective parts can be estimated from the present experimental result. For this purpose the ground state of ^{147}Pm is taken from Kisslinger and Sorenson and the wave function of the 531 keV state is taken to be predominently determined by the particle state 5/2 and the particle 7/2 + phonon state thus:

$$\left|\tfrac{7}{2}\right\rangle = 0.71\left|\tfrac{7}{2}\right\rangle - 0.63\left|2\tfrac{7}{2}\tfrac{7}{2}\right\rangle - 0.08\left|2\tfrac{5}{2}\tfrac{7}{2}\right\rangle - 0.08\left|2\tfrac{3}{2}\tfrac{7}{2}\right\rangle$$

$$\left|\tfrac{5}{2}\right\rangle_{531} = A\left|\tfrac{5}{2}\right\rangle + \sqrt{1-A^2}\left|2\tfrac{7}{2}\tfrac{5}{2}\right\rangle$$

From these functions the M1 transition probability is obtained in terms of A and equated to the present experimental value.

The value of A thus obtained is given by

$$A = 0.99 \pm 0.16$$

$$\text{and} \sqrt{1 - A^2} = 0.05 \pm 0.02$$

These values are employed to predict B (E2) as

$$B(E2)_{predicted} = (2.1 \pm 1.0) \times 10^{-3}$$

while the corresponding experimental value is given by

$$B(E2)_{exp.} = (4.95 \pm 0.83) \times 10^{-3}$$

It can be seen from these values that the agreement is only approximate. However in estimating the experimental value of B(E2) the error in δ^2 is not taken into account. In view of that the agreement seems to be satisfactory. It therefore appears that the 531 keV state in ^{147}Pm contains a large 5/2 particle part and a small collective part.

REFERENCES:

1. K.M.M.S. Ayyangar et. al. Current Science 34, 606 (1965)
2. L.S. Kisslinger and R.A. Sorenson, Rev. Mod. Phys. 35, 853 (1963)
3. R.E. Green and R.E. Bell, Nucl. Inst. 3, 127 (1958)
4. Hans-Dietrich et. al. Nucl. Phys. 20, 169 (1960)
5. G.A. Westernberger et. al. Phys. Rev. 123, 1812 (1961)
6. E. Spring Phys. Lett. 7, 218 (1963)
7. A. de-Shalit, Phys. Rev. 122, 1530 (1961)

DISCUSSION:

P. Sen: With such a crude resolution, the value of τ by peak shift method is not valid unless moment calculations are made?

V. Lakshminarayana: Yes. But the value of δ^2 is not also known to sufficient accuracy. More accurate values are of course needed for accurate estimates of A. The present values, however, throw some light on the structure of the state.

BRANCHING RATIO IN THE ELECTRON CAPTURE TRANSITIONS OF ^{65}Zn

H.K. Sahoo and U.C. Gupta
Bhabha Atomic Research Centre, Trombay

ABSTRACT.

Branching ratio in the electron capture transitions of ^{65}Zn has been measured using a coincidence set up developed in this Laboratory in conjunction with a gamma ray spectrometer. The setup employs a high pressure 4π-proportional counter for the detection of X-rays and Auger electrons. Gamma rays are detected in a NaI(Tl) crystal placed outside the proportional counter.

The coincidence measurement gave the total electron capture rate while the gamma spectrometer gave the gamma emission rate. The branching ratio was calculated from these two measurements and was found to be (0.53 ± 0.03). This value is in good agreement with the values obtained by other methods (1,2).

REFERENCES:

1. G.I Gleason, Phys. Rev. 113, 287 (1959)

2. J.G.V. Taylor and J.S. Merritt, Phys. Canada 19, No.3,17 (1963)

DECAY OF ^{99}Mo

P. Jagam and V Lakshminarayana
Laboratories for Nuclear Research
Andhra University, WALTAIR.

The radioactive decay of ^{99}Mo was studied by a few investigators (1,2). Recent investigations of Cretzu and Hohmuth (3) have effected a few changes in the earlier results. They also found evidence for 2 new gamma rays 410 and 620 keV in coincidence with the 370 keV gamma ray. The results of Crowther and Elridge (4) are in good agreement with these results except for the 2 new gamma rays. sum (5) and sum-peak (6) coincidence techniques being ideally suited for studies on cascade modes of decay the present study is undertaken.

Five samples of carrier-free liquid source of ^{99}Mo are obtained at different times from AEET and studied with the experimental arrangements shown in Fig. 2. The two channels are assembled with DuMont 6292 photo-multipliers and Harshaw type NaI(Tl) crystals of dimensions $1\frac{3}{4}$" (dia.) x 2". The experimental arrangement is of the conventional fast-slow type with a 100-channel analyser. The spectra are recorded in sum coincidence, 7 cm sum-peak and 4π sum-peak coincidence modes of operation. The zero-bias 7 cm sum-peak coincidence spectrum is shown in Fig. 3. It shows peaks at 1270, 1150, 920 and 280 keV. Peaks in 7 cm sum-peak coincidence arrangement can only occur for two gamma cascade events. It therefore appears possible that the highest energy level fed in the beta decay of ^{99}Mo is 1270 keV. The same figure also shows the 200 keV bias spectrum in which the presence

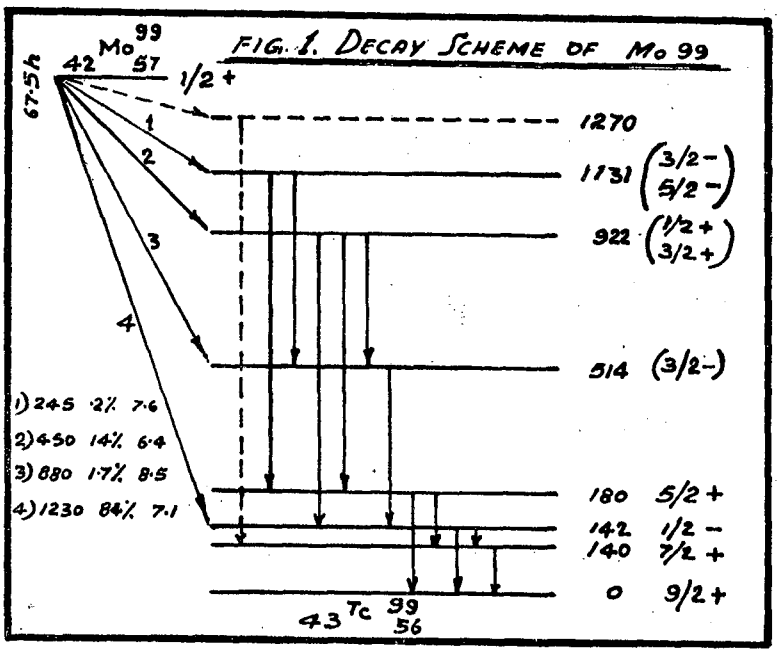

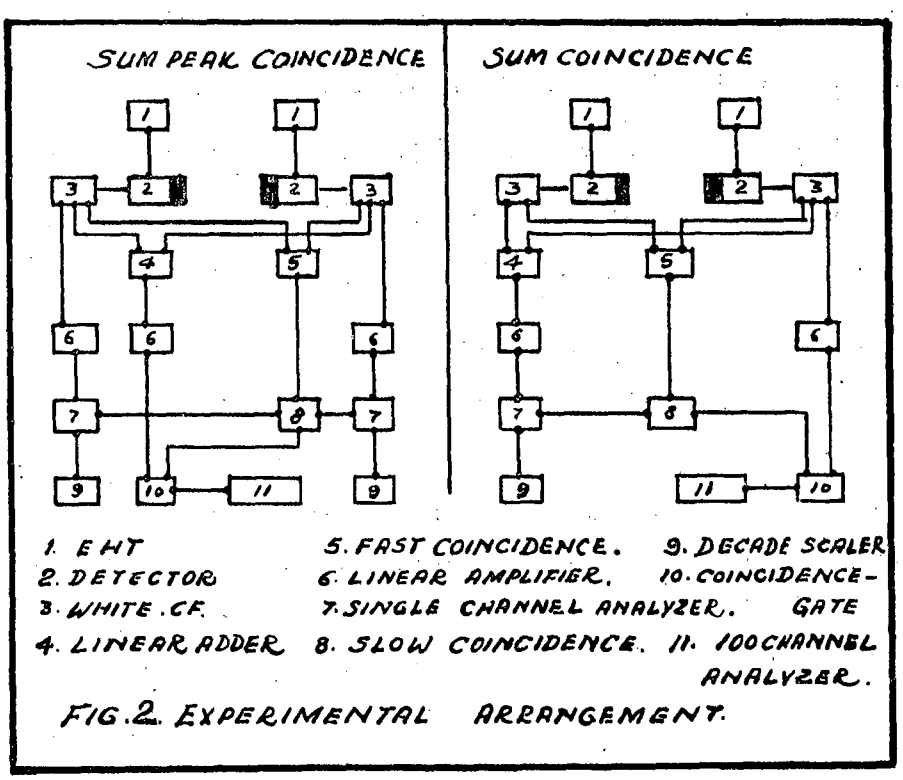

FIG. 2. EXPERIMENTAL ARRANGEMENT.

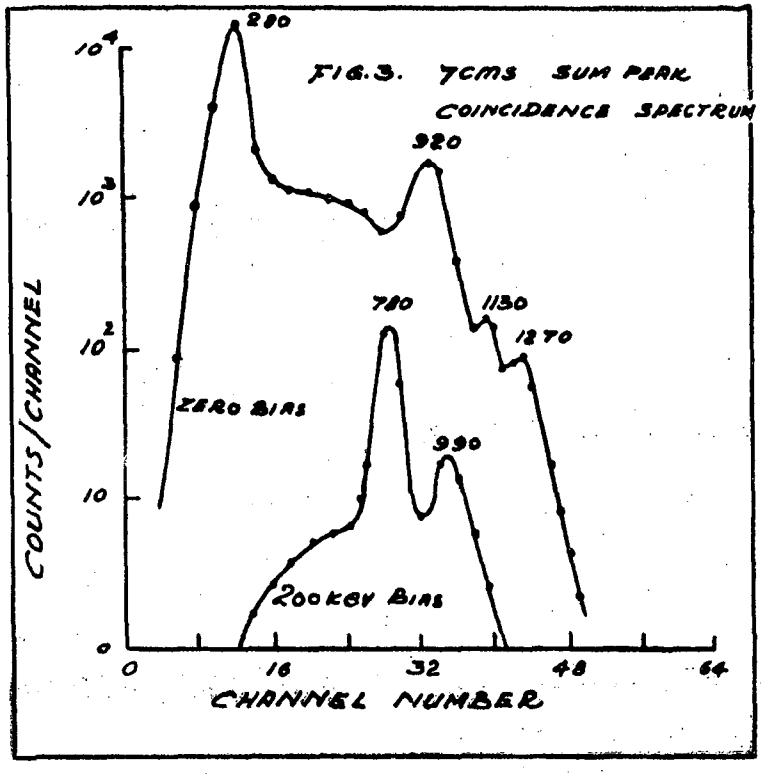
FIG.3. 7CMS SUM PEAK
COINCIDENCE SPECTRUM
280
920
780
1130
1270
990
ZERO BIAS
200 KEV BIAS
COUNTS/CHANNEL
CHANNEL NUMBER
0
16
32
48
64
10
10^2
10^3
10^4

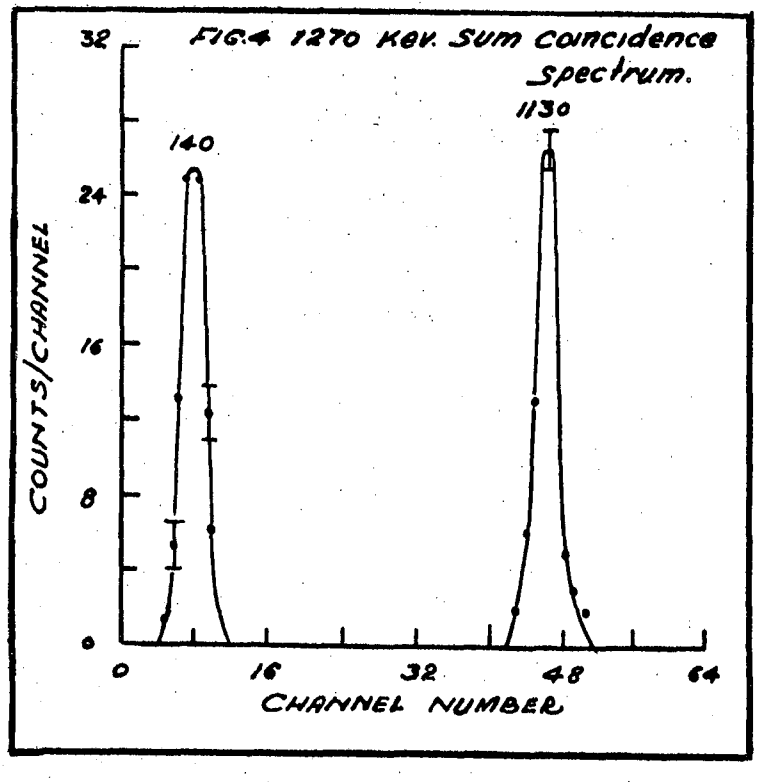
FIG.4 1270 KEV. SUM COINCIDENCE
SPECTRUM.
140
1130
COUNTS/CHANNEL
CHANNEL NUMBER
0
8
16
24
32
48
64

of peaks at energies 730 and 990 keV supports the evidence for the two new gamma lines recently observed (3). The sum coincidence spectrum with gate at 1270 keV is recorded and shown in Fig. 4. Two lines at energies 140 and 1130 keV suggest that the 1270 keV state predominently decays to the 140 keV state. The sum coincidence spectra recorded for gates at 1130 and 920 keV confirmed the cascade relations proposed earlier (3). The halflife of the source is followed in the 4π sum-peak mode and the various components are found to decay with a half-life of 65$\pm$2 hours. The decay scheme is shown in Fig.1. with the new level and gamma line now being introduced shown by dotted lines.

REFERENCES:

1. B.S. Dzelepov and L.K. Peker, Decay schemes of Radioactive nuclei : Pergamon Press (1961).
2. E. Bodenstedt et. al., Z. Phys. 153, 423 (1959)
3. T. Cretzu and K. Hohmuth , Nucl. Phys. 66, 391 (1965)
4. P. Crowther and J.S. Eldridge, Nucl. Phys. 66, 472 (1965)
5. A.M. Hoogenboom, Nucl. Inst. 3, 57 (1958)
6. J. Kantele and R.W. Fink, Nucl. Inst. & Meth. 17, 33 (1962)

DISCUSSION:

N. Nath: When one tries to do sum-coincidence or even simple coincidence studies involving a high energy and a very low energy γ-ray (as is the case for your level predictions at 1270 keV with 1130 and 140 keV as cascades) it is better to try a selective

absorption experiment to eliminate the possibility of summing in the crystal resulting in an erraneous conclusion?

V. Lakshminarayana: We have, of course, not done that. But we have ensured that the effect of summing events to be small.

S.P. Sud: Could you estimate the beta feeding to the 1270 keV levels?

V. Lakshminarayana: No. Intensity estimates are not attempted in view of poor statistics.

P.C. Mangal: How did you take care of the chance coincidence contributions in sum-peak coincidence study?

V. Lakshminarayana: Simple. Taking the resolving time and the singles rates.

P.C. Mangal: Did you find any difference in the chance rate in simple coincidence study and in sum-peak coincidence study?

V. Lakshminarayana: Chance rate should be about the the same. But true-to-chance ratio of the sum-peak arrangement is better.

DECAY OF ^{97}Zr

P. Jagam and V. Lakshminarayana
Laboratories for Nuclear Research
Andhra University
Waltair.

ABSTRACT.

The sum-and sum-peak-coincidence techniques with a 100 channel analyser are used for the investigation of the decay scheme of ^{97}Zr. The 7 cm-sum-peak arrangement eliminates completely the singles gammas in the zero bias sum-peak spectrum and records only cascade events. In the case of ^{97}Zr such a zero bias sum peak coincidence spectrum shows a peak at 2580 keV. The sum-coincidence spectrum with gate at this energy shows the decay as arising out of two cascades. The half life is followed in the 4π sum-peak arrangement and is found to be consistent with the accepted half life of 17 hours. A thousand keV component observed in the spectrum however is found to decay with a half-life of about 80 hours and is tentatively assigned to the decay of ^{95m}Nb.

BETA-GAMMA DIRECTIONAL CORRELATION STUDIES IN THE DECAY OF ^{160}Tb.

V. Seshagiri Rao and V. Lakshminarayana
Laboratories for Nuclear Research,
Andhra University
Waltair.

ABSTRACT.

Beta-Gamma directional correlations are studied for the 3^-, 2^+, 860 keV beta transition in the decay of ^{160}Tb accepting the following gammas of energies 880 keV and 970 keV in the gamma channel. The reduced correlation coefficients after allowing for the combined effect of the two gammas are obtained and plotted against energy. The best fit through the various points gives the energy-dependent and independent coefficients as

$$R_3 = 0.110 \pm 0.011 \text{ and}$$

$$e = 0.000110 \pm 0.000062$$

These values indicate a strong support for the approximation while the large log-ft (8.8) value is inconsistent with this conclusion.

ANGULAR CORRELATION STUDIES IN THE DECAY OF ^{115}Cd AND ^{192}Ir USING SUM COINCIDENCE TECHNIQUES

N. Ramakumar and V. Lakshminarayana
Laboratories for Nuclear Research,
Andhra University
Waltair.

ABSTRACT.

Angular correlations are studied on the 232 + 260 keV cascade between the levels 827 and 335 keV in In-115 using the 200 keV bias sum-peak spectrum. The correlation could be fitted as

$$W(\theta) = 1 - (0.243 \pm 0.015)\ P_2(\cos\theta) + (0.000 \pm 0.015)\ P_4(\cos\theta)$$

The zero value for the A_4 coefficient suggests a spin assignment of $3/2^-$ for the 595 keV state. Angular correlations are also measured for the cascades 588 + 612 keV and 316 + 884 keV simultaneously using the sum-coincidence spectrum with gate at 1200 keV in the decay of ^{192}Ir. The values obtained for these cascades are

$$W(\theta)=1+(0.097\pm0.010)\ P_2(\cos\theta)+(0.001 \pm 0.010)\ P_4(\cos\theta)$$

and

$$W(\theta)=1+(0.086\pm0.010)\ P_2(\cos\theta)+(0.000 \pm 0.010)\ P_4(\cos\theta)$$

These results indicate a spin assignment of 4^+ for 1200 keV state in ^{192}Pt.

GAMMA-GAMMA ANGULAR CORRELATION MEASUREMENTS BY SUM-PEAK COINCIDENCE METHOD*

S.P. Sud, K.K. Suri, P.C. Mangal and P.N. Trehan
Department of Physics,
Panjab University,
Chandigarh.

ABSTRACT.

Sum-peak coincidence method has been used for the gamma-gamma angular correlation measurements. This set up has been found to have some special advantages over the conventional slow-fast Coincidence method. The sum-peak spectrometer being fully symmetrical registers all the wanted coincidences and has therefore almost double coincidence dtection efficiency. The performance of the spectrometer is insensitive to minor electronic drifts. Slight electronic drifts donot change the area under the sum-peak but only broaden it. This makes it particularly useful in angular correlation studies involving weak cascades where long runs are needed to obtain good statistics. By stuying several sum-peaks at the same time, it is possible to measure several angular correlation functions simultaneously. If a sum-peak is due to more than one cascade, the set-up can be used to determine the contributions of the unwanted cascades in the sum-peak.

The feasibility of the technique was checked by studying 1.17 Me V-1.33 MeV gamma cascade in ^{60}Ni. The angular

This work was done under the sponsorship of National Bureau of Standards washington, D.C.

correlation function obtained by a least squares fit (2) of the data after correcting for the attenuation due to finite solid angle of the dtectors (3) was found to be

$$W(\theta) = 1 + (0.0995 \pm 0.0103) P_2(\cos\theta) + (0.0095 \pm 0.0013) P_4(\cos\theta)$$

The 356-82 keV gamma Cascade in ^{133}Cs was studied using this technique. The angular correlation function corrected for finite solid angle of the detectors was found to be

$$W(\theta) = 1 + (0.0350 \pm 0.0015) P_2(\cos\theta) - (0.0048 \pm 0.0030) P_4(\cos\theta)$$

The results are in agreement with the results of other authors (4-9), and favour $1/2^+$ spin assignment to the 438 keV level in ^{133}Cs. B.N. Subba Rao (10) assigns $3/2^+$ spin to this level on the basis of 82K-356 KeV electron gamma angular correlation, but R.Othaz (11) on the basis of 82K-356 keV electron gamma angular correlation assigns a spin $1/2^+$ to this level.

REFERENCES:

1. J. Kantele and R.W. Fink, Nucl. Insts. 15, 69-73 (1962)
2. M.E. Rose, Phys. Rev. 92, 610 (1953)
3. M.J.L. Yates in Alpha Beta - Gamma-rays spectroscopy edited by K.Siegbahn Vol. 2.
4. A.P. Arya. Phys. Rev. 122, 549 (1961)
5. F.M. Clikemand and M.G. Stewart Phys. Rev. 114, 1052 (1960)

6. E. Bodenstedt, J.H. Korner and E. Mathias Nucl. Phys. 11, 584 (1959)

7. F. Munich, K. Fricke and U. Welner, Zeits Phys. 174, 68 (1963)

8. L.I. Yin & Wiedenbeck, Nucl. Phys. 54, 86 (1964)

9. J.E. Thun et al, Nucl. Phys. 88, 289 (1966)

10. B.N. Subba Rao, Nucl. Phys. 27, 28 (1961)

11. R. Othaz Proc. Intern. Conf. Internal Conv. Processes, edited by J.H. Hamilton.

GAMMA-GAMMA DIRECTIONAL CORRELATIONS IN ^{82}Kr

M.M. Bajaj, S.L. Gupta and N.K. Saha
Department of Physics and Astrophysics,
University of Delhi Delhi.

INTRODUCTION:

The energy level structure of ^{82}Kr following the beta decay of 36h ^{82}Br has been investigated by many workers (1-10). Recent studies (4,6-10) have confirmed the existence of a highly excited level in ^{82}Kr at 2425 keV which depopulates by a weak gamma quantum emission of energy 1648 keV leading to the first excited state at 777 keV (fig.1). Recently Etherton and Kelly (6) studies the energy level structure of ^{82}Kr using high resolution Ge(Li) detectors and permanent magnet electron spectrometers. Their measurements suggest three possible spin values to the 2425 keV level, namely, 2,3 and 4. We have made directional correlation measurements on 1648-777 keV cascade to arrive at a unique spin value of the 2425 keV level and also to investigate the multipolarity of the 1648 keV transition. In addition directional correlation measurements are made on the 1317-777 and the 619-1475 keV cascades and the E2 lifetimes of the 1317 and 619 keV transitions are estimated from their observed mixing ratio analysis.

All coincidence and directional correlation measurements were carried out using a fast-slow NaI(Tl) scintillation coincidence spectrometer with an effective resolving time of $\approx$ 30ns.

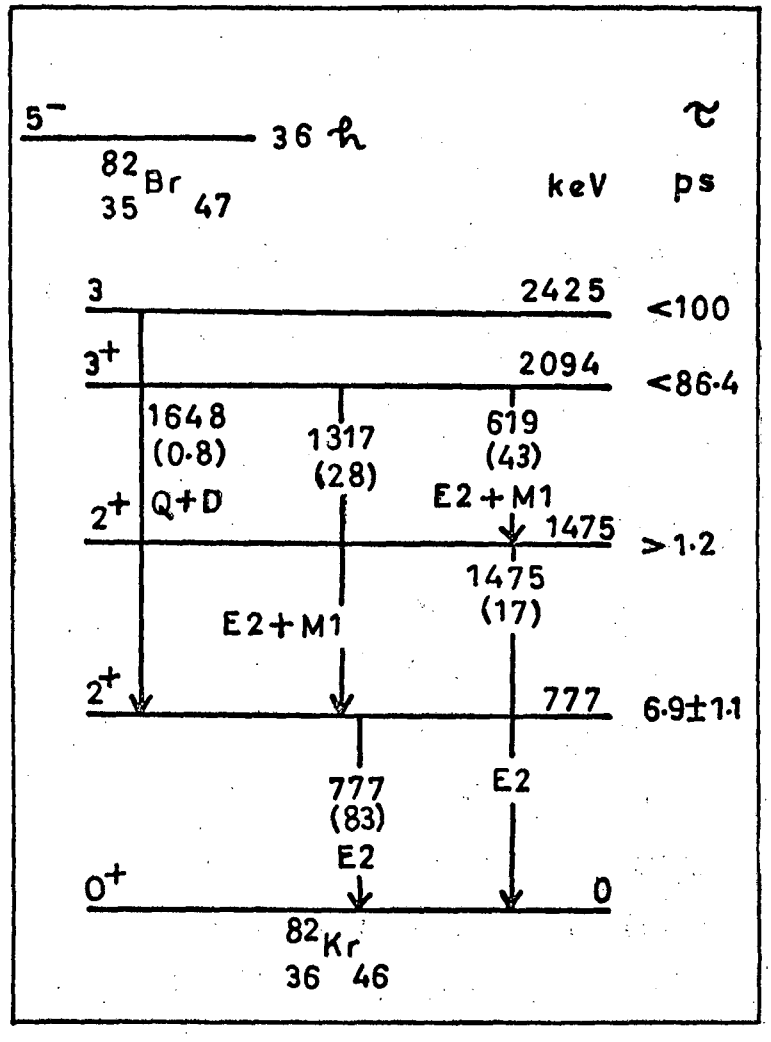
5⁻
36 h
τ
82 Br 35 47
keV
ps
3
2425
<100
3+
2094
<86·4
1648
(0·8)
Q+D
1317
(28)
619
(43)
E2+M1
2+
1475
>1·2
1475
(17)
E2+M1
2+
777
6·9±1·1
777
(83)
E2
E2
0+
0
82 Kr 36 46

RESULTS:

The solid angle corrected directional correlation function for the 1648-777 keV cascade was found to be $W(\Theta) = 1 + (0.0427 \pm 0.0152)P_2(\cos\Theta) - (0.0517 \pm 0.0308)P_4(\cos\Theta)$ (1)

This cascade, also recently studied by Koch et al., is practically free from all interfering contributions, because the three high energy gamma rays 1777, 1871 and 2052 keV also cascading with γ 777 are extremely weak. As mentioned earlier, Etherton and Kelly (6), assigned three spin values 2,3 or 4 to the 2425 keV level. The spin and parity of the ground state of even-even ^{82}Kr is 0^+ and that of the first excited state 2^+, which decays by a pure E2 transition. Three possible spin sequences, therefore, follow for the above cascade: (i) 2(D,Q)2(Q)0, (ii) 3(D,Q)2(Q)0 and (iii) 4(Q)2(Q)0. The (iii) spin sequence is not compatible with eq. (1) because the theoretical expansion coefficients for this sequence are $A_2 = +0.1020$ and $A_4 = +0.0091$. The observed A_2 coefficient alone appears to be consistent with the sequence (i), if the 1648 keV gamma transition is assumed to contain a mixture of either ~ 93% dipole and ~ 7% quadrupole or ~ 98% quadrupole and ~ 2% dipole radiations. But in both these cases, the finite negative value (-0.0517 ± 0.0308) of the observed A_4 coefficient cannot be accounted for. Therefore, the only possible spin sequence which could be assigned to this cascade is 3(D,Q)2(Q)0. Mixing ratio analysis of the observed A_2 expansion coefficient in terms of this spin sequence leads to the quadrupole content of $Q_{1648} = 0.0210 \pm 0.0035$ or 0.9025 ± 0.0125 for the 1648 keV

radiation. Therefore the 1648 keV gamma ray is either predominantly dipole in character with a quadrupole admixture of $(2.10 \pm 0.35)\%$ or predominantly quadrupole in character with a dipole admixture of $(9.75 \pm 1.25)\%$. As the internal conversion coefficient of this radiation is not known, nothing definite can be said about its multipolarity. However a similar mixing ratio analysis made on the observed A_4 expansion coefficient favours a predominantly quadrupole character for the 1648 keV gamma ray. This conclusion is in contrast with the results of Koch et al. (10) who prefer a predominantly dipole character for this transition from their directional correlation measurements.

For the 1317-777 keV cascade, the solid angle corrected directional correlation function is

$$W(\theta)=1-(0.0301\pm 0.0069)P_2(\cos\theta)-(0.0452\pm0.0140)P_4(\cos\theta) \qquad (2)$$

The contribution of the 1648-777 keV cascade to the present one has been estimated to be $\leq 2.5\%$ from a careful analysis of our singles and coincidence spectra. As this is quite negligible, we have made no corrections for it.

According to eq. (2), the most likely spin sequence for this cascade is 3(D,Q)2(Q)0. As a result, the mixing ratio analysis shows that the E2 and M1 contents of γ 1317 are $(95.5\pm0.5)\%$ and $(4.5\pm0.5)\%$, respectively. These conclusions are in excellent agreement with those reported by Etherton & Kelly (6) and Benczer-Koller (2).

For the 619-1475 keV cascade the solid angle corrected directional correlation function is

$$W(\theta)=1+(0.0992\pm0.0029)P_2(\cos\theta)-(0.0022\pm 0061)P_4(\cos\theta) \quad (3)$$

With the channel settings and energy windows used, the contribution of the interfering cascades 554-(619)-1475, 554=1317, 1317-777 and 1648-777 keV to the investigated one, has been estimated to be $\leq 2\%$ each. Therefore eq. (3) needs no correction.

The directional correlation data are consistent with the spin sequence 3(D,Q)2(Q)0. The mixing ratio analysis carried out in terms of this spin sequence shows that γ 619 is (84.5±0.5)% E2 with a M1 admixture of (15.5±0.5)%. These results are quite compatible with the earlier studies (1,2,6) made on this cascade.

Table I shows the E2 lifetimes for the 619 and the 1317 keV gamma transitions, computed by us, using the measured values of δ^2, $T_{1/2}$ (expt) (5) and the α_K(2). The E2 component, in the case of γ619, appears to be enhanced by a factor $\sim$2, whereas in the case of γ1317, it is retarded by a factor of $\sim$ 10. The E2 lifetime values seem to follow the order of the single particle values and thus do not reflect the many-body collective behaviour of even - even nuclei. Usually the collective transition involving many particles are considerably faster than the single particle ones. The above results, therefore, seem to follow the simple shell model considerations for these transitions.

Table I.

Energy of the transition (keV)	Mixing ratio (δ)	τ(E2) expt $\times 10^{-11}$ sec	τ(E2) expt $\times 10^{-11}$ sec	E2 enhancement $= \frac{\tau(E2)_W}{\tau(E2)_{Expt}}$
619	-2.34 ± 0.05	< 23.52	41.67	$\gtrsim 1.8$
1317	-4.61 ± 0.26	< 11.23	0.96	$\gtrsim 0.09$

REFERENCES:

1. R.C. Waddell and E.N. Jensen, Phys. Rev. 102, 816 (1956)
2. N. Benczer-Koller, CU-177 (1958)
3. V.S. Dubey, C.E. Mandeville and M.A. Rothman, Phys. Rev. 103, 1430 (1956)
4. L. Simons, S. Bergstrom and A. Anttila, Nuclear Physics, 54, 683 (1964)
5. W. Flauger and H. Schneider, Nuclear Physics 55, 207 (1964)
6. R. C. Etherton and W.H. Kelly, Nuclear Physics 34, 129 (1966)
7. T.J. Kennett, I.B. Webster and W.V. Prestwich, Nuclear Physics 58, 56 (1964)
8. L.Mo, F. Hsu and C.S. Wu, Bull. Amer. Phys. Soc. 10, 81 (1965)
9. E.B. Nieschmidt, C.E. Mandeville and L.D. Ellsworth, Bull. Amer. Phys. Soc. 10, 129 (1965)
10. J. Koch et al., Zeit. fur Naturforsch. 20a, 845 (1965)

DISCUSSION:

J. Rama Rao: Have you used the 'pealing off' technique for the measurement of gamma ray intensities? If so, what is the order of accuracy?

M.M. Bajaj: Yes. Order of accuracy is $\sim 5\%$.

P.C. Mangal: What was the percentage contribution in the coincidence rate for 1648 - 777 keV cascade because of the other three interfering cascades?

M.M. Bajaj: The other three cascades (1777 - 777, 1871 - 777 and 2052 - 777 keV) are extrmely weak. The contribution due to these are expected to be $< 0.005\%$ in the present cascade.

R.P. Varshneya: What are your results for angular correlation of 1317 - 777 and 619 - 1475 keV cascades?

M.M. Bajaj: Directional correlation functions for the 1317 - 777 and 619 - 1475 keV cascades are

$$W(\theta)=1-(0.0301\pm0.0069)P_2(\cos\theta) - (0.0452\pm0.0140)P_4(\cos\theta)$$

$$W(\theta)=1+(0.0992\pm0.0029)P_2(\cos\theta) - (0.0022\pm0.0061)P_4(\cos\theta)$$

GAMMA-GAMMA ANGULAR CORRELATIONS IN ^{147}Nd

M.S. Rajput and M.L. Sehgal
Department of Physics, Aligarh Muslim University, Aligarh

INTRODUCTION:

The energy levels of ^{147}Pm from the beta decay of ^{147}Nd have been studied by several workers (1-14). Spin and parity assignments have been made on the basis of calculated log ft values by Wendt and Kleihentz (1) and nuclear alignment experiments by Westenbareger and Shirley (2). Some assignemnts have also been made on the basis of directional correlation studies by Arya (10), Saraf (12) and Bodenstedt (3). But the spin assignments of all these workers are not in good agreement with each other. There is ambuigity about the spin assignments of the levels at 91,182,533 and 690 keV respectively. Hence it was felt worthwhile to reinvestigate the angular correlation of some gamma cascades in ^{147}Nd.

2. RESULTS AND ANALYSIS:

2,1. Angular Correlation of 91 - 91 keV cascade.

After applying the geometrical correction, the correlation function was obtained to be,

$$W(\theta) = 1 + (0.055 \pm 0.013)\, P_2(\cos\theta) - (0.033 \pm 0.021)\, P_4(\cos\theta)$$

Due to the complex level structure of ^{147}Pm, the correlation coefficients are to be corrected for the interferring cascades. The interferring coincidences are observed between the lower 91 keV gamma ray and the gamma rays of energy 120,199,320,400,442 and 599 keV. The contributions for these cascades are calculated from

their relative contribution in the 91 - 91 keV coincidence. It was estimated that the contributions due to these cascades are: 320 - 91 keV = (2.5 ± 0.5)%, 400 - 91 keV = (1.5 ± 0.40)%, 442 - 91 keV = (1.6 ± 0.4)% and 599 - 91 keV = (1.2 ± 0.4)%. Other interfrrences were found negligible. After applying corrections for these interferrences, the correlation function became.

$$W(\theta) = 1 + (0.058 \pm .029)P_2(\cos\theta) - (0.049 \pm 0.042)\ P_4(\cos\theta)$$

The ground state spin of ^{147}pm has been measured by Cabezas (5) to be 7/2. The K-conversion coefficient of the lower 91 keV gamma ray is measured to be 1.6 ± 0.2 by Rajput and Sehgal (9). This value of conversion coefficient agrees with M_1, E_2 or $M_1 + E_2$ nature of this gamma ray. So the possible spins of the first excited state can be 3/2, 5/2, 7/2, 9/2 and 11/2. The nucleus ^{147}Nd decays 65% to the first excited state of ^{147}Pm and the ground state spin of ^{147}Nd is $5/2^-$. So from the beta intensity considerations the possible spins of the first excited state can only be 3/2 or 5/2, as the log ft value of the beta transitions feeding this level is 7.6. The life time of this level is measured to be 4.73 ± 0.04 ns by Beekhuiss (3). This agrees with the l-forbidden M_1 transition. Thus the spin of the level at 91 keV can only be 5/2. The second excited state of ^{147}Pm is at 182 keV and this level is populated only through the beta decay of ^{147}Nd with log ft value 8.1 as measured by Wendt and confirmed by Rajput and Sehgal (9). From the beta log ft value considerations, the possible, spins of this level can be 1/2,3/2,5/2,7/2, and 9/2. If the spin of this level is either 5/2, 7/2 or 9/2, in that case the cross over transtion of 182 keV transition should be more prominent than the upper 91 keV gamma ray, as about 10% of the transitions of ^{147}Nd

decays to this level. In the singles or in coincidence we have not seen any 182 keV gamma - ray. So the possible spin of this level can be only 1/2 or 3/2. If the spin of this level is 1/2, the log ft value of the beta transition are stisfied but it requires an appreciable life time of the order of few microseconds. We have performed the β-γ delayed coincidences in ^{147}Nd with 91 keV gamma rays and did not find any life time of this order. Hence the spin of this level cannot be 1/2 and the most probable spin of this level is $3/2^{+}$.

By the graphical analysis of the correlation function in terms of 3/2 (1,2) 5/2 (1,2) 7/2 spin sequence the quadrupole admixture in the upper 91 keV gamma rays was obtained to be (1.75 $\pm$ 1.25)%. The limits for the lower transition were taken from the work of Westenbarger and Shirley (2).

2.2. Angular Correlation of 442 - 91 keV Cascade.

After applying the geometrical corrections the angular correlation function was found to be;

$$W(\theta) = 1 + (0.053 \pm 0.012)\, P_2(\cos\theta) - (0.032 \pm 0.016)\, P_4(\cos\theta)$$

In the above function the interferring coincidences are present due to 400 - 91 keV and 599 - 91 keV cascades. An estimate of these interferrences was made and were found to be negligible. No correction was applied for them. The above correlation function is in agreement with other measurements (3,10,12).

The spins of the ground state and the first excited state are 7/2 and 5/2. The following spins are possible for this cascade: 1/2,3/2,5/2,7/2 and 9/2. Since the level at 533 keV is populated

by the first forbidden beta decay with log ft value 7.1 as measured by Wendt (1), it excludes the possibilities of the spins 1/2 and 9/2 for this level. If one takes the spin values 3/2 or 7/2 for this level, they require a positive A_4 term in the angular correlation function. Hence the only possible spin of this level can be 5/2. This assignments is consistent with the β-γ angular correlation experiments (13). The correlation coefficiets when analysed in terms of the spin sequence 5/2 (1,2) 5/2 (1,2) 7/2, yielded (32 $\pm$ 8)% quadrupole admixture in the 442 keV gamma ray.

2.3 Angular correlation of 599-91 keV cascade.

After applying various corrections the angular correlation function was found to be,

$$W(\theta) = 1 + (0.061 \pm 0.018)\, P_2(\cos\theta) - (0.052 \pm 0.022)\, P_4(\cos\theta)$$

The above function is in good agreement with that of Saraf (12). Since the log ft value of the beta transition feeding the 690 keV level is measured to be 6.5 by Wendt and Kleinhentz (1), this requires this beta group to be of first forbidden in nature. It therefore excludes the possibilities of the spins 1/2 or 9/2 for this level, as the ground state of ^{147}Nd is 5/2$^-$. Thus the possible spins of this level are 3/2, 5/2 and 7/2 only. If one takes the spins 3/2 or 7/2 for this level, they require a positive A_4 term in the angular correlation, but the experimental value is negative. Hence the spin of the 690 keV level is probably 5/2. By the graphical analysis of the correlation coefficient in terms of the 5/2 (1,2) 5/2 (1,2) 7/2 spin sequence, the quadrupole admixture

in the 599 keV gamma-rays was found to be (37.5 ± 12.5)%

REFERENCES:

1. H.D. Wendt and P. Kleinhentz Nucl. Phys. 20, 167 (1960)
2. G.A. Westenbarger and D.A. Shirley. Phys. Rev. 123,1812 (1961)
3. E. Bodenstedt et al Z. Physik. 160, 33 (1960)
4. J.M. Coerk et al, Phys,Rev. 110, 526 (1958)
5. C.A. Cabezas et al Nucl. Phys. 20, 509 (1960)
6. M.R. Gunve et al Phys. Rev. 124, 176 (1961)
7. A.C.G. Mitchel et al, Phys. Rev. 111, 1343 (1958)
8. H.S. Hans et al. Phys. Rev. 97, 1267 (1955)
9. M.S. Rajput and M.L. Sehgal Ind. J. Phys. Accepted for publication in 1966.
10. V.V.G. Shastry et al Ind.J. Pure and Appl.Phys. 2,307 (1964)
11. A.P. Arya. Phys. Rev. 122, 124 (1961)
12. B.L. Saraf. et al Phys. Rev. 124, 184 (1961)
13. H. Beekhuiss Physics, 28, 119 (1962)
    H. Beekhuiss, Nuc. Phys. 79, 220 (1966)
14. D. Bernye, Nucl. Phys. 8, 607 (1958)

DISCUSSION:

T.S. Mudhole: What are the dimensions of the crystal for detection of 38 keV energy peak?

M.S. Rajput: The size of the NaI(Tl) crystal was 2" x 2".

V. Lakshminarayana: (1) The existence or otherwise of the 182 keV state has been a subject of great dispute. How well did you establish its existence? (2) What is the contribution of 91 - 91 keV chances to your coincidence rate?

M.S. Rajput: (1) For the existence or non existence of this level we have performed the efficiency experiments. By comparing the total detection-efficiency of the NaI(Tl) crystal in a fixed geometry with standard value of the detector efficiency, we obtained that another 91 keV gamma ray exists and it comes from the 182 keV level. This level is fed with the beta decay of ^{147}Nd only. The percentage of the beta group feeding this level is (10 $\pm$ 2). (2) The contribution is less than 10%.

GAMMA-GAMMA ANGULAR CORRELATION IN ^{75}As

R.P. Varshneya and M.L. Sehgal
Physics Department
Aligarh Muslim University, Aligarh.

ABSTRACT

Gamma-gamma angular correlations for the two interfering cascades 121-280 keV and 136-265 keV and the weaker cascades 66-199 keV, 66-136 keV and 136-199 keV following the decay of ^{75}Se have been studied using the coincidence method. The results of the angular correlations are the following:

$$W(\theta, 121\text{-}280) = 1 - (0.395 \pm 0.020)\, P_2(\cos\theta) - (0.015 \pm 0.026) P_4(\cos\theta)$$
$$W(\theta, 136\text{-}265) = 1 - (0.035 \pm 0.015)\, P_2(\cos\theta) + (0.012 \pm 0.020)\, P_4(\cos\theta)$$
$$W(\theta, 66\text{-}199) = 1 - (0.019 \pm 0.020)\, P_2(\cos\theta) - (0.008 \pm 0.025)\, P_4(\cos\theta)$$
$$W(\theta, 136\text{-}199) = 1 - (0.015 \pm 0.018)\, P_2(\cos\theta) - (0.006 \pm 0.022)\, P_4(\cos\theta)$$
$$W(\theta, 66\text{-}136) = 1 + (0.019 \pm 0.010)\, P_2(\cos\theta) - (0.003 \pm 0.013)\, P_4(\cos\theta)$$

The 66-199 keV and 136-199 keV gamma-gamma angular correlations have been found consistent with the spin 1/2 for the 199 keV level in ^{75}As. The multipole E_2 admixtures of (2.9 ± 1.9)% (13.0±4.3)% and (1.6 ± 0.3)% have been obtained in 66 keV, 280 keV and 265 keV transitions respectively from the graphical analysis of the angular correlation data.

NUCLEAR STRUCTURE EFFECTS IN INTERNAL CONVERSION

G. Nageswara Rao and R. Janaki Raman,
Indian Institute of Technology,
Kanpur.

ABSTRACT

The mixing ratios for the M1 and E2 transitions in $2^{+1} \rightarrow 2^{+}$ transitions in even nuclei obtained from the (gamma-gamma) angular correlation measurements are used to obtain the theoretical K and L shell Internal Conversion Coefficients making use of Sliv and Bands values. These values are compared with the available accurate experimental data of the Internal Conversion Coefficients of the K and L shells. The experimental and theoretical values of the pure M1 transitions are also compared. These studies showed the existence of some nuclear structure effects in Internal Conversion.

POSITRON RADIAL WAVE FUNCTIONS FOR THE ANALYSIS OF β-DECAY*

S. C. K. Nair
Saha Institute of Nuclear Physics, Calcutta.

In connection with the extraction of Gv, the polar vector β-decay coupling constant from the experimental data on super allowed β-decays we have recalculated the positron radial wave functions including both the finite nuclear size effect and the screening due to atomic electrons. The tentative ft values calculated with our radial wave functions are given in this and the possible implications discussed. A mistake in the previous work of Bhalla and Rose (where the screening effect was neglected) pointed out recently by Buhring is confirmed and it is found that the error in the Bhalla-Rose table for positron radial wave functions for heavy nuclei and for large values of momentum is as much as 4%.

---

* A short account of the work is to be found in R.J. Blin-Stoyle and S.C.K. Nair, Advances in Physics 15, 521 (1966). More detailed report is to be published elsewhere.

DEVELOPMENT OF A FAST TIME-TO-AMPLITUDE CONVERTER SYSTEM FOR LIFE TIME MEASUREMENTS

P. Sen and A.P. Patro
Saha Institute of Nuclear Physics
Calcutta-9.

ABSTRACT.

A fast time-to-amplitude converter (T.A.C), similar to that of Bell, Tao and Green has been constructed. The linearity range is 120 nano seconds. With electronic pulse generator a resolution (f.w.h.m.) of better than 7.0×10^{-11} sec. has been observed. When utilising scintillation pulses from plastic phosphors (1" x 1") and RCA 6810A photomultipliers, a resolution of only 0.72×10^{-9} sec. is usually achieved, the limiting factor being mainly in the phosphor, photomultiplier combination. These factors influencing the resolution have been considered. A resolution of 0.64×10^{-9} sec. has been achieved by reducing the factors influencing the tube. Further improvements to improve the resolution will be discussed and some typical life time measurements will be presented.

Z-DEPENDENCE OF EXTERNAL BREMSSTRAHLUNG

T.S. Mudhole and N. Umakantha
Department of Physics, Karnatak University, Dharwar

ABSTRACT.

Integrated intensity of external bremsstrahlung due to beta particles from a Sr-Y-90 source falling on foils of different atomic numbers (29,34,48,82), is measured for different thicknesses of radiators. It is found that for a thickness of radiator less than about 0.4 times the range of beta particles, the intensity can be expressed as $I = K Z^n N e^{-\Sigma t}$ where Z is atomic number, N the number of atoms, t the thickness of radiator in mg/cm^2 and K,n and Σ are constants. Log(I/N) versus t is found to be a straight-line with a slope independent of Z. A plot of Log (KZ^n) versus Log Z is found to be a straight line having a slope $n = 1.97 \pm 0.06$ showing that the external bremsstrahlung intensity is proportional to Z^2 as expected from Bethe-Heitler theory. The experiment is repeated for bremsstrahlung spectrum above 400 keV and it is found that $n = 2.05 \pm 0.07$.

As the thickness of the radiator is increased beyond about 0.4 times the range of the beta particles, the bremsstrahlung intensity falls due to self absorption strongly depends on the atomic number of the radiator, showing that all measurements with a thickness of radiator sufficient to stop all beta particles, are subject to heavy self absorption effects, and do not represent

true bremsstrahlung spectrum. The Z-dependence of the observed bremsstrahlung spectra reported in literature may be attributed to the neglect of self absorption.

ELASTIC SCATTERING OF 1.33 MEV GAMMA RAYS AT HIGH MOMENTUM TRANSFER AS A FUNCTION OF ATOMIC NUMBER [6]

G. Basavaraju and P.P. Kane
Physics Department,
Indian Institute of Technology, Bombay - 76.

Measurements have been made of the atomic differential cross sections for the elastic scattering of 1.33 MeV gamma rays through 124.5°. Scattering from aluminium, copper, zirconium, molybdenum, silver, tantalum, tungsten, mercury and lead was studied. The work was undertaken with a view to determining the variation of the Rayleigh scattering cross section with atomic number at a relatively high momentum transfer (4.6 mc units in our case) and, if possible, the presence of the Delbruck scattering at an energy only slightly above the pair-production threshold. Previous experiments of a similar kind (1), carried out between 0.280 MeV and 1.12 MeV but with a poor angular resolution, extended only upto about 3.5 mc momentum transfer. Since the expected cross sections were of the order of microbarns per steradian, background had to be reduced as much as possible. Conventional 'scattering geometry' was used. Under the given experimental conditions, 124.5° was the largest angle that could be studied. To reduce the importance of secondary effects as far as practicable, an effort was made to carry out the measurements in good geometry, with thin scatterers and a relatively weak source. The selected Cobalt-60 beam source has a nominal strength of 1.3 curies. The

[6] Work assisted in part by a grant from the National Bureau of Standards, Washington, D.C.

distances of the scaterer from the source and the 3/2" x 2" sodium iodide counter were 56.7 cm and 46.5 cm respectively. In most cases, the thicknesses of the scatterer were about $1/3\mu$, where μ is the linear attenuation coefficient of the scatterer. Only in the case of tungsten and mercury, the thicknesses wereas high as $1/(1.45)\mu$ and $1/(0.784)\mu$ respectively. The homogeneity of the beam in the plane of the scatterer was ascertained by a study of the counts from an auxiliary lead scatterer of dimensions 11.5 cm x 6.00 cm x 0.547 cm for different positions in the beam.

The differential elastic scattering cross section was determined by an application of the well-known equation

$$\left(\frac{d\sigma}{d\Omega}\right)_{el} = \left(\frac{r^2}{NT}\right) \times \left(\frac{S_{calib}}{S}\right) \times \left(\frac{C_{Scatt}}{C_{calib}}\right) \times f_{el} \qquad .. (1)$$

where r is the distance of the scatterer from the source, N is the number of scattering atoms, T is the average transmission of the scatterer, S_{calib} and s are the strengths of the calibration and the beam sources respectively, C_{scatt} and C_{calib} are the counts due to the scattered gamma rays and the calibration source in the scatterer position respectively and f_{el} is the fraction of C_{scatt} attributable to elastic scattering.

The ratio, $\frac{S_{calib}}{S}$, was determined by a comparison of the counts in the sodium iodide counter placed 2.1 meters from the calibration and the beam sources under indentical collimator conditions. In the case of the beam source, an absorption curve had

to be taken and the results extrapolated to zero absorber thickness. In separate runs, the collimator aperture was varied between 3/4 inch and 1 - 1/2 inches. Twenty five independent measurements give an average value for the ratio of 1/1770 with a standard deviation of 4 per cent. The attenuation coefficient of lead turns out to be 0.0538 cm^2/gm and is in good agreement with standard values.

For the determination of C_{scatt} and C_{calib}, a windo, about 90 keV in width and extending upwards from a voltage a little above the 1.33 MeV photopeak height, was used. C_{calib} was determined several times during a day. This determination helped also in a check of pulse height shifts, which were less than 1 per cent. Counts C_{scatt} with the lead scatterer were taken at regular intervals both as an integral part of the main experiment and as an additional check on the overall operation. Background was about 20 per cent of the counts with the lead scatter in place. The final statistical precision is about 1.5 per cent in the case of lead and 10 per cent in the case of the others.

The fraction, f_{el}, was determined both by a detailed pulse height analysis of the counts due to the scatterer and by absorption measurements on C_{scatt}. The pulse height spectrum of counts due to processes other than elastic scattering is expected to have a smooth continuum type structure and to fall off with increasing pulse height. f_{el} was determined with the help of this criterion

and the expected distribution for 1.33 MeV gamma rays. Absorption measurements confirmed the correctness of these estimates of f_{el}. The errors in f_{el} cannot be determined accurately but are about 10 per cent to 15 per cent. The results for f_{el}, $(\frac{d\sigma}{d\Omega})_{el}$, and calculated $(\frac{d\sigma}{d\Omega})$ for a coherent combination of nuclear Thomson and Rayleigh scattering are summarized in Table 1.

Table I
Data at 124.5° and 1.33 MeV

Element	Al	Cu	Zr	Mo	Ag	Ta	W	Hg	Pb
f_{el}	0.65	0.60	0.60	0.60	0.60	0.55	0.55	0.50	0.50
$(\frac{d\sigma}{d\Omega})_{el}$ experimental, in 10^{-30} cm^2/Sr	0.89	3.66	6.30	6.96	8.28	35.0	36.5	40.0	58.5
$(\frac{d\sigma}{d\Omega})_{R+T}$ calculated in 10^{-30} cm^2/Sr.	0.65	3.55	-	-	-	-	-	99.0	111.0

DISCUSSION:

In the case of aluminium and copper, the Rayleigh scattering amplitudes are certainly less than 4 per cent and 17 per cent respectively of the corresponding nuclear Thomson scattering ampli-

tudes. Therefore, irrespective of uncertainties in Rayleigh scattering calculations, the cross sections for these elements can be computed to a good accuracy. Our experimental values are in agreement with the computed ones, and with those of Standing and Yovanovich (2) if allowance is made in a straightforward way for variation with angle. Thus, the correctness of our procedure is established.

Yet, our results for medium Z elements are somewhat lower than the values obtained by extrapolations from the results of other workers for tin. In the case of mercury and lead, our results are lower than those of the others by a factor of at least two. The results for some of the medium Z elements and for the other high Z elements have not been published earlier.

Since the disagreement depends on Z, the possibility of a systematic error in S_{calib}/S cannot be its cause. If f_{el} is arbitrarily taken to be unity, our cross sections for high Z will be brought into better agreement with the earlier values. But such a high value of f_{el} is extremely unlikely in view of the many competing processes and the absorption data. Further, in that case, a serious discrepancy of the opposite sign will result especially in the case of the medium Z elements. A careful analysis of the possible systematic errors in C_{scatt}/C_{calib} shows that they cannot be responsible for the observed trend of our data. So we conclude

that the disagreement with some of the earlier data is genuine and that it is probably due to an increased accuracy in our experiment. The theoretical implications of the results will be discussed subsequently.

---

1. N. Cindro and K. Ilakovac, Nucl.Phys. 5, 647 (1958); and M. Singh and B.S. Sood, Nucl. Phys. 64, 502 (1965)

2. K.G. Standing and J.V. Yovanovich, Can. J. Phys. 40, 622 (1962)

REAL PART OF THE DELBRUCK SCATTERING AMPLITUDE AND ITS EXPERIMENTAL VERIFICATION AT 124.5°.

P.P. Kane,
Physics Department,
Indian Institute of Technology
Powai, Bombay.

ABSTRACT.

Measurements of the differential elastic scattering cross section of lead for gamma rays of 1.33 MeV at 124.5°, made by Basavaraju and the author, are definitely in disagreement with (in particular much lower than) those of Standing and Yovanovich, and of Hara et al. The implication of the disagreement is either that our measurements may involve unsuspected systematic errors or that the effect of the dispersive Delbruck scattering amplitude is being detected for the first time. Detailed arguments will be presented for the rejection of the first alternative. These include the accuracy of the measured cross sections in the case of elements of low atomic number. The conclusions regarding the detection of the dispersive Delbruck effect do not depend sensitively upon the details of Rayleigh scattering calculations.

RAYLEIGH SCATTERING OF POLARISED PHOTONS

D.R.S. Somayajulu and V. Lakshminarayana
Laboratories for Nuclear Research
Andhra University, WALTAIR.

Two theories exist for the description of Rayleigh Scattering of gamma radiation - one due to Franz (1) (from factor approximation) and the other due to Brown and Mayers(2). Studies on polarisation effects are more sensitive tests of theories than measurements of cross-sections. Brini (3) et. al. therefore measured asymmetry in Rayleigh scattering of partially polarised photons. ($h\nu = 0.64$ mc^2, $\xi = 0.307$ and $h\nu = 1.28$ mc^2, $\xi = 0.322$). In both cases they used a 2-curie 60 Co source and a single crystal scintillation spectrometer arrangement. They measured the asymmetry by placing the same counter successively in different orthogonal planes. The present study is an attempt to extend their investigations to $\xi = 0.5$ and 0.6 with an improved experimental arrangement.

A 10-curie ^{137}Cs source is used in the present study with two counters in the two orthogonal planes to collect the data simultaneously. The experimental arrangement is shown in Fig. 1. The primary photons, after collimation, are scattered by an aluminium target ($\frac{1}{2}$" dia. x $\frac{3}{4}$" high.). The Compton scattered partially polarised photon beams at 2 angles ($\theta = 90^\circ$, $h\nu = 0.56$ mc^2, $\xi = 0.58$ and $\theta = 60^\circ$, $h\nu = 0.78$ mc^2, $\xi = 0.50$) are used to measure the asymmetry ratios. These partially polarised photon beams

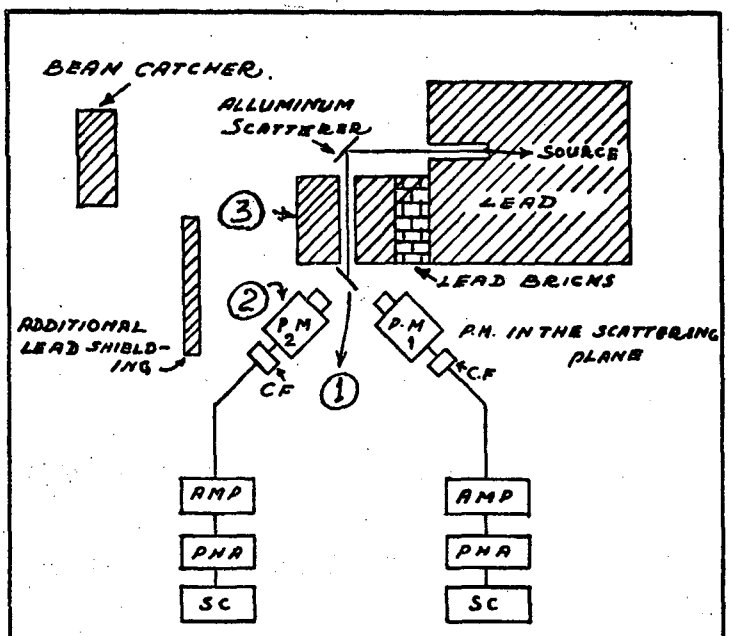

1. LEAD SCATTERER
2. P.M.2 IN THE ORTHOGONAL PLANE
3. LEAD BLOCK WITH 1" CENTRAL HOLE.

FIG. 1. GEOMETRICAL ARRANGEMENT AND BLOCK DIAGRAM OF THE EXPERIMENTAL SET-UP.

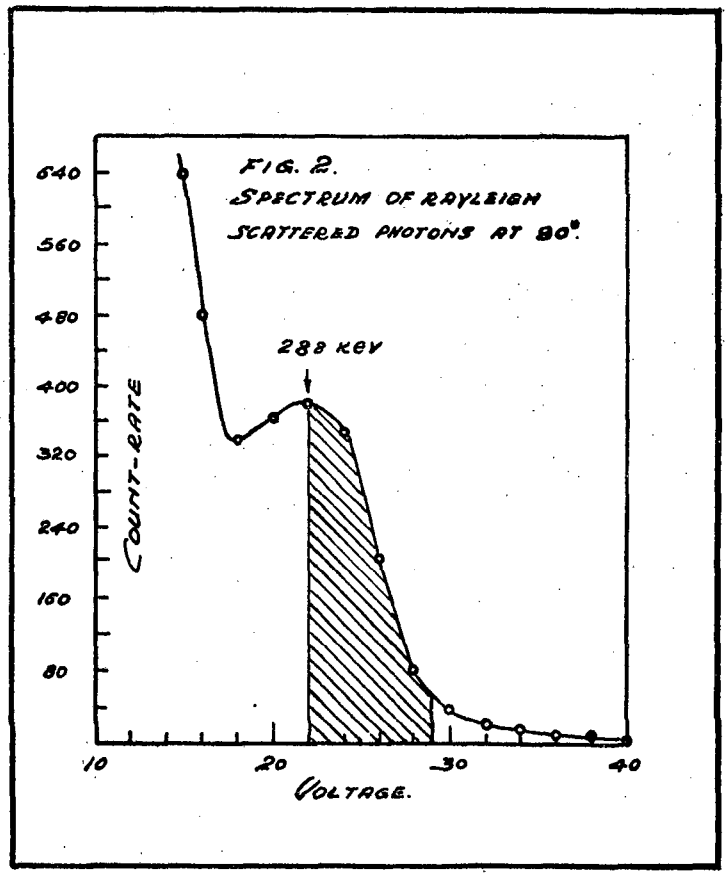

FIG. 2. SPECTRUM OF RAYLEIGH SCATTERED PHOTONS AT 80°.

are further collimated and made incident on a hollow lead cylindrical target of wall thickness 1 mm. The Rayleigh scattered photon beams are detected by two NaI(Tl) crystals placed in the scattering and orthogonal planes. Initially the two counters are adjusted to minimise the intrinsic asymmetry using a ^{203}Hg source in target position.

The scattered spectrum of photons recorded in the scintillation counter placed in the scattering plane at $\Theta = 90^{\circ}$ is shown in Fig. 2. It shows a broad peak at 290 keV, the low energy side of which increases steeply. This spectrum contains 4 types of events - : elastic-elastic, elastic-inelastic, inelastic-elastic and inelastic-inelastic types. The magnitudes of these events are in increasing order and in the ratios 10^{-10}: 10^{-3}; 1 : 32 for the present case (90°-90° scattering). Thus the effect of the first two types of events could be neglected. The high energy part of the recorded spectrum (shaded area in Fig. 2.) is accepted in the channel to minimise the interference of type 4 events. Auxiliary experiments are conducted to asses the role of background and target holder effects. The asymmetry ratios are obtained by collecting a minimum of about 10,000 true counts in the counter placed in the orthogonal plane (except in the case of 105° scattering for which 4,000 counts are collected). The experiments are conducted at 45°, 60°, 75°, 90°, and 105°. The resulting asymmetry ratios are shown in Table I.

Table I

Values of Asymmetry Ratios

S.No.	Scattering angle	Experimental values	Theoretial Values Franz	Brown et.al.
1.	45°	1.50 ± 0.02	1.48	1.56
2.	60°	2.17 ± 0.04	2.06	2.26
3.	75°	2.99 ± 0.07	3.04	3.13
4.	90°	3.36 ± 0.11	3.73	3.55
5.	105°	2.15 ± 0.21	3.04	2.44
1.	45°	1.41 ± 0.02	1.40	1.46
2.	60°	1.91 ± 0.03	1.85	1.99
3.	75°	2.48 ± 0.06	2.55	2.60
4.	90°	2.63 ± 0.09	2.99	2.79
5.	105°	1.76 ± 0.13	2.55	2.00

The first part of the table refers to the data at primary scattering anlge of 90° (ξ = 0.58) while the second part refers to the scattering angle 60° (ξ = 0.50). The theoretical values included in the table are obtained in a manner similar to that of Brini et. al. It can be seen from the table that the present experimental values for scattering anlges 60°, 90° and 105° support the theoretical values of Brown et. al. At other angles however the differences between the theoretical values themselves are small.

REFERENCES:

1. Franz W., Z. Physik 95, 652 (1935) ibid. 98, 314 (1936)

2. Brown et. al., Proc. Phys. Soc. (London) 242A, 89 (1957) and other references mentioned therein

3. Brini et. al., Nuovo Cimento 7, 877 (1958) ibid. 11, 533 (1959)

AN EXPIRICAL FORMULA FOR COHERENT SCATTERING OF GAMMA RAYS.

A. Nath and A.M.Ghose
Nuclear Physics Laboratory,
Bose Institute,
Calcutta.

ABSTRACT.

An empirical formula for the differential coherent scattering cross sections of gamma rays of various energies and Z of the scatterers applicable for momentum transfers upto several m c will be presented. Comparison will be made with the experimental data available in this field.

DETERMINATION OF K-SHELL PHOTOELECTRIC CROSS-SECTIONS FOR ^{60}Co GAMMA RAYS

B.S. Ghumman, S. Anand and B.S. Sood
Punjabi University, Patiala

ABSTRACT.

The technique of absolute intensity measurements of the K-shell fluorescent radiation that follow the photoelectric interaction has been further employed to measure the photoelectric cross-sections for ^{60}Co gamma rays. The efficiency of 1" x 1" NaI(Tl) detector used in the experiment has been dtermined experimentally from the β-X coincidence measurements using a ^{198}Au source and its value agrees well with that obtained from the correction factors of iodine escape peak, absorption in the air and absorption in the crystal container. The cross-sections obtained are 3.9 $\pm$ 0.5, 3.3 $\pm$ 0.5 and 2.7 $\pm$ 0.4 barns respectively for lead, gold and tungsten which show a good agreement with the available data within the range of experimental uncertainty.

ISOMERIC CROSS-SECTION RATIO FOR (n,γ)REACTION AT 24 KEV

A.K. Chaubey and M.L. Sehgal
Department of Physics
Aligarh Muslim University, Aligarh, India

I. INTRODUCTION:

The isomeric cross-section ratio has been studied by a number of authors (1,7). The isomeric cross-section ratios have been used to have an idea about nuclear level density parameter σ. The earlier reported work (1,7) gives the information about σ mostly at thermal energies. Obviously any other information about σ at higher energies will be very important. The aim of the present measurement was to determine the energy dependence of σ.

CALCULATION OF ISOMERIC CROSS-SECTION RATIO:

The isomeric cross-section ratio (defined as σ_h/σ_T, where σ_h and σ_T are the cross-sections for the population of isomeric and for both the states respectively) for isomeric pairs produced by (n, γ) reaction is calculated in two main parts following the method of Huizenga and Vandenbosch (1,2). The first part includes the formation of the compound nucleus having different values of J, the total spin of the compound nucleus, and second the computation of the spin distribution following gamma ray emission. The method of calculation of isomeric cross-section ratios was same as given in reference (7). In this method of isomeric cross-section ratio calculation, the number of gamma rays, $\bar{\nu}$,

emitted in the process of compound nucleus de-excitation, and the parameter σ , are variable. If one of these two parameters is known the other can be calculated, by comparing the experimentally measured value of the isomeric cross-section ratio with theoretically computed value. The average number of gamma ray (multiplicity, $\bar{\nu}$) in the de-excitation process can be evaluated from the relation (8)

$$\bar{\nu} = \sqrt{a E_0}/2 \qquad (1)$$

where E_0 is the excitation energy of the compound nucleus and a is the level density parameter which gives the dependence of level density on the atomic weight A. Therefore knowing the value of $\bar{\nu}$, σ can be calculated.

RESULTS AND DISCUSSION:

Table I shows the isomeric cross-section ratio for all the cases reported in earlier papers (9,10). Table I also shows the cross-section ratio at thermal energies for all the above cases and at 1 MeV for some cases taken from other papers (4-7, 11-14). From this table it is clear that σ increases with the increases in incident neutron energy. This is so because as neutron energy increases, higher value of angular momentum starts taking part and these will populate higher spin states more.

In Table II the values of E_0 and a are given which were taken from reference (15). The value of σ which gives the cal-

culated value of σ_h/σ_T equal to the experimental value of σ_h/σ_T for given value of $\bar{\nu}$ are also listed in same table. In the case of 68-Zn, 76-Ge, and 130-Te the values of E_0 and a are not given. For 68-Zn the value of σ is given for two values of multiplicity. In 76-Ge if $\bar{\nu}$ is taken 2 them σ comes out to be 4 and if $\bar{\nu}$ is taken as 3 then the upper limit of σ comes out to be 2. If $\bar{\nu}$ is further increased σ will decrease. In 130-Te if $\bar{\nu}$ is taken 5 as is the value in the neighbouring nuclei then the value of comes out to be equal to 5. If lower values of $\bar{\nu}$ are taken then these will further increase the value of σ, when $\bar{\nu}$ is taken 6 the lower limit of σ shifts to 4. In general it is seen that in all the above cases σ lies in the range 3 $\pm$ 1.

In the case of 79-Br the value of level density parameter was also computed at various energies of neutron lying in between 0-3 MeV. The experimental values of isomeric cross-section ratios (σ_h/σ_T) were taken from the results of Bacso et al (7) and Johnsurd et al (12). An error of 15% was taken in the results of Johnsurd et al. Using the method (7) as described previously the cross-section ratios were calculated. From relation (1) it is seen that at thermal energies $\bar{\nu}$ = 4.79 and at 3 MeV $\bar{\nu}$ = 5.76, but we have taken $\bar{\nu}$ = 5 at all the excitation energies upto 3 MeV and have calculated the value of σ. The value of σ versus energy is shown in fig. 1. It is seen that as energy increases σ also increases slowly. At 2.6 MeV we have also calculated the value of σ taking ν = 6, which is equal to $3.5 \pm {}^{0.8}_{0.5}$ and is very near to

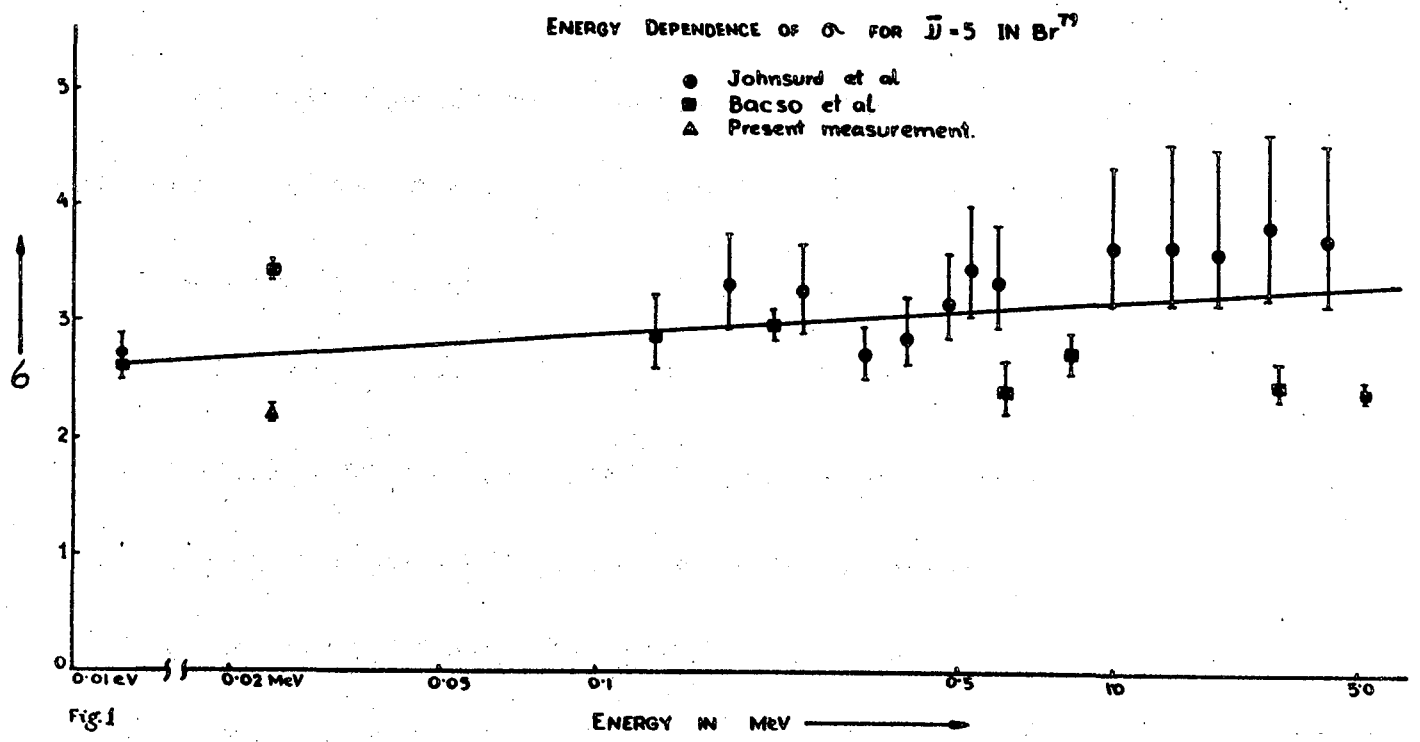
ENERGY DEPENDENCE OF σ FOR ν̄ = 5 IN Br79
Johnsurd et al
Bacso et al
Present measurement.
6
0
1
2
3
4
5
0·01 eV
0·02 MeV
0·05
0·1
0·5
1·0
5·0
ENERGY IN MeV

Fig. 1

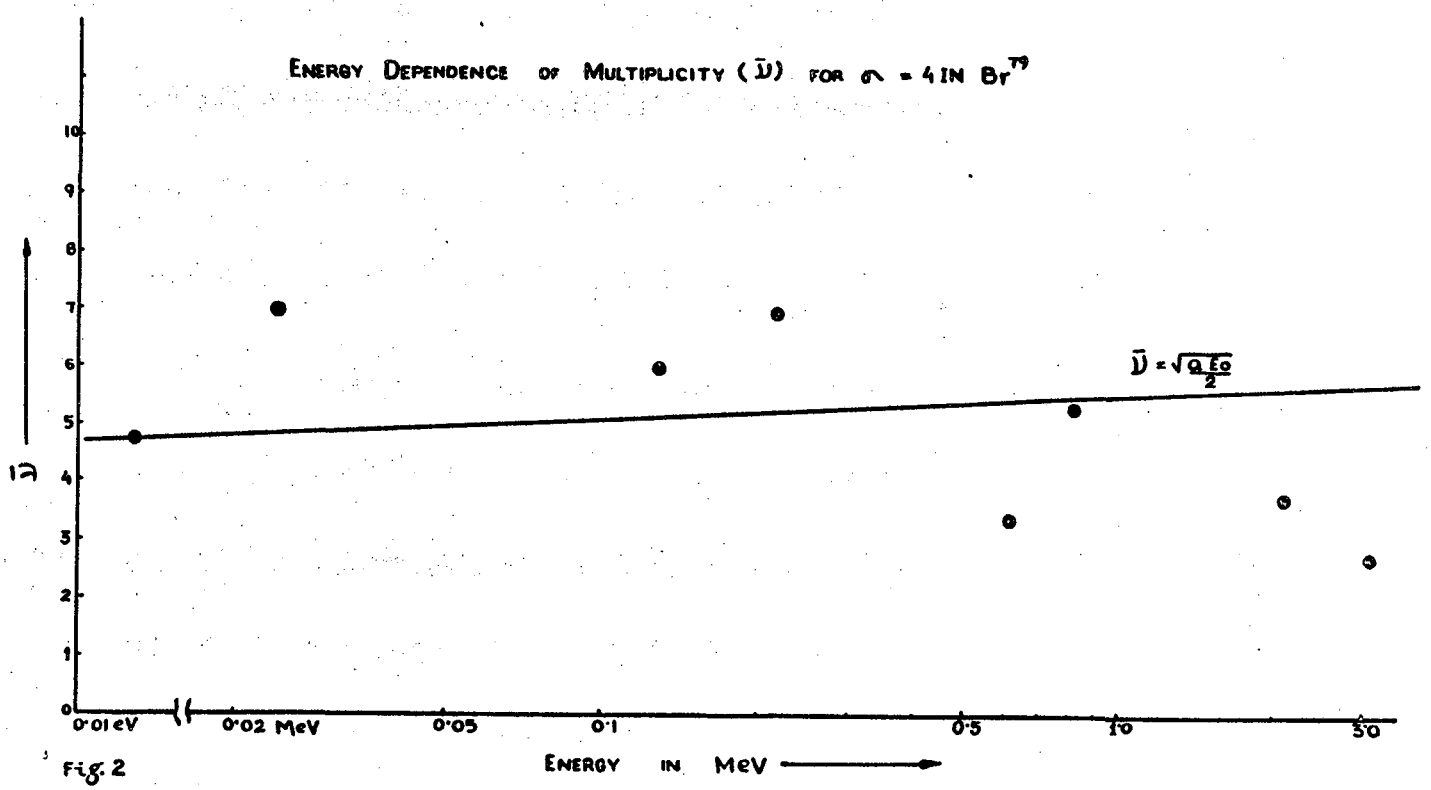
ENERGY DEPENDENCE OF MULTIPLICITY (ν̄) FOR σ = 4 IN Br79
ν̄ = √(aE₀/2)
12
0
1
2
3
4
5
6
7
8
9
10
0·01 eV
0·02 MeV
0·05
0·1
0·5
1·0
5·0
ENERGY IN MeV

Fig. 2

the value for $\bar{\nu} = 5$.

While calculating the isomeric cross-section ratio the values of transmission coefficients were taken from the tables of Moldauer (16). The contribution of ℓ = 2 neutrons was taken into account from 24 keV to 350 keV and at higher energies T_ℓ values upto ℓ = 4 were used. Bacso et al ( ) have also calculated the values of σ at different energies. Using their experimental values for σ_n/σ_T we have also calculated the value of σ which is different from their value. The main reason of this is probably that they have taken old values of transmission coefficients. Also they have not mentioned upto what value of ℓ they have taken into account.

Bacso et al have calculated the value of σ from the expression:

$$\sigma^2 = 8.89 \times 10^{-2}\, a T A^{2/3} \qquad (2)$$

In this expression a is the same parameter as defined previously and T is the temperature of the residual nucleus. The value of σ for 79-Br from the above expression comes out to be 4 as calculated by Bacso et al. Taking this value of σ we have seen the energy dependence of multiplicity, from their graphs. In fig. 2 is plotted the multiplicity versus energy for σ = 4 obtained from the results of Bacso et al. The line shown in the same figure represents the line from eq. (2). From figure it is clear that at

Table I.

A comparison of isomeric cross-section ratios at different energies

Target	Spin	Spin of isomeric levels	Half life of levels		σ high / σ total (σ_h/σ_T) Thermal energies	24 keV	1 MeV
68-Zn	0	$9/2^+$	13.9	h	0.09 ± 0.01[4]	0.185 ± 0.04[10]	0.652[13]
		$1/2^-$	52	m			
76-Ge	0	$1/2^-$	59	s	0.23 ± 0.02[11]	0.181 ± 0.04*	
		$7/2^+$	11.3	h			
80-Se	0	$7/2^+$	57	m	0.17 ± 0.02[4]	0.538 ± 0.14[10]	
		$1/2^-$	18	m			
79-Br	3/2	5^-	4.5	h	0.24 ± 0.02[4]	0.123 ± 0.013[10]	
		1^+	18	m		0.28 ± 0.01[7]	0.424±063[12]
103-RH	1/2	5^+	4.4	m	0.07 ± 0.007[6]	0.108 ± 0.05[10]	
		1^-	42	s		0.106[14]	0.137[13]
115-In	9/2	5^+	2.5 s and 54 m				
		1^-	13	s	0.74[13]	0.725 ± 0.744[13]	
130-Te	0	$11/2^-$	1.2	d	0.129[5]	0.234 ± 0.07*	
		$3/2^+$	25	m			

* Present measurements

Table II.

Level density parameter (σ) at 24 keV

Target	a (MeV^{-1})	E_0 (B + E) (MeV)	$\bar{\nu}$	σ
68-Zn			3	2.85 + 0.55 − 0.40
76-Ge			4	2.35 + 0.20 − 0.15
			2	4.0 + 3.0 − 1.8
			3	$<$ 2
80-Se	14.96	6.845	5	3.75 + 2.0 − 1.25
79-Br	13.77	6.672	5	2.22 + 0.07 − 0.05
103-Rh	15.69	6.814	5	2.5 ± 0.05
115-In	18.15	6.634	5	3.25 + 0.60 − 0.40
130-Te			5	$>$ 5
			6	3.8

thermal energies two values of the $\bar{\nu}$ are same while at higher energies the multiplicity starts decreasing. This means that the number of gamma rays emitted in the de-excitation of the compound nucleus decreases as the excitation energy increases. But it is not possible, when other channels are absent the number of gamma rays in the de-excitation process should not decrease. This means that if $\bar{\nu}$ decreases with energy either eq. (2) is wrong or the experimental results of Bacso et al are wrong. Similar type of calculations are in progress in 103-Rh and 115-In.

REFERENCES:

1. J.R. Huizenga and R. Vandenbosch Phys. Rev. 120, 1305 (1960)
2. R. Vandenbosch and J.R. Huizenga Phys. Rev. 120, 1313 (1960)
3. C.T. Bishop, ANI-6405 (1961)
4. B. Keisch, Phys. Rev. 129, 769 (1963)
5. M.L. Sehgal, Phys. Rev. 128, 761 (1962)
6. S.K. Mangal and P.S. Gill Nucl. Phys. 41, 372 (1963)
7. J. Bacso et al, Nucl. Phys. 67, 443 (1965)
8. L.V. Groshev et al, Proc. conf. on the peaceful uses of Atomic Energy Geneva, paper P/2029, 15, 138 (1958)
9. A.K. Chaubey and M.L. Sehgal Nucl. Phys. 66, 267 (1965)
10. A.K. Chaubey and M.L. Sehgal Phys. Rev. 152, 1055 (1966)

11. R.S. Iyer et al, Progress report on nuclear data activities in India III AEET-267 (1966)

12. A.E. Johnsurd et al Phys. Rev. 116, 927 (1959)

13. D.J. Hughes et al Phys. Rev. 91, 1423 (1953)

14. J. Csikai et al Nucl. Phys. 41, 316 (1963)

15. E. Erba et al Nuovo Cimento 22, 1237 (1961)

16. P.A. Modauer ANL-6323 (1961)

NANOSECOND LIFETIMES OF EXCITED STATES THROUGH NEUTRON INELASTIC SCATTERING WITH INTENSE PULSED BEAMS

N. NATH*, A.K.M. SIDDIQ** AND G. MURRAY
Nuclear Physics Division, AERE, Harwell.

Low intensities and background problems associated with neutron scattering greatly restricted its utility in the study of nuclear excited states. Recent availability of intense proton beams from the IBIS Van de Graaff at Harwell with pulse durations of $\leq$ 1 ns at repetition rate of 1 Mc/sec and 5-10 μA mean currents provides variable energy neutron pulsed-beams to facilitate such studies.

Figure 1 gives the experimental set-up for looking at the gamma rays that follow excitation of levels in a given sample by neutron inelastic scattering. Cylindrical samples could be suspended in from of a neutron producing target while an appropriately shielded scintillation detector coupled to a 56 AVP photomultiplier looked at the gamma rays as well as scattered neutrons reaching it mainly from the sample. Fast pulses from the photomultiplier were fed to the "Start" input of a TPH convertor whose "Stop" input was derived from a beam pick - up loop through a variable delay. The output of the convertor was observed in coincidence with a suitable gate on the gamma-ray energy spectrum derived from the slow linear output of the photomultiplier. It could be displayed on a multichannel analyzer.

* Present Address: Dept. of Physics, Banaras Hindu University, Varanasi (India)

* Present Address: Physics Dept., Dacca University, Dacca (E.Pakistan)

Figure 2 shows the time-spectrum observed with an iron sample when a 'gamma' gate was set on the first level of ^{56}Fe at 845 keV ('no sample' backgound contribution already subtracted). It indicates well-separated contributions in time due to gamma-rays following (n,n') reaction in ^{56}Fe and those produced in the scintillator on the arrival of scattered neutrons. The time distribution due to the former was observed to be symmetrical in accordance with fast lifetime of the 845 keV level. A measureable lifetime shall produce an exponential tail in this distribution. As a test of the method, measurements were made on the 582 keV first excited state in ^{25}Mg which is known to possess a half -life of 3.5 ns (1). Using a scattering sample of natural magnesium at 1 MeV neutron bombarding energy, only this state could be excited by inelastic scattering. Time spectrum as shown in Figure 3 was observed by setting a gate on the 582 keV photopeak. ('No sample' contribution already subtracted). Comparison was made using the same energy gate on the Compton distribution of the 845 keV transition from ^{56}Fe (n,n') reaction to obtain a prompt distribution. Time calibration was effected by observing the displacement of the prompt curve as a function of known variable nanoseconds delay. The mean lifetime of the 582 keV state in ^{25}Mg was then computed from the slope of the exponential part of the delayed distribution to be 4.9 $\pm$ 0.3 ns in agreement with the known value.

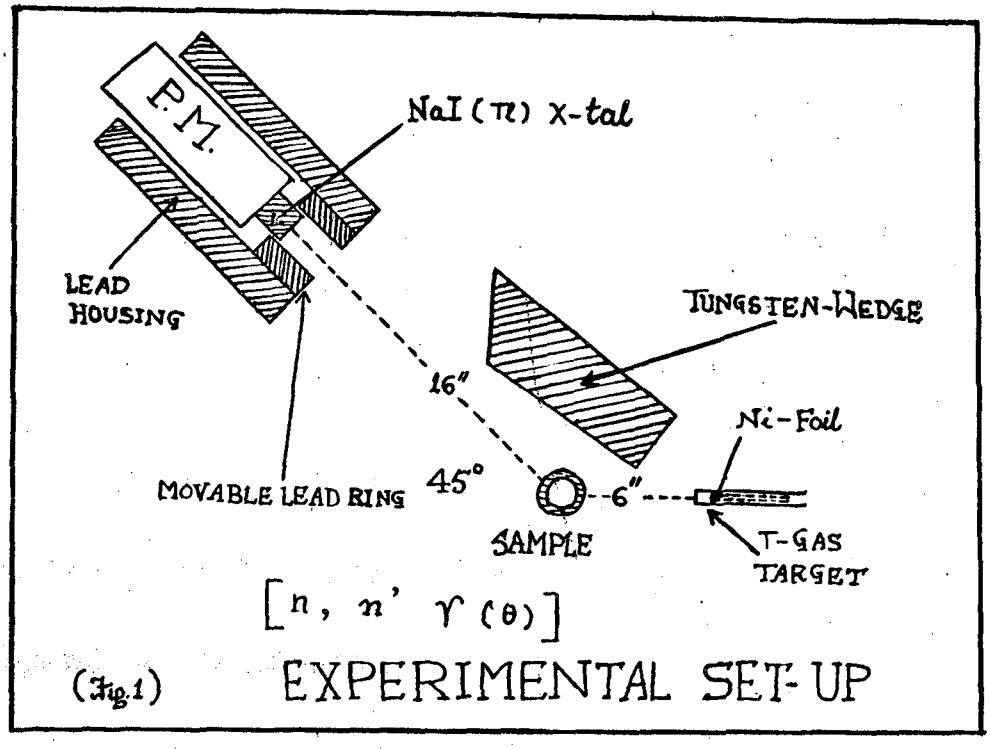

(Fig.1) EXPERIMENTAL SET-UP

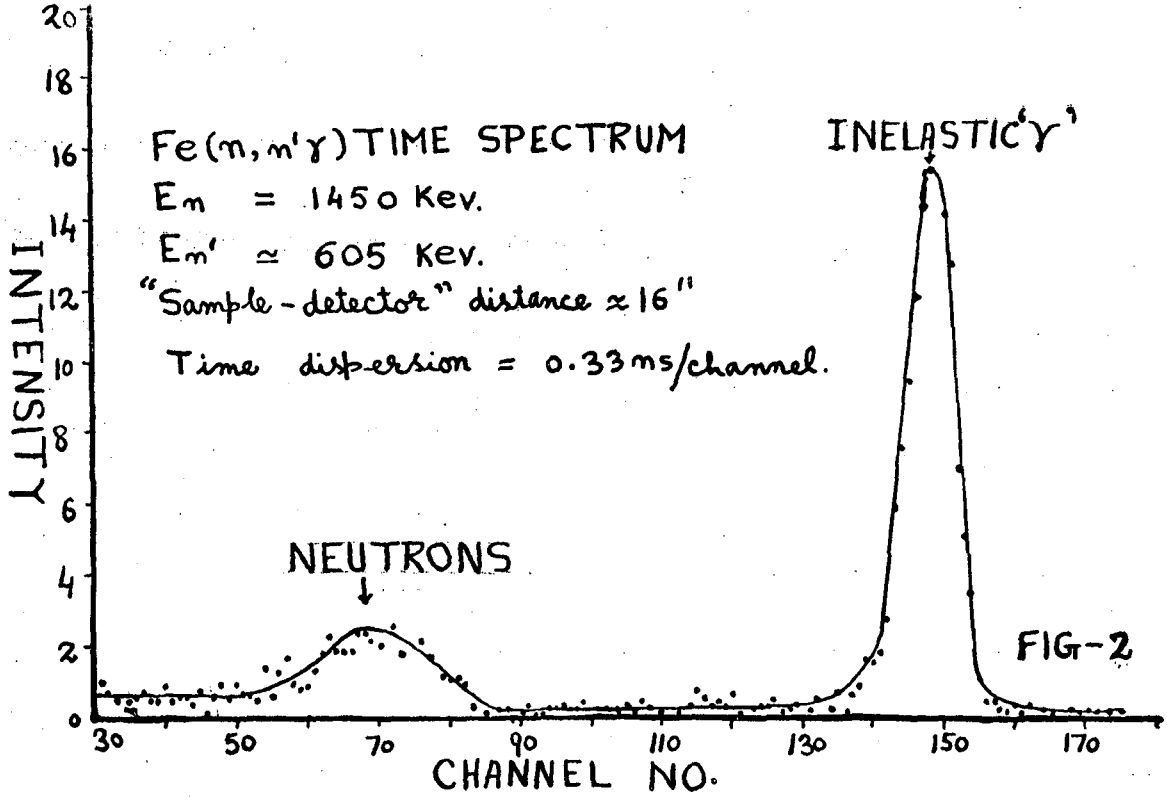

FIG-2

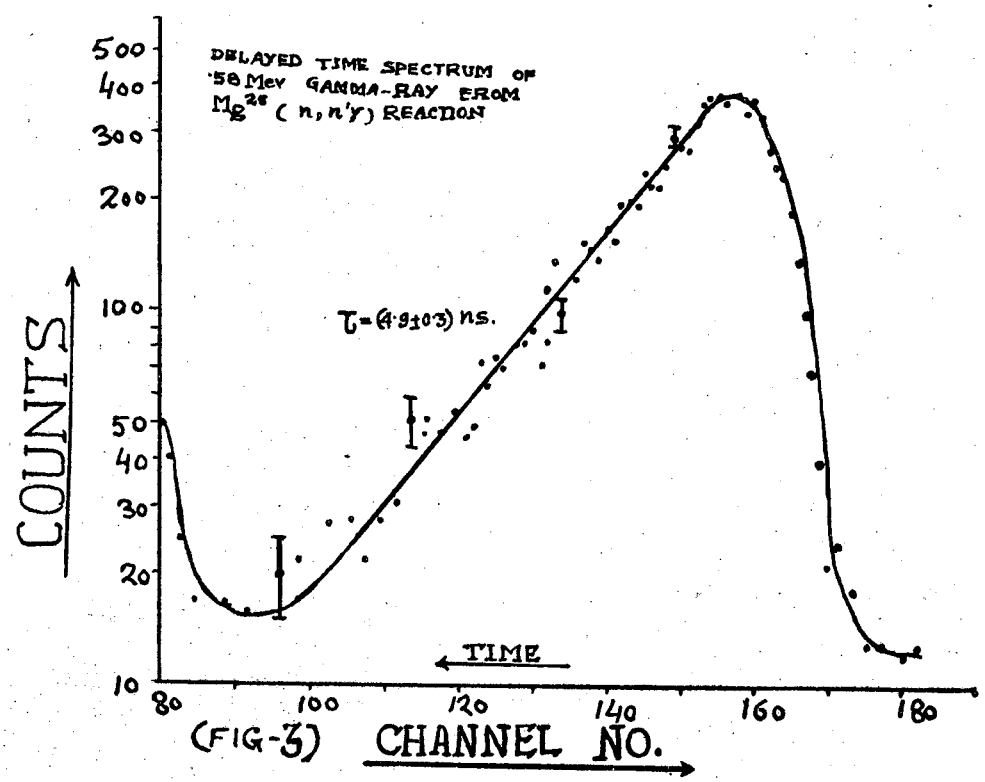
DELAYED TIME SPECTRUM OF
·58 Mev GAMMA-RAY FROM
Mg^{26} (n, n'γ) REACTION
τ = (4·9±0·3) ns.
COUNTS
500
400
300
200
100
50
40
30
20
10
80
100
120
140
160
180
TIME
CHANNEL NO.

(FIG-3)

The 1130 keV state in ^{121}Sb was attributed a half-life of (11 ± 2.5) ns (2). It was considered a good case to confirm using the technique mentioned here. A gamma ray of energy 1.12 MeV was first established as arising from the Sb(n,n') reaction in the time-gated gamma-ray spectrum obtained with a sample of natural antimony at neutron energy of about 1.35 MeV. A narrow gate was then set on its peak and the time distribution was looked for the predicted delayed nature. It was however observed to be prompt to the limit $\tau \leq 1.0$ ns in contradiction with the reported measurement.

REFERENCES:

1. Ferguson, Grace and Newton, Nuclear Physics 17, 1 (1960)
2. Bhattacharya R. and Shastry S., Nuclear Physics 41, 184 (1963)

DISCUSSION:

A.S. Divatia: What was the resolution for 1 MeV neutrons in keV or per cent?

N. Nath: Under the best conditions it could be as good as 1-2%.

S.S. Kapoor: What was the time resolution in your measurement?

N. Nath: Nearly 2.5 ns for the prompt γ ray peak. Considering that the time resolution here arises out of neutron energy spread, sample size as well as the detector, it was not much.

S.K. Gupta: I feel the gamma peak which you get in the time spectrum should be a sum of spurious gamma prompt peak plus a peak having a life time character? How do you eliminate the prompt peak contribution in your measurement?

N. Nath: The prompt contribution depends on the gamma-gate selection. In our experiment we could control neutron energy and thereby the excitation of states in the sample. In the case of ^{25}Mg we only excited the 582 keV state, the first excited states in ^{24}Mg and ^{26}Mg, the more abundant isotopes in our natural magnesium sample, were not excited. There could be prompt contributions if the (n,γ) reaction is significant in the sample as the contribution of such γ rays shall lie in the same time peak as obtained due to (n,n') γ-rays. This was negligible in our particular case. However, when we did the experiment with antimony, (n,γ) cross section was significant to cause prompt contributions but unfortunately the 1147 keV state de-excitation was also found to be prompt.

THIN CARBON FILMS FOR TARGET BACKINGS

S.S. Kerekatte, K.K. Sekharan and K.B. Nambiar
Bhabha Atomic Research Centre, Trombay

ABSTRACT.

Thin carbon films are useful as target backings in charged particle reactions involving fine energy resolution. Such films have been made in our laboratory in the following way. A layer of sodium chloride was evaporated on to glass slides in a vacuum chamber. The carbon films were then deposited on the sodium chloride layer by evaporation from an electric arc struck between two carbon electrodes. The films were floated off in water and picked up on suitable frames.

The thickness of a carbon film was measured as follows. Five MeV alpha particles from the accelerator were scattered from a carbon film. A spectrum of the elastically scattered alpha particles at 150° and of 1.37 MeV energy, was taken with an without the sample carbon film in the path of the scattered beam. The energy lost by the alphas in passing through the film, was given by the shift in the spectrum, and was found to be 17.6 keV with an error of 1.3%. However, when the energy loss was converted to $\mu gm/cm^2$, an error of 20% was introduced due to errors in the published tables of atomic stopping cross-sections. The thickness of the films was found to be $10 \pm 2\ \mu gm/cm^2$.

A SIMPLE NEW DEVICE FOR A MOSSBAUER SPECTROMETER

P.K. Iyengar and P.S. Parvathanathan
Bhabha Atomic Research Centre, Trombay

One of the vital parts of a Mossbauer spectrometer is the modulator that provides a means of shifting the energy of a nuclear gamma ray by a precisely controlled amount, making it possible to examine a region in the vicinity of the nuclear transition energy.

In principle the energy shift is introduced by a Doppler shift in the frequency of the gamma ray as observed by the absorber nucleus given by the relation

$$\nu' = \nu \left[1 - \frac{v}{c} \cos\theta \right]$$

where ν is the frequency of the emitted radiation, v is the velocity of the absorbing nucleus, and θ the angle w.r.t. the incident gamma ray. This is illustrated in Fig. 1. Many of the existing methods of Mossbauer spectroscopy use a continuous variation in the Doppler velociety v ignoring the angular factor θ. It occurred to the first author that this angular factor could be advantageously varied keeping v constant.

Confining oneself to uniform circular motion, the component of velocity of a particle executing uniform circular motion along a direction as shown in Fig.1 is

$$v\cos\theta = r\omega\cos\theta = \omega x$$

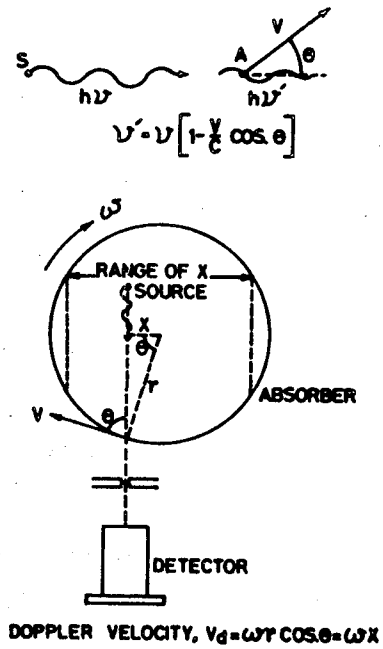

FIG. 1

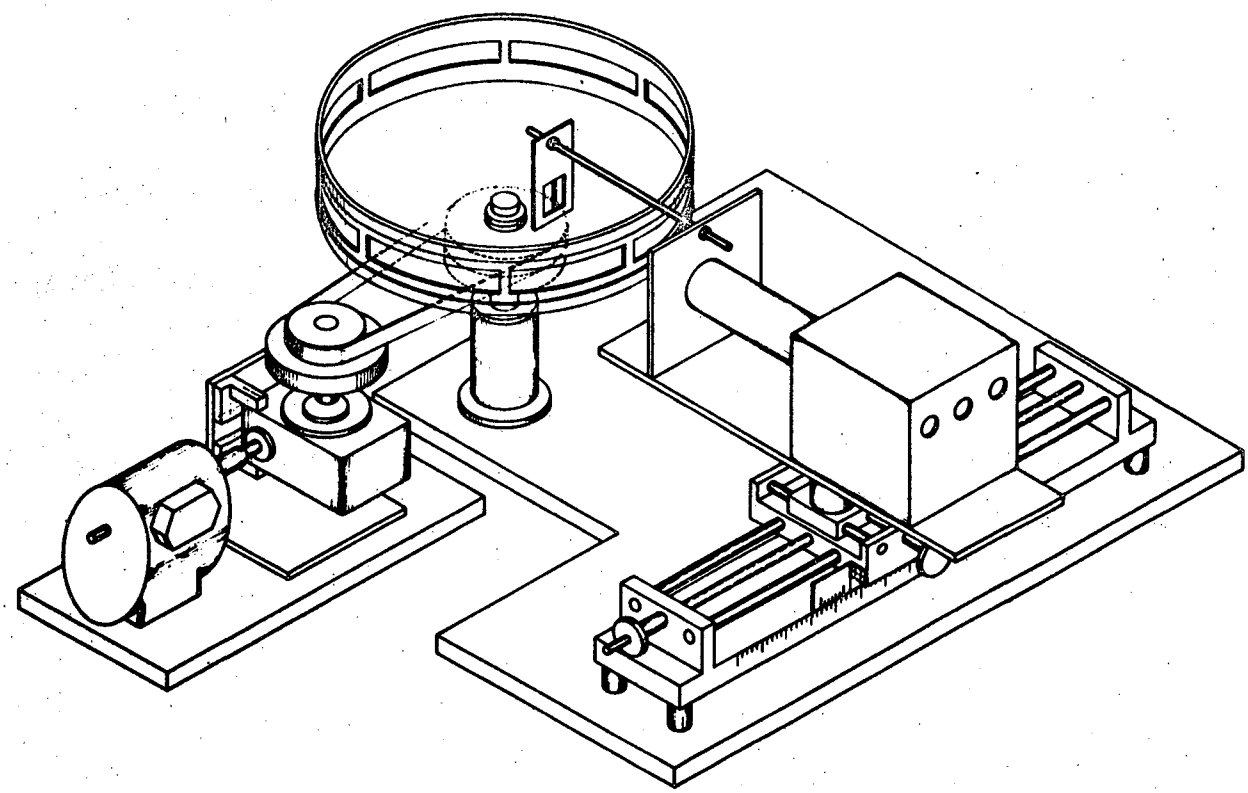

MÖSSBAUER SPECTROMETER

FIG. 2

Thus if the gamma rays are observed along parallel directions displaced from the centre of rotation by equal increments in x, the absorber will present different Doppler velocities as a function of x. For a typical value of $\omega = 0.1$ roughly corresponding to a rotation speed of 1 r.p.m. and X ranging from 0 to 20 cms, Doppler velocities in the range 0 to 20 mm/sec are obtained. This is quite an interesting range for the study of hyperfine strucutre effects. It is easily possible to change ω to cover different Doppler velocity ranges.

Fig.2 illustrates the experimental set up: a fractional horse power induction motor is geared down to provide a rotational speed of about 1 r.p.m. It is connected by an endless belt to the main rotating shaft. The absorber is struck to a circular frame. The detector consisting of 1 mm NaI(Tl) scintillator coupled to a photomultiplier is carried on a lead screw arrangement such that it could be made to traverse in the desired direction. The source is rigidly attached to this carriage as shown. The recording device is a conventional gamma ray spectrometer using automatic time control. A typical measurement using a 200 microcurie ^{57}Co on stainless steel source and on thou thick stainless steel absorber is shown in Fig.3.

The method is perhaps extremely simple. It could be easily automated by just coupling a motor drive to the detector lead screw and controlling its position in steps. One main advantage arises from the fact that the speed of the motor

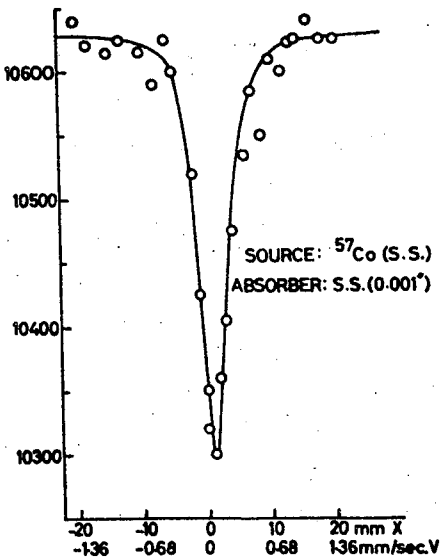

X : DISTANCE OF THE SOURCE DETECTOR SYSTEM FROM THE CENTRE OF ROTATION.
V : THE RELATIVE VELOCITY OF THE ABSORBER w.r.t. SOURCE.

FIG. 3

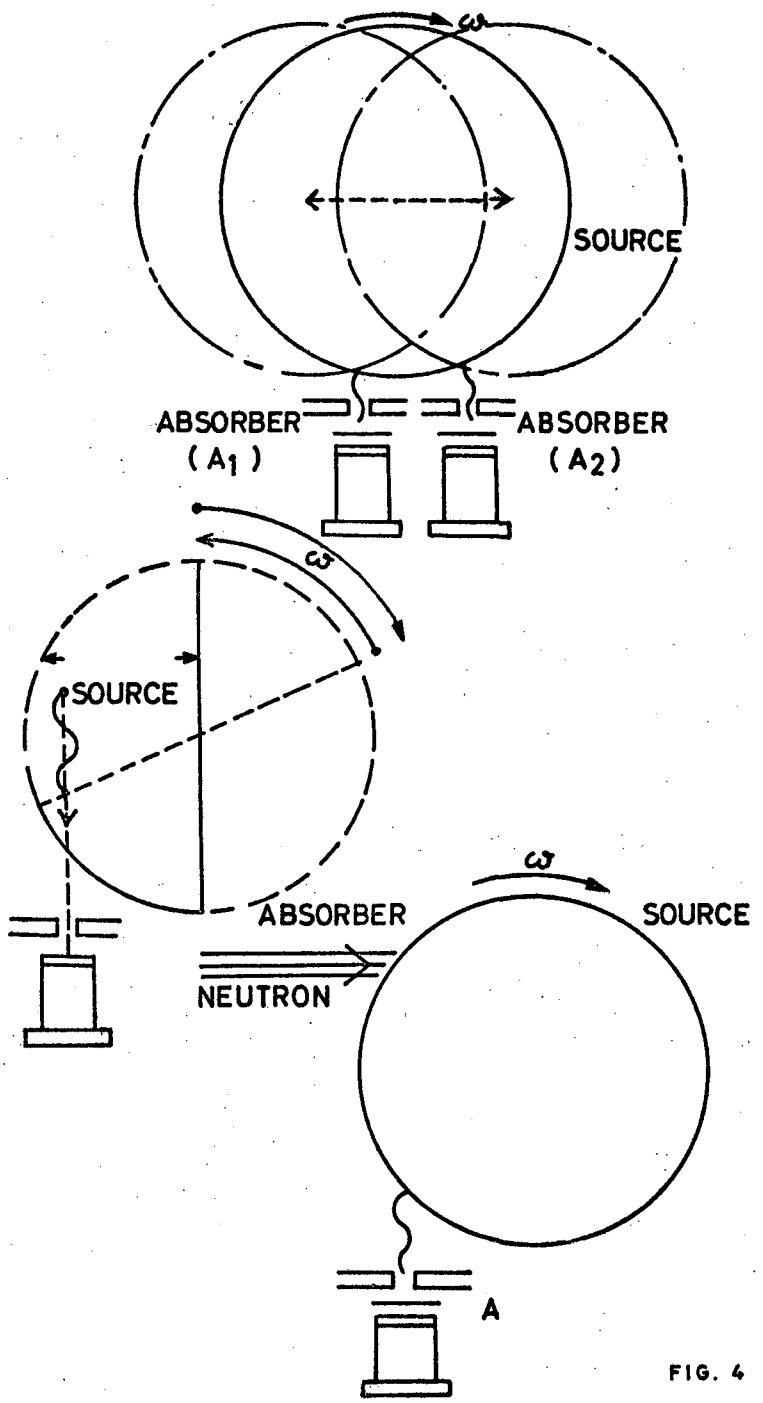

FIG. 4

does not have to be varied as in the case of cam devices and in principle, a uniform circular motion is very much easier to obtain than a complicated motion cam device needs to generate.

The only limitation to this device is the fact that a long piece of absorber is being used around the circumference of the 15 cm radius circle. It is possible to overcome this by several means. A few adaptations of this principle are shown in the Fig.4. The source can be coated on the periphery of the revolving frame. It is then possible to do several experiments using the same source and several absorbers simultaneously. The absorber and the photomultiplier are together moved to different positions enabling different Doppler shifts or the centre of rotation of the source can be displaced. However, to avoid the limitation that a fairly large source is required, it is possible to coat the source over a short length of the periphery and use the oscillation mode.

The method has also quite interesting applications when used in conjunction with Mossbauer nuclei which are being continuously produced through either a neutron beam or charged particle beam. In the case of neutron beam, some of the short lived nuclei could be explored for any possible Mossbauer resonances.

DICUSSION:

V.S. Indurkar: (1) Is there any feed back employed to obtain the compensation for the instantaneous changes in velocity e.g. these due to the supply variations? (2) In the oscillatory motion does there exist any nonlinearity of motion in the peak amplitude positions, where it changes the direction?

P.K. Iyengar: (1) We use an induction motor operating on line frequency and has proved satisfactory. (2) When used, in the oscillatory mode, the counting will be gated such that the end effects are eliminated.

V.G. Bhide: Since the absorber will be all round the circumference, the thickness will not be uniform and this will cause line broadening.

P.K. Iyengar: The effect of non-uniformity in the thickness of the foil is the same for all positions, since the counts are accumulated on several rotations for each value of χ. There is of course a known variation in thickness as a function of χ. However, if the source is coated on the rotating drum this method is in no way different from other methods in that small samples could be used.

A STUDY OF THE METHOD OF SEPARATION OF ISOTOPES USING TIME-OF-FLIGHT PRINCIPLE

J.V. Ramana and M.P. Navalkar
Bhabha Atomic Research Centre, Trombay

INTRODUCTION:

The conventional method of separation and detection of isotopes is by observing its trajectories in a combination of electrostatic and electromagnetic fields. A method which measures charge-to-mass ratio of an ion by its transit time was first used by Wilson (1) and later by Glenn (2) and Michel (3). An instrument based on this principle is constructed and some of its features are reported in this paper.

In conventional electromagnetic machines, for good resolution the transmission rarely exceeds 2 per-cent of the ions formed. The time-of-flight method offers reasonably good resolution combined with increased transmission of about 20 per-cent. This gain in transmission is of great importance, added advantages being its physical simplicity and the ease with which it can be decontaminated while working with radio-active samples.

PRINCIPLE OF OPERATION:

A block-diagram of the apparatus is shown in Fig. 1. Positive ions from the sample are formed at the thermal source S(4) and are accelerated to the first buncher grid G_1. Ion source S, all the accelerator Plates A, and buncher grid G_1 are applied an additional saw -tooth voltage over and above D.C. acceleration

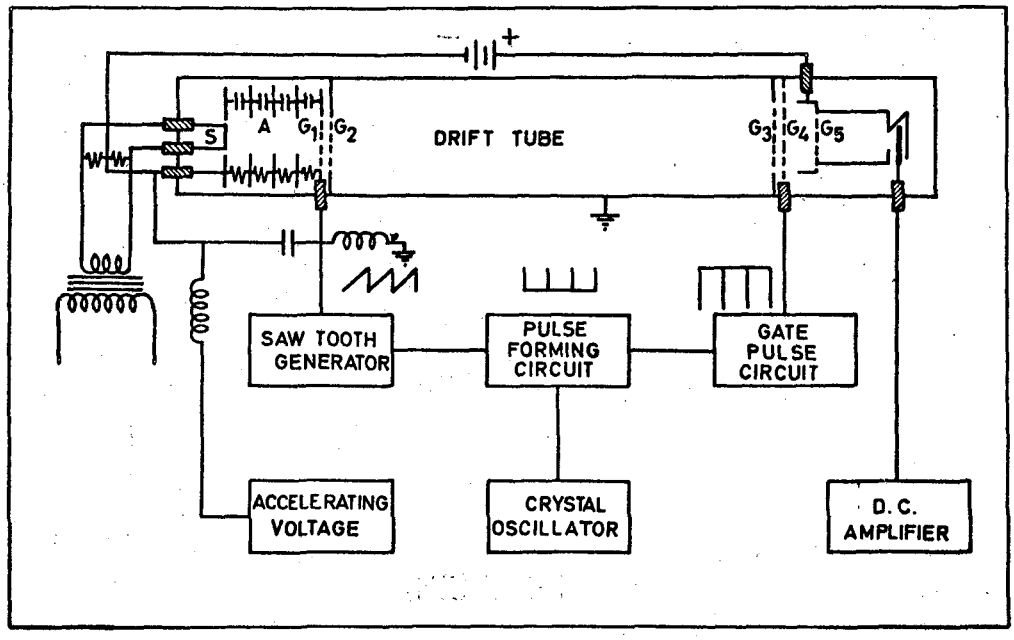

FIG. 1 BLOCK DIAGRAM OF THE APPARATUS

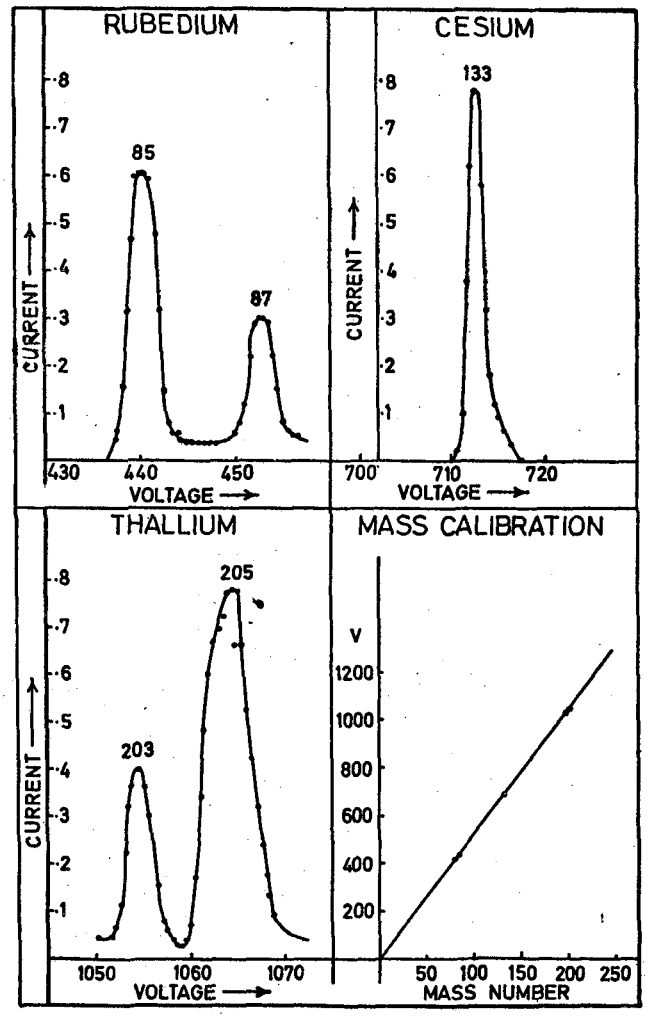

FIGURE-2

voltage. As ions cross between buncher grids G_1-G_2, they receive an additional acceleration voltage varying linearly with time. The ions then enter drift tube. Those that leave the buncher in the early part of the saw-tooth cycle have lower velocity and those arriving later in the cycle receive additional acceleration enabling them to overtake ions which have passed earlier in the cycle. Thus all ionsof a given mass bunch down the drift tube. A theoritical analysis of Ion Bunching has been given by Dutt (). The conditions for bunching is such that not only the desired mass but adjacent masses will also be bunched. It will be noted that the time of arrival of ion bunch will be proportional to the square root of mass of ion. As shown in Fig.1, repeller grid G_5 is placed at a positive potential above the maximum value of accelerating voltage plus bunching voltage. Hence no ions pass through G_5 unless they acquire an additional energy greater than that due to repelling potential. As ions pass between G_3-G_4, coincident with the arrival of the desired bunch of ions, a sharp negative pulse is applied to accelerate the ions. Those ions which have been accelerated during this pulse duration can now pass through G_5 and get collected on a collector plate. The resulting current is measured on a D.C. amplifier. The ions of undesired mass which do not receive accelerating pulse are repelled back the drift-tube by G_5 and eventually discharged on the walls.

CONSTRUCTIONAL DETAILS:

The fundamental choice in the design of this instrument is the size of drift tube which has been chosen as 60 cms length and 10 cms diameter. Inner side of the drift tube is polished to

reduce the effect of coulomb force exerted on the beam by any stray charge collected on the walls. Ion source consists of a 1 cm wide tantallum ribbon mounted flush with accelerator assembly. Bunching grids are separated by 25 mils so that ion travel time between grids becomes a negligible fraction of saw-tooth cycle. Similarly gate-grids are separated by 20 mils. The grids are constructed of 2 mil wire, 8 mils apart would on a copper ring. Each grid will have a transparency of about 70 per cent. Since the ions must go through four grids, the total transparency of the system will be about 24 per cent. The transit time has been chosen as 40 times the saw-tooth period (0.455 u Sec) in order to similify bunching requirements. Accelerating voltage is about 1000 volts, sufficiently high so that thermal energy spread of ions is negligible.

RESULTS:

The sample is coated on the filament and its temperature raised by passing A.C. current. Accelerating and bunching voltages are optimised for proper bunching of ions as indicated on D.C. amplifier. Ion current intensities were measured as a function of accelerating voltage for Rubedium, Cesium, and Thallium and the results are shown in Fig. 2. As seen from the graph the resolution is about one mass unit. The areas under curves compare with natural abundances. A graph of mass versus acceleration voltage shows the linearity of mass scale calibration.

REFERENCES:

1. R.R. Wilson, United States Atomic Commission, Declassified Document AECD-3373 (May 1952)

2. W.E. Glenn, Ph.d. Thesis, University of California, Radiation Laboratory, Declassified UCRL - 1928 (January 1953).

3. M.C. Michel, Ph.D. Thesis, University of California, Radiation Laboratory, Unclassified Report UCRL -2267 (July 1953)

4. J.P. Blewett and E.J. Jones Phy. Rev. 50, 464 (1936)

5. P.K. Dutt, Nuclear Instrument and Methods 38 Vol. 10 (1961)

DISCUSSION:

S. Chatterjee: What is the order of magnitude of peak currents in Rubidium isotopes?

J.V. Ramana: Rubidium is very suitable for thermal ion source. We have gone to ion peak current of about 8×10^{-8} with a filament current of about 40 Amp.

P.K. Patwardhan: What is the drift in your D.C. amplifier?

J.V. Ramana: We do not expect any drift in D.C. amplifier as it is stabilised over a long time before the start of the experiment. There can be a drift due to variations in accelerating voltage which can be controlled to a high degree.

ON A METHOD FOR THE STUDY OF ANGULAR AND ENERGY DISTRIBUTION OF FISSION FRAGMENTS

L.R. Khare
Department of Physics
Indian Institute of Technology, Kanpur. U.P

Roy (1) and others (2,3) have studied the fission fragments using a gridded ionization chamber. Our chamber was designed on the same principle.

Since the analysis of photograps is both inaccurate and time-consuming, we use an electronic technique to determine all the parameters with good accuracy and good statistics in a shorter time.

When a gas like argon is ionized by radiation, there is a time-delay of the order of a few milli-secs between the collection of electrons and + ions. Also, since the projection of the range R of the fission fragment on the electric field is given by $p = R \cos\theta$ and since $P \propto T_c$, the time of collection of + ions and $R \propto h$, the height of the + ion pulse, therefore $\cos\theta = K (Tc/h)$. The value of constant K is determined by the maximum value of Tc/h, when $\theta = 0^\circ$.

We can differentially select a γ-ray coming parallel to the electric field and look at the coincident fission fragments.

The information required to determine the energies and the angles of emission θ and $(180-\theta)$ (See CRO picutre in figure1) are t_1, t_2, h and t_1', t_2', h' (t_1, t_1' are the time for the first + ion to reach the cathodes or the delay-times between the collect-

ion of electrons and + ions; t_2, t_2' are the times of collection of the + ions; h,h' are their pulse heights). However, since the fragments are emitted approximately in opposite directions, it was considered sufficient to determine only t_1, t_2, h and h'.

A γ-e coincidence pluse starts the first (time delay) counter and opens different gates (Fig. 1). The + ion pulse from gate 1 triggers a univibrator, a differentiator and a memory circuit. The Univibrator stops the counter No. 1 (time t_1) and starts the second (rise-time) counter, which is stopped by a sharp pulse from the differentiator occuring at the peak of the + ion pulse (time t_2). The 'memory' converts the pulse to a voltage level proportional to the peak of the pulse which is recorded on a digital voltmeter. When the scanner is triggered, the above information (t_1, t_2, h, h') is fed to a printer for automatic recording, after which a singnal is sent out by the scanner, which resets all equipment.

The pulse height was calibrated using (a) alphas of known energy from ^{235}U and other alpha-sources and (b) by plotting a double-humped yield curve of the fragments and identifying the peaks of the heavy and light fragments and the valley with the corresponding values of Fowler (2). Sums and ratios of the kinetic energies were determined, the latter giving the mass-ratio. Thus, yield curves of mass-ratio and total energy (or a graph of total energy Vs. mass-ratio) could be plotted (Fig.2) and their most probable values determined.

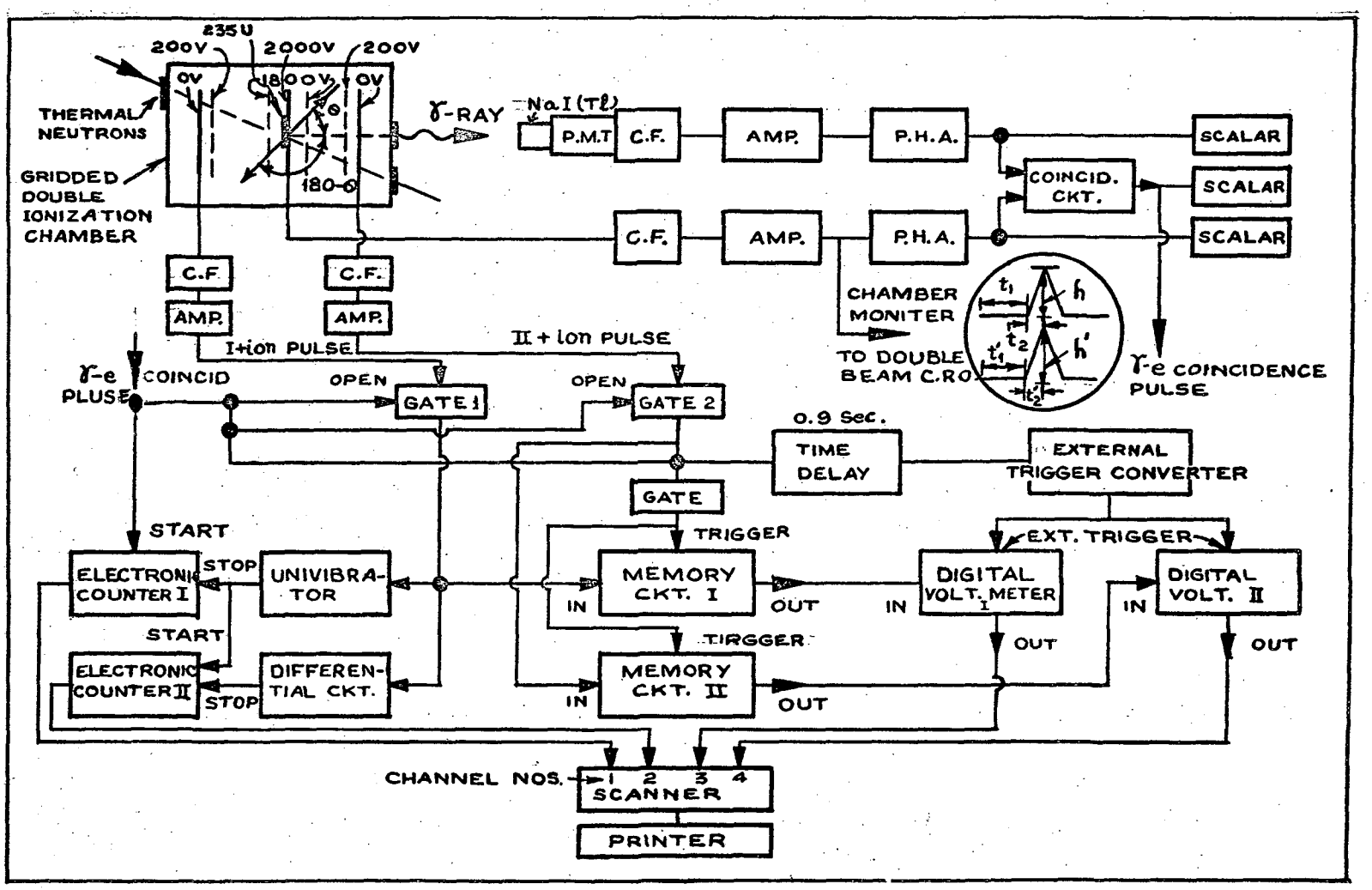
235U
200V
2000V
200V
0V
1800V
0V
THERMAL NEUTRONS
GRIDDED DOUBLE IONIZATION CHAMBER
180-θ
γ-RAY
NaI (Tl)
P.M.T
C.F.
AMP.
P.H.A.
COINCID. CKT.
SCALAR
SCALAR
SCALAR
C.F.
AMP.
P.H.A.
C.F.
AMP.
C.F.
AMP.
CHAMBER MONITER
TO DOUBLE BEAM C.RO
γ-e COINCIDENCE PULSE
I+ion PULSE
II + ion PULSE
γ-e PLUSE
COINCID
OPEN
GATE 1
OPEN
GATE 2
0.9 Sec.
TIME DELAY
EXTERNAL TRIGGER CONVERTER
GATE
TRIGGER
EXT. TRIGGER
START
ELECTRONIC COUNTER I
STOP
UNIVIBRA-TOR
MEMORY CKT. I
IN
OUT
DIGITAL VOLT. METER I
IN
DIGITAL VOLT. II
IN
OUT
OUT
START
TIRGGER
ELECTRONIC COUNTER II
STOP
DIFFEREN-TIAL CKT.
MEMORY CKT. II
IN
OUT
CHANNEL NOS.
1 2 3 4
SCANNER
PRINTER

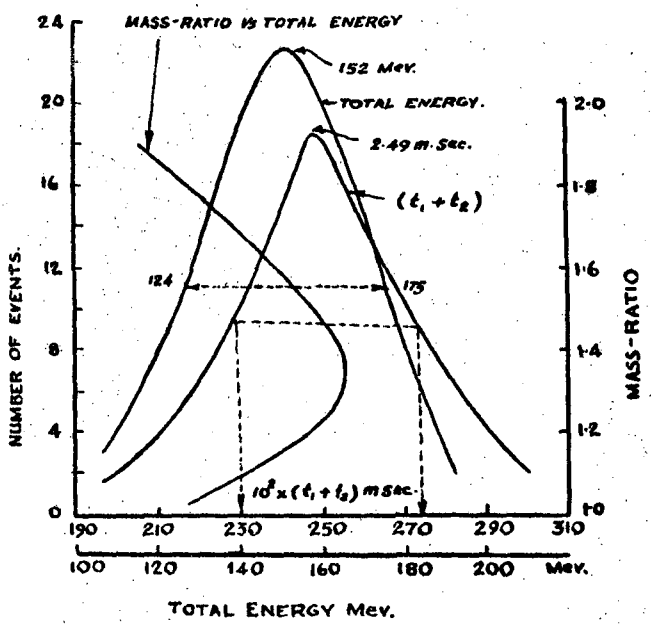
MASS-RATIO Vs TOTAL ENERGY
152 MeV.
TOTAL ENERGY.
2.49 m.sec.
$(t_1 + t_2)$
124
175
$10^3 \times (t_1 + t_2)$ m sec.
NUMBER OF EVENTS.
MASS-RATIO
TOTAL ENERGY Mev.
Mev.

FIG. 2.

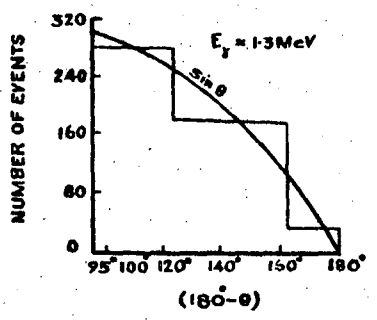
$E_\gamma \approx 1.3$ MeV
Sin θ
NUMBER OF EVENTS
(180°-θ)

FIG. 3.

Knowing the average number of neutrons emitted per fission and the sum and the ratio of masses, one can get the absolute values of fragment masses. Angular distribution graph (fig.3) is found to be isotropic.

Since the sum of $(t_1 + t_2)$ = a constant, so a Gaussian yield curve was plotted and only the data corresponding to the half-width limits were taken as the valid data (fig.2).

More information can be obtained by differentially selecting one fragment and looking at the integrally selected fragment on the other side coming in coincidence with it. One could measure angles in both the chambers by determining t_1, t_2 and t'_1m t'_2 and could use electron pulses in place of + ion pulses.

The method is also suitable for fast neutron fission and Photo-fission studies and for recording time-intervals (0.001 m.Sec.) and pulse heights (accuracy 0.2%). The scanner can handle information from 25 channels.

REFERENCES:

1. R.R. Roy, II International Conference on the peaceful uses of At.En. Geneva Vol. 15 (1958)

2. Fowler and Rosen, Phys.Rev. 72, 929 (1947).

3. Brunton, DC and Hanna, GC.- Canad. J. Res. 28A, 190 (1950)

DISCUSSION:

P.K. Patwardhan: What was time factor involved in data logging?

L.R. Khare: 5 coincidences/min.

S.S. Kapoor: What is the angular resolution obtained by this method?

L.R. Khare: Error in $\delta(\cos\theta) = .347$. So, $\delta\theta = 0.347/\sin\theta$.

V.S. Indurkar: What is the effect of the finite size of the source ^{235}U foil. What is the error introduced?

L.R. Khare: Error estimated from the yield curve of the total energy peak was 1.42%.

RANGE MEASUREMENTS OF FISSION FRAGMENTS IN THERMAL FISSION OF ^{235}U

R. Rangarajan, K.N. Iyengar and M.R. Hiranandani
Tata Institute of Fundamental Research,
Colaba, Bombay.

INTRODUCTION:

Ranges of fission fragments are usually studied either by radiochemical methods or using nuclear emulsions. Radiochemical studies of the various fragments in thermal fission of ^{235}U have been attempted by several workers (1). Experimental data are confined to the most probable groups of fission fragments (2).

This paper reports a work using "LEXAN" as a detector of the fission fragments (3). The method, as in the nuclear emulsion technique, suffers from the disadvantage of not being

able to identify either the fragment (mass, charge etc.) or its energy. The disadvantage is discounted by the easy handling and the lack of background in these "specific-ionisation-threshold" detectors. Here the ranges of the two fragments are found simultaneously by using a "sandwich technique". A mass-yield distribution is obtained by employing a general range-energy relationship for heavy ions and an iteration method.

EXPERIMENT:

A sandwich of natural uranium was prepared by pressing a drop of 10% uranium nitrate between two layers of Lexan joined together at one end. The layers which were held pressed between two perspex plates with screws were exposed to a beam of neutrons in the thermal column of CIRUS for about a day where the thermal neutron flux is about 3×10^7 n/cm^2/sec. After exposure the sandwich was washed in water and etched in a 6N solution of NaOH at 70°C for about 30 min. The fragment tracks were measured by viewing the sandwich under a magnification of about 1000 X. It was found that a drop of sandal wood oil between the layers kept the two surfaces in close contact. The introduction of commercially available dyes like "Nigrosine" enhanced the contrast characteristics. Greater accuracy in measurement was thus possible. The two surfaces of the sandwich were found to have a lateral displacement of between 5 and 40 microns. This did not affect the identification of

correlated tracks, since the correlation could be obtained by the similarity in direction. All range measurements were corrected for an error due to the etching - a factor connected with the dip of the track (3).

RESULTS:

The range distributions of the light and heavy groups as obtained by measurements of correlated fragments are shown in fig.1. It can be seen that the ranges of the light and heavy groups are well separated. The average ranges of the light and heavy groups obtained in Lexan with total statistics of 1000 are found to be $20.1 \pm 0.038\mu$ and $16.3 \pm 0.037\mu$ respectively.

DISCUSSION:

The assumption of a direct proportionality between range energy of a fragment has been used by Manley (4) to get the relation

$$R_L M_L = R_H M_H \qquad (1)$$

which is implied in assuming that the range ratio is a measure of the mass ratio. Lindhard et al (5) using a Thomas-Fermi model of the atom calculated theoretically a range-energy relationship for fission fragments. Aras et al (6) used these formulae in their measurements of fragment ranges and found that the energies thus obtained are true with minor variations for

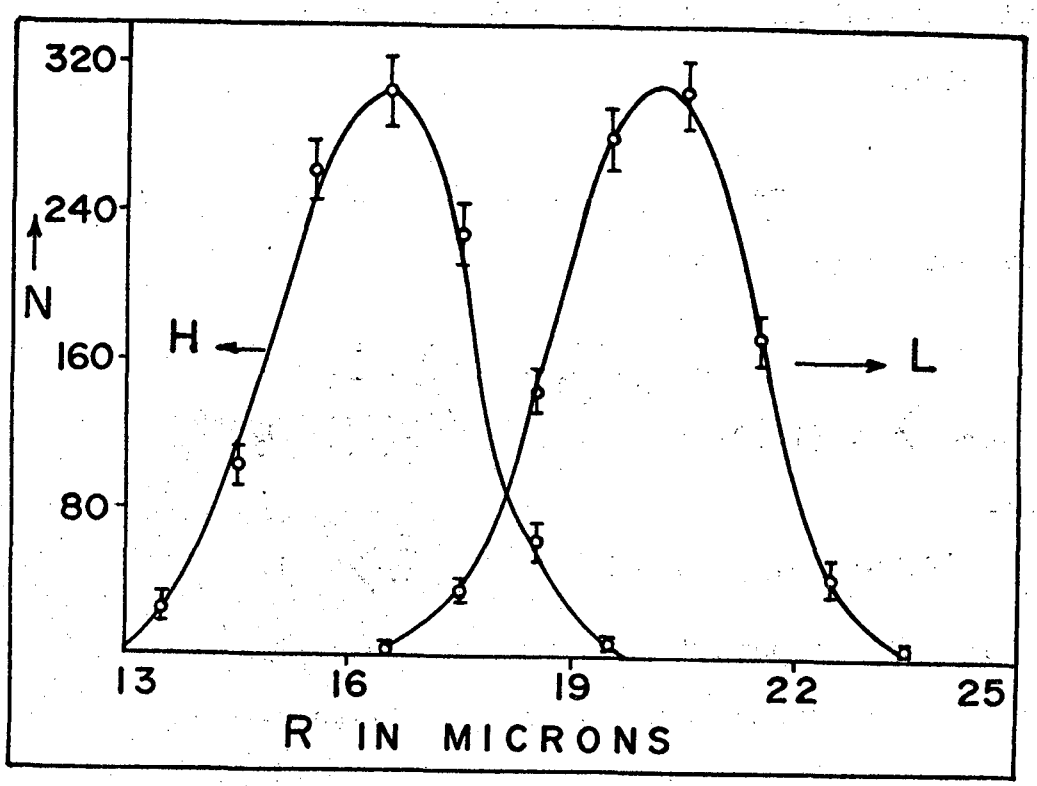
320
240
160
80
N
H
L
13
16
19
22
25
R IN MICRONS

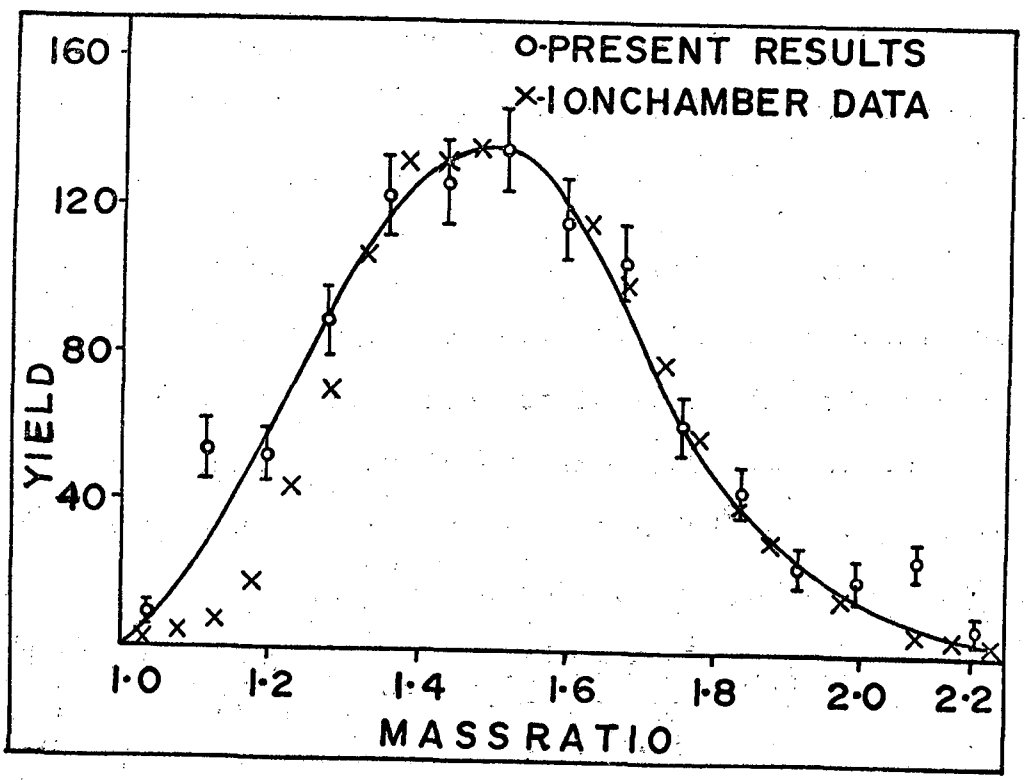
O-PRESENT RESULTS
X-IONCHAMBER DATA
160
120
80
40
YIELD
1·0
1·2
1·4
1·6
1·8
2·0
2·2
MASSRATIO

alumium but are not applicable in the varied form for air or uranium.

We have used a composite range-energy relationship given by Barkas (7) of the form

$$R = \frac{M}{Z^2} \quad (\lambda + B_Z) \tag{2}$$

where $\lambda \approx (11.01 + 1.34\ I_{adj}^{5/3}) \langle \frac{A}{Z} \rangle \beta^{10/3}$ g/cm^2 (2a)

and

$$B_Z \approx (48.0 + 5.3\ I_{adj}^{5/3}) \langle \frac{A}{Z} \rangle \times 10^{-5}\ Z^{5/3} \quad \text{g/cm}^2 \tag{2b}$$

where Z and beta the charge and velocity of the ion and $\langle \frac{A}{Z} \rangle$ refers to average mass to charge ratio of the stopping medium. To check the accuracy to which this relation held we calculated the range of protons of various energies in emulsion using a value of I_{adj} = 300 eV (8). We found about 25% discrepancy for 0.4 MeV protons and less than 9% for 1 MeV protons. Using the composition of Lexan as $H_{18}C_{16}O_3$ we determined I_{Lexan} to be 68.45 eV

From Eqn. (1) and constancy of total mass (233.5), an approximate value of mass was obtained. We assumed constant charge distribution equal to that of the fissioning nucleus $^{235}_{92}U$ i.e. 0.394. This was the starting point of iteration. Eqn. (2) together with the experimental range gave a value of β. New values of the mass given by

$$M_1 = \frac{\beta_2 \times 233.5}{\beta_1 + \beta_2} \quad \text{and} \quad M_2 = \frac{\beta_1 \times 233.5}{\beta_1 + \beta_2} \tag{3}$$

were used in Eqn. (2) for fresh values of β and so on. The iteration, written in FORTRAN for computer CDC 3600 was done thrice and the result thus obtained is shown in fig.2. It is seen to compare well with ionisation measurements (9).

FIGURE CAPTIONS:

Fig.1. Range-frequency plot of correlated tracks.

Fig.2. Plot of mass ratio vs. yield (See text)

REFERENCES:

1. J. Alexander, M.F. Gazdik, A.R. Trips and S. Wasif, Phys. Rev. 129, 2659 (1963)
2. C.B. Fulmer and B.L. Cohen, Phys. Rev. 109, 94 (1958)
3. R.L. Fleischer, P.B. Price, R.M. Walker and E.L. Hubbard, Phys. Rev. 133, A1443 (1964).
4. J.H. Manley, Nucl. Phys. 33, 70 (1962)
5. J. Lindhard, M. Scharff and H.E. Schiott, Mat. Fys. Medd. Dan. Vid. Selsk. 33, no. 14, (1963)
6. N.K. Aras, M.P. Menon and G.E. Gordon, Nucl. Phys. 69, 337 (1965)
7. W.H. Barkas and M.J. Berger, "NASA" Report No. SP-3013.
8. W.H. Barkas "Nuclear Research Emulsions" Vol. 1, p.366.
9. D.C. Brunton and W.B. Thompson, Can. J. Res. 28A, 498 (1950)

DISCUSSION:

M.L. Jhingan: You pointed out the advantages of threshold detector over nuclear emulsion. One of the advantages is that emulsion has got a shrinkage factor of 2.5. But this disadvantage of emulsion can be eliminated by non shrinkage development technique.

K.N. Iyengar: This is true if the shrinkage is inhibited completely and the other advantages weigh more in favour of the solid state detector at least in the case of fission studies.

MASS DISTRIBUTION SPECTRUM OF ^{235}U EMPLOYING A RATIO-CIRCUIT

P.K. Patwardhan and V.S. Indurkar
Bhabha Atomic Research Centre
Electronics Division
Trombay - Bombay

I. INTRODUCTION:

Although the radiometric and mass spectrometeric techniques are practiced for the study of yield-mass distribution of fission fragments, there is a lacuna in terms of a more elegant and efficient method which will employ faster electronic techniques and will lend itself to quicker diagnostics of experimental conditions. The newly developed Ratio-Circuits (pulse-voltage-dividing-circuits) are promising in this respect (1,6).

II. BASIC RATIO-CIRCUIT:

The present system is based on the comparision of a ramp voltage with a stretched pulse (6). The output pulses from two independent detectors (Frisch double grid ionization chamber or solid state detectors placed back-to-back), after suitable amplification are algebraically added. This sum-pulse is then stretched (pulse width = Tμsec.) and allowed to charge a capacitor with constant current, thus generating the ramp. This is compared with another stretched pulse (also Tμsecs.) from one of the detectors. The comparator yields an "Index Pulse" at the instant equality is achieved. This divides the total time Tμsec. into two parts (t_1 and t_2 μsec.) carrying the information regarding the ratio of the two input pulses. It has been shown

earlier (6) that t_2 is given by

$$t_2 = \frac{V_A}{V_{(A+B)}} \cdot T + \frac{V_B}{V_{(A+B)}} \left(\frac{G_A - G_B}{G_A}\right) \cdot T \quad \ldots\ldots\ldots \quad (1)$$

where V_A and V_B are the two pulses proportional to the energy of the fragments and

$$V_{(A+B)} = V_A + V_B$$

If the amplifiers have indentical gains $G_A = G_B$ then it follows

$$t_2 = \frac{V_A}{V_{(A+B)}} \cdot T \quad \ldots\ldots\ldots\ldots\ldots\ldots\ldots \quad (2)$$

III. PRE-TREATMENT AND PULSE-SHAPING:

Although, there can be many ways of achieving pulse voltage addition, a simple passive attenuation network with a common attenuation point is used, Fig. 1. The analytical treatment of the possible effects of attnuation are discussed elsewhere (7).

The two pulse stretchers have to fulfill stringent design requirements in order to provide for the identical performance, in terms, of rise time, stretching time, percentage droop and fall time. Further, the percentage attenuation of both the pulse stretchers should be equal and should remain constant for all working ranges of input pulse height and frequency.

The emitter followers Q_1 and Q_1' admit the two pulses to the memory capacitor C_1 and C_2 respectively which are discharged simultaneously after a time T/μsec., through the

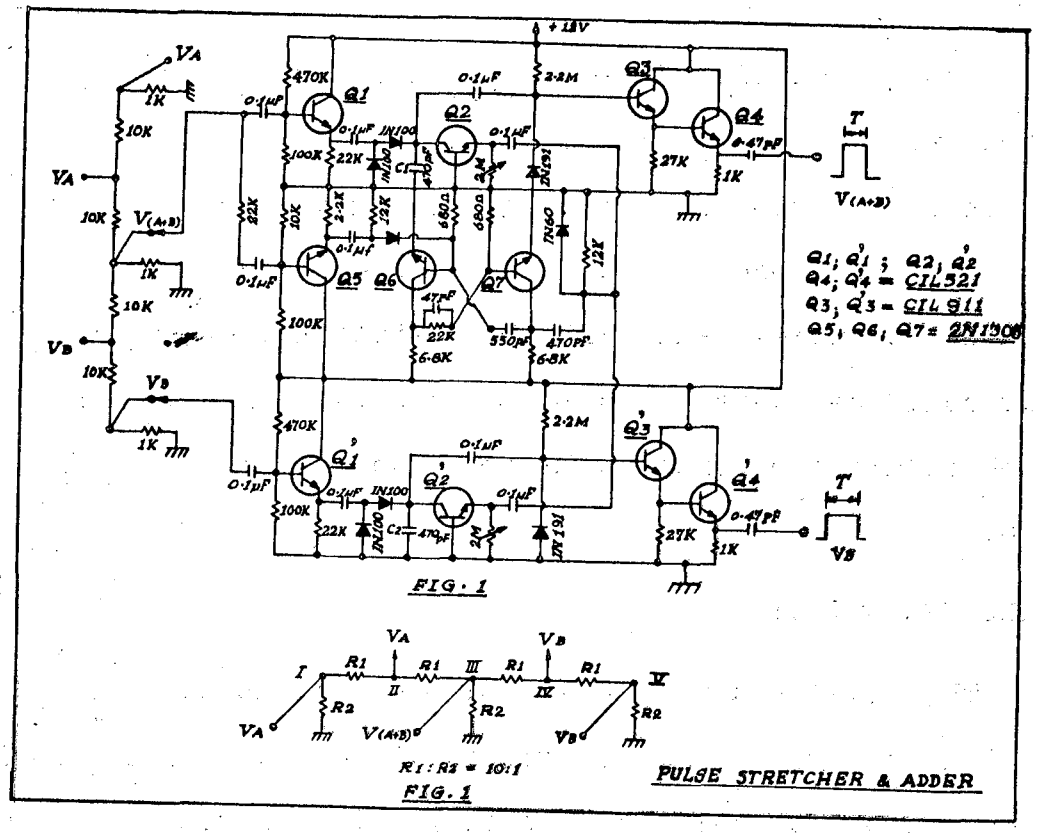
+18V
Q1; Q1' ; Q2, Q2'
Q4; Q4' = CIL521
Q3; Q3' = CIL911
Q5, Q6, Q7 = 2N1308
FIG. 1
R1 : R2 = 10:1
FIG. 1
PULSE STRETCHER & ADDER

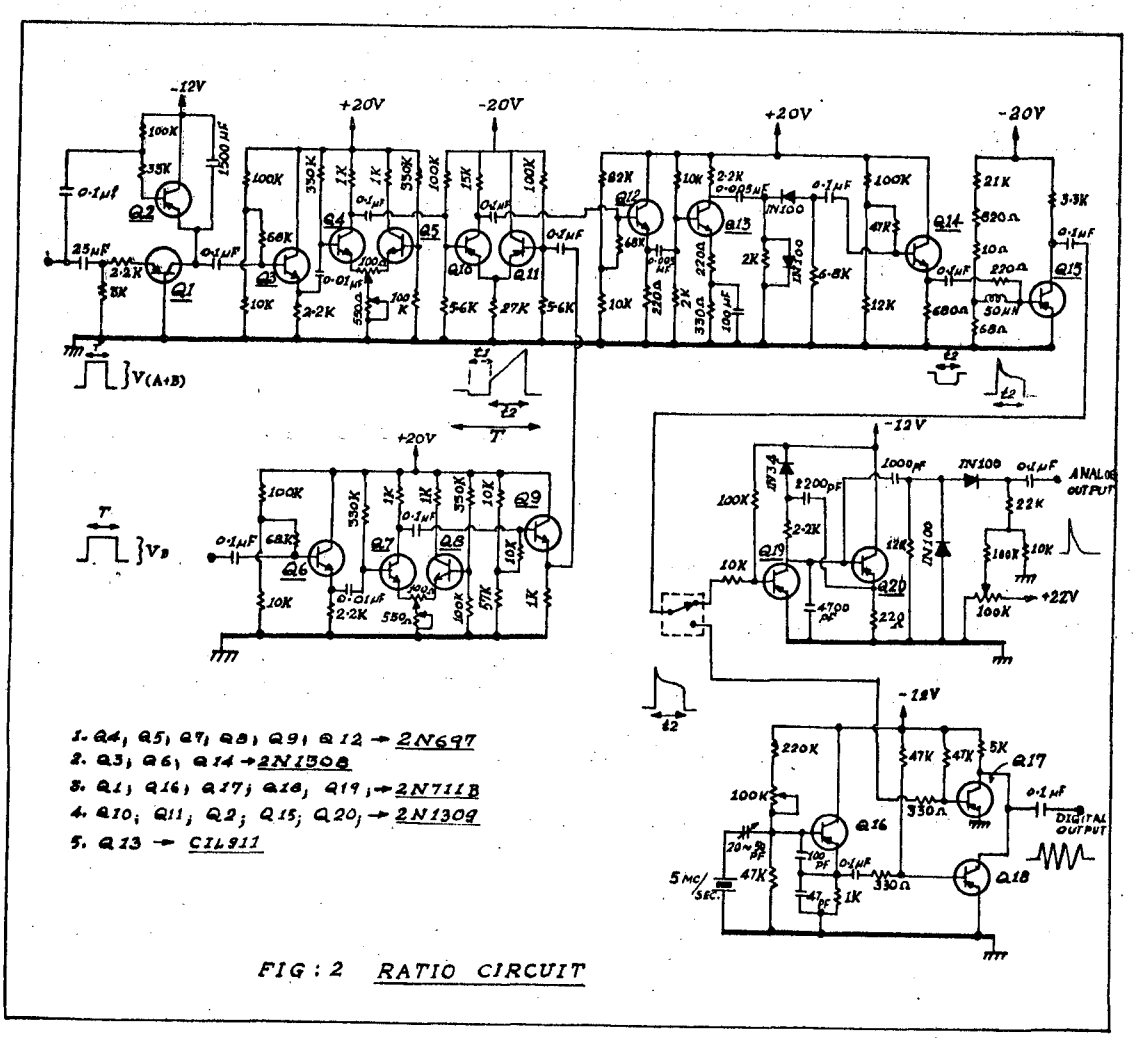
-12V
+20V
-20V
+20V
-20V
+20V
-12V
-12V
-12V
ANALOG OUTPUT
DIGITAL OUTPUT
5 MC/SEC.
1. Q4, Q5, Q7, Q8, Q9, Q12 → 2N697
2. Q3, Q6, Q14 → 2N1308
3. Q1, Q16, Q17, Q18, Q19 → 2N711B
4. Q10, Q11, Q2, Q15, Q20 → 2N1309
5. Q13 → CIL911
FIG : 2 RATIO CIRCUIT

transistors Q_2 and Q_2'. Pulse $V_{(A+B)}$ also triggers the delay time univibrator, which gives out a discharge pulse after time, $T = 8\mu$sec. The choice of the stretching time T, μsec. is a matter of convenience. Discharge switches Q_2 and Q_2' operate in common base mode. The variable resistances at the emitters of them could be adjusted to compensate for the slight mismatch which might be present in order to equalize the pulse heights.

IV. ADC TECHNIQUE:

The novel feature of present design was to incorporate the analog-to-digital conversion technique, namely to make the ratio time proportional, thus utilizing the pricision obtainable from time measurements. Provision is made, either to obtain the digital output or, an analog pulse, as output of the Ratio-Circuit. In case the digital output is required, the rectangular pulse of duration t_2 gates a crystal controlled oscillator. When multichannel analyser facility is available analog output is preferred.

Schematic of the present Ratio-Circuit is shown in Fig.2. and indicates fairly straight forward logic, illustrated with appropriate waveforms. Used in common base mode Q_1 is a constant current generator. The transistors Q_{10} and Q_{11} constitute a comparator in difference configuration with a common mode rejection to improve the thermal stability. Q_{13} and Q_{15} constitute the rate-of-rise amplifier and a high speed switch,

which converts the waveform to give a rectangular pulse with a duration equal to $t_2 \mu$secs. Q_{19} and Q_{20} constitute the time-to-pulse height converter for obtaining analog output, in which high linearity exists because of boot-strapping. The performance of the Ratio-Circuit gives the maximum deviation from linearity to be 2% for the ratio 0.2 to 0.9 and maximum fluctuations to be $\pm$ 2%.

V. ELECTRONIC SIMULATION:

The electronic simulation of fission experimental conditions are brought about by deriving two simultaneous pulses from a single pulse obtained from a mercury pulser. Emitter followers are used for the adequate isolation of each other and minimizing their pulse-height-interdependance. The two coincident pulses fed to the pre-amplifers, amplifiers, adder, pulses-stretchers and Ratio-circuit assembly are varied independently to achieve amplitude randomization to near experimental conditions. The added pulse is kept within the total dynamic working range of the system $-1.5\ V \leq V_{(A+B)} \leq 5.5\ V$.

The ratio curcuit output V_{out} is plotted against $\left(\frac{V_A}{(V_A + V_B)}\right)$ calculated from the observed values of V_A and V_B at the adder Nodes (I) and (V). It is observed that the deviation from linearity and fluctuations are less than 4% for the overall system (including the pulse-stretchers and the adder) for

the ratio 0.2 to 0.9 which compares favourably with that reported in the literature. It should be noted that electronic simulation and subjecting the overall system for such tests brings to light the real performance of the system. This aspect will be discussed elsewhere (7).

VI. MASS DISTRIBUTION MEASUREMENT:

The experiment was carried out at APSARA swimming pool reactor site. The fission fragment induced pulses are obtained from the solid state detectors and the output voltages proportional to energies of the corresponding fragments are amplified. The two sets of preamplifier and amplifier, chosen for the two channels, should be nearly identical from the point of view of gain, rise time, and the RC-time constant. Fig.3 shows the mass-distribution spectrum for thermal neutron induced fission of ^{235}U, using a T.M.C. 1024 channel analyser, in a single parameter moade. The area under the light and heavy mass-groups, was given by 26977 counts and 27299 counts respectively and shows that the areas under the peaks are nearly equal. The results obtained, using the Ratio-circuit compare well with the standard mass-distribution profile for thermal neutron fission of ^{235}U, obtained by other methods.

VII. OTHER APPLICATION:

Besides the main use of Ratio-circuit for mass distribution measurements in low-yield situation, such as photofission, it finds application in multiparameter fission ex-

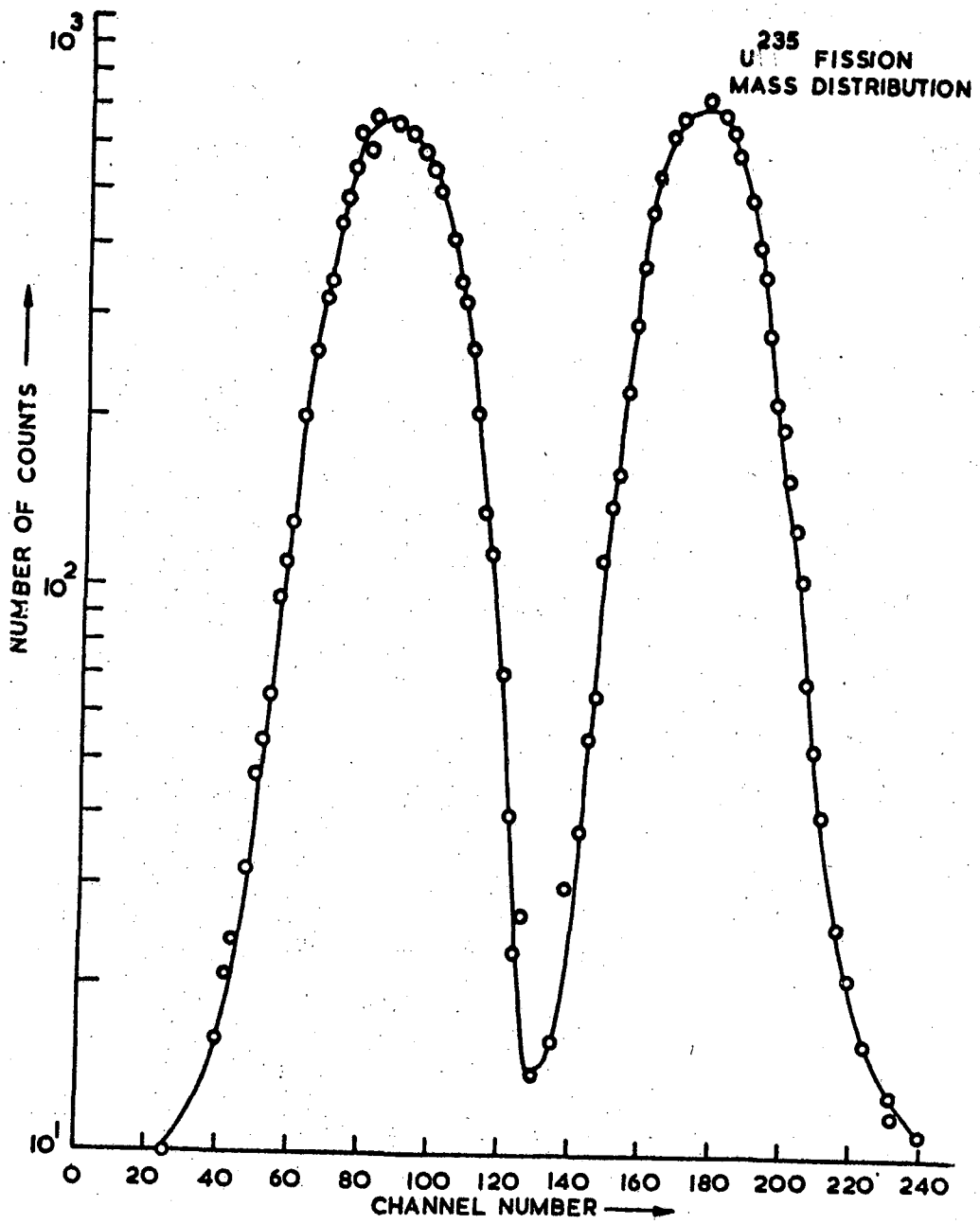

FIG.3 MASS DISTRIBUTION SPECTRUM

periments, such as, fission angular correlation or, fission associated gamma ray spectra etc. This is an important advantage of Ratio-circuit.

It can also be easily adapted to monitor the amplifier gain-spread, while an experiment involving long time periods is in progress. Further, it can be put to use for the measurement of gain or, attenuation factor in various experimental set-ups, such as the attenuation measurements in Inospheric Back-Scatter studies.

VIII. ACKNOWLEDGEMENT:

The authors are thankful to the members of the Nuclear Physics Division of B.A.R.C. for their help in connection with ^{235}U mass distribution measurements. They are also thankful to Shri A.S. Rao, Director, Electronics Group and Shri G.H. Vaze, Head, Electronics Division for their interest in this work.

REFERENCES:

1. Griffiths R.J. and Knight K.M., Nucl. Instr. & Meth. 15, 309 (1962)
2. Bennett E.F., USAEC Rep. ANL-6479 (1962)
3. Bayer R., Nuclear Electronics II, IAEA., Vienna 337-344 (1962)
4. Roeland L.W., et. al. Proc. 2nd U.N. Int. Conf. PUAE 15, 440 (1958)
5. Tsukuda M., Nucl. Instr. & Meth. 25, 265-268 (1964)

6. Patwardhan P.K., and Indurkar V.S., Nuclear Electronics, Proc. of Conf. on Nucl. Electronics, Bombay. IAEA, Vienna 341-350 (1966)

7. Patwardhan P.K. and Indurkar V.S., Being communcated elswhere.

SOME OBSERVATION ON THE SCINTILLATION PERFORMANCE CHARACTERISTICS OF SODIUM IODIDE THALLIUM ACTIVATED CRYSTALS

G.K. Bhide, G.V.N. Ramamurthy & S.C. Karandikar
Technical Physics Division

INTRODUCTION:

Ever since the Sodium Iodide-Thallium activated crystals are used in gamma ray spectrometry, considerable effort has been put in to understand the complexities involved in the resolution (FWHM) attainable with this scintillator.

According to Breitenberger (1) inhomogenous luminescence process itself contributes to the instrumental line width via a non normal (non propertional) scintillation variance. According to Shamovskii (2) the activator, which can be present as a separate phase in the crystal causes quenching and hence deterieration in performance.

Harshaw et al have reported that the pulse height is independent of impurity centre concentration within fairly wide limits (3).

Our earlier studies (4) have indicated that there is a decrease in the pulse heights of NaI(tl) crystals with increase in Thallium Iodide concentration higher than 0.20 percent by weight. NaI being considerably hygroscopic, inorder to eliminate the additional uncertainties involved such as polishing and canning the characteristics of a large number of crystals have been reviewed on a statistical basis in the present text.

EXPERIMENTAL DETAILS:

Starting materials our crystals are granular Sodium Iodide (Regent Grade of Banker and Adamson). All the 105 crystals were grown employing the technique based on Stockbarger's modification of Bridgeman's method (5) under identical conditions of initial doping concentration, rate of growth, temperature gradients in the growing furnaces, polishing canning and testing of the crystals within practical limits. The crystals were tested on an automatic recording gammaray spectrometer employing the RCA 8054 multiplier tube with 662 keV gammarays from ^{137}Cs. The photo peak pulse heights were normalised by expressing as a percentage to that of a Harshaw crystal of 1½" dia and 1" height.

RESULTS:

All the 105 crystals studied are grouped into five categories, their averages and mean deviations as regards to photo peak pulse heights and $FWHM_s$ are presented in table I. Photo peak pulse height VS FWHM for crystals under category 4 of table I is shown in Figure I.

Table I.

Category.	Details	Average photo-peak pulse ht.	Average FWHM
1.	14 crystals of 1½" dia.-1½" ht.	75.37 ± 12.54	11.3 ± 2.0
2.	14 Crystals of 1½" dia. 1" ht. obtained from Category (1)	73.1 ± 10.1	9.76± 1.1

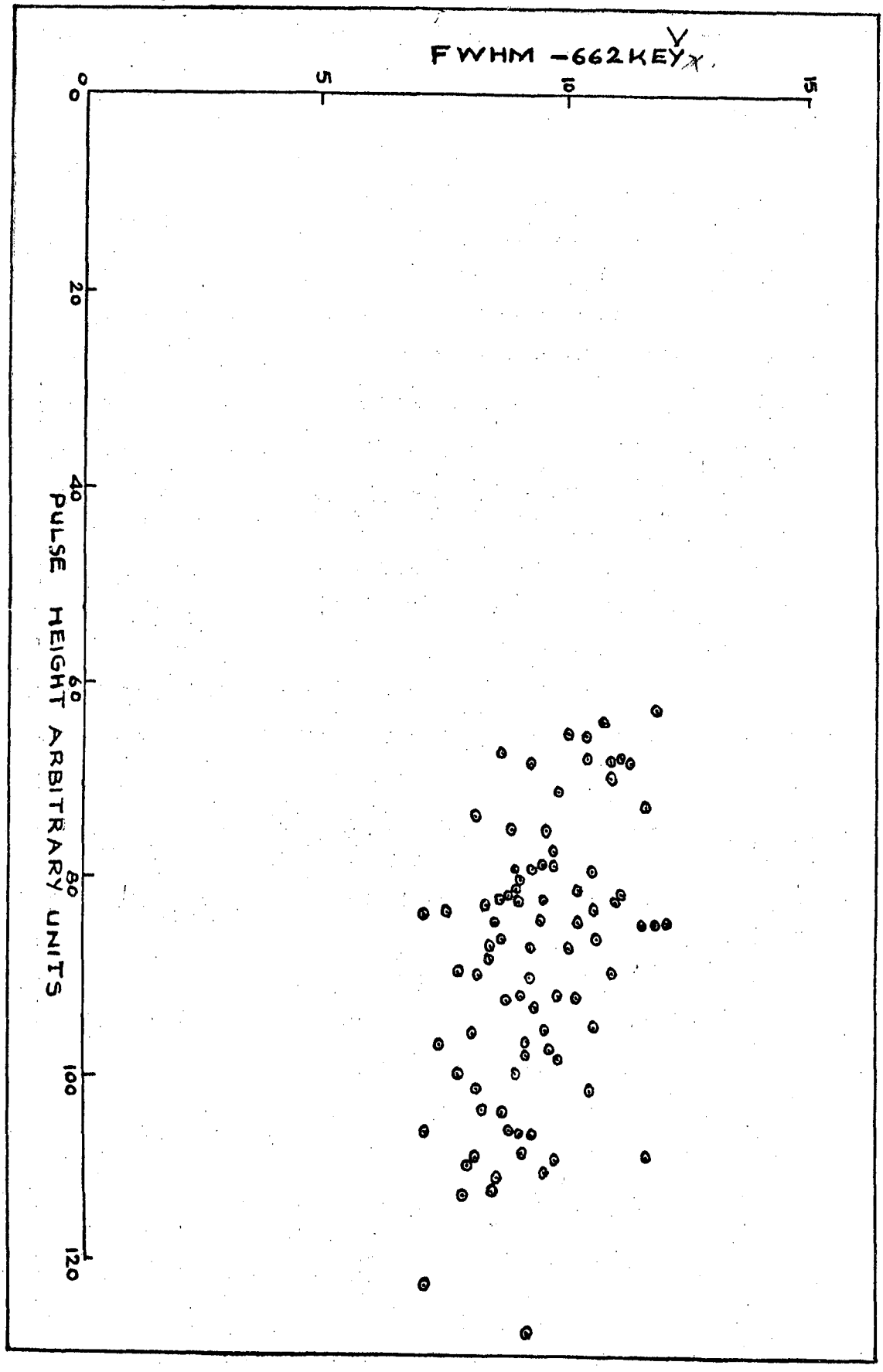
FWHM -662KEV
0
5
10
15
0
20
40
60
80
100
120
PULSE HEIGHT ARBITRARY UNITS

3.	14 Crystals of $1\frac{1}{2}$" dia 1" ht. obtained from $1\frac{3}{4}$" dia. ingot	95.6 ± 10.45	9.1 ± 0.83
4.	All 88 Crystals of $1\frac{1}{2}$" dia and 1" ht. whose $FWHM_s$ lie between 7 & 12%	88.8 ± 11.7	9.3 ± 0.95
5.	17 Crystals of $1\frac{1}{2}$" dia 1" ht. whose $FWHM_s$ are 12%	70.2 ± 10.4	14.3 ± 1.57

DISCUSSION:

It will be observed from the table that the average FWHM of the crystals of category 2 is very much better than that of the crystals of category 1, though the improvement in the pulse height is only very little. It has been pointed out by the authors that smaller crystals give larger pulse heights probably because the attentation suffered by the light pulses within the crystal is smaller in a small crystal. The slight improvement in the pulse height is due to this effect. The average performance of the crystals belonging to category 3 is the best of all. This is also felt to be in keeping with the expectation that the crystals having been machined out of larger ingots ($1\frac{3}{4}$" dia. x 2" ht. in this instance) exhibit much better uniformity of the activator concentrations. This leads to a more uniform light output from individual scintillations and hence a good FWHM. However .. the light output is not uniform as is likely to be the case if the nonuniformity in the activator concentration is pronounced, the shape of the photo peak will no longer be a single gaussian, but will be a number of gaussian distributions superimposed over each other and the effect will be to broaden the FWHM.

It is well known that the FWHM of a scintillator improves with the energy of the incident gamma ray. G.G. Kelly (6) et al have reported FWHM values ranging from 13.5% for 113 keV through 7.7% for 661 keV to 5.45% for 1850 keV gamma rays, using a good crystal photo tube combination. In this range the pulse heights can be assumed to be proportional to the incident energies. A certain deterioration in FWHM with lower photo peak pulse heights is thus to be anticipated. Our values of the average FWHM and pulse heights for eactegories 2 , 3 and 4 are closely compatible with the extent of expected deterioration, while the FWHM and pulse heights of category 5 are quite incompatible. A source of uncertainty viz. the part of the ingot from which the crystals were machined may lead to a greater degree of nonuniformity of the activator thereby producing the observed pronounced deterioration in the FWHM of crystals in this category.

According to Shamovskii (2) the periodic deposition of the activator as a separate phase is mainly responsible in effecting the performance of the scintillator adversely. According to him this can be avoided and crystals of spectrometry grade can be grown only under high temperature gradients. We are not certain whether the temperature gradients employed in the present work are adequate to avoid the deposition of the activator as a separate phase in our crystals.

CONCLUSION:

The FWHM & pulse height of a scintillator are quite likely to be influenced by various factors such as, uniformity of the activator distribution over the crystal, presence of the activator crystal, strains in the crystal, etc.

ACKNOWLEDGEMENTS:

Thanks are due to Kum. R.P. Hassani for the patient job of canning all the crystals. Authors are very much grateful to Prof. D.Y. Phadke and Shri C. Ambasankaran for their encouragement in this work.

REFERENCES:

1. E. Brietenberger, Progress in Nuclear Physics Vol. 4, 56-94.
2. L.M. Shamovskii, Growth of Crystals Vol.4, Reports of the second Conference on Crystal Growth Moscow March 23-April 1-1959, Authorised translation from Russian, pp.223.
3. Harshaw J.A., Kremers H.C., Stewart E.C., Warburton E.K. and Hay J.O., Report on preparation and performance of some scintillation crystals. NYO 1577 (U.S. Atomic Energy Commission Washington) (1952)
4. G.V.N. Ramamurty & G.K. Bhide, Indian Journal of Pure and applied Physics Vol. 4 No. 1 pp 24-26 (1966)
5. G.K. Bhide, AEE/TP/3/1963 (Atomic Energy Establishment Trombay, Bombay (1963)
6. G.G. Kelly, I.R.E. Transaction on Nuclear Science Vol.No.53No.4.

DISCUSSION:

S.K. Gupta: The resolution of NaI(Tl) or any other scintallator depends strongly upon the method of polishing of the crystal as described by Gonmethal in his book "Applied gamma ray spectroscopy". He has described a technique of lathe polishing of the crystals in dry atomosphere which consistently results in optimum resolution of about 8%. Bad polishing by emery papers results in the resolution between 9% and 12%.

G.K. Bhide: Though this is true, the large variation from crystal to crystal observed still needs explanation, as all the crystals were processed for encapsulation, under indentical conditions as far as was practical and hence the crystals should have been performing uniformly.

A.S. Divatia (Comment):

Machining a crystal and polishing a crystal should be separated. It is the machining that may make a difference. The polishing averages out.

P.K. Patwardhan: Have you studied the basic scintillation pulse profile, such as life time etc?

G.K. Bhide: In my opinion the pulse decay time is characteristic of the host material. However, we have not studied the scintillation pulse profile as we do not presently have sufficient facilities with us for doing this.

THE SOURCE INTRINSIC EFFICIENCY OF A NaI(Tl) CRYSTAL FOR A CYLINDRICAL SOURCE HAVING ITS AXIS PERPENDICULAR TO THAT OF THE CRYSTAL

S.M. Bharathi and M.L. Jhingan
Tata Institute of Fundamental Research, Bombay

ABSTRACT.

In (n, γ) experiments using the reactor as the source of thermal neutrons, the target to be studied is usually chosen to be cylindrical and is placed in the thermal column such that the axis of the detector is perpendicular to that of the target and passes through its centre. With a view to find out the optimum source to detector distance and hence to maximise the signal to background ratio, a formula has been derived for computing the source intrinsic efficiencies of a NaI crystal placed at different distances from the source for different photon energies. A knowledge of the variation of the average solid angle Ω subtended by the certain preliminary experiments with thermal neutron induced capture gamma rays at CIRUS, Trombay. First, a formula was derived to calculate Ω , which was later modified to give the source intrinsic efficiency of a NaI crystal for monochromatic gamma readiation.

The integrals appearing in the derived expression could be numerically evaluated using the CDC 3600 computer of the Tata Institute of Fundamental Research, Bombay. Efficiency calculations have been made for different source to detector distances and source and detector dimensions.

DISCUSSION:

S.K. Gupta: What is the geometry for which you made the calculations and where do you require it?

S.M. Bharathi: (a) The geometry is one in which the axis of the detector is perpendicular to that of the target and passes through its centre.

(b) This type of geometry is usually chosen in (n,γ) experiments.

GAMMA RAY RESPONSE OF PLASTIC SCINTILLATORS

Arun Chatterjee and A.M. Ghose
Nuclear Physics Laboratory
Bose Institute
Calcutta.

ABSTRACT.

Gamma ray response of plastic scintillators have been analysed theoretically taking nonlinearity of electron energy pulse height relationship, escape from the edges etc. into account. The result of experimental tests on the theory will be presented.

A UNIFORM SENSITIVITY PHOTON COUNTER FOR LOW ENERGY PHOTONS

A.R. Dasgupta and A.M. Ghose
Nuclear Physics Laboratory
Bose Institute
Calcutta.

ABSTRACT.

Design and Performance of a uniform sensitivity photon counter suitable for photons of energy less than 1.5 MeV will be discussed.

DESIGN AND PERFORMANCE OF HIGH INTENSITY GAMMA LINEAR COMPTON POLARIMETER

N. Rudra and A.M. Ghose
Nuclear Physics Laboratory,
Bose Institute
Calcutta.

ABSTRACT.

Design considerations of a high intensity linear Compton polarimeter with small altitudinal and aximulthal spreads will be discussed.

ON THE DESIGN OF A SPLIT POLE MAGNETIC SPECTROGRAPH

M.N. Viswesvariah and N. Sarma
Bhabha Atomic Research Centre,
Trombay, Bombay.

In the following the ion optical performance of the split pole magnetic spectrograph (SPMS) and a brief description of its major components are presented.

We have worked out expressions using the first order theory as given by Herzog and Hintenberger and Calculated values for various ion optical parameters on the electronic computer CDC 3600.

Figures 1 to 2 show the expected ion optical performance of the split pole spectrograph. The main features are the comparative straightness of the focal plane and the momentum resolution curves. Results of calculation involving the shifting of the source away from the SPMS shows variations in focal plane and resolution. It is found that the change in the position of the focal plane is relatively small, whereas there is considerable change in resolution R. It is clear that the resolution wanted can be obtained by choosing the proper source distance.

Design work connected with the construction of SPMS has been carried out, the major components constituting the SPMS being:

A. The split pole Electromagnet.
B. The stabilised DC power supply.
C. The vacuum chamber assembly.
D. The magnet support and turn table.

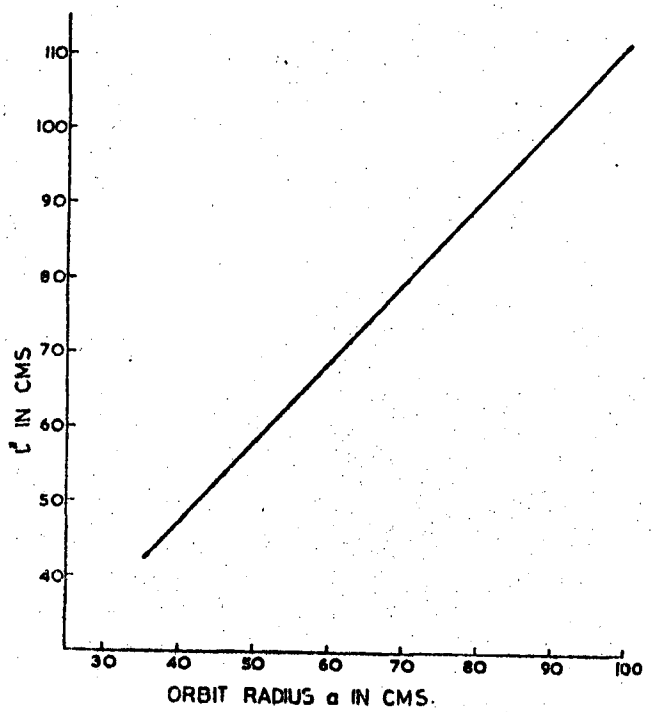

FIG·1

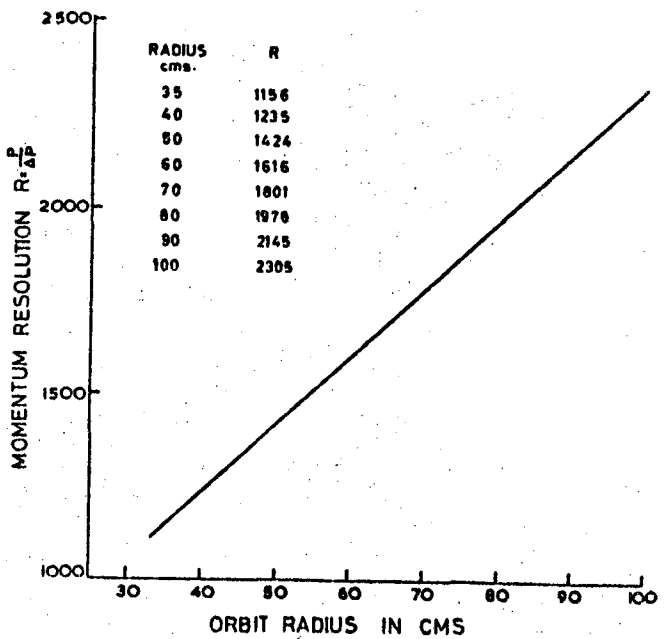

FIG - 2

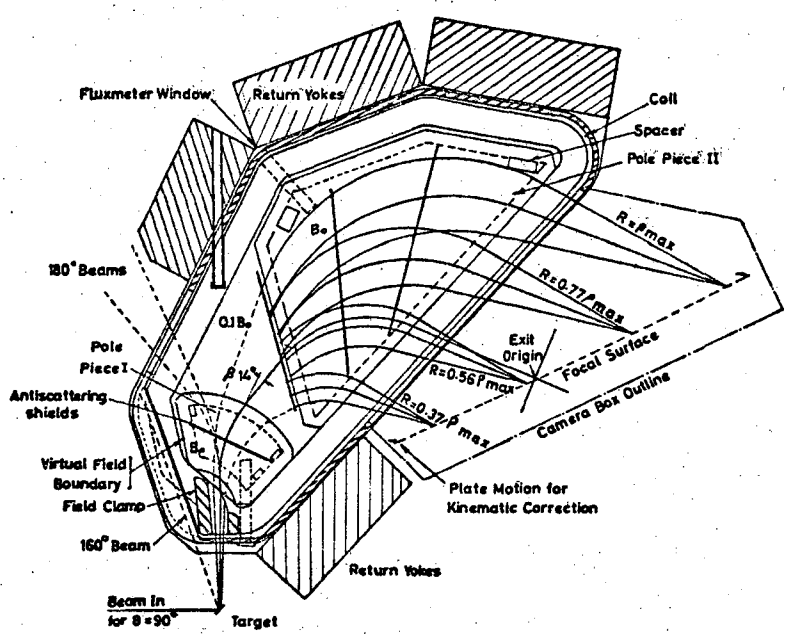

FIG - 3

A. ELECTROMAGNET:

The pole face layout and the elevation of the electromagnet are shown in fig. 3 and 4. The magnet is made of high permeability low carbon magnetic steel approximating to Tata A Grade. The field strength is nearly 10 kilogauss (maximum) in a pole gap of 4 cms and an excitation of 50 kiloampere-turns are needed to produce this field. The return flux is distributed over 5 return paths. The top and bottom pole pieces serve as lids of the vacuum chamber in the magnetic gap. The magnet coil is made of 200 turns of ½" square electrical grade aluminium tubing with a central hole to permit the flow of cooling water through the coil.

B. FIELD STABILISED DC POWER SUPPLY:

The DC power is supplied by a 3 phase power transformer. Variation in current is brought about by varying the phase angle at which the silicon controlled rectifiers start conducting. Stabilisation of 1 part in 10^4 is brought about by a sensor which is a temperature compensated hall probe. A standard chopper amplifier with a current output amplifier will deliver the phase control signal. Use is also made of an electronic filter which reduces the bulk of capacitances used in conventional filters to cut down AC ripple.

C. THE VACUUM CHAMBER ASSEMBLY:

This consists of the target chamber, vacuum chamber and the camera. The target chamber consists of a phospher-Bronze or stainless steel vacuum seal, giving variable contact between the rot-

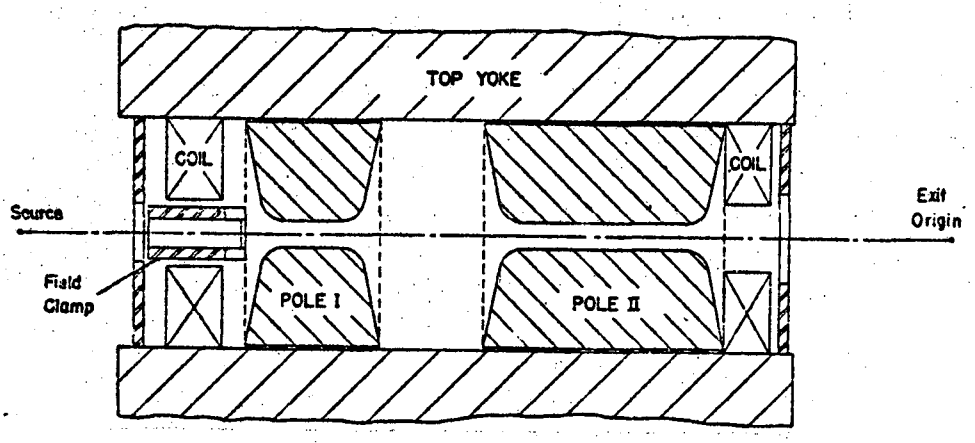

b) Folded-out cross section

FIG-4

ating vacuum chamber and the beam tube.

The camera chamber has arrangements to hold a number of nuclear emulsion plates to be brought in the focal plane one after another for exposure without breaking the vacuum.

D. MAGNET SUPPORT AND TURN TABLE.

The magnet support has to handle about 30 tons of weight which is a fixed load without involving any tilting. For measurements at the back angle of 180° the magnet carrier has to be provided with a facility to give a translatory movement to the magnet in a direction parallel to the beam direction.

A FIVE PORT SWITCHING MAGNET FOR USE WITH THE 5.5 MeV VAN DE GRAAFF ACCELERATOR AT TROMBAY

T.P. David, N. Sarma, M. Bhatia and P.R. Sunder Rao
Bhabha Atomic Research Centre
Trombay, Bombay.

ABSTRACT.

A Five port switching magnet has been built at the Van de Graaff Laboratories at Trombay with beam exit ports at + 45°, + 25°, 0°, - 25° and -45°. The magnet yoke and pole pieces have been fabricated from low carbon Tata 'A' Grade steel having a magentic saturation around 21,000 gauss. Electrical Grade Aluminium tubing of 12.7 mm. sq. section has been used for making the magnet coils. Cooling water will be passed through these tubing thus obtaining maximum cooling efficiency. A high current (max .175 amps at 20 volts) variable D.C. supply feeds the main coils. This supply is stabilized by a bank of series controlled transistors. Each exit port is provided with a pair of adjustable insulated pick up slits. The amplified signals picked up by these slits control a low current power supply feeding an auxiliary coil. Apart from giving an additional stabilization, this also enables small range energy scanning without manually

adjusting the switching magnet current.

It is estimated that the cost of a complete beam switching system including a pair of electromagnetic quarupole focusing lenses in each of the five ports vacuum system and power supplies will be approximately Rs. 150,000 with only Rs. 10,000 in foreign exchange. A much smaller magnet and power supply able to bend a maximum of 2.75 MeV alpha beam has been quoted at Rs. 180,000 in Foreign Exchange.

DISCUSSION:

S.K. Gupta: What type of coil have you used in the switching magnet ?

T.P. David: Half inch Aluminium tubing of the square section is found in the form of pole shape and the cooling water is passed through these coils.

STATISTICAL ANALYSIS OF PULSE SEQUENCES AS A TECHNIQUE OF DETECTION OF DELAYED COINCIDENCES IN THE PRESENCE OF LARGE BACKGROUND

M. Srinivasan and S.L. Mehta,
Bhabha Atomic Research Centre,
Tromaby, Bombay.

ABSTRACT.

In radioactive counting it is common knowledge that the statistical accuracy of counting is measured by the square root of the total counts collected. This rule is valid only if the pulses being counted follow a Poisson distribution or in other words form a time sequence of uncorrelated random pulses. There are however circumstances when the sequence of pulses issuing from a nuclear particle detector may not obey Poisson statistics. This would be the case for example when short half life delayed coincidence pairs are present amongst the pulses. In such cases a measurement of the deviation from poissonian behaviour of the statistical properties of the pulse series would give information on the nature and magnitude of the correlation (or time-relation) between the pulses. As an example the determination of the mean life time of prompt neutrons in a neutron multiplying medium by such techniques is discussed and the results of some measurements presented. The possible applications of statistical methods in nuclear physics work is breiefly reviewed.

BeO ABSORPTION CROSS-SECTION MEASUREMENT BY OULSED NEUTRON METHOD

B.V. Joshi, V.R. Nargundkar and K. Subbarao
Bhabha Atomic Research Centre
Trombay, Bombay.

ABSTRACT.

The use of the pulsed neutron method for the precise determination of absorption cross-section of moderators is described. The absorption cross-sections of BeO with empty channels are obtained by this method. The neutron bursts were produced by a cascade accelerator by pulsing the ion source and using Be(d,n) reaction. An enriched BF_3 counter was used as a detector of neutrons. By avoiding space and time harmonics, constant background effecrs, it was possible to determine the decay constant of the fundamental mode of thermal neutron population to a high degree of accuracy. A proper choice of the number of terms to be used in the decay constant expression, rendered an accurate determination of the absorption cross-section.

RESONANCE SELF-SHIELDING IN ^{235}U AND ^{239}Pu

R. Shankar Singh
Reactor Engineering Division
Bhabha Atomic Research Centre, Trombay

INTRODUCTION:

The need of resonance parameters for evaluating the self-shielded cross sections of nuclei which exhibit resonance behaviour in their reaction cross sections is well known. Resonance parameters of fissile nuclei is one field where many descrepancies and inconsistencies still exist between the experiment and theory of resonance reactions. The object here is to illustrate for ^{235}U and ^{239}Pu, how the lack of knowledge of proper resonance parameters could significantly affect the computed effective cross sections and thereby introduce considerable uncertainties in the predicted behaviour of a nuclear reactor.

RESONANCE PARAMETERS AND EFFECTIVE CROSS SECTIONS:

The basic resonance parameters which are required in the computation of effective cross sections are : the energy at which the resonance occurs (Eo); the total (Γ) and partial level widths such as Γ_n the neutron width, Γ_γ the capture width, Γ_f the fission width and the spin of the level (to get the statistical g-factor). In the unresolved resonance region, parameters to be described by statistical distributions are, the average strength function $\langle \Gamma_n^o/D \rangle$ for s and p-wave, the average level spacings $\bar{D}$ for

different spin states, the type of statistical distributions and their number of degrees of freedom etc. For fissile nuclei like ^{233}U, ^{235}U and ^{239}Pu, difficulties have been encountered not only in the experiments, but also in the analysis of resonance parameters. Levels of fissile nuclei are very closely spaced and several of their level shapes cannot be fitted by a single level Briet-Wigner function and require multilevel analysis. The data hitherto published (1) show the resonances to be resolved upto 60 eV for ^{233}U, 150 eV for ^{235}U and 300 eV for ^{239}Pu. Hence, with the present available information on the resolved resonance data for these nuclei, it is difficult to determine the average parameters with sufficient accuracy in the unresolved resonance region. The situation is illustrated here for ^{235}U and ^{239}Pu while such an attempt for ^{233}U would be futile at this time.

Self-shielded cross sections are evaluated through the resonance integral calculations using the resonance parameters. Such calculations have been made here using a computer code DOPINT (2) on CDC-3600, under the narrow resonance approximation for a homogeneous mixture.

EFFECT OF UNCERTAINTIES IN RESONANCE PARAMETERS:

Uncertainties in the resonance parameters are reflected in the computed self-shielded cross sections which in turn would affect the predicted reactivity coefficients of a nuclear reactor. The status will be exemplified here for ^{235}U and ^{239}Pu.

^{235}URANIUM.

A review of the resonance properties of the main fertile and fissile nuclei made recently by J.J. Schmidt (1) has shown that for ^{235}U many inconsistencies and descrepencies exist between the theoretical predictions of channel theorey and the experimental data. Spins have not been determined for many of the resolved resonances so far. Hence resonance integral calculations have been done only with the unresolved average parameters.

The fission widths estimated for the resolved resonances in the experiment are low ($\sim$65 mV) compared to those resulting from the statistical theory fits to 'α', the capture to fission cross section ratio, in the unresolved resonance region. The results of extrapolating the low value of Γ_f to the unresolved resonance region are shown in Table I where in the capture and fission cross sections as well as 'α' have been computed for few groups in a 22-group structure (3) for a specific case of σ_p the potential scattering cross section per absorber atom = 200 barns and temperature = 300 K. It is seen that the 'α' values are greater than unity for all groups if Γ_f = 65 mV is used. This is contrary to the experimental results and the results of a choice (4) of Γ_f = 120 mV are also given in Table I where in the 'α' values agree with the experimental results. This illustrates the serious errors that may result due to extrapolating the parameters at lower energies to higher energies.

^{239}PLUTONIUM

The situation for this material is slightly better as pointed out by Schmidt, but still far from satisfactory. Resonances upto 300 eV are resolved and resonance integral calculations are made and cross sections computed for the last two groups (21 and 22), results of which (RRP) are shown in Table 2.

It has been observed by Schmidt (1) and also by Michaudon et. al, (5) that the statistical study of the fission widths actually shows the existence of two families of resonances, one with a higher value of Γ_f and another with a lower value. These have been indentified as corresponding to the two spin states J = 0 and J = 1. Results of using the spin-dependent values of Γ_f suggested by Schmidt (URP1) have been given in Table 2 for the two groups with the unresolved parameters for calculations. For comparision, results of calculations using a single value of Γ_f for both the spin states (URP2) have also been given in Table 2. It is seen from comparison that by using unresolved resonance parameters for the last two groups in which resonance are resolved, the computed effective cross sections are not very much different, provided the spin dependence of Γ_f is taken into account. It is observed that the capture and fission cross sections with the (URP_1) parameters are closer to those with (RRP), than the results obtained with (URP_2) parameters.

REFERENCES:

1. J.J. Schmidt, "Resonance properties of main fertile and fissile nuclei" paper presented at the ANS Topical Meeting on Reactor Physics in Resonance and Thermal Regions, February (1966)

2. R.S. Singh and G.A. Desai, "DOPINT" - A program to calculate resonance integrals and multigroup cross section". Internal Report, RED/TRP/117 (1966)

3. R.S. Singh and G.A. Desai, "Self-shielded cross sections for the Main Fertile and Fissile Nuclei". To be published as an AEET report (1966).

4. R.N. Hwang, "Doppler Effect Calculation for fissile materials" ANL - 6792, p. 727 (1964).

5. A. Michaudon, et. al, "Total and Fission Cross-Sections of ^{239}Pu, statistical study of 0-500 eV Resonance Parameters". Paper submitted at the IAEA Conference on Nuclear Data, October (1966).

Table I.

Effective Cross Sections of ^{235}U (barns)

(σ_p = 200 barns ; T = 300 K)

Group J	EL (keV)	Schmidt's Data* σ_c	σ_f	$\alpha = \sigma_c/\sigma_f$	Hwang's Data** σ_c	σ_f	$\alpha = \sigma_c/\sigma_f$
13	9.1	1.362	1.307	1.042	0.845	1.889	0.448
15	2.8	2.841	2.645	1.074	1.824	3.875	0.471
19	0.55	6.214	5.644	1.097	4.068	8.311	0.489
21	0.10	11.356	10.344	1.098	7.308	14.909	0.490

*Schmidt's Data

$\Gamma_n^o/D = 0.915 \times 10^{-4}$; $\nu = 2$

D 3 = D 4 = 1.06 eV

$\Gamma_f = 0.0651$ eV; $\Gamma_\gamma = 0.0479$ eV.

**Hwang's Data

$\Gamma_n^o/D = 1 \times 10^{-4}$; $\nu = 2$

D 3 = D 4 = 1.72 eV.

$\Gamma_f = 0.120$ eV; $\Gamma_\gamma = 0.033$ eV.

Table II.

Effective Cross Sections of ^{239}Pu (barns)

(σ_p = 300 barns ; T = 300 K)

Group J	E_L (eV)	σ_c RRP*	σ_c URP_1**	σ_c URP_2***	σ_f URP*	σ_f URP_1**	σ_f URP_2
21	100.0	6.879	6.955	7.359	12.832	13.361	11.013
22	30.0	11.386	11.103	10.156	20.862	20.250	15.626

* RRP - Resolved Resonance Parameters as given in reference (2)

** URP_1 - Unresolved Resonance Parameters *** URP_2

$\Gamma_n^o/D = 1.07 \times 10^{-4}$; $\nu = 2$

$D_o = 8.78$ eV ; $\Gamma_f^o = 2.8$ eV

$D_1 = 3.12$ eV ; $\Gamma_f^1 = 0.057$ eV

$\Gamma_\gamma = 0.0387$ eV.

All parameters same as for URP_1 except that $\Gamma_f^o = \Gamma_f^1 = 0.09$ eV

CALCULATION OF HETEROGENEOUS RESONANCE INTEGRAL USING AN INTERMEDIATE RESONANCE APPROXIMATION TAKING INTO ACCOUNT THE OVERLAP AND DOPPLER BROADENING OF RESONANANCES

G.V. Acharya
Reactor Engineering Division
Bhabha Atomic Research Centre,
Trombay, Bombay.

ABSTRACT.

The paper presents the computation of effective heterogeneous resonance integral of Thorium doublet at 21.84 ev and 23.48 ev at a temperature of 300°K using an intermediate resonance approximation. The method is an extension of the formulation of Cohen and Goldstein for homogeneous mixtures. The resonance integral of each member of the doublet has been calculated with and without interference from the other. The results of the computation have been compared with those of RIFF - RAFF, an ANL programme of Kier.

RESONANCE INTEGRAL OF U-238 AND Th-232

H.C. Huria
Reactor Engineering Division
Bhabha Atomic Research Centre
Trombay, Bombay.

ABSTRACT

A programme to obtain the effective resonance integral of ^{238}U and ^{232}Th rods in cylindrical, lattices has been undertaken. The method used is the one formulated by Driggers which makes use of multigroup-multiregion technique. This has been programmed for CDS-3600. Some modifications were made in the original version to eliminate certain observed discrepancies in the results e.g. non-conservation of neutrons in energy groups. The alterations, however, do not change the resonance integral appreciably but considerably change the values of resonance escape probability. The results obtained so far show a fairly good agreement with Hellstrand's experimental values.